Polyphénols de la vigne et du vin et dégénérescence maculaire liée à l'âge

Clarisse Cornebise

THESE DE DOCTORAT DE L'ETABLISSEMENT UNIVERSITE BOURGOGNE FRANCHE-COMTE

PREPAREE A L'INSERM UMR 1231 (LIPIDES, NUTRITION, CANCER), équipe TIReCs

Ecole doctorale n°554

Environnements-Santé

Doctorat de Biochimie et Biologie moléculaire

Par

Clarisse CORNEBISE

Polyphénols de la vigne et du vin et dégénérescence maculaire liée à l'âge.

Thèse présentée et soutenue à Dijon, le 3 octobre 2023

Composition du Jury :

Pr. Laurent Martiny	Directeur de recherche, CNRS, Reims	Président
Dr. Niyazi Acar	Directeur de recherche, INRAE, CSGA, Dijon	Examinateur
Dr. Stéphanie Krisa	Maitre de conférences, INRAE, Université de Bordeaux	Rapporteur
Pr. Cédric Saucier	Professeur, Université de Montpellier	Rapporteur
Pr. Dominique Delmas	Professeur, Université de Bourgogne, Dijon	Directeur de thèse
Dr. Virginie Aires	Maitre de conférences, Université de Bourgogne, Dijon	Co-directrice de thèse
M. Christian Vanier	Directeur du bureau Interprofession des vins de Bourgogne	Invité

Thèse financée avec l'aide :

Du Bureau Interprofessionnel des Vins de bourgogne

Du FEDER (European Funding for Regional Economic Development)

De l'université de Bourgogne

De l'INSERM

Remerciements

Je tiens en premier lieu à remercier les membres de mon jury de thèse, qui me font l'honneur de juger mon travail. Je remercie le Dr. Stéphanie Krisa et le Pr. Cédric Saucier pour leur temps consacré à mon travail en leur qualité de rapportrice et rapporteur de thèse.

Je souhaite également remercier chaleureusement le Pr. Laurent Martigny et le Dr. Niyazi Acar pour leur implication dans mon comité de suivi de thèse et pour avoir accepté de faire partie de mon jury de thèse en qualité d'examinateur. Je vous remercie pour le temps que vous m'avez accordé tout au long de ces années.

Je tiens à remercier le Dr. Niyazi Acar pour son implication et son soutien dans l'élaboration de mes expérimentations *in vivo*. Je tiens aussi à remercier Benedicte Buteau pour m'avoir fait bénéficier de son expertise dans la récupération des rétines.

Je tiens ensuite à remercier mes deux directeurs de thèse le Pr. Dominique Delmas et le Dr. Virginie Aires pour m'avoir donné l'opportunité de réaliser cette thèse. Je vous remercie pour m'avoir guidée dès mes premiers pas en recherche et de m'avoir accueillie dans votre équipe dès mon stage de master 1. Je tiens à vous remercier pour la confiance que vous m'avez accordée tout au long de mon doctorat.

Je tiens également à remercier le Dr. David Monchaud de m'avoir accueillie au sein de son équipe dans laquelle j'ai pu réaliser l'extrait sec de vin rouge. Je tiens particulièrement à remercier Marc Pirrotta pour son accueil chaleureux ainsi que pour son aide et son expertise dans l'extraction des polyphénols.

Je tiens à remercier chaleureusement le Dr. François Hermetet pour avoir partagé avec moi son (mon ?) bureau durant ses deux dernières années de doctorat. Tout d'abord un grand merci pour ton aide dans l'expérimentation animale, tant dans sa conception que dans sa réalisation. Merci pour ton temps consacré à mon projet. Merci d'avoir pris le temps de toujours répondre à mes très nombreuses *petites* questions. Merci de m'avoir fait bénéficier de ton expérience et de toute ouverture d'esprit tant sur le plan scientifique qu'humain. Enfin, je tiens à te remercier pour ta bonne humeur quotidienne, ton humour et ton rire communicatif ! Merci d'avoir supporté mes bougonnements et ma frustration. Un grand merci pour m'avoir reboostée quand j'en avais besoin, tu as toujours su trouver les mots justes lors de mes moments de doute.

Je tiens ensuite à remercier mes acolytes de paillasse Flavie, Aline, Maude et Aurélie. Merci à Flavie d'avoir été là lors de mes premiers pas au laboratoire. Merci pour nos échanges et pour ton aide. Merci à Aline qui m'a accompagnée dans cette aventure dès le début de mon stage de M1.

Un grand merci à Maude, je l'ai dit mais je vais le répéter, ton arrivée en thèse dans l'équipe m'a donné un second souffle. Tu as été mon coup de foudre professionnel dès le premier jour de ta thèse, tout ça grâce à un gel de western blot, qui l'eut cru que le western pouvait forger des amitiés ! Un grand merci pour ton temps passé sur mon article de thèse. Je tiens aussi à te remercier pour nos échanges tant scientifiques que personnels, cela aura été un véritable bonheur de travail dans la bonne humeur ! En parlant de bonne humeur… Je tiens à remercier la petite ronchonneuse de l'équipe, Aurélie. Merci d'avoir été là pour ronchonner avec moi. Merci pour nos échanges scientifiques et pour nos petites pauses café. Merci de m'avoir fait découvrir de nouveaux bars (*Ah oui oui oui*). Un grand merci à vous deux pour votre soutien quotidien, cette thèse n'aurait pas été la même sans vous. Je tiens tout de même à rappeler que

si vous avez la moindre question, n'oubliez pas que : « c'*est écrit dans le protocole* ». Enfin, je tiens à remercier toutes les personnes qui sont passées par l'équipe. Merci à Marie, Mahassen, Sahla, Randa, Elodie M., Vivien, Héloïse, Elodie G, Alicia et Léna.

Je tiens également à remercier tous les membres du troisième étage ! Merci à tous pour la bonne humeur qui règne au troisième. Je tiens à remercier Cindy, qui a toujours répondu à toutes mes questions en termes de sécurité. Un grand merci à Lisa et à Jimena pour leur aide dans l'isolation des PBMC. Merci à Cassandre et Dasha pour leur présence quotidienne au laboratoire. Et comment de ne pas remercier Elise, je te compte parmi le 3ème étage (en même temps on ne peut pas vraiment dire que tu l'aies vraiment quitté). Merci pour nos échanges, tu m'auras fait comprendre qu'un western c'est quand même un peu plus que juste une protéine de ménage bien homogène… Je suis triste que nous ne redevenions pas collègues pour plus longtemps.

Last but not leats, je n'oublie bien évidement pas Flavie… Merci d'être un peu moins ronchon que ta sœur, ça me permet de vous différencier !

Je remercie également l'équipe « d'en face », les FG… Mannon, Christophe, Théo et Joséphine ! Merci pour ces pauses repas animées et pour votre bonne humeur. Merci à Théo pour nos échanges scientifiques et personnels au tour d'un café ou d'une bière. À bientôt au détour d'un pub londonien ?

Je tiens à remercier chaleureusement Joséphine. De collègue à amie, tu m'as accompagnée tout au long de ma thèse. Un grand merci pour ton soutien sans faille. Nos petits après-midi thés~~/crêpe/cidre/bière~~ m'auront permis d'évacuer la pression. Je n'ai pas les mots pour exprimer toute ma gratitude envers toi. Merci d'avoir écouté mes longs monologues. Tu auras su me comprendre et m'épauler dans les moments les plus dures et pour cela un grand merci, je te dois la survie de ma santé mentale.

Enfin, je souhaite adresser mes plus profonds remerciements à toute ma famille. Merci à mes parents de m'avoir soutenue durant toutes mes études et ma thèse. Vous avez su me soutenir et être présents durant les moments les plus durs. Merci pour vos encouragements, votre écoute et votre intérêt pour mon sujet. Je tiens aussi à remercier mon grand frère et sa compagne pour leur soutien et leur présence tout au long de cette thèse. Merci pour ces moments partagés et pour la famille soudée que nous formons. Merci à ma tante, Anne-Marie, pour ton soutien, tes relectures, et surtout pour tes super sauces tomates et tes butternuts ! Enfin, je tiens à remercier mon compagnon, tu auras été mon plus grand soutien durant toute cette aventure. Merci d'avoir été là au quotidien et de m'avoir épaulée durant toutes mes études. Merci de m'avoir encouragée à poursuivre en thèse. Merci d'avoir soutenu mon projet, et d'avoir su calmer mes doutes. Merci infiniment pour ton écoute et ta patience sans faille.

Table des matières

Table des figures

Table des tableaux

Liste des abréviations

𝒜

A2E	: N-retinylidene-N-retinylethanolamine
AAPH	: 2,20 -Azobis(2-methylpropionamidine) dihydrochloride
ADNc	: ADN complémentaire
ADNmt	: ADN mitochondrial
ADP	: Adénosine di phosphate
AGPI	: Acides gras poly-insaturés
ApoE	: Alipoprotéine
ARE	: Elément de réponse antioxydante
ARMS2	: Age-Related Maculopathy Susceptibility 2
ARNm	: ARN messager
ATP	: Adénosine triphosphate

ℬ

BHR	: Barrière hémato-rétinienne
BIVB	: Bureau Interprofessionnel des Vins de Bourgogne
BSA	: Sérum-albumine bovine

𝒞

Cat	: Catalase
CCL2	C-C motif chemokine ligand 2
CFH	: Facteur H du complément
CLHP	: Chromatographie Liquide Haute Performance
CMH	: Complexe majeur d'histocompatibilité
Cul3	: Cullin 3
Cyt c	: Cytochrome c

𝒟

DMEM	: *Dulbecco's Modified Eagle Medium*
DMLA	: Dégénérescence maculaire liée à l'âge

ℰ

EFS	: Etablissement Français du Sang
ELISA	: *Enzyme-Linked Immuno Sorbant Assay*
EPR	: Epithélium rétinien pigmentaire
ERK	: *Extracellular Regulated Kinase 1/2*
ERO	: Espèce réactive de l'oxygène
ETDRS	: *Early treatment diabetic retinopathy study*

𝒢

GLUT	: *Glucose transportor*
GM-CSF	: *Granulocyte-macrophage colony-stimulating factor*
GPx	: Glutathion peroxydase
GSH	: Glutathion réduit
GSSH	: Disulfure de glutathion

ℋ

HAS	: Haute autorité de santé
HBSS	: *Hanks' Balanced Salts Solution*
HIF	: Hypoxia inducible factor
HO-1	: Hème oxygénase

ℐ

ICMUB	: Institut de Chimie Moléculaire de l'Université de Bourgogne
IL	: Interleukine
IMC	: Indice de masse corporelle
INFγ	: Interferon gamma

IRPB	: *Interphotoreceptor retinoid-binding protein*

K

Keap1	: Kelch-like ECH-associated protein 1

L

LPS	: Lipopolysaccharides

M

MCP-1	: Chimiotactiques monocytaire-1
MDA	: Malondialdéhyde
MEK	: *Mitogen-activated Extracellular signal-regulated protein Kinase*
MerTK	: c-Mer Proto-Oncogene Tyrosine Kinase
MLA	: Maculopathie liée à l'âge
MTC	: *Monocarboxylate transporter*

N

NLRP3	: *NOD-like receptor family*
Nrf2	: Facteur nucléaire érythroïde-2

O

OTC	: Tomographie par cohérence optique

P

PBMC	: Cellules mononucléaires du sang périphérique
PBS	: *Phosphate-buffered saline solution*
PEDF	: *Pigment epithelium-derived factor*
PGF	: *Placental growth factor*

Q

qPCR	: Reaction en chainne par polymerase quantitative

R

RLBP-1	: Retinaldehyde binding protein 1
RPE65	: *Retinal pigment epithelium-specific protein 65*
RSV	: Resvératrol
rVEGF	: *Vascular Endothelial Growth Factor human recombinant*
RWE	: *Red wine extract* (extrait sec de vin rouge)

S

SOD	: Superoxyde dismutase
SVF	: Sérum de veau fœtal

T

TL-R	recepteur Toll-like
TNF	: *Tumor necrosis factor*

U

u.a.	: Unité arbitraire
UV	: Ultra-violet

V

VEGF	: *Vascular Endothelial Growth Factor*
VEGF-R	: Recepteur du *vascular Endothelial Growth Factor*

Introduction

A. Physiologie de l'œil

A.1. Anatomie générale de l'œil

L'œil est l'organe de la vision, il permet la transformation d'un signal lumineux en signal nerveux ainsi que sa transmission au cerveau par le nerf optique. Chez l'homme, l'œil a un diamètre d'environ 25 mm et pèse environ 7 grammes (Kels et al., 2015). Il est composé de **trois tuniques** renfermant **trois milieux transparents** et forme ainsi une lentille convergente (Figure 1) :

- La **tunique externe** est composée de la sclère et de la cornée.
    - **La sclère** recouvre la majorité de l'œil (4/5). C'est une tunique fibreuse composée de collagène dense lui permettant de contenir la pression interne de l'œil et de conférer sa forme plutôt ronde au globe oculaire ainsi que de le protéger des lésions mécaniques externes. Peu innervée et vascularisée, elle est cependant traversée à l'arrière par le nerf optique, et latéralement par des vaisseaux sanguins et lymphatiques ainsi que des nerfs. Elle permet l'ancrage des muscles oculomoteurs sur le globe oculaire et ainsi permet la mobilité de ce dernier. La partie antérieure de la sclère est recouverte d'une fine couche de mucus (**conjonctive**) composée de cellules caliciformes produisant du mucus participant à la sécrétion du liquide lacrymal. La conjonctive recouvre la face interne des paupières et s'étend jusqu'au bord de la cornée (Snell and Lemp, 2013).
    - **La cornée** recouvre la partie centrale de l'œil (1/5). Sa structure non innervée et transparente permet la transmission de la lumière à l'intérieur de l'œil et ainsi constitue le premier élément réfractif de l'œil (DelMonte and Kim, 2011).
- L'**uvée, tunique moyenne**, composée de l'iris, des corps ciliaires et de la choroïde.
    - **L'iris** est composé de fibres pigmentées qui confèrent sa couleur à l'œil. Il entoure la pupille et régule son ouverture par l'intermédiaire du sphincter de l'iris afin d'ajuster la quantité de lumière entrante dans l'œil (McDougal and Gamlin, 2015). L'iris est relié à la choroïde par les corps ciliaires.
    - **Les corps ciliaires** assurent à la fois la jonction entre l'iris et la choroïde, ainsi que la sécrétion de **l'humeur aqueuse**. Ils contiennent les **muscles ciliaires**

permettant de changer la forme du **cristallin** afin de focaliser la lumière sur la rétine et de faire la mise au point de la vision (Warjri and Senthil, 2022).

- **La choroïde** est située entre la sclère et l'intérieur de l'œil. Elle assure la nutrition des parties de l'œil qui sont peu vascularisées telles que l'iris et les photorécepteurs. De plus, elle bloque la majorité des rayons lumineux, ce qui protège l'intérieur de l'œil et permet de maintenir ce dernier en chambre noire (Nickla and Wallman, 2010).

- La **tunique interne ou rétine** est composée du tissu nerveux.
  - **La rétine** recouvre la surface interne de l'œil. Elle est composée de photorécepteurs capables de capter les rayons lumineux et de les transformer en signal nerveux afin de les transmettre au cerveau grâce au nerf optique. Le **corps vitré,** localisé entre le cristallin et la rétine, permet le maintien de cette dernière contre les parois de l'œil. Le corps vitré, avec le cristallin et l'humeur aqueuse, forme une lentille convergente qui focalise la lumière sur la zone centrale de la rétine appelée **macula**. La macula présente en son centre une légère dépression d'un demi-millimètre, **la fovéa** (Jackson et al., 2002). Du fait d'une concentration élevée en photorécepteurs, la fovéa est la zone où l'acuité visuelle est à son maximum, c'est cette zone qui permet la vision la plus précise en éclairage diurne.

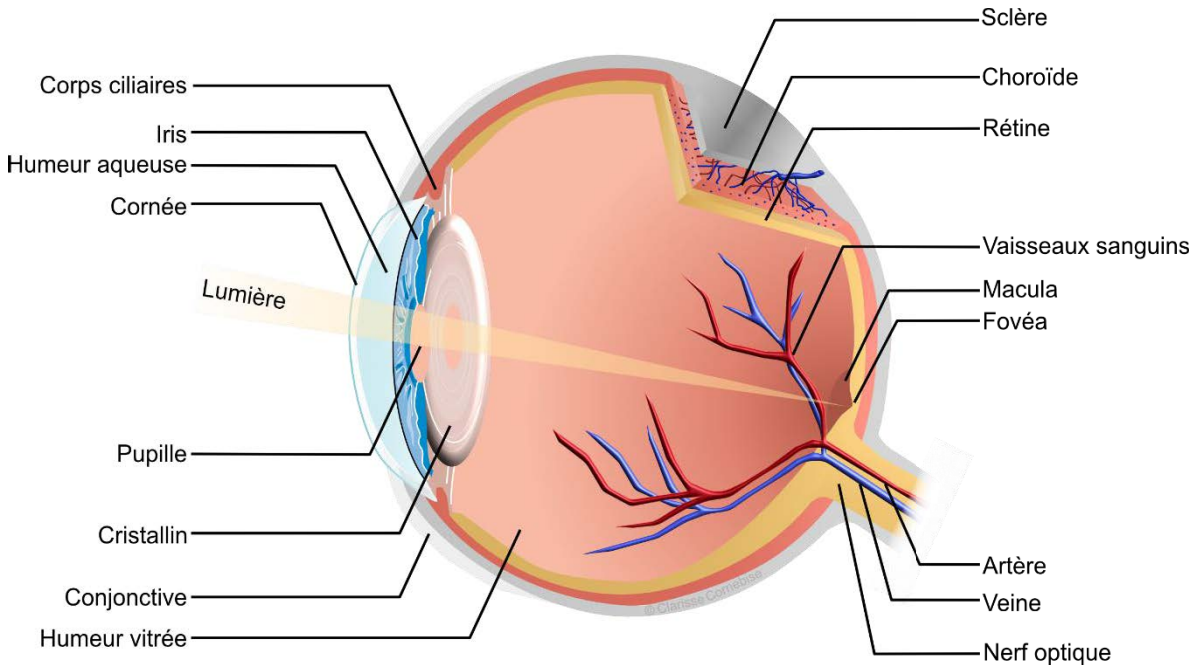

Figure 1. Anatomie générale de l'œil

Coupe sagittale schématique de l'œil humain montrant la disposition des trois tuniques principales : tunique externe (sclère et cornée), l'uvée (iris, corps ciliaires et choroïde) et la tunique interne (rétine) ainsi que les trois milieux transparents, l'humeur aqueuse, le cristallin et l'humeur vitrée.

A.2. La rétine

A.2.1. Anatomie

La rétine assure la **première étape de la vision** (Behar-Cohen et al., 2009; von Hanno et al., 2017). Elle s'organise en couches de noyaux cellulaires et de couches cellulaires. Ces dernières s'alternent avec des couches plexiformes formées par des synapses et les prolongements de cellules gliales (Figure 2).

La couche la plus interne de la rétine est la **membrane limitante interne**, elle sépare l'humeur vitrée de la rétine. Elle est constituée de la partie proximale des cellules de Müller (pieds) qui participent au maintien de l'homéostasie rétinienne (Bringmann et al., 2006). La seconde couche, la **couche de fibres optiques rétiniennes**, est composée des prolongements des cellules de Müller, des astrocytes ainsi que des axones des cellules ganglionnaires. Les noyaux de ces dernières forment la **couche granuleuse interne** (couche ganglionnaire). À l'arrière de l'œil, les axones des cellules ganglionnaires se rejoignent afin de former le **nerf optique** et permettent ainsi la transmission du signal nerveux au cerveau (Selhorst and Chen, 2009). Les cellules ganglionnaires vont former des synapses avec les cellules bipolaires et amacrines ce qui va former la **couche plexiforme interne**. Le corps des cellules horizontales,

des cellules amacrines et des cellules bipolaires forment la **couche granuleuse moyenne** (couche nucléaire interne). Ces dernières fonctionnent comme des canaux permettant la transmission de l'information entre les photorécepteurs et les cellules ganglionnaires (Demb et al., 2001). Les cellules horizontales jouent quant à elle un rôle de régulation en formant des synapses avec à la fois les photorécepteurs et les cellules bipolaires. Ces synapses permettent une régulation latérale de l'influx nerveux provenant afin d'éliminer tous les signaux superflus favorisant ainsi le contraste des images (Boije et al., 2016). Les synapses entre les projections des photorécepteurs, des cellules bipolaires et des cellules horizontales se situent dans la **couche plexiforme externe**. Le corps des photorécepteurs forme la **couche granuleuse externe**. L'interaction des photorécepteurs avec les cellules de Müller va créer des jonctions et ainsi former la **membrane limitante externe**. Cette membrane composée de jonctions adhérentes et serrées joue un rôle de barrière hématorétinienne (BHR) en permettant les interactions entre les cellules tout en bloquant la diffusion de grosses molécules (<100 kDa) (Cunha-Vaz et al., 2011). Les segments internes et externes des photorécepteurs forment la **couche des photorécepteurs**. Le segment externe des photorécepteurs est quant à lui juxtaposé aux cellules de **l'épithélium pigmentaire rétinien** qui forment la dernière couche de la rétine (Nguyen et al., 2023).

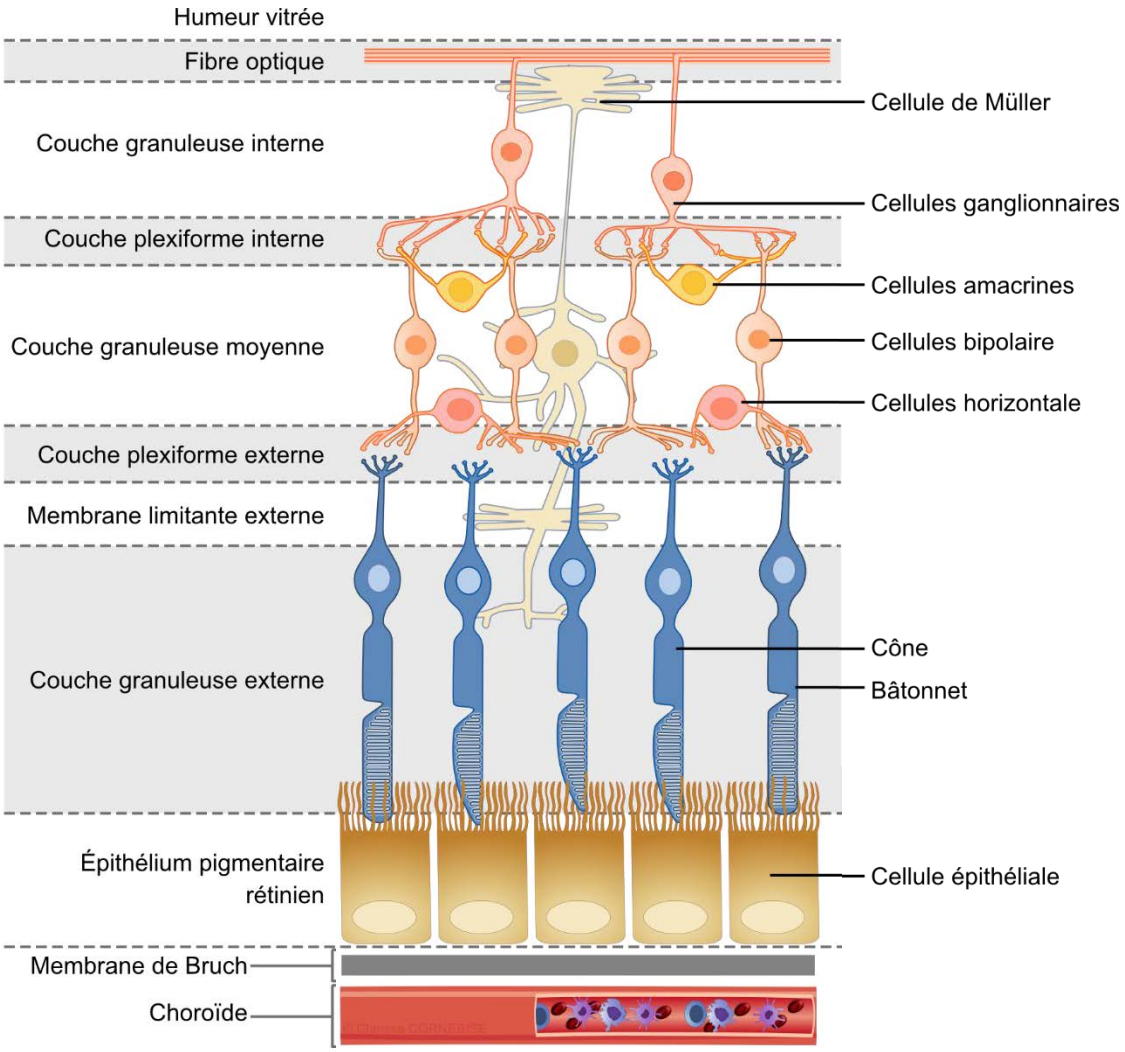

Figure 2. Anatomie de la rétine : schéma illustrant les différentes couches histologiques
La rétine est composée de 10 couches distinctes qui comprennent des noyaux cellulaires ainsi que des couches cellulaires alternant avec des couches plexiformes contenant des synapses et les prolongements cellulaires. La rétine est positionnée sur la choroïde dont elle est séparée par la membrane de Bruch. (Adapté de Akhtar-Schäfer et al., 2018; Graw, 2010).

A.2.2. Les photorécepteurs

Les photorécepteurs, les **cônes** et les **bâtonnets** sont des cellules **neurosensorielles**, leur principale fonction est de capter un signal lumineux (photon) et de le transformer en signal électrique. Ils possèdent une organisation commune qui se décompose en quatre régions :

- La **terminaison synaptique** qui permet la transmission du signal électrique aux cellules bipolaires *via* une synapse.
- Le **corps cellulaire** contenant les noyaux des photorécepteurs.

- Le **segment interne** composé de différents organites cellulaires et notamment des mitochondries soutenant l'activité métabolique élevée des photorécepteurs.
- Le **segment externe** contenant les pigments visuels sensibles à la lumière.

A.2.2.1. Les cônes

Les **cônes** sont impliqués dans la vision de jour en couleur. Ils sont **peu sensibles** à la lumière cependant chaque cône transmet l'information électrique à **plusieurs fibres optiques**. Cela leur permet de ne pas être saturés par une trop forte intensité lumineuse et de transmettre un signal électrique important lors d'un éclairage **diurne**.

La vision en couleur est obtenue grâce à la diversité des pigments de la famille des **opsines** retrouvée dans les cônes. Chez l'homme, il existe trois types de pigments, **l'érythropsine** sensible au rouge (cônes L, absorption maximale λ = 560 nm), la **chloropsine** sensible au vert (cônes M, absorption maximale λ = 530 nm) et la **cyanopsine** sensible au bleu (cônes S, absorption maximale λ = 430 nm). Ces pigments confèrent aux cônes une sensibilité à la couleur.

Les cônes sont **répartis de manière inégale** au sein de la rétine. Leur concentration est à son maximum au niveau de la **fovéa** (150 000/mm²) puis diminue à la périphérie (5 000/mm²) au-delà de 20° d'excentricité (Figure 3) (Curcio et al., 1990; Zouache, 2022). De plus, au niveau de la fovéa, de par l'absence des couches supérieures de la rétine, les cônes ont directement accès au signal lumineux. Cette organisation permet d'obtenir une acuité visuelle de **très haute définition** et en couleur au centre de la vision.

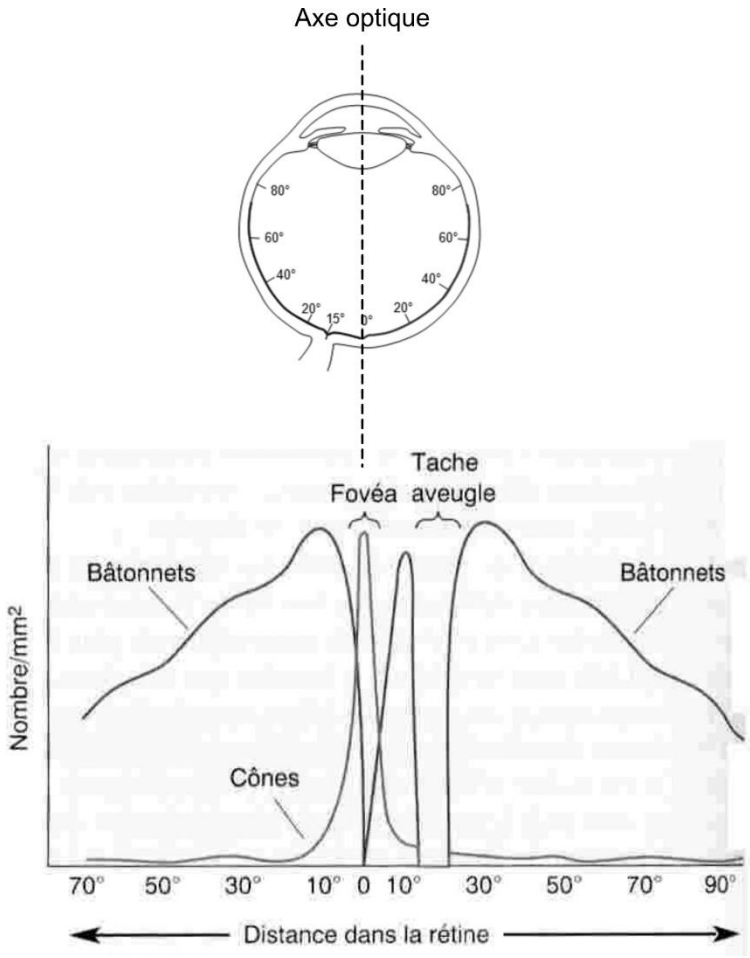

Figure 3. Répartition des cônes et des bâtonnets sur la rétine
En haut, représentation schématique des degrés d'excentricité de l'œil. En bas, histogramme de la répartition des cônes et des bâtonnets en fonction du degré d'excentricité sur la rétine. Adapté de Sawadogo, 2023; Zouache, 2022.

A.2.2.2. Les bâtonnets

Les **bâtonnets** sont à l'origine de la **vision périphérique et nocturne**. Ne possédant qu'un seul pigment visuel, la **rhodopsine**, ils confèrent une **vision achromatique**. La rhodopsine est **très sensible à la lumière** ce qui permet la vision nocturne. En revanche, lorsque le signal lumineux est trop intense, les bâtonnets vont être saturés et ne pourront pas transmettre de signaux visuels. Par conséquent, ils ne peuvent pas être utilisés pour une vision diurne.

Les bâtonnets sont répartis de manière inégale sur la rétine (Figure 3) (Curcio et al., 1990; Zouache, 2022). Leur répartition permet l'acquisition d'une **vision périphérique**. Cependant, cette vision est **moins précise** que celles fournies par les cônes. En effet, plusieurs bâtonnets ne sont reliés qu'à une **seule fibre optique,** ce qui limite leur capacité à distinguer les détails.

A.2.2.3. La phototransduction

La phototransduction est un processus permettant de **transformer l'énergie lumineuse (photon) en un signal électrique** interprétable par le cerveau (Fu, 1995). Les deux catégories de photorécepteurs, les cônes et les bâtonnets possèdent des pigments différents, les iodopsines et la rhodopsine. Ces pigments ont une composition similaire, ils sont constitués d'un **chromophore**, le 11-*cis*-rétinal, et d'une opsine (protéine transmembranaire).

- Le **11-*cis*-rétinal** est synthétisé à partir de la vitamine A (ou rétinol) d'origine animale ou du β-carotène d'origine végétale. Un signal lumineux va induire son isomérisation permettant la conversion du signal lumineux en signal nerveux.
- Les **opsines** sont des protéines constituées d'une chaîne polypeptidique qui s'enroule sur elle-même pour former sept hélices α transmembranaires. Il existe différentes opsines, chacune ayant une composition en acide aminé distincte. Dans les cônes on retrouve trois types d'opsines avec une composition proche, mais qui présentent une sensibilité différente selon les longueurs d'onde. En revanche, l'opsine présente dans les bâtonnets a une composition très différente que celle présente dans les cônes. Elle se distingue par une très forte sensibilité à la lumière et ce peu importe les longueurs d'onde (Terakita, 2005).

Les iodospines et la rhodopsine possèdent un mécanisme d'action identique. Tout d'abord, l'absorption d'un photon induit l'**isomérisation** du **11-*cis*-rétinal** en **tout-*trans*-rétinal**. Ce changement de conformation induit la dissociation de la liaison rétinal/opsine ce qui provoque une cascade de réactions biochimiques induisant une modification de la concentration ionique intracellulaire. Les canaux membranaires GMPc (Guanosine MonoPhosphate cytoplasmique) des photorécepteurs répondent à ce changement de concentration en modifiant l'influx d'ions calcium (Ca^{2+}) et sodium (Na^{+}) à travers la membrane entraînant une **hyperpolarisation** des photorécepteurs au niveau des synapses.

La vision à faible intensité lumineuse, à l'obscurité, est rendue possible grâce à la forte **sensibilité des bâtonnets**. Leurs canaux membranaires sont constamment ouverts, entraînant une **dépolarisation constante**. Ces canaux vont se refermer lors de l'activation de la cascade moléculaire engendrée par l'isomérisation du 11-*cis*-rétinal en tout-*trans*-rétinal et ainsi induire une hyperpolarisation des photorécepteurs.

Les photorécepteurs ne sont pas capables d'isomériser à nouveau le tout-*trans*-rétinal en 11-*cis*-rétinal. Ce processus va être assuré par les cellules de l'épithélium rétinien pigmentaire (EPR).

A.2.3. L'épithélium pigmentaire rétinien

A.2.3.1. Organisation

L'épithélium pigmentaire rétinien (EPR) est formé par une couche **cellulaire monostratifiée** située entre la choroïde et la rétine. Elle repose, du côté basolatéral, sur la **membrane de Bruch** et est en contact avec les photorécepteurs du côté apical. Les cellules de l'EPR sont **polarisées**, elles possèdent, du côté basolatéral, leur noyau ainsi que leurs mitochondries et du côté apical des extensions du réticulum endoplasmique lisse et rugueux, des mélanosomes, des phagosomes, des liposomes et ainsi que des granules de lipofuscine dérivées des déchets de la phagocytose. La membrane des cellules est également polarisée. La membrane basolatérale est caractérisée par de nombreuses invaginations courtes qui permettent d'augmenter la surface d'échange entre les cellules de l'EPR et la membrane de Bruch. La membrane au pôle apical possède deux types de **microvillosités** : de longues microvillosités permettant d'augmenter la surface d'échange entre les cellules de l'EPR et les photorécepteurs, ainsi que des microvillosités courtes impliquées dans la phagocytose. L'EPR joue un rôle crucial au sein de la rétine tant dans le maintien de l'intégrité structurelle que dans l'intégrité fonctionnelle des photorécepteurs. Les cellules de l'EPR réalisent plusieurs fonctions essentielles à la vision.

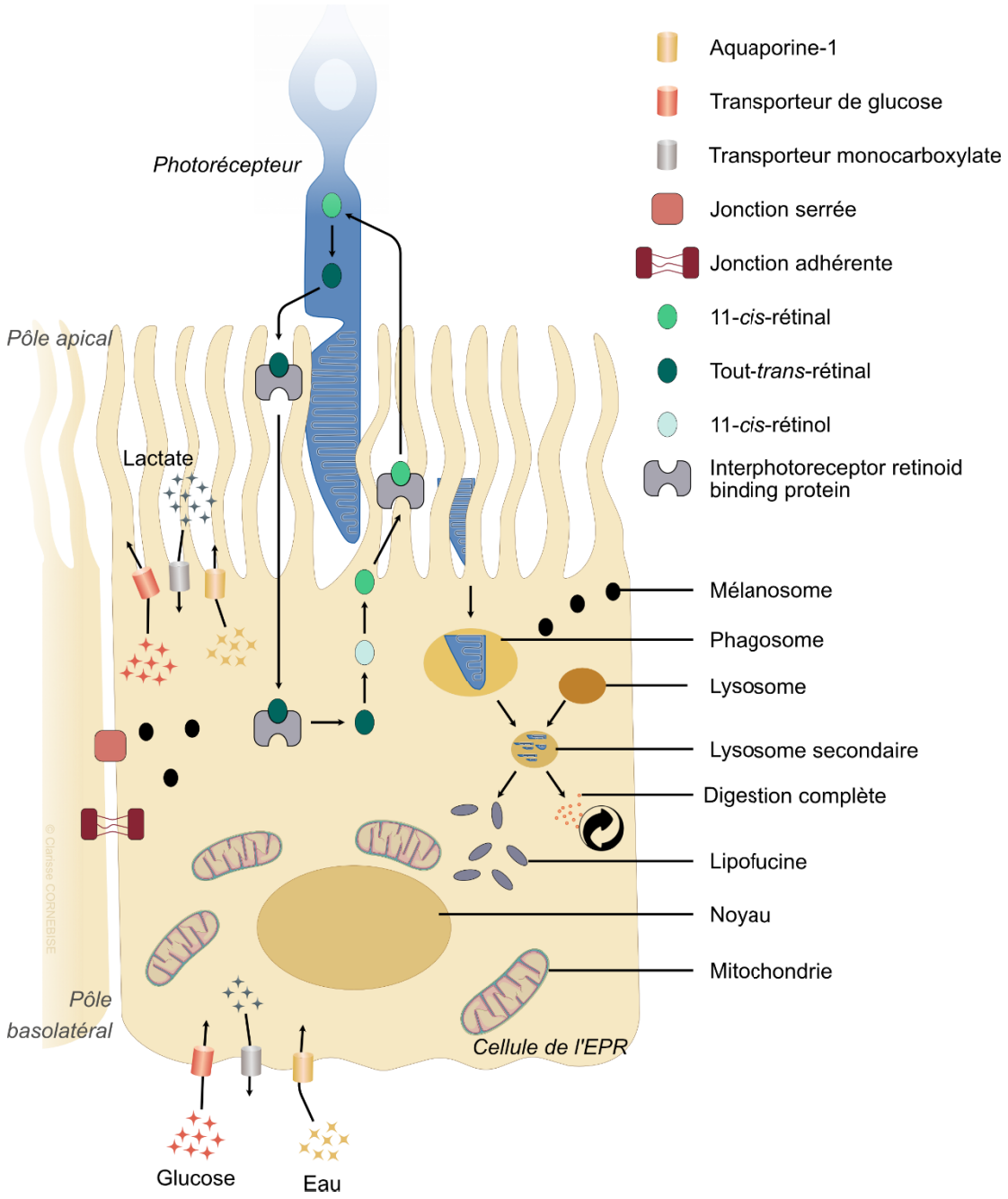

Figure 4. Représentation schématique des cellules de l'épithélium pigmentaire rétinien (EPR) Les cellules de l'EPR sont impliquées dans divers mécanismes permettant le maintien de la rétine : elles permettent le transport de molécules *via* divers transporteurs (aquaporine-1, transporteur du glucose et transporteur de type monocarboxylate). Elles phagocytent l'extrémité des photorécepteurs. Les déchets de la digestion complète de ces dernières sont recyclés tandis que les produits de la digestion incomplète sont stockés sous forme de lipofuscine. Les cellules de l'EPR isomérisent le tout-*trans*-rétinal en 11-*cis*-rétinol puis en 11-*cis*-rétinal et le redonnent aux photorécepteurs à l'aide de l'*interphotorecptor retinoid binding protein*. Les jonctions serrées et adhérentes entre les cellules de l'EPR forment une barrière hématorétinienne.

A.2.3.2. Cycle visuel

L'épithélium pigmentaire rétinien joue un rôle crucial dans le **cycle visuel**. En effet, lors de l'acquisition du signal visuel, les photorécepteurs (cônes et bâtonnets) captent un photon ce qui induit le changement de conformation du 11-*cis*-rétinal en **tout-*trans*-rétinal**. Ne possédant pas de *cis*-*trans* isomérase, les photorécepteurs ont besoin des cellules de l'EPR pour reformer du 11-*cis*-rétinal.

Le cycle visuel du rétinal dans les cellules de l'EPR permet d'**isomériser le tout-*trans*-rétinal en 11-*cis*-rétinal**. Pour cela, le tout-*trans*-rétinal est transformé par une déshydrogénase dans les photorécepteurs en tout-*trans*-rétinol. Ensuite, le tout-*trans*-rétinol est pris en charge par une **protéine cargo IRBP** (*interphotoreceptor retinoid-binding protein*) afin d'être transporté à travers la matrice inter-photorécepteur et de rentrer dans les cellules de l'EPR (Jin et al., 2009). Le tout-*trans*-rétinol peut ainsi être isomérisé à nouveau en 11-*cis*-rétinol grâce à **l'isomérase RPE65** (retinal pigment epithelium-specific protein 65) présente dans le cytoplasme des cellules de l'EPR pour ensuite être oxydé en 11-*cis*-rétinal (Kaushik et al., 2023; Moiseyev et al., 2005). Pour finir, le 11-*cis*-rétinal est pris en charge par la protéine cargo IRBP afin de retourner dans les photorécepteurs (Figure 4).

A.2.3.3. Transport transépithélial

L'épithélium pigmentaire rétinien réalise le transport transépithélial de l'**eau**, des **nutriments** ainsi que des **ions** entre les photorécepteurs et la choroïde. En effet, les photorécepteurs, de par leur haute activité métabolique, sont à l'origine de l'augmentation du volume d'eau au sein de l'œil. La pression oculaire ainsi que les cellules gliales de Müller permettent de diriger l'eau vers le fond de l'œil. Les jonctions serrées de l'EPR ne permettant pas l'élimination de l'eau par voie *para*-cellulaire, des canaux (**aquaporines-1**) sont présents dans les membranes apicales et basolatérales des cellules de l'EPR favorisant ainsi son élimination (Stamer et al., 2003). Du côté apical de l'EPR, une **Na^+-K^+-ATPase** permet l'apport d'énergie nécessaire au transport transépithélial et ainsi de créer un gradient ionique favorisant le passage de plusieurs ions (ions chlore et potassium) et d'eau de la rétine à la choroïde. L'EPR est aussi essentiel dans l'**élimination des déchets** produits par les photorécepteurs tels que le **lactate** grâce aux *monocarboxylate transporter 1* (**MCT-1**) au pôle apical et **MCT-3** au pôle basolatéral (Bonilha et al., 2020; Philp et al., 2003). De plus, l'EPR

permet l'approvisionnement en nutriments des photorécepteurs notamment par le transport du glucose par les glucose transporter 1 et 3 **(GLUT1** et **GLUT3)** (Ban and Rizzolo, 2000; Samra et al., 2023) (Figure 4).

A.2.3.4. Phagocytose

La **phagocytose des photorécepteurs** par l'EPR permet le **renouvellement** des segments externes des photorécepteurs et limite le stress oxydant généré par les photons. Chaque cellule de l'EPR interagit avec 20 à 30 photorécepteurs (Yang et al., 2021; Young, 1971). La **taille des photorécepteurs est constante** due à leur dégradation par phagocytose de leur partie distale et de leur croissance par la partie proximale (Boesze-Battaglia and Goldberg, 2002; Young, 1971). La phagocytose est un processus diurne qui comprend trois récepteurs. Dans un premier temps, la liaison entre l'EPR et les photorécepteurs est réalisée par l'**intégrine αVβ5** et déclenche une cascade de signalisation entrainant l'activation du **récepteur tyrosine kinase MerTK** (c-Mer Proto-Oncogene Tyrosine Kinase). L'activation de ce dernier permet d'augmenter la concentration calcique intracellulaire et ainsi mène à l'activation du **récepteur CD36**. Ce dernier va ensuite adresser un signal afin d'internaliser les débris externes par les **phagosome**s et les mener aux **lysosomes** où ils vont être digérés (Figure 4).

Lors de la phagocytose, certaines molécules nécessaires aux photorécepteurs sont **recyclées** comme le 11-*cis*-rétinal tandis que d'autres sont entièrement digérées et éliminées dans le sang *via* la choroïde comme les opsines. Certaines molécules, ne pouvant pas être totalement digérées, restent piégées dans les cellules du EPR sous forme de **granules de lipofuscine** (Figure 4). Ces granules sont composés de résidus issus de la **digestion incomplète** de lipides, de protéines et de molécules photo-réactives. Ces résidus peuvent engendrer un stress oxydant et donc être photo-toxique (Manley et al., 2023; Sparrow and Boulton, 2005). Lors du vieillissement, les granules de lipofuscine s'accumulent dans les cellules de l'EPR et peuvent induire certaines pathologies oculaires tels que la dégénérescence maculaire liée à l'âge (DMLA).

A.2.3.5. Fonction anti-oxydante de l'EPR

L'œil est un environnement propice à la production d'**espèces réactives de l'oxygène** (ERO) de par son exposition à la **lumière** et sa grande **consommation d'oxygène**, et aussi par la présence de **molécules photosensibles** (opsines, lipofuscine…) et d'acides gras poly-insaturés facilement oxydables. De plus, des ERO peuvent aussi être produites lors de certains processus physiologiques tels que la phagocytose.

Afin de protéger l'œil de la photo-oxydation, les cellules de l'EPR produisent et stockent des pigments, de la **mélanine**, sous forme de granules fusiformes appelées **mélanosomes** (Figure 4). La mélanine permet d'**absorber l'excès de photons** et ainsi limiter la lumière réfléchie au sein de l'œil.

De plus, les cellules de l'EPR possèdent des **enzymes anti-oxydantes** capables d'inactiver les radicaux libres tels que les superoxydes dismutases (SOD) (Hashizume et al., 2008, p. 1), la catalase, le glutathion réduit **(**GSH) et l'hème oxygénase 1 (HO-1) (Kensler et al., 2007). Les cellules de l'EPR synthétisent aussi de nombreuses **molécules détoxifiantes**, des caroténoïdes (lutéine, zéaxanthine, β carotène, vitamine, …) (Plafker et al., 2012). Ensemble, ces défenses permettent de neutraliser le stress oxydant et ainsi de restaurer l'homéostasie redox au sein de la rétine.

A.2.3.6. Maintien de l'environnement rétinien

Les cellules de l'EPR sont en liaison constante avec leur environnement grâce à des protéines de surfaces telles que les intégrines mais elles sont aussi capables de sécréter des **facteurs de croissance**. En effet, l'EPR est connu pour produire et sécréter des facteurs impliqués dans le maintien de l'intégrité de la rétine ainsi que de la choroïde. Dans un œil sain, les cellules de l'EPR sécrètent le *pigment epithelium-derived factor* (**PEDF**) qui permet le maintien de la rétine et de la choroïde de deux manières. Premièrement, il a une action **neuroprotectrice** qui limite l'apoptose des neurones, notamment due à l'hypoxie. Deuxièmement, le PEDF a une action **anti-angiogénique** qui permet de réguler la prolifération des cellules endothéliales et de stabiliser la choroïde. Par ailleurs, les cellules de l'EPR sécrètent le *Vascular Endothelial Growth Factor* (**VEGF**) qui est surtout impliqué dans le **développement embryonnaire**. Cependant, il est aussi sécrété faiblement, mais de manière constante chez l'adulte afin de stabiliser la choroïde et de protéger les cellules de l'endothélium contre l'apoptose (Imanishi et al., 2023).

De plus, le VEGF joue un rôle prépondérant dans la stabilisation de la **fenestration de l'endothélium** et ainsi régule les échanges entre la rétine et la choroïde. Ces deux facteurs de croissance, le VEGF et le PEDF sont sécrétés aux **pôles opposés** de l'EPR. Le PEDF est sécrété au pôle apical et ainsi protège les photorécepteurs tandis que le VEGF est sécrété au pôle basolatéral afin d'agir sur la choroïde.

A.2.3.7. EPR et immunité

Les cellules de l'épithélium pigmentaire rétinien forment un épithélium jointif et étanche participant à la formation de la **barrière hématorétinienne** (BHR). Cette barrière permet d'isoler la rétine des cellules immunitaires présentes dans les vaisseaux sanguins de la choroïde et ainsi participe au **privilège immun de l'œil**. En effet, l'œil fait partie des rares organes qui bénéficient d'un statut immunitaire privilégié qui permet de **limiter les dommages liés à l'inflammation** afin de conserver leurs fonctions principales (la vision pour l'œil) (Pescarmona et al., 2023).

Les cellules de l'EPR possèdent aussi des fonctions immunosuppressives. En effet, dans un œil sain, les cellules de l'EPR sécrètent des facteurs médiateurs du système immunitaire tel que des interleukines, le **facteur H du complément** ou des protéines chimiotactiques monocytaire-1 (MCP1). De plus, les cellules de l'EPR possèdent à leur surface des récepteurs tels que les récepteurs du complexe majeur d'histocompatibilité (**CMH**), les récepteurs du TNF-α (tumor necrosis factor α), les récepteurs Fas ligand ou encore les récepteurs toll-like. L'activation de ces récepteurs entraîne la sécrétion des cascades de signalisation menant à la sécrétion d'interleukines pro-inflammatoires telles que l'IL-6 et l'IL-8 ainsi que la sécrétion du facteur MCP-1 permettant ainsi le recrutement de la microglie ou des cellules immunitaires présentes au niveau de la choroïde (Austin et al., 2009; Taylor et al., 2021).

A.2.4. Les réseaux vasculaires de la rétine

La rétine est irriguée *via* deux systèmes vasculaires distincts : le réseau rétinien assure la **vascularisation directe** des couches rétiniennes internes et le réseau choroïdien assure la **vascularisation indirecte** de la rétine (Figure 5).

Le **réseau vasculaire rétinien**, localisé dans la couche des fibres optiques, est constitué de **capillaires rétiniens** issus de l'artère centrale (Figure 5). Il fournit l'apport en **besoins métaboliques des couches internes de la rétine**. Il est formé par des cellules endothéliales à jonctions serrées formant une **barrière hématorétinienne interne (BHR)**.

Le **réseau vasculaire choroïdien**, localisé sous l'EPR, est constitué d'un ensemble de capillaires (**choriocapillaires**) (Figure 5). Les choriocapillaires sont formés d'une couche de cellules endothéliales à **jonctions serrées** possédant de larges **fenestrations** favorisant le passage de **macromolécules et de protéines** jusqu'à l'EPR *via* la **membrane de Bruch**. L'ouverture de ces fenestrations est régulée par le VEGF, lequel est principalement sécrété par les cellules de l'EPR permettant le passage des nutriments de la choroïde aux photorécepteurs. Lors du vieillissement, la membrane de Bruch s'épaissit ce qui perturbe les échanges entre la choroïde et l'EPR, en empêchant notamment l'élimination de certains déchets pouvant engendrer une cytotoxicité pour la rétine.

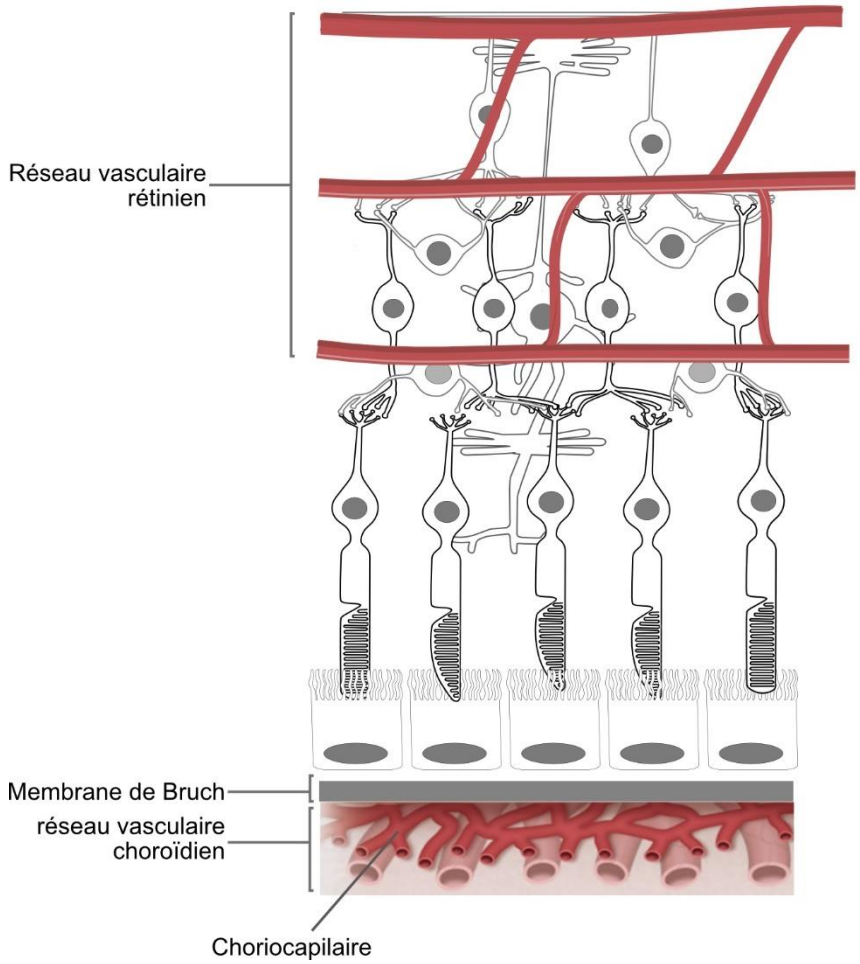

Figure 5. Représentation schématique des réseaux vasculaires de la rétine
Le réseau vasculaire rétinien se situe dans la partie extérieure de la rétine tandis que le réseau vasculaire choroïdien est juxtaposé à la membrane de Bruch, sur la partie la plus interne de la rétine.

Adapté de Akhtar-Schäfer et al., 2018 et Jampol et al., 2020. (La description de l'anatomie de la rétine est décrite figure 2.)

B. La dégénérescence maculaire liée à l'âge (DMLA)

B.1. Généralité/épidémiologie

La dégénérescence maculaire liée à l'âge (DMLA) est la **première cause de handicap visuel** chez les personnes âgées de **plus de cinquante ans** dans les pays industrialisés (Deng et al., 2021; Wong et al., 2014). En France, d'après la Haute Autorité de Santé (HAS), la DMLA **touche 8 % de la population française** en 2022 et sa prévalence augmente fortement avec l'âge (Tableau 1) :

Tableau 1. Prévalence de la DMLA en fonction de l'âge

Âge	***50-55 ans***	***65-75 ans***	***Plus de 75 ans***
Prévalence	1 %	10 %	25-30 %

Décrite pour la première fois en 1874, la DMLA connait une prévalence croissante en raison du **vieillissement de la population mondiale**. Ce phénomène s'accélère rapidement et ainsi pose un défi majeur en matière de santé publique. En effet, le nombre de personnes âgées de **65 ans et plus dans le monde passera de 771 millions en 2019 à 1,6 milliard d'ici 2050** (United Nations, 2022). En France, on estime qu'en 2070, les personnes âgées de 65 ans et plus représenteront 28,7 % de la population, contre 20,5 % en 2020 (Institut national de la statistique et des études économiques (INSEE), projection de population 2013-2070). Par conséquent, avec le vieillissement croissant de la population, il est également prévu que la **prévalence de la DMLA augmente**.

B.1.1. Symptômes

Le principal symptôme de la DMLA est une **perte progressive de la vision centrale** avec un **maintien de la vision périphérique.** Dans un premier temps, elle peut se développer de manière unilatérale, c'est-à-dire qu'elle n'affecte qu'un seul œil. Puis, elle peut progresser et atteindre le second œil (atteinte bilatérale).

Les premiers symptômes sont souvent subjectifs et discrets, ce qui retarde le diagnostic ainsi que le début des traitements. Les premiers symptômes sont majoritairement une **diminution de la perception des contrastes**, une sensation d'**éblouissement**, une **modification de la vision des couleurs**, une **gêne lors de la vision nocturne** et une **déformation des lignes** (Figure 6). Par la suite, une simple baisse de l'acuité visuelle au centre de la vision est souvent observée avec l'apparition d'un ou plusieurs **scotome**s (taches sombres dans le champ visuel) et évolue généralement par la **perte de la vision centrale**. L'évolution de la maladie dépend fortement de sa **forme clinique**.

Figure 6. Illustration des dommages de la vision perçus par une personne atteinte de la DMLA
Adapté de l'infographie de Pascal Marseaud, Les signes fonctionnels permettant d'établir un diagnostic de la DMLA, Haute Autorité de Santé.

B.2. Les différents types de DMLA

La DMLA est classée en **trois formes cliniques** : **une forme précoce** appelée maculopathie liée à l'âge (MLA) et **deux formes tardives** (DMLA atrophique et DMLA néovasculaire).

B.2.1. Maculopathie lié à l'âge

La **phase précoce** de la maladie, **maculopathie liée à l'âge** (MLA) se caractérise par l'apparition de **drusen** au niveau de la macula (Figure 7). Les drusen sont constitués de dépôts lipido-protéiques situés entre l'EPR et la membrane de Bruch. Ces dépôts s'accumulent lors de la phagocytose des photorécepteurs par les cellules de l'EPR. Leur élimination est de plus en plus difficile au cours du vieillissement ce qui entraîne leur accumulation et ainsi la formation

de **drusen.** Souvent **sans influence sur l'acuité visuelle**, l'observation de drusen lors d'un examen du fond de l'œil constitue le principal critère de diagnostic chez les patients de plus de 50 ans. Cet examen permet en effet de quantifier et de mesurer la taille des drusen présents sur la rétine. Un patient atteint de MLA va présenter de **nombreux drusen de petite taille** (< 63 µm) ainsi que **quelques drusen de tailles intermédiaires** (compris entre 63 et 125 µm) (Belmouhand et al., 2022; Sarks et al., 1999). Par ailleurs, une **altération de la pigmentation** (hypo- ou hyper-pigmentation) de l'EPR peut aussi être observée (Figure 7). L'évolution de la MLA peut stagner au cours de la vie, mais environ **50 % des cas évoluent** vers une forme dégénérative tardive (DMLA).

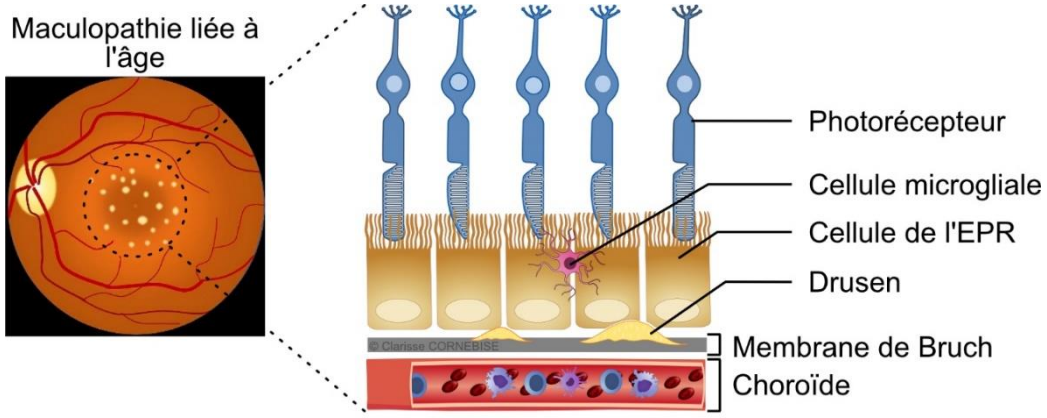

Figure 7. Représentation schématique de la maculopathie liée à l'âge (MLA)
EPR : épithélium pigmentaire rétinien. A gauche, représentation schématique d'une image de fond d'œil d'un patient atteint de MLA. A droite représentation schématique simplifiée de la rétine d'un patient atteint de MLA avec la présence de drusen au niveau des cellules de l'ERP. Adapté de Akhtar-Schäfer et al., 2018 et Delmas et al., 2021; Ruan et al., 2021.

B.2.2. DMLA atrophique

La **DMLA atrophique**, également appelée forme « sèche », se caractérise par une augmentation de la fréquence et de la taille des **drusen (>125 µm**) suivie d'une **perte progressive et irréversible des photorécepteurs** et des **cellules de l'EPR** au niveau de la macula. Les cellules de l'EPR disparaissent par un processus d'**apoptose** entraînant l'altération des photorécepteurs. Dans un premier temps, les cellules restantes de l'EPR vont s'étaler afin de compenser la perte de cellules. Lorsqu'un trop grand nombre de cellules ont disparu, la compensation n'est plus possible, ce qui entraîne la formation d'**atrophies géographiques.**

L'évolution de cette forme de DMLA est lente et peut s'étendre sur plusieurs années. Initialement, de petites atrophies géographiques peuvent être observées, puis l'atrophie peut évoluer avec la formation de **nouvelles zones** ou **s'étendre avec l'élargissement des zones d'atrophie** existantes induisant un amincissement de la rétine. Aux stades les plus avancés de la maladie, le centre de la fovéa est atteint, entraînant une perte de la vision centrale (Figure 8). Lors d'un examen du fond d'œil, l'amincissement de la membrane va laisser apparaître les vaisseaux sanguins de la choroïde (Figure 8).

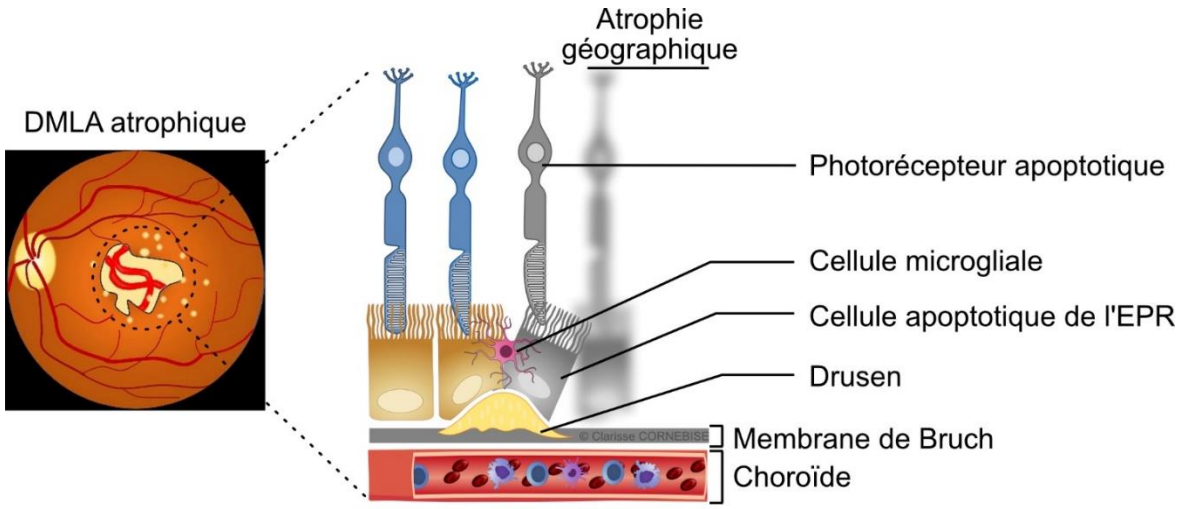

Figure 8. Représentation schématique de la dégénérescence maculaire liée à l'âge (DMLA) atrophique

A gauche, représentation schématique d'une image de fond d'œil d'un patient atteint de DMLA atrophique caractérisé par la présence de drusen et de zone d'atrophie géographique laissant apparaître les vaisseaux sanguins de la choroïde. A droite, représentation schématique simplifiée de la rétine d'un patient atteint de DMLA atrophique. On distingue la présence de drusen de taille importante ainsi que la création d'une atrophie géographique avec la perte par apoptose de photorécepteur et de cellules de l'épithélium pigmentaire rétinien (EPR). Adapté de Akhtar-Schäfer et al., 2018 et Delmas et al., 2021; Ruan et al., 2021.

B.2.3. DMLA néovasculaire

La **DMLA néovasculaire**, également appelée forme "humide" se caractérise par la présence de **néovaisseaux anormaux** au niveau de la macula. Ces néovaisseaux proviennent de la choroïde et traversent la membrane de Bruch, perturbant ainsi la rétine. En raison de leur **fragilité** et de leur **perméabilité**, ces nouveaux vaisseaux peuvent laisser passer du sang et des fluides, entraînant des complications telles que **des œdèmes intrarétiniens** de la macula, des **hémorragies rétiniennes** et des **accumulations de fluides** qui désorganisent la structure de la

rétine (Figure 9). De plus, ces nouveaux vaisseaux contribuent au maintien d'un environnement **pro-inflammatoire** au niveau de la rétine, favorisant l'accumulation de macrophages au sein de la rétine.

L'**évolution** de la DMLA néovasculaire est **rapide**. Un examen du fond d'œil permet de diagnostiquer rapidement cette forme de DMLA en observant les néovaisseaux vasculaires choroïdiens et les hémorragies.

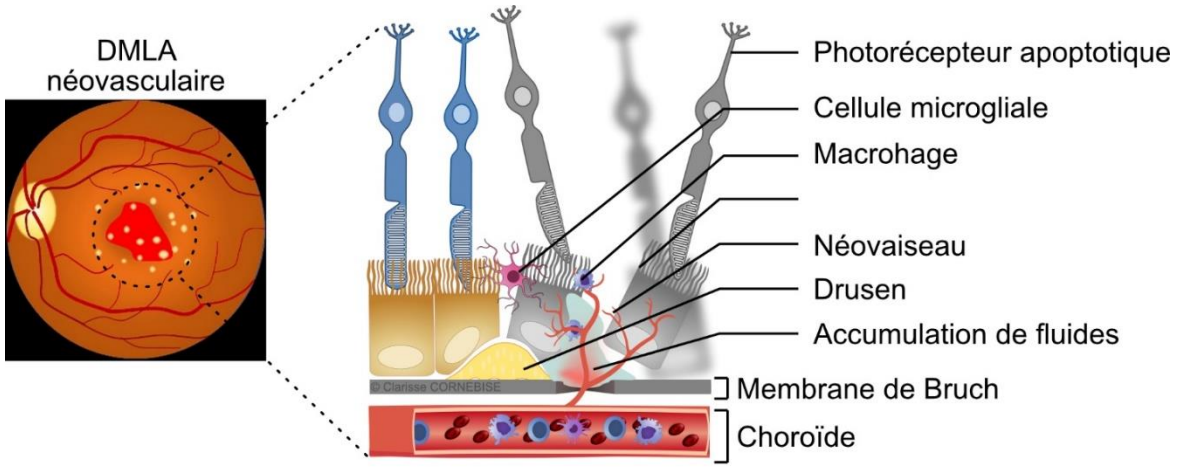

Figure 9. Représentation schématique de la dégénérescence maculaire liée à l'âge (DMLA) néovasculaire

A gauche, représentation schématique d'une image de fond d'œil d'un patient atteint de DMLA néovaculaire caractérisée par la présence de drusen de taille importante ainsi qu'une hémorragie rétinienne induite par de nouveaux vaisseaux. A droite, représentation schématique simplifiée de la rétine d'un patient atteint de DMLA néovasculaire. On distingue l'accumulation de fluides induite par la formation de nouveaux vaisseaux. L'altération de la rétine engendre la mort par apoptose des cellules de l'épithélium pigmentaire rétinien (EPR) ainsi que des photorécepteurs. Adapté de Akhtar-Schäfer et al., 2018 et Delmas et al., 2021; Ruan et al., 2021.

B.3. Diagnostic et examen clinique

Le diagnostic de la DMLA ainsi que la détermination du stade et de la forme de DMLA sont réalisés par différents tests. Dans un premier temps, une simple **mesure de l'acuité** visuelle permet de déterminer si le patient présente des signes de DMLA. Par la suite, des **examens du fond d'œil** permettent d'établir un diagnostic précis en déterminant la forme de DMLA, mais surtout le stade de développement de la maladie. Afin de suivre précisément l'avancée de la maladie, l'AREDS a créé une **classification simplifiée des différentes catégories de DMLA** (Tableau 2).

Tableau 2. Classification simplifiée de l'AREDS

Catégorie	***Caractéristiques cliniques***
Catégorie 1	Aucun ou peu de drusen (< 63 µm).
Catégorie 2 : maculopathie liée à l'âge	Le patient présente un ou plusieurs des éléments suivants : • De nombreux petits drusen (<63 µm) • Quelques drusen de taille intermédiaire (63 µm > drusen intermédiaire < 125 µm) • Anomalie de l'EPR
Catégorie 3 : DMLA modérée	Le patient présente un ou plusieurs des éléments suivants : • De nombreux drusen de taille intermédiaires (63> drusen intermédiaire< 125 µm) • Au moins un grand drusen (> 125 µm) • Atrophie géographique excluant la fovéa
Catégorie 4 : DMLA tardive	Le patient présente un ou plusieurs des éléments suivants : • Atrophie géographique touchant la fovéa • Présence d'une DMLA néovasculaire

B.3.1. Mesure de la vision

La **mesure de l'acuité visuelle** est réalisée à l'aide de **l'échelle ophtalmique** (ETDRS : *Early treatment diabetic retinopathy study*) sur un **œil indépendamment de l'autre**. Elle permet de mesurer l'acuité visuelle lettre par lettre afin d'observer les plus fines pertes de vision, et elle est utilisée lors du diagnostic ainsi que pour le suivi de l'évolution de la maladie. L'échelle ETDRS (Figure 10) est composée de 3 planches différentes : ETDRS R permet de déterminer la **réfraction** pour l'œil gauche et droit. Les deux autres planches permettent de mesurer l'acuité visuelle de l'œil droit (ETDRS 1) et de l'œil gauche (ETDRS 2). En complément de l'acuité visuelle, la **vision des contrastes** est mesurée à l'aide de l'échelle Pelli Robson (Figure 10). Cette échelle est composée de lettres de même taille possédant des contrastes par rapport au fond différent.

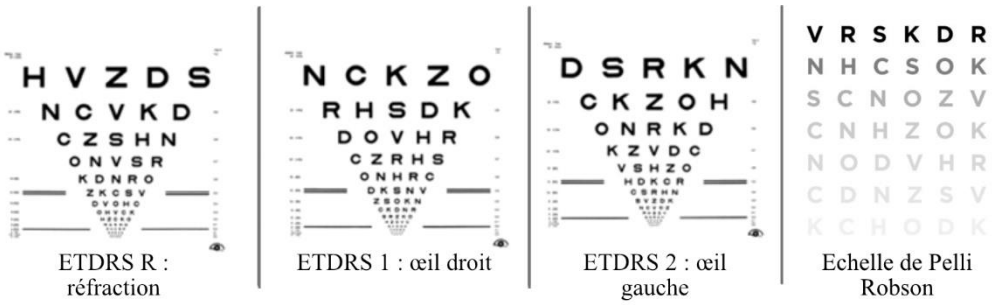

Figure 10. Échelles ophtalmiques (adapté de Kaiser, 2009)

Une **métamorphopsie** (déformation des lignes) ou un **scotome** (tâche sombre dans le champ visuel) peuvent être observés lors d'un examen simple, réalisé en autosurveillance ou chez un médecin à l'aide d'une grille d'Amsler (Figure 11). Cette grille est constituée d'un quadrillage régulier avec un point noir en son centre. La grille doit être observée avec un seul œil afin de vérifier que le patient voit toutes les lignes droites avec des angles droits à chaque intersection lorsqu'il fixe le point central.

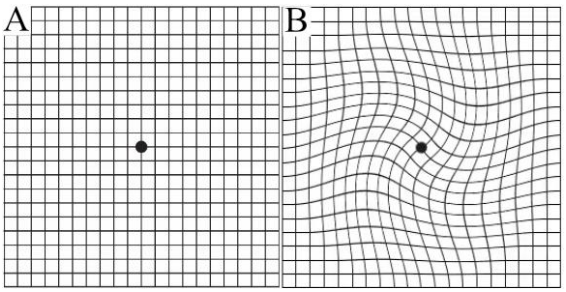

Figure 11. Grille d'Amsler
A) Grille d'Amsler **B)** Simulation d'une perception de métamorphopsie

B.3.2. Examen du fond d'œil

Bien que la perte de la vision centrale soit une caractéristique de la DMLA, un examen clinique plus approfondi est nécessaire afin d'établir un diagnostic précis sur la forme ainsi que le stade de la maladie.

La **rétinographie** permet d'obtenir une image du fond de l'œil du patient. La pupille du patient est dilatée puis une photo d'un fond de l'œil est prise à l'aide d'une lampe à fentes. Cet examen permet d'observer et de mesurer la taille des drusen, d'observer les zones d'atrophie, la néovascularisation ainsi que les hémorragies rétiniennes (Figure 12). La rétinographie est généralement complétée par une analyse par **auto-fluorescence du fond d'œil**. Cet examen

consiste à visualiser la **lipofuscine** présente dans l'épithélium rétinien pigmentaire excitable par la lumière bleue. Les drusen vont renvoyer un signal augmenté ou diminué, l'atrophie se traduira par une hypofluorescence, les néovaisseaux pourront se traduire par une hyperfluorescence (Figure 12).

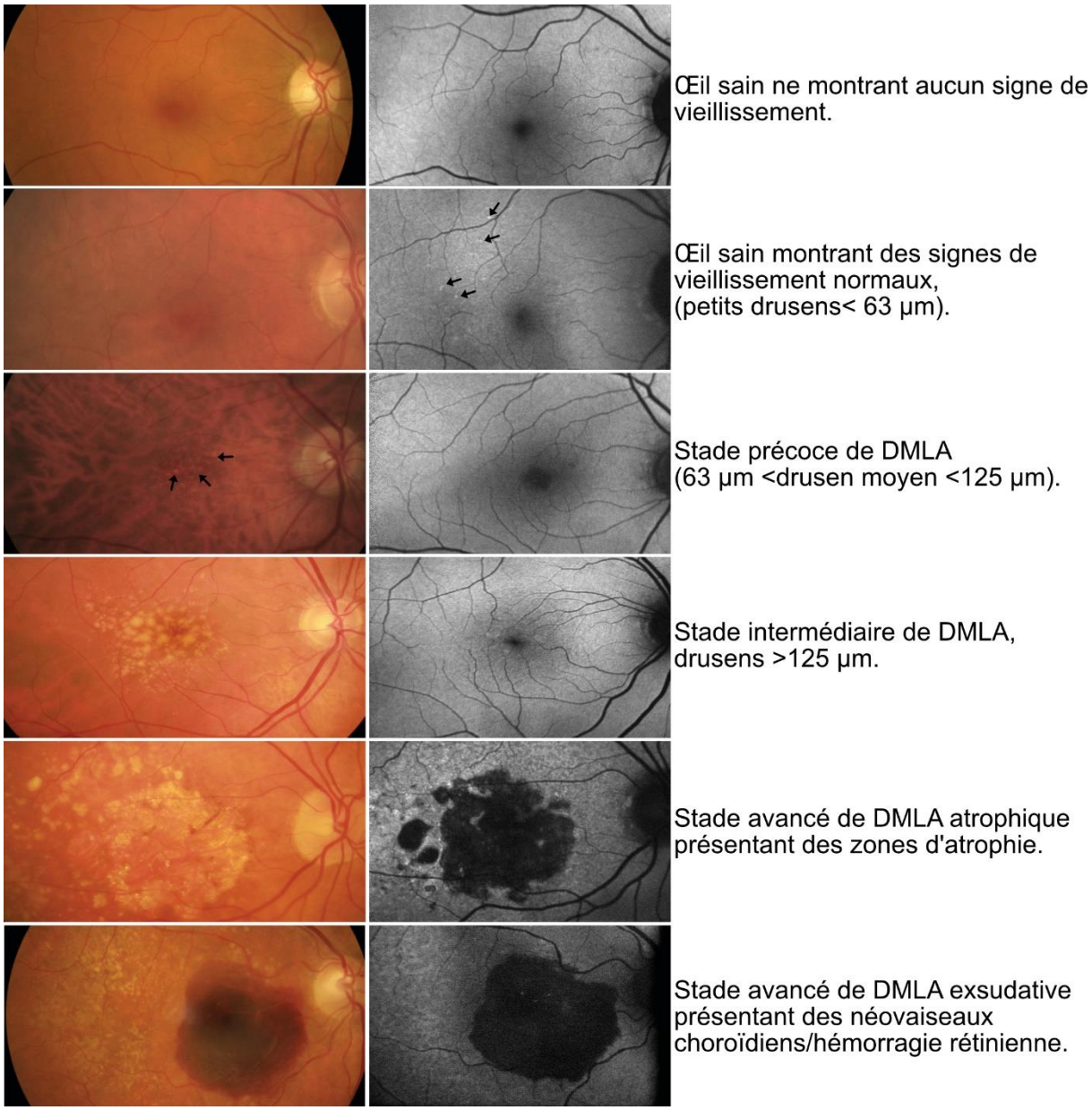

Figure 12. Examen du fond d'œil chez des patients atteints des différents stades de DMLA
Panel de gauche réalisé par rétinophotographie. Panel de droite réalisé par autofluorescence du fond d'œil. Adapté de Hart et al., 2020.

B.3.3. Tomographie par cohérence optique

La **tomographie par cohérence optique** (OTC) permet de visualiser toutes les couches de la rétine. Cet examen est principalement utilisé lors du suivi des traitements. Chez les patients atteints de MLA, des **drusen sont visibles** et forment de **légers soulèvements de l'EPR**. La **DMLA atrophique** se caractérise par une **hyperréflectivité des couches choroïdiennes** et l'évolution des drusen induit des décollements de l'EPR sans accumulation liquidienne. La **DMLA néovasculaire** se traduit, dans un premier temps, par un **épaississement hyperréflectif du complexe EPR-chorio-capillaire** et dans un second temps, par une **accumulation de liquide** sous rétinien induisant un décollement de la rétine pouvant être accompagné d'œdèmes. (Figure 12).

B.3.4. Angiographie

L'angiographie rétinienne permet de visualiser la néovascularisation choroïdienne à la suite d'une injection d'un **produit de contraste** par voie intraveineuse (fluorescéine et de vert d'indocyanine). Cette technique est principalement utilisée après le diagnostic d'une DMLA à un **stade tardif** (DMLA atrophique ou néovasculaire). Cet examen permet **de suivre l'évolution de l'atrophie** dans le cas de DMLA atrophique. Dans les cas de **DMLA néovasculaire**, cet examen permet de **visualiser les lésions, la taille et l'étendue des néovaisseaux**.

B.4. Facteurs de risques

Bien que l'**âge** joue un rôle prépondérant dans l'apparition de la maladie, la DMLA est une **pathologie multifactorielle**, impliquant à la fois des **facteurs génétiques** et **environnementaux**.

B.4.1. Facteurs génétiques

L'**hérédité** semble être liée à l'apparition de la maladie. Une personne ayant un parent atteint de DMLA possède un risque 4 fois plus élevé de développer une DMLA. Des recherches ont permis d'identifier des variants génétiques associés à la maladie (Leveziel et al., 2010) :

- Variants du gène codant pour le **facteur H du complément** impliqué dans la réponse inflammatoire : Ces variants sont associés à une dérégulation de la réponse immunitaire avec notamment une accumulation de macrophages au niveau de la rétine participant au maintien d'un environnement pro-inflammatoire dans la rétine (Hallam et al., 2022; Klein et al., 2005)
- Différents allèles de **l'apolipoprotéine E** (ApoE) : L'ApoE est impliquée dans le transport des phospholipides et du cholestérol. Ces protéines pourraient non seulement être impliquées dans la formation des drusen, mais aussi interagir avec le système du complément et ainsi soutenir un environnement pro-inflammatoire (Hu et al., 2021; Klaver et al., 1998).
- Les variants du gène ABCA. Les protéines ABCA font partie de la famille des transporteurs impliqués dans le cycle visuel.
- Le gène **Age-Related Maculopathy Susceptibility** 2 est impliqué dans le stress cellulaire. Une surexpression de ce gène serait à l'origine de la dégradation de la membrane de Bruch et ainsi participerait à la formation de drusen dans la rétine. Il favoriserait principalement la forme néovasculaire. (Chakravarthy et al., 2013; Supanji et al., 2021)

Depuis quelques années, les nouvelles technologies de séquençage du génome humain ont permis d'identifier de nombreux variants génétiques associés au risque de la survenue de la maladie. Au total, **52 polymorphismes nucléotidiques** ont été identifiés (Fritsche et al., 2016, 2013; Wang et al., 2023).

B.4.2. Facteurs environnementaux

Le mode de vie semble impacter la survenue de la maladie. En effet, **les apports nutritionnels** et notamment un régime pauvre en acides gras poly-insaturés (oméga-3) riche en cholestérol et en acide gras saturés et mono-insaturés augmentent la prévalence de la DMLA. Ces acides gras vont remplacer les acides gras poly-insaturés (AGPI) présents au niveau de la membrane des cellules rétiniennes. Difficilement éliminables par les cellules de l'EPR, ils vont s'accumuler au sein de la rétine et perturber son homéostasie. De plus l**'indice de masse corporelle** (IMC) est aussi lié à l'apparition de la maladie. Un patient possédant un

IMC supérieur à 30 voit son risque doublé par rapport à un patient ayant un IMC inférieur à 25.

Néanmoins, le facteur environnemental impactant le plus la prévalence de la maladie est le **tabagisme**. Il constitue le second facteur de risque le plus important après l'âge. Il semble que le tabagisme soit un facteur dose dépendant, la prévalence de la maladie étant augmentée par 3 chez un patient fumant 20 à 39 paquets/an et par 5 chez un patient fumant plus de 40 paquets/an.

C. Physiopathologie de la DMLA

Les facteurs environnementaux et génétiques jouent un rôle clef dans la physiopathologie de la DMLA. En effets, ils peuvent influer sur les **trois composantes de la DMLA**, à savoir, l'apparition d'un **stress oxydant**, la formation et le maintien d'un **environnement pro-inflammatoire** ainsi que la création de nouveaux vaisseaux par **néo-angiogenèse**.

La DMLA est caractérisée par diverses **altérations tissulaires** dues au vieillissement telle que **l'accumulation de lipofuscine** dans les cellules de l'EPR, un **épaississement** et une **détérioration de la membrane de Bruch**, l'apparition de **drusen**. Bien que les mécanismes moléculaires conduisant à ces altérations ne soient pas encore totalement élucidés, il est de plus en plus évident que le stress oxydant et l'inflammation soient des éléments initiateurs de la DMLA tandis que l'angiogenèse survient plus tardivement.

C.1. DMLA et stress oxydant

Le stress oxydant se définit par une agression des cellules par des **radicaux libres** appelés **espèces réactives de l'oxygène** (ERO). Ces radicaux libres peuvent être produits de manière endogène par les cellules dans les mitochondries au niveau de la chaine respiratoire lors de la phosphorylation oxydative (ou respiration mitochondriale). Cette dernière représente 90 % de notre consommation d'oxygène et permet la conversion de l'ADP et Pi (adénosine diphosphate + phosphate) en ATP (adénosine triphosphate) fournissant ainsi l'énergie nécessaire aux cellules. La consommation d'oxygène n'est pas sans conséquence, elle peut induire la formation d'ERO tels que l'anion superoxyde ($O2^{\bullet -}$), le peroxyde d'hydrogène (H_2O_2), le radical hydroxyle ($^{\bullet}OH$), le radical pyroxyle ($ROO^{\bullet}$), ou encore le radical alkoxyl ($RO^{\bullet}$) (Figure

13). Les ERO sont radicalaires à l'exception du peroxyde d'hydrogène, qui par la réaction de fenton, peut aussi générer des radicaux libres (Figure 13).

Afin de lutter contre les radicaux libres, certaines cellules de la rétine expriment de manière endogène des **enzymes détoxifiantes** (Figure 13) :

- La **catalase (Cat)**, présente dans les cellules de l'EPR et dans les photorécepteurs, catalyse la conversion de l'H_2O_2 en eau et oxygène. C'est l'un des enzymes anti-oxydantes les plus rapides, elle est capable de convertir plusieurs centaines de milliers de molécules d'H_2O_2 par seconde en eau.
- Les **superoxydes dismutase**s (SOD), présentent dans les cellules de l'EPR et dans les photorécepteurs sont des métalloprotéinases qui catalysent la **dismutation des anions superoxydes** et eau et oxygène. Il existe deux types de SOD, la SOD manganèse présente principalement dans les mitochondries et une SOD à zinc et cuivre présente dans le cytosol.
- Le **glutathion peroxydase** (GPx) est une enzyme du métabolisme glutathion. Cette enzyme utilise le glutathion réduit (GSH) comme donneur d'électrons et va former du disulfure de glutathion (GSSG) lors de la **détoxification d'hydroperoxyde**.

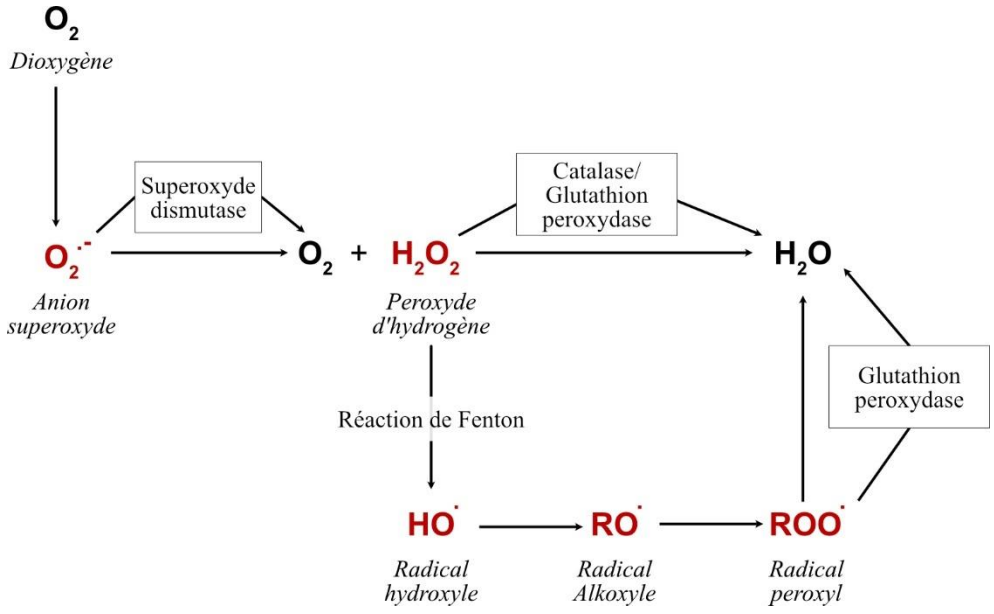

Figure 13. Espèces réactives de l'oxygène et enzymes anti-oxydantes
La quantité importante en oxygène (O_2) peut induire la formation d'anion superoxyde. La superoxyde dismutase (SOD) va convertir ce dernier en oxygène et en peroxyde d'hydrogène. Le peroxyde d'oxygène va être, à son tour, converti en eau à l'aide de la catalase ou du glutathion

peroxydase (GSH). Lorsque le peroxyde d'oxygène n'est pas détoxifié, il va induire la formation de radicaux, le radical hydroxyle puis le radical alkoxyle et pour finir le radical peroxyl. Ce dernier pourra être converti en eau par le glutathion peroxydase.

C.1.1. Les origines du stress oxydant au sein de la rétine

L'œil est un des tissus du corps humain le plus **consommateur d'oxygène** permettant ainsi la transformation d'un signal lumineux en signal visuel et sa transmission au cerveau (Yu and Cringle, 2005). Cette grande consommation d'oxygène combinée à d'autres facteurs environnementaux peut induire la formation d'ERO. Au niveau de la rétine, divers mécanismes sont impliqués dans la formation des ERO.

C.1.1.1. Le vieillissement

Le **vieillissement** est défini par la somme des altérations délétères d'un organisme diminuant ses capacités à maintenir l'homéostasie (Finch and Ruvkun, 2001; Harman, 1981). Le processus de vieillissement est initié par des **dommages moléculaires** conduisant à la **dégradation** des cellules et des tissus engendrant *in fine* la **perte de fonctionnalité d'un organe ou d'un tissu**.

Lors du vieillissement, une augmentation des ERO a été observée au sein de la rétine (Torres et al., 2023; Zhang et al., 2015). Cette augmentation pourrait être expliquée par une altération de la chaine respiratoire mitochondriale ainsi que par une diminution des capacités anti-oxydantes et notamment par une diminution de l'activité enzymatique telle que la catalase et la SOD (Torres et al., 2023; Zhang et al., 2015) (Figure 14). En raison de leur rôle dans le maintien de la rétine, les cellules de l'EPR possèdent une activité métabolique élevée nécessitant une quantité importante d'énergie. Afin de répondre à leur demande énergétique, les cellules de l'EPR possèdent un grand nombre de mitochondries. Ainsi, l'altération des fonctions mitochondriales des cellules de l'EPR peut leur être fatale entraînant non seulement leur propre dysfonctionnement, mais aussi le dysfonctionnement des photorécepteurs.

Le vieillissement des cellules de l'EPR est aussi caractérisé par une **accumulation d'agrégats de débris lipidiques et protéiques** connus sous le nom de **lipofuscine** provenant de la **phagocytose** des photorécepteurs.

C.1.1.2. La phagocytose

La **phagocytose** permet de maintenir la taille des photorécepteurs tout en recyclant les éléments nécessaires aux photorécepteurs et aux cellules de l'EPR. Cependant, certains lipides et certaines protéines ne sont pas complètement phagocytés, et ne peuvent être **ni recyclés, ni dégradés, ni excrétés,** ce qui induit leur **accumulation** sous forme de **lipofuscine**.

La lipofuscine est stockée sous forme de granules dans le cytoplasme des cellules de l'EPR. Elle est composée de protéines autofluorescentes : le N-retinylidene-N-retinylethanolamine, la bis-rétinoïde pyrimidine, la protéine carboxyéthylpyrrole, le malondialdéhyde (MDA), etc. De plus, une trop grosse quantité de lipofuscine peut être fatale pour les cellules de l'EPR dûe à la **toxicité** de certains composés tels que le N-retinylidene-N-retinylethanolamine (**A2-E**), un dérivé toxique du rétinol. L'A2-E est un inhibiteur de la pompe à proton et **altère la membrane des lysosomes**. Ces altérations entrainent une perturbation des fonctions lysosomales provoquant une diminution des capacités de phagocytoses des cellules de l'EPR. L'altération de ces fonctions lysosomales peut induire un relargage d'ERO dans le cytoplasme provoquant non seulement des dommages oxydatifs, mais aussi l'accumulation de lipofuscine. Une accumulation de ces agrégats au sein du cytoplasme des cellules de l'EPR serait délétère pour ces dernières et jouerait un rôle dans les maladies rétiniennes dégénératives telles que la DMLA. Ces agrégats contiennent des fluorochromes **sensibles à la lumière**. Ainsi, lors d'une exposition à la lumière, ces fluorochromes peuvent induire la formation d'ERO.

C.1.1.3. Le stress oxydatif induit par la lumière

La lumière est au cœur des premières hypothèses émises sur l'origine des ERO au sein de la rétine (Chalam et al., 2011; Noell et al., 1966; Terao et al., 2022).

La lipofuscine n'est pas le seul chromophore présent dans la rétine. En effet, l'acquisition du signal lumineux est réalisée par les photorécepteurs à l'aide de différents **chromophores** (Ivanov et al., 2018). L'absorption d'un photon par ces chromophores induit leur excitation ainsi que leurs interactions rapides avec d'autres molécules y compris l'oxygène, ce qui peut former des ERO (Chalam et al., 2011; Ivanov et al., 2018).

Par ailleurs, certains rayonnements (**ultraviolet**, UV) sont connus pour leurs effets délétères sur l'ADN. Certaines études ont montré qu'une exposition aux UV pouvait induire des dommages à l'ADN (Blasiak et al., 2017; Kciuk et al., 2020; Szaflik et al., 2009).

C.1.1.4. Dommages à l'ADN

Les **dommages à l'ADN** présents au sein des cellules de l'EPR peuvent provenir des ERO produits de manière **endogène** par le métabolisme cellulaire, mais aussi par des facteurs **exogènes** tels que les **UV** ainsi que certains produits chimiques contenus dans la **fumée de cigarette**.

Les dommages à l'**ADN mitochondrial** (ADNmt) sont un des marqueurs des maladies dégénératives. Il a été montré que les personnes atteintes de DMLA présentaient des dommages à l'ADNmt sur l'ensemble du génome mitochondrial alors que lors d'un vieillissement physiologique, les dommages sont localisés dans les régions communes de délétion de l'ADNmt. Les régions communes de délétions regroupent 4977 paires de bases (pb) localisées sur deux sites, de 8 470 à 8 482 et de 13 447 à 13 459. (Karunadharma et al., 2010; Peng et al., 2006). L'altération de l'ADNmt induit des dysfonctionnements notamment sur la **chaîne respiratoire mitochondriale** ce qui provoque une **diminution de la production d'énergie** ainsi qu'une **diminution des défenses anti-oxydantes** des cellules (Figure 14) (Hyttinen et al., 2018).

C.1.2. Stress oxydatif et EPR

L'EPR possède un système anti-oxydant complexe afin de **contrer les dommages oxydatifs endogènes**. Ces systèmes anti-oxydants sont régulés par différentes voies de signalisation et divers facteurs de transcription.

Parmi ses facteurs de transcription, on retrouve un facteur de transcriptions des enzymes anti-oxydantes, le **facteur nucléaire érythroïde-2 (Nrf2)**. En absence de stress oxydatif, Nrf2 est associé à la Kelch-like ECH-associated protein 1 (**Keap1**) ce qui le bloque dans le cytosol et l'empêche de rentrer dans le noyau. De plus, Keap1 interagit aussi avec le **complexe E3** d'une ubiquitine ligase dépendant de cullin 3 (Cul3). Cette dernière permet de réguler la quantité de Nrf2 *via* sa protéolyse par le protéasome (Datta et al., 2017). En condition physiologique, l'expression des gènes anti-oxydants est basse afin de maintenir un pouvoir redox minimal. Lors **d'un stress oxydant**, Keap1 subit un changement de conformation **libérant Nrf2** et ainsi permet la **translocation de ce dernier dans le noyau**. Nrf2 sera ensuite capable de se lier à

l'élément de réponse anti-oxydant (ARE) et ainsi initier la transcription des gènes anti-oxydants (Datta et al., 2017; Sun et al., 2023). Il a été montré que **Nrf2 diminue avec l'âge** altérant la réponse anti-oxydante des cellules de l'ERP et ainsi favorise certaines maladies oculaires telles que la DMLA (Datta et al., 2017).

L'accumulation des dommages oxydatifs va mener à l'oxydation de macromolécules et ainsi mener au **dysfonctionnement des cellules de l'EPR**. L'oxydation protéique conduit à une altération plus au moins rapide de la fonction des protéines ce qui aboutit à des dysfonctionnements cellulaires et tissulaires (Negre-Salvayre et al., 2008). De plus, l'oxydation des lipides mène à des altérations membranaires avec une diminution de la fluidité membranaire, augmentation de la perméabilité, gonflement des mitochondries induisant une inhibition de la chaine respiratoire et le relargage du **cytochrome c**. Le relargage de ce dernier entraine la disparition des cellules de l'ERP par apoptose (Figure 14). L'accumulation d'ERO va aussi induire des dommages à l'ADN nucléaire ce qui va activer la phosphorylation d'ATM, Chk2 et p53 et ainsi provoquer un arrêt du cycle cellulaire. In fine, l'arrêt de cycle cellulaire va mener à l'apoptose des cellules de l'EPR (Figure 14).

Par ailleurs, ces dysfonctionnements vont aussi activer certaines voies de signalisation impliquées dans la DMLA. En effet, il a été montré *in vitro* que l'induction d'ERO dans des cellules de l'EPR active la voie Nf-κB c'est-à-dire la dégradation de IκBα par le protéasome libérant ainsi p50 et p65 qui vont induire l'activation de gènes impliqués dans l'inflammation (Figure 14). De plus, il a aussi été montré que l'augmentation d'ERO intracellulaire induisant la phosphorylation de protéines (p38, ERK1/2 et JNK1/2) impliquées dans l'angiogenèse et ainsi dans la production et la sécrétion de VEGF-A (Figure 14). Ainsi, le stress oxydant est un élément crucial dans la pathogénicité de la DMLA, il va induire l'apoptose des cellules et aussi participer à l'inflammation et l'angiogenèse (Figure 14).

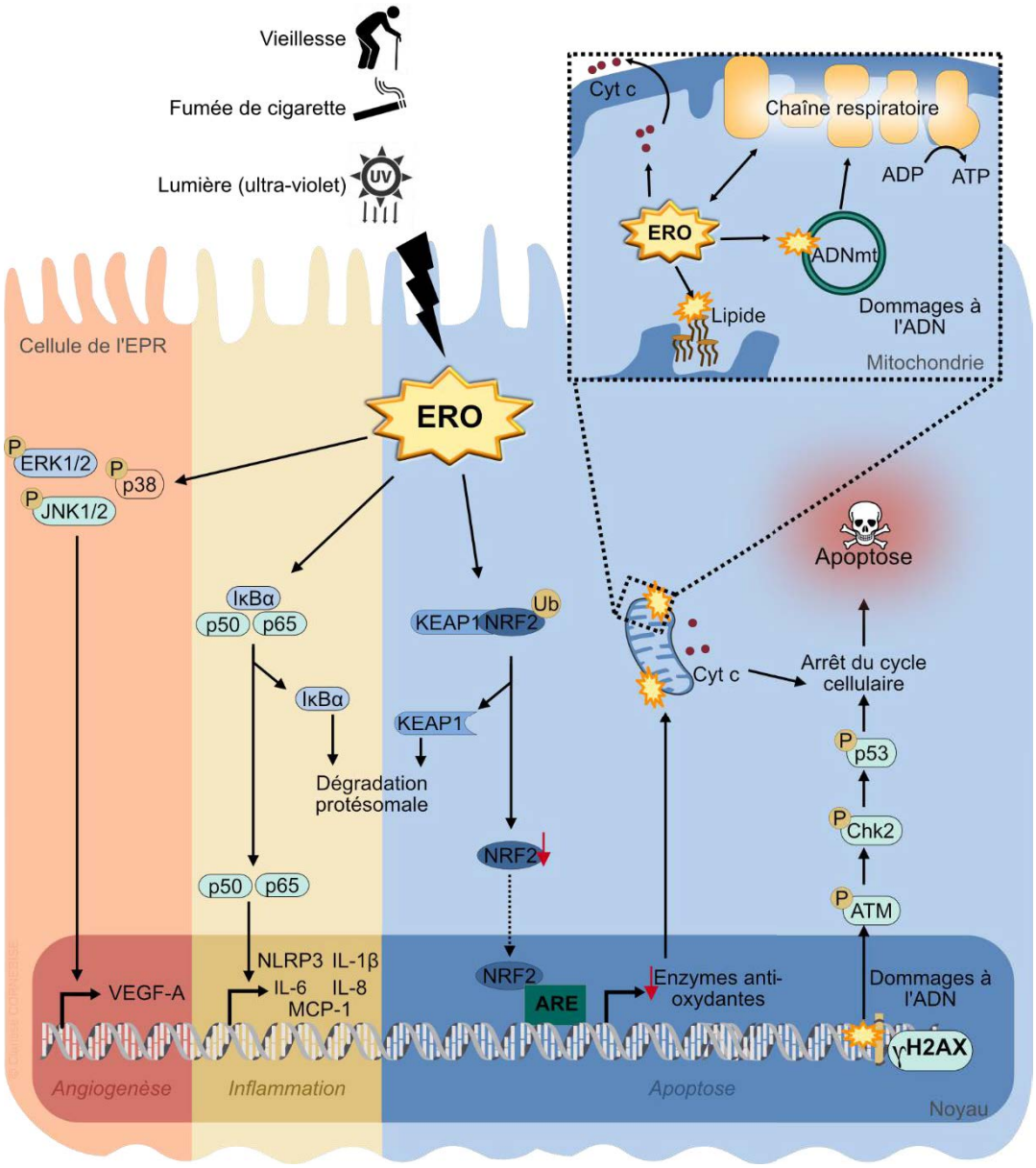

Figure 14. Représentation schématique du stress oxydant au sein des cellules de l'épithélium pigmentaire rétinien (EPR)

Les espèces réactives de l'oxygène (ERO) générées par divers facteurs (UV, fumée de cigarette, vieillissement …) vont activer diverses voies de signalisation impliquées dans la DMLA. Les ERO vont induire la phosphorylation (activation) des protéines ERK1/2, JNK1/2 et p38 qui vont à leur tour induire la transcription du gène VEGF-A impliqué dans l'angiogenèse. Les ERO vont aussi induire la dégradation par le protéasome d'IκBα libérant ainsi p65 et p50. Une fois libérées, ces protéines vont induire des gènes impliqués dans l'inflammation. Par ailleurs, les ERO vont induire la dégradation de KEAP1 libérant ainsi NRF2 impliqué dans la régulation positive des enzymes anti-oxydantes. Lors du vieillissement, l'expression d'NRF2 diminue ce qui entraîne une altération des défenses anti-oxydantes et ainsi ne protègent plus les mitochondries des ERO. Les dommages à l'ADN induits dans les mitochondries provoquent le relargage de cytochrome c (cyt C) dans le cytosol ce qui provoque la mort par apoptose des cellules de l'EPR. L'augmentation des ERO va aussi induire des dommages à l'ADN nucléaire induisant ainsi l'augmentation de γH2AX ainsi que la phosphorylation d'ATM, Chk2 et p53 menant à l'arrêt du cycle cellulaire. In fine, l'arrêt du cycle cellulaire va induire l'apoptose des cellules.

C.2. DMLA et inflammation

L'inflammation joue un rôle prépondérant dans la progression de la DMLA. **Habituellement**, l'inflammation est un **processus biologique bénéfique** qui permet de mobiliser le système immunitaire afin d'éliminer un agent indésirable identifié comme nocif par l'organisme. Cependant, chez les patients atteints de **DMLA**, l'inflammation induite par divers stimuli contribue à la **destruction des cellules de la rétine**.

C.2.1. Cellules immunitaires

Les **cellules microgliales** sont les **macrophages résidents** du système nerveux central que l'on retrouve dans le cerveau, mais aussi dans la rétine et qui constituent la première ligne de défense de la rétine. En **condition physiologique**, les cellules microgliales jouent un **rôle de sentinelles**. Elles sont aussi impliquées dans la **fonction visuelle**, elles participent à la **clairance des cellules apoptotiques** et au maintien de l'**intégrité ainsi qu'à l'élagage** (élimination) **des synapses** (Dixon et al., 2021). Chez les patients atteints de **DMLA**, les cellules microgliales vont être **activées** par divers médiateurs sécrétés par les cellules de l'EPR, mais aussi par l'accumulation d'A2E présent dans la lipofuscine ou bien par l'accumulation de drusen perçue comme **signal de danger** par les cellules. Leur activation va induire une **phagocytose excessive** des photorécepteurs et ainsi leur disparition.

Les **macrophages** sont des cellules hématopoïétiques provenant de la moelle osseuse et qui voyagent dans la **circulation systémique** sous forme de monocytes. Ces cellules jouent un rôle dans la **phagocytose**, le nettoyage des débris, la **présentation d'antigène** ainsi que dans la **sécrétion de cytokines.** Les macrophages circulants sont activés et acquièrent des phénotypes fonctionnels spécialisés en fonction des stimuli : les **macrophages pro-inflammatoire de type M1** et les **macrophages anti-inflammatoires de type M2** (Figure 15). Les patients atteints de DMLA présentent une accumulation de macrophages au sein de la rétine. Ces macrophages présentent principalement un profil pro-inflammatoire de type M1 et se caractérisent par une **phagocytose accrue** ainsi qu'une **libération d'ERO**, et de **cytokines pro-inflammatoires** (IL-1β, IL-6)(Behnke et al., 2020)(Figure 15). Leur activité de phagocytose ainsi que la libération d'ERO induit la disparition des photorécepteurs ainsi que des cellules de l'ERP.

Outre leur activité de phagocytose, les phagocytes peuvent aussi agir en tant que **cellules présentatrices d'antigène** et ainsi faire le **lien entre l'immunité innée et adaptative** (Behnke et al., 2020).

Il est maintenant bien établi que l'**immunité adaptative** joue aussi un rôle dans la DMLA. En effet, l'analyse des sérums de patients atteints de DMLA montre l'implication des **lymphocytes B** dans la DMLA à travers la présence d'anticorps anti-rétiniens (Korb et al., 2023b)(Figure 15). De plus, il a été montré que les patients de DMLA néovasculaire et atrophique présentent des taux élevés de lymphocytes $CD8^+$ (Lymphocytes T cytotoxiques) (Ezzat et al., 2008; Faber et al., 2013; Krogh Nielsen et al., 2019; Subhi et al., 2017; Subhi and Lykke Sørensen, 2017). La présence accrue de lymphocytes T CD8+ semble être associée aux deux formes de DMLA, soutenant l'hypothèse selon laquelle la DMLA pourrait avoir une composante immunitaire systémique importante (Behnke et al., 2020). Néanmoins, le rôle de ces lymphocytes ainsi que les mécanismes moléculaires impliqués dans la DMLA restent inconnus (Behnke et al., 2020).

C.2.1.1. Médiateurs pro-inflammatoires

Interleukine 1β (IL-1 β)

L'**IL-1β** est une cytokine pro-inflammatoire, sa sécrétion nécessite deux composantes : l'induction de l'expression de la pro-IL-1β et l'activation de l'inflammasome. Ce dernier va permettre le clivage par la caspase 1 de la pro- IL-1β en IL-1β mature qui pourra être sécrétée. L'IL-1β active joue un rôle dans l'initiation et la propagation de l'inflammation (Wooff et al., 2019), incluant le **recrutement des macrophages** (Rider et al., 2011), **l'activation de l'interleukine-6** (IL-6) (McGeough et al., 2012; Tomani et al., 2020), ainsi que la **régulation de l'expression des chimiokines** (Natoli et al., 2017). De plus, il a été montré que l'IL-1β influence fortement la formation de néovaisseaux (Fahey and Doyle, 2019) favorisant ainsi la colonisation de la rétine par de nouvelles cellules immunitaires. En effet, la liaison de l'IL-1β avec son récepteur va induire l'activation de la voie des MAPKs et ainsi induire la phosphorylation de protéines clefs impliquées dans l'activation de la transcription du VEGF-A (Chen et al., 2018).

L'interleukine 6 (IL-6)

L'**IL-6** possède, tout comme l'IL-1β, des propriétés pro-inflammatoires et pro-angiogéniques. L'IL-6 **inhibe l'expression de FasL** au niveau de la membrane des cellules de l'EPR **diminuant ainsi le privilège immun**. Il a aussi été montré que l'IL-6 pouvait avoir un rôle dans la DMLA néovasculaire. En effet, les patients atteints de DMLA néovasculaire présentent une concentration intraoculaire d'IL-6 très élevée (Lechner et al., 2017; Mao et al., 2022). Des études cliniques ont montré que les taux d'IL-6 dans l'humeur aqueuse sont corrélés à la survenue d'œdème maculaire, et ce de manière plus importante que les niveaux de VEGF (Chalam et al., 2014; Ulhaq et al., 2020). Néanmoins, il reste à élucider les mécanismes moléculaires sous-jacents.

Monocyte chemoattractant protein 1 (MCP-1)

MCP-1 aussi appelé CCL-2 (C-C motif chemokine ligand 2) permet de **recruter les macrophages** pro-inflammatoires exprimant fortement le récepteur CCR2. Il a été montré, chez les patients atteints de DMLA, une augmentation de MCP-1 ainsi qu'une infiltration de macrophages CCR2+ (Murenu et al., 2022; Roubeix et al., 2020; Sennlaub et al., 2013). Le recrutement de ces macrophages est corrélé à la mort des photorécepteurs. Des études précliniques ont étudié le rôle de MCP-1 dans le **recrutement des macrophages**. Ainsi, une étude réalisée dans un modèle murin néovascularion choroïdienne induite par impact laser a montré que l'inhibition de MCP-1 avec un inhibiteur (liposomal clodronate) prévenait la formation de nouveaux vaisseaux (Roubeix et al., 2020; Sakurai et al., 2003). De plus, une seconde étude a complété les investigations sur le rôle de MCP-1 dans la DMLA. Elle a montré par marquage histochimique qu'une délétion du gène CCR2 chez des souris prévenait la disparition des photorécepteurs (Roubeix et al., 2020; Sennlaub et al., 2013). Ainsi, ces études suggèrent que le recrutement des macrophages CCR2+ et leur activation par MCP-1 sont impliqués dans la dégénérescence maculaire et plus spécifiquement dans la DMLA néovasculaire (Roubeix et al., 2020).

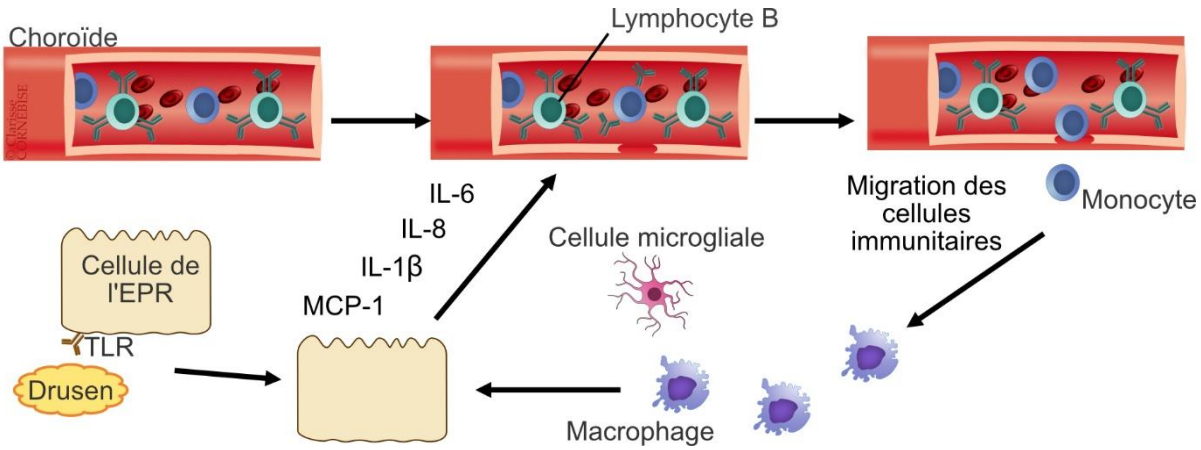

Figure 15. Initiation de la réponse immunitaire.
La reconnaissance des signaux de danger tels que les drusen par les récepteurs Toll-like (TLR) présents à la surface des cellules de l'épithélium pigmentaire rétinien (EPR) entraine la production de cytokines pro-inflammatoires et chimiokines (IL-6, IL-8, IL-1β, MCP-1 : *monocyte chemoattractant protein 1*). Ces médiateurs contribuent à l'activation et le recrutement de cellules immunitaires (macrophages pro-inflammatoires) ainsi que la sécrétion d'auto-anticorps par les lymphocytes B. (adapté de Behnke et al., 2020; Kauppinen et al., 2016).

C.2.2. Inflammation et EPR

Bien que les cellules de l'EPR ne soient pas des cellules immunitaires, elles jouent cependant un rôle crucial dans la **régulation de l'inflammation** au sein de la rétine. Lorsque ces cellules sont exposées à des facteurs de stress tels que des ERO, elles peuvent sécréter des cytokines et chimiokines pro-inflammatoires (IL-6, IL-8, MCP-1…) et ainsi favoriser le **recrutement et l'activation des cellules immunitaires**. La réponse inflammatoire de l'EPR est étroitement liée au stress oxydant qu'il subit. En effet, les ERO ainsi que l'activation des récepteurs membrane de l'IL-1β et des récepteurs Toll -like activent la voie de signalisation **NF-κB** induisant la dégradation par le protéasome d'IκBα et ainsi libère p50 et p65 qui vont promouvoir la transcription de gènes de cytokine pro-inflammatoire et de NRLP-3 (Figure 16). L'induction de ce dernier va induire l'oligomérisation de l'inflammasome NLRP3 et ainsi le clivage de la pro-IL-1β en IL-1β qui va ensuite être sécrétée et participer à l'environnement pro-inflammatoire de la rétine (Figure 16).

Par ailleurs, des études épidémiologiques ont permis de démontrer que certains **variants du gène codant pour le facteur H du complément** (CFH) augmentent la prévalence de la maladie. Le CFH est un régulateur clé du système du complément. Ce dernier est constitué d'un groupe de protéines dont leur activation en cascade permet la formation d'un **complexe d'attaque**

membranaire induisant des pores dans la membrane plasmique de la cellule. L'activation du système du complément permet notamment l'**opsonisation** des organismes étrangers ou des cellules hôtes en favorisant leur **phagocytose** ainsi que leur **lyse**. L'altération du gène du CFH est délétère pour ses fonctions de régulation, ce qui provoque une **dérégulation à la hausse de l'activité du système du complément** soutenant un **environnement pro-inflammatoire** (Behar-Cohen, 2018).

Les cellules de l'EPR sont aussi sensibles à leur environnement. Elles vont détecter les **drusen** comme signaux de danger *via* l'activation des **récepteurs toll-like 4** (TL-R4) présents à leur surface. L'activation de ces récepteurs va activer la **voie de signalisation Nf-κB** et ainsi la sécrétion de cytokines et chimiokines inflammatoires (IL-8, IL-6, IL1β) (Klettner and Roider, 2021)(Figure 16).

Il est important de rappeler que l'EPR forme grâce à des jonctions adhérentes et des jonctions serrées une **barrière hématorétinienne** (BHR). Ainsi, la détérioration des cellules de l'EPR induite par un stress oxydant entraîne la **perte de la BHR**. Cette perte permet aux cellules immunitaires présentes dans la choroïde de migrer dans la rétine. Ainsi, la **migration des cellules immunitaires** ainsi que la **sécrétion de médiateurs inflammatoires** (IL-6, IL-8, MCP-1…) vont créer un environnement pro-inflammatoire au sein de la rétine corrélée à la progression de la maladie (Krogh Nielsen et al., 2019).

Dans la DMLA, **l'inflammation et l'angiogenèse sont étroitement liées** et contribuent à la progression de la maladie. L'inflammation va stimuler la production de facteurs de croissance et de cytokines pro-inflammatoires, tels que le facteur de **croissance endothélial vasculaire** (VEGF) favorisant ainsi l'angiogenèse.

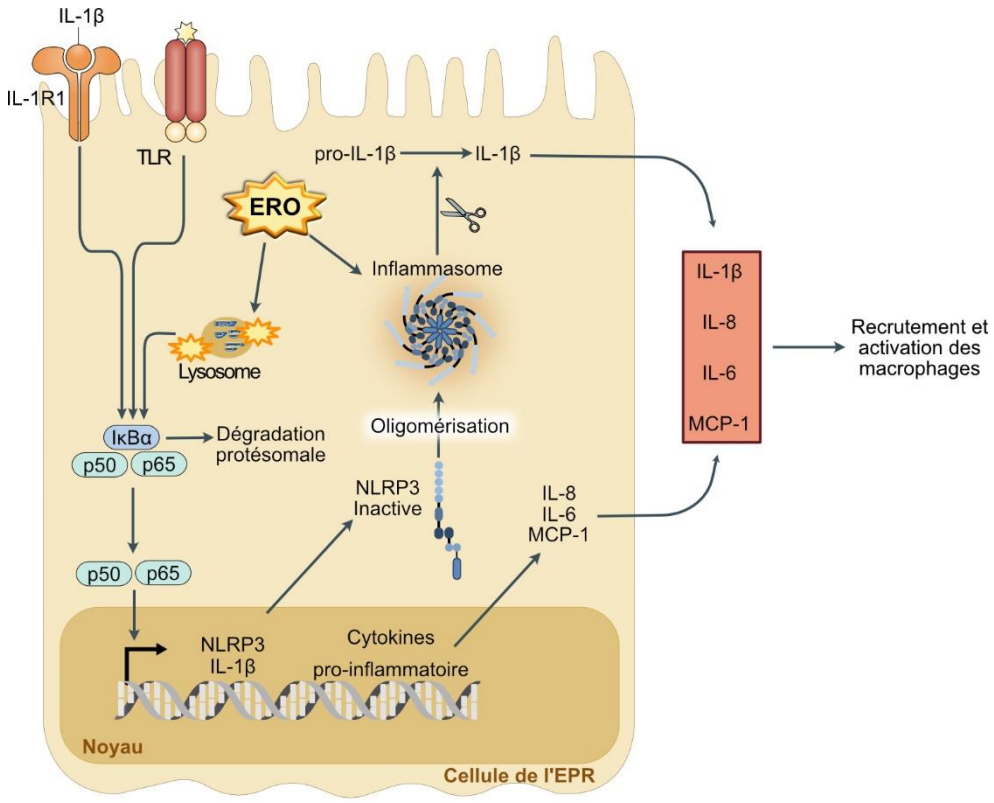

Figure 16. Représentation schématique de l'inflammation au sein des cellules de l'épithélium pigmentaire rétinien

L'IL-1β et les signaux de danger tels que les drusen vont être détectés par le récepteur IL-1β (IL-1R1) et les récepteurs Toll-like (TLR) présents au niveau de la membrane des cellules de l'épithélium pigmentaire rétinien (EPR). Cela va activer la dégradation d'IκBα induisant la libération de p65 et p50. Ces derniers vont activer la transcription de gènes pro-inflammatoire induisant l'activation de l'inflammasome ainsi que la sécrétion de cytokines pro-inflammatoires.

C.3. DMLA et angiogenèse

L'angiogenèse est le processus qui permet la **formation de nouveaux vaisseaux sanguins** à partir d'un réseau vasculaire préexistant (Adair and Montani, 2010; Folkman, 1971). L'angiogenèse est très présente au **stade embryonnaire** puis est **extrêmement régulée** et ne s'active que dans certains cas chez l'adulte. Une dysrégulation de ces mécanismes peut conduire à certaines pathologies telles que la DMLA. On distingue donc l'angiogenèse physiologique de l'angiogenèse pathologique. Dans le cas de la DMLA néovasculaire, l'angiogenèse se caractérise par le développement de **nouveaux vaisseaux sanguins**, issus de la choroïde, qui s'étendent vers la **rétine à travers la membrane de Bruch** (Green and Enger, 1993; Hammadi et al., 2023). Les néovaisseaux choroïdiens se forment comme des capillaires avec plusieurs points d'origine et peuvent entraîner des **brèches dans l'EPR** et des

accumulations de fluides. Ces accumulations vont désorganiser l'EPR et induire un décollement de la rétine (Chen et al., 2021). Dans les stades les plus avancés, les nouveaux vaisseaux peuvent induire des œdèmes ainsi que des hémorragies au niveau de la rétine.

La formation des nouveaux vaisseaux est induite par la libération de facteurs angiogéniques de la choroïde (Korb et al., 2023a). Ces facteurs angiogéniques vont **activer les cellules endothéliales** *via* des récepteurs membranaires, ce qui va déclencher des signaux intracellulaires induisant la migration ainsi que la différenciation de ces cellules (Carmeliet and Jain, 2011). L'origine exacte de ces signaux n'a pas été clairement identifiée, il semblerait que l'initiation de la maladie par un stress oxydant ainsi qu'une inflammation couplée à des facteurs génétiques et environnementaux participent au développement de la DMLA néovasculaire. Bien que son origine ne soit pas totalement élucidée, les médiateurs de l'angiogenèse sont clairement identifiés. Le facteur de croissance, **Vascular Endothelial Growth Factor** (VEGF) est le plus important et le plus étudié dans le processus de l'angiogenèse (Guillonneau et al., 2017).

C.3.1. Les médiateurs angiogéniques

C.3.1.1. Vascular Endothelial Growth Factor (VEGF)

Le VEGF est une glycoprotéine signalétique impliquée dans la vasculogenèse et l'angiogenèse. Son expression et sa sécrétion sont régulées par diverses voies de signalisations.

Le VEGF est impliqué dans la restauration de l'apport en oxygène des tissus, ainsi, il est très sensible à l'hypoxie. Lorsque les cellules manquent d'oxygènes, elles produisent un facteur, l'**hypoxia inducible factor** (HIF) qui va stimuler la transcription du VEGF (Ladoux and Frelin, 1993). Lors du vieillissement, la membrane de Bruch est altérée, elle s'épaissit, ce qui perturbe les échanges entre les cellules de l'EPR et la choroïde favorisant l'hypoxie et ainsi le VEGF (Rittié et al., 1999).

La famille du VEGF est composée de diverses isoformes générées par **épissage alternatif** (VEGF-A, VEGF-B, VEGF-C, VEGF-D, VEGF-E, VEGF-F et le *placental growth factor* (PGF). Ces **différentes isoformes peuvent se lier à trois récepteurs** à activité tyrosine kinase : VEGFR-1, VEGFR-2 et VEGFR-3.

C.3.1.2. Les récepteurs au VEGF

Le **VEGF récepteur 1** (VEGF-R1) possède une **forte affinité** pour le VEGF-A, B, F et le PIGF, cependant la **réponse** cellulaire suite à sa stimulation est **très faible** comparée à celle du VEGF-R2. Le VEGF-R1 peut aussi être **internalisé avec son ligand,** ce qui permet d'éviter la stimulation d'un autre récepteur (Boucher et al., 2017). Il semblerait que VEGF-R1 ait un rôle de **régulateur**. En effet, des études ont montré que les souris n'exprimant pas VEGF-R1 ne peuvent pas se développer correctement dû à une hypervascularisation. (Ho and Fong, 2015).

Le **VEGF récepteur 2** (VEGF-R2) peut se lier avec le VEGF-A, -C, -D, -E ainsi que le -F. Il semble que ce récepteur soit le **principal responsable des effets cellulaires du VEGF**. (Ferrara, 2004). L'activation de ce récepteur induit la **phosphorylation** de différentes tyrosines (en position 951, 1054/1059, 1175 ou 1214), impliquées dans plusieurs voies de signalisations et conduit donc à des réponses biologiques différentes impliquées dans la survie cellulaire, la migration, la prolifération cellulaire ainsi que la perméabilité cellulaire. De plus, son activation induit une cascade de signalisation (MAPK) régulant l'expression du gène VEGF-A et ainsi forme une boucle de rétrocontrôle positif.

Le **VEGF récepteur 3** (VEGF-R3) se lie aux VEGF-C et D. Ce récepteur est responsable de la lymphangiogenèse. (Como et al., 2023; Tammela et al., 2008). Principalement étudié en cancérologie, il a été montré que VEGF-C et D pouvaient faciliter la migration des cellules cancéreuses, néanmoins, les mécanismes moléculaires restent méconnus (Stacker et al., 2014). De plus, le rôle de VEGF-R3 n'a pas été démontré dans un contexte de DMLA.

C.3.1.3. Les ligands

VEGF-A

Le **VEGF-A** joue un rôle crucial dans l'angiogenèse pathologique. Il induit la **prolifération** des cellules endothéliales et facilite leur **migration**. De plus, il augmente la **perméabilité** des vaisseaux sanguins en provoquant une vasodilatation et une formation de fenêtres dans les capillaires (Esser et al., 1998). Le VEGF-A peut se lier aux récepteurs VEGF-R1 et -R2. Il existe 4 isoformes de ce ligand, VEGF-A121, 165, 189, 206 (Robinson and Stringer, 2001). Le VEGF-A 165 est la forme la plus abondante, on la retrouve dans tout l'organisme et dans les cellules de l'EPR (Ferrara, 2004; Ford et al., 2011).

Le VEGF-A est produit par les cellules de l'EPR (Nitzsche et al., 2022; Shibuya, 2001), il est impliqué dans les signaux paracrine entre l'EPR et la choroïde. En effet, il est impliqué dans la fenestration endothéliale (Zhao et al., 2023). La fenestration endothéliale est caractérisée par la présence de petites ouvertures, appelées fenêtres, dans l'endothélium qui tapisse les vaisseaux sanguins. Ces fenêtres permettent les échanges rapides de fluides et de molécules entre la choroïde et l'EPR (Zhao et al., 2023).

La sécrétion de VEGF-A par les cellules de l'EPR est polarisée. En conditions physiologiques (normoxiques), le VEGF-A sécrété est plus abondant au pôle basolatéral (du côté de la membrane de Bruch) comparé au pôle apical (de côté des photorécepteurs) (Blaauwgeers et al., 1999). Cette différence est amplifiée en cas d'**hypoxie** (Mammadzada et al., 2020). Cela soutient le fait que le VEGF-A joue un rôle prépondérant dans le développement de la DMLA néovasculaire. En effet, une surexpression du VEGF-A a été observée dans l'EPR et dans l'humeur aqueuse des yeux de patients atteints de DMLA comparé aux patients sains et aux patients atteints de DMLA précoce(Frank et al., 1996; Lopez et al., 1996; Vilkeviciute et al., 2022).

VEGF-B

Le **VEGF-B**, tout comme le VEGF-A, possède différentes **isoformes** (VEGF-B 167 et VGEF-B 186). Bien que ses effets restent mal connus, il semblerait qu'il ait un **rôle indirect** sur l'angiogenèse. Il permettrait de **saturer le VEGF-R1** afin de laisser la place au VEGF-A sur le récepteur 2 (VEGF-R2) (Zhang et al., 2009).

VEGF-C et VEGF-D

Le VEGF-C et -D sont dans un premier temps exprimés sous forme de **précurseurs protéiques**. Ils doivent subir une maturation protéolytique afin de pouvoir être excrétés et ainsi se fixer aux récepteurs VEGF-R2 et -R3 (Karkkainen et al., 2004). Il semblerait que leur action affecte principalement la **lymphangiogenèse** due à leur liaison avec le VEGF-R3. (Pazgal et al., 2007).

C.4. Angiogenèse et EPR

Les cellules de l'EPR vont jouer un rôle crucial dans l'angiogenèse. En effet, les cellules de l'EPR vont produire et sécréter du VEFG-A. A la suite d'un stress oxydant, l'augmentation des ERO intracellulaires va être corrélée à la phosphorylation de MEK. La phosphorylation de cette dernière va induire des cascades de signalisations dépendantes de cJUN et de ERK1/2 ce qui va induire la sécrétion de VEGF-A (Figure 17) (Courtaut et al., 2021a; Delmas et al., 2021; Sghaier et al., 2022). La liaison de VEGF-A avec son récepteur, le VEGF-R2 va induire un rétrocontrôle positif des voies de signalisations de MEK et de PI3K permettant ainsi la survie et la prolifération ainsi que la sécrétion de VEGF-A (Figure 17) (Courtaut et al., 2021a; Delmas et al., 2021; Sghaier et al., 2022). L'activation de ces voies va aussi induire la production de métalloprotéinase (MMP-2 et MMP-9) capable de digérer la membrane de Bruch (Hussain et al., 2011). *In fine*, la sécrétion de VEGF-A va induire la formation de nouveaux vaisseaux et ainsi la progression de la DMLA néovasculaire.

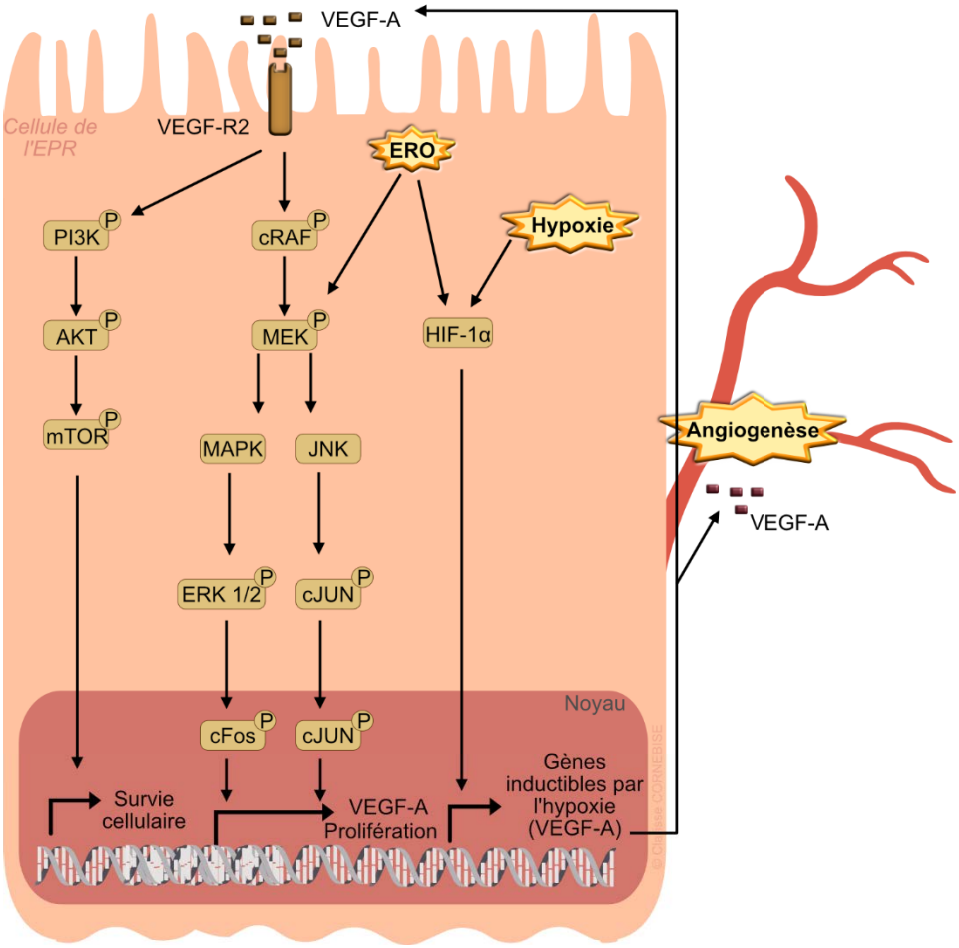

Figure 17. Représentation schématique de l'angiogenèse au sein des cellules de l'épithélium pigmentaire rétinien (EPR)

L'hypoxie ainsi que les espèces réactives de l'oxygène vont induire l'activation de gènes inductibles par l'hypoxie tels que le VEGF-A. De plus, la liaison du VEGF-A au récepteur VEGF-R2 va induire des cascades de phosphorylation induisant la survie ainsi que la prolifération cellulaire et la sécrétion de VEGF-A impliqué dans l'angiogenèse.

C.5. Le processus d'angiogenèse

Le processus d'angiogenèse commence par la formation du **bourgeonnement** des **cellules de front** (tip cells). Ces **cellules** vont bourgeonner à partir de vaisseaux existants et se diriger vers la source du signal angiogénique. De plus, les **cellules de soutien** (stalk cells) vont **proliférer** afin de permettre l'**allongement des vaisseaux** (Figure 18). Par ailleurs, les jonctions cellulaires sont réduites dues à l'internalisation de la cadhérine endothéliale permettant ainsi la migration des cellules. Le VEGF va aussi stimuler la prolifération cellulaire afin de former les nouveaux vaisseaux. Lorsque deux cellules de front se rejoignent, les **deux bourgeons**

fusionnent et ainsi forment un vaisseau connecté. *In fine*, la barrière endothéliale est rétablie grâce aux jonctions entre les cellules endothéliales (Figure 18).

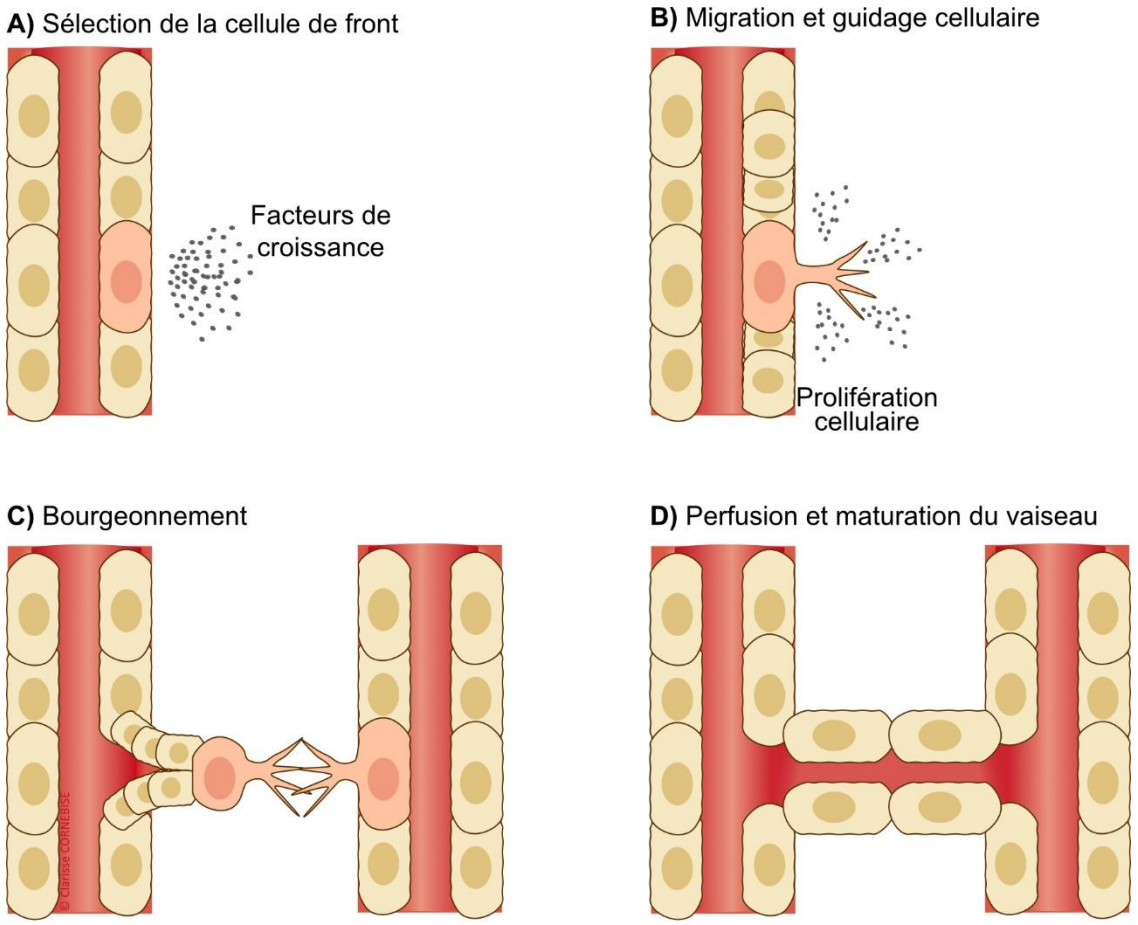

Figure 18. Schéma formation nouveau vaisseau

A) L'augmentation de la concentration intercellulaire de VEGF-A permet le recrutement de cellule de front. B) En réponse à la sécrétion de VEGF-A, les jonctions endothéliales de la cellule de front sont diminuées, elle acquiert un phénotype invasif. C) Les cellules de soutien prolifèrent et permettent la croissance des futurs bourgeons. D) La fusion des vacuoles endothéliale conduit à la formation de la lumière et permet la perfusion du nouveau vaisseau. Adapté de Treps and Gavard, 2015.

D. Traitements

D.1. Traitements curatifs

D.1.1. Injection d'anti-VEGF

Les injections d'anti-VEGF constituent le **traitement de première intention de la DMLA néovasculaire**. Les injections réalisées en intravitréenne permettent de délivrer des anticorps dirigés contre le VEGF impliqué dans la formation des néovaisseaux. Ces anticorps vont **bloquer le VEGF** et ainsi l'activation de leur récepteur inhibant ainsi la sécrétion de VEGF

conduisant in fine à **l'inhibition** du développement et de la progression des **néovaisseaux**. Il existe aujourd'hui trois traitements commercialisés, bévacizumab (ou Avastin®), ranibizumab (ou Lucentis®) et alfibercept (EYLEA®). Le **bévacizumab** est un **anticorps monoclonal** (149 kDa) qui a été **humanisé** et qui cible le **VEGF-A**. Le **ranibizumab** est quant à lui constitué de **fragments d'anticorps monoclonal humanisé** ce qui lui confère une taille plus petite (48 kDa) et ainsi une **meilleure pénétration** dans la rétine. L'**alfibercept** est composé de f**ragments de domaine extracellulaire du récepteur 1 et 2** du VEFG. Il va se lier au VEGF-A avec une affinité plus forte que les récepteurs naturels et ainsi réduire leur activation.

Les traitements avec ces molécules débutent généralement par **3 injections à 1 mois** d'intervalle puis d'autres doses sont administrées en fonction du protocole de traitement choisi par l'ophtalmologiste ainsi qu'en fonction de l'évolution de la maladie. Certaines études à grande échelle ont démontré que les injections d'anti-VEGF permettaient de **stabiliser l'acuité visuelle dans 60 % et de l'améliorer dans 30 % des cas.** (Leveziel et al., 2009). Cependant, certains patients **ne répondent pas ou peu** aux traitements ou bien montrent une diminution de l'efficacité des traitements. Il n'existe pas de définition précise pour diagnostiquer la résistance aux anti-VEGF. Néanmoins, de nombreux scientifiques déclarent que la **résistance** se traduit par la **persistance** d'un **exsudat** intra ou sous-rétinien à la suite de 3 injections et ce malgré une réponse positive observée lors des premières injections (Yang et al., 2016). Certaines études décrivent une tolérance (diminution de la réponse au traitement) aux injections d'anti-VEGF qui peut aussi apparaître dès les premières injections (tachyphylaxie). Une augmentation des doses administrées ainsi qu'une augmentation de la fréquence des injections est généralement proposée afin de contrer la diminution de l'efficacité lorsqu'une tolérance est observée. Un changement de traitement peut aussi être proposé afin d'alterner entre deux molécules différentes.

Des études cliniques ont montré que certains **polymorphismes de gènes** impliqués dans la survenue de la maladie (CFH et ARMS2) étaient corrélés à une mauvaise réponse aux traitements. Ainsi, une étude de la littérature réalisée par Chen, Yu et Xu a révélé que des patients portant les polymorphismes **Y402H ou Y1277C du gène CFH** présentent une réponse au ranibizymab et bevacizumab diminuée par rapport au patient portant le polymorphisme ancestral du gène (Chen et al., 2012). De plus, une étude clinique réalisée sur 156 patients atteints de DMLA néovasculaire traités au ranibizumab a montré que les patients portant le

polymorphisme **Y402H du CFH** avaient 37 % de risque de nécessité de plus d'injections que les patients ayant le polymorphisme ancestral (Lee et al., 2009). Une autre étude clinique réalisée sur 111 patients a confirmé ces résultats et étudié d'autres polymorphismes du gène. Ainsi, les polymorphismes **R102G** et **E318D** ont aussi été corrélés avec une diminution de l'efficacité des traitements (ranibizumab et bévacizumab) (Kubicka-Trząska et al., 2022). Ces études suggèrent que ces polymorphismes pourraient être utilisés afin d'adapter les stratégies de traitement, néanmoins, d'autres études plus approfondies sont nécessaires afin de valider ces diagnostics (Kozhevnikova et al., 2022).

Ces polymorphismes sont connus pour **altérer l'inflammation** chez les patients, ainsi, ils pourraient induire une inflammation chronique plus importante entrainant des dommages structurels permanents sur le réseau vasculaire (Kozhevnikova et al., 2022; Yang et al., 2016). De plus, un environnement pro-inflammatoire augmente le risque de fibrose qui agit comme une barrière et ainsi diminue la sensibilité des patients aux anti-VEGF (Yang et al., 2016). Des études portant sur les mécanismes moléculaires de résistance ont révélé que la neuropiline-1 (un corécepteur du VEGF) était surexprimée lors des traitements avec les anti-VEGF et était associée à une augmentation de la sécrétion de VEGF-A (Dumond et al., 2020; Lorés-Motta et al., 2016). De plus, il a été montré que des patients traités avec de l'alfibercept montraient une diminution de VEGF-A, mais une augmentation de PIGF (Zehetner et al., 2015). Ainsi, des systèmes compensatoires pourraient être à l'origine des résistances aux traitements par anti-VEGF. Cependant, ces mécanismes restent encore mal connus et des études complémentaires sont nécessaires afin d'approfondir nos connaissance sur ces mécanismes (Sharma et al., 2023).

D.1.2. Photocoagulation

La **photocoagulation au laser thermique** est la technique la plus ancienne, elle a été pendant longtemps le seul recours face à la DMLA néovasculaire. Ce traitement n'est effectif que dans les cas de DMLA néovasculaire, il consiste à produire une **brûlure thérapeutique** dans une zone précise afin de **stopper les saignements** et de **limiter la croissance des néovaisseaux**. Ce traitement impacte non seulement les néovaisseaux, mais aussi l'EPR et le reste de la rétine produisant un scotome irréversible. Il n'est donc utilisé qu'en dernier recours pour traiter la DMLA néovasculaire extrafovéolaire. Il reste cependant utilisé dans les formes très avancées de DMLA présentant des résistances au traitement anti-VEGF.

D.2. Traitements préventifs

D.2.1. Suppléments alimentaires

Des études à grande échelle (Age-related disease study, **AREDS**) ont mis en évidence les **bénéfices d'une supplémentation** en vitamines et minéraux dans le cadre de la prévention de la DMLA avec une **réduction de 25 %** du risque de bi-latérisation à cinq ans (Age-Related Eye Disease Study Research Group, 2001). Suite à ces études, la Haute Autorité de Santé (HAS) recommande une supplémentation alimentaire en anti-oxydants (vitamines C & E, β carotène, lutéine, zéaxanthine), oligo-éléments (zinc, cuivre) et des oméga-3 dans les cas de DMLA uni-latérale afin de prévenir l'atteinte du deuxième œil. Ainsi, une supplémentation de molécules anti-oxydantes et oméga-3 semble être un axe de recherche prometteur pour prévenir l'apparition de la maladie.

Ces études ont ouvert la voie à de nombreuses recherches sur le rôle de l'alimentation et notamment sur les molécules anti-oxydantes dans la prévention de la maladie. Parmi ces **molécules anti-oxydantes**, **les polyphénols** connus pour leurs multiples actions biologiques semblent être de bons candidats. En effet, les polyphénols ont été connus à la suite de la découverte du « *French paradoxe* » qui faisait l'observation d'une faible incidence des maladies cardiovasculaires chez les Français. L'hypothèse principale du paradoxe suggère que la consommation de vin rouge était bénéfique en raison de sa forte teneur en resvératrol (Jeandet et al., 1993).

D.2.2. Le resvératrol

Le **resvératrol** (RSV) est l'un des polyphénols les plus emblématiques dans le domaine de la santé. Très largement étudiés, les bienfaits du resvératrol ont été démontrés dans diverses maladies telles que les maladies oculaires (Delmas et al., 2021). En raison de son pouvoir anti-oxydant, le RSV pourrait protéger les tissus oculaires contre le stress oxydatif de la même manière que les anti-oxydants présents dans les fruits et légumes (vitamines C, E et caroténoïdes) pour lesquels des études ont démontré que leur consommation pouvait retarder ou empêcher le développement de maladies rétiniennes (Age-Related Eye Disease Study Research Group, 2001). Il a été démontré, *in vitro*, que le RSV pouvait protéger les cellules de

l'EPR (ARPE-19) contre les effets néfastes d'un inducteur du stress oxydant, l'H_2O_2 (King et al., 2005). En effet, le RSV, peut non seulement **piéger les radicaux libres** des espèces réactives de l'oxygène (ERO) (Leonard et al., 2003), mais aussi **moduler,** de manière dose dépendante**, l'activité d'enzymes anti-oxydantes** telles que le superoxyde dismutase (SOD), le glutathion peroxydase (GPx) et la catalase (Yang et al., 2019). Par ailleurs, le RSV est aussi capable **d'augmenter l'activité** bioénergétique **mitochondriale** (Neal et al., 2020). La régulation positive de ces enzymes permet l'élimination des espèces réactives de l'oxygène (ERO) et ainsi protège les cellules des dommages oxydatifs et de l'apoptose (Figure 19). En effet, différentes études réalisées *in vitro*, dans des cellules de l'EPR (ARPE-19) ont démontré que les RSV avaient un effet anti-oxydant sur les cellules de l'EPR lors d'une induction de stress oxydant par divers facteurs **H_2O_2** (King et al., 2005) , **UV** (Chan et al., 2015), **pollution** et **fumée de cigarette** (Kode et al., 2008). Le RSV peut activer **Nrf2** permettant ainsi d'augmenter les enzymes anti-oxydantes présentes dans les mitochondries. De plus, ces études ont aussi montré que le RSV pouvait réguler positivement **Sirt1** et ainsi augmenter l'activité mitochondriale (Zhou et al., 2021).

Par ailleurs, le RSV est aussi connu pour son activité **anti-inflammatoire**. Tout d'abord, grâce à son activité anti-oxydante, le RSV peut **diminuer la sécrétion de cytokines pro-inflammatoires** telles que l'IL-8 et l'IL-6 induites lors d'un stress oxydant. (Bhattarai et al., 2020; Neal et al., 2020). Le RSV peut aussi réguler des facteurs moléculaires clés de l'inflammation impliqués dans de nombreuses voies de signalisation régulant la réponse inflammatoire (Figure 19). Ces données mettent en évidence que le RSV pourrait être utilisé pour prévenir les stades précoces de la maladie en limitant le stress oxydant et l'inflammation impliqués dans l'initiation de la DMLA. De plus, le RSV est aussi connu pour ses effets anti-angiogéniques, ces effets ont notamment été démontrés dans un modèle murin d'angiogenèse choroïdienne induite par impact laser (Courtaut et al., 2021a).

L'ensemble de ces études met en lumière les effets bénéfiques que pourrait avoir l'apport de resvératrol chez les patients. Bien que le resvératrol soit l'un des polyphénols les plus étudiés, il n'est pas le seul présentant des effets bénéfiques. En effet, les polyphénols forment une grande famille de molécules, l'étude de ces diverses molécules semble être prometteur dans le cadre de la santé et notamment dans le contexte de la DMLA.

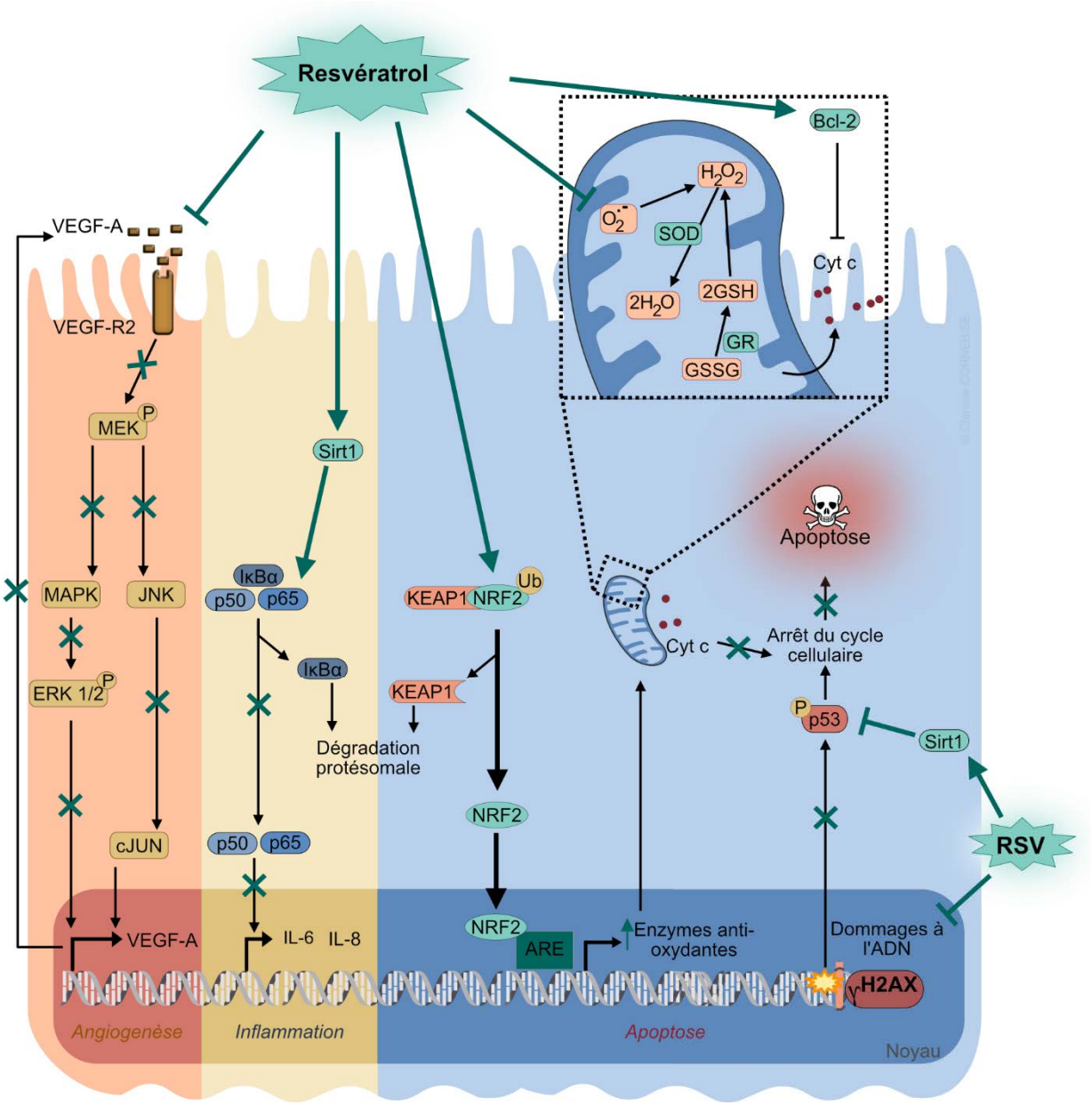

Figure 19. Effets du resvératrol dans un contexte de dégénérescence maculaire liée à l'âge (DMLA) néovasculaire.

Le resvératrol pourrait prévenir le stress oxydatif impliqué dans le développement et la progression de la maladie. Divers facteurs environnementaux produisent des radicaux libres, entraînant un stress oxydatif dans les tissus oculaires et provoquant par conséquent l'apparition de maladies telles que la DMLA. D'une part, le RSV est capable de piéger les radicaux libres ($O2^{-}$) et d'activer le superoxyde dismutase (SOD) ou le glutathion réductase (GR), d'autre part, il inhibe l'inflammation par la réduction de diverses cytokines pro-inflammatoires et bloque la voie de signalisation induite par le facteur de croissance de l'endothélium vasculaire-A (VEGF-A) laquelle joue un rôle majeur dans l'angiogenèse (adapté de Delmas et al., 2021).

E. Polyphénol de la vigne et du vin & DMLA

Les polyphénols sont une grande famille de molécules organiques produites par de nombreuses plantes en réponse à un **stress biotique ou abiotique** (Ahuja et al., 2012; Serag et al., 2023). Étudié dans un premier temps en biologie végétale, l'intérêt des polyphénols a surtout porté sur leurs activités **antifongiques**. Les polyphénols ont généré beaucoup d'engouement pendant les années 90 à la suite du postulat « *French paradox* ». Depuis ce jour, les polyphénols suscitent beaucoup d'intérêt dans le domaine de la santé. Certaines études ont démontré que le vin rouge contenait non seulement une quantité importante de resvératrol (Tableau 3), mais aussi une grande variété de composés phénoliques qui pourraient eux aussi avoir un effet bénéfique sur la santé et notamment sur la DMLA.

Tableau 3. Concentration en resvératrol dans divers aliments. Adapté de (Delmas et al., 2021; Weiskirchen and Weiskirchen, 2016)

Aliments	***Quantité en resvératrol***	***Référence***
Vin rouge	0,362-1,979 mg/L	(Jeandet et al., 1993)
Pomme	400 µg/Kg	(Farneti et al., 2015)
Vin blanc	0,057-0,390 mg/L	(Romero-Pérez et al., 1996)
Chocolat noir	350 µg/Kg	(Hurst et al., 2008)
Peau du raisin	27,5 µg/g	(Careri et al., 2003)
Cacahuète	0,03-0,14 µg/g	(Sanders et al., 2000)
Myrtille	0,03 µg/g	(Lyons et al., 2003)

E.1. Structure chimique

Les polyphénols possèdent une **structure commune** composée d'un **noyau aromatique** avec un ou plusieurs groupements hydroxyles (Pietta et al., 2003). Les variations de leurs squelettes chimiques ont permis de les classifier en différentes classes comprenant les non-flavonoïdes et les flavonoïdes. Ces derniers sont divisés en plusieurs sous-classes comprenant les

stilbenoïdes, les lignanes, les tanins, les diarylheptanoïdes, les amides polyphénoliques, les anthraquinones (Rambaran, 2020).

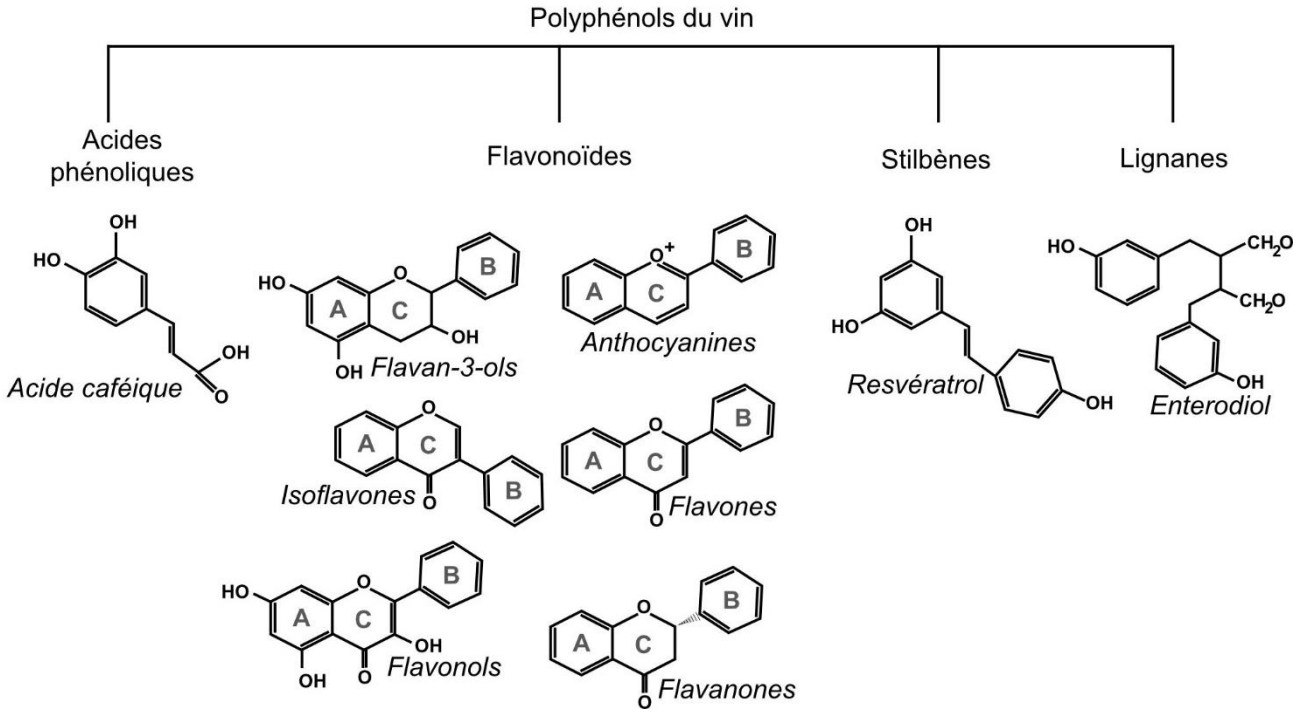

Figure 20. Structure chimique des polyphénols du vin

Les polyphénols du vin se divisent en quatre classes : les acides phénoliques, les flavonoïdes, les lignanes et les stilbènes. Adapté de Delmas et al., 2021.

E.1.1. Les non-flavonoïdes

Les **acides phénoliques** sont composés d'un **cycle aromatique** possédant au moins une fonction carboxylique et un hydroxyle phénolique. Les principaux acides phénoliques retrouvés dans le vin sont les acides galliques, caféiques, acide férulique.

Les **stilbènes,** dont le plus connu reste le resvératrol, se caractérisent par **deux cycles aromatiques** reliés entre eux par un **pont d'éthylène**. Principalement présent dans la **pellicule** des raisins, il a été observé que les **formes *trans*** étaient majoritaires par rapport aux formes *cis*. Les stilbènes sont synthétisés par les plantes lors d'un stress biotique ou abiotique, ils font partie des phytoalexines (Parage et al., 2012).

E.1.2. Les flavonoïdes

Les flavonoïdes sont les polyphénols les plus abondants dans le règne végétal (Manach et al., 2004). Ils sont composés de **deux cycles aromatiques** (A et B) reliés par un **hétérocycle** (C).

Les flavonoïdes sont subdivisés en différents groupes en fonction de l'état d'oxydation de l'hétérocycle comprenant les flavanols, les anthocyanes, les flavonones, les flavonols ainsi que les flavones et isoflavones :

Les **flavanols ou flavan-3-ols** se caractérisent par une hydroxylation sur l'hétérocycle. Ils se déclinent ensuite en différents degrés d'hydroxylation sur les deux cycles aromatiques. Présents sous forme de monomère, les flavanols peuvent aussi former des oligomères ou des polymères pour former des tanins condensés ou des proanthocyanidines. Les flavan-3-ols les plus répandus sont les dérivés de la catéchine et de l'épicatéchine. On les retrouve principalement dans les pépins ainsi que dans la peau des raisins, et sont responsables de la sensation d'astringence lors de leur interaction avec la salive (Aron and Kennedy, 2008).

Les **anthocyanes** sont des hétérosides d'anthocyanidines. Ils présentent différents nombres d'hydroxyles et de méthoxyles. Les glycosides de la malvidine sont les anthocyanes les plus répandues dans les raisins rouges et leurs dérivés (vin rouge). On retrouve les anthocynes uniquement dans la peau des raisins et ils sont responsables de leur couleur (He and Giusti, 2010).

Les **flavanones** se caractérisent par un **hétérocycle saturé** et sont différenciés grâce au nombre ainsi qu'à la position des groupements hydroxyles et méthoxy (Gopinath et al., 2018).

Les **flavonols** se caractérisent par un **groupe hydroxyle ainsi qu'une insaturation sur l'hétérocycle**. Ils sont présents au niveau de la peau du raisin. Bien que la quantité de flavonols soit moindre que celle d'anthocynes, les flavonols sont les phénols les plus présents dans la pellicule du raisin (Gopinath et al., 2018)..

Les **flavones** se caractérisent par un **hétérocycle insaturé et** ne possèdent pas de groupe hydroxyle (Gopinath et al., 2018)..

Les **isoflavones** sont des **isomères des flavones**. Comme ces derniers, les isoflavones possèdent un cycle aromatique (B) relié à un hétérocycle (C). Cependant, l'hétérocycle est relié au second cycle aromatique (A) en position 2 et non en **position 3** (Li et al., 2023).

E.2. Les polyphénols du vin rouge et santé

Dans le **domaine de la santé**, le vin rouge est surtout connu pour ses fortes teneurs en **resvératrol** qui est le polyphénol le plus emblématique. Il est vrai que le vin rouge contient une grande quantité de ce polyphénol. Cependant, ce n'est pas le seul polyphénol présent. En

effet, les vins rouges possèdent une **grande variété** de composés phénoliques et ce plus que d'autres boissons telles que le jus de raisin. La **vinification** joue un rôle très important dans la composition du vin rouge. Si l'on compare la composition du vin rouge avec un jus de raisin, on constate que le **vin possède davantage de composés phénoliques** que les autres produits dérivés du raisin (Manach et al., 2004).

Les polyphénols sont principalement localisés dans la **peau et les pépins du raisin**, ainsi, lors de la vinification, les composés phénoliques sont extraits. Il est aussi important de noter que la qualité et la quantité de polyphénols dans le vin rouge dépendent des cépages, du type de raisin et du temps de conservation. La variabilité de la composition des vins rouges rend plus difficile la généralisation des études concernant leurs effets bénéfiques sur la santé. Certaines études permettent néanmoins d'avoir une idée globale de la composition de différents vins rouges. Bien que les études actuelles se soient principalement focalisées sur le resvératrol (voir partie D.2), de nombreux autres composés phénoliques du vin rouge possèdent eux aussi des effets bénéfiques.

E.3. Extrait sec de vin rouge enrichi en polyphénols

Les études antérieures de notre équipe ont montré qu'un **extrait sec de vin rouge** (*red wine extract,* RWE) enrichi en polyphénols peut agir sur l'**inflammation** en réduisant la sécrétion de certaines cytokines pro-inflammatoires produites par les cellules immunitaires (Chalons et al., 2020), ainsi qu'en atténuant la formation d'un complexe inflammatoire dans les macrophages tels que NLRP3 (NOD-like receptor family, pyrin domain-containing 3) (Chalons et al., 2018). Ces effets ont été confirmés par d'autres études, où le RWE a démontré sa capacité à **réduire la croissance tumorale** de cellules cancéreuses CT26 chez les souris BALB/c ainsi que l'expression du facteur de croissance endothélial vasculaire (VEGF) (Walter et al., 2010). Ce facteur est non seulement essentiel pour la néo-angiogenèse, impliqué dans la croissance tumorale ainsi que dans la propagation des cellules métastatiques, mais est également impliqué dans d'autres pathologies telles que la dégénérescence maculaire liée à l'âge (DMLA).

Les effets bénéfiques d'une alimentation riche en polyphénols ont été démontrés dans diverses pathologies y compris dans les maladies oculaires telles que la DMLA (Delmas et al., 2021; Gopinath et al., 2018) (Tableau 4).

E.3.1. Effet anti-oxydant des polyphénols du vin rouge

L'effet santé le plus connu des polyphénols reste leur pouvoir **anti-oxydant**. De nombreuses études ont montré les effets bénéfiques de divers polyphénols contre le stress oxydant (Tableau 4). Ces études ont, dans un premier temps, montré *in vitro* sur des cellules humaines de l'EPR (ARPE-19) que différents polyphénols (acide caféique, cyanidine, malvidine, resvératrol, epicatéchine, querctine, piceaténol, delphidine,…) avaient un effet protecteur en **augmentant la survie cellulaire** lors d'une induction du stress oxydant par divers stimuli (H_2O_2, lumière bleue, iodate de sodium, fumée de cigarette, nicotine ; voir Tableau 4). De plus, ces études ont montré que cette survie était accompagnée d'une **diminution des ERO intracellulaires**. Certaines études ont aussi permis d'approfondir les mécanismes d'action des polyphénols. En effet, certains polyphénols (acide caféique, delphinidine, malvidine, viniférine, tableau 4) peuvent **augmenter l'activité des enzymes anti-oxydantes** (catalase, superoxyde dismutase) lors d'un stress oxydant provoqué par (H_2O_2, lumière bleue, tableau 4). L'augmentation de l'activité enzymatique pourrait être expliquée par l'augmentation de **Nrf2**. En effet, il a été montré *in vitro* que la quercétine, le piceatannol et la delphidine pouvaient augmenter l'expression protéique de NRF2 à la suite d'un stress oxydant (H_2O_2 ou fumée de cigarette, voir tableau 4).

L'effet anti-oxydant des polyphénols du vin a été confirmé dans quelques études *in vivo*. En effet, il a été montré que l'épicatéchine pouvait **réduire les pertes mitochondriales** induites par l'iodate de sodium (40 mg/Kg) dans des souris C57BL/6 (Peng et al., 2022; tableau 4). Par ailleurs, la quercétine permet aussi **d'augmenter l'activité enzymatique** de la SOD, de la catalase et de la GSH dans des rétines de souris Balb/C traitées avec de l'iodate de sodium (40 mg/Kg ; Hsu et al., 2021, 2021; tableau 4).

E.3.2. Effet anti-inflammatoire des polyphénols du vin rouge

Le stress oxydant et l'inflammation sont deux processus intrinsèquement liés dans la progression de la DMLA. En effet, l'induction d'un stress oxydant *in vitro* dans différents modèles cellulaires (cellules de l'EPR de singe, hESC-EPR, ARPE-19, voire tableau 4) et différents inducteurs (H_2O_2, lumière bleue, fumée de cigarette, voire tableau 4) provoquent une augmentation de la sécrétion de **cytokines pro-inflammatoire** (IL-6, IL-8, IL-1β, TNF-α,

MCP-1) ainsi que l'augmentation de leur expression ARNm. Certaines études ont montré que plusieurs polyphénols (acide gallique, quercétine, cyanidine, viniférine) étaient capables de réduire l'expression d'ARNm ainsi que la sécrétion de ces cytokines et ainsi **réduire l'inflammation induite par stress oxydant** (Tableau 4).

Afin de comprendre les mécanismes moléculaires impliqués dans la diminution de la sécrétion de cytokines pro-inflammatoires, certaines études *in vitro* ont montré que certains polyphénols (viniférine, acide gallique, cyanidine, tableau 4) pouvaient diminuer l'expression de l'ARNm de **Nf-κB** et de **NLRP-3**. Néanmoins, d'autres études seraient nécessaires pour approfondir les mécanismes moléculaires impliqués dans cette réduction de l'inflammation.

E.3.3. Effet anti-angiogénique des polyphénols du vin rouge

En supplément de leurs effets anti-oxydants et anti-inflammatoires, les polyphénols sont aussi connus pour leurs effets **anti-angiogénique** dans diverses pathologies telles que le cancer (Bhosale et al., 2020). Dans le contexte de la DMLA, il a été montré que les polyphénols pouvaient réduire la néo-angiogenèse induite dans la rétine (Tableau 4). En effet, *in vivo*, il a été montré que l'acide caféique, la quercétine et un extrait contenant de la viniférine et de l'acide gallique permettaient de prévenir la dégénérescence induite dans la rétine de modèles murins (tableau 4). Kim *et al* ont montré que l'acide gallique pouvait **réduire l'angiogenèse** induite par hypoxie dans des souris C57BL/6 (tableau 4). Du point de vue moléculaire, de nombreuses études ont permis de montrer que plusieurs polyphénols (acide caféique, quercétine, extrait contenant de la viniférine et de l'acide gallique) pouvaient diminuer la sécrétion ainsi que l'expression d'ARNm du **VEGF-A** dans des cellules de l'EPR traitées avec des molécules pro-oxydantes (H_2O_2, lumière bleue) ou avec du VEGF recombinant (tableau 4). Les études de Lee *et al.* ont permis de montrer *in vitro*, que la quercétine pouvait diminuer l'expression de protéique de **VEGF-R2** et ainsi diminuer la sécrétion de VEGF-A dans des cellules dérivées de photorécepteurs traitées avec du VEGF recombinant (tableau 4). De plus, Shanmuganathan et Angayarkanni ont montré que l'acide gallique pouvait diminuer l'expression de **ERK** et de **p38** impliqués dans l'angiogenèse.

Ainsi, l'ensemble de ces études *in vitro* et *in vivo* suggèrent que les polyphénols pourraient être utilisés afin de prévenir ou de ralentir la survenue de la maladie ainsi que de ralentir sa

progression. Néanmoins, des études complémentaires sont nécessaires afin d'élargir ces connaissances sur les mécanismes moléculaires régulés par les polyphénols.

Tableau 4. Effets des polyphénols de la vigne et du vin dans des modèles *in vivo* et *in vitro* de dégénérescence maculaire liée à l'âge.

Composé phénolique	***Espèce***	***Model***	***Effets***	***Référence***
Acide gallique	Singe et poulet	*In vitro* : RF/6A (Cellules endothéliales choroïdiennes rétiniennes de singe) (dérivé de sérum 16 h, acide gallique 50-100 µM & TNFα ; 5 ng/mL ; 48 h) *Ex vivo* : embryon de poule (acide gallique ; 25 µM et TNF-α ; 20 ng ; 6h)	*In vitro* : • Diminution de la sécrétion de TNF-α, d'IL-6, d'IL-8 et de MCP-1. *Ex vivo :* • Diminution de l'angiogenèse	(Shanmuganathan and Angayarkanni, 2018)
Acide caféique (dérivé nitré)	Homme	*In vitro* : ARPE-19 (lignée cellulaire de l'épithélium pigmentaire rétinien humain) (acide caféique (dérivé nitré) ; 1-100 µM & H_2O_2, 2 mM ; 2 h)	*In vitro* : • Diminution d'ERO intracellulaires • Augmentation de la survie cellulaire • Augmentation de l'activité de l'hème oxygénase.	(Pittalà et al., 2017)
Acide caféique (Ester phénéthylique)	Homme	*In vitro* : ARPE-19 (Acide caféique (Ester phénéthylique) ; 5-30 µM ; 24 h puis H_2O_2, 600 µM ; 16 h)	*In vitro* : • Diminution de l'expression d'ARNm et de la sécrétion de VEGF-A	(Dinc et al., 2017)
Acide caféique	Homme, Souris	*In vitro* : Cellules endothéliales	*In vitro* :	(Kim et al., 2009)

		microvasculaires de la rétine humaine (HRMEC) (acide caféique ; 100 µM puis VEGF recombinant ; 20 ng/mL ; 24 h ou H_2O_2 ; 100 nM ; 12 h) *In vivo :* Souris C57BL/6, (néovascularisation de la rétine induite par hypoxie ; 5 jours puis injection intravitréenne d'acide caféique (100 µM)	• Diminution de la sécrétion de VEGF-A • Diminution de la migration cellulaire. • Diminution des ERO intracellulaires *In vivo :* • Diminution de la néovascularisation	
cyanidine, delphinidine, malvidine, trans-resvératrol, et procyanidine B2 (extrait polyphénolique de myrtille)	Homme	*In vitro* : ARPE-19 (extrait ; 30 µg/mL & exposées à la lumière bleue (470 nm ; 500 lumens) durant 24 h	*In vitro* : • Diminution de l'apoptose • Diminution des ERO intracellulaire	(Ogawa et al., 2023)
Epicatechine	Souris	*In vivo :* Souris C57BL/6 (supplémentation orale épicatechine (100 mg/Kg/jour ; gavage) et iodate de sodium (40 mg/Kg) durant 7 jour	*In vivo :* • Protection de la dégénérescence rétinienne • Réduction des drusen • Prévention partielle des fonctions visuelles • Réduction des pertes mitochondriales	(Peng et al., 2022)

Epicatechine	Homme, rat	*In vitro* : ARPE-19 et R28 (cellule précurseur de la rétine de rat) (épicatéchine ; 5 µM ; 1h puis 7-cétocholestérol ; 30 µg/mL ; 24h supplémentaires.	*In vitro* : • Diminution de l'apoptose sur les ARPE-19 • Pas d'effets sur l'apoptose des cellules R28.	(Neekhra et al., 2020)
Epicatechine	Homme	*In vitro* : ARPE-19, cellules endothéliales microvasculaires humaines (HMVEC) et R28 (épicatéchine ; 5 - 10 µM ; 4h puis nicotine ; 0,1-10 mM ; 24h)	*In vitro* : • Diminution de l'apoptose.	(Patil et al., 2009)
Quercétine	Homme	*In vitro* : Cellules embryonnaires humaines dérivées en cellule de l'EPR (hESC-RPE) (quercétine ; 5 µM et H_2O_2; 200 µM ; 2 h.	*In vitro* : • Diminution de l'expression d'ARNm d'IL-6 et TGF-β	(Gao et al., 2022)
Quercétine	Homme, Souris	*In vitro* : ARPE-19 (quercétine ; 1,25 à 5 µM ; 1h30 puis iodate de sodium ; 3 mM ; 15 h) *In vivo :* Souris BALB/c (iodate de sodium ; 40 mg/Kg et quercétine ; 100 mg/Kg ; une seule injection intraveinneuse)	*In vitro* : • Diminution de l'apoptose. • Diminution des ERO intracellulaires *In vivo :* • Protection de la dégénérescence rétinienne • Augmentation de l'activité enzymatique de SOD, catalase et GSH	(Hsu et al., 2021)

Quercétine	Homme	*In vitro* : ARPE-19 (quercétine ; 1-100 nM et fumée de cigarette ;4 % ; 24 h.	*In vitro* : • Diminution de l'apoptose. • Diminution de la sécrétion d'IL-1β, IL-6, IL-8, MCP-1 • Augmentation de l'expression protéique de Nrf2 et KEAP1	(Zhu et al., 2019)
Quercétine		*In vitro* : Cellules 661W dérivées de photorécepteurs coniques de souris (quercétine ; 100 nM et VEGF recombinant ; 20 ng ; 16h)	*In vitro* : • Diminution de l'expression de protéine impliquée dans les voies de signalisation de Nf-κB, du récepteur VEGF -R2	(Lee et al., 2017)
Quercétine	Homme	*In vitro* : ARPE-19 (quercétine ; 20 μM et H_2O_2 ; 300 μM ; 24h)	*In vitro* : • Diminution de l'apoptose • Diminution d'ERO intracellulaire • Augmentation de l'expression protéique de Nrf2	(Weng et al., 2017)
Quercétine	Homme	*Ex vivo :* Cellules de l'EPR obtenues de donneurs post-mortem (quercétine 100 μM ; hyperosmolarité)	*Ex vivo :* • Diminution du stress oxydatif	(Veltmann et al., 2016)
Piceatanol	Homme	*In vitro* : ARPE-19 (piceatanol ; 5-15 μM ; 24h puis H_2O_2 ; 300 μM ; 24 h)	*In vitro* : • Diminution de l'apoptose • Augmentation de l'expression	(Hao et al., 2019)

			protéique d'enzymes anti-oxydantes • Augmentation de l'expression protéique de Nrf2 et Keap1	
Piceatanol, resvératrol et lutéine	Homme	*In vitro* : ARPE-19 (A2E ;20 µM durant 7 jours ; à J3 et J10 : piceatanol (3,75-60 µM) ou resveratrol (3,75-60 µM) ou lutéine (30 µM) et à j11 : lumière bleue ; 430 nm ; 4,02 J/cm² ; 7 min)	*In vitro* : • Diminution de l'apoptose • Diminution du stress oxydant	(Kang and Choung, 2016)
Delphindine	Homme	*In vitro* : ARPE-19 (Delphinidine 25-100 µG et H_2O_2 500 µM ; 4 h)	*In vitro* : • Diminution de l'apoptose • Diminution d'ERO intracellulaire • Augmentation de l'activité enzymatique de SOD, catalase, GSH • Augmentation de l'expression nucléaire de Nrf2	(Ni et al., 2019)
Delphindine, cyanidine ou lutein	Homme	*In vitro* : ARPE-19 (5µM de delphinidine, cyanidine ou lutéine ; 60 min puis lumière bleue ; 90 s ; 312 nm ; 5,8 W/m)	*In vitro* : • Diminution de l'apoptose • Diminution d'ERO intracellulaire	(Silván et al., 2016)

Cyanidine 3-glucoside	Homme	*In vitro* : ARPE-19 (cyanidine-3-glucoside ; 10-100 μM ; 2h puis 4-hydroxyhexenal ; 50 μM ; 24 h)	*In vitro* : • Diminution de l'apoptose • Diminution de la sécrétion d'IL-1β • Diminution de l'expression d'ARNm d'IL-1β, NLRP3 et caspase 1	(Jin et al., 2018)
Malvidin, Malvidin-3-glucoside et Malvidin-3-6-O-glucoside	Homme	*In vitro* : ARPE-19 (H_2O_2)	*In vitro* : • Diminution d'ERO intracellulaire • Augmentation de l'activité enzymatique de SOD	(Liu et al., 2021)
Dipterocarpus tuberculatus extract contenant notamment ε-viniférine et l'acide gallique	Human Souris	*In vitro* : ARPE-19 (extrait ; 50-200 μg/mL ; 24h puis A2E ; 20 μM ; 24 h & lumière bleue ; 430 nm ; 6000 Lux ; 10 min) *In vivo :* Souris Balb/c (extrait ; 100-200 mg/Kg/jour ; administration oral durant 4 jours et lumière bleue ; 2 h)	*In vitro* : • Diminution d'ERO intracellulaire • Augmentation de l'activité de SOD. • Augmentation de la survie cellulaire • Diminution de l'expression des MMP-2 et -9et de l'expression de VEGF et NLRP3 • Diminution de l'expression d'ARNm de TNF-a, IL-1β, IL-6 et NF-kB. *In vivo :* • Protection de la dégénérescence	(Lee et al., 2023)

induite sur la rétine.

International Journal of
Molecular Sciences

MDPI

Review

New Highlights of Resveratrol : A Review of Properties against Ocular Diseases

Dominique Delmas [1,2,3,*], Clarisse Cornebise [1,2], Flavie Courtaut [1,2], Jianbo Xiao [4,5,6] and Virginie Aires [1,2]

1 Université de Bourgogne Franche-Comté, F-21000 Dijon, France; clarisse.cornebise@gmail.com (C.C.); flavie.courtaut@gmail.com (F.C.); virginie.aires02@u-bourgogne.fr (V.A.)
2 INSERM Research Center U1231, Cancer and Adaptive Immune Response Team, Bioactive Molecules and Health Research Group, F-21000 Dijon, France
3 Centre anticancéreux Georges François Leclerc, F-21000 Dijon, France
4 Nutrition and Bromatology Group, Department of Analytical Chemistry and Food Science, Faculty of Food Science and Technology, University of Vigo-Ourense Campus, E-32004 Ourense, Spain; jianboxiao@yahoo.com
5 College of Food Science and Technology, Guangdong Ocean University, Zhanjiang 524088, China
6 International Research Center for Food Nutrition and Safety, Jiangsu University, Zhenjiang 212013, China
* Correspondence: dominique.delmas@u-bourgogne.fr; Tel.: +33-380-39-32-26

Résumé : Les maladies oculaires constituent actuellement un problème majeur de santé publique en raison du vieillissement de la population ainsi que des nouveaux modes de vie. Ainsi, de nouvelles stratégies de traitement ont été développées ces dernières décennies avec notamment des injections intraoculaires d'anticorps monoclonaux. Les études portant sur la prévention des maladies oculaires ont permis de souligner l'importance du régime alimentaire dans la survenue de ces maladies. Récemment, des molécules anti-oxydantes telles que le resvératrol ont fait l'objet d'une grande attention en tant qu'outils potentiels contre diverses maladies oculaires. Dans cette revue, nous nous concentrons sur les mécanismes du resvératrol contre les maladies oculaires, en particulier la dégénérescence maculaire liée à l'âge (DMLA), le glaucome, la cataracte, la rétinopathie diabétique et la vitréorétinopathie. Nous analysons, en relation avec les différentes étapes de chaque maladie, les propriétés du resvératrol à de multiples niveaux, tels que la signalisation cellulaire et moléculaire ainsi que les effets physiologiques. Nous montrons et discutons des effets du resvératrol sur les espèces réactives de l'oxygène, la régulation des processus inflammatoires, ainsi que de son rôle dans la prévention de ces maladies grâce à une action épigénétique potentielle par l'activation de la sirtuine-1. Enfin, quelques essais cliniques permettent d'approfondir les connaissances sur les différents modes d'administration du resvératrol chez l'homme. Cette revue permet de mettre en lumière le rôle que pourrait avoir le resvératrol dans la prévention des maladies oculaires. Cependant, d'autres études précliniques et cliniques sont nécessaires afin de mieux comprendre l'activité potentielle du RSV chez l'homme.

Mots clés : Resvératrol, polyphénols, nutraceutique, maladies oculaires, œil, DMLA, angiogenèse, rétinopathie diabétique, cataracte.

Citation: Delmas, D.; Cornebise, C.; Courtaut, F.; Xiao, J.; Aires, V. New Highlights of Resveratrol: A Review of Properties against Ocular Diseases. Int. J. Mol. Sci. 2021, 22, 1295. https://doi.org/10.3390/ijms22031295

Academic Editors: Janusz Blasiak and Kai Kaarniranta
Received: 10 December 2020
Accepted: 24 January 2021
Published: 28 January 2021

Abstract: Eye diseases are currently a major public health concern due to the growing number of cases resulting from both an aging of populations and exogenous factors linked to our lifestyles. Thus, many treatments including surgical pharmacological approaches have emerged, and special attention has been paid to prevention, where diet plays a preponderant role. Recently, potential antioxidants such as resveratrol have received much attention as potential tools against various ocular diseases. In this review, we focus on the mechanisms of resveratrol against ocular diseases, in particular age-related macular degeneration, glaucoma, cataract, diabetic retinopathy, and vitreoretinopathy. We analyze, in relation to the different steps of each disease, the resveratrol properties at multiple levels, such as cellular and molecular signaling as well as physiological effects. We show and discuss the relationship to reactive oxygen species, the regulation of inflammatory process, and how resveratrol can prevent ocular diseases through a potential epigenetic action by the activation of sirtuin-1. Lastly, various new forms of resveratrol delivery are emerging at the same time as some clinical trials are raising more questions about the future of resveratrol as a potential tool for prevention or in therapeutic strategies against ocular diseases. More preclinical studies are required to provide further insights into RSV' s potential adjuvant activity.

Keywords: resveratrol; polyphenols; nutraceutical; ocular diseases; eyes; AMD; angiogenesis; diabetic retinopathy; cataract

1. Introduction

The number of visually impaired people of all ages is estimated to be 285 million worldwide, of whom 39 million are blind [1]. The leading causes of blindness and low vision are primarily age-related eye diseases such as age-related macular degeneration (AMD), cataract, diabetic retinopathy (DR), and glaucoma. The molecular mechanisms seem to be involved in many common steps, such as early oxidative stress, an inflammatory-associated process, and often over-angiogenesis. Visual impairment is a major global health issue, partly due to an aging world population, and the search for preventive or therapeutic strategies is therefore an important issue. Thus, of the dietary microcomponents that can participate in these strategies against ocular diseases, polyphenols could be good candidates (Figure 1). Indeed, various studies have shown that polyphenols may protect against numerous diseases (i.e., vascular diseases, cancers, and associated inflammatory disorders) [2–4]. These phytomolecules have cellular targets similar to those of the new drugs developed by pharmaceutical companies. Indeed, more than 1600 patents are currently reported concerning flavonoids and 3000 patents concerning polyphenols. Pleiotropic pharmaceutical activities are claimed in fields such as cancer, inflammatory arthritis, eye diseases, and many other domains. One of the best known is the polyphenol resveratrol, which is a *trans*-3,4′,5-trihydroxystilbene (*Trans*-RSV) (Figure 1) and appears to be of great interest in the prevention of these pathologies. Resveratrol (RSV) presents a myriad of beneficial health effects and acts at multiple levels such as cellular signaling, enzymatic pathways, apoptosis, and gene expression to prevent or fight coronary heart damage, cancer, and

degenerative diseases in in vitro and in vivo studies [5–8]. Due to its multiple biological properties, RSV could help fight the main molecular events of ocular pathologies through its antioxidant power, as well as its anti-inflammatory and anti-angiogenic properties. In this review, we focus only on RSV with whom we have been working for more than 20 years on the elucidation of biological properties and also because it is one of the only polyphenols so that there are both very many robust studies on the molecular mechanisms on several ocular pathologies but also some clinical studies. Thus, this present review concentrates on the current knowledge of the mechanism of RSV on some of the main ocular disorders such as AMD, glaucoma, cataract, and DR. We describe cellular and molecular actions of RSV, as well as its potential epigenetic action in ocular disease prevention. Furthermore, a number of clinical trials have been conducted to test the efficacy of RSV in some cases of AMD. Lastly, we discuss the potential use of RSV and its new formulations in association with other therapeutic drugs.

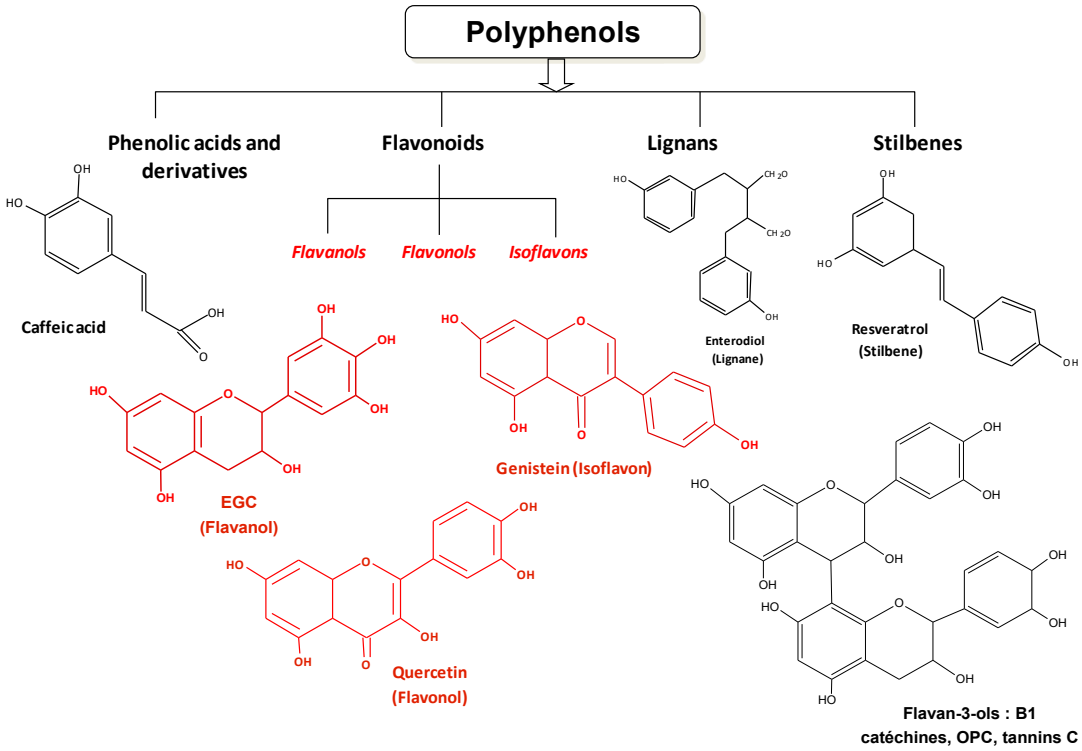

Figure 1. Chemical structures of polyphenols. Polyphenols that are ubiquitous in plants can be divided into four classes: phenolic acids such as caffeic acid, flavonoids including quercetin and genistein, the lignans, and the stilbenes, to which resveratrol belongs.

2. The origins of Resveratrol

RSV is a secondary metabolite produced in a small number of plant species. It was first isolated in 1940 from the root of Veratrum grandiflorum, which is a common flower of the Eurasian grasslands [9]. The root of the word "resveratrol" is a combination of the Latin prefix Res, meaning "which comes from", veratr, from the plant "Veratrum", and the suffix ol, indicating that it contains "alcohol" chemical groups. Veratrum grandiflorum has been reported to synthesize RSV and analogues. It is interesting to note that root powder of Veratrum album has long been used at medium altitude in

Northern Europe, Asia, and Japan to treat rheumatism and nervous diseases. However, Veratrum album contains potent toxic alkaloids: the protoveratrines A & B. The RSV precursor is phenylalanine and the Int. J. Mol. Sci. 2021, 22, 1295 3 of 29 key cellular enzyme is stilbene synthase, which initiates the synthesis pathway toward RSV instead of toward flavonoids through chalcone synthase [10]. Therefore, RSV can be classified either as a stilbene or as a polyphenol (Figure 1). Firstly, a significant amount is found in the leaves when the plant is damaged by chemical treatments [11]; secondly, the roots and rhizomes are relatively rich in RSV and, as such, were used as a crude preparation to treat hypertension in the East (Table 1) [12]. One of the richest sources of RSV is Japanese knotweed (barnbuo japonaise) Polygonum cuspidatum, root extract. These roots play an important role in ancient Chinese and Japanese natural medicine [13,14]. Its presence has been reported in many trees including eucalyptus [15,16], the spruce [17], and tropical trees like Bauhinia racemosa [18]. RSV has been identified in a small number of flowering plants; only two species of hellebore, Veratrum grandiflorum and Veratrum formosanum, are able to synthesize this compound. RSV is also present in Pterolobium hexapetallum, a legume [19]. Cotyledons such as peanut Arachis hypogaea synthesize a set of stilbene—phytoalexins including RSV with concentrations significantly increased in response to infection, injury, and ultra-violet (UV) irradiation [20–24]. The importance of RSV in plant biology lies in its ability to inhibit the growth of fungal infection, a property that has allowed it to be included in the class of antibiotic plants: phytoalexins. Due to its function as a phytoalexin and its role as a marker of infection by various pathogens, this interest in RSV mainly concerns vines (Vitaceae). The first report describing the structure and presence of RSV in grapes and its induction by infection with a fungus such as Botrytis cinerea [25–27] showed that this hydroxystilbene can exist in two forms: *trans*-RSV, the most organic form actively blocking the development of Botrytis cinerea, and *cis*-RSV obtained by the action of light on the *trans*-form. Most grape varieties contain varying quantities of this natural fungicide molecule, with grape skin containing about 50–100 μg of RSV per gram. It follows that during maceration, which takes place in the process of red wine vinification, RSV is dissolved in the hydro-alcoholic medium and then found in abundance in red wine, i.e., up to 20 mg/L [28]. Furthermore, RSV can be converted into viniferin by the action of vacuolar peroxidases [27,29]. Methyl-transferase and glucosyl-transferase activities have been identified to explain the biosynthesis of pterostilbene and RSV glucosides (including piceid and RSV-3-O-β-D-glucoside) [30–32].

Table 1. *Trans*-resveratrol (*Trans*-RSV) concentration in various food sources

Sources	*Trans*-RSV (μg/g)	References
Hop	0.5	[33]
Peanuts	5.1	[34]
Peanut butter	0.3	[34]
Grape skin	27.5	[35]
Kojo-Kon	523	[34]
Blueberries	0.03	[36]

Like many other plant polyphenols, RSV is considered to be a preventive food microcomponent in the same way as the flavonoids and epicatechins of green tea or cocoa [37]. In fact, RSV attracted little interest until 1992, when it was postulated to explain some cardioprotective effects of red wine, with interest then increasing from 1997 when Pezzuto's team published a seminal paper reporting the ability of RSV to inhibit carcinogenesis at multiple stages [38]. Since then, the number of papers and citations have increased in an exponential manner due to the pleiotropic effects of RSV on various diseases (Figure 2). The main properties of RSV were found to relate to its antioxidant power, its anti-inflammatory properties, and its ability to modulate various targets in numerous pathologies (Figure 2) such as:

(1) Coronary heart diseases, *via* scavenging of reactive oxygen species (ROS) [39–41], prevention of the oxidation of low-density lipoproteins (LDL) [42–44], a decrease in foam cell formation and pro-inflammatory molecules [45,46], as well as a reduction in platelet aggregation [47–49].

(2) Cancers, through its ability to inhibit carcinogenesis at multiple stages (initiation, promotion, and tumor progression) in in vivo models of skin tumors [38]. Systemic administration of RSV has since been shown to inhibit the initiation and growth of tumors in a wide variety of rodent cancer models through various mechanisms, including cell cycle arrest, induction of apoptosis, and inhibition of angiogenesis (see for review [7,50]).

(3) Inflammatory diseases, where RSV is able to modulate both the adaptive and the innate immune response and consequently decrease the production of various proinflammatory cytokines in response to a wide range of exogenous stimuli [2,6].

(4) Age-related degenerative diseases, through its capacity to activate an important actor, sirtuin-1 (Sirt-1), which exhibits down-regulated expression in multiple organs during aging [51,52].

Therefore, these properties of polyphenol could participate in a chemopreventive or chemotherapeutic strategy against ocular diseases such as age-related macular degeneration (AMD), cataract, retinal degeneration, optic neuritis, glaucoma, and retinoblastoma through common mechanisms, as well as through specificities that characterize individual ocular diseases.

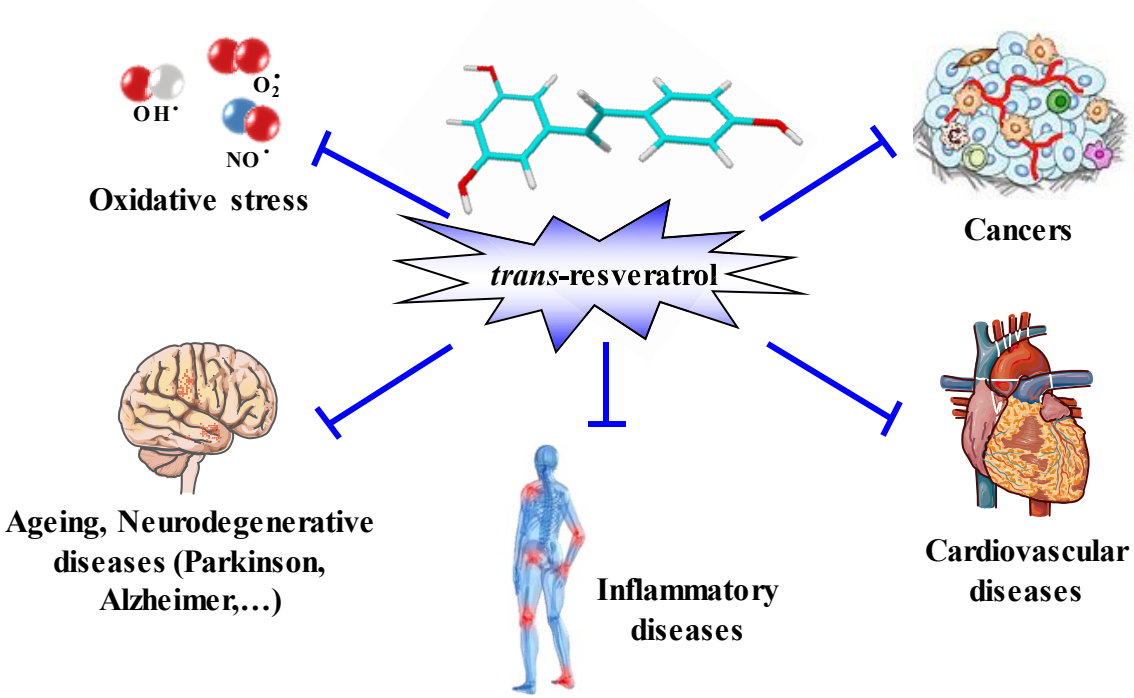

Figure 2. Pleiotropic action of RSV. The 3,4′,5-trihydroxystilbene is able to prevent coronary heart diseases, inflammatory pathologies, oxidative stress in aging, neurodegenerative diseases, as well as cancers.

3. Age-Related Macular Degeneration and RSV Action

3.1. AMD and the Key Actors

AMD is one of the main causes of deterioration of vision in elderly people in developed countries [53], resulting in a loss of vision in the center of the visual field due to damage to the retina. It is usually classified as one of two forms: a dry form characterized by the appearance of drusen, which are proteinaceous collections at the level of the retinal pigment epithelium (RPE); and a wet form, in which neovascularization complicates retinal changes. At present, some therapies are used for wet AMD to inhibit the abnormal growth of blood vessels with VEGF inhibitors or laser photocoagulation, but a number of side effects to these therapies are seen, as is resistance. Concerning dry AMD, currently only nutritional supplementation is given; no therapies have shown efficacy. The aim of non-exudative AMD treatment is to delay the loss of visual function. Int. J. Mol. Sci. 2021, 22, 1295 5 of 29 Some therapies that modulate risk factors are able to prevent the development or progression of the pathology, but do not completely cure patients affected by AMD. Consequently, new therapies are needed and RSV could act on this disease at different levels. Indeed, keys processes have been identified in AMD such as oxidative damage, impaired activity or function of the RPE, increased apoptosis, and chronic inflammation (Figure 3). Moreover, neovascularization seems to play a very important role in AMD complications. RVS could act on these different steps mainly through its antioxidant power, anti-inflammatory action, or through its anti-angiogenic effects.

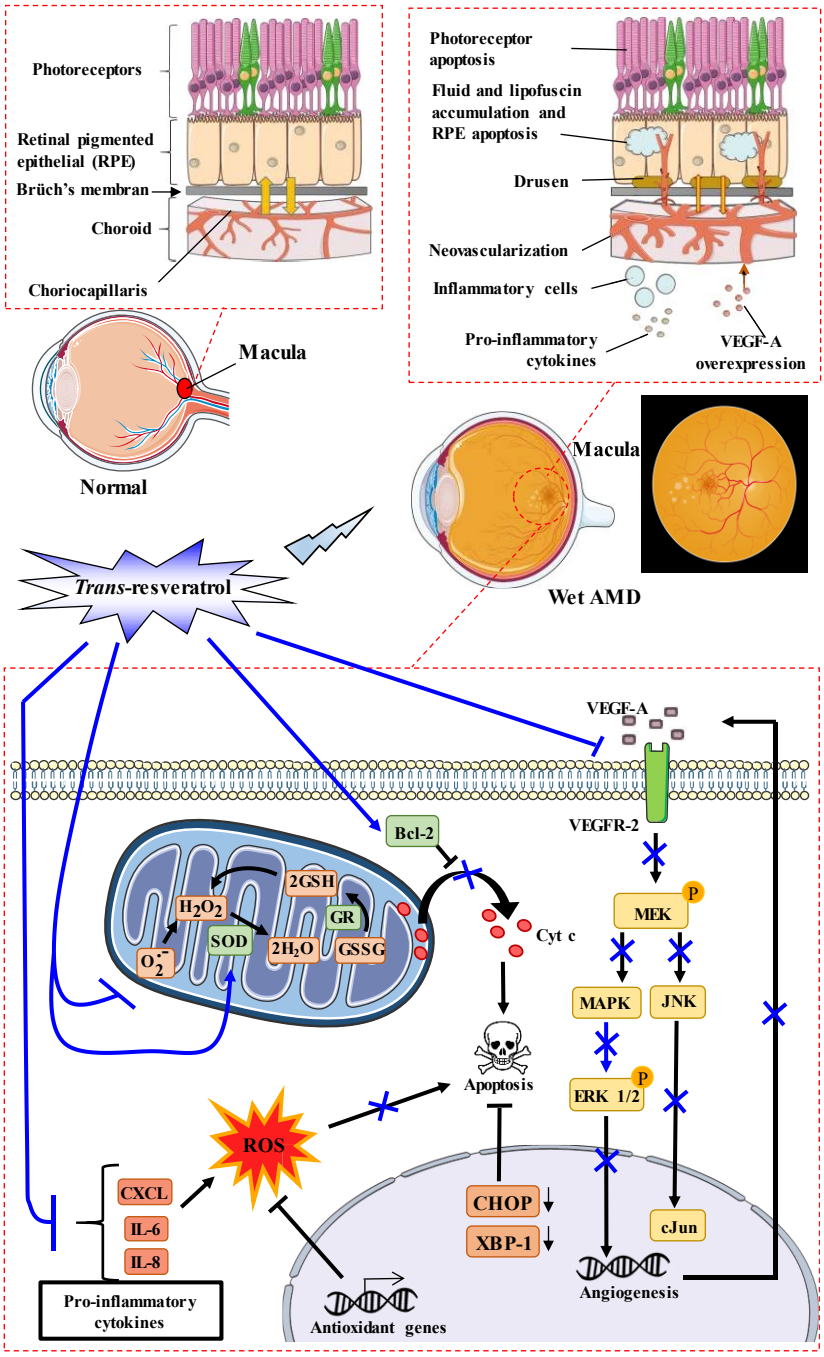

Figure 3. RSV could prevent oxidative stress involved in the development and progression of ocular diseases such as age-related macular degeneration (AMD). Various environmental factors produce free radicals, leading to oxidative stress in ocular tissues and consequently provoking the initiation of diseases such as AMD. On the one hand, RSV is able to scavenge free radicals (O2 −) and activate superoxide dismutase (SOD) or glutathione reductase (GR), while on the other, it inhibits inflammation through the reduction of various pro-inflammatory cytokines and blocks the signaling pathway induced by vascular endothelial growth factor-A (VEGF-A) to promote neoangiogenesis.

3.2. RSV and AMD Initiation

AMD is a multifactorial disease with both environmental and genetic risk factors [54]: air pollution, smoking, UV radiation, metabolic diseases (e.g., diabetes, hypertension, obesity), dietary fat consumption [55–58], and genetic polymorphisms such as cfh, arms2/hrta1 genes [59]. Alone or in combination, these factors could contribute to initiating AMD through the production of free radicals such as superoxide anion (O2 ·–), nitric oxide (NO·), and hydroxyl radical (OH·), which create oxidative stress and inflammation in ocular tissues. It is now well-established that oxidative stress and inflammation play a critical role in the initiation and development of AMD [60].

Due to its antioxidant power and ability to scavenge free radicals, RSV could protect ocular tissues against oxidative stress (Figure 3). RPE cells, which form the cell layer responsible for maintaining retinal health by providing structural and nutritional support, are the primary target for AMD-associated oxidative stress [61]. Due to its antioxidant power, RSV could be effective at reducing the risk of AMD in the same manner as antioxidants commonly found in fruits and vegetables (vitamins C, E, and carotenoids) for which studies have demonstrated that their intake may delay or prevent the development of retinal diseases [62]. Indeed, the treatment of RPE cells with RSV prevents ROS production, both in the basal state (around 20% compared to untreated controls) and when cells are treated with an inducer of oxidative stress such as hydrogen peroxide (H_2O_2). Secondly, RSV protects or delays cell death induced by H_2O_2 in RPE cells. Indeed, King et al. have shown that the pretreatment of cells with RSV followed by treatment with H_2O_2 prevents the inhibition of cell proliferation [63]. Moreover, polyphenol protected against the oxidative damage of RPE cells by modulating SOD/MDA (malondialdehyde) activity and activating Bcl-2 expression [64]. These protective actions of RSV could involve the inhibition of mitogen-activated protein kinase (MAPK) pathways induced by oxidative stress. At the basal level, RSV was able to decrease the phosphorylation of extracellular signal-regulated kinase 1/2 (ERK 1/2), phospho-ERK1/2, in a dose-dependent manner, as well as the tyrosine/threonine mitogen-activated kinase kinase (MEK), especially with 25 and 50 μM RSV compared to cells treated with H_2O_2 alone [63]. This ability to reduce MAPK activation could contribute to a reduction in the effect of H_2O_2 on this pathway.

Other environmental factors, such as acrolein found in cigarette smoke, induce oxidative stress in human retinal cells. A study performed at the ophthalmology department in Taiwan showed that RSV pretreatment can also prevent damage caused by exposure to acrolein for 7 days followed by H_2O_2 treatment [65,66]. In the same way, other studies have shown that RSV, alone or in combination with polyunsaturated fatty acids (PUFA; Resvega®), was able to improve RPE cell viability upon cigarette smoke-derived hydroquinone exposure and reduce the release of interleukin (IL)-8 and monocytic chemoattractant protein (MCP)-1 from RPE cells [67,68]. Under these conditions, RSV upregulated C/EBP homologous protein (Chop) and spliced X-box binding protein 1 (XBP1), thereby improving mitochondrial bioenergetics, upregulating antioxidant genes, and stimulating the unfolded protein response [68,69].

UV radiation, especially UVA, can also penetrate the lens, reach the retina, and induce oxidative stress in RPE cells. RSV was able to: (i) reduce the UVA-induced

decrease in RPE cell viability, (ii) reduce the generation of intracellular H_2O_2, and (iii) decrease the activation of UVA-induced extracellular signal-regulated kinase, c-jun-NH2 terminal kinase, and p38 kinase in RPE cells, as well as cyclooxygenase-2 (COX-2) expression [70].

In a similar manner at our laboratory, we have shown that the toxic effects of oxysterols, which come from the diet or from cholesterol catabolism and play important roles in AMD, could be counteracted by RSV [71]. Indeed, when retinal cells (ARPE-19) were treated with 7-beta-hydroxycholesterol (7β-OH) or with 7-ketocholesterol (7KC), we observed a decrease in viable cells after 24 h and more strongly after 40 h. RSV, which has no toxic effect on retinal cells, can protect these cells from the toxic effects of oxysterols.

Other antioxidant mechanisms of RSV may be involved. Indeed, we have shown in various cell lines that RSV could act on ROS production *via* its action on mitochondrial enzymatic pathways [7].

RSV can interfere with mitochondrial electron transport and promotes a fall in the mitochondrial transmembrane potential $\Delta\psi m$ [72,73], a decrease in ATP production, and the generation of ROS (Figure 3) [74]. RSV has also been described to: (1) decrease complex III activity by competing with coenzyme Q, whose complex is the site of ROS production, (2) inhibit ATPase activity, and (3) scavenge superoxide anions [75]. Furthermore, O2 − radicals are converted to H_2O_2 by superoxide dismutase (SOD), and H_2O_2 detoxification normally occurs according to two different reactions, i.e., either by the thioredoxine reductase (TR) or by reacting with glutathione reductase (GSH) and glutathione peroxidase (GPx). The latter reaction produces water and oxidized glutathione (GSSG), and GSSG is recycled to GSH by glutathione reductase (GR). Therefore, in addition to scavenger O2 −, RSV accelerates the detoxification of O2 − by inducing an increase in glutathione levels and also by inducing GPx, GR, glutathione-S-transferase (GST), and catalase (CAT) activities [76–80], as well as their mRNAs levels [81]. This modulation of antioxidant enzymes could explain the inhibition of DNA damage in human lymphocytes induced by various toxic drugs (i.e., H_2O_2, 1,2-dimethylhydrazine, bleomycin) [82–84].

Metabolic diseases can also play an essential role in the production of oxidative stress. It is now well-defined that diabetes and obesity have numerous effects on ocular diseases [85]. A wide range of evidence implies that dietary hyperglycemia is etiologically related to human aging and diseases, including DR and AMD. In this context, these diseases can be considered as retinal metabolic diseases. A number of clinical trials have been published investigating the effects of RSV on whole-body energy metabolism in relation to the multiple health factors that are affected by obesity and type 2 diabetes [86–90]. Indeed, daily administration of 2.5 or 5 g RSV for 28 days shows a decrease of fasting and postprandial glucose and insulin. At low concentrations such as 5 mg twice daily for 4 weeks, RSV significantly decreased insulin resistance [91]. Timmers et al. showed that 75 mg of RSV twice daily for 30 days improved the metabolic profile in a healthy obese man: RSV reduced sleeping and resting metabolic rates [88]. In muscle, RSV activated the AMPK–SIRT1–PGC1α axis, reduced blood glucose and insulin levels, reduced liver fat, improved muscle mitochondrial function,

and reduced inflammatory markers in the blood [88]. Consequently, through the pleiotropic action of RSV on metabolic diseases, this polyphenol could contribute to reducing the collateral effects of metabolic diseases on eye disorders, especially AMD.

A final and important mechanism in this step of AMD initiation is the accumulation of lipofuscin or cellular debris in RPE. Lipofuscin, an aging pigment, is considered to be a credible marker for the aging of cells. Lipofuscin tends to accumulate even at an early age, but rapidly progresses with the advancement of the aging process, suggesting the inability of autophagy to handle the waste disposal capacity. The decline of autophagy during aging appears to be the cause for lipofuscin accumulation. Morselli et al. showed that transgenic expression of Sirt-1 induces autophagy in human cells in vitro and in C. elegans in vivo [92]. Caloric restriction and RSV promotes longevity through the Sirt-1-dependent induction of autophagy [93]. Moreover, RSV induced autophagy in ARPE-19 cells, as determined by the increased presence of autophagic vacuoles, increased the LC3II/I ratio, and decreased p62 expression [94]. In this study, RSV acted similarly to proteasomal inhibition downstream of the mammalian target of rapamycin (mTOR), since upstream inhibition of autophagy by 3-methyladenine was not able to inhibit autophagy in ARPE19 cells. This effect on autophagy is also found with a combination between RSV and PUFA (especially omega-3), where 288 ng of Resvega®, containing 30 mg of *trans*-RSV and 665 mg of omega-3 fatty acids, among other nutrients, was able to induce autophagy and contribute to the survival of ARPE-19 cells exposed to detrimental protein waste triggered by proteasome inhibition [95].

RSV was also able to prevent the toxic effects of N-retinyl-N-retinylidene ethanolamine (A2E), a major lipofuscin component that accumulates in RPE cells with age. Indeed, polyphenol pretreatment strengthened cell monolayer integrity through the preservation of *trans*-epithelial electrical resistance, maintained the intracellular redox balance, and prevented A2E-induced mitochondrial network fragmentation [96]. Moreover, RSV and its metabolite, piceatannol, reduced intracellular A2E accumulation in RPE cells [97].

3.3. RSV and Inflammatory Processes Related to AMD

We and others have shown that RSV is an efficient anti-inflammatory compound in various models of cardiovascular disease, cancer, and chronic inflammatory diseases [5,50,98]. Inflammation also plays a central role in ocular pathologies, especially in AMD [99–101], and thus the use of RSV to counteract inflammatory processes could be relevant herein.

Based on the important role played by interleukins, a study has shown that RSV was able to reduce the production of interleukin-6 (IL-6) and interleukin-8 (IL-8) induced by glucose in retinal cells [102]. This latter interleukin, IL-8, has been shown to be an important risk factor for AMD [101]. Furthermore, RSV substantially inhibited pro-inflammatory cytokine-induced CXCL11 production, which is an important chemokine involved in inflammatory cell recruitment [103]. Indeed, RPE cells adjacent to drusen deposits in the AMD eye are known to contain CXCL11. This is not the only chemokine modulated by RSV—this polyphenol was also able to inhibit the cytokine-induced expression of chemokines CXCL9, CCL2, and CCL5.

Another mechanism could involve peroxisome proliferator-activator receptors (PPAR). Indeed, RSV protects RPE cells from sodium iodate injury (increasing levels of ROS and IL-8) through the activation of PPARα and alteration of PPARδ conformation [104].

3.4. RSV Can Prevent Complications of AMD

The ultimate step in the AMD process is neovascularization, which constitutes a major complication of AMD. The molecular mechanisms involve vascular endothelial growth factor A (VEGF-A) and an increase in vascular permeability that results in loss of vision [105]. Anti-angiogenic therapies targeting VEGF have proven to be highly effective in treating neovascular AMD, but they cause a number of side effects. In this approach of angiogenesis inhibition, RSV could counteract AMD through its action on VEGF contributing to the abnormal growth of blood vessels. To test this hypothesis, we tested the protective effect of RSV on the VEGF secretion induced by oxysterols in RPE cells [71]. Oxysterols induced VEGF-A secretion after 24 and 40 h of treatment with 7β-hydroxycholesterol and 25-hydroxycholesterol. Interestingly, cotreatment with RSV at 1 μM decreased VEGF-A secretion induced by these oxysterols both at 24 and 40 h [71].

Consequently, RSV could reduce neovascularization or protect against various factors that induce VEGF-A production and promote neovascularization such as diabetes, which is known to induce VEGF and which is linked to the progression of vision loss (see below). In this regard, Kim et al. have shown, in retinal tissues, that RSV pretreatment can prevent diabetes-induced rises in VEGF secretion [106]. Notably, they observed an increase in VEGF levels between the outer plexiform layer and the nerve fiber layer on retinal sections of mice 2 months after the induction of diabetes compared to control mice. Indeed, the authors showed that RSV pretreatment of mice by oral gavage at 20 mg/kg once a day for 4 weeks prevents VEGF secretion as well as VEGF expression. Moreover, RSV was able to reduce both epidermal growth factor-A (EGF-A) and VEGF-C secretion by human RPE cells stimulated with a mixture of inflammatory cytokines (interferon [IFN]-γ, tumor necrosis factor [TNF]-α, IL-1β) and to decrease tumor growth factor (TGF-β) and cobalt chloride [107]. This potential effect on hypoxia has been raised in several other studies where RSV inhibited hypoxic choroidal vascular endothelial cell proliferation through activation of the stress-activated protein kinase (SAPK)/Jun amino-terminal kinase (JNK) pathway [108]. The development of choroidal neovascularization (CNV) is a critical step in the pathogenesis of AMD, and laser photocoagulation has been described to induce CNV in mice. A preclinical study has shown that CNV volume was significantly lower in the RSV-treated mice 1 week after laser treatment compared with vehicle-treated animals. Very interestingly, RSV inhibited macrophage infiltration into RPE–choroid and suppressed the expression of inflammatory and angiogenic molecules, including VEGF, monocyte chemotactic protein-1 (MCP-1), and intercellular adhesion molecule-1 (ICAM-1) [109]. The underlining molecular mechanism appeared to involve the maintenance of adenosine monophosphate-activated protein kinase (AMPK) levels, this latter exerting its inhibitory effect on the nuclear factor-κB (NFκB) in the RPE–choroid complex.

4. Glaucoma and RSV Action

4.1. Glaucoma and the Key Actors

Glaucoma is a progressive optic neuropathy defined by damage to the optic nerve associated with the degeneration of retinal ganglion cells (RGC), causing visual field damage and subsequent blindness. Ocular hypertonia (OH) is the first known risk factor that contributes in most cases to the pathology and remains to date the only pathogenic event accessible to medical or surgical treatment. Glaucoma is the second leading cause of blindness in the world after cataracts. It has been projected to affect 80 million people worldwide by 2020 [110] and 112 million people by 2040 [111]. The pathological elevation of intra-ocular pressure (IOP) is due to alteration and then degeneration of the trabecular meshwork. Aqueous humor (AH) is eliminated at a rate of 90% by the trabecular route through the trabeculum and at a rate of 10% by the so-called uveoscleral route. The trabeculum is considered a dynamic filter that drains AH out of the anterior chamber of the eye. It is located in the iridocorneal angle over its entire circumference. Therapy is based on either medical, laser, or surgical intervention. However, recent works tend to show that a nutritional prevention strategy could be interesting. Indeed, certain lifestyle habits could influence glaucoma progression or its prevention. For exemple, frequency of coffee intake may be associated with disease progression [112].

4.2. RSV and the Oxidative Stress in Glaucoma

Oxidative stress is known to be an early event in hydrostatic pressure-induced RGC damage involved in glaucoma. Indeed, several studies have revealed that oxygen metabolism, and more particularly, ROS are crucial in the development of glaucoma. As described previously, RSV has antioxidant properties that, through its hydroxyl groups, have the ability to react with ROS in glaucoma [113]. Nevertheless, this is not RSV's only antioxidant ability. In fact, many studies have demonstrated that RSV can reduce ROS in glaucoma models (in vitro and in vivo) through several pathways (Figure 4) [114–116]. This downregulation of ROS could be due to the modulation of the endogenous antioxidant system [117], such as induction of nuclear factor erythroid-2-related factor 2 (Nrf2) translocation into the nucleus, where it binds to antioxidant response elements (ARE). This latter leads to the production of heme oxygenase-1 (HO-1), an antioxidant enzyme [117,118].

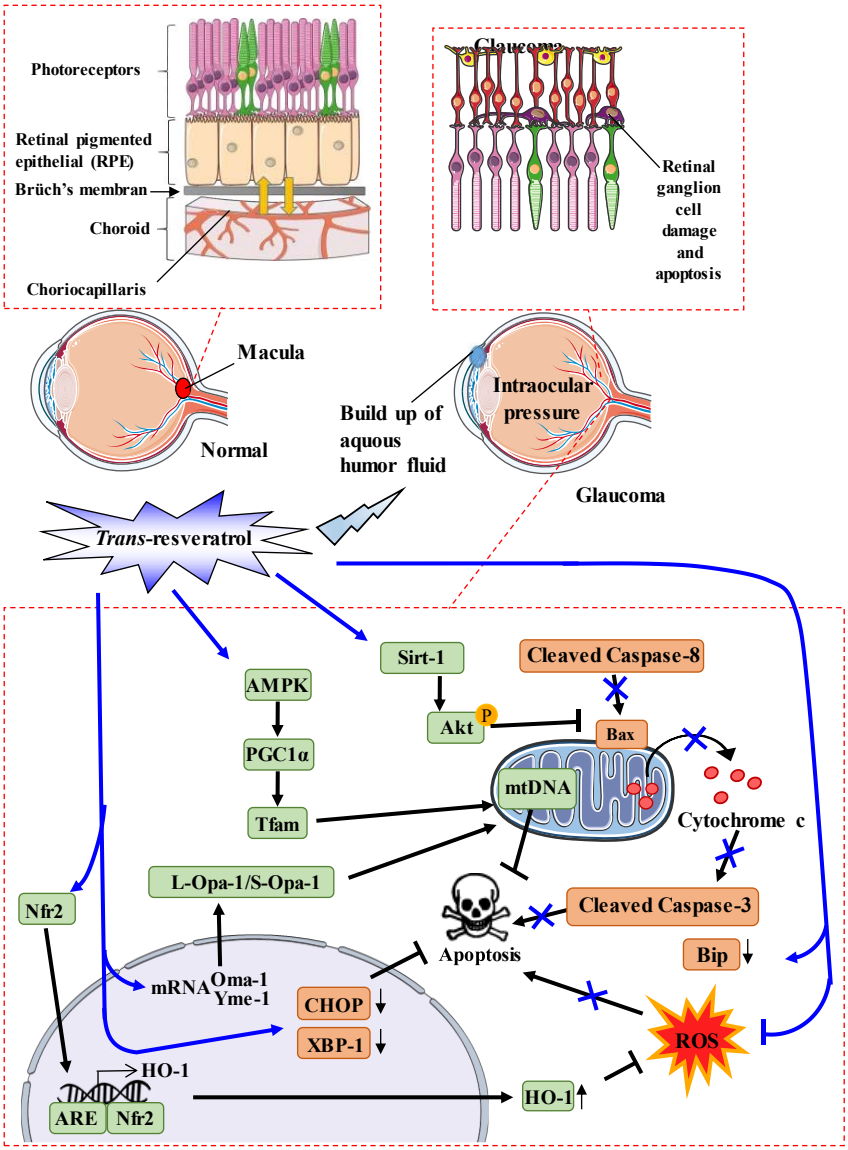

Figure 4. Proposed model of resveratrol action during oxidative stress in glaucoma. *Trans*-resveratrol (RSV) activates sirtuin-1 (Sirt-1), which leads to the phosphorylation of Akt and inhibits Bax activity. RSV also activates the AMPK pathway, which leads to mitochondrial DNA transcription and replication. RSV is also able to alter Oma-1 and Yeme-1 mRNA expression, leading to the alteration of the L-Opa-1/S-Opa-1 (long-optical autophagy 1/short optical autophagy) ratio. In addition, RSV also lowers ROS levels not only by activating the scavenger pathway, but also by facilitating the translocation of Nrf2 into the nucleus, thereby favoring interaction between Nfr2 and the antioxidant response element (ARE) leading to HO- production.

Another important pathway regulating ROS production is the mitochondrial pathway. Indeed, mitochondria are crucial organelles in glaucoma, and oxidative stress can be produced by an imbalance between ROS production and ROS defenses. A significant decrease in the activity of detoxifying enzymes such as SOD and GPx has been shown in the aqueous humor of patients with glaucoma [119]. Thus, targeting mitochondrial homeostasis could be a potential therapy for glaucoma. Some studies have shown that RSV can alter not only the quantity but also the quality of mitochondria in RGC. Indeed, it has been shown that RSV is able to increase the number of

mitochondria present in one cell [120] and can affect pathways leading to mitochondrial biogenesis. In this way, RSV is able to downregulate the Oma-1 gene and upregulate the Yeme-1 gene, which increase the ratio L-Opa-1/S-Opa-1 (long-optical autophagy 1/short optical autophagy 1) involved in mitochondrial fusion (Figure 4) [121]. Moreover, RSV is able to restore protein levels that are decreased in glaucoma and which are involved in mitochondrial biogenesis, such as AMPK, peroxisome proliferator-activated receptor γ coactivator-1α (PGC-1α), and mitochondrial transcription factor A (Tfam), which leads to mitochondrial DNA transcription and replication [115]. Zhang et al. have also shown that RSV modifies not only the number but also the quality of mitochondria by maintaining mitochondrial integrity. Indeed, RSV are able to decrease the membrane potential depolarization induced by pressure.

4.3. RSV and the Cell Death Process in Glaucoma

RGCs are the main cell type affected in optic neuropathies, with degeneration of these cells leading to profound phenotypes and eventual loss of vision. It has been reported that the pathways of RGC loss have been explored in depth after acute high IOP injury, such as apoptosis, autophagy, and necrosis. Furthermore, pyroptosis, a novel type of pro-inflammatory cell programmed necrosis, plays a crucial role in retinal neuronal death, especially in the ganglion cell layer, by acute high IOP injury that peaks at 6 h [122]. Several other in vitro and in vivo studies have shown that RSV treatment or pre-treatment before inducing stress reduces cell apoptosis. For instance, in various glaucoma models, RSV has been demonstrated to reduce the activation of caspase-3, as evidenced by the decrease in cleaved caspase-3 protein expression levels [121,123,124]. In a mouse model of ischemia/reperfusion (I/R) injury, RSV was shown to alter the extrinsic apoptosis pathway by reducing caspase-8 mRNA levels and proteolytic cleavage in mice retina [123]. Furthermore, other studies have investigated the mitochondrial apoptosis pathway, and showed that RSV can also reduce the expression of Bax and decrease cytochrome c release. Similarly, another study has been carried out to investigate the effect of RSV on the endoplasmic reticulum (ER) stress apoptosis pathway [125]. This study revealed that RSV reduces the level of cytosolic Bip and also reduces the nuclear quantity of XBP-1 and CHOP, which consequently reduces apoptotic rates [125]. In a preclinical study, C57BL/6J male mice were injected with RSV for 2 consecutive days before I/R retinal injury, which induces apoptosis in RGCs. In this model, RSV treatment significantly reduced the loss of retinal morphology and downregulated mRNA expression and activation of caspase-8 and caspase-3 protein and subsequently reduced apoptosis [123]. These observations were also confirmed in vitro by others [126].

4.4. RSV and the Inflammatory Process in Glaucoma

Neuro-inflammation in glaucomatous pathology is a component due to the role of immune and glial cells in the early stages of the pathology. In fact, astrocytes, microglia, and monocytic cells are defined as being critical players in the neuro-inflammatory response in glaucoma. Therefore, a number of studies have investigated the potential inflammatory effect of RSV on trabecular meshwork (TM) endothelial cells. Indeed, it

has been shown that the induction of the inflammatory markers IL-1α, IL-6, IL-8, and endothelial leucocyte adhesion molecule-1 (ELAM-1) in TM cells subjected to chronic oxidative stress is dependent on the activation of intracellular ROS (iROS) generated by the mitochondria. RSV could be used to reduce the iROS production that results from oxidative stress. A study recently demonstrated that RSV could be used to lower IL-1α levels. In this study, authors showed that IL-1α levels were unrelated to those of ELAM-1 [127]. This suggests that other mechanisms could be affected in glaucomatous TM cells. Furthermore, Luna et al. showed that RSV prevents inflammatory markers such as IL-6 and IL-8 in TM cells under chronic oxidative stress conditions [128]. Another mechanism that could be involved is the activation of adenosine A1 receptors, which may lead to increased matrix metalloproteinase 2 (MMP-2) activity. Razzali et al. have shown that the repeated topical application of RSV for 21 days in steroid-induced ocular hypertensive (SIOH) rats significantly reduces IOP and TM thickness [129]. In these in vivo experiments, RSV also significantly increased ganglion cell layer thickness, the linear cell density in these cells, and inner retinal thickness. Furthermore, it also significantly reduced retinal oxidative stress compared to the SIOH vehicle-treated group. Interestingly, pretreatment with an A1 antagonist abolished the oculohypotensive effect of RSV, suggesting that its oculohypotensive action involves its agonistic activity at the A1 adenosine receptor [130]. In a model of IOP-induced retinal ischemia in rats, RSV was able to reduce detrimental effects due to ischemia through a potential downregulation of MMP-9 and inducible nitric oxide synthase (iNOS), as well as through the upregulation of HO-1 [116].

5. Cataract and RSV Action

Cataract is the partial or total clouding of the lens. It is a ubiquitous condition that affects an increasing number of people around the world every year. The risk factors of cataract development are similar to those of AMD and include a wide range of lifestyle parameters (i.e., smoking, alcohol, fatty diet, stress, etc.), although there are also rarer etiologies, as well as traumatic and congenital factors. Furthermore, the main risk factors for age-related cataracts are glaucoma and diabetes, which can lead to secondary cataracts. The extent of cataract formation significantly increases with age in ad libitum-fed mice. Strikingly, this increase was attenuated by RSV treatment, which was more effective than in the every-other-day-feeding group at 30 months of age [131]. In an experimental model of naphthalene (1 g/kg/day, po)-induced age-related cataract in rats, RSV (20 and 40 mg/kg/day, i.p.) retarded lenticular opacity, restored antioxidants (CAT, SOD, GPX, GSH), Ca2+ ATPase function, protein contents, and reduced lipid peroxidation in the lenses of RSV-treated rats [132]. RSV was able to significantly inhibit the TGFβ2-induced expression of the myofibroblast marker, α-SMA, in a human lens cell line (FHL124) and human capsular bags following simulated cataract surgery, indicating the ability of RSV to prevent the EMT associated with posterior capsule opacification (PCO). [133]. Interestingly, in cultured lens epithelial cells, RSV inhibited apoptosis and decreased acetyl-p53 levels under oxidative stress induced by H_2O_2 [134].

6. Diabetic Retinopathy and RSV Action

DR is one of the most common complications of type I and type II diabetes. About 80% of patients who have lived with diabetes for 15 years have clinical signs of retinopathy and more than 10% of them are affected by vision loss. This latter is the consequence of slow and progressive alterations in the microvessels of the retina, leading to the opening of the blood–retinal barrier (BRB), the pathological proliferation of blood vessels, and the formation of fibrous tissue in the vitreous cavity, resulting in retinal detachment. During this pathology, neuroglial dysfunction, significant oxidative stress, as well as inflammation and angiogenesis are found. In addition, an increase in the permeability of the retinal vasculature is observed, as well as migration of leukocytes into the retina. Moreover, alterations in biochemical pathways, such as increased flux of advanced glycation end products/receptors (AGE/RAGE), the polyol pathway, protein kinase C (PKC) activation, and the hexosamine pathway induced by hyperglycemia, produce oxidative stress and cause the rupture of the BRB, pericyte loss, and increased vascular permeability [135]. At present, the recommended treatment for severe non-proliferative and proliferative DR is photocoagulation and intravitreal injections of anti-VEGF, with or without focal laser treatment for diabetic macular edema.

RSV is able to prevent oxidative stress due to its pleiotropic actions on various key actors. Indeed, RSV was shown to be able to significantly decrease ROS production by increasing retinal SOD activity, which is one of the most important antioxidant defense systems in the retina [136–138]. Conversely, RSV decreased retinal 8-iso-prostaglandin F2α (iPF2α), a marker of oxidative damage, and reduced glutathione levels [138–140]. Very interestingly, RSV was able to affect the MAP kinase pathway by inducing phosphorylation of protein kinase B (Akt), for which a reduction is observed in retinal neurodegeneration [138,141], phosphorylation of AMPK, Sirt-1 expression, and PGC-1α protein expression [137], and decreasing phosphorylation of ERK 1/2 (Figure 5) [138]. Consequently, RSV increased the thickness of both the whole retina and the inner nuclear layer in diabetic rats [138].

RSV significantly attenuated diabetes-induced downregulation of occludin and diabetesinduced upregulation of high-mobility group box-1 (HMGB1), as well as the receptor for advanced glycation end products and BRB breakdown in diabetic retina [142].

Very interestingly, RSV restored the insulin level and paraoxonase 1 (PON1) expression and activity, as well as clearly reducing retinal vascular permeability, retinal AGEs, low-density lipoprotein (LDL), oxidized LDL (Ox-LDL), caspase-3 activity, and retinal damage in STZ-induced diabetic rats [139,143]. Moreover, in the same model, RSV decreased various pro-inflammatory cytokines such as IL-1β, IL-6, TNFα, VEGF, IFNγ, MCP-1 [143], and NFκB, as well as TNFα and apoptosis [144]. In this pathway involving NFκB, RSV prevented the increase in p65 acetylation, the binding of p65 at the metalloproteinase MMP-9 promoter, and MMP-9 activation, as well as mitochondrial damage and retinal endothelial cell apoptosis [145]. In another model using high-glucose (HG)-stimulated rat retinal endothelial cells (RRECs), RSV reduced

caspase-3 activity and Ox-LDL expression [143]. Thus, hyperglycemia and oxidative-osmotic nitrosative stress play a role in the pathophysiology of diabetic cataract (Figure 5). RSV in combination with nicotinamide exhibits strong effects; it was shown that RSV (10 or 30 mg/kg/day) was not able to prevent the onset of diabetic cataract, but significantly delayed its progression compared to the control group [146].

Mechanistically, the delayed progression due to RSV was shown to be linked to a decrease in protein carbonyl levels in diabetic lenses [146], to the inhibition of the aldose reductase enzyme, and to the reduction in the formation of glycation end products in rat lens [147]. Moreover, in a glucose-induced lens opacity model, RSV displayed a protective effect by preventing opacification in cattle lens. These results suggest that RSV partially delays diabetic cataracts through the attenuation of oxidative damage to lens proteins [146]. This prevention of oxidative damage in lens epithelial cells seemed to be mediated by various processes, such as SOD-1, HO-1, CAT, forkhead box O (FoxO) activity, in particular FoxO1A, FoxO3A, and FoxO4, or inhibition of P38 and JNK phosphorylation [148,149].

Very interestingly, RSV at a dose of 40 mg/kg/day (i.p. injection) in a model of naphthalene (1 g/kg/day, po)-induced age-related cataract (ARC), prevented cataract formation associated with aging through an increase in soluble proteins and Ca2+ homeostasis (i.e., Ca2+ ATPase pump activities in the lens) [132].

By acting on the key actors of the cellular matrix, RSV could prevent posterior capsule opacification (PCO), which is a common complication of cataract surgery. Indeed, RSV was able to inhibit suppressed expression of TGF-β2-induced genes associated with fibrotic disease, including in the treatment of STZ-induced diabetic cataract [150]. In general, the cellular pathways induced by DR lead to apoptosis of retinal cells. RSV was able to suppress STZ-induced apoptosis of retinal cells in the inner nuclear layer of retina after administration of 10 mg/kg/day for 7 months.

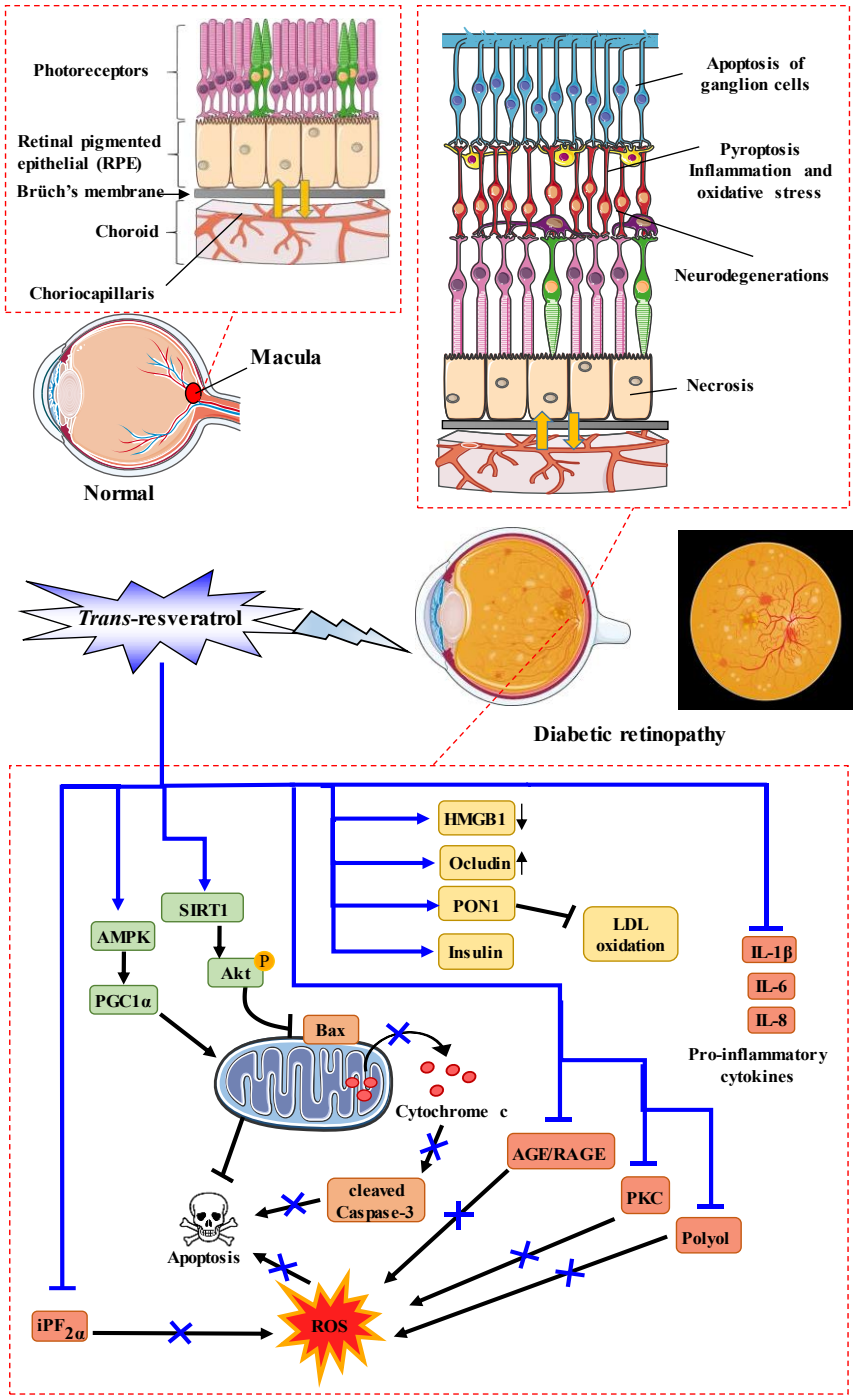

Figure 5. RSV action and process of diabetic retinopathy. RSV activates sirtuin-1 (Sirt-1), which leads to the phosphorylation of Akt and inhibits the mitochondrial apoptosis pathway. Furthermore, RSV stimulates mitochondrial activity through the AMPK–PGC1α pathway, which reduces apoptosis. RSV also lowers ROS through the iPf2α, AGE/RAGE, PKC, and polyol pathways, and downregulates pro-inflammatory cytokines such as IL-1β, IL-6, and IL-8.

Very interestingly, these beneficial effects were inhibited by the miR-29b inhibitor [151]. RSV inhibited the high-glucose-induced decreases in glutamate uptake, glutamine synthase activity, glutamate transporters, and glutamine synthase expression in high-glucose-treated Müller cell cultures compared to controls [152].

Moreover, RSV (10 mg/g/day) alleviated hyperglycemia in diabetic rats and attenuated diabetes-induced decreases in the amplitude of a-wave in rod response, decreases in the amplitude of a- and b-waves in the cone and rod response, and decreases in amplitude of OP2 in oscillatory potentials [152].

Immune cells seem to be involved in the inflammatory process found in DR through the release of IL-17 by lymphocyte T helper 17 (Th17). Indeed, serum of patients with DR exhibit higher IL-17 expression than non-diabetic control groups [153,154]. Moreover, peripheral blood mononuclear cells (PBMCs) exhibited increased expression levels of IL-17 in the DR group of patients, whereas Sirt-1 protein expression decreased in the PBMCs of patients with DR [154]. Interestingly, RSV was able to reduce IL-17 secretion levels in PBMC cultures from patients with proliferative DR, as well as restore Sirt-1 expression in both genic and protein expression [154]. These results obtained on cultured PBMCs echo the results that we have been able to demonstrate directly on Th17 immune cells, where resveratrol was able to reduce the production of IL-17, as well as alter the process of differentiation of naive T lymphocytes into pro-inflammatory Th17 immune cells [155]. In addition, in numerous in vivo models, we have been able to show that resveratrol is able to decrease not only the secretion of IL-17, but also the key factors involved in lymphocyte differentiation. This process is associated with a highly significant decrease in angiogenesis by reducing VEGF-A secretion. This mechanism is dependent on the Sirt-1 protein, where the conditional invalidation of Sirt-1 in T CD4 cells demonstrated that this effect on the production of IL-17 and VEGF was under the control of the Sirt-1 protein and the nuclear transcriptional factor STAT3 [155].

7. Vitreoretinopathy and RSV Action

Proliferative vitreoretinopathy (PVR) is the main cause of failure following retinal detachment surgery. The membrane cells seen in PVR are of the pseudofibroblastic type, but they have several origins, in particular astrocytes and RPE cells. The importance of RPE cells in VRP likely stems from the access of RPE cells to the vitreous due to retinal invasion and the dispersion of viable RPE cells into the vitreous during cryopexy treatment of retinal tears. There are various key actors involved in the development of PVR, which is dependent on the migration and proliferation of RPE cells, glial cells, and inflammatory cells [156]. In this way, TGF-β2-induced epithelial-to-mesenchymal transition (EMT), and EMT inhibition decreases collagen gel contraction and fibrotic membrane formation, resulting in the prevention of PVR. Moreover, numerous cytokines such as IL-1β and IL-6 are considered to be key factors in the development of PVR.

In a model of ARPE-19 cells, RSV suppressed the decrease of zona occludens-1 (ZO1) and caused an increase of alpha-smooth muscle actin expression in TGF-β2-treated cells and increased vimentin expression [157]. Very interestingly, RSV decreased TGFβ2-induced wound closure and cell migration, as well as collagen gel contraction and the phosphorylation of Smad2 and Smad3 in TGF-β2-treated ARPE-19 cells [157]. With regard to Smad protein, another study in RPE cells has shown that RSV induced EMT and inhibited TGF-β2-induced EMT of RPE cells by deacetylation of

Smad4 [158]. TGF-β2 is not the only growth factor involved: platelet-derived growth factor (PDGF) has been shown to enhance the proliferation and migration of RPE cells in PVR. RSV was also able to inhibit PDGF-BB, an isoform of PDGF and PI3K/Akt, ERK, and p38 pathways, but had no effect on RPE cell adhesion to fibronectin [63,159].

8. Corneal Infection and RSV Action

Corneal infection represents a group of serious and blind ocular diseases. The cornea, in its normal condition, is highly resistant to microbial invasion. Nevertheless, pathogens may invade the cornea if epithelial integrity is breached. Corneal infection is a common ocular infection that can lead to ocular morbidity and blindness. These infections can be caused by several bacteria, virus, or fungi, with the common treatment being antibiotic drops.

Some studies have investigated the potential antibiotic action of RSV on corneal infection. An in vivo study revealed that RSV can reduce the cytotoxicity of Acanthamoeba castellanii on the HBMEC cell line [160]. Marino et al. showed that RSV can have a beneficial effect on Staphylococcus aureus-induced keratitis in an ex vivo culture model of rabbit cornea [161]. Indeed, this study demonstrated that RSV treatment can downregulate cell surface TLR2 on cells and reduce the expression of the interleukin-8 gene and, therefore, reduce the action of Staphylococcus aureus. In order to better understand the action of RSV on corneal infection, Tsai et al. investigated its antioxidant action on a human corneal epithelial cell line exposed to levofloxacin or moxifloxacin. They demonstrated that RSV not only increased cell survival, but also reduced intracellular accumulation of oxidative stress [162]. Unfortunately, the mechanism of RSV on corneal infection remains poorly understood, and further studies are required in order to gain deeper insight into the mechanism of RSV on corneal infection.

9. Potential Epigenetic Action of RSV in AMD and Cataract Prevention

RSV could also act by other mechanisms, particularly through sirtuins, which have recently been described as essential targets in various processes such as cellular stress resistance, genomic stability, tumorigenesis, and energy metabolism [8]. Sirt-1 is found in various organs and tissues regulating a variety of pathways such as glucose production in liver, fat mobilization and lipid metabolism in adipose tissue, as well as angiogenesis in blood vessels or other processes in the brain, pancreas, and intestine. Sirt-1 is expressed in almost all ocular tissues, including the cornea, lens (epithelial cells), iris, ciliary body, and retina. Particularly in the cornea, Sirt-1 is located in the corneal epithelial cells, keratocytes, and corneal endothelial cells. In the retina, Sirt-1 is found in the RPE, outer nuclear layer (ONL), inner nuclear layer (INL), and ganglion cell layer (GCL). In eyes, Sirt-1 seems to protect the retinal cells from DNA damage such as oxidative stress-related retinal damage, apoptotic retinal death, and anti-inflammation. In addition, the breakdown of Sirt-1 causes retinal damage through multiple mechanisms. Thus, RSV, which is described as an agonist of sirtuins, could protect the eye by Sirt-1 activation. In this way, Kubota et al. showed that oral RSV pretreatment at a dose of 50 mg/kg for 5 days reverses retinal Sirt-1 activity to restore

its basal activity in BALB/c mice exposed to 5000-lux white light for 3 h [163]. These events are associated with a significant decrease in the number of apoptotic cells in the ONL. Moreover, recent studies have shown that RSV inhibits hypoxia-inducible factor (HIF)-1α accumulation and VEGF secretion induced by cobalt chloride (CoCl2) through Sirt-1 in human RPE cells [108,164]. In this way, RSV downregulated VEGF-R2 phosphorylation and activation induced by VEGF in endothelial cells *via* Sirt-1 and, thus, could contribute to reducing choroidal neovascularization. Furthermore, RSV restored the activity of DNA methyltransferases (DNMTs), which catalyze the methylation process, in ARPE-19 cells, and, more specifically, restored LINE-1 methylation in retinal cells under oxidative and inflammatory conditions [165]. These results are not surprising, partly since Sirt-1 regulates the activity of DNMTs, especially DNMT1 [166]. The overexpression of Sirt-1 is associated with an induction by RSV of AMPK phosphorylation and an overexpression of PGC-1α protein [137]. Indeed, the beneficial effects of RSV were suppressed by inhibitors of AMPK and Sirt-1, as well as by treatment with PGC-1α siRNA. This AMPK pathway is also demonstrated in a mice model of STZ-induced diabetes [167]. Nevertheless, Michan et al. showed that neither overexpression of Sirt-1 by a genetic approach (i.e., conditional Sirt-1 overexpression in retinal neurons or vessels by breeding Sirt-1 overexpressing flox mice with Nestin-Cre or Tie2-Cre mice, respectively) or by a pharmacological approach with Sirt-1 agonists (i.e., RSV) provides additional protection against retinopathy in mice [168]. In transformed retinal Müller (glial) cells in hyperglycemia-like conditions, RVS decreased acetylation of histone H3 and could thus prevent the inflammatory changes that contribute to various ocular diseases such as DR [169]. Further studies are needed to examine whether RSV could modulate epigenetic alterations in ocular diseases.

10. New RSV Formulations and Clinical Trials

10.1. New Formulations of RSV

Several formulations have been developed to efficiently deliver RSV in the eye, including nanoparticle complexation and lipid-based encapsulation. For instance, RSV-loaded polyethylene glycols (PEGs) modified chitosan (CS) nanoparticles (NPs) by an ionic gelation method that was developed and tested both in vitro and in vivo in a rabbit model of glaucoma [170,171]. Data showed that this formulation improved corneal permeation compared with RSV dispersion, and that NPs can evoke an initial burst of RSV release of 45%, followed by a controlled release [165]. In vivo, the formulation was shown to efficiently reach the cornea and retinal choroid, and to significantly reduce IOP by 4.3 ± 0.5 mm Hg for up to 8 h in normotensive rabbits [170,171]. In a cellular model of AMD (ARPE-19 cells), it was also demonstrated that the use of RSV-loaded poly(lactic-co-glyolic acid) (PLGA) nanoparticles (optimized formulation with a particle size of 102.7 nm) improved RSV cellular uptake and increased RSV-induced inhibition of VEGF expression [172]. Although not tested as yet in vivo, this RSV formulation, either alone or in combination with conventional anti-VEGF therapies, may be promising in reducing VEGF-induced neovascularization in an AMD context. In epithelial D407 cells, Rugina et al. ˇ [173] used a microencapsulated RSV formulation based on porous CaCO3 templates and polyelectrolyte layers covered by rhodamine 6G

(Rh6G). Their so-called as-designed PMs-Rv-Rh6G microcapsules were internalized by D407 cells grown in normal and high glucose-induced inflammation conditions (to mimic DR), and reached the cell nucleus within 24 h. This formulation bioavailability was correlated with the inhibition of the expression and secretion of VEGF as assessed by ELISA. Additionally, the use of RSV loaded into lipid-cyclodextrin-based nanoparticles also seems to increase RSV bioavailability and to potentiate RSV-induced ROS scavenging capacities compared to RSV alone [174]. Besides nanoparticles or delivery vehicles, the design of an RSV prodrug formulation has also emerged. For instance, Valdés-Sánchez et al. [175] developed an RSV prodrug, 3,40 -diglucosyl resveratrol (JC19), and tested its efficiency in an experimental mouse model (autosomal recessive RP.Rd10 mice). They injected JC19 subretinally on postnatal day 13, and showed, 15 days post-injection, that JC19 significantly delayed the loss of rod photoreceptors associated with the maintenance of rhodopsin expression and the preservation of their electrical responses to light stimuli. Mechanistically, the authors suggest that Sirt1 activation by JC19 could explain the beneficial effects of the formulation.

10.2. RSV and Clinical Trials

Over the past decade, preclinical and clinical trials (Table 2) have shown that RSV could have a beneficial effect on health. Indeed, clinical trial has revealed that RSV supplementation in normal and healthy subjects can have antioxidant and anti-inflammatory properties in response to a high-fat, high-carbohydrate
meal [176], which supports the fact that RSV could be used clinically in humans without toxicity.

Table 2 : clinical trials with resveratrol with ocular measurements

Author	*Year*	*Region*	*Study design*	*No. of participants per group Age (mean±SD)*	*Dose / frequency / duration / follow-up*	*Effects*	*Ref*
Lin, C.T. et al.	2016	China	Randomized double-blinded trial	*n* = 72	(150 or 450 mg/d) *trans*-RSV or placebo during 12-week treatment Visits were scheduled at 0, 4, 8, and 12 weeks after treatment	Appearance rates of VEGF, Flk-1, and Ang-2 were more significantly reduced in the high-dose group versus the placebo group, but not in the low-dose group.	[177]
Wang S. et al.	2016	China	Randomized and divided into two groups matched by age and gender	34 participants randomly divided into two groups by age and gender matched, 11 women and seven men with a mean age of 25.44 ± 1.46 years (age range, 23–29 years) for the study group; eight women and eight men aged between 23 and 28 years with a mean age of 24.88 ± 1.26 for the control group.	Longenivex (100 mg of *trans*-RSV per capsule) against placebo All OCT scans were performed at the same time of day (between 9:00 a.m. and 12:00 p.m.).	A statistical increase in choroidal thickness (by EDI-OCT) 1 h after Longevinex ingestion compared with baseline measurements.	[180]
Richer S. et al.	2014	USA		*n* = 3 (two males and one female): Case 1: 64 y/o Caucasian with suspected glaucoma and photophobia, atrophic AMD, and diabetes with declining visual function in the right eye, had been on L/RV for 2.5 years and was maintaining visual function; Case 2: 89 y/o Caucasian with chronic kidney disease and cataracts, had been on L/RV for 3 years maintaining his visual function requirements to retain his driver's license; Case 3: 67 y/o Caucasian with bilateral polypoidal choroidal vasculopathy (PCV), a treatment–resistant AMD variant, worse in the right eye. Improved retinal/choroid structure was observed.	Cases 1, 2 : 2, 5 years Case 3: 2 years with Longevinex containing 100 mg of RSV)	Broad bilateral improvements in retina and choroid structure and function,visual acuity, contrast sensitivity, and glare recovery over a long time period, contrary to what might be expected due to aging and the natural progression of the patient's pathophysiology. No side effects were observed.	[179]
Richer S. et al.	2013	USA		*n* = 3 (two males and one female): Case 1: 86 y/o morbidly obese male and advanced AMD; Case 2: 88 y/o female with bilateral wet AMD; Case 3: 75 y/o male with diabetes and dry AMD who developed wet AMD.	100 mg micronized/micro-encapsulated *trans*-RSV in Longevinex formulations.	Case 1 showed a Snellen visual acuity improvement by seven lines at 6 weeks and better IR choroidal circulatory images during the same period. Case 2 showed bilateral improvement in visual function and near resolution of retinal fluid after 2 weeks. Case 3 reported better vision in 5 days with L/RV, and objective retinal and visual restoration similar to anti-VEGF therapy wasobserved after 52 days of treatment	[178]

Preclinical studies have shown that RSV has beneficial effects in ocular diseases, particularly AMD, glaucoma, cataract, DR, and vitreoretinopathy. Indeed, in vivo and in vitro studies have shown the anti-angiogenic potential of RSV in AMD [71] and DR [106]. One randomized and double-blinded clinical trial including 72 patients showed that supplementation with *trans*-resveratrol can lower VEGF levels in peritoneal effluent [177], thereby supporting the notion that RSV could be effective at reducing neovascularization in patients. Another clinical trial performed in the USA in octogenarians also showed that oral administration of Longevinex®, which is a combination of RSV with quercetin, ferulic acid together with vitamin D3 and a cooper/iron/calcium binding molecule called IP6 (inositol hexaphosphate), could improve retinal structure and visual function [178] as well as reduce neovascularization [179]. Moreover, a clinical trial on 19 type 2 diabetic patients supplemented with RSV revealed that it can not only be used to reduce oxidative stress and activate the AKT pathway, but also to improve insulin sensitivity [91]. Indeed, preclinical trials have shown that RSV can restore insulin levels in vitro.

10.3. RSV and Association with Other Therapeutics

Much evidence has been provided with regard to the bioactivities of RSV alone, both in vitro and in vivo. Nevertheless, RSV could also be useful in combination with conventional therapies. Indeed, in a cancer context, it was shown that RSV can act as a therapeutic adjuvant and is able to potentiate the efficacy of chemotherapies. Some studies have also shown the adjuvant potential of RSV in ocular diseases. For instance, in an experimental model of glaucoma, treatment with RSV either alone or in combination with riluzole significantly delayed RGC loss [181]. Very interestingly, Subramani et al. showed that RSV was able to reverse the adverse effects of bevacizumab on cultured ARPE-19 cells [182]. Indeed, numerous patients treated with anti-VEGF therapies show clinical complications due to repeated intravitreal injections [183,184]. In the presence of RSV, Notch signaling gets activated. This activation, along with dephosphorylation of Erk 1/2 and MEK, has been shown to be a major driver of the functional restoration of RPE cells treated with a RSV/bevacizumab combination compared to those treated with bevacizumab alone [182].

11. Safety of RSV

Concerning the toxicity of RSV, various studies have shown that RSV does not exhibit cytotoxicity in animal models and normal cells at the concentrations usually used in vitro (up to 100 μM) or in vivo (up to 500 mg/kg/day; see Table III) [185–188]. Moreover, some clinical studies have shown that RSV is safe in humans at various doses. Indeed, after daily RSV administration (0.5, 1.0, 2.5, or 5.0 g) for 29 days in 40 healthy volunteers, no significant adverse effects were observed, only mild to moderate gastrointestinal symptoms at 2.5 and 5.0 g RSV [189]. Other reports on trials of RSV in humans after single [190,191] or multiple daily doses of up to 600 mg/d administered over 2 or 3 days [192,193] show that RSV is safe under the tested conditions. Recent clinical studies have shown that patients with confirmed colorectal cancer present high levels of RSV metabolites, especially RSV-3-Osulphate, RSV-3-O-glucuronide, and RSV-

4-O-glucuronide, accumulated in the colorectum, and we have recently shown that these metabolites have anticarcinogenic properties. Thus, this poses the question as to whether RSV or RSV metabolites could be accumulated in eyes and ocular tissues and whether it is the aglycone molecule or its metabolites that are active. In fact, Wang et al. measured *trans*-RSV and its main metabolites in human eyes in patients with rhegmatogenous retinal detachment that were orally supplemented with Longevinex® (containing 100 mg of *trans*-RSV; one capsule daily for a total of three doses prior to surgical tissue resection) [194]. HPLC/MS-MS was performed to quantify *trans*-RSV, RSV-3-O-sulfate, RSV-3-O-glucuronide, and RSV-40 -O-glucuronide on tissue samples. The investigators showed that RSV and its main metabolites were detectable in conjunctiva, aqueous humor, and vitreous humor (i.e., 17.19 ± 15.32 nmol/g RSV in conjunctiva and 62.95 ± 41.97 nmol/L RSV-3-O-sulfate in aqueous humor). These data suggest that RSV and its main metabolites can be found in human eyes after supplementation and could potentially participate at the tissue level in the treatment of ocular diseases.

12. Conclusions

There is compelling evidence that RSV can act on various pathologies in vivo such as coronary heart damage, cancer, and degenerative disease, by affecting various pathways. Along these pathways, RSV is able to act on common targets such as reactive oxygen species, lipids mediators, apoptosis, pro-inflammatory mediators, and angiogenesis. Through these mechanisms, RSV could prevent age-related ocular diseases (i.e., AMD, glaucoma, cataract, and DR) and could protect eyes against environmental factors (such as diabetes, hypertension, stress, UV light, acrolein found in cigarette smoke, and air pollution). Finally, through its pleiotropic properties/mechanisms of action, RSV could constitute a good candidate to prevent ocular diseases and may provide a novel strategy to enhance the efficacy of therapy currently used. More preclinical studies are required to provide further insights into RSV's potential adjuvant activity.

13. Methods

For this review, a systematic search of PubMed (https://pubmed.ncbi.nlm.nih.gov/) was conducted to identify studies on RSV in ocular cells, experimental animals, or humans in relation to ocular diseases up to December 2020. The search term "resveratrol" was used in combination with "ocular diseases," "eye diseases," "retinal cells," "oxidative stress," "reactive oxygen species" (ROS), "age-related macular degeneration," "AMD," "glaucoma," "cataract," "diabetic retinopathy," "corneal infection," "vitreoretinopathy," "epigenetic," and "clinical trials." The search was limited to English-language studies.

Author Contributions: Conceptualization, D.D. and V.A. writing—original draft preparation, D.D.; writing—review and editing, C.C., F.C. and J.X.; visualization, C.C. and J.X.; supervision, D.D.; funding acquisition, D.D. All authors have read and agreed to the published version of the manuscript.

Funding: This work was supported by grants from the ANRT N◦2016/0003, by a French Government grant managed by the French National Research Agency under the program "Investissements d'Avenir," reference ANR-11-LABX-0021, the Conseil Régional Bourgogne, Franche-Comte, the FEDER (European Funding for Regional Economic Development), and the "Bureau Interprofessionnel des Vins de Bourgogne" (BIVB). The authors thank Miss Isabella Athanassiou for valuable English corrections.

Conflicts of Interest: The authors declare that there are no conflicts of interest

References

1. Pascolini, D.; Mariotti, S.P. Global estimates of visual impairment: 2010. *Br. J. Ophthalmol.* **2012**, *96*, 614–618, doi:10.1136/bjophthalmol-2011-300539.
2. Ghiringhelli, F.; Rebe, C.; Hichami, A.; Delmas, D. Immunomodulation and anti-inflammatory roles of polyphenols as anticancer agents. *Anticancer Agents Med. Chem.* **2012**, *12*, 852–873, doi:10.2174/187152012802650048.
3. Afaq, F.; Adhami, V.M.; Ahmad, N.; Mukhtar, H. Botanical antioxidants for chemoprevention of photocarcinogenesis. *Front. Biosci.* **2002**, *7*, d784–d792.
4. Delmas, D.; Xiao, J. Natural Polyphenols Properties: Chemopreventive and Chemosensitizing Activities. *Anticancer Agents Med. Chem.* **2012**, *12*, 835, doi: 10.2174/187152012802650093.
5. Delmas, D.; Jannin, B.; Latruffe, N. Resveratrol: Preventing properties against vascular alterations and ageing. *Mol. Nutr. Food Res.* **2005**, *49*, 377–395.
6. Delmas, D.; Limagne, E.; Ghiringhelli, F.; Aires, V. Immune Th17 lymphocytes play a critical role in the multiple beneficial properties of resveratrol. *Food. Chem. Toxicol.* **2020**, *137*, 111091, doi:10.1016/j.fct.2019.111091.
7. Delmas, D.; Solary, E.; Latruffe, N. Resveratrol, a phytochemical inducer of multiple cell death pathways: Apoptosis, autophagy and mitotic catastrophe. *Curr. Med. Chem.* **2011**, *18*, 1100–1121.
8. Baur, J.A.; Sinclair, D.A. Therapeutic potential of resveratrol: The in vivo evidence. *Nat. Rev. Drug. Discov.* **2006**, *5*, 493–506.
9. Takaoka, M. Of the phenolic substances of white hellebore (Veratrum grandiflorum Loes. fil.). *J. Fac. Sci. Hokkaido Imp. Univ.* **1940**, *3*, 1–16.
10. Lanz, T.; Tropf, S.; Marner, F.J.; Schroder, J.; Schroder, G. The role of cysteines in polyketide synthases. Site-directed mutagenesis of resveratrol and chalcone synthases, two key enzymes in different plant-specific pathways. *J. Biol. Chem.* **1991**, *266*, 9971–9976.
11. Hanawa, F.; Tahara, S.; Mizutani, J. Antifungal stress compounds from Veratrum grandiflorum leaves treated with cupric chloride. *Phytochemistry* **1992**, *31*, 3005–3007.
12. Chung, M.I.; Teng, C.M.; Cheng, K.L.; Ko, F.N.; Lin, C.N. An antiplatelet principle of Veratrum formosanum. *Planta Med.* **1992**, *58*, 274–276.
13. Nomura, S.; Kanagawa, H.; Makimoto, A. Chemical constituents of polygonaceous plants. I. Studies on the components of Ko-jo-kon. (Polygonum cuspitadum SIEB et ZUCC). *Yakugaku Zasshi* **1963**, *83*, 988–990.
14. Kubo, M.; Kimura, Y.; Shin, H.; Haneda, T.; Tani, T.; Namba, K. Studies on the antifungal substance of crude drug (II). On the roots of Polygonum cuspidatum Sieb. et Zucc. (Polygonaceae). *Shoyakugaku Zashi* **1981**, *35*, 58–61.
15. Hathway, D.E.; Seakins, J.W. Hydroxystilbenes of Eucalyptus wandoo. *Biochem. J.* **1959**, *72*, 369–374.
16. Hillis, W.; Hart, J.; Yazaki, Y. Polyphenols of Eucalyptus sideroxylon wood. *Phytochemistry* **1974**, *13*, 1591–1595.

17. Rolfs, C.; Kindl, H. Stilbene synthase and chalcone synthase. Two different constitutive enzymes in cultured cells of Picea excels. *Plant Physiol.* **1974**, *75*, 489–492.
18. Anjaneyulu, A.; Reddy, A.; Reddy, D.; Ward, R.; Adhikesavalu, D.; Cameron, T. Prachin: A new dibenzo (2,3-6,7) oxepin derivative from Bauhinia racemosa lamk. *Tetrahedon* **1984**, *40*, 4245–4252.
19. Kumar, R.; Jyostna, D.; Krupadanam, G.; Srimannarayana, G. Phenanthrene and stilbenes from Pterolobium hexapetallum. *Phytochemistry* **1988**, *27*, 3625–3626.
20. Ingham, J. 3,5,4′-Trihydroxystilbene as aphytoalexin from groundnuts (arachis hypogaea). *Phytochemistry* **1976**, *15*, 1791–1793.
21. Rolfs, C.; Fritzemeier, K.; Kindl, H. Cultured cells of arachis hypogaea susceptible to induction of stilbene synthase (resveratrol-forming). *Plant Cell Rep.* **1981**, *1*, 83–85.
22. Fritzemeier, K.; Rolfs, C.; Pfau, J.; Kindl, H. Action of ultraviolet-C on stilbene formation in callus of Arachis hypogaea. *Planta* **1983**, *159*, 25–29.
23. Schoppner, A.; Kindl, H. Purification and properties of a stilbene synthase from induced cell suspension cultures of peanut. *J. Biol. Chem.* **1984**, *259*, 6806–6811.
24. Ibern-Gomez, M.; Roig-Perez, S.; Lamuela-Raventos, R.M.; de la Torre-Boronat, M.C. Resveratrol and piceid levels in natural and blended peanut butters. *J. Agric. Food Chem.* **2000**, *48*, 6352–6354.
25. Langcake, P.; Pryce, R.J. A new class of phytoalexins from grapevines. *Experientia* **1977**, *33*, 151–152.
26. Langcake, P.; Cornford, C.; Pryce, R. Identification of pterostilbene as a phytoalexin from Vitis vinifera leaves. *Phytochemistry* **1979**, *66*, 1025–1027.
27. Langcake, P.; Pryce, R. The production of resveratrol and the viniferins by grapevines in response to ultra-violet irradiation. *Phytochemistry* **1977**, *16*, 1193–1196.
28. Jeandet, P.; Bessis, R.; Maume, B.; Sbaghi, M. Analysis of resveratrol in selected California wines by a new HPLC method. *J. Wine Res.* **1993**, *4*, 79–85.
29. Hoos, G.; Blaich, R. Metabolism of stilbene phytoalexins in grapevines: Oxidation of resveratrol in single cell culture. *Vitis* **1988**, *27*, 1–12.
30. Jeandet, P.; Bessis, R.; Sbaghi, M.; P, M. Occurence of a resveratrol-∂-D-glucoside in wine. *Vitis* **1994**, *33*, 183–184.
31. Waterhouse, A.; Lamuele-Raventos, R. The occurence of piceid, a stilbene glucoside in grape berries. *Phytochemistry* **1994**, *37*, 581–573.
32. Goldberg, D.; Karumanchiri, A.; Diamandis, E.; Soleas, G. The assay of resveratrol glycosides and isomers in wine by direct-injection HPLC. *J. Chromatogr. A* **1995**, *708*, 89–98.
33. Callemien, D.; Jerkovic, V.; Rozenberg, R.; Collin, S. Hop as an Interesting Source of Resveratrol for Brewers: Optimization of the Extraction and Quantitative Study by Liquid Chromatography/Atmospheric Pressure Chemical Ionization Tandem Mass Spectrometry. *J. Agric. Food Chem.* **2005**, *53*, 424–429.
34. Burns, J.; Yokota, T.; Ashihara, H.; Lean, M.E.; Crozier, A. Plant foods and herbal sources of resveratrol. *J. Agric. Food Chem.* **2002**, *50*, 3337–3340.
35. Careri, M.; Corradini, C.; Elviri, L.; Nicoletti, I.; Zagnoni, I. Direct HPLC analysis of quercetin and trans-resveratrol in red wine, grape, and winemaking byproducts. *J. Agric. Food Chem.* **2003**, *51*, 5226–5231.
36. Lyons, M.M.; Yu, C.; Toma, R.B.; Cho, S.Y.; Reiboldt, W.; Lee, J.; van Breemen, R.B. Resveratrol in raw and baked blueberries and bilberries. *J. Agric. Food Chem.* **2003**, *51*, 5867–5870.
37. Kris-Etherton, P.M.; Keen, C.L. Evidence that the antioxidant flavonoids in tea and cocoa are beneficial for cardiovascular health. *Curr. Opin Lipidol.* **2002**, *13*, 41–49.
38. Jang, M.; Cai, L.; Udeani, G.O.; Slowing, K.V.; Thomas, C.F.; Beecher, C.W.; Fong, H.H.; Farnsworth, N.R.; Kinghorn, A.D.; Mehta, R.G.; et al. Cancer chemopreventive activity of resveratrol, a natural product derived from grapes. *Science* **1997**, *275*, 218–220.
39. Belguendouz, L.; Fremont, L.; Linard, A. Resveratrol inhibits metal ion-dependent and independent peroxidation of porcine low-density lipoproteins. *Biochem. Pharm.* **1997**, *53*, 1347–1355.

40. Fremont, L.; Belguendouz, L.; Delpal, S. Antioxidant activity of resveratrol and alcohol-free wine polyphenols related to LDL oxidation and polyunsaturated fatty acids. *Life Sci.* **1999**, *64*, 2511–2521.
41. Fauconneau, B.; Waffo-Teguo, P.; Huguet, F.; Barrier, L.; Decendit, A.; Merillon, J.M. Comparative study of radical scavenger and antioxidant properties of phenolic compounds from Vitis vinifera cell cultures using in vitro tests. *Life Sci.* **1997**, *61*, 2103–2110.
42. Orallo, F.; Alvarez, E.; Camina, M.; Leiro, J.M.; Gomez, E.; Fernandez, P. The possible implication of trans-Resveratrol in the cardioprotective effects of long-term moderate wine consumption. *Mol. Pharm.* **2002**, *61*, 294–302.
43. Leiro, J.; Alvarez, E.; Arranz, J.A.; Laguna, R.; Uriarte, E.; Orallo, F. Effects of cis-resveratrol on inflammatory murine macrophages: Antioxidant activity and down-regulation of inflammatory genes. *J. Leukoc Biol.* **2004**, *75*, 1156–1165.
44. Shigematsu, S.; Ishida, S.; Hara, M.; Takahashi, N.; Yoshimatsu, H.; Sakata, T.; Korthuis, R.J. Resveratrol, a red wine constituent polyphenol, prevents superoxide-dependent inflammatory responses induced by ischemia/reperfusion, platelet-activating factor, or oxidants. *Free Radic. Biol. Med.* **2003**, *34*, 810–817.
45. Zhong, M.; Cheng, G.F.; Wang, W.J.; Guo, Y.; Zhu, X.Y.; Zhang, J.T. Inhibitory effect of resveratrol on interleukin 6 release by stimulated peritoneal macrophages of mice. *Phytomedicine* **1999**, *6*, 79–84.
46. Feng, Y.H.; Zou, J.P.; Li, X.Y. Effects of resveratrol and ethanol on production of pro-inflammatory factors from endotoxin activated murine macrophages. *Acta Pharm. Sin.* **2002**, *23*, 1002–1006.
47. Pace-Asciak, C.R.; Rounova, O.; Hahn, S.E.; Diamandis, E.P.; Goldberg, D.M. Wines and grape juices as modulators of platelet aggregation in healthy human subjects. *Clin. Chim. Acta* **1996**, *246*, 163–182.
48. Olas, B.; Wachowicz, B.; Stochmal, A.; Oleszek, W. Anti-platelet effects of different phenolic compounds from Yucca schidigera Roezl. bark. *Platelets* **2002**, *13*, 167–173.
49. Bertelli, A.A.; Giovannini, L.; Giannessi, D.; Migliori, M.; Bernini, W.; Fregoni, M.; Bertelli, A. Antiplatelet activity of synthetic and natural resveratrol in red wine. *Int. J. Tissue React.* **1995**, *17*, 1–3.
50. Delmas, D.; Lancon, A.; Colin, D.; Jannin, B.; Latruffe, N. Resveratrol as a chemopreventive agent: A promising molecule for fighting cancer. *Curr. Drug. Targets* **2006**, *7*, 423–442.
51. Han, L.; Zhou, R.; Niu, J.; McNutt, M.A.; Wang, P.; Tong, T. SIRT1 is regulated by a PPAR{gamma}-SIRT1 negative feedback loop associated with senescence. *Nucleic Acids Res.* **2010**, *38*, 7458–7471, doi:10.1093/nar/gkq609.
52. Khan, R.S.; Fonseca-Kelly, Z.; Callinan, C.; Zuo, L.; Sachdeva, M.M.; Shindler, K.S. SIRT1 activating compounds reduce oxidative stress and prevent cell death in neuronal cells. *Front. Cell Neurosci.* **2012**, *6*, 63, doi:10.3389/fncel.2012.00063.
53. Klein, R.; Peto, T.; Bird, A.; Vannewkirk, M.R. The epidemiology of age-related macular degeneration. *Am. J. Ophthalmol.* **2004**, *137*, 486–495, doi:10.1016/j.ajo.2003.11.069. S0002939403015095 [pii].
54. AREDS. Risk factors associated with age-related macular degeneration. A case-control study in the age-related eye disease study: Age-Related Eye Disease Study Report Number 3. *Ophthalmology* **2000**, *107*, 2224–2232, doi:S0161642000004097 [pii].
55. Seddon, J.M.; Willett, W.C.; Speizer, F.E.; Hankinson, S.E. A prospective study of cigarette smoking and age-related macular degeneration in women. *JAMA* **1996**, *276*, 1141–1146.
56. Cackett, P.; Yeo, I.; Cheung, C.M.; Vithana, E.N.; Wong, D.; Tay, W.T.; Tai, E.S.; Aung, T.; Wong, T.Y. Relationship of smoking and cardiovascular risk factors with polypoidal choroidal vasculopathy and age-related macular degeneration in Chinese persons. *Ophthalmology* **2011**, *118*, 846–852, doi:10.1016/j.ophtha.2010.09.026.
57. Seddon, J.M.; George, S.; Rosner, B. Cigarette smoking, fish consumption, omega-3 fatty acid intake, and associations with age-related macular degeneration: The US Twin Study of Age-Related Macular Degeneration. *Arch. Ophthalmol.* **2006**, *124*, 995–1001, doi:10.1001/archopht.124.7.995.

58. Seddon, J.M.; Cote, J.; Davis, N.; Rosner, B. Progression of age-related macular degeneration: Association with body mass index, waist circumference, and waist-hip ratio. *Arch. Ophthalmol.* **2003**, *121*, 785–792, doi:10.1001/archopht.121.6.785.
59. Chen, Y.; Bedell, M.; Zhang, K. Age-related macular degeneration: Genetic and environmental factors of disease. *Mol. Interv.* **2010**, *10*, 271–281, doi:10/5/271 [pii]. 10.1124/mi.10.5.4.
60. Jarrett, S.G.; Boulton, M.E. Consequences of oxidative stress in age-related macular degeneration. *Mol. Asp. Med.* **2012**, *33*, 399–417, doi:10.1016/j.mam.2012.03.009.
61. Cai, J.; Nelson, K.C.; Wu, M.; Sternberg, P., Jr.; Jones, D.P. Oxidative damage and protection of the RPE. *Prog. Retin. Eye Res.* **2000**, *19*, 205–221, doi:S1350-9462(99)00009-9 [pii].
62. Group, A.-R.E.D.S.R. A randomized, placebo-controlled, clinical trial of high-dose supplementation with vitamins C and E, beta carotene, and zinc for age-related macular degeneration and vision loss: AREDS report no. 8. *Arch. Ophthalmol.* **2001**, *119*, 1417–1436, doi:ecs10161 [pii].
63. King, R.E.; Kent, K.D.; Bomser, J.A. Resveratrol reduces oxidation and proliferation of human retinal pigment epithelial cells via extracellular signal-regulated kinase inhibition. *Chem. Biol. Interact* **2005**, *151*, 143–149.
64. Yang, Y.; Wu, Z.Z.; Cheng, Y.L.; Lin, W.; Qu, C. Resveratrol protects against oxidative damage of retinal pigment epithelium cells by modulating SOD/MDA activity and activating Bcl-2 expression. *Eur. Rev. Med. Pharm. Sci* **2019**, *23*, 378–388, doi:10.26355/eurrev_201901_16786.
65. Sheu, S.J.; Liu, N.C.; Chen, J.L. Resveratrol protects human retinal pigment epithelial cells from acrolein-induced damage. *J. Ocul. Pharm.* **2010**, *26*, 231–236.
66. Mimura, T.; Kaji, Y.; Noma, H.; Funatsu, H.; Okamoto, S. The role of SIRT1 in ocular aging. *Exp. Eye Res.* **2013**, *116C*, 17–26, doi:10.1016/j.exer.2013.07.017.
67. Bhattarai, N.; Korhonen, E.; Toppila, M.; Koskela, A.; Kaarniranta, K.; Mysore, Y.; Kauppinen, A. Resvega Alleviates Hydroquinone-Induced Oxidative Stress in ARPE-19 Cells. *Int. J. Mol. Sci.* **2020**, *21*, doi:10.3390/ijms21062066.
68. Neal, S.E.; Buehne, K.L.; Besley, N.A.; Yang, P.; Silinski, P.; Hong, J.; Ryde, I.T.; Meyer, J.N.; Jaffe, G.J. Resveratrol Protects Against Hydroquinone-Induced Oxidative Threat in Retinal Pigment Epithelial Cells. *Invest. Ophthalmol. Vis. Sci.* **2020**, *61*, 32, doi:10.1167/iovs.61.4.32.
69. Sheu, S.J.; Liu, N.C.; Ou, C.C.; Bee, Y.S.; Chen, S.C.; Lin, H.C.; Chan, J.Y. Resveratrol stimulates mitochondrial bioenergetics to protect retinal pigment epithelial cells from oxidative damage. *Invest. Ophthalmol. Vis. Sci.* **2013**, *54*, 6426–6438, doi:10.1167/iovs.13-12024.
70. Chan, C.M.; Huang, C.H.; Li, H.J.; Hsiao, C.Y.; Su, C.C.; Lee, P.L.; Hung, C.F. Protective effects of resveratrol against UVA-induced damage in ARPE19 cells. *Int. J. Mol. Sci.* **2015**, *16*, 5789–5802, doi:10.3390/ijms16035789.
71. Dugas, B.; Charbonnier, S.; Baarine, M.; Ragot, K.; Delmas, D.; Menetrier, F.; Lherminier, J.; Malvitte, L.; Khalfaoui, T.; Bron, A.; et al. Effects of oxysterols on cell viability, inflammatory cytokines, VEGF, and reactive oxygen species production on human retinal cells: Cytoprotective effects and prevention of VEGF secretion by resveratrol. *Eur. J. Nutr.* **2010**, *49*, 435–446, doi:10.1007/s00394-010-0102-2.
72. Vayssiere, J.L.; Petit, P.X.; Risler, Y.; Mignotte, B. Commitment to apoptosis is associated with changes in mitochondrial biogenesis and activity in cell lines conditionally immortalized with simian virus 40. *Proc. Natl. Acad. Sci. USA* **1994**, *91*, 11752–11756.
73. Zamzami, N.; Marchetti, P.; Castedo, M.; Zanin, C.; Vayssiere, J.L.; Petit, P.X.; Kroemer, G. Reduction in mitochondrial potential constitutes an early irreversible step of programmed lymphocyte death in vivo. *J. Exp. Med.* **1995**, *181*, 1661–1672.
74. Wallace, D.C. Mitochondrial diseases in man and mouse. *Science* **1999**, *283*, 1482–1488.
75. Zini, R.; Morin, C.; Bertelli, A.; Bertelli, A.A.; Tillement, J.P. Effects of resveratrol on the rat brain respiratory chain. *Drugs Exp. Clin. Res.* **1999**, *25*, 87–97.
76. Yen, G.C.; Duh, P.D.; Lin, C.W. Effects of resveratrol and 4-hexylresorcinol on hydrogen peroxide-induced oxidative DNA damage in human lymphocytes. *Free Radic Res.* **2003**, *37*, 509–514.

77. Kampa, M.; Hatzoglou, A.; Notas, G.; Damianaki, A.; Bakogeorgou, E.; Gemetzi, C.; Kouroumalis, E.; Martin, P.M.; Castanas, E. Wine antioxidant polyphenols inhibit the proliferation of human prostate cancer cell lines. *Nutr. Cancer* **2000**, *37*, 223–233.
78. Sainz, R.M.; Mayo, J.C.; Tan, D.X.; Lopez-Burillo, S.; Natarajan, M.; Reiter, R.J. Antioxidant activity of melatonin in Chinese hamster ovarian cells: Changes in cellular proliferation and differentiation. *Biochem. Biophys. Res. Commun.* **2003**, *302*, 625–634.
79. Lopez-Burillo, S.; Tan, D.X.; Mayo, J.C.; Sainz, R.M.; Manchester, L.C.; Reiter, R.J. Melatonin, xanthurenic acid, resveratrol, EGCG, vitamin C and alpha-lipoic acid differentially reduce oxidative DNA damage induced by Fenton reagents: A study of their individual and synergistic actions. *J. Pineal Res.* **2003**, *34*, 269–277.
80. Kasdallah-Grissa, A.; Mornagui, B.; Aouani, E.; Hammami, M.; El May, M.; Gharbi, N.; Kamoun, A.; El-Fazaa, S. Resveratrol, a red wine polyphenol, attenuates ethanol-induced oxidative stress in rat liver. *Life Sci.* **2006**., *80*, 1033–1039.
81. Hu, Y.; Rahlfs, S.; Mersch-Sundermann, V.; Becker, K. Resveratrol modulates mRNA transcripts of genes related to redox metabolism and cell proliferation in non-small-cell lung carcinoma cells. *Biol. Chem.* **2007**, *388*, 207–219.
82. Sengottuvelan, M.; Deeptha, K.; Nalini, N. Resveratrol ameliorates DNA damage, prooxidant and antioxidant imbalance in 1,2-dimethylhydrazine induced rat colon carcinogenesis. *Chem. Biol. Interact* **2009**, *181*, 193–201.
83. Sengottuvelan, M.; Senthilkumar, R.; Nalini, N. Modulatory influence of dietary resveratrol during different phases of 1,2-dimethylhydrazine induced mucosal lipid-peroxidation, antioxidant status and aberrant crypt foci development in rat colon carcinogenesis. *Biochim. Biophys. Acta* **2006**, *1760*, 1175–1183.
84. Sener, G.; Topaloglu, N.; Ozer Sehirli, A.; Ercan, F.; Gedik, N. Resveratrol alleviates bleomycin-induced lung injury in rats. *Pulm. Pharm.* **2006**, *20*, 642–649.
85. Jeganathan, V.S.; Wang, J.J.; Wong, T.Y. Ocular associations of diabetes other than diabetic retinopathy. *Diabetes Care* **2008**, *31*, 1905–1912, doi:10.2337/dc08-0342.
86. Bhatt, J.K.; Thomas, S.; Nanjan, M.J. Resveratrol supplementation improves glycemic control in type 2 diabetes mellitus. *Nutr. Res.* **2012**, *32*, 537–541, doi:10.1016/j.nutres.2012.06.003.
87. Poulsen, M.M.; Vestergaard, P.F.; Clasen, B.F.; Radko, Y.; Christensen, L.P.; Stodkilde-Jorgensen, H.; Moller, N.; Jessen, N.; Pedersen, S.B.; Jorgensen, J.O. High-dose resveratrol supplementation in obese men: An investigator-initiated, randomized, placebo-controlled clinical trial of substrate metabolism, insulin sensitivity, and body composition. *Diabetes* **2013**, *62*, 1186–1195, doi:db12-0975 [pii]. 10.2337/db12-0975.
88. Timmers, S.; Konings, E.; Bilet, L.; Houtkooper, R.H.; van de Weijer, T.; Goossens, G.H.; Hoeks, J.; van der Krieken, S.; Ryu, D.; Kersten, S.; et al. Calorie restriction-like effects of 30 days of resveratrol supplementation on energy metabolism and metabolic profile in obese humans. *Cell Metab.* **2011**, *14*, 612–622.
89. Yoshino, J.; Conte, C.; Fontana, L.; Mittendorfer, B.; Imai, S.; Schechtman, K.B.; Gu, C.; Kunz, I.; Rossi Fanelli, F.; Patterson, B.W.; et al. Resveratrol supplementation does not improve metabolic function in nonobese women with normal glucose tolerance. *Cell Metab.* **2012**, *16*, 658–664, doi:10.1016/j.cmet.2012.09.015.
90. Crandall, J.P.; Oram, V.; Trandafirescu, G.; Reid, M.; Kishore, P.; Hawkins, M.; Cohen, H.W.; Barzilai, N. Pilot study of resveratrol in older adults with impaired glucose tolerance. *J. Gerontol. A Biol. Sci. Med. Sci.* **2012**, *67*, 1307–1312, doi:10.1093/gerona/glr235.
91. Brasnyo, P.; Molnar, G.A.; Mohas, M.; Marko, L.; Laczy, B.; Cseh, J.; Mikolas, E.; Szijarto, I.A.; Merei, A.; Halmai, R.; et al. Resveratrol improves insulin sensitivity, reduces oxidative stress and activates the Akt pathway in type 2 diabetic patients. *Br. J. Nutr.* **2011**, *106*, 383–389.
92. Morselli, E.; Maiuri, M.C.; Markaki, M.; Megalou, E.; Pasparaki, A.; Palikaras, K.; Criollo, A.; Galluzzi, L.; Malik, S.A.; Vitale, I.; et al. The life span-prolonging effect of sirtuin-1 is mediated by autophagy. *Autophagy* **2010**, *6*, 186–188, doi:10817 [pii].

93. Gurusamy, N.; Lekli, I.; Mukherjee, S.; Ray, D.; Ahsan, M.K.; Gherghiceanu, M.; Popescu, L.M.; Das, D.K. Cardioprotection by resveratrol: A novel mechanism via autophagy involving the mTORC2 pathway. *Cardiovasc Res.* **2010,** *86*, 103–112.
94. Josifovska, N.; Albert, R.; Nagymihaly, R.; Lytvynchuk, L.; Moe, M.C.; Kaarniranta, K.; Vereb, Z.J.; Petrovski, G. Resveratrol as Inducer of Autophagy, Pro-Survival, and Anti-Inflammatory Stimuli in Cultured Human RPE Cells. *Int. J. Mol. Sci.* **2020**, *21*, doi:10.3390/ijms21030813.
95. Koskela, A.; Reinisalo, M.; Petrovski, G.; Sinha, D.; Olmiere, C.; Karjalainen, R.; Kaarniranta, K. Nutraceutical with Resveratrol and Omega-3 Fatty Acids Induces Autophagy in ARPE-19 Cells. *Nutrients* **2016**, *8*, doi:10.3390/nu8050284.
96. Alaimo, A.; Di Santo, M.C.; Dominguez Rubio, A.P.; Chaufan, G.; Garcia Linares, G.; Perez, O.E. Toxic effects of A2E in human ARPE-19 cells were prevented by resveratrol: A potential nutritional bioactive for age-related macular degeneration treatment. *Arch. Toxicol.* **2020**, *94*, 553–572, doi:10.1007/s00204-019-02637-w.
97. Kang, J.H.; Choung, S.Y. Protective effects of resveratrol and its analogs on age-related macular degeneration in vitro. *Arch. Pharm. Res.* **2016**, *39*, 1703–1715, doi:10.1007/s12272-016-0839-0.
98. Limagne, E.; Lancon, A.; Delmas, D.; Cherkaoui-Malki, M.; Latruffe, N. Resveratrol Interferes with IL1-beta-Induced Pro-Inflammatory Paracrine Interaction between Primary Chondrocytes and Macrophages. *Nutrients* **2016**, *8*, doi:10.3390/nu8050280.
99. Parmeggiani, F.; Romano, M.R.; Costagliola, C.; Semeraro, F.; Incorvaia, C.; D'Angelo, S.; Perri, P.; De Palma, P.; De Nadai, K.; Sebastiani, A. Mechanism of inflammation in age-related macular degeneration. *Mediat. Inflamm.* **2012**, *2012*, 546786, doi:10.1155/2012/546786.
100. Chen, J.; Smith, L.E. Protective inflammasome activation in AMD. *Nat Med* **2012**, *18*, 658–660, doi:nm.2761 [pii]. 10.1038/nm.2761.
101. Rosenbaum, J.T. Eyeing macular degeneration--few inflammatory remarks. *N. Engl. J. Med.* **2012**, *367*, 768–770, doi:10.1056/NEJMcibr1204973.
102. Losso, J.N.; Truax, R.E.; Richard, G. trans-resveratrol inhibits hyperglycemia-induced inflammation and connexin downregulation in retinal pigment epithelial cells. *J. Agric. Food Chem.* **2010**, *58*, 8246–8252.
103. Kutty, R.K.; Samuel, W.; Abay, R.; Cherukuri, A.; Nagineni, C.N.; Duncan, T.; Jaworski, C.; Vijayasarathy, C.; Redmond, T.M. Resveratrol attenuates CXCL11 expression induced by proinflammatory cytokines in retinal pigment epithelial cells. *Cytokine* **2015**, *74*, 335–338, doi:10.1016/j.cyto.2015.03.016.
104. Qin, S.; Lu, Y.; Rodrigues, G.A. Resveratrol protects RPE cells from sodium iodate by modulating PPARalpha and PPARdelta. *Exp. Eye Res.* **2014**, *118*, 100–108, doi:10.1016/j.exer.2013.11.010.
105. Ferrara, N. Vascular endothelial growth factor and age-related macular degeneration: From basic science to therapy. *Nat. Med.* **2010**, *16*, 1107–1111, doi:nm1010-1107 [pii]. 10.1038/nm1010-1107.
106. Kim, Y.H.; Kim, Y.S.; Roh, G.S.; Choi, W.S.; Cho, G.J. Resveratrol blocks diabetes-induced early vascular lesions and vascular endothelial growth factor induction in mouse retinas. *Acta Ophthalmol.* **2011**, *89*, e31–e37.
107. Nagineni, C.N.; Raju, R.; Nagineni, K.K.; Kommineni, V.K.; Cherukuri, A.; Kutty, R.K.; Hooks, J.J.; Detrick, B. Resveratrol Suppresses Expression of VEGF by Human Retinal Pigment Epithelial Cells: Potential Nutraceutical for Age-related Macular Degeneration. *Aging Dis.* **2014**, *5*, 88–100, doi:10.14366/AD.2014.050088.
108. Balaiya, S.; Murthy, R.K.; Chalam, K.V. Resveratrol inhibits proliferation of hypoxic choroidal vascular endothelial cells. *Mol. Vis.* **2013**, *19*, 2385–2392.
109. Nagai, N.; Kubota, S.; Tsubota, K.; Ozawa, Y. Resveratrol prevents the development of choroidal neovascularization by modulating AMP-activated protein kinase in macrophages and other cell types. *J. Nutr. Biochem.* **2014**, *25*, 1218–1225, doi:10.1016/j.jnutbio.2014.05.015.
110. Quigley, H.A.; Broman, A.T. The number of people with glaucoma worldwide in 2010 and 2020. *Br. J. Ophthalmol.* **2006**, *90*, 262–267, doi:10.1136/bjo.2005.081224.

111. Barkana, Y.; Dorairaj, S. Re: Tham et al.: Global prevalence of glaucoma and projections of glaucoma burden through 2040: A systematic review and meta-analysis (Ophthalmology 2014;121:2081-90). *Ophthalmology* **2015**, *122*, e40–e41, doi:10.1016/j.ophtha.2014.11.030.
112. Hecht, I.; Achiron, A.; Man, V.; Burgansky-Eliash, Z. Modifiable factors in the management of glaucoma: A systematic review of current evidence. *Graefes Arch. Clin. Exp. Ophthalmol.* **2017**, *255*, 789–796, doi:10.1007/s00417-016-3518-4.
113. Bola, C.; Bartlett, H.; Eperjesi, F. Resveratrol and the eye: Activity and molecular mechanisms. *Graefes Arch. Clin. Exp. Ophthalmol.* **2014**, *252*, 699–713, doi:10.1007/s00417-014-2604-8.
114. Cao, K.; Ishida, T.; Fang, Y.; Shinohara, K.; Li, X.; Nagaoka, N.; Ohno-Matsui, K.; Yoshida, T. Protection of the Retinal Ganglion Cells: Intravitreal Injection of Resveratrol in Mouse Model of Ocular Hypertension. *Invest. Ophthalmol. Vis. Sci.* **2020**, *61*, 13, doi:10.1167/iovs.61.3.13.
115. Zhang, X.; Feng, Y.; Wang, Y.; Wang, J.; Xiang, D.; Niu, W.; Yuan, F. Resveratrol ameliorates disorders of mitochondrial biogenesis and dynamics in a rat chronic ocular hypertension model. *Life Sci.* **2018**, *207*, 234–245, doi:10.1016/j.lfs.2018.06.010.
116. Ammar, D.A.; Hamweyah, K.M.; Kahook, M.Y. Antioxidants Protect Trabecular Meshwork Cells From Hydrogen Peroxide-Induced Cell Death. *Transl. Vis. Sci. Technol.* **2012**, *1*, 4, doi:10.1167/tvst.1.1.4.
117. Ghosh, A.K.; Rao, V.R.; Wisniewski, V.J.; Zigrossi, A.D.; Floss, J.; Koulen, P.; Stubbs, E.B., Jr.; Kaja, S. Differential Activation of Glioprotective Intracellular Signaling Pathways in Primary Optic Nerve Head Astrocytes after Treatment with Different Classes of Antioxidants. *Antioxid. (Basel)* **2020**, *9*, doi:10.3390/antiox9040324.
118. Chen, S.; Fan, Q.; Li, A.; Liao, D.; Ge, J.; Laties, A.M.; Zhang, X. Dynamic mobilization of PGC-1alpha mediates mitochondrial biogenesis for the protection of RGC-5 cells by resveratrol during serum deprivation. *Apoptosis* **2013**, *18*, 786–799, doi:10.1007/s10495-013-0837-3.
119. Goyal, A.; Srivastava, A.; Sihota, R.; Kaur, J. Evaluation of oxidative stress markers in aqueous humor of primary open angle glaucoma and primary angle closure glaucoma patients. *Curr. Eye Res.* **2014**, *39*, 823–829, doi:10.3109/02713683.2011.556299.
120. Abu-Amero, K.K.; Kondkar, A.A.; Chalam, K.V. Resveratrol and Ophthalmic Diseases. *Nutrients* **2016**, *8*, 200, doi:10.3390/nu8040200.
121. Pang, Y.; Qin, M.; Hu, P.; Ji, K.; Xiao, R.; Sun, N.; Pan, X.; Zhang, X. Resveratrol protects retinal ganglion cells against ischemia induced damage by increasing Opa1 expression. *Int. J. Mol. Med.* **2020**, *46*, 1707–1720, doi:10.3892/ijmm.2020.4711.
122. Yu, Z.; Yanxia, H.; Limin, G.; Yun, Z.; Mingxuan, Z.; Fuyao, X.; Cheng, T.; Jufang, H.; Dan, C. Melatonin alleviates pyroptosis of retinal neurons following acute intraocular hypertension. *Cns Neurol. Disord. Drug Targets* **2020**, doi:10.2174/1871527319666201012125149.
123. Seong, H.; Ryu, J.; Yoo, W.S.; Kim, S.J.; Han, Y.S.; Park, J.M.; Kang, S.S.; Seo, S.W. Resveratrol Ameliorates Retinal Ischemia/Reperfusion Injury in C57BL/6J Mice via Downregulation of Caspase-3. *Curr. Eye Res.* **2017**, *42*, 1650–1658, doi:10.1080/02713683.2017.1344713.
124. Luo, H.; Zhuang, J.; Hu, P.; Ye, W.; Chen, S.; Pang, Y.; Li, N.; Deng, C.; Zhang, X. Resveratrol Delays Retinal Ganglion Cell Loss and Attenuates Gliosis-Related Inflammation From Ischemia-Reperfusion Injury. *Invest. Ophthalmol. Vis. Sci.* **2018**, *59*, 3879–3888, doi:10.1167/iovs.18-23806.
125. Lindsey, J.D.; Duong-Polk, K.X.; Hammond, D.; Leung, C.K.; Weinreb, R.N. Protection of injured retinal ganglion cell dendrites and unfolded protein response resolution after long-term dietary resveratrol. *Neurobiol. Aging* **2015**, *36*, 1969–1981, doi:10.1016/j.neurobiolaging.2014.12.021.
126. Pasovic, L.; Eidet, J.R.; Lyberg, T.; Messelt, E.B.; Aabel, P.; Utheim, T.P. Antioxidants Improve the Viability of Stored Adult Retinal Pigment Epithelial-19 Cultures. *Ophthalmol* **2014**, *3*, 49–61, doi:10.1007/s40123-014-0024-9.
127. Avotri, S.; Eatman, D.; Russell-Randall, K. Effects of Resveratrol on Inflammatory Biomarkers in Glaucomatous Human Trabecular Meshwork Cells. *Nutrients* **2019**, *11*, doi:10.3390/nu11050984.

128. Luna, C.; Li, G.; Liton, P.B.; Qiu, J.; Epstein, D.L.; Challa, P.; Gonzalez, P. Resveratrol prevents the expression of glaucoma markers induced by chronic oxidative stress in trabecular meshwork cells. *Food Chem. Toxicol.* **2009**, *47*, 198–204, doi:10.1016/j.fct.2008.10.029.
129. Razali, N.; Agarwal, R.; Agarwal, P.; Tripathy, M.; Kapitonova, M.Y.; Kutty, M.K.; Smirnov, A.; Khalid, Z.; Ismail, N.M. Topical trans-resveratrol ameliorates steroid-induced anterior and posterior segment changes in rats. *Exp. Eye Res.* **2016**, *143*, 9–16, doi:10.1016/j.exer.2015.09.014.
130. Razali, N.; Agarwal, R.; Agarwal, P.; Kumar, S.; Tripathy, M.; Vasudevan, S.; Crowston, J.G.; Ismail, N.M. Role of adenosine receptors in resveratrol-induced intraocular pressure lowering in rats with steroid-induced ocular hypertension. *Clin. Exp. Ophthalmol.* **2015**, *43*, 54–66, doi:10.1111/ceo.12375.
131. Pearson, K.J.; Baur, J.A.; Lewis, K.N.; Peshkin, L.; Price, N.L.; Labinskyy, N.; Swindell, W.R.; Kamara, D.; Minor, R.K.; Perez, E.; et al. Resveratrol delays age-related deterioration and mimics transcriptional aspects of dietary restriction without extending life span. *Cell Metab.* **2008**, *8*, 157–168, doi:10.1016/j.cmet.2008.06.011.
132. Singh, A.; Bodakhe, S.H. Resveratrol delay the cataract formation against naphthalene-induced experimental cataract in the albino rats. *J. Biochem. Mol. Toxicol.* **2020**, *34*, e22420, doi:10.1002/jbt.22420.
133. Smith, A.J.O.; Eldred, J.A.; Wormstone, I.M. Resveratrol Inhibits Wound Healing and Lens Fibrosis: A Putative Candidate for Posterior Capsule Opacification Prevention. *Invest. Ophthalmol. Vis. Sci.* **2019**, *60*, 3863–3877, doi:10.1167/iovs.18-26248.
134. Zheng, T.; Lu, Y. SIRT1 Protects Human Lens Epithelial Cells Against Oxidative Stress by Inhibiting p53-Dependent Apoptosis. *Curr. Eye Res.* **2016**, *41*, 1068–1075, doi:10.3109/02713683.2015.1093641.
135. Semeraro, F.; Morescalchi, F.; Cancarini, A.; Russo, A.; Rezzola, S.; Costagliola, C. Diabetic retinopathy, a vascular and inflammatory disease: Therapeutic implications. *Diabetes Metab.* **2019**, *45*, 517–527, doi:10.1016/j.diabet.2019.04.002.
136. Al-Shabrawey, M.; Smith, S. Prediction of diabetic retinopathy: Role of oxidative stress and relevance of apoptotic biomarkers. *Epma J.* **2010**, *1*, 56–72, doi:10.1007/s13167-010-0002-9.
137. Li, J.; Yu, S.; Ying, J.; Shi, T.; Wang, P. Resveratrol Prevents ROS-Induced Apoptosis in High Glucose-Treated Retinal Capillary Endothelial Cells via the Activation of AMPK/Sirt1/PGC-1alpha Pathway. *Oxid. Med. Cell Longev.* **2017**, *2017*, 7584691, doi:10.1155/2017/7584691.
138. Fathalipour, M.; Eghtedari, M.; Borges, F.; Silva, T.; Moosavi, F.; Firuzi, O.; Mirkhani, H. Caffeic Acid Alkyl Amide Derivatives Ameliorate Oxidative Stress and Modulate ERK1/2 and AKT Signaling Pathways in a Rat Model of Diabetic Retinopathy. *Chem. Biodivers* **2019**, *16*, e1900405, doi:10.1002/cbdv.201900405.
139. Soufi, F.G.; Mohammad-Nejad, D.; Ahmadieh, H. Resveratrol improves diabetic retinopathy possibly through oxidative stress-nuclear factor kappaB-apoptosis pathway. *Pharm. Rep.* **2012**, *64*, 1505–1514, doi:10.1016/s1734-1140(12)70948-9.
140. Yar, A.S.; Menevse, S.; Dogan, I.; Alp, E.; Ergin, V.; Cumaoglu, A.; Aricioglu, A.; Ekmekci, A.; Menevse, A. Investigation of ocular neovascularization-related genes and oxidative stress in diabetic rat eye tissues after resveratrol treatment. *J. Med. Food* **2012**, *15*, 391–398, doi:10.1089/jmf.2011.0135.
141. Reiter, C.E.; Wu, X.; Sandirasegarane, L.; Nakamura, M.; Gilbert, K.A.; Singh, R.S.; Fort, P.E.; Antonetti, D.A.; Gardner, T.W. Diabetes reduces basal retinal insulin receptor signaling: Reversal with systemic and local insulin. *Diabetes* **2006**, *55*, 1148–1156, doi:10.2337/diabetes.55.04.06.db05-0744.
142. Mohammad, G.; Abdelaziz, G.M.; Siddiquei, M.M.; Ahmad, A.; De Hertogh, G.; Abu El-Asrar, A.M. Cross-Talk between Sirtuin 1 and the Proinflammatory Mediator High-Mobility Group Box-1 in the Regulation of Blood-Retinal Barrier Breakdown in Diabetic Retinopathy. *Curr. Eye Res.* **2019**, *44*, 1133–1143, doi:10.1080/02713683.2019.1625406.

143. Chen, Y.; Meng, J.; Li, H.; Wei, H.; Bi, F.; Liu, S.; Tang, K.; Guo, H.; Liu, W. Resveratrol exhibits an effect on attenuating retina inflammatory condition and damage of diabetic retinopathy via PON1. *Exp. Eye Res.* **2019**, *181*, 356–366, doi:10.1016/j.exer.2018.11.023.
144. Ghadiri Soufi, F.; Arbabi-Aval, E.; Rezaei Kanavi, M.; Ahmadieh, H. Anti-inflammatory properties of resveratrol in the retinas of type 2 diabetic rats. *Clin. Exp. Pharm. Physiol.* **2015**, *42*, 63–68, doi:10.1111/1440-1681.12326.
145. Kowluru, R.A.; Santos, J.M.; Zhong, Q. Sirt1, a negative regulator of matrix metalloproteinase-9 in diabetic retinopathy. *Invest. Ophthalmol. Vis. Sci.* **2014**, *55*, 5653–5660, doi:10.1167/iovs.14-14383.
146. Higashi, Y.; Higashi, K.; Mori, A.; Sakamoto, K.; Ishii, K.; Nakahara, T. Anti-cataract Effect of Resveratrol in High-Glucose-Treated Streptozotocin-Induced Diabetic Rats. *Biol. Pharm. Bull.* **2018**, *41*, 1586–1592, doi:10.1248/bpb.b18-00328.
147. Ciddi, V.; Dodda, D. Therapeutic potential of resveratrol in diabetic complications: In vitro and in vivo studies. *Pharm. Rep.* **2014**, *66*, 799–803, doi:10.1016/j.pharep.2014.04.006.
148. Li, G.; Luna, C.; Navarro, I.D.; Epstein, D.L.; Huang, W.; Gonzalez, P.; Challa, P. Resveratrol prevention of oxidative stress damage to lens epithelial cell cultures is mediated by forkhead box O activity. *Invest. Ophthalmol. Vis. Sci.* **2011**, *52*, 4395–4401, doi:10.1167/iovs.10-6652.
149. Zheng, Y.; Liu, Y.; Ge, J.; Wang, X.; Liu, L.; Bu, Z.; Liu, P. Resveratrol protects human lens epithelial cells against H2O2-induced oxidative stress by increasing catalase, SOD-1, and HO-1 expression. *Mol. Vis.* **2010**, *16*, 1467–1474.
150. Singh, A.; Bodakhe, S.H. Biochemical Evidence Indicates the Preventive Effect of Resveratrol and Nicotinamide in the Treatment of STZ-induced Diabetic Cataract. *Curr. Eye Res.* **2020**, 1–12, doi:10.1080/02713683.2020.1782941.
151. Zeng, K.; Wang, Y.; Yang, N.; Wang, D.; Li, S.; Ming, J.; Wang, J.; Yu, X.; Song, Y.; Zhou, X.; et al. Resveratrol Inhibits Diabetic-Induced Muller Cells Apoptosis through MicroRNA-29b/Specificity Protein 1 Pathway. *Mol. Neurobiol.* **2017**, *54*, 4000–4014, doi:10.1007/s12035-016-9972-5.
152. Zeng, K.; Yang, N.; Wang, D.; Li, S.; Ming, J.; Wang, J.; Yu, X.; Song, Y.; Zhou, X.; Yang, Y. Resveratrol Prevents Retinal Dysfunction by Regulating Glutamate Transporters, Glutamine Synthetase Expression and Activity in Diabetic Retina. *Neurochem. Res.* **2016**, *41*, 1050–1064, doi:10.1007/s11064-015-1793-9.
153. Nadeem, A.; Javaid, K.; Sami, W.; Zafar, A.; Jahan, S.; Zaman, S.; Nagi, A. Inverse relationship of serum IL-17 with type-II diabetes retinopathy. *Clin. Lab.* **2013**, *59*, 1311–1317, doi:10.7754/clin.lab.2013.121140.
154. Liu, S.; Lin, Y.U.; Liu, X. Protective effects of SIRT1 in patients with proliferative diabetic retinopathy via the inhibition of IL-17 expression. *Exp. Med.* **2016**, *11*, 257–262, doi:10.3892/etm.2015.2877.
155. Limagne, E.; Thibaudin, M.; Euvrard, R.; Berger, H.; Chalons, P.; Vegan, F.; Humblin, E.; Boidot, R.; Rebe, C.; Derangere, V.; et al. Sirtuin-1 Activation Controls Tumor Growth by Impeding Th17 Differentiation via STAT3 Deacetylation. *Cell Rep.* **2017**, *19*, 746–759, doi:10.1016/j.celrep.2017.04.004.
156. Charteris, D.G. Proliferative vitreoretinopathy: Pathobiology, surgical management, and adjunctive treatment. *Br. J. Ophthalmol.* **1995**, *79*, 953–960, doi:10.1136/bjo.79.10.953.
157. Chen, C.L.; Chen, Y.H.; Tai, M.C.; Liang, C.M.; Lu, D.W.; Chen, J.T. Resveratrol inhibits transforming growth factor-beta2-induced epithelial-to-mesenchymal transition in human retinal pigment epithelial cells by suppressing the Smad pathway. *Drug Des. Devel.* **2017**, *11*, 163–173, doi:10.2147/DDDT.S126743.
158. Ishikawa, K.; He, S.; Terasaki, H.; Nazari, H.; Zhang, H.; Spee, C.; Kannan, R.; Hinton, D.R. Resveratrol inhibits epithelial-mesenchymal transition of retinal pigment epithelium and development of proliferative vitreoretinopathy. *Sci. Rep.* **2015**, *5*, 16386, doi:10.1038/srep16386.
159. Chan, C.M.; Chang, H.H.; Wang, V.C.; Huang, C.L.; Hung, C.F. Inhibitory effects of resveratrol on PDGF-BB-induced retinal pigment epithelial cell migration via PDGFRbeta, PI3K/Akt and MAPK pathways. *PLoS ONE* **2013**, *8*, e56819, doi:10.1371/journal.pone.0056819.

160. Aqeel, Y.; Iqbal, J.; Siddiqui, R.; Gilani, A.H.; Khan, N.A. Anti-Acanthamoebic properties of resveratrol and demethoxycurcumin. *Exp. Parasitol.* **2012**, *132*, 519–523, doi:10.1016/j.exppara.2012.09.007.
161. Chan, M.M. Antimicrobial effect of resveratrol on dermatophytes and bacterial pathogens of the skin. *Biochem. Pharm.* **2002**, *63*, 99–104, doi:10.1016/s0006-2952(01)00886-3.
162. Tsai, T.Y.; Chen, T.C.; Wang, I.J.; Yeh, C.Y.; Su, M.J.; Chen, R.H.; Tsai, T.H.; Hu, F.R. The effect of resveratrol on protecting corneal epithelial cells from cytotoxicity caused by moxifloxacin and benzalkonium chloride. *Invest. Ophthalmol. Vis. Sci.* **2015**, *56*, 1575–1584, doi:10.1167/iovs.14-15708.
163. Kubota, S.; Kurihara, T.; Ebinuma, M.; Kubota, M.; Yuki, K.; Sasaki, M.; Noda, K.; Ozawa, Y.; Oike, Y.; Ishida, S.; et al. Resveratrol prevents light-induced retinal degeneration via suppressing activator protein-1 activation. *Am. J. Pathol.* **2010**, *177*, 1725–1731, doi:10.2353/ajpath.2010.100098.
164. Zhang, H.; He, S.; Spee, C.; Ishikawa, K.; Hinton, D.R. SIRT1 mediated inhibition of VEGF/VEGFR2 signaling by Resveratrol and its relevance to choroidal neovascularization. *Cytokine* **2015**, *76*, 549–552, doi:10.1016/j.cyto.2015.06.019.
165. Maugeri, A.; Barchitta, M.; Mazzone, M.G.; Giuliano, F.; Basile, G.; Agodi, A. Resveratrol Modulates SIRT1 and DNMT Functions and Restores LINE-1 Methylation Levels in ARPE-19 Cells under Oxidative Stress and Inflammation. *Int. J. Mol. Sci.* **2018**, *19*, doi:10.3390/ijms19072118.
166. Peng, L.; Yuan, Z.; Ling, H.; Fukasawa, K.; Robertson, K.; Olashaw, N.; Koomen, J.; Chen, J.; Lane, W.S.; Seto, E. SIRT1 deacetylates the DNA methyltransferase 1 (DNMT1) protein and alters its activities. *Mol. Cell Biol.* **2011**, *31*, 4720–4734, doi:10.1128/MCB.06147-11.
167. Kubota, S.; Ozawa, Y.; Kurihara, T.; Sasaki, M.; Yuki, K.; Miyake, S.; Noda, K.; Ishida, S.; Tsubota, K. Roles of AMP-activated protein kinase in diabetes-induced retinal inflammation. *Invest. Ophthalmol. Vis. Sci.* **2011**, *52*, 9142–9148, doi:10.1167/iovs.11-8041.
168. Michan, S.; Juan, A.M.; Hurst, C.G.; Cui, Z.; Evans, L.P.; Hatton, C.J.; Pei, D.T.; Ju, M.; Sinclair, D.A.; Smith, L.E.; et al. Sirtuin1 over-expression does not impact retinal vascular and neuronal degeneration in a mouse model of oxygen-induced retinopathy. *PLoS ONE* **2014**, *9*, e85031, doi:10.1371/journal.pone.0085031.
169. Kadiyala, C.S.; Zheng, L.; Du, Y.; Yohannes, E.; Kao, H.Y.; Miyagi, M.; Kern, T.S. Acetylation of retinal histones in diabetes increases inflammatory proteins: Effects of minocycline and manipulation of histone acetyltransferase (HAT) and histone deacetylase (HDAC). *J. Biol. Chem.* **2012**, *287*, 25869–25880, doi:10.1074/jbc.M112.375204.
170. Pandian, S.; Jeevanesan, V.; Ponnusamy, C.; Natesan, S. RES-loaded pegylated CS NPs: For efficient ocular delivery. *Iet. Nanobiotechnol.* **2017**, *11*, 32–39, doi:10.1049/iet-nbt.2016.0069.
171. Natesan, S.; Pandian, S.; Ponnusamy, C.; Palanichamy, R.; Muthusamy, S.; Kandasamy, R. Co-encapsulated resveratrol and quercetin in chitosan and peg modified chitosan nanoparticles: For efficient intra ocular pressure reduction. *Int. J. Biol. Macromol.* **2017**, *104*, 1837–1845, doi:10.1016/j.ijbiomac.2017.04.117.
172. Bhatt, P.; Fnu, G.; Bhatia, D.; Shahid, A.; Sutariya, V. Nanodelivery of Resveratrol-Loaded PLGA Nanoparticles for Age-Related Macular Degeneration. *Aaps Pharmscitech* **2020**, *21*, 291, doi:10.1208/s12249-020-01836-4.
173. Rugina, D.; Ghiman, R.; Focsan, M.; Tabaran, F.; Copaciu, F.; Suciu, M.; Pintea, A.; Astilean, S. Resveratrol-delivery vehicle with anti-VEGF activity carried to human retinal pigmented epithelial cells exposed to high-glucose induced conditions. *Colloids Surf. B Biointerfaces* **2019**, *181*, 66–75, doi:10.1016/j.colsurfb.2019.04.022.
174. Vora, D.; Heruye, S.; Kumari, D.; Opere, C.; Chauhan, H. Preparation, Characterization and Antioxidant Evaluation of Poorly Soluble Polyphenol-Loaded Nanoparticles for Cataract Treatment. *Aaps Pharmscitech* **2019**, *20*, 163, doi:10.1208/s12249-019-1379-y.
175. Valdes-Sanchez, L.; Garcia-Delgado, A.B.; Montero-Sanchez, A.; de la Cerda, B.; Lucas, R.; Penalver, P.; Morales, J.C.; Bhattacharya, S.S.; Diaz-Corrales, F.J. The Resveratrol Prodrug JC19 Delays Retinal Degeneration in rd10 Mice. *Adv. Exp. Med. Biol.* **2019**, *1185*, 457–462, doi:10.1007/978-3-030-27378-1_75.

176. Ghanim, H.; Sia, C.L.; Korzeniewski, K.; Lohano, T.; Abuaysheh, S.; Marumganti, A.; Chaudhuri, A.; Dandona, P. A resveratrol and polyphenol preparation suppresses oxidative and inflammatory stress response to a high-fat, high-carbohydrate meal. *J. Clin. Endocrinol. Metab.* **2011**, *96*, 1409–1414, doi:10.1210/jc.2010-1812.
177. Lin, C.T.; Sun, X.Y.; Lin, A.X. Supplementation with high-dose trans-resveratrol improves ultrafiltration in peritoneal dialysis patients: A prospective, randomized, double-blind study. *Ren Fail.* **2016**, *38*, 214–221, doi:10.3109/0886022X.2015.1128236.
178. Richer, S.; Stiles, W.; Ulanski, L.; Carroll, D.; Podella, C. Observation of human retinal remodeling in octogenarians with a resveratrol based nutritional supplement. *Nutrients* **2013**, *5*, 1989–2005, doi:10.3390/nu5061989.
179. Richer, S.; Patel, S.; Sockanathan, S.; Ulanski, L.J., 2nd; Miller, L.; Podella, C. Resveratrol based oral nutritional supplement produces long-term beneficial effects on structure and visual function in human patients. *Nutrients* **2014**, *6*, 4404–4420, doi:10.3390/nu6104404.
180. Wang, S.; Moonasar, N.; Xiao, X.; Yin, T.; Weinreb, R.N.; Sun, X. Effect of Resveratrol-Based Nutritional Supplement on Choroidal Thickness: A Pilot Study. *Curr. Eye Res.* **2016**, *41*, 1339–1345, doi:10.3109/02713683.2015.1119282.
181. Pirhan, D.; Yuksel, N.; Emre, E.; Cengiz, A.; Kursat Yildiz, D. Riluzole- and Resveratrol-Induced Delay of Retinal Ganglion Cell Death in an Experimental Model of Glaucoma. *Curr. Eye Res.* **2016**, *41*, 59–69, doi:10.3109/02713683.2015.1004719.
182. Subramani, M.; Ponnalagu, M.; Krishna, L.; Jeyabalan, N.; Chevour, P.; Sharma, A.; Jayadev, C.; Shetty, R.; Begum, N.; Archunan, G.; et al. Resveratrol reverses the adverse effects of bevacizumab on cultured ARPE-19 cells. *Sci. Rep.* **2017**, *7*, 12242, doi:10.1038/s41598-017-12496-z.
183. Pozarowska, D.; Pozarowski, P. The era of anti-vascular endothelial growth factor (VEGF) drugs in ophthalmology, VEGF and anti-VEGF therapy. *Cent. Eur. J. Immunol.* **2016**, *41*, 311–316, doi:10.5114/ceji.2016.63132.
184. Kwong, T.Q.; Mohamed, M. Anti-vascular endothelial growth factor therapies in ophthalmology: Current use, controversies and the future. *Br. J. Clin. Pharm.* **2014**, *78*, 699–706, doi:10.1111/bcp.12371.
185. Billard, C.; Izard, J.C.; Roman, V.; Kern, C.; Mathiot, C.; Mentz, F.; Kolb, J.P. Comparative antiproliferative and apoptotic effects of resveratrol, epsilon-viniferin and vine-shots derived polyphenols (vineatrols) on chronic B lymphocytic leukemia cells and normal human lymphocytes. *Leuk Lymphoma* **2002**, *43*, 1991–2002.
186. Clement, M.V.; Hirpara, J.L.; Chawdhury, S.H.; Pervaiz, S. Chemopreventive agent resveratrol, a natural product derived from grapes, triggers CD95 signaling-dependent apoptosis in human tumor cells. *Blood* **1998**, *92*, 996–1002.
187. Lu, J.; Ho, C.H.; Ghai, G.; Chen, K.Y. Resveratrol analog, 3,4,5,4'-tetrahydroxystilbene, differentially induces pro-apoptotic p53/Bax gene expression and inhibits the growth of transformed cells but not their normal counterparts. *Carcinogenesis* **2001**, *22*, 321–328.
188. Colin, D.; Gimazane, A.; Lizard, G.; Izard, J.C.; Solary, E.; Latruffe, N.; Delmas, D. Effects of resveratrol analogs on cell cycle progression, cell cycle associated proteins and 5fluoro-uracil sensitivity in human derived colon cancer cells. *Int. J. Cancer* **2009**, *124*, 2780–2788.
189. Brown, V.A.; Patel, K.R.; Viskaduraki, M.; Crowell, J.A.; Perloff, M.; Booth, T.D.; Vasilinin, G.; Sen, A.; Schinas, A.M.; Piccirilli, G.; et al. Repeat dose study of the cancer chemopreventive agent resveratrol in healthy volunteers: Safety, pharmacokinetics, and effect on the insulin-like growth factor axis. *Cancer Res.* **2010**, *70*, 9003–9011.
190. Walle, T.; Hsieh, F.; DeLegge, M.H.; Oatis, J.E., Jr.; Walle, U.K. High absorption but very low bioavailability of oral resveratrol in humans. *Drug. Metab. Dispos.* **2004**, *32*, 1377–1382.
191. Boocock, D.J.; Faust, G.E.; Patel, K.R.; Schinas, A.M.; Brown, V.A.; Ducharme, M.P.; Booth, T.D.; Crowell, J.A.; Perloff, M.; Gescher, A.J.; et al. Phase I dose escalation pharmacokinetic study in healthy volunteers of resveratrol, a potential cancer chemopreventive agent. *Cancer Epidemiol. Biomark. Prev.* **2007**, *16*, 1246–1252.

192. Almeida, L.; Vaz-da-Silva, M.; Falcao, A.; Soares, E.; Costa, R.; Loureiro, A.I.; Fernandes-Lopes, C.; Rocha, J.F.; Nunes, T.; Wright, L.; et al. Pharmacokinetic and safety profile of trans-resveratrol in a rising multiple-dose study in healthy volunteers. *Mol. Nutr. Food. Res.* **2009**, *53*, S7–S15.
193. Nunes, T.; Almeida, L.; Rocha, J.F.; Falcao, A.; Fernandes-Lopes, C.; Loureiro, A.I.; Wright, L.; Vaz-da-Silva, M.; Soares-da-Silva, P. Pharmacokinetics of trans-resveratrol following repeated administration in healthy elderly and young subjects. *J. Clin. Pharm.* **2009**, *49*, 1477–1482.
194. Wang, S.; Wang, Z.; Yang, S.; Yin, T.; Zhang, Y.; Qin, Y.; Weinreb, R.N.; Sun, X. Tissue Distribution of trans-Resveratrol and Its Metabolites after Oral Administration in Human Eyes. *J. Ophthalmol.* **2017**, *2017*, 4052094, doi:10.1155/2017/4052094

Objectifs

La dégénérescence maculaire liée à l'âge (DMLA) est la **première cause de handicap visuel** chez les personnes âgées de plus de 65 ans dans les pays industrialisés. Les traitements actuels se concentrent principalement sur la DMLA néovasculaire en utilisant des **injections d'anticorps bloquant** le facteur de croissance endothéliale (VEGF) responsable de la formation des nouveaux vaisseaux. Cependant, ces traitements ne ciblent que la phase active de la maladie c'est-à-dire lors de la formation des nouveaux vaisseaux. Au cours des deux dernières décennies, des études ont examiné le rôle de **l'alimentation** dans la **prévention** de la DMLA, démontrant ainsi que l'alimentation peut jouer un rôle important dans sa prévention et sa progression. En effet, les études AERDS ont démontré qu'une alimentation riche en **oméga-3 et anti-oxydant** permettait de **réduire** significativement le risque de développer la DMLA. Ainsi, certains patients atteints de la maladie se voient prescrire des **compléments alimentaires** contenant des anti-oxydants et des oméga-3 pour renforcer leur apport quotidien.

Parmi les molécules anti-oxydantes présentes naturellement dans l'alimentation, le **resvératrol** (RSV), un polyphénol de la vigne et du vin, est déjà connu pour ses effets protecteurs dans certaines maladies et nettement dans les maladies cardiovasculaires. Plus récemment, certaines études ont montré que le RSV pouvait être un bon candidat pour la prévention de maladies oculaires telles que la DMLA. Son pouvoir **anti-oxydant** permet non seulement de réduire les espèces réactives de l'oxygène (ERO), mais aussi de renforcer les défenses anti-oxydantes enzymatiques des cellules. En plus de son pouvoir anti-oxydant, le RSV présente aussi des bénéfices **anti-inflammatoires** dans les maladies oculaires. Ses effets anti-inflammatoires et anti-oxydants pourraient permettre de prévenir ou bien de ralentir les phases précoces de la maladie. De plus, le RSV pourrait aussi permettre de réduire la progression de la maladie grâce à ses effets **anti-angiogéniques**. En effet, diverses études menées sur le RSV dans des maladies telles que le cancer ont permis de montrer qu'il était capable de diminuer l'expression de protéines clefs impliquées dans l'angiogenèse ainsi que de ralentir la formation de nouveaux vaisseaux. Ainsi, ces études *in vitro* et préclinique ont permis de montrer les effets pléiotropies du resvératrol dans le contexte de la DMLA.

Bien que le RSV soit l'un des polyphénols, le plus étudié, d'autres polyphénols et composés phénoliques issus de la vigne et du vin présentent des effets bénéfiques sur la santé. **Le vin rouge**, en particulier, est l'une des sources les plus riches en polyphénols. Il contient non seulement une **concentration élevée de resvératrol**, mais aussi une **diversité de polyphénols** extrêmement intéressante. De plus, certaines études ont mis en évidence que des combinaisons de polyphénols pouvaient avoir des actions biologiques plus importantes que l'utilisation de polyphénol seul. Dans ce contexte, nous avons, au sein de l'axe transversal concernant « l'Apport des polyphénols dans le domaine de la santé » entre le Centre INSERM U1231 et l'IUVV (Institut universitaire de la vigne et du vin) initié un projet de recherche concernant l'impact d'anti-oxydants tels que les polyphénols de la vigne et du vin dans la DMLA. Cette étude vise à établir si un extrait sec de vin rouge riche en polyphénols peut exercer une action bénéfique dans le cadre de la survenue et de la progression de la DMLA et de comparer ses effets aux effets du resvératrol seul. Cette étude a porté sur un vin rouge issu des procédures de vinification établies par le Bureau interprofessionnel des Vins de Bourgogne (BIVB), dont nous avons réalisé un extrait sec enrichi en polyphénols. Après avoir caractérisé l'extrait, nous avons cherché à démontrer que cet extrait pouvait avoir un effet bénéfique dans le contexte de la DMLA. **Ainsi, nous nous sommes posé la question si l'extrait sec de vin rouge pouvait prévenir, voire protéger l'œil sain face à divers inducteurs de la DMLA. Pour cela nous nous sommes demandé si l'extrait sec de vin rouge pouvait : 1) Altérer la sécrétion ainsi que la voie de signalisation du VEGF-A dans les cellules de l'épithélium pigmentaire rétinien en condition non pathologique ; 2) Altérer la sécrétion de VEGF-A en condition pathologique induite par différents inducteurs ; 3) Prévenir la production d'espèces réactives de l'oxygènes ainsi que leur dommage dans les cellules de l'EPR ; 4) Prévenir la sécrétion de cytokine pro-inflammatoire en condition pathologique dans les cellules de l'EPR ainsi que dans des cellules immunitaires (macrophages).**

Matériels et Méthodes

Extrait sec de vin rouge

Extraction des polyphénols

Le vin rouge utilisé dans cette étude a été sélectionné par le Bureau Interprofessionnel des Vins de Bourgogne (BIVB), il s'agit d'un Santenay 1er cru, Les gravières 2012, dont le cépage principal est le Pinot Noir. La réalisation de l'extrait sec de ce vin a été réalisée en collaboration avec le Dr. David Monchaud de l'Institut de Chimie Moléculaire de l'Université de Bourgogne (ICMUB) selon la méthode décrite par Chalons et al., 2018.

Dans un premier temps, l'alcool et l'eau contenus dans le vin ont été évaporés à l'aide d'un évaporateur rotatif (Rotavapor RII, BUCHI) couplé à une pompe à vide et un bain-marie chauffé à 37°C. Le concentré de vin obtenu a ensuite été déposé sur une colonne d'absorption composée d'une matrice de billes de vinyl-divinyl benzène ; Diaion® HP20 (Supelco). Après avoir été rincés quatre fois avec de l'eau, les polyphénols ont été élués par une solution d'éthanol/acide acétique glacial 0,1%. Par la suite, l'éluant a été concentré et séché à l'aide d'un évaporateur rotatif (Rotavapor RII, BUCHI) couplé à une pompe à vide et un bain-marie chauffé à 37°C. Une poudre fine a été obtenue, extrait sec de vin rouge (*red wine extract* : RWE) stocké à -20°C à l'abri de la lumière.

Analyse qualitative et quantitative de l'extrait sec de vin rouge

La composition de l'extrait sec de vin rouge a été analysée par Chromatographie Liquide Haute Performance (CLHP) selon la méthode décrite par Chalons et al. 2018, et en collaboration avec le Pr. Tristan Richard et le Dr. Josep Valls-Fonayet de l'Université de Bordeaux. Cette analyse a été réalisée à l'aide d'un système CLHP équipé d'une colonne C18 pour la séparation des composés, d'un détecteur à barrette de diodes pour la quantification des anthocyanes, des flavonols et des acides phénoliques, et d'un détecteur de fluorescence pour la catéchine et analyse des stilbènes. L'échantillon de vin a été injecté en trois exemplaires. Pour les anthocyanes et les flavonols, la phase mobile est constituée d'eau contenant 5 % d'acide formique (v/v) et de méthanol en proportions variables à un débit de 1 mL /min. Les anthocyanes ont été quantifiées à 520 nm sous forme de malvidine-3-glucoside [limite de détection (LOD) = 0,074 mg/L, limite de quantification (LOQ) = 0,240 mg/L]. Les flavonols ont été quantifiés à 360 nm sous forme de quercétine-3-rutinoside. Les flavan-3-ols, les acides phénoliques et les stilbènes ont été analysés à l'aide d'un gradient contenant de l'eau avec 2 %

d'acide acétique (v/v) et du méthanol/eau/acide acétique (90 :8 :2, v/v/v). Les acides phénoliques ont été quantifiés à 320 nm sous forme d'acide caféique. Les flavan-3-ols ont été quantifiés en tant que catéchine en utilisant le signal de fluorescence avec la longueur d'onde d'excitation à 290 nm et la longueur d'onde d'émission à 320 nm. Les stilbènes ont été quantifiés en tant que resvératrol par détection de fluorescence avec la longueur d'onde d'excitation à 330 nm et la longueur d'onde d'émission à 320 nm. Des solutions standard ont été injectées en trois exemplaires et les moyennes des données ont été utilisées pour construire la courbe standard. Les concentrations totales ont été calculées selon chaque courbe standard. Toutes les anthocyanes quantifiées sont des dérivés 3-glucosyl qui peuvent être acylés en position 6 du glucose. Pour les flavonols, seule la quercétine-3-rutinoside a été quantifiée.

Réactifs

Le ***trans*-resvératrol** (Sigma-Aldrich, St. Quentin Fallavier, France) a été dissout dans de l'éthanol 70% de sorte à obtenir une solution mère de 20 mM pour les expérimentations *in vitro* et une solution mère à 80 mM dans du DMSO a été réalisée pour les expérimentations *in vivo*. Une solution mère de **lipopolysaccharides** d'Escherichia coli O55:B5 (LPS, Sigma-Aldrich, St. Quentin Fallavier, France) a été réalisée dans de l'eau à une concentration de 5 mg/mL. L'**interféron gamma** (INFγ, preprotech, Neuilly-Sur-Seine, France) a été solubilisé dans de l'eau à une concentration de 25 µg/mL. Le **VEGF-165 recombinant humain** (rVEGF, Invitrogen, Waltham, MA, USA) a été solubilisé dans de l'eau afin de réaliser une solution mère à 50 µg/mL. La sonde **2',7'-Dichlorofluorescin diacetate** (DCFH-DA, Sigma-Aldrich, St. Quentin Fallavier, France) a été dissoute dans du DMSO afin de réaliser une solution mère à 50 mM. Une solution mère de **2,2'-Azobis(2-methylpropionamidine) dihydrochloride** (AAPH, MERCK) a été préparée dans de l'eau à une concentration de 600 mM. Ces solutions mères ont été stockées à -20°C.

Le **peroxyde d'hydrogène** (H_2O_2) a été obtenu chez MERCK (Darmstadt, Germany) et a été préparé dans du milieu de culture cellulaire à une concentration de 300 mM.

Pour les analyses de western blot, les anticorps ont été préparés dans une solution de saturation (PBS 1X, tween20 0,1% et 5% de BSA ou de lait). Les anticorps suivants ont été obtenus chez cellsignaling Technology : VEGF-R2 (1/1 000 ; #2479), p-VEGF-R2 Y951 (1/1 000 ; #4991), p65 (1/1 000 ; #8242), p50 (1/1 000, #13586). L'anticorps dirigé contre p-VEGF-R2 Y1054

(1/1 000 ; 04-893) a été obtenu chez millipore et l'anticorps HSC70 (1/2 000, sc7298) a été obtenu chez santa cruz technology.

Culture cellulaire

ARPE-19

Les cellules ARPE-19 proviennent de l'American Type Culture Collection (CRL-2302, ATCC). C'est une lignée cellulaire spontanée de l'épithélium pigmentaire rétinien (EPR) isolée à partir de la rétine d'un homme de 19 ans décédé à la suite d'un traumatisme crânien.

Culture cellulaire

Les cellules ont été cultivées dans un mélange (1:1, *v/v*) *Dulbecco's Modified Eagle Medium* (DMEM) et de milieu F-12 contenant du GlutaMAX™ (Thermo Fisher, Waltham, MA, USA) contenant 10 % de sérum de veau fœtal (SVF ; Dutscher, France) et maintenu à 37 ◦C dans une atmosphère contenant 5 % de CO_2. Les cellules sont passées deux fois par semaine ou avant qu'elles n'atteignent 80-85 % de confluence. Pour cela, le tapis cellulaire est rincé avec du tampon *Hanks' Balanced Salts Solution* (HBSS ; Dutscher) puis les cellules sont décollées par l'action de trypsine-EDTA (Dutscher). Une fraction de la suspension cellulaire (1/10ème) est ensuite repiquée dans une nouvelle flasque. La contamination par les mycoplasmes a été testée une fois toutes les deux semaines à l'aide du test MycoAlertTM (Lonza).

Ensemencement

Les cellules sont ensemencées à une densité constante de 7 500 cellules/cm² dans du DMEM/F12 supplémenté avec 10 % de SVF. Après 72 h de culture, le milieu de culture est éliminé et le tapis cellulaire rincé avec de l'HBSS. Du milieu frais supplémenté avec 1 % de SVF est ensuite ajouté. Après 24h de culture supplémentaire, les différents traitements ont été ajoutés dans le milieu de culture.

ARPE-19 "différenciées"

Les cellules ARPE-19 différenciées, décrites par Dunn et al., en 1996, présentent un phénotype épithélial qui se rapproche des cellules physiologiques retrouvées dans l'épithélium rétinien pigmentaire.

Afin d'induire leur différenciation, les cellules ARPE-19 ont été cultivées à 100 % de confluence durant 8 semaines dans du milieu DMEM/F12 supplémenté avec 1 % de SVF. Le milieu a été renouvelé 2 fois par semaine et la contamination au mycoplasme a été testée une fois toutes les deux semaines avec le test MycoAlertTM (Lonza).

A la fin des 8 semaines de différenciation, les différents traitements ont été ajoutés dans les milieux de culture. La différenciation cellulaire a, par la suite été vérifiée par mesure de l'ARNm de gènes marqueurs de l'EPR, à savoir *retinal pigment epithelium-specific 65* (RPE65) et *retinaldehyde binding protein 1* (RLBP-1).

Macrophages

Les macrophages ont été isolés à partir de sang de patient. Pour cela, des *buffy coat* ont été obtenus auprès de l'Etablissement Français du Sang (EFS). Afin d'isoler les cellules mononucléaires du sang périphérique (PBMC), le sang a été déposé sur du milieu de séparation des lymphocytes (EUROBIO, Les Ulis, France) après avoir été dilué (1:1, *v*/*v*) au préalable dans une solution tamponnée avec du phosphate (*phosphate-buffered saline*, PBS, Dutscher, Brumath, France). Le sang a ensuite été centrifugé 20 min à température ambiante à une vitesse de 700x g (sans décélération). L'anneau formé par les PBMC a été récupéré et lavé deux fois avec du PBS. Les cellules ont ensuite été incubées 5 min à température ambiante dans un tampon de lyse (150 mM NH_4Cl ; 10 mM $KHCO_3$, 0,1 mM EDTA). Cette étape permet d'éliminer tous les érythrocytes résiduels afin de ne conserver que les PBMC. Les cellules ont ensuite été ensemencées à une densité de 800 000 cellules/cm² dans du milieu DMEM/F12 sans sérum. Après deux heures, le tapis cellulaire a été rincé deux fois avec du milieu sans sérum afin de ne garder que les cellules adhérées. Enfin, les cellules ont été maintenues durant 6 jours dans du milieu frais DMEM/F12 contenant 10 % de SVF et 100 ng/mL GM-CSF (*granulocyte-macrophage colony-stimulating factor*, MiltenyiBiotec, Bergisch Gladbach, Germany). Le milieu

de culture a été renouvelé tous les deux jours. Après 6 jours de culture, les différents traitements ont été ajoutés aux milieux de culture.

Mesure de la viabilité cellulaire

La viabilité cellulaire a été mesurée par coloration au cristal violet. A la fin des traitements, le milieu de culture a été éliminé et les tapis cellulaires rincés avec du PBS avant d'être incubé 15 min dans une solution de cristal violet (2.3% cristal violet, 0.1% oxalate d'ammonium et 20% alcool éthylique, Sigma-Aldrich, St. Quentin Fallavier, France). La solution de coloration a ensuite été éliminée et les tapis cellulaires rincés trois fois avec de l'eau. Après l'évaporation totale de l'eau, le cristal violet a été dissout dans de l'acide acétique 33% et l'absorbance lue à 590 nm à l'aide du lecteur de plaque PerkinElmer®, Envision. L'absorbance des cellules traitées avec le solvant (cellules contrôles) a été utilisée comme référence et rapportée à 100 % de viabilité, l'absorbance des différentes conditions de traitement est exprimée en pourcentage moyen par rapport au contrôle ± SEM.

Western Blot

Extraction protéique

A la fin des traitements, les cellules ont été collectées (350x g, 5 min, 4°C), lavées 3 fois dans du PBS puis lysées dans un tampon *radioimmunopecipitation assay* (RIPA, 50 mM Tris-HCl ; 150 mM chlorure de sodium ; 0.1% dodécyl sulfate de sodium ; 0.5% désoxy cholate de sodium; 1% NP40; pH 8) associé à des inhibiteurs de phosphatase (fluore de sodium 50 mM) et de protéase (fluorure de phenylmethylsulfonyl ; PMSF ; 100 µM, Sigma-Aldrich,St. Quentin Fallavier, France), et un cocktail d'inhibiteur de protéase (Roche, Boulogne-Billancourt, France). Après 30 min de lyse sur glace, les échantillons ont été centrifugés 20 min à 16 000x g à 4°C afin d'éliminer les débris cellulaires. La concentration protéique des lysats a été mesurée à l'aide du kit QuantiPro™ BCA (Sigma, Aldrich, St. Quentin Fallavier, France). Les échantillons, contenant entre 25-60 µg de protéine, ont ensuite été dilués avec un tampon Leammli (60 mM Tris HCl, 10% glycérol, 2% dodécyl sulfate de sodium, 100 mM désoxy cholate de sodium, et 0.002% bleu de bromophénol, pH 6,8) puis chauffés 5 min à 95 °C.

Dépôt, migration et transfert

Les échantillons ainsi que des marqueurs de poids moléculaire (PageRuler™, ThermoFisher Scientific) ont été déposés sur des gels d'acrylamide (7,5-12%) TGX Stain-Free™ FastCast™ (Bio-Rad, Marnes-la-Coquette, France).

La migration a été réalisée dans un système d'électrophorèse (BioRad) dans un tampon de migration (Tris base 25 mM, glycine 190 mM, SDS 0,1 %, pH 8,8). A la fin de la migration, les protéines ont été transférées sur une membrane de nitrocellulose (Bio-Rad) grâce au système TransBlot Turbo (BioRad).

Par la suite, les sites aspécifiques ont été saturés à l'aide d'une solution contenant soit 5% sérum-albumine bovine (BSA) ou 5% lait dans du PBS contenant 0,1 % tween 20 (PBS-T) durant 1 heure à température ambiante sous agitation. Puis les membranes ont été incubées avec les anticorps primaires durant une nuit à 4°C sous agitation. Après trois lavages de 10 minutes sous agitation avec une solution de PBS et 0,1% de tween, les membranes ont été incubées sous agitation à température ambiante durant 1 heure avec des anticorps secondaires couplés HRP (Horseradish Peroxidase) dirigés spécifiquement contre l'isotope de l'anticorps primaire utilisé. Pour finir, les membranes ont été lavées 3 fois comme décrit précédemment avant d'être révélées par chimioluminescence en utilisant du Clarity Western ECL (BioRad), les images ont été acquises avec un Chemidoc MP Imaging System. Les images ont ensuite été analysées grâce au logiciel Image Lab™ v6.0 (BioRad).

Certaines membranes ont été utilisées deux fois consécutives afin de révéler deux protéines de poids moléculaires similaires. Pour cela, les membranes ont été déshybridées entre la première et la seconde protéine à l'aide de deux bains successifs de 10 min dans du tampon de déshybridation (Glycine 25 mM, SDS 1 %, pH 2). Le pH a ensuite été remonté lors de 3 lavages avec du PBS-T, puis les membranes ont été saturées avant d'incuber le second anticorps primaire.

Mesure des espèces réactives de l'oxygène intracellulaire

Avant le traitement des cellules avec de l'H_2O_2 ou de l'AAPH, les cellules ont été incubées avec 10 µM de 2',7'-dichlorofluorescin diacétate (DCFH-DA, Sigma-Aldrich, St. Quentin, France). Après 30 minutes d'incubation, les cellules ont été rincées deux fois avec de l'HBSS,

puis du milieu de culture contenant les différents traitements a été ajouté sur les cellules. A la fin des traitements, la fluorescence de la sonde DCFH-DA a été mesurée à l'aide du lecteur de plaque PerkinElmer Envision (excitation = 488 nm; émission = 528 nm) et la viabilité cellulaire a été mesurée par cristal violet.

Enzyme-Linked Immuno Sorbant Assay : ELISA

Les taux de cytokines sécrétées (IL-6, IL-8, VEGF-A) dans le milieu de culture ont été mesurés par ELISA à l'aide des kits commercialisés par BioLegend (Amsterdam, Pays-Bas). Des plaques 96 puits ont été incubées à 4°C sur la nuit avec les anticorps de captures. Après avoir été rincés 4 fois avec 400 µL de PBS 1X contenant 0,1% de tween20, les sites aspécifiques ont été saturés avec la solution de saturation fournie dans les kits. Par la suite, les échantillons ainsi que les standards ont été ajoutés dans les plaques. Après 2 heures d'incubation sous agitation à température ambiante, les puits ont été rincés et incubés avec l'anticorps de détection durant 1 heure. Les puits ont ensuite été rincés comme décrit précédemment et une solution de stréptavidine conjuguée à HRP (peroxydase de raifort) a été incubée 30 min avant l'ajout de son substrat. 10 min après l'ajout de ce dernier, une solution stop (H2SO4, 1N) a été ajoutée et l'absorbance a été lue à 450 nm grâce au lecteur de plaque PerkinElmer™ Envision. Enfin, la concentration cytokinique a été calculée à l'aide du logiciel GraphPad Prism v8.3.0.

Mesure de l'expression d'ARN

Isolation des ARN

Les ARN ont été isolés à l'aide du kit commercialisé par Zymo Research (Californie, USA). A la fin des traitements, le milieu de culture cellulaire a été éliminé et le tampon de lyse a été ajouté sur les tapis cellulaires et les cellules ont été grattées dans le tampon de lyse. Par la suite, un volume d'éthanol 70% équivalent au volume du tampon de lyse a été ajouté dans chaque échantillon. Le mélange tampon de lyse et éthanol a ensuite été placé sur une colonne d'extraction avant d'être centrifugé 30 secondes à 16 000x g. Afin d'éviter les contaminations par l'ADN, ce dernier a été digéré grâce à l'ADNase fourni dans le kit durant 15 min à température ambiante. Les colonnes ont ensuite été rincées 3 fois avant l'élution des ARN avec 15 µL d'eau. Enfin, les ARN ont été dosés grâce au Nanodrop 2 000 (Thermo Scientific).

Reverse transcription

Les 400 ng d'ARN ont été rétrotranscrits en ADN complémentaires (ADNc) à l'aide du kit *high capacity cDNA reverse transcription (*4368813, Fisher scientific). Dans un premier temps, les ARN ont été dénaturés 5 min à 65°C en présence d'amorces aléatoires et de 0,5 mM de désoxyribonucléotides triphosphates (dNTP). Ensuite, une enzyme de rétrotranscription a été ajoutée. Les échantillons ont été chauffés dans un thermocycler, 2 heures à 37°C puis 5 minutes à 70°C et enfin conservés à 4°C.

Réaction en chaine par polymerase quantitative (qPCR)

Afin de mesurer l'expression de gène cible, les ADNc ont été incubés dans un mix contenant un couple d'amorces spécifique du gène d'intérêt (Tableau 5) et du SYBR green (15310939, Applied biosystem, Thermofisher). La qPCR a été réalisée à l'aide d'un thermocycleur ViiaTM 7 Real – Time PCR System (Applied Biosystems) (10 minutes à 95 °C ; 40 cycles : 15 secondes à 95 °C ; 1 minute à 60 °C ; 15 secondes 0 à 95 °C ; 10 minutes à 95 °C ; 15 secondes à 95 °C).

Les valeurs de *cycle threshold* (Ct) des gènes cibles ont été rapportées aux valeurs des gènes de ménages (L27 et GAPDH). L'expression transcriptionnelle relative a ensuite été calculée en utilisant la formule 2^(-ΔCt).

Tableau 5. Liste des amorces utilisées pour les PCR

Gène	***Amorce sens (5′-3′)***	***Amorce antisens (5′-3′)***
RPE65	GATGTGGGCCAGGACTCTTT	AGTGCGGATGAACCTTCTGT
RLBP1	GGCAGGGGAACAACCAAGACT	AGTCAGGGCCAAGTTGTGAC
VEGF-A	ATCTTCAAGCCATCCTGTGTG	GAGGTTTGATCCGCATAATCTG
IL-10	TCTCCGAGATGCCTTCAGCAGA	TCAGACAAGGCTTGGCAACCCA
IL-6	AGACAGCCACTCACCTCTTCAG	TTCTGCCAGTGCCTCTTTGCTG
IL-8	GAGAGTGATTGAGAGTGGACCAC	CACAACCCTCTGCACCCAGTTT
MCP-1	CATGAAAGTCTCTGCCGCCC	GGGCATTGATTGCATCTGGCTG
CD206	CCAAACGCCTTCATTTGCCA	ACCTTCCTTGCACCCTGATG
L27	ACCTAATGCCCACAAGGTACTC	TCGGGCCTTGCGTTTAAGAG

Analyse statistique

La moyenne des valeurs est exprimée ± SEM (*Standard Error of the Mean*) issue de trois expériences indépendantes. Les analyses statistiques ont été calculées à l'aide du logiciel GraphPad Prims 8.3.0 (GraphPad Software, La Jolla, San Diego, CA, USA). La distribution normale des données entre les groupes a été calculée à l'aide du test de Shpiro-Wilk. Un test ANOVA suivi d'un test à comparaison multiple de Dunnett a été utilisé lorsque les valeurs suivent la loi normale. Un test ANOVA suivi d'un test à comparaison multiple de Kruskal-Wallis a été utilisé lorsque les valeurs suivent la loi normale. p-value ≤ 0,05 a été considérée comme significative, n.s. = non significatif; *p<0,05, **p<0,01 ;*** p<0,0001.

Résultats

Etude 1 : Analyse de l'effet d'un extrait sec de vin rouge sur la sécrétion et la signalisation intracellulaire du facteur de croissance endothéliale (VEGF-A) dans les cellules de l'épithélium pigmentaire rétinien.

A. Contexte général et objectifs de l'étude

La DMLA est une maladie dégénérative de la rétine qui se traduit par la perte de la vision centrale. Dans sa forme tardive et la plus sévère, elle se caractérise par une néo-angiogenèse anarchique, conduisant à la formation de nouveaux vaisseaux sanguins qui perturbent l'organisation de la rétine. Ces nouveaux vaisseaux proviennent de la choroïde et traversent la membrane de Bruch, ce qui altère l'homéostasie de la rétine et notamment de l'épithélium pigmentaire rétinien. Ces cellules servent d'ancrage aux cônes et bâtonnets, leur destruction entraîne une perte localisée et permanente de cette vision. De plus, la formation de ces nouveaux vaisseaux peut induire de graves complications telle que des hémorragies rétiniennes ou encore un décollement de la rétine entraînant une perte très rapide de la vision centrale. La néovasclarisation est principalement induite par un facteur de croissance, le VEGF. Ainsi, la surexpression de ce facteur (VEGF-A) est de mauvais pronostic pour l'évolution de la maladie. De nombreuses stratégies de traitement utilisent des anticorps anti-VEGF afin d'inhiber l'angiogenèse. Cependant, ces anticorps ne sont efficaces que lors des phases actives de la maladie, c'est-à-dire lors de la formation des nouveaux vaisseaux. Afin de compléter ces traitements, certaines études ont montré que l'alimentation joue un rôle important dans sa survenue ainsi que dans la progression de la maladie. Ainsi, dans certains cas, les médecins ophtalmologues prescrivent des compléments alimentaires afin de renforcer les apports nutritionnels des patients en anti-oxydants et oméga-3. Parmi les composés naturellement anti-oxydants, les polyphénols pourraient présenter un intérêt pour la santé et notamment pour la DMLA. En effet, certaines études ont été réalisées afin de prouver l'effet de plusieurs préparations enrichies en extrait de polyphénol de raisin ou en polyphénols de vin sur les maladies dégénératives liées à l'âge (Mendes et al., 2018) et les maladies oculaires (Dugas et al., 2010; Kang and Choung, 2016; Sheu et al., 2010). Plus particulièrement, le resvératrol, un polyphénol de la vigne, empêchait la sécrétion de VEGF induite par les oxystérols des cellules rétiniennes humaines (Dugas et al., 2010). Cependant, qu'en est-il d'un

mélange complexe plus polyphénolique comme le vin rouge, qui contient une grande variété de polyphénols ? Considérant le rôle fondamental du VEGF dans le développement et la progression de la DMLA, nous avons étudié l'effet potentiel d'un extrait de vin rouge (*Red wine extract*, RWE) sur la sécrétion de VEGF-A dans les cellules rétiniennes humaines ARPE-19. **L'objectif principal est de déterminer si l'extrait peut diminuer la sécrétion de VEGF-A et altérer sa voie de signalisation et ainsi influencer la progression de la DMLA.**

B. Résumé de l'étude

B.1. Extraction et caractérisation des polyphénols de vin rouge

En partenariat avec le **Bureau Interprofessionnel des Vins de Bourgogne** (BIVB) nous avons sélectionné un vin rouge de la région viticole de la Côte de Beaune, un **Santenay 1er cru, Les gravières 2012**. Pour cette étude, l'extraction des composés phénoliques a été réalisée en collaboration avec le **Dr. David Monchaud de l'Institut de Chimie Moléculaire de l'Université de Bourgogne** (ICMUB) selon la méthode décrite par Chalons et al. (2018). Brièvement, l'alcool a été éliminé par évaporation à l'aide d'un évaporateur rotatif (Rotavapor RII, BUCHI) couplé à une pompe à vide et à un bain-marie à 37 °C. Ensuite, les composés du vin rouge ont été séparés en utilisant une **colonne d'absorption** contenant des **billes de vinyl-divinyl benzène** (Diaion® HP20, Supelco). La colonne a ensuite été lavée avec de l'eau distillée afin d'éliminer les impuretés puis les polyphénols ont été élués avec une solution d'éthanol/acide acétique glacial 0,1 %. Pour finir, les fractions d'éluant recueillies ont été **concentrées à sec** à l'aide d'un ensemble d'évaporateurs rotatifs (Rotavapor RII, BUCHI) couplé à une pompe à vide et à un bain-marie à 37 °C.

L'analyse quantitative et qualitative du RWE a été effectuée en utilisant la technique de **Chromatographie Liquide Haute Performance** (CLHP) selon la méthode de Chalons et al. (2018), en collaboration avec le **Pr. Tristan Richard et le Dr. Josep Valls-Fonayet de l'Université de Bordeaux.** L'analyse a été réalisée grâce à un système CLHP équipé d'une colonne C18 pour la séparation des composés, d'un détecteur à barrette de diodes pour la quantification des anthocyanes, des flavonols et des acides phénoliques, et d'un détecteur de fluorescence pour la catéchine et l'analyse des stilbènes. La caractérisation de l'extrait montre une forte teneur en **acides phénoliques** et **flavan-3-ols**, ces derniers représentant respectivement 49,2 et 36 % de l'extrait total. À cela s'ajoute une quantité moindre, mais non

négligeable d'**anthocyanines** (9 %), de **flavanols** (2 %) et de **stilbènes** (3,2 % au total dont 1,5 % de **resvératrol**).

B.2. Évaluation du potentiel santé de l'extrait sec de vin rouge

Afin d'évaluer les effets de l'extrait sec de vin rouge (*red wine extract*, RWE), nous avons utilisé des cellules humaines de l'épithélium pigmentaire rétinien (EPR), ARPE-19. Dans un premier temps, nous avons évalué l'innocuité de l'extrait ainsi que celui du resvératrol (RSV) seul. Ainsi, après 24 h et 48 h de traitement avec des concentrations croissantes en RWE et RSV allant de 0 à 250 µg/mL, nous n'avons observé **aucune cytotoxicité**.

Pour la suite de l'étude, nous avons choisi trois doses de RWE, à savoir **30**, **50** et **100 µg/mL**. Nous avons mis en évidence que ces doses avaient un effet biologique dans d'autres types cellulaires (Chalons et al., 2020, 2018). De plus, nous avons également choisi une dose de **RSV à 20 µM**. Les précédents travaux de notre équipe ont montré l'effet bénéfique du RSV utilisé à cette dose contre la toxicité induite par des oxystérols (Dugas et al., 2010).

Comme décrit précédemment, le principal acteur de la progression de la DMLA néovasculaire est le facteur de croissance *vascular endothelial growth factor-A* (**VEGF-A**). La voie classique de signalisation médiée par le VEGF-A passe par sa fixation sur ses récepteurs VEGF-R1 et VEGF-R2 (R2 étant le récepteur de signalisation majeur), ce qui déclenche l'activité de plusieurs kinases qui vont réguler la sécrétion de VEGF-A, la prolifération, la migration, la survie et la perméabilité vasculaire. L'inhibition de la sécrétion et de la voie de signalisation du VEGF-A par des molécules naturelles peut être bénéfique dans la DMLA.

Afin d'analyser les effets du RWE, nous avons cherché à mesurer l'expression protéique ainsi que la sécrétion de VEGF-A dans les cellules rétiniennes traitées en présence ou en absence de RWE (0, 30, 50 et 100 µg/mL) ou de RSV à 20 µM. Ces analyses ont montré que le **RWE peut diminuer significativement l'expression ainsi que la sécrétion du VEGF-A, et ce de manière plus importante que le RSV seul.**

La sécrétion de VEGF-A par les cellules rétiniennes résulte de l'activation de la voie de signalisation impliquant les récepteurs à tyrosines kinases spécifiques du VEGF. La liaison du VEGF-A se produit principalement sur le récepteur **VEGF-R2**, qui induit sa **phosphorylation** et une cascade de signalisation intracytoplasmique passant par la phosphorylation de **MEK** (*Mitogen-activated Extracellular signal-regulated protein Kinase*), et avec l'activation de la

phosphorylation des kinases **ERK 1/2** (*Extracellular Regulated Kinase 1/2*). La phosphorylation de ces protéines active divers facteurs de transcription nécessaires à l'activation transcriptionnelle du gène codant pour le VEGF-A. Ainsi, en accord avec la capacité du RWE à diminuer la sécrétion de VEGF-A, nous avons aussi montré qu'il est capable de diminuer significativement la phosphorylation du récepteur VEGF-R2 sur la **tyrosine 951** ainsi que la phosphorylation de MEK et de ERK 1/2. Le resvératrol seul diminue uniquement l'expression protéique de VEGF-R2 sans toutefois modifier significativement sa phosphorylation (activation), ni celles des kinases MEK et ERK 1/2. Ainsi, il semble que **l'extrait sec de vin rouge présente un effet anti-angiogénique plus prometteur que le resvératrol seul**.

C. Article publié

Red Wine Extract Inhibits VEGF Secretion and Its Signaling Pathway in Retinal ARPE-19 Cells to Potentially Disrupt AMD

Clarisse Cornebise[†], Flavie Courtaut[†], Marie Taillandier-Coindard, Josep Valls Fonayet, Tristan Richard, David Monchaud, Virginie Aires et Dominique Delmas*

molecules

MDPI

Article

Red Wine Extract Inhibits VEGF Secretion and Its Signaling Pathway in Retinal ARPE-19 Cells to Potentially Disrupt AMD

Clarisse Cornebise [1,2,†], Flavie Courtaut [1,2,†], Marie Taillandier-Coindard [1,2], Josep Valls Fonayet [3], Tristan Richard [3], David Monchaud [1,4], Virginie Aires [1,2] and Dominique Delmas [1,2,5,*]

1 Université de Bourgogne Franche-Comté, F-21000 Dijon, France; clarisse.cornebise@gmail.com (C.C.); flavie.courtaut@gmail.com (F.C.); marie.taillandiercoindard@gmail.com (M.T.); david.monchaud@u-bourgogne.fr (D.M.); virginie.aires02@u-bourgogne.fr (V.A.) ; dominique.delmas@u-bourgogne.fr (D.D)

2 INSERM Research Center U1231—Cancer and Adaptive Immune Response Team, Bioactive Molecules and Health research group, F-21000 Dijon, France; clarisse.cornebise@gmail.com (C.C.); flavie.courtaut@gmail.com (F.C.); marie.taillandiercoindard@gmail.com (M.T.); virginie.aires02@u-bourgogne.fr (V.A.) ; dominique.delmas@u-bourgogne.fr (D.D)

3 Unité de recherche Oenologie, EA 4577, USC 1366 INRA-ISVV, F-33882 Villenave d'Ornon, France; Josep.Valls-Fonayet@U-Bordeaux.Fr (J.V.F.); tristan.richard@u-bordeaux.fr (T.R.)

4 Institut de Chimie Moléculaire (ICMUB), CNRS UMR6302, UBFC, F-21078 Dijon, France ; david.monchaud@u-bourgogne.fr (D.M.)

5 Centre anticancéreux Georges François Leclerc, F-21000 Dijon, France ; dominique.delmas@u-bourgogne.fr (D.D)

* Correspondence: Dominique.delmas@u-bourgogne.fr; Tel.: +33-380-39-32-26

† These authors contributed equally to this work.

Academic Editors: Paula Silva and Norbert Latruffe
Received: 5 November 2020; Accepted: 25 November 2020; Published: 27 November 2020

Abstract: Age-related macular degeneration (AMD) is a degenerative disease of the retina where the molecular mechanism involves the production of vascular endothelial growth factor (VEGF), a factor of poor prognosis of the progression of the disease. Previous studies have shown that resveratrol, a polyphenol of grapevines, can prevent VEGF secretion induced by stress from retinal cells. Considering the fundamental role played by VEGF in development and progression of AMD, we investigate the potential effect of red wine extract (RWE) on VEGF secretion and its signaling pathway in human retinal cells ARPE-19. To examine the effect of RWE in ARPE-19, a quantitative and qualitative analysis of the RWE was performed by HPLC MS/MS. We show for the first time that RWE decreased VEGF-A secretion from ARPE-19 cells and its protein expression in concentration-dependent manner. RWE-induced alteration in VEGF-A production is associated with a down of VEGF-receptor 2 (VEGF-R2) protein expression and its phosphorylated intracytoplasmic domain. Subsequently, the activation of kinase pathway is disturbing and RWE prevents the phosphorylation of MEK and ERK 1/2 in human retinal cells ARPE-19. Finally, this study sheds light on the interest that the use of polyphenolic cocktails could represent in a prevention strategy.

Keywords: polyphenols; red wine extract; AMD; retinal cells; ARPE-19; degenerative diseases; ocular diseases

1. Introduction

Since the last decade, several epidemiological studies have shown an inverse relation between the incidence of coronary diseases and wine consumption, compared to wine abstinence [1,2]. In France, despite of a fat-containing diet, the incidence of coronary heat diseases is lower than other western countries with a similar diet, which is partly attributed to the moderation consumption of red wine [3]. This apparent discrepancy is called the "French paradox". However, since the 1990s, some studies have shown that this "French paradox" is more likely resulting from a Mediterranean-type diet [4,5].

In this context, we have previously shown in a controlled environment in hospital that a moderate consumption of red wine (250 mL/day), even for a short period (2 weeks), associated with a "Western prudent" diet, improves various blood parameters in the lipid and antioxidative status in patients with previous coronary ischemic accidents in comparison to patients receiving water [6]. This "Western prudent" diet has also been proposed to prevent other pathologies such as degenerative diseases or diseases linked to oxidative stress or even cancer. Very recently, we were able to demonstrate that a red wine extract (RWE) made it possible to act on inflammation by reducing the level of certain proinflammatory cytokines produced by immune cells [7] but also by reducing the formation of an inflammatory complex in macrophages such as NLRP3 (NOD-like receptor family, pyrin domain containing 3) [8], or to reduce intestine polyp preneoplasia development in mice [9]. These effects have been confirmed in other studies, where RWE can reduce tumoral C26 growth in BALB/c mice and vascular endothelial growth factor (VEGF) [10]. The latter factor is not only important for the neoangiogenesis, which is necessary for tumor growth and the spread of metastatic cells, but it is also involved in other disease processes such as age-related macular degeneration (AMD).

Indeed, AMD is a degenerative disease of the retina characterized by progressive loss of central vision. This disease selectively affects the macula, which is the central region of the retina, which explains why only the central vision is affected, and not the peripheral vision. The formation of new blood vessels through the membrane destroys the cells lining the back of the retina. These cells serve as an anchor for the cones and rods, which allow vision, their destruction leads to a localized and permanent loss of this vision. Thus the overexpression of this vascular factor is a factor of poor prognosis of the progression of the disease and many strategies are put in place to counter the production of VEGF in particular the use of anti-VEGF antibodies. Alongside these pharmacological strategies for which resistance sometimes appears, numerous studies have been able to show the influence of nutrition on the occurrence of this type of pathology and its evolution [11,12]. Among natural compounds, polyphenols could present interest to counteract AMD. Indeed, some studies have performed in order to prove the effect of several preparations enriched with polyphenol grape extract or wine polyphenols on age-related degenerative diseases [13] and ocular diseases [14–16]. More specifically, we have shown that resveratrol, a polyphenol of grapevines, prevented VEGF secretion induced by oxysterols from human retinal cells [15]. However, what about a more polyphenolic complex mixture such as red wine, which

contains a wide variety of polyphenols? Considering the fundamental role played by VEGF in development and progression of AMD, we investigated the potential effect of a red wine extract (RWE) on VEGF-A secretion in human retinal cells ARPE-19 having an AMD phenotype. The main goal is to determine whether RWE could decrease VEGF-A secretion and alter this signaling pathway and thus influence the progression of AMD. We show here for the first time that RWE inhibits VEGF-A secretion in a dose-dependent manner in human retinal cells. This reduction is associated with a decrease in VEGF-A protein expression. Very interestingly, RWE affects the signaling pathway leading VEGF production, particularly, RWE decreases activation of the receptor to VEGF-A, VEGF-R2 and the associated-protein kinases such as the mitogen-activated protein kinase (MEK) and extracellular regulated kinase 1/2 (ERK 1/2)

2. Results

2.1. Qualitative and Quantitative Analysis of RWE and Its Toxicity on ARPE-19 Retinal Cells

The wine vinification processes can affect, by many factors, the wine. Indeed, the climate, the vine, the country and the year can alter the quantity and the quality of polyphenols in wine, which also varies between white and red wines. Red wine present a higher quantity of polyphenols estimated to be around 900–2500 mg/L in contrary to white wine composition estimated to be around 190–290 mg/L. As we previously demonstrated in a previous study, the quantitative and qualitative wine composition of bioactive molecules such as polyphenolic compounds is essential in the biological effects that can be observed whether there are antagonistic or synergistic [9]. The Figure 1 summarizes the extraction of red wine (Santenay 1er cru Les Gravières 2012 (Côte d'Or, France), to obtain a power of red wine namely red wine extract (RWE), which was diluted in 70% ethanol at a rate of 100 mg/mL.

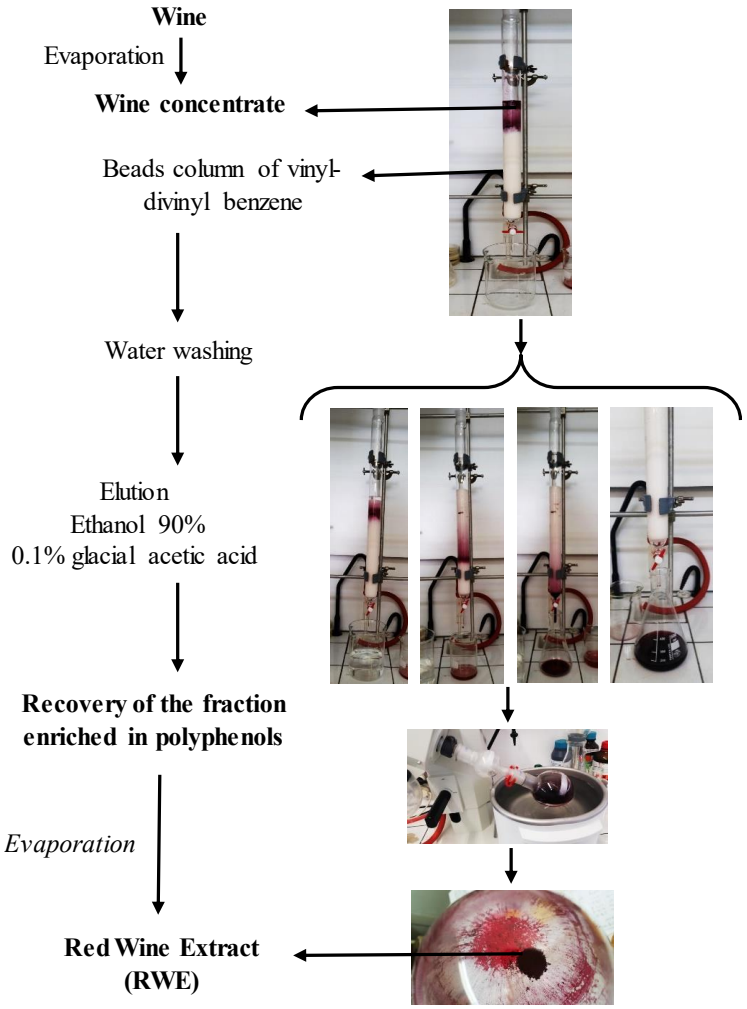

Figure 1. A preparative column was used to adsorb phenolic compounds present in red wine, and after alcohol evaporation, the concentrated residue was lyophilized to be finally sprayed in order to obtain the phenolic extract dry powder.

A qualitative and quantitative analysis performed by HPLC of the RWE was carried out in order to determine its polyphenolic content. As illustrated in Figure 2, we obtained different spectra allowing identifying with MRM transitions and by UV (λ = 520 nm) the main compounds contained in the extract by differentiating the main phenolic non-anthocyanin compounds (Figure 2a) and the main anthocyanins (Figure 2b). Figure 1. A preparative column was used to adsorb phenolic compounds present in red wine, and after alcohol evaporation, the concentrated residue was lyophilized to be finally sprayed in order to obtain the phenolic extract dry powder. A qualitative and quantitative analysis performed by HPLC of the RWE was carried out in order to determine its polyphenolic content. As illustrated in Figure 2, we obtained different spectra allowing identifying with MRM transitions and by UV (λ = 520 nm) the main compounds contained in the extract by differentiating the main phenolic non-anthocyanin compounds (Figure 2a) and the main anthocyanins (Figure 2b).

The qualitative and quantitative determination of polyphenolic compounds in RWE is crucial to evaluate its biological activities since we have previously demonstrated that

composition of bioactive compounds of the wine could impact its antiproliferative and anti-inflammatory activities [7,8]. In fact, we have shown that an association of resveratrol and quercetin can have a synergetic effect against the proliferation of colon cancer cells, which is not the case for other combinations such as resveratrol/catechin or resveratrol/catechin/quercetin [9]. The evaluation of the polyphenolic content revealed an important proportion of phenolic acids and flavan-3-ols. Indeed, we identified 49% of phenolic acids (gallic acid, caftaric acid and caffeic acid) and 36% of flavan 3-ols (catechin, epicatechin, procyanidins B1, B2, B3 and B4) of the total content (Figure 3). To this is added in a smaller but not insignificant quantity, 9% of anthocyanins (delphinidin 3-glucoside, cyanidin 3-glucoside, petunidin 3-glucoside, peonidin 3-glucoside and malvidin 3-glucoside); 2% of flavonols (quercetin, quercetin-3-glucoside and quercetin-3-rhamnoside) and 4% of stilbenes (*cis*- and *trans*-resveratrol, *cis*- and *trans*-piceid, *trans*-piceatannol, ε-viniferin, Ω-viniferin, pallidol and isohopeaphenol).

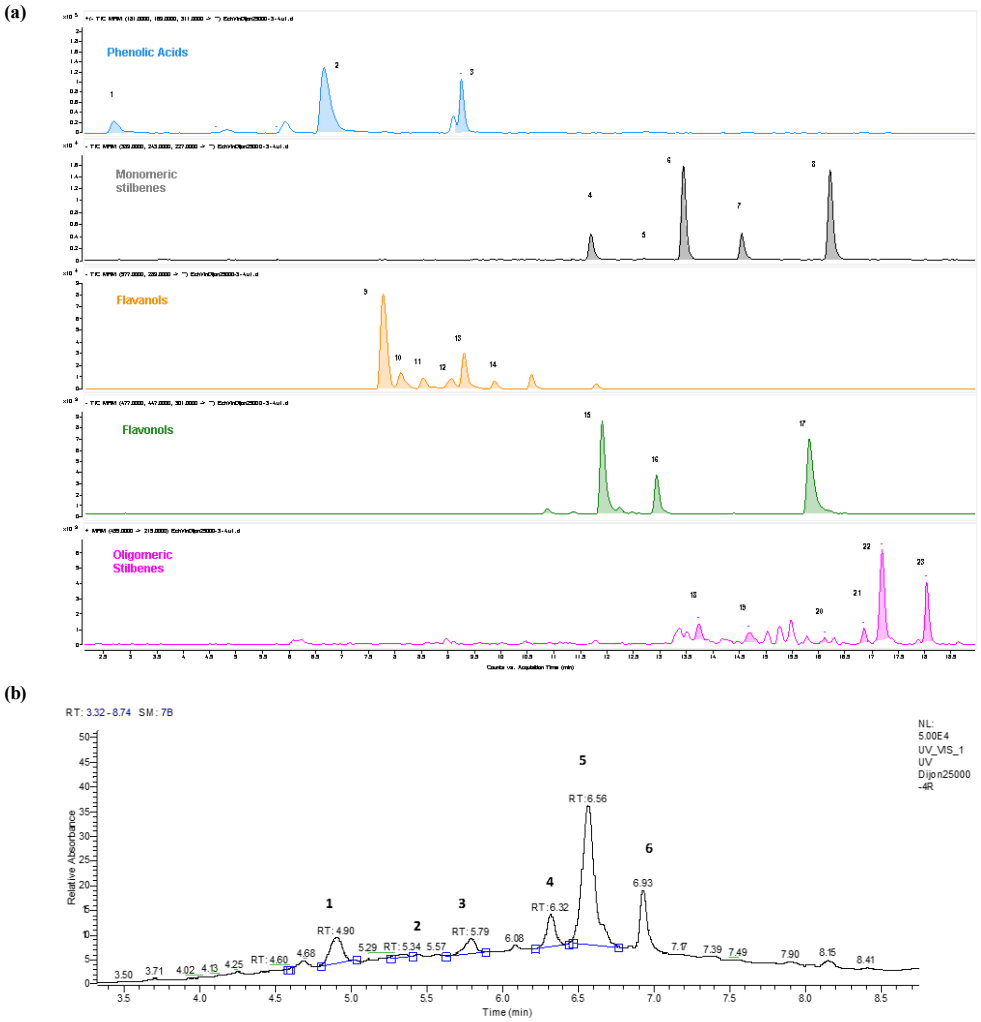

Figure 2. (a) Extracted ion chromatogram of the MRM transitions belonging to the main phenolic non-anthocyanin compounds detected in the wine extract. 1 = Gallic Acid; 2 = Caftaric Acid; 3 = Caffeic Acid; 4 = t-Piceid; 5 = t-Piceatannol; 6 = c-Piceid; 7 = t-Resveratrol; 8 = c-Resveratrol; 9 = Procyanidin B1; 10 = Procyanidin B3; 11 = Catechin; 12 = Procyanidin B4; 13 = Procyanidin B2; 14 = Epicatechin; 15 = Quercetin-3-glucuronide; 16 = Quercetin-3-rhamnoside; 17 = Quercetin; 18 = Pallidol; 19 = Parthenocisin A; 20 = Isohopeaphenol; 21 = c-E-viniferin; 22 = t-E-viniferin, 23 = t-w-viniferin. (b) UV520 Chromatogram of the

main anthocyanins detected in the red wine extract. 1 = Delphinidin 3-glucoside; 2 = Cyanidin 3-glucoside; 3= Petunidin 3-glucoside; 4= Peonidin 3-glucoside; 5= Malvidin 3-glucoside; 6 = Malvidin acylated derivative.

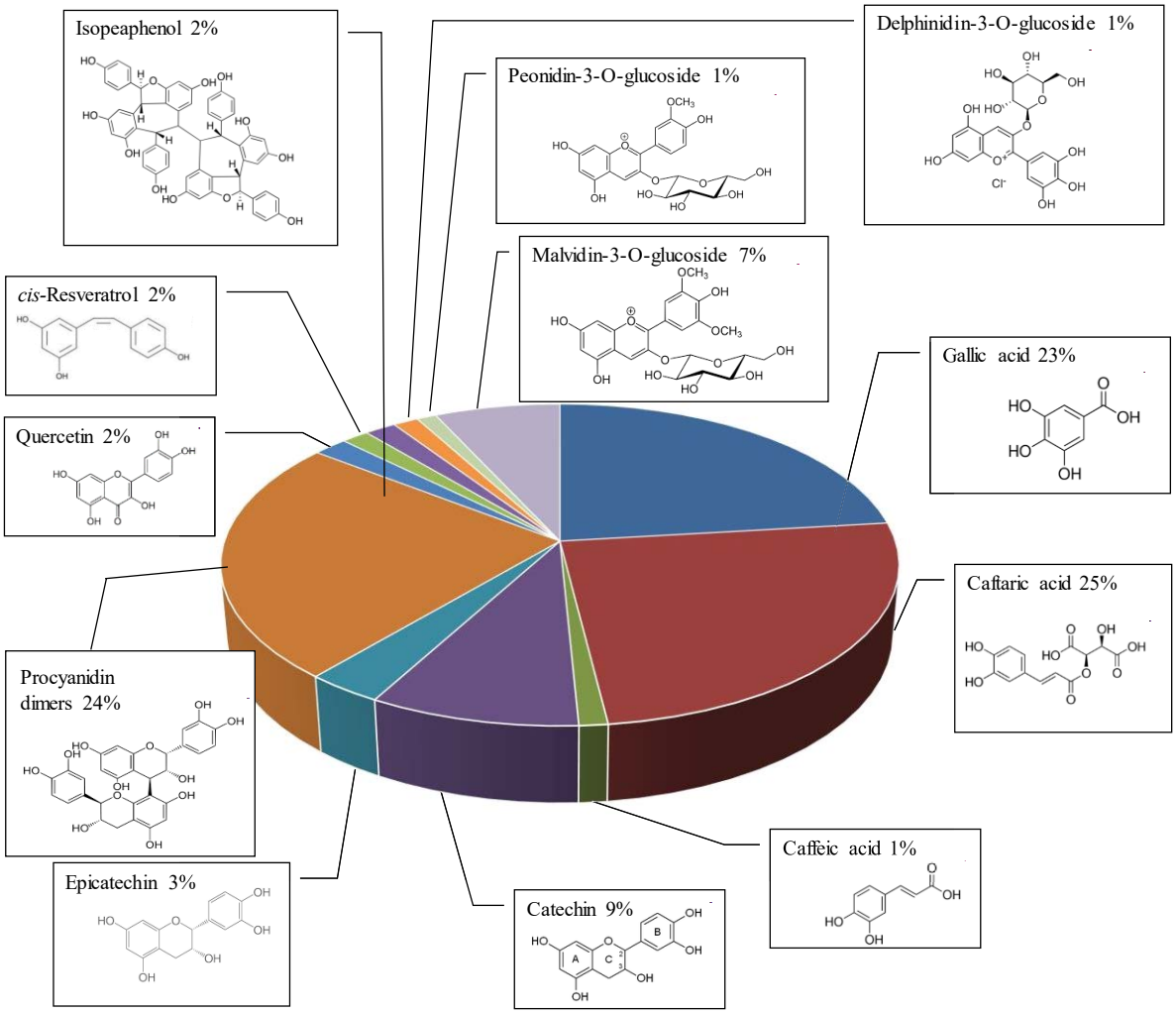

Figure 3. Quantitative analysis of red wine extract content and chemical structures of the main polyphenolic compounds

To specify the potential role of RWE in AMD and more particularly against VEGF, we first evaluated its toxicity on undifferentiated ARPE-19 retinal cells mimicking cells affected by AMD [17]. As revealed by cytotoxic curves that whatever the time of treatment, 24 and 48 h, RWE had no significant impact on the cellular viability of human retinal cells ARPE-19 with a game of increasing concentrations of RWE to 0 up to 250 µg/mL (Figure 4a). In the same manner, resveratrol (RSV) used in our experiment as a reference compound, presented no significant toxicity at the time of treatment and concentrations used (Figure 4b). In the following experiments, RWE was therefore used at three concentrations namely 30, 50 and 100 µg/mL in ARPE-19 cell lines. These concentrations were chosen both because they are noncytotoxic on retinal cells and because we have previously shown with these same concentrations that RWE was able to present significative properties (i.e., inhibition of proinflammatory cytokines

production from macrophages [8], prevention of naïve T lymphocytes differentiation into proinflammatory T helper 17 cells [7] and inhibition of polyps development [9]). Furthermore, the secretion of VEGF by retinal cells being a rapid process with an early response of the kinase cascade activation, we explored the effect of RWE after 24 h of treatment of APRE-19 cells. In this experiment, RSV was used as a comparison at a concentration of 30 μM, which is non cytotoxic on the cell line ARPE-19. Indeed, we have previously shown a protective effect of RSV against toxic effects of oxysterols in retinal cells after 24 h and 48 h of treatment [15].

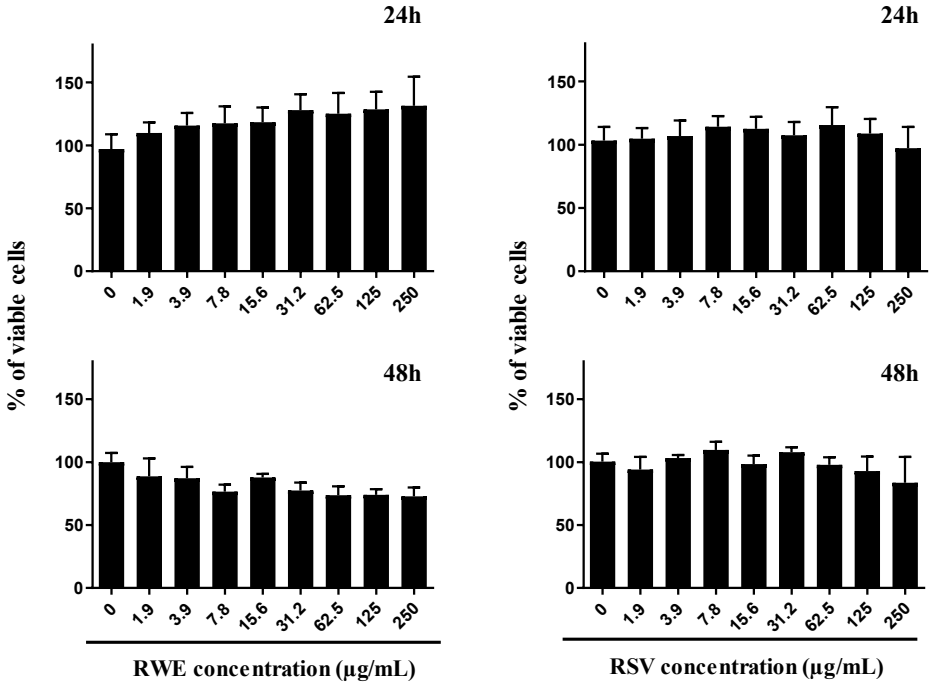

Figure 4. Safety assessment of red wine extract (RWE) and RSV on human retinal cell line ARPE-19. Crystal violet staining was performed in order to analyzed the cell viability of ARPE-19 after 24, 48 and 72 h of the (a) RWE treatment (starting concentration up to 250 μg/mL, 1:2 serial dilutions) and (b) RSV (starting concentration up to 250 μg/mL, 1:2 serial dilutions). Data are expressed as mean percentages ± s.d. of three independent experiments.

2.2. RWE Prevents VEGF Secretion from ARPE-19 Cells and Its Protein Expression

Since VEGF is the main factor involved in the neoangiogenesis and the progression of AMD, we firstly determined whether RWE was able to affect its expression. Immunoblotting analysis shown that after 24 h of treatment, RWE strongly decreased VEGF protein expression in ARPE-19 cells in a concentration-dependent manner as compared to the control (Figure 5a). Interestingly, RWE at 50 μg/mL presented the same inhibitory effect of VEGF expression as RSV at 30 μM, and a more effect at 100 μg/mL (Figure 5a). These results suggested that polyphenolic compounds present into RWE at lower concentrations act in a synergistic manner to decrease VEGF expression. This is in agreement with what we previously found regarding the effect of RWE in other models such as macrophages or immune cells [7,8]. This decrease in VEGF protein expression by RWE should normally be accompanied by a decrease in VEGF secretion

by retinal cells. In order to verify this hypothesis, we quantified using an ELISA method, the levels of VEGF released into the culture medium. As assumed, 24 h of treatment, RWE decreased the levels of VEGF in a very significant manner for the concentrations of 50 and 100 μg/mL (Figure 5b). Surprisingly, the RSV at the concentrations of 30 μM after 24 h of treatment failed to decrease the production of VEGF in retinal cells.

2.3. RWE Prevents VEGF-A Secretion from ARPE-19 Cells and Its Protein Expression

Secretion of VEGF-A by retinal cells results from the activation of the signaling pathway involving VEGF-specific tyrosine kinase receptors whose activation loop results from a phosphorylation cascade through the induction of successive kinases [18]. Indeed, the binding of VEGF-A occurs mainly on the VEGF-R2 receptor, which induces its phosphorylation and the intracytoplasmic signaling cascade, passing through the phosphorylation of the mitogen-activated protein kinase kinase (MEK) protein, and with the ultimate activation of the phosphorylation of the extracellular regulated kinase 1/2 (ERK 1/2) protein. The latter once phosphorylated could then activate various nuclear transcription factors making it possible to activate the gene coding for VEGF. We observed by immunoblotting that RWE since low concentration at 30 μg/mL was able to strongly inhibit VEGF-R2 protein expression and its phosphorylated form (Figure 6). This disruption in VGEF-R2 activation through its intracytoplasmic phosphorylation leads to a decrease of activation of the MEK and ER 1 2 pathway. As shown by the immunoblotting 24 h of treatment with RWE decreased significantly the phosphorylation of MEK and ERK 1/2 in ARPE-19 cells (Figure 6). Although RSV decreased significantly the expression of VEGF-R2, the polyphenol failed to prevent the phosphorylation of VEGF-R2 and subsequently then allowed the phosphorylation cascade to take place.

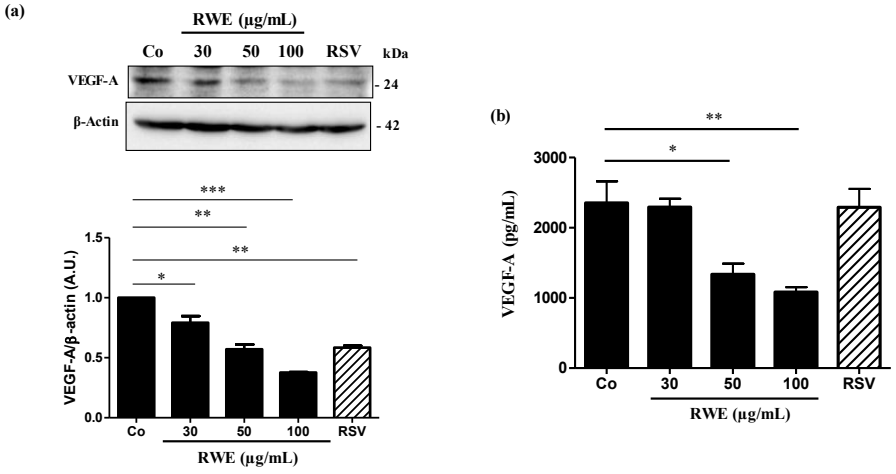

Figure 5. RWE decreases VEGF-A protein expression and its secretion from ARPE-19 cells. (a) Upper panel: representative immunoblot of VEGF6A protein expression from three independent experiments in human retinal ARPE-19 cells after 24 h of treatment without (Co) or with 30, 50 and 100 μg/mL of RWE or with RSV 20 μM. β-actin was used as a loading control. Down panel: densitometry quantification of Western blotting. Data are expressed as the mean folds' induction ± SEM of three independent experiments. p values were determined by a one-way ANOVA followed by Tukey's multiple comparison test. * $p < 0.05$, ** $p < 0.01$ and *** $p < 0.001$. (b) As in (a) VEGF-A secretion was measured in the cell medium by ELISA. The data are the mean ± S.D. of four independent

experiments with n = 10. p values were determined by a one-way ANOVA followed by Tukey's multiple comparison test. * = $p < 0.05$; ** = $p < 0.01$; *** = $p < 0.001$.

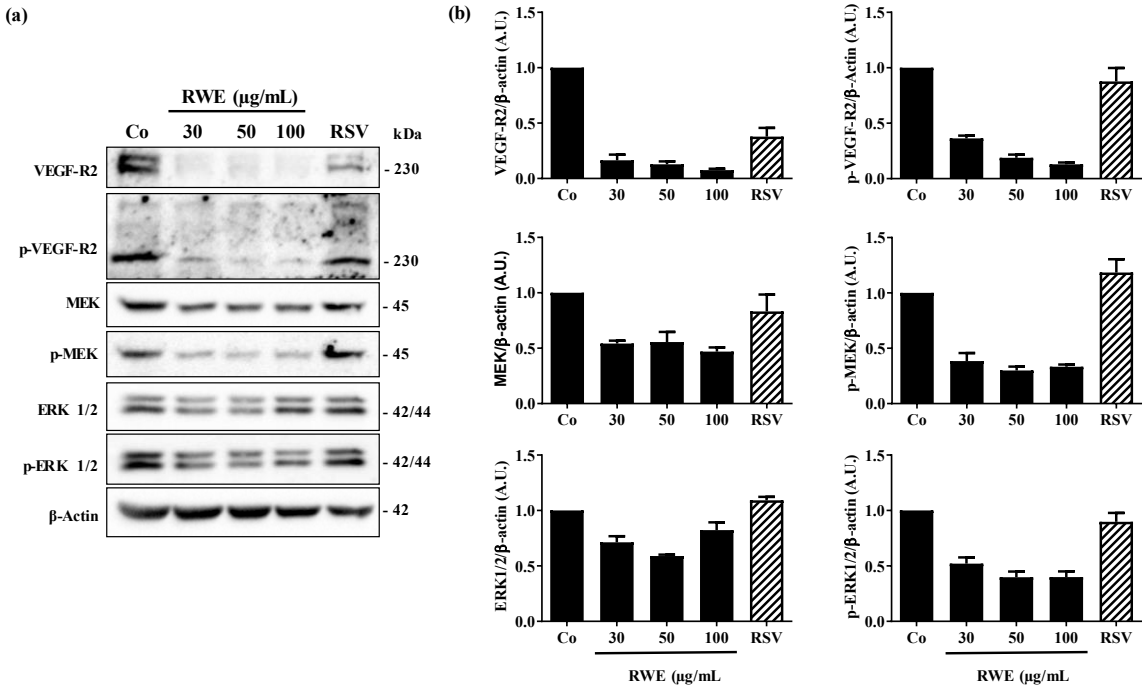

Figure 6. RWE disrupts VEGF-R2 kinase activation pathways. (a) Immunoblotting analysis of VEGF-R2, phospho VEGF-R2 (p-VEGF-R2), MEK, phospho MEK (p-MEK), ERK 1/2 and phospho-ERK 1/2 (p ERK 1/2) in RWE-treated ARPE-19 cells with increasing concentration (30, 50 and 100 µg/mL) or with RSV (20 µM) for 24 h. β-actin was used as a loading control. (b) Densitometry quantification of Western blotting. Data are expressed as the mean folds induction ± SEM of three independent experiments. p values were determined by a one-way ANOVA followed by Tukey's multiple comparison test. * $p < 0.05$, ** $p < 0.01$ and *** $p < 0.001$.

3. Discussion

AMD is a multifactorial degenerative pathology, which results from the conjunction of several risk factors. The most important of these is age, with a sharp increase after the sixth decade, but there are also genetic, ethnic or environmental factors. Indeed, smoking, obesity and diet are linked to this disease [19]. Studies have shown that in developed countries, AMD is the leading cause of visual impairment and blindness affecting people over 65 years [20]. The molecular mechanism of AMD involved a growth factor, namely VEGF-A, for which the secretion induces the appearance of new immature and poor quality blood vessels that invade the different histological layers that make up the retina. This results in the destruction of the thin membrane separating the retina from the bloodstream [21]. This invasion combined with the fact that these vessels, of poor quality, allow serum to diffuse causes a progressive loss of vision by the destruction of the underlying cells. It therefore appears essential to control the secretion of VEGF in order to limit the phenomenon of neoangiogenesis and thus limits the disappearance of retinal cells. To overcome this VEGF-A secretion by retinal cells affected by AMD, there is a growing research interest to develop various antibodies against VEGF-A [22], but this strategy failed in one form of AMD, the dry form for

which there is no treatment at present apart from recommendations in particular in terms of nutrition or supplementation [23]. Moreover, some resistance to anti-VEGF-A antibodies is highlighted in patients with an exudative form [24]. Thus some studies have tried to demonstrate the action of nutrition or supplementation against VEGF-A secretion from retinal cells such as oral nutritional supplementation in patients with intermediate or advanced AMD, where the risk of vision loss of three or more line was reduced by 19% with this supplementation [11]. In this way, we tested the ability of a polyphenol-enriched extract (RWE) from a red wine to act on the VEGF-A pathway in human retinal cells, which is an AMD phenotype. The present study highlights that RWE was able to prevent secretion of VEGF-A from ARPE-19 cells in a dose-dependent manner, which is associated with a decrease of VEGF-A protein expression. Usually, its activity is linked to its binding to the surface of tyrosine kinase receptors (VEGF-R or vascular endothelial growth factor receptor). The binding is done on the extracellular part of the transmembrane receptors. There are three isoforms of receptors that bind VEGFs with different affinities: VEGF-R1, VEGF-R2 and VEGF-R3. Each of them activates different signaling channels resulting in different effects. It has thus been possible to demonstrate the role of VEGF-R1 and VEGF-R2 in the process of angiogenesis, while that of VEGF-R3 is more linked to lymphangiogenesis [25]. More generally, VEGF-A binds to VEGF-R1 and VEGF-R2. These have 44% homology in their sequence, but their affinity for their ligand differs, and they induce different cellular and biological effects. The receptor with the strongest affinity for VEGF-A is VEGF-R1, but the receptor predominantly present on the surface of epithelial cells is VEGF-R2, so it is the latter that appears to be the main mediator of angiogenic activity. In addition, VEGF-R1 has been shown to have lower activity due to the presence of an inhibitory sequence, the absence of which in VEGF-R2 leads to an improvement in tyrosine kinase activity. VEGF binding to its receptor leads to phosphorylation of its intracytoplasmic domain for engaging the mitogen-activated protein kinase (MAP kinase) activation cascade including MEK and ERK (Figure 7).

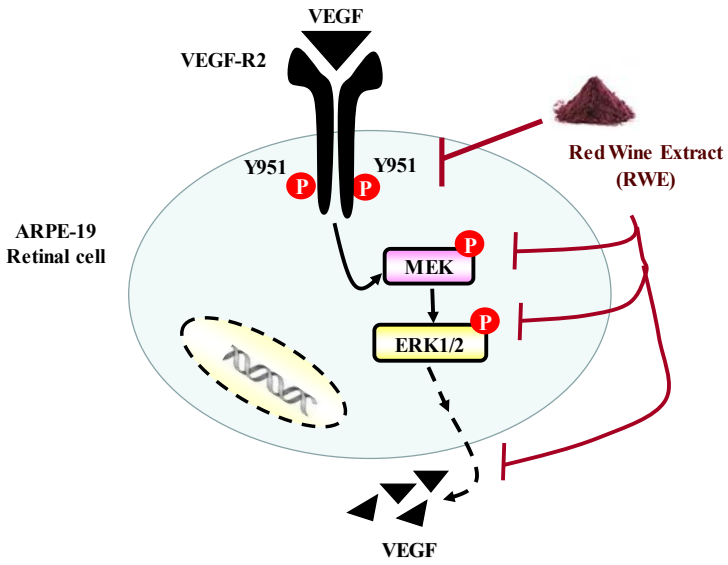

Figure 7. RWE prevents VEGF production by disruption of VEGF-R2 activation. RWE decreases the phosphorylation of VEGF-R2 (P-VEGF-R2) and subsequently prevents the phosphorylation of MEK (P-MEK) and ERK 1/2 (P-ERK 1/2) in human retinal cells ARPE-19.

We show in the present report that RWE was able to alter the phosphorylation of intracytoplasmic domain of VEGF-R2 leading a disrupting in kinase pathway (Figure 7). By disrupting the phosphorylation of MEK and ERK in retinal cells, RWE could alter the pathway inducing the VEGF production.

It is very surprising that the polyphenol RSV alone was not able to prevent this pathway at 20 μM. This absence of effect on VEGF secretion by retinal cells was with a lack of effect on the MAPK activation pathway. This could be explained by the fact that RWE contains many polyphenolic compounds that, even at very low concentrations, could act in synergy in order to exert an action against the activation of the VEGF-R2 pathway. Analysis of polyphenolic composition revealed a high content of phenolic acid (49%) and flavan 3-ols (36%). These compounds were particularly important since separately they were shown to exert an action on VEGF-A production. For example, among phenolic acids, gallic acid exerted an antiangiogenic effect in ovarian cancer cells [26] or in vascular smooth muscle cells [27], and caffeic acid reduces the VEGF secretion in human retinal pigment epithelial cells under hypoxic conditions [28]. Similarly, delphinidin has been shown to inhibit angiogenesis through the suppression of VEGF expression in lung cancer cells [29]. The presence of quercetin could explain a potential mechanism of synergism. Indeed, resveratrol + quercetin association increases resveratrol uptake by colon carcinoma cells, and in combination with RWE this combination increases the influx of resveratrol [9,30,31]. In a similar manner, the presence of quercetin in RWE could increase the uptake of some polyphenols and favors the synergism between the bioactive compounds to potentiate their action against neoangiogenesis in AMD.

4. Materials and Methods

4.1. Cell Lines and Cell Culture

The human retinal pigmented epithelial cell line ARPE-19, purchased from the American Type Culture Collection (Manassas, VA, USA), were maintained in Dulbecco's modified Eagle's F12 medium (DMEM/F12) supplemented with 10% fetal bovine serum (Dutscher, Brumath, France), 1% penicillin/streptomycin in a humidified atmosphere of 5% CO2 at 37 ◦C. Cells were seeded and grown to a subconfluence of 60–70% in normoxia. Twenty four hours after seeding, the medium was removed and the cells were washed once with Hank's Balanced Salt Solution (HBSS, Dutscher, Brumath, France) before reincubating in DMEMF12 with 1% FBS and 1% penicillin/streptomycin. The following day, cells were treated with DMSO, RWE with indicated concentrations or resveratrol 20 μM.

4.2. Chemical Reagents and Antibodies

Resveratrol (RSV) was purchased from Sigma-Aldrich (St. Quentin Fallavier, France) and dissolved in ethanol 70%. VEGFR2 (sc-2479, 1:1000); p-VEGFR2 TYR951 (sc-4991, 1:1000); ERK1/2 (sc-4695, 1:1000); p-ERK1/2 (sc-9101, 1:1000); MEK1/2 (sc-91226, 1:1000) and p-MEK1/2 (Ser221; sc-2338, 1:1000) were obtained from Santa Cruz Biotechnology (Nanterre, France) and p-VEGFR2 (TYR 1054; 267,398, 1:1000) was obtained from EMD Millipore Corporation. B-Actin (A1978, 1:5000) was obtained from Abcam. (Paris, France). (+)-Catechin (>99%), (−)-epicatechin (>99%), procyanidin B1 (>90%), procyanidin B2 (>90%) and quercetin as a dihydrate (>99%) were obtained from Extrasynthese (Genay, France). Gallic acid (>97.5%) and caffeic acid (>98%) were obtained from Sigma-Aldrich (St Quentin Favrallier, France). Caftaric acid (>98%) was purchased from Carl Roth (Karslruhe, Germany). E-resveratrol, hopeaphenol and malvidin 3-glucoside were purified as standards in the MIB laboratory using a Varian Pro Star preparative HPLC. Purity was assessed to be over 90% by HPLC.

4.3. Preparation of the Red Wine Extract

The red wine extract (RWE) was obtained from French red wine, Santenay 1er cru Les Gravières 2012 (EARL Capuano-Ferreri Santenay, Côte-d'Or, France) selected by BIVB (Bureau Interprofessionnel des Vins de Bourgogne, Beaune, France) and provided by CTIVV (Centre Technique Interprofessionnel de la Vigne et du Vin, Beaune, France). Red wine extract dry powder was prepared and analyzed as previously described [7,8]. Briefly, the phenolic compounds contained in the wine were separated from the liquid using an absorption column and solubilized in alcohol. After evaporation of the alcoholic eluent using a rotary evaporator, the concentrated residue was deposited on the column (Diainon® HP-20, Supelco, Germany). For the retention phase, the column reservoir was filled with distilled water, and the flow rate was adjusted to approximately 20 drops/min. Then the polyphenol fraction retained was eluted using a solution of ethanol and 0.1% glacial citric acid, and the flow rate was adjusted to about 40 drops/min. The fractions collected after elution were concentrated to dryness with a rotary evaporator. In this way, we obtained, from 1 L of red wine, 104 g of phenolic extract in powder form, containing 5.04 mg g−1 of total phenolic compounds expressed as the gallic acid equivalent.

4.4. High-Performance Liquid Chromatography Analysis

Triplicates of 5 mg freeze-dried extract was dissolved with 200 µL of a mixture water:methanol (1:1) and centrifuged for 5 min at 10,000× g before anthocyanins and polyphenols analysis. Anthocyanins were analyzed with a Thermo Scientific Vanquish UHPLC equipped with a Thermo Scientific MWL detector operating at 520 nm. Of the sample 1 µL was injected in Agilent Zorbax SB-C18 (100 mm × 2.1 mm × 1.8 µm) column at 35◦ using the following conditions of separation: solvent A (5% formic acid in MilliQ water) and solvent B (5% formic acid in acetonitrile); flow: 0.35 mL/mi and gradient: 2.5% B (0–1 min), 17% B (5–7 min), 45% B (10–11 min), 95% B (11–12.5 min) and 2.5% B (13–15 min). A calibration curve in the range of 6.25–80 mg/L was built with malvidin 3-glucoside previously purified in our laboratory. The 5 quantified anthocyanins (delphinidin 3-glucoside, cyanidin 3-glucoside, petunidin 3-glucoside, peonidin 3-

glucoside and malvidin 3-glucoside) were quantified as malvidin 3-glucoside. The rest of the polyphenols was analyzed by HPLC–MS/MS methodology previously published [32] with slight modifications. The compounds were separated with an Agilent 1260 HPLC instrument. Of samples 4 μL were eluted on an Agilent Zorbax SB-C18 (100 mm × 2.1 mm × 1.8 μm) column at 40 ◦C with a binary solvent system of solvent A (0.1% formic acid in water) and solvent B (0.1% formic acid in acetonitrile). The chromatographic separation was conducted with a flow rate of 0.4 mL/min and the following gradient: 10–18% B (0–1 min), 18–33% B (1–6.5 min), 33% B (6.5–9.5 min), 33–40% B (9.5–15 min), 40–90% B (15–16 min), 90% B (16–19 min) and 90–10% B (19–20 min). The HPLC was coupled to an Agilent 6430 Triple Quadrupole mass spectrometer, which operated under the following parameters: alternate positive/negative mode; drying gas (nitrogen), 11 L/min; nebulizer pressure, 15 psi; temperature, 350 ◦C and capillary voltage, 3000 V. Specific MRM transitions were used for the detection and quantification of each compound. Calibration curves were established with pure standards in the range of 0.03–15.00 mg/L except for catechin, gallic acid and caftaric acid (range 0.03–100 mg/L). All compounds were quantified as their corresponding standard except flavan 3-ol dimers B3 and B4, which were expressed as dimer B1 and B2 respectively, and isomers c-resveratrol and c-piceid, which were determined as their respective t-isomer.

4.5. Cell Viability Assays

The viability assays were assessed by crystal violet staining (Sigma Aldrich, St. Quentin Fallavier, France). Retinal ARPE-19 cells were seeded into 96-well plates after 24 h, the medium was replaced by new medium containing different concentrations of RWE or RSV and incubated for 24, 48 and 72 h. Then, cells were washed with phosphate-buffered saline (PBS) and fixed with ethanol for 10 min at 4 ◦C. Finally, cells were stained with a crystal violet solution (0.5% (w/v) crystal violet in 25% (v/v) methanol) for 15 min at room temperature, then the absorbance was measured at 590 nm using a Biochrom Assays UVM 340 microplate reader, following extraction of the dye using an acetic acid 33% solution.

4.6. Measurement of VEGF Secretion

Cell culture media were saved from the final 24 h of treatment of ARP-19 with RWE (30, 50 or 100 μg·mL−1) or RSV (20 μM). VEFG levels in cell culture conditioned medium were measured using the enzyme-linked immunosorbant assay (ELISA; BMS277-2 eBioscience) with antibodies mainly specific to VEGF-121; VEGF-165 and VEGF-189.

4.7. Immunoblotting Analysis

ARPE-19 cells were treated as described above. Next, cells were collected and lysed in radioimmunoprecipitation assay (RIPA) buffer (50 mM Tris-HCl, 150 mM sodium chloride, 0.1% sodium dodecyl sulfate, 0.5% sodium deoxycholate, 1% NP40 and pH 8) containing a protease inhibitor, phenylmethylsulfonyl fluoride (PMSF; 100 μM, Sigma-Aldrich, St. Quentin Fallavier, France), phosphatase inhibitor, sodium fluoride (50 mM)

and a protease inhibitor cocktail (Roche, Boulogne-Billancourt, France). Protein concentrations were measured using the QuantiPro™ BCA (Bicinchoninic Acid; Sigma Aldrich, St. Louis, MO, USA; bovine serum albumin (BSA) was used as a standard). Fifty micrograms of proteins were prepared in the Laemmli gel loading buffer (50 mM Tris-HCl, 10% glycerol, 5% 2-mercaptoethanol, 2% sodium dodecyl sulfate, pH 6.8 and 0.1% bromophenol blue). After being boiled 5 min at 95 ◦C, samples were loaded and separated on sodium dodecyl sulfate–polyacrylamide gel electrophoresis (SDS-PAGE). Protein size markers (Thermo Fisher Scientific, Illkirch-Graffenstaden, France) were loaded without heating. Then, proteins were separated on sodium dodecyl sulfate–polyacrylamide gel electrophoresis (SDS-PAGE). Proteins separated on gels were transferred to nitrocellulose membrane (Amersham, Les Ulis, France). Membranes were blocked for 1 h at room temperature in either 5% of bovine serum albumin (BSA) or 5% of skimmed milk powder dissolved in PBS-T (PBS containing 0.1% Tween 20) and incubated with the primary antibody on a rocker platform at 4 ◦C overnight. Primary antibodies for Western blot listed in chemical reagents and antibodies were diluted with 5% w/v non-fat milk or 5% BS PBS-T. After three 10 min in PBS-T, primary antibodies were detected using appropriate horseradish peroxidase (HRP)-conjugated secondary antibodies (Jackson ImmunoResearch, Interchim, Montlucon, France) for 1 h at room temperature, followed by exposure to enhanced chemiluminescence (ECL; Bio-Rad, Marnes-la-Coquette, France). Detection of immunoreactive bands was performed by ChemiDocTM XRS + imaging system (Bio-Rad, Marnes-la-Coquette, France), and blots were analyzed with Image LabTM version 6.0.1 software (Bio-Rad).

4.8. Statistical Analysis

Statistical analysis was conducted using the GraphPad6.0 Prism software (GraphPad Software, La Jolla, San Diego, CA, USA). Data are represented as means ± standard deviation (SD) for triplicate assay samples (otherwise mentioned), of at least three independent experiments. The difference between mean values was determined by the multiple Student's t test or by Mann–Whitney U test. All p values are two-tailed; $p < 0.05$ was considered significant (* $p < 0.05$, ** $p < 0.01$ and *** $p < 0.001$).

5. Conclusions

Increasing life expectancy will continue to increase the prevalence of age-related eye diseases in economically developed countries. Its chronic course is currently impossible to cure, but it can be delayed. In this, the search for new bioactive molecules of low toxicity could represent a major interest for the prevention or for delaying the progression of AMD. In this study we showed for the first time that a polyphenol-enriched extract, RWE, could decrease VEGF-A secretion for human retinal ARPE-19 cells mimicking the AMD phenotype. This disturbing of VEGF-A production is associated with a decrease of its protein expression. Very interestingly, RWE affects the MAP kinase pathway through downregulation of phosphorylated forms of MAK and ERK1/2 proteins. Thus the use of polyphenolic cocktails could represent a potential interest in a therapeutic strategy. Nonetheless, further studies should better clarify the

role of each of the polyphenols present, but also to specify more precisely the molecular mechanisms involved and their effects in preclinical models of AMD.

Author Contributions: C.C., F.C. and M.T.-C. performed the experiments and analyzed the data; J.V.-F. and T.R. investigated the qualitative and quantitative polyphenols composition, D.M. helped for RWE extract methods; V.A. Methodology Project administration, D.D.; Supervision, D.D.; Writing—original draft, D.D. All authors have read and agreed to the published version of the manuscript.

Funding: This work was supported by grants from the ANRT N◦2016/0003, by a French Government grant managed by the French National Research Agency under the program "Investissements d'Avenir", reference ANR-11-LABX-0021, the Conseil Régional Bourgogne, Franche-Comte (PARI grant) and the FEDER (European Funding for Regional Economic Development), the "Bureau Interprofessionnel des Vins de Bourgogne" (BIVB), and by the Bordeaux Metabolome Facility and MetaboHUB (ANR-11-INBS-0010) project. Acknowledgments: The authors thank Ruth Hornedo Ortega for supplying the malvidin 3-glcuoside standard. Conflicts of Interest: The authors declare no conflict of interest

References

1. Renaud, S.C.; Gueguen, R.; Schenker, J.; d'Houtaud, A. Alcohol and mortality in middle-aged men from eastern France. *Epidemiology* **1998**, *9*, 184–188.
2. Goldberg, D.M.; Soleas, G.J.; Levesque, M. Moderate alcohol consumption: The gentle face of Janus. *Clin. Biochem.* **1999**, *32*, 505–518.
3. St Leger, A.S.; Cochrane, A.L.; Moore, F. Ischaemic heart-disease and wine. *Lancet* **1979**, *1*, 1294.
4. Parodi, P.W. The French paradox unmasked: The role of folate. *Med. Hypotheses* **1997**, *49*, 313–318.
5. Criqui, M.H.; Ringel, B.L. Does diet or alcohol explain the French paradox? *Lancet* **1994**, *344*, 1719–1723.
6. Rifler, J.P.; Lorcerie, F.; Durand, P.; Delmas, D.; Ragot, K.; Limagne, E.; Mazue, F.; Riedinger, J.M.; d'Athis, P.; Hudelot, B.; et al. A moderate red wine intake improves blood lipid parameters and erythrocytes membrane fluidity in post myocardial infarct patients. *Mol. Nutr. Food Res.* **2012**, *56*, 345–351.
7. Chalons, P.; Courtaut, F.; Limagne, E.; Chalmin, F.; Cantos-Villar, E.; Richard, T.; Auger, C.; Chabert, P.; Schini-Kerth, V.; Ghiringhelli, F.; et al. Red Wine Extract Disrupts Th17 Lymphocyte Differentiation in a Colorectal Cancer Context. *Mol. Nutr. Food Res.* **2020**, e1901286, doi:10.1002/mnfr.201901286.
8. Chalons, P.; Amor, S.; Courtaut, F.; Cantos-Villar, E.; Richard, T.; Auger, C.; Chabert, P.; Schni-Kerth, V.; Aires, V.; Delmas, D. Study of Potential Anti-Inflammatory Effects of Red Wine Extract and Resveratrol through a Modulation of Interleukin-1-Beta in Macrophages. *Nutrients* **2018**, *10*, doi:10.3390/nu10121856.
9. Mazue, F.; Delmas, D.; Murillo, G.; Saleiro, D.; Limagne, E.; Latruffe, N. Differential protective effects of red wine polyphenol extracts (RWEs) on colon carcinogenesis. *Food Funct.* **2014**, *5*, 663–670.

10. Walter, A.; Etienne-Selloum, N.; Brasse, D.; Khallouf, H.; Bronner, C.; Rio, M.C.; Beretz, A.; Schini-Kerth, V.B. Intake of grape-derived polyphenols reduces C26 tumor growth by inhibiting angiogenesis and inducing apoptosis. *FASEB J.* **2010**, *24*, 3360–3369.
11. Marshall, L.L.; Roach, J.M. Prevention and treatment of age-related macular degeneration: An update for pharmacists. *Consult. Pharm.* **2013**, *28*, 723–737.
12. Querques, G.; Benlian, P.; Chanu, B.; Portal, C.; Coscas, G.; Soubrane, G.; Souied, E.H. Nutritional AMD treatment phase I (NAT-1): Feasibility of oral DHA supplementation in age-related macular degeneration. *Eur. J. Ophthalmol.* **2009**, *19*, 100–106.
13. Mendes, D.; Oliveira, M.M.; Moreira, P.I.; Coutinho, J.; Nunes, F.M.; Pereira, D.M.; Valentao, P.; Andrade, P.B.; Videira, R.A. Beneficial effects of white wine polyphenols-enriched diet on Alzheimer's disease-like pathology. *J. Nutr. Biochem.* **2018**, *55*, 165–177.
14. Kang, J.H.; Choung, S.Y. Protective effects of resveratrol and its analogs on age-related macular degeneration in vitro. *Arch. Pharm. Res.* **2016**, *39*, 1703–1715.
15. Dugas, B.; Charbonnier, S.; Baarine, M.; Ragot, K.; Delmas, D.; Menetrier, F.; Lherminier, J.; Malvitte, L.; Khalfaoui, T.; Bron, A.; et al. Effects of oxysterols on cell viability, inflammatory cytokines, VEGF, and reactive oxygen species production on human retinal cells: Cytoprotective effects and prevention of VEGF secretion by resveratrol. *Eur. J. Nutr.* **2010**, *49*, 435–446.
16. Sheu, S.J.; Liu, N.C.; Chen, J.L. Resveratrol protects human retinal pigment epithelial cells from acrolein-induced damage. *J. Ocul. Pharmacol. Ther.* **2010**, *26*, 231–236.
17. Ablonczy, Z.; Dahrouj, M.; Tang, P.H.; Liu, Y.; Sambamurti, K.; Marmorstein, A.D.; Crosson, C.E. Human retinal pigment epithelium cells as functional models for the RPE in vivo. *Invest. Ophthalmol. Vis. Sci.* **2011**, *52*, 8614–8620.
18. Koch, S.; Tugues, S.; Li, X.; Gualandi, L.; Claesson-Welsh, L. Signal transduction by vascular endothelial growth factor receptors. *Biochem. J.* **2011**, *437*, 169–183.
19. Clemons, T.E.; Milton, R.C.; Klein, R.; Seddon, J.M.; Ferris, F.L.; Age-Related Eye Disease Study Research Group. Risk factors for the incidence of Advanced Age-Related Macular Degeneration in the Age-Related Eye Disease Study (AREDS) AREDS report no. 19. *Ophthalmology* **2005**, *112*, 533–539.
20. Tranos, P.; Vacalis, A.; Asteriadis, S.; Koukoula, S.; Vachtsevanos, A.; Perganta, G.; Georgalas, I. Resistance to antivascular endothelial growth factor treatment in age-related macular degeneration. *Drug Des. Dev. Ther.* **2013**, *7*, 485–490.
21. Siemerink, M.J.; Augustin, A.J.; Schlingemann, R.O. Mechanisms of ocular angiogenesis and its molecular mediators. *Dev. Ophthalmol.* **2010**, *46*, 4–20.
22. Kovach, J.L.; Schwartz, S.G.; Flynn, H.W., Jr.; Scott, I.U. Anti-VEGF Treatment Strategies for Wet AMD. *J. Ophthalmol.* **2012**, *2012*, 786870.
23. Krishnadev, N.; Meleth, A.D.; Chew, E.Y. Nutritional supplements for age-related macular degeneration. *Curr. Opin. Ophthalmol.* **2010**, *21*, 184–189.
24. Yang, S.; Zhao, J.; Sun, X. Resistance to anti-VEGF therapy in neovascular age-related macular degeneration: A comprehensive review. *Drug Des. Dev. Ther.* **2016**, *10*, 1857–1867.
25. Kaipainen, A.; Korhonen, J.; Mustonen, T.; van Hinsbergh, V.W.; Fang, G.H.; Dumont, D.; Breitman, M.; Alitalo, K. Expression of the fms-like tyrosine kinase 4 gene becomes restricted to lymphatic endothelium during development. *Proc. Natl. Acad. Sci. USA* **1995**, *92*, 3566–3570.
26. He, Z.; Chen, A.Y.; Rojanasakul, Y.; Rankin, G.O.; Chen, Y.C. Gallic acid, a phenolic compound, exerts anti-angiogenic effects via the PTEN/AKT/HIF-1alpha/VEGF signaling pathway in ovarian cancer cells. *Oncol. Rep.* **2016**, *35*, 291–297.
27. Yang, H.L.; Huang, P.J.; Liu, Y.R.; Kumar, K.J.; Hsu, L.S.; Lu, T.L.; Chia, Y.C.; Takajo, T.; Kazunori, A.; Hseu, Y.C. Toona sinensis inhibits LPS-induced inflammation and

migration in vascular smooth muscle cells via suppression of reactive oxygen species and NF-kappaB signaling pathway. *Oxidative Med. Cell. Longev.* **2014**, 901315.

28. Paeng, S.H.; Jung, W.K.; Park, W.S.; Lee, D.S.; Kim, G.Y.; Choi, Y.H.; Seo, S.K.; Jang, W.H.; Choi, J.S.; Lee, Y.M.; et al. Caffeic acid phenethyl ester reduces the secretion of vascular endothelial growth factor through the inhibition of the ROS, PI3K and HIF-1alpha signaling pathways in human retinal pigment epithelial cells under hypoxic conditions. *Int. J. Mol. Med.* **2015**, *35*, 1419–1426.
29. Kim, M.H.; Jeong, Y.J.; Cho, H.J.; Hoe, H.S.; Park, K.K.; Park, Y.Y.; Choi, Y.H.; Kim, C.H.; Chang, H.W.; Park, Y.J.; et al. Delphinidin inhibits angiogenesis through the suppression of HIF-1alpha and VEGF expression in A549 lung cancer cells. *Oncol. Rep.* **2017**, *37*, 777–784.
30. Delmas, D.; Aires, V.; Limagne, E.; Dutartre, P.; Mazue, F.; Ghiringhelli, F.; Latruffe, N. Transport, stability, and biological activity of resveratrol. *Ann. N. Y. Acad. Sci.* **2011**, *1215*, 48–59.
31. Delmas, D.; Lin, H.Y. Role of membrane dynamics processes and exogenous molecules in cellular resveratrol uptake: Consequences in bioavailability and activities. *Mol. Nutr. Food Res.* **2011**, *55*, 1142–1153.
32. Loupit, G.; Prigent, S.; Franc, C.; De Revel, G.; Richard, T.; Cookson, S.J.; Fonayet, J.V. Polyphenol Profiles of Just Pruned Grapevine Canes from Wild Vitis Accessions and Vitis vinifera Cultivars. *J. Agric. Food Chem.* **2020**, doi 10.1021/acs.jafc.9b08099.

Sample Availability: Samples of the compounds ..... are available from the authors.

Publisher's Note: MDPI stays neutral with regard to jurisdictional claims in published maps and institutional affiliations.

D. Résultats complémentaires

La DMLA est une pathologie qui est généralement uni-latérale. Cela signifie qu'au stade précoce de la maladie, un seul œil est atteint. Ainsi, il est primordial de conserver le plus longtemps possible l'œil sain en bonne santé. Nous nous sommes donc demandé si l'extrait sec de vin rouge pouvait protéger les cellules de l'EPR en condition basale. Dans notre première étude, nous avons montré que l'extrait était capable de diminuer la sécrétion ainsi que l'expression protéique de VEGF-A ainsi que l'expression de protéines clefs impliquées dans la signalisation de son récepteur (VEGF-R2). Afin de compléter cette étude, nous avons mesuré l'expression génique de VEGF-A lorsque ces dernières sont traitées avec l'extrait sec de vin rouge. En accord avec les résultats de ce premier article, **l'expression d'ARNm de VEGF-A est inhibée par le RWE** (Figure 21).

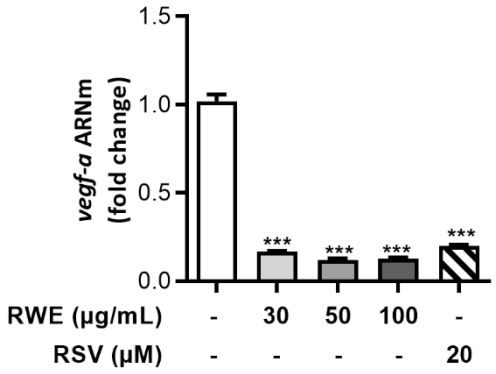

Figure 21. L'extrait sec de vin rouge diminue l'expression de VEGF-A dans les cellules ARPE-19
Les cellules ARPE-19 ont été traitées durant 24 h avec un extrait sec de vin rouge (*red wine extract* : RWE, 30 ; 50 ; 100 µg/mL) ou avec 20 µM de resvératrol (RSV). A la fin des traitements, l'expression de VEGF-A a été mesurée par qPCR. Les résultats sont exprimés en valeurs moyennes ± SEM de trois expériences indépendantes (u.a. : unité arbitraire). Les *p*-values ont été calculées par un test ANOVA suivi d'un test de Dunnett. *** $p<0,0001$ (valeurs comparées aux valeurs des cellules traitées avec le solvant (-)).

Comme décrit précédemment, le **stress oxydant** est l'un des éléments initiateurs de la maladie. Nous nous sommes donc demandé si l'extrait sec de vin rouge était capable de diminuer la production basale d'ERO dans les cellules ARPE-19. Ainsi, nous avons mesuré les ERO présents dans les cellules ARPE-19 après les avoir traités durant 24h avec du RWE ou du RSV. Les résultats suggèrent que **ni le RWE ni le RSV n'impactent la production basale d'ERO** dans les cellules ARPE-19 (Figure 22)

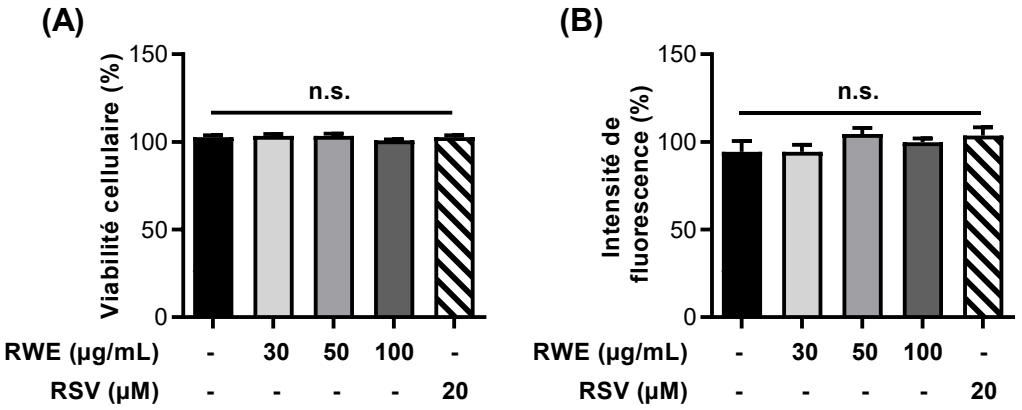

Figure 22. L'extrait sec de vin rouge n'altère pas la production basale d'ERO dans les ARPE-19
Les cellules ARPE-19 ont été traitées avec des concentrations croissantes d'extrait sec de vin rouge (*red wine extract* : RWE; 30; 50; 100 µg/mL) ou avec 20 µM de resvératrol (RSV). Après 24h de traitement, les cellules ont été incubées avec la sonde DCFDA sensible aux espèces réactives de l'oxygène (ERO), (10 µM) durant 30 minutes. Après rinçage, la viabilité cellulaire a été mesurée par cristal violet **(A)** et les ERO ont été mesurés grâce à l'intensité de fluorescence de la sonde DCFDA (em/ex : 490/520) **(B)**. Les résultats sont exprimés en pourcentage moyen rapporté aux cellules contrôles ± SEM de trois expériences indépendantes. Les *p*-values ont été calculées par un test ANOVA suivi d'un test de Dunnett. *p*-value ≤ 0,05 a été considérée comme significative, n.s. = non significatif (valeurs comparées aux valeurs des cellules traitées avec le solvant (-)).

Afin de poursuivre notre étude de l'effet protecteur de RWE en condition basale, nous nous sommes intéressés à son caractère **anti-inflammatoire** en condition basale. Ainsi, nous avons quantifié la sécrétion de cytokine pro-inflammatoire ainsi que leurs expressions d'ARNm. **L'extrait n'altère ni la sécrétion ni l'expression de l'interleukine 6** (IL-6). Cependant, nous avons montré que le RWE peut **diminuer de manière dose dépendante la sécrétion d'IL-8** (Figure 23). Cette diminution de sécrétion est corroborée par une **diminution de l'expression d'ARNm d'IL-8.** De manière intéressante, le RSV seul n'altère pas la sécrétion d'IL-8 néanmoins il diminue de manière significative l'expression d'ARNm d'IL-8 (Figure 23). Ainsi, il semblerait que **l'extrait sec de vin rouge pourrait altérer l'inflammation basale** des cellules ARPE-19.

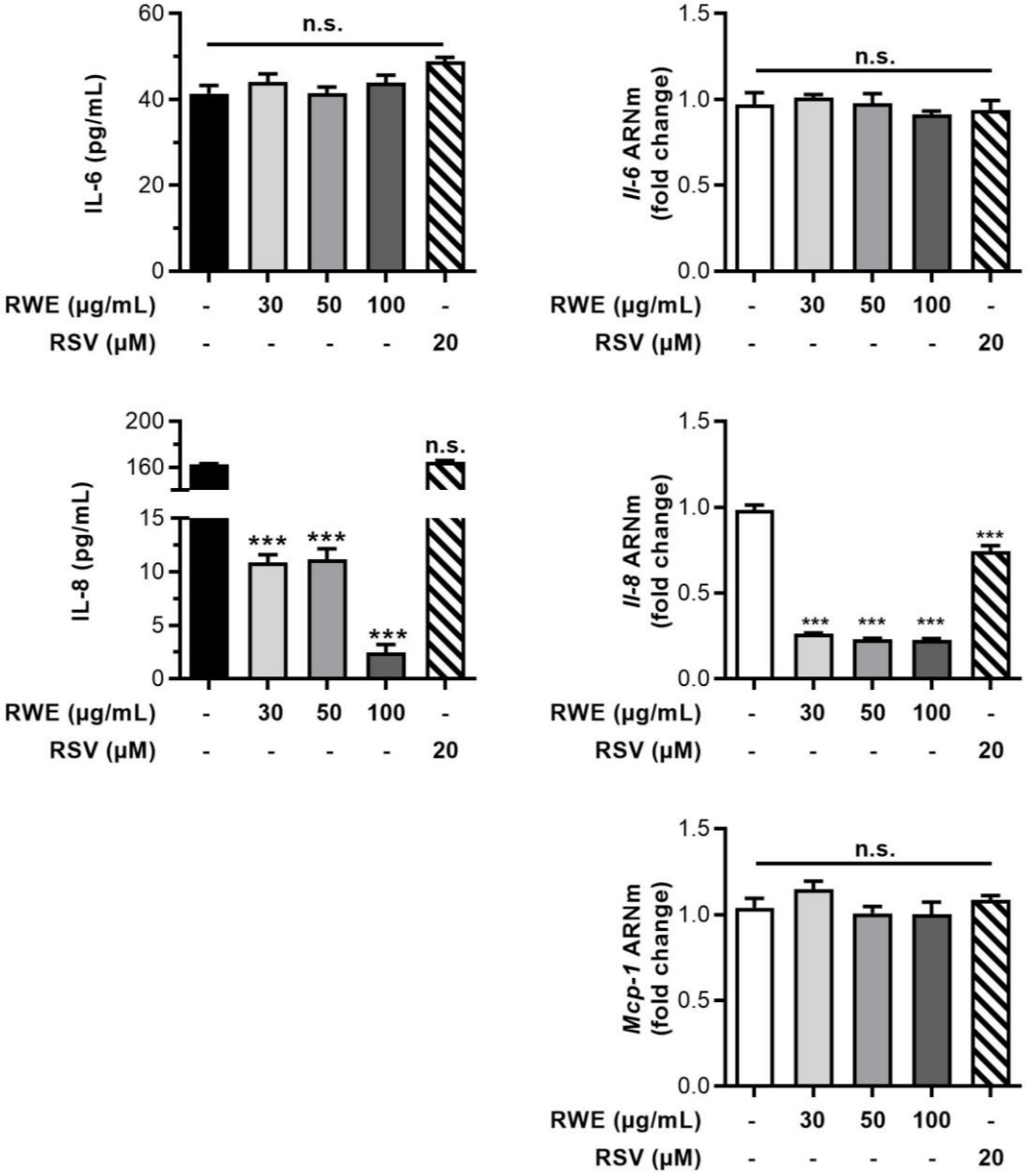

Figure 23. Mesure du caractère anti-inflammatoire de l'extrait en conditions basales

Les cellules ARPE-19 ont été traitées durant 24 h avec différentes concentrations d'extrait sec de vin rouge (*red wine extract* : RWE; 30; 50; 100 µg/mL) ou avec 20 µM de resvératrol (RSV). **(A)** La sécrétion de cytokines pro-inflammatoire, Interleukine 6 et 8 (IL-6, IL-8) a été mesurée par ELISA. **(B)** Les expressions d'ARNm de cytokine pro-inflammatoire, IL-6, IL-8 et MCP-1 (Chimiotactiques monocytaire-1) ont été mesurées par qPCR. Les résultats d'ELISA sont exprimés en valeurs moyennes ± SEM de trois expériences indépendantes. Et les résultats de PCR sont exprimés en pourcentage moyen rapporté aux cellules contrôles (traitées avec le solvant (-)) ± SEM de trois expériences indépendantes (u.a. : unité arbitraire). Les *p*-values ont été calculées par un test ANOVA suivi d'un test de Dunnett. *p*-value ≤ 0,05 a été considérée comme significative, n.s. = non significatif; *** $p<0,0001$ (valeurs comparées aux valeurs des cellules contrôles).

E. Conclusion

Les résultats de ces études ont montré que l'extrait sec de vin rouge (RWE) pouvait **inhiber l'expression d'ARNm** et protéique de VEGF-A ainsi que sa **sécrétion**. Cette inhibition est couplée à une **altération de la voie de signalisation de VEGF-A.** En effet, RWE est capable de diminuer l'activation (phosphorylation) de protéines clefs impliquées dans la voie du VEGF. De plus, bien que l'extrait ne diminue pas la production basale d'ERO, il semblerait qu'il pourrait avoir un effet **anti-inflammatoire** *via* la diminution de certaines cytokines pro-inflammatoires telles que l'IL-8. Il est important de retenir que le **RWE présente un effet plus important que le RSV seul**. Ainsi, il semble être un bon candidat dans la lutte contre la DMLA. Par la suite, il conviendra de mesurer ses caractères anti-angiogéniques, anti-inflammatoires et anti-oxydants dans un contexte pathologique.

Etude 2 : Effets préventifs de l'extrait sec de vin rouge sur les évènements précoces de la DMLA, i.e. Stress oxydatif et inflammation dans les cellules rétiniennes ARPE-19

A. Contexte général et objectifs de l'étude

Bien que les mécanismes moléculaires conduisant à la DMLA ne soient pas encore totalement élucidés, il apparait clairement que trois éléments majeurs conduisent à la pathogénie de la DMLA : un **stress oxydatif** lié au vieillissement, qui peut induire des dommages à l'ADN des cellules RPE et provoquer leur mort (Abokyi et al., 2020; Ruan et al., 2021; Toma et al., 2021; van Lookeren Campagne et al., 2014) ; **l'inflammation chronique**, qui est, en partie, caractérisée par le recrutement et l'infiltration de cellules immunitaires pro-inflammatoires telles que les macrophages; la **néo-angiogenèse**, provoquée par des cytokines pro-angiogéniques ; et les chimiokines, produites par les cellules immunitaires pro-inflammatoires (Ambati et al., 2013; Blasiak et al., 2020).

Comme décrit précédemment, l'**alimentation** peut jouer un rôle important dans la prévention de la maladie. Ainsi, certaines molécules anti-oxydantes présentes naturellement dans l'alimentation pourrait être utilisées afin de limiter la progression de la maladie. Parmi les molécules anti-oxydantes, le resvératrol (RSV), un polyphénol de la vigne, pourrait présenter un intérêt majeur en raison de ses propriétés pléiotropes dans le stress oxydatif, l'inflammation et la dégénérescence (Delmas et al., 2020, 2011, 2006, 2005). Nous avons montré dans la précédente étude qu'un cocktail polyphénolique (un extrait sec de vin rouge) pouvait être plus efficace que le RSV seul contre certains aspects de la maladie. Afin de mieux caractériser le potentiel santé de l'extrait sec de vin rouge dans la DMLA, nous avons cherché à déterminer son impact ainsi que celui du RSV seul sur deux éléments initiateurs de la DMLA à savoir le stress oxydant et l'inflammation (Shen et al., 2023).

B. Résumé de l'étude

B.1. Effets anti-angiogéniques du RWE dans les cellules ARPE-19

Lors de notre première étude, nous avons montré que le RWE était capable de diminuer le niveau basal de VEGF-A dans les cellules ARPE19. Lors de notre seconde étude, nous nous

sommes demandé quel était l'effet du RWE lorsque la production de VEGF-a était induite par des facteurs exogènes. Pour cela, nous avons utilisé deux inducteurs à savoir le VEGF recombinant (rVEGF) et le peroxyde d'hydrogène (H_2O_2). Ainsi, nous avons pu montrer que le RWE prévenait la sécrétion de VEGF-A. Nous avons aussi comparé l'effet du RWE à celui du RSV seul et nous avons montré que ce dernier était significativement moins efficace que l'extrait.

B.2. Effets anti-oxydants du RWE

Afin de compléter notre étude sur les effets protecteurs du RWE, nous nous sommes intéressés à un des **événements précoces de la DMLA,** à savoir le stress oxydant. De par sa composition riche en anti-oxydants, il nous est apparu intéressant d'évaluer la capacité de l'extrait de vin rouge à contrecarrer les mécanismes associés à ce stress précoce. Ainsi, comme attendu, nous avons pu montrer que les deux inducteurs utilisés (H_2O_2 et AAPH) génèrent une forte augmentation d'**ERO intracellulaire laquelle est significativement diminuée lorsque les cellules sont traitées avec le RWE**. Comme ce qui a été observé précédemment, le RSV seul présente un effet moindre comparé au RWE.

Il a été clairement établi que l'augmentation d'ERO intracellulaire était à l'origine de **dommage à l'ADN** entraînant le dysfonctionnement des cellules de l'EPR. Pour poursuivre notre recherche sur les effets anti-oxydants du RWE, nous avons évalué son effet protecteur sur les dommages à l'ADN induits par l'H_2O_2 et l'AAPH. Nous avons montré par microscopie ainsi que par cytométrie en flux que le **RWE pouvait prévenir les dommages à l'ADN** induit par un stress oxydant et ce toujours de manière plus importante que le RSV seul. Afin de compléter ces résultats, nous nous sommes intéressés à l'activation de protéines clés impliquées dans la voie de réponse aux dommages à l'ADN. Ainsi, nous avons montré que le RWE permettait de prévenir l'activation de protéines impliquées dans les voies de dommages à l'ADN.

Ces résultats mettent en évidence que le RWE peut prévenir le stress oxydant induit par H_2O_2 ou par l'AAPH dans les cellules humaines ARPE-19 RPE de manière dose-dépendante et, ainsi, protège les cellules RPE contre les dommages à l'ADN.

B.3. Effet anti-inflammatoire du RWE

Il est maintenant bien connu que le stress oxydatif menant à la production d'ERO et de dommages à l'ADN contribue aux processus **inflammatoires**. En effet, lors du vieillissement ou de l'exposition à des facteurs exogènes et endogènes, la production d'ERO est associée à une augmentation de la sécrétion de cytokines pro-inflammatoires, et en particulier l'IL-6 et l'IL-8 (Marazita et al., 2016). Dans ce contexte, nous nous sommes demandé si le RWE présentait des bénéfices anti-inflammatoires sur les cellules ARPE-19 lors d'une inflammation induite par un stress oxydant (H_2O_2) et lors d'une inflammation induite par un produit pro-inflammatoire tel que de LPS. Dans les deux cas, nous avons pu montrer que le **RWE permettait de prévenir la sécrétion d'IL-6 et d'IL-8 de manière dose dépendante**.

Des études cliniques ont mis en évidence la présence de cellules inflammatoires au niveau de la rétine chez les patients atteints de DMLA. Nous nous sommes donc intéressés à l'effet anti-inflammatoire du RWE sur des **cellules immunitaires**, à savoir des **macrophages**. Nous avons activé des macrophages primaires humains en macrophages de type M1 (pro-inflammatoire) afin d'étudier l'effet du RWE sur ces cellules. Ces analyses nous ont permis de montrer que, comme dans les ARPE-19, le **RWE était capable de prévenir la sécrétion d'IL-6 et d'IL-8 dans des macrophages pro-inflammatoires**. Ces résultats suggèrent que le RWE pourrait être utilisé dans la prévention des événements précoces de la DMLA avec la diminution du stress oxydant et de l'inflammatoire et pourrait aussi agir sur les stades plus tardifs de la maladie avec une diminution de l'angiogenèse.

C. Article publié

Red Wine Extract Prevents Oxidative Stress and Inflammation in ARPE-19 Retinal Cells

Clarisse Cornebise, Maude Perus, Farnçois Hermetet, Josep Valls-Fonayet, Transtan Richard, Virginie Aires et Dominique Delmas.

cells

MDPI

Article

Red Wine Extract Prevents Oxidative Stress and Inflammation in ARPE-19 Retinal Cells

Clarisse Cornebise [1,2], Maude Perus [1,2], François Hermetet [1,2], Josep Valls-Fonayet [3], Tristan Richard[3], Virginie Aires [1,2,†] and Dominique Delmas [1,2,4,*,†]

[1] UFR des Sciences de Santé, Université de Bourgogne, 21000 Dijon, France; clarisse.cornebise@gmail.com (C.C.); maude.perus@u-bourgogne.fr (M.P.); francois.hermetet@u-bourgogne.fr (F.H.); virginie.aires02@u-bourgogne.fr (V.A.)
[2] INSERM Research Center U1231—Cancer and Adaptive Immune Response Team, Bioactive Molecules and Health Research Group, 21000 Dijon, France
[3] Université de Bordeaux, Bordeaux Sciences Agro, Bordeaux INP, INRAE, OENO, UMR 1366, ISVV, 33140 Villenave d'Ornon, France; josep.valls-fonayet@u-bordeaux.fr (J.V.-F.); tristan.richard@u-bordeaux.fr (T.R.)
[4] Centre de Lutte Contre le Cancer Georges François Leclerc Center, 21000 Dijon, France
* Correspondence: dominique.delmas@u-bourgogne.fr; Tel.: +33-380-39-32-26
† These authors have contributed equally to this work.

Abstract: Age-related macular degeneration (AMD) is one of the most commonly occurring ocular diseases worldwide. This degenerative condition affects the retina and leads to the loss of central vision. The current treatments are focused on the late stage of the disease, but recent studies have highlighted the importance and benefits of preventive treatments and how good dietary habits can reduce the risk of progression to an advanced form of the disease. In this context, we studied whether resveratrol (RSV) or a polyphenolic cocktail, red wine extract (RWE), are able to prevent the initiating events of AMD (i.e., oxidative stress and inflammation) in human ARPE-19 retinal pigment epithelial (RPE) cells and macrophages. This study highlights that RWE and RSV can prevent hydrogen peroxide (H_2O_2) or 2,2′-Azobis(2-methylpropionamidine) dihydrochloride (AAPH)-induced oxidative stress and can subsequently prevent DNA damage *via* the inhibition of the ATM (ataxia telangiectasia-mutated)/Chk2 (checkpoint kinase 2) or Chk1 signaling pathways, respectively. Moreover, ELISA assays show that RWE and RSV can prevent the secretion of proinflammatory cytokines in RPE cells and in human macrophages. Interestingly, RWE exhibits a greater protective impact compared to RSV alone, even though RSV was more concentrated when used alone than in the red wine extract. Our results suggest that RWE and RSV may have potential interest as preventive nutritional supplementations against AMD.

Keywords: polyphenol; red wine extract; resveratrol; AMD; oxidative stress; inflammation; prevention

Citation: Cornebise, C.; Perus, M.; Hermetet, F.; Valls-Fonayet, J.; Richard, T.; Aires, V.; Delmas, D. Red Wine Extract Prevents Oxidative Stress and Inflammation in ARPE-19 Retinal Cells. Cells 2023, 12, 1408.

https://doi.org/10.3390/ cells12101408

Academic Editor: Paola Bagnoli

Received: 6 April 2023
Revised: 12 May 2023
Accepted: 15 May 2023
Published: 17 May 2023

1. Introduction

Age-related macular degeneration (AMD) is currently the leading cause of visual impairment in people over the age of 50 in developed countries, affecting hundreds of millions of individuals worldwide [1]. The risk of AMD occurrence increases with age to exceed 25% of the population after the age of 75 [2]. This disease mainly affects the macula, which is localized in the center of the retina and surrounds the fovea, responsible for the high quality and color central vision. AMD can therefore cause blurred vision in the center of the visual field but hardly affects the peripheral vision. Patients with AMD develop one or more of the following retinal abnormalities: drusen (whitish/yellowish deposits of lipid and lipoprotein material between the retinal pigment epithelium (RPE) and Bruch's membrane, variable in size, shape, and number); alteration or geographic atrophy (GA) of the RPE, or choroidal neovascularization (CNV). These abnormalities depend on the stage of the disease and can be unilateral (only one eye is affected) or bilateral (both eyes are affected). The term AMD corresponds to the most advanced stages of the disease. There are generally three major clinical forms [3,4]. The first is age-related maculopathy (AML), corresponding to the early stage of the disease (appearing around 50 years of age) and characterized by the accumulation of precursors such as drusen of variable shape, size, and number, an accumulation of photoreceptor phagocytosis residues by RPE cells (slowing down of the elimination capacities due to the aging of the retina) that seems to be the origin of the disease. The second is atrophic or "dry" AMD, which is one of the two severe forms of AML, evolving very slowly over time and characterized by a progressive loss of RPE cells due to their degeneration by apoptosis. These events cause the disappearance of the choriocapillaris and photoreceptors in the macular region, leading to severe vision loss. The third is neovascular AMD (nAMD, also called wet or exudative AMD), characterized by neovascularization of the choroid, which accounts for 90% of severe vision loss caused by AMD [5]. The new blood vessels tend to be very fragile and lead to a diffusion of the serum and blood, causing hemorrhages within the retina that disrupt its organization, particularly due to the appearance of exudates, intraretinal edema, scars, or retinal detachment. Since the 2000s, nAMD has been treated by repeated injections of antibodies directed against the major factor regulating angiogenesis, vascular endothelium growth factor A (VEGF-A), directly into the eye *via* the intravitreal route (on average, seven shots per year). Over the last few years, these targeted therapies have supplanted thermal laser photocoagulation techniques or photodynamic therapies used to destroy new vessels or by creating direct damage to abnormal vessels while preserving healthy retinal tissue [6–8]. However, persistent fluid or recurrent exudation may persist despite anti-VEGF therapy, and patients can develop mechanisms of resistance to anti-VEGF treatments in the long term, which consequently reduces the therapeutic efficacy [9,10]. The numerous molecular mechanisms underlying AMD are complex and still not fully understood. However, there are three major elements that lead to the pathogenesis of AMD: major oxidative stress linked to aging, which can induce DNA damage in RPE cells and cause their death, which appears be the triggering factor for AMD [11–14]; chronic inflammation, which is,

in part, characterized by the recruitment and infiltration of proinflammatory immune cells such as macrophages; neoangiogenesis, caused by proangiogenic cytokines; and chemokines, produced by proinflammatory immune cells, which a common feature of the most advanced and severe stages of the disease [15,16]. Many data from the literature also suggest that preventive treatments and/or good eating habits can reduce the risk of progression to an advanced form of the disease: regular consumption of fruits; green vegetables rich in lutein (spinach, broccoli, cabbage curly fish, etc.); fatty fish (salmon, tuna, mackerel, etc.); regular physical activity; etc. Indeed, the controlled, randomized Age-Related Eye Disease Study 1 and 2 (AREDS-1 and AREDS-2) clinical studies demonstrated that nutritional supplementation with antioxidant vitamins such as vitamins C or E, zinc, polyunsaturated fatty acids from the omega-3 family, or lutein can significantly reduce the risk of developing severe forms of the disease [17]. Among antioxidants, resveratrol (RSV), a grapevine polyphenol, could be of major interest due to its pleiotropic properties in oxidative stress, inflammation, and degeneration [18–21]. Recently, we highlighted the use of this hydroxystilbene as a potential preventive tool against various ocular diseases—in particular, AMD, glaucoma, cataract diabetic retinopathy, and vitreoretinopathy [22]. Through its antioxidant and anti-inflammatory properties, RSV could protect against several deleterious environmental factors that initiate AMD [23], such as air pollution; smoking; ultraviolet radiation; metabolic diseases (e.g., diabetes, hypertension, and obesity); dietary fat consumption [24–27]; and genetic polymorphisms such as cfh and arms2/hrta1 genes [28]. Alone or combined, these factors could contribute to the initiation of AMD through the production of free radicals such as superoxide anion ($O_2^{\cdot -}$), nitric oxide ($NO^{\cdot}$), or hydroxyl radical ($OH^{\cdot}$), which generate oxidative stress and inflammation in ocular tissues. More recently, we showed that a mixture of polyphenols, rather than RSV alone, could be more efficient in counteracting some aspects of AMD pathogenesis. We demonstrated that a dry extract of red wine (RWE), containing low amounts of RSV, was able to reduce the secretion of VEGF-A by the human RPE cell line ARPE-19 to a greater extent than 20 μM RSV alone [27]. This effect could be explained by synergic interactions between the compounds present in the mixture, as we previously observed for RSV and the flavonoid quercetin in a colorectal cancer context [29]. Mechanistically, the reduction of the secreted VEGF-A levels resulted from the action of the polyphenol mixture on the VEGF receptor (VEGF-R)/mitogen-activated protein kinases (MAPKs) molecular pathway [30]. Hence, the use of such a formulation may be of value for an AMD prevention strategy.

To better characterize the potential of RWE in AMD, we sought to determine the impact of RWE and RSV on oxidative stress and inflammation, two well-recognized primary triggers of AMD [31]. Herein, we show that RWE was able to significantly decrease the secretion of VEGF-A induced by the recombinant human VEGF-A (rVEGF) protein but, also, by oxidative stress. This inhibition of VEGF-A secretion is associated with a significant reduction in reactive oxygen species (ROS) induced by oxidative agents. Moreover, the decrease of total ROS by RWE is associated with a disruption in the DNA damage pathway. Very interestingly, we demonstrate for the first time that

RWE prevents inflammation, a second key initiator of AMD, by reducing the secretion of interleukin (IL)-6 and IL-8 in both RPE cells and immune cells such as macrophages. These findings provide new evidence that a polyphenol combination could be a robust and promising tool to prevent the development of AMD in at-risk populations and to develop innovative prevention strategies.

2. Materials and Methods

2.1. Red Wine Extract (RWE) Extraction, Purification, and Characterization

Red wine extract (RWE) was obtained from red wine, a Santenay 1er Cru Les gravières 2012 (EARL Capuano-Ferrari Santenay, Côte-d'Or, France) that was selected by the Bureau Interprofessionnel des Vins de Bourgognes (BIVB, Beaune, France) and provided by the Centre Technique Interprofessionnel de la Vigne et du Vin (CTIVV, Beaune, France). A dry red wine powder was extracted and analyzed as previously described [30,32,33]. Briefly, alcohol and water were evaporated using a rotary evaporator; then, phenolic compounds were purified using an absorbance column (Diaion® HP-20, 13606, Merck, Darmstadt, Germany) and eluted in alcohol. After elution, a rotary evaporator was used to evaporate all the alcoholic eluent, and the extract was then concentrated to dryness.

The composition of RWE was characterized as previously described [30]. Briefly, Thermo Scientific Vanquich UHPLC equipped with a Thermo Scientific MWL detector was used to analyze the anthocyanins. The other polyphenols were analyzed by highperformance liquid chromatography coupled to an Agilent 6430 triple-quadrupole mass spectrometer (HPLC-MS/MS), as previously published [30]. In brief, compounds were separated with an Agilent 1260 HPLC and eluted on an Agilent Zorbax SB-C18 column. Specific Multiple Reaction Monitoring (MRM) transitions and retention times were used for the detection and quantification of each compound. All compounds were quantified as their corresponding standard except flavan 3-ol dimers B3 and B4, which were expressed as dimers B1 and B2, respectively, and *cis*-resveratrol and *cis*-piceid, which were quantified as their respective *trans*-isomer forms [30].

2.2. Chemical Reagents and Antibodies

Trans-resveratrol (RSV, R5010, Sigma-Aldrich, St. Quentin Fallavier, France) stock solution was prepared at 20 mM in 70% ethanol and stored at −20 ◦C. A stock solution of lipopolysaccharides from Escherichia coli O55:B5 (LPS, L2880, Sigma-Aldrich, St. Quentin Fallavier, France) was prepared in H2O at 5 mg/mL and stored at −20 ◦C. Human recombinant interferon gamma (IFN-γ, 300-02, preprotech, Neuilly-Sur-Seine, France) stock solution was prepared in H2O at 25 µg/mL and stored at −20 ◦C. Recombinant human VEGF-165 (rVEGF) protein (11858821, Invitrogen, Waltham, MA, USA) was solubilized in H2O at 50 µg/mL and stored at −20 ◦C. 20 ,70 -Dichlorofluorescin diacetate (DCFH-DA, D6863, Sigma-Aldrich, St. Quentin Fallavier, France) was prepared in dimethyl sulfoxide (DMSO); the stock solution was prepared at 50 mM and stored at −20 ◦C. Hydrogen peroxide (H_2O_2) was purchased from MERCK (H1009, Darmstadt,

Germany), and a stock solution was extemporaneously prepared at 300 mM in culture medium for cell treatments. 2,20 -Azobis(2-methylpropionamidine) dihydrochloride (AAPH; 440914, MERCK) was prepared as a stock solution at 600 mM in water and was stored at −20 ◦C.

For the Western blot analyses, the following antibodies were used: ATM (#2873, 1:1000); p-ATR (#2853, 1:1000); Chk1 (#2360, 1:1000); p-Chk1 (#2348, 1:1000); Chk2 (#2662, 1:1000); p-Chk2 (#2197, 1:1000); p53 (#2524, 1:1000); and p-p53 (#9284, 1:1000), purchased from Cell Signaling Technology (Ozyme, Saint-Cyr-l'Ecole, France). ATR (Sc-1887, 1:200); p21 (Sc756, 1:500); and heat shock cognate (HSC70) (sc-7298; 1:10,000) were purchased from Santa Cruz Biotechnology (Nanterre, France). p-ATM (ab81292, 1:50,000) was purchased from Abcam (Cambridge, UK). For the immunofluorescence analyses, p-Histone H2A.X (#80312, 1:200) was purchased from Cell Signaling Technology (Ozyme, Saint-Cyr-l'Ecole, France), and anti-mouse 488 fluorophore-conjugated secondary antibody (SAB4600387, 1:500) was obtained from Sigma-Aldrich (St. Louis, MO, USA). For flow cytometry, Alexa Fluor® 647 anti-p-histone H2A.X (Ser139) antibody was purchased from BioLegend (San Diego, CA, USA).

2.3. Cell Culture and Treatments

2.3.1. Human Retinal Cell Line ARPE-19

The human RPE cells (ARPE-19, CRL-2302TM) were purchased and validated by the American-type Cell Culture Collection (ATCC) (Manassas, MD, USA). Nonpolarized cells were cultured in Dulbecco's modified Eagle's medium; the nutrient mixture F12 (DMEM/F12) was supplemented with GlutaMAX (Thermo Fisher, Waltham, MA, USA) and with 10% fetal bovine serum (FBS, Dutscher, Brumath, France) and maintained at 37 ◦C in an atmosphere containing 5% CO2. Cells were routinely tested for mycoplasma contamination using the MycoAlertTM (Lonza) test and passaged twice per week before they reached 80–85% confluency. The ARPE-19 cells were seeded at a density of 7500 cells/cm2 into 75 cm2 flasks (Sarstedt, Marnay, France) for the immunoblotting experiments, 12-well plates (Sarstedt, Marnay, France) for flow cytometry, 24-well plates (Sarstedt, Marnay, France) for immunofluorescence, or 48-well plates (Sarstedt, Marnay, France) for the ELISA and DCFDA assays, in DMEM/F12 supplemented with 10% FBS. After 72 h of cell culture, nonpolarized ARPE-19 cells (60–70% confluence) were washed twice with Hank's balanced salt solution (HBSS, Dutscher, Brumath, France) and then incubated in DMEM/F12 supplemented with 1% of FBS for 24 h. Cells were further incubated with an increasing concentration of RWE (30, 50, and 100 μg/mL) or RSV (20 μM) or with the solvent alone (0.1% of ethanol 70% v/v). After 24 h of pretreatment, cells were further treated with rVEGF, H_2O_2, AAPH, or LPS + IFN-γ at the indicated concentrations and times of treatments. In any of the experimental conditions, control cells were treated with the corresponding solvents (used for compound solubilization) alone and did not exceed 0.1% for ethanol 70%, 0.02% for DMSO, and 0.2% for H2O.

2.3.2. PBMC-Derived Macrophages

Buffy coats of fresh blood from four healthy male donors with different blood types (B+, A−, O+, and AB+) were obtained from the Etablissement Français du Sang (EFS). In order to separate peripheral blood mononuclear cells (PBMC), buffy coats were diluted with phosphate-buffered saline (PBS, Dutscher, Brumath, France) 1× (1:1, v/v) and loaded on the top of a Ficoll (CMSMCLO1, Eurobio, Les Ulis, France). After 20 min of centrifugation at 700× g (without deceleration), PBMC were collected and washed twice with PBS 1×. PBMC were then seeded at a density of 800,000 cells/cm2 into 48-well plates in DMEM/F12 without FBS. After 2 h, the cells were washed twice, and adherent monocytes were cultivated in DMEM/F12 10% FBS with 100 ng/mL GM-CSF (130-093-866, Miltenyi Biotec, Bergisch Gladbach, Germany). After 6 days of culture (medium was changed every 2 days), the cells were further treated with the solvent (0.1% ethanol 70%) alone as a control or with increasing concentrations of red wine extract (RWE, 30, 50, and 100 μg/mL) or resveratrol (RSV, 20 μM). After 24 h, cells were activated with LPS O55:B5 (10 ng/mL) and IFN-γ (25 ng/mL) or water as the control. After 4 h of LPS + IFN-γ stimulation, cells were again challenged with increasing concentrations of RWE, RSV, or solvent alone, as described above, for an additional 20 h.

2.4. ELISA

Cells (ARPE-19 or PBMC) were seeded and treated in 48-well plates, as previously described. At the end of the treatments, cell culture supernatants were collected, and the secretion levels of human VEGF-A (446504, BioLegend, Amsterdam, the Netherlands), IL-6 (430504, BioLegend, Amsterdam, the Netherlands), and IL-8 (431504, BioLegend, Amsterdam, the Netherlands) were measured by ELISA according to the manufacturer's protocols. Briefly, 96-well plates were coated with anti-VEGF-A, anti-IL-6, or anti-IL-8 capture antibodies overnight (O/N) at 4 ◦C. After washing, the standards provided in the kits were prepared in the assay diluent according to the manufacturer's protocols. Cell supernatants of each experimental condition were diluted with a sample diluent, loaded onto a 96-wells plate, and incubated for 2 h at room temperature (RT) on a microplate shaker. At the end of incubation, individual wells were washed twice, and then, 100 μL of anti-VEGF-A, anti-IL-6, or anti-IL-8 detection antibodies were added and incubated at RT for 1 h on a microplate shaker. After washing, 100 μL of avidin conjugated to horseradish peroxidase (HRP) were loaded onto the plate and incubated for 30 min at RT in the dark; then, 100 μL of substrate were added and incubated for an additional 10 min. The reaction was stopped by adding 100 μL of stop solution (H2SO4, 1N), and then, the absorbance was measured at 450 nm using Perkin Elmer Multimode Plate Reader Envision. To calculate the cytokine concentrations, the standard curves for each assay were plotted with GraphPad Prism 8.3.0 software (GraphPad Software, La Jolla, San Diego, CA, USA) using the 4-parameter sigmodal curve fit.

2.5. Western Blot Analysis

ARPE-19 cells were seeded and treated in 75 cm2 flasks (562,500 cells/flask). Cells were collected; washed twice with cold PBS 1×; centrifuged (5 min, 450× g, 4 ◦C); and then lysed

30 min on ice with radioimmunopecipitation assay (RIPA) buffer (50 mM Tris-HCl, 150 mM sodium chloride, 0.1% sodium dodecyl sulfate, 0.5% sodium deoxycholate, 1% NP40, and pH8) supplemented with a phosphatase inhibitor, sodium fluoride (50 mM), protease inhibitor phenylmethylsulfonyl fluoride (PMSF) (100 µM, Sigma-Aldrich, St. Quentin Fallavier, France), and protease inhibitor cocktail (Roche, Boulogne-Billancourt, France). After centrifugation (20 min, 16,000× g, 4 ◦C), cell debris was eliminated, and protein quantification was performed using the QuantiProTM BCA assay kit (QPBCA, Sigma-Aldrich, St. Quentin Fallavier, France) and by using bovine serum albumin (BSA) as a standard. Samples containing 25–60 µg of proteins were prepared in Laemmli loading buffer (60 mM Tris HCl, 10% glycerol, 2% sodium dodecyl sulfate, pH6.8, 100 mM dithiothreitol, and 0.002% bromophenol blue) and were then heated for 5 min at 95 ◦C. Proteins were resolved by 7.5–12.5% Acrylamide TGX Stain-Free™ FastCast™ (Bio-Rad, 1610185, Marnes-la-Coquette, France) and then transferred onto 0.2 µm nitrocellulose membrane Trans-Blot Turbo (Bio-Rad, 1704271, Marnes-la-Coquette, France). Nonspecific binding sites were blocked using either 5% of bovine serum albumin (BSA) or 5% of skimmed milk in Tris-buffered saline (TBS)–Tween 20 0.1% for 1 h at RT before O/N incubation at 4 ◦C with specific primary antibodies. Primary antibodies were then detected with appropriate HRPconjugated secondary antibodies (111-035-144 and 115-035-146, Jackson ImmunoResearch, Interchim, Montlucon, France) for 1 h at RT, followed by exposure to enhanced chemiluminescence (ECL, 1705032, Bio-Rad, Marnes-la-Coquette, France). The signal was acquired with the ChemiDocTM XRS imaging system (Bio-Rad, Marnes-la-Coquette, France). The densitometry of the blot was analyzed with Image LabTM version 6.0.1 software (Bio-Rad), and HSC70 was used as the internal loading control.

2.6. Cell Viability Assays

Cell viability was determined by crystal violet staining (Sigma-Aldrich, St. Quentin Fallavier, France). After treatments, cells were washed twice with PBS 1× and then stained with crystal violet solution (2.3% crystal violet, 0.1% ammonium oxalate, and 20% ethyl alcohol, #HT90132, Sigma-Aldrich, St. Quentin Fallavier, France) for 15 min at RT and then rinsed with water. After drying, crystal violet stain was dissolved in acetic acid 33%, and then, the absorbance was read at 590 nm using a PerkinElmer® Multimode Plate Reader, Envision.

2.7. Intercellular Reactive Oxygen Species (ROS) Measurement

ARPE-19 cells were seeded at a density of 7500 cells/cm2 in 48-well plates in DMEM/F12 supplemented with 10% FBS. After 72 h of cell culture, the culture medium was removed, and cells were washed twice with Hank's balanced salt solution (HBSS, Dutscher, Brumath, France) and then incubated in DMEM/F12 supplemented with 1% of FBS for 24 h. Cells were further incubated with ethanol 70% (vehicle control) and increasing concentrations of RWE (30, 50, 100 µg/mL) or RSV (20 µM). After 24 h of treatment, the cells were washed twice with HBSS and incubated with 10 µM of 20 ,70 -

dichlorofluorescin diacetate (DCFH-DA, D6863, Sigma-Aldrich, St. Quentin, France) or with the solvent alone (DMSO, 0.02%) as a control for 30 min at 37 ◦C. After washing, ARPE-19 cells were treated with H_2O_2 or AAPH at the indicated concentrations or with the culture medium or H2O as the control. At the end of the treatments, the fluorescence intensity (excitation = 488 nm; emission = 528 nm) was measured using PerkinElmer Multimode Plate Reader Envision, and the cell viability was assessed by crystal violet staining.

2.8. Immunofluorescence

ARPE-19 cells (7500 cells/cm2) were cultured in 24-well plates on coverslips. After treatment, cells were washed twice with PBS 1× and then fixed and permeabilized for 10 min on ice with glacial methanol. After washing cells twice with Tris-buffered saline (TBS) 1×, nonspecific sites were blocked for 1 h at RT with a solution containing 1% BSA and 0.2% Triton 100×. Next, cells were incubated O/N at 4 ◦C with anti-p-histone H2A.X (Ser139) primary antibody (#80312, Cell Signaling Technology, Ozyme, Saint-Cyr-l'Ecole, France) diluted at 1:200 in TBS 1× containing 1% BSA and 0.2% Triton 100×. After washing with TBS 1× containing 0.2% Triton 100×, the cells were incubated with secondary Alexa Fluor goat anti-mouse 488 (SAB4600387, Sigma-Aldrich, St. Quentin Fallavier, France) diluted at 1:500 in TBS 1× containing 1% BSA and 0.2% Triton 100×. After washing with TBS 1× containing 0.2% Triton 100×, coverslips were mounted in Prolong® Gold Antifade with DAPI (P36941, Invitrogen, Thermo Fisher, Waltham, MA, USA) in the dark for 24 h. Images were acquired with AxioImager M2 (Zeiss) and analyzed with Zen 3.6 (blue edition, Zeiss, Rueil Malmaison, France) and Icy (v2.4, Institut Pasteur and France-BioImaging, Paris, Montpellier, France) software.

2.9. Flow Cytometry

ARPE-19 cells were seeded and treated in 12-well plates as previously described. After treatments, cells were collected and viable cells were stained with fixable viability stain 520 (564407, Becton Dickinson, Franklin Lakes, NJ, USA) for 15 min at RT in the dark. After washing, cells were permeabilized with glacial methanol for 10 min on ice. Nonspecific sites were blocked for 10 min at RT with a saturation buffer (PBS 1×, 1% BSA, and 0.2% Triton 100×), and then, cells were incubated with Alexa Fluor® 647 anti-p-histone H2A.X (Ser139) antibody (613408, BioLegend, San Diego, CA, USA) in the saturation buffer (1:100) for 30 min at RT. After washing, an analysis was performed using an Aurora cytometer (Cytek® Biosciences, Fremont, CA, USA) with Spectroflo® software (Biosciences, Torrance, CA, USA), and the data were analyzed using FlowJo v10 software (version 10, Tree Star, Ashland, OR, USA).

2.10. Statistics

Data were expressed as the means ± standard error of the mean (SEM) for at least three independent experiments (2–4 biological replicates per independent experiment). Statistical analyses were carried out with GraphPad Prism 8.3.0 software (GraphPad

Software, La Jolla, San Diego, CA, USA). Data were compared among experimental groups using oneway ANOVA followed by Tukey's multiple comparison test, two-way ANOVA followed by Dunnett's multiple comparison test, or the Kruskal–Wallis test with Dunn's post hoc analysis as appropriate after having checked the data for normal distribution (Shapiro–Wilk test) and variance homogeneity. All *p*-values were two-tailed, and *p*-values less than 0.05 were considered significant (* $p < 0.05$, ** $p < 0.01$, *** $p < 0.001$, and **** $p < 0.0001$).

3. Results

3.1. RWE Prevents VEGF-A Production Induced by rVEGF and H_2O_2 in ARPE-19 Cells

We have previously demonstrated that the contents of bioactive substances in wine and, more specifically, polyphenols could influence the biological effects observed in various biological systems. These qualitative and quantitative variations mainly result from the conditions of vinification but, also, from the grape variety and from exogenous factors (biotic or abiotic stress) [29,32,33]. In order to compare the activity of our red wine dry extract to a standard which properties are now well established, RSV, we determined the quality and quantity of the phenolic compounds contained in the extract by HPLC, as previously described [30]. We can observe in Table 1 the different polyphenols characterized in the dry extract and their respective concentrations. This table shows a high proportion of phenolic acids and flava-3-ols compared to the amounts of anthocyanins, flavonols, and stilbenes (Table 1).

In order to determine whether RWE could affect the different molecular steps leading the development and progression of AMD, we first evaluated the ability of RWE to prevent the secretion of VEGF-A contributing to neoangiogenesis, which is the final step of the AMD process. We previously showed that this extract was able to decrease the basal level of VEGF-A in ARPE19 cells. However, what is the effect of RWE when its production is induced by exogenous factors? First, we evaluated the toxicity of increasing concentrations of recombinant human VEGF-165 (rVEGF) protein (10, 25, 50, and 75 ng/mL) after 1, 6, 10, 16, and 24 h of treatment. As shown in Figure 1A, none of the concentrations and time of treatment used had an impact on the cell viability, which was assessed by crystal violet staining. In the same experimental conditions, we further measured the secretion levels of VEGF-A in the cell supernatants. As shown in Figure 1B, rVEGF induced a maximal VEGF-A secretion by ARPE-19 cells after 6 h of treatment when used at 75 ng/mL. Based on this observation, we next evaluated the ability of RWE to counteract the increase in VEGF-A induced by 75 ng/mL of rVEGF after an optimal stimulation of 6 h. Very interestingly, 24 h of pretreatment with RWE was able to significantly decrease VEGF-A secretion in a concentration-dependent manner in ARPE-19 cells. Indeed, rVEGF-induced VEGF-A secretion was reduced by 42%, by 59%, and by 67% when cells were, respectively, pretreated with 30, 50, and 100 μg/mL RWE (Figure 1D) without impacting the cell viability (Figure 1C). Although RSV decreased VEGF-A secretion significantly (32% with 20 μM of RSV compared to the control), the percentage of inhibition was clearly lower compared to the RWE and whatever the concentration

tested. Extracellular VEGF-A is not the only inducer able to stimulate the secretion of VEGF-A by RPE cells. Indeed, the molecules responsible for oxidative stress such as hydrogen peroxide (H_2O_2) are also at the origin of the increase in VEGF-A. To evaluate the ability of RWE to counteract oxidative stress-induced VEGF-A secretion by ARPE-19 cells, we first determined the optimal concentrations and time of treatment with H_2O_2. We thus treated the cells with increasing concentrations of H_2O_2 (150, 300, 450, and 600 μM) for 1, 6, 10, 16, and 24 h and determined the cell viability (Figure 1E) and, in cell supernatants, the VEGF-A levels by ELISA (Figure 1F). Only 150 μM H_2O_2 was able to significantly increase VEGF-A secretion as compared to the control cells after 24 h of treatment without impacting the ARPE-19 cell viability (Figure 1E,F). Next, cells were treated for 24 h with increasing concentrations of RWE or RSV, as previously described, and were then treated with 150 μM H_2O_2 for an additional 24 h. In these experimental conditions, no significant toxicity was observed with any of the treatments (Figure 1G). Nevertheless, the data showed that VEGF-A secretion induced by 150 μM H_2O_2 was significantly reduced by the RWE pretreatment in a concentration-dependent manner, with 100 μg/mL RWE being the most efficient (reduction of VEGF-A secreted levels by 67% compared to H_2O_2 alone) (Figure 1H). Regarding RSV, it reduced, to a similar extent, the H_2O_2-induced VEGF-A levels (29% vs. 20% for RSV and 30 μg/mL RWE, respectively) but was less efficient than RWE at 50 and 100 μg/mL.

Table 1. Doses (μg/mL) of red wine extract (RWE) used in the study.

		Concentration (nM) of Compounds from Used Doses of RWE		
Compounds	**mg/g of Extract**	**30 μg/mL**	**50 μg/mL**	**100 μg/mL**
Phenolic Acids	51.25×10^{-1}			
Gallic Acid	24.07×10^{-1}	424.49	707.49	1414.98
Caftaric Acid	25.93×10^{-1}	249.18	415.31	830.61
Caffeic Acid	12.44×10^{-2}	20.72	34.54	69.08
Flavan-3-ols	37.78×10^{-1}			
Catechin	90.98×10^{-2}	94.04	156.74	313.47
Epicatechin	33.30×10^{-2}	34.42	57.36	114.73
Procyanidin B1	16.72×10^{-1}	84.40	140.66	281.33
Procyanidin B2	49.92×10^{-2}	25.20	41.99	83.98
Procyanidin B3	18.76×10^{-2}	9.47	15.78	31.57
Procyanidin B4	17.52×10^{-2}	8.84	14.74	29.48
Flavonols	2.35×10^{-1}			
Quercetin	19.62×10^{-2}	19.48	32.47	64.94
Quercetin 3-glucuronide	2.69×10^{-2}	1.69	2.82	5.64
Quercetin 3-rhamnoside	1.16×10^{-2}	0.78	1.30	2.59
Stilbenes	5.61×10^{-1}			
cis-Resveratrol	15.70×10^{-2}	20.64	34.39	68.79
trans-Resveratrol	4.69×10^{-2}	6.16	10.27	20.55
cis-Piceid	4.57×10^{-2}	3.52	5.86	11.73
trans-Piceid	1.25×10^{-2}	0.96	1.60	3.20
trans-Piceatanol	1.53×10^{-2}	1.88	3.13	6.27
cis-epsilon-viniferin	1.21×10^{-3}	0.08	0.13	0.27
epsilon-viniferin	6.79×10^{-3}	0.45	0.75	1.50
omega-viniferin	3.57×10^{-3}	0.24	0.39	0.79
Pallidol	5.74×10^{-2}	3.79	6.31	12.62
Parthenocissin	3.48×10^{-2}	2.30	3.83	7.65
Isohopeaphenol	17.97×10^{-2}	5.94	9.91	19.81
Anthocyanins	10.54×10^{-1}			
Delphindin 3-glucoside	14.48×10^{-2}	8.68	14.46	28.92
Cyanidin 3-glucoside	5.53×10^{-3}	0.34	0.57	1.14
Petunidin 3-glucoside	7.36×10^{-2}	4.29	7.15	14.30
Peonidin 3-glucoside	11.20×10^{-2}	6.74	11.23	22.45
Malvidin 3-glucoside	71.76×10^{-2}	40.70	67.84	135.68

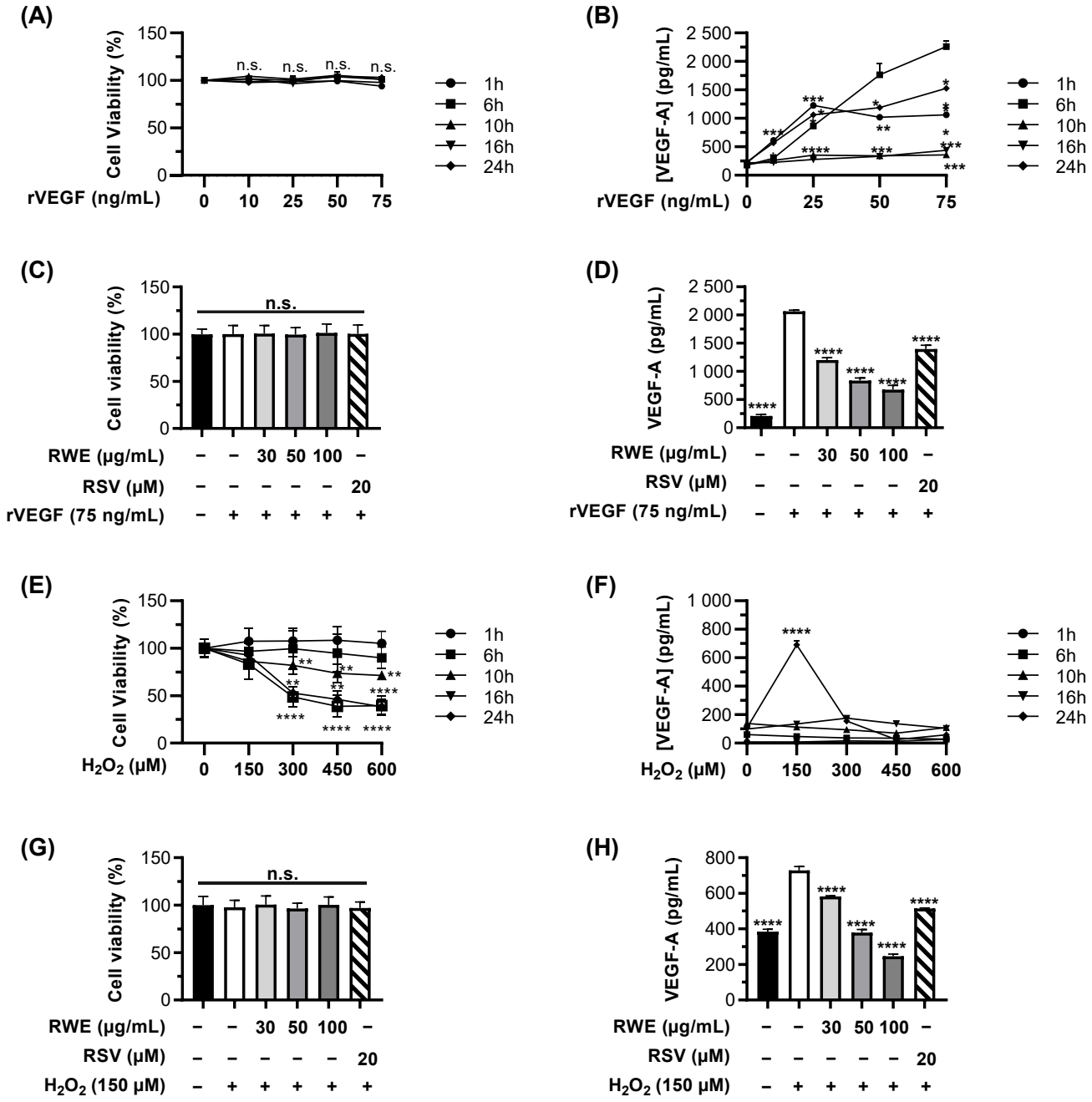

Figure 1. RWE prevents both rVEGF and H_2O_2 -induced VEGF-A secretion in ARPE-19 cells. (A,B) ARPE-19 cells were treated for 1, 6, 10, 16, and 24 h with increasing concentrations of human recombinant VEGF (rVEGF) (0, 10 25, 50, and 75 ng/mL) or with the vehicle alone (0.1% H2O). After treatments, the cells' viability was assessed by crystal violet staining (A), and the VEGF-Asecreted levels were measured in cell supernatants by ELISA (B). (C,D) ARPE-19 cells were treated for 24 h with increasing concentrations of RWE (30, 50, and 100 µM); RSV (20 µM); or with the vehicle alone (0.1% ethanol 70%) and then treated for 6 h with 75 ng/mL rVEGF or with the vehicle alone (0.1% H2O). After treatments, the cells' viability was assessed by crystal violet staining (C), and the VEGF-A-secreted levels were measured in cell supernatants by ELISA (D). (E,F) Cells were treated for 1, 6, 10, 16, and 24 h with increasing concentrations of H_2O_2 (0, 150, 300, 450, and 600 µM) or with the vehicle alone. After treatments, the cells' viability was assessed by crystal violet staining (E), and the VEGF-A-secreted levels were measured in cell supernatants by

ELISA (F). (G,H) Cells were treated for 24 h with increasing concentrations of RWE (30, 50, and 100 μM); RSV (20 μM); or with the vehicle alone (0.1% ethanol 70%) and then treated for 24 h with 150 μM H_2O_2 or with the vehicle alone

After treatments, the cells' viability was assessed by crystal violet staining (G), and the VEGF-Asecreted levels were measured in cell supernatants by ELISA (H). For the viability assays, data are expressed as a mean percentage relative to the control cells (treated with vehicles alone) ± SEM of three independent experiments (4 biological replicates per independent experiment). For kinetics (A,B,E,F), the *p*-values were determined by a two-way ANOVA followed by Dunnett's multiple comparison test and compared to the 6 h timepoint. (C,G) The *p*-values were determined by a one-way ANOVA followed by Tukey's multiple comparison test. The *p*-values ≤ 0.05 were considered significant (n.s. nonsignificant). For the ELISA assays (D,H), the data are expressed as a mean in pg/mL ± SEM of 3–5 independent experiments (2–4 biological replicates per independent experiment). The *p*-values were determined by a one-way ANOVA followed by Tukey's multiple comparison test. The *p*-values ≤ 0.05 were considered significant (* $p < 0.05$, ** $p < 0.01$, *** $p < 0.001$, and **** $p < 0.0001$ comparing data to rVEGF- or H_2O_2 -treated cells).

3.2. RWE Inhibits ROS Levels Induced by Oxidative Stress in ARPE-19 Cells

Therefore, H_2O_2 can contribute to the progression of the later processes of the disease through the production of VEGF-A. Furthermore, oxidative stress has been described as crucial in the early events of AMD with, in particular, the production of ROS, which induces several harmful effects. In order to show the ability of RWE to disrupt the production of ROS in human RPE cells, we first sought to determine the optimal conditions for oxidative stress-induced ROS production in the ARPE-19 cell line. Thus, we achieved kinetics from 1 to 24 h by stimulating ARPE-19 RPE cells with two well-known oxidative stress inducers, H_2O_2 and 2,20 -azobis(2-methylpropionamidine) dihydrochloride (AAPH) (Figure 2A,B,E,F). The cells were treated with increasing concentrations of H_2O_2 and AAPH as indicated, and then, the cell viability was assessed by crystal violet staining and ROS production by flow cytometry using the ROS-sensitive probe DCFDA. As a control, the cells were treated with the vehicles alone (−). Compared to AAPH, which do not induce cytotoxicity in the ARPE-19 cell line, H_2O_2, when used at high concentrations and for long times of incubation (10 to 24 h), reduced the cell viability by around 50% (Figure 2A,E), which translated into lower H_2O_2-induced ROS production (Figure 2B). According to the ROS curves obtained by the DCFDA assays, we thus selected 300 μM for H_2O_2 and 600 μM for AAPH in the subsequent experiments, since they induced significant ROS production as compared to the control cells (increases by 7- and 17-fold, respectively) without affecting the cell viability. We found that the pretreatment of cells with RWE significantly and strongly reduced H_2O_2 and AAPH-induced ROS production from the lowest concentration, 30 μM, allowing ROS to return to the basal levels (Figure 2D,H). As expected, the effect of RWE on ROS production was not related to cytotoxicity (Figure 2C,G). In this case, RSV also induced a significant reduction in the H_2O_2 and AAPH-induced production of ROS by 49% and 69% respectively, but it was not able to return to the basal level, as seen with RWE.

The oxidative stress induced by H_2O_2 was associated with increases in the protein expression of nuclear factor erythroid 2-related factor 2 (Nrf2), a key transcription factor that regulates gene expressions for antioxidant enzymes such as Heme-Oxygenase 1 (HO-1) [34] (Supplementary Figure S1). RWE, to a greater extent than RSV alone, tended to rescue H_2O_2- induced Nrf2 expression but not that of HO-1. This suggests that the protective effects of RWE against oxidative stress may occur through the activation of cellular antioxidant defenses (Supplementary Figure S1).

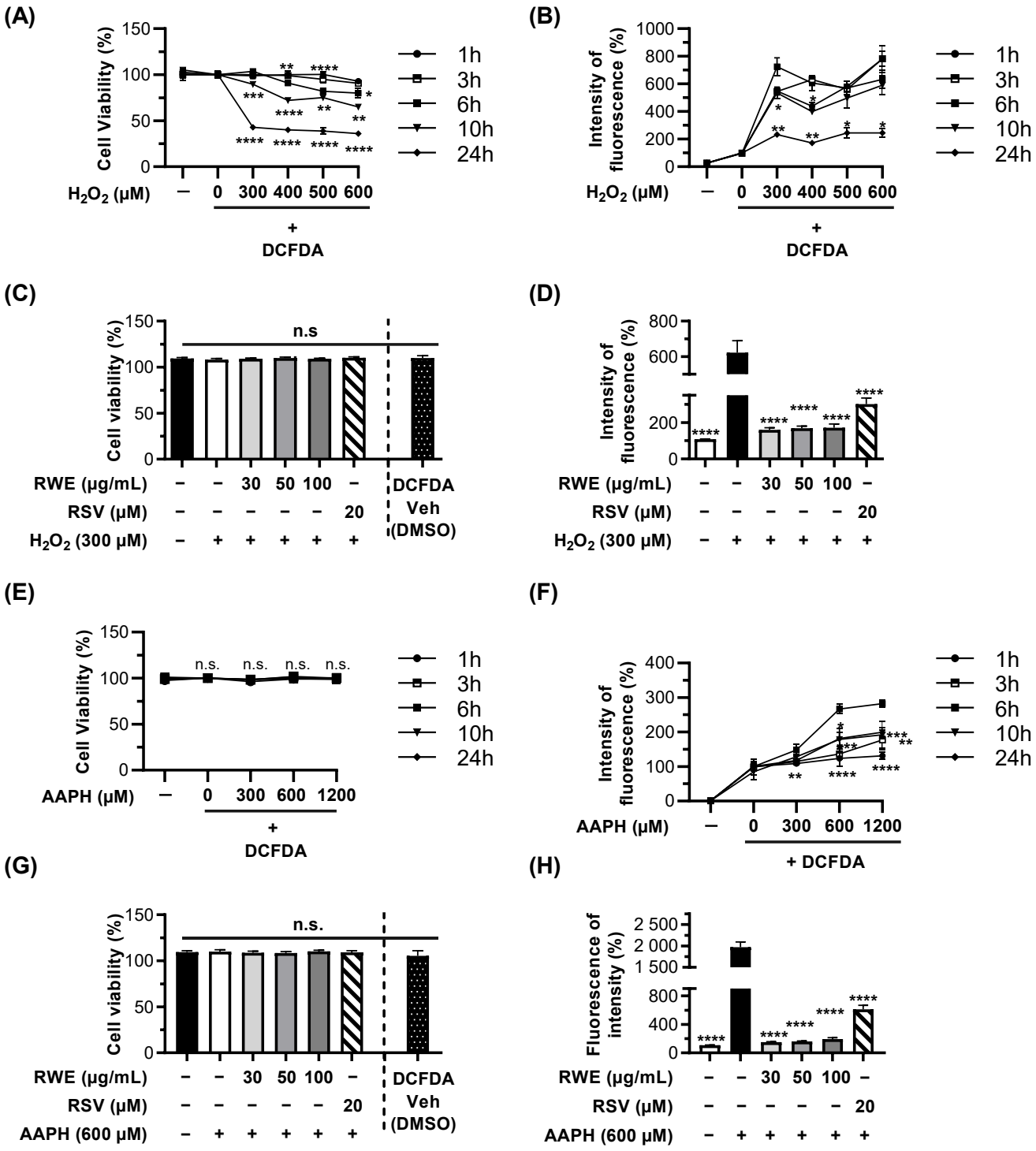

Figure 2. RWE prevents H_2O_2 - and AAPH-induced oxidative stress in ARPE-19 cells. (A,B) ARPE-19 cells were incubated for 30 min with the ROS-sensitive probe DCFDA (10 µM) or with the vehicle alone (0.02% DMSO). Then, cells were treated for 1, 6, 10, 16, and 24 h with increasing concentrations of H_2O_2 (0, 300, 400, 500, and 600 µM) or with the vehicles alone (0.2% culture medium; -DCFDA: −). After treatments, the cells' viability was assessed by crystal violet staining (A), and the ROS levels were quantified by flow cytometry (B). (C,D) Cells were treated 24 h with increasing concentrations of RWE (30, 50, and 100 µg/mL); RSV (20 µM); or with the vehicle alone (0.1% ethanol 70%).

After 24 h, the cells were incubated with 10 μM DCFDA or the vehicle alone (0.02% DMSO) for 30 min, followed by 6 h of treatment with H_2O_2 (300 μM). Thereafter, the cells' viability and ROS levels were determined as in (A,B). (E,F) ARPE-19 cells were incubated for 30 min with the ROS-sensitive probe DCFDA (10 μM) or with the vehicle alone (0.02% DMSO). Then, the cells were treated for 1, 6, 10, 16, and 24 h with increasing concentrations of AAPH (0, 300, 600, 1200, and 2400 μM) or with the vehicles alone (0.2% H2O; -DCFDA: −). After treatments, the cells' viability was assessed by crystal violet staining (E), and the ROS levels were quantified by flow cytometry (F). (G,H) Cells were treated 24 h with increasing concentrations of RWE (30, 50, and 100 μg/mL); RSV (20 μM); or with the vehicle alone (0.1% ethanol 70%). After 24 h, the cells were incubated with 10 μM DCFDA or the vehicle alone (0.02% DMSO) for 30 min, followed by 6 h of treatment with AAPH (600 μM). After treatments, the cells' viability was assessed by crystal violet staining (G), and the ROS levels were quantified by flow cytometry (H). For the kinetics in (A,B,E,F), the *p*-values were determined by a two-way ANOVA followed by Dunnett's multiple comparison test and compared to the 6 h timepoint. (C,G) The *p*-values were determined by a one-way ANOVA followed by Tukey's multiple comparison test. The *p*-values ≤ 0.05 were considered significant (n.s. nonsignificant). (D,H) The data are expressed as the mean DCFDA fluorescence intensity ± SEM of 3–5 independent experiments (2–4 biological replicates per independent experiment). The *p*-values were determined by a oneway ANOVA followed by Tukey's multiple comparison test. The *p*-values ≤ 0.05 were considered significant (* $p < 0.05$, ** $p < 0.01$, *** $p < 0.001$, and **** $p < 0.0001$ comparing the data to H_2O_2 - or AAPH-treated cells)

3.3. RWE Prevents Oxidative Stress-Induced DNA Damage in RPE Cells

In the first steps of AMD, oxidative stress can induce progressive retinal cellular damage, which leads to protein misfolding, functional anomalies, and DNA damage that trigger RPE cell dysfunctions. One of the most commonly used DNA oxidative stress markers is histone H2AX phosphorylation. Indeed, the phosphorylated histone H2AX (γH2AX), is usually used to assess DNA damage levels, being a marker of single- and double-stranded DNA breaks [35,36]. Firstly, we explored the ability of RWE to prevent DNA damage induced by oxidative stressors (i.e., H_2O_2 and AAPH) in ARPE-19 cells. Microscopic analyses highlighted the typical γH2AX foci after H_2O_2 treatment with 300 μM for 6 h, which was concomitant to ROS production (Figure 3A). Similarly, AAPH induced the same foci of γH2AX after 6 h of treatment with 600 μM of AAPH (Figure 3B). Interestingly, pretreatment with three concentrations of RWE (30, 50, and 100 μM) for 24 h before oxidative stress induction prevented the appearance of green fluorescence, reflecting the increase in γH2AX foci (Figure 3A,B). A quantitative analysis of MFI measured with Icy software (v2.4) showed that H_2O_2 and AAPH induced significant increases in γH2AX foci by +108% and +37% compared to the control cells (cells treated with the vehicle alone). In addition, we observed that RWE pretreatment, whatever the concentration used, significantly prevented H_2O_2- and AAPH-induced rises in γH2AX foci by, respectively, around 25% and 30% (Figure 4A,C). In order to confirm the induction of DNA damage, we stained RPE cells with Alexa Fluor® 647 anti-γH2A.X, and the MFI were measured by flow cytometry. These results confirmed the microscopic observations, showing that the treatment with 300 μM of H_2O_2 induces a strong increase in γH2AX staining compared to the control cells (by six-fold) (Figure 4B). The pretreatment with RWE significantly decreased H_2O_2-induced γH2AX in a concentration-dependent manner (33% for 30 μM, 38% for 50 μM, and 47% for 100 μM) compared to the H_2O_2 treatment (Figure 4B). RSV treatment with 20 μM had a modest inhibition of γH2AX (22%) compared to the

RWE treatments. Similarly, AAPH induced a two-fold increase in the γH2AX level compared to the control cells, and the pretreatment with RWE decreased γH2AX even at the lowest concentration (30 μg/mL) and allowed a return to the basal levels (Figure 4D).

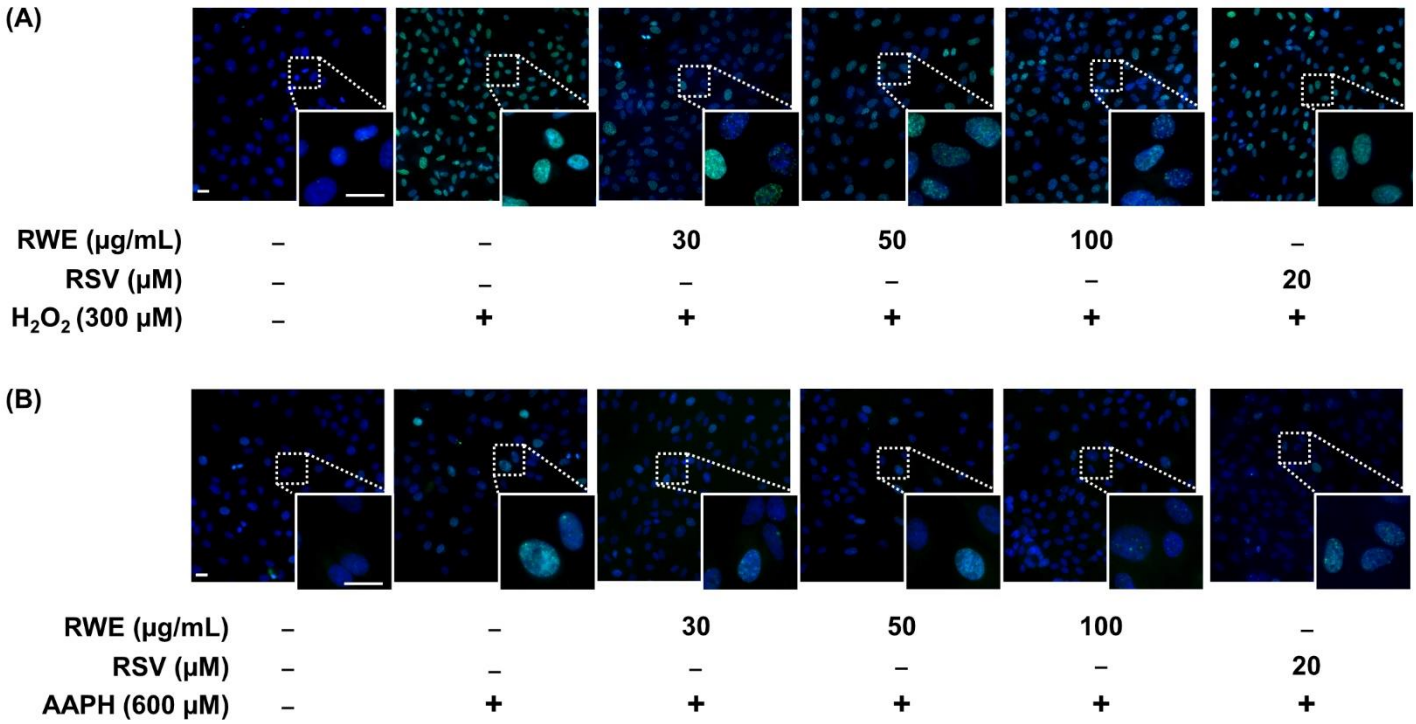

Figure 3. RWE prevents oxidative stress-induced DNA damage in ARPE-19 cells. Cells were treated with increasing concentrations of RWE (30, 50, and 100 μg/mL); RSV (20 μM); or with the vehicle alone (0.1% ethanol 70%). After 24 h, the cells were incubated with (A) H_2O_2 (300 μM) or with (B) AAPH (600 μM) for 6 h. γH2AX expression was analyzed by fluorescence microscopy (×20 and ×63 Figure 3. RWE prevents oxidative stress-induced DNA damage in ARPE-19 cells. Cells were treated with increasing concentrations of RWE (30, 50, and 100 μg/mL); RSV (20 μM); or with the vehicle alone (0.1% ethanol 70%). After 24 h, the cells were incubated with (A) H_2O_2 (300 μM) or with (B) AAPH (600 μM) for 6 h. γH2AX expression was analyzed by fluorescence microscopy (×20 and ×63 magnifications, scale bar = 20 μm). Nuclei (blue fluorescence) and γH2AX green fluorescence. Representative images of three independent experiments are shown.

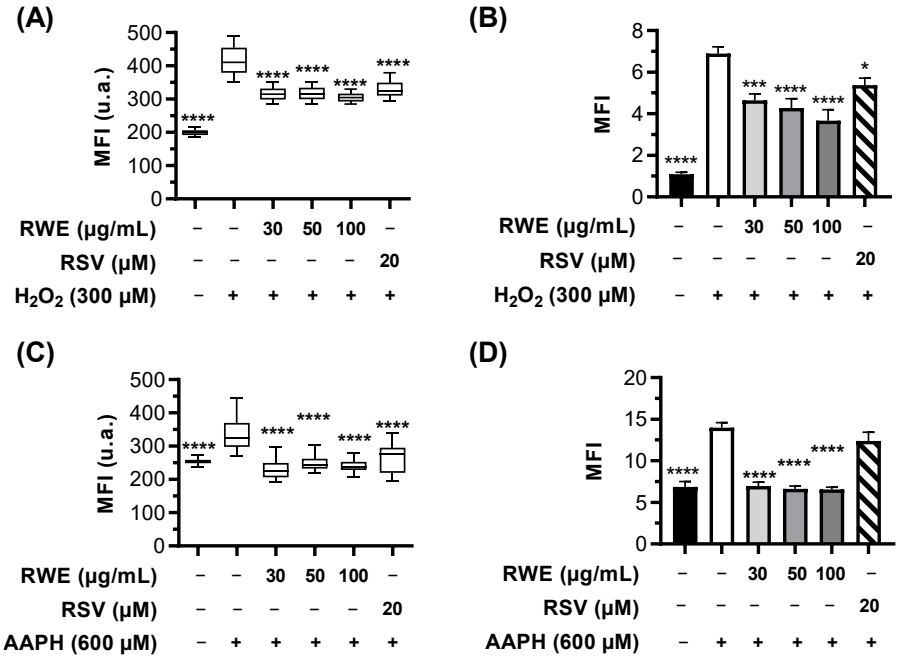

Figure 4. RWE prevents oxidative stress-induced DNA damage in ARPE-19 cells. (A,B) Cells were treated with increasing concentrations of RWE (30, 50, and 100 µg/mL); RSV (20 µM); or with the vehicle alone (0.1% ethanol 70%). After 24 h, the cells were incubated with H_2O_2 (300 µM) for 6 h. (A) Histograms of the mean fluorescence intensity (MFI) of γH2AX staining shown in Figure 3A. (B) Analysis of γH2AX staining in cells by flow cytometry. (C,D) Cells were treated with increasing concentrations of RWE (30, 50, and 100 µg/mL); RSV (20 µM); or with the vehicle alone (0.1% ethanol 70%). After 24 h, the cells were incubated with AAPH (600 µM) for 6 h. (C) Histograms of the mean fluorescence intensity (MFI) of γH2AX staining shown in Figure 3B. (D) Analysis of γH2AX staining in cells by flow cytometry. Fluorescence microscopy analyses were performed by measuring the MFI on merged pictures (n > 60 cells) with Icy software (v2.4) and were expressed as the mean MFI ± SEM of three independent experiments. The *p*-values were determined by Kruskal–Wallis followed by Dunn's multiple comparison test and comparing the data to H_2O_2 - or AAPH-treated cells. The *p*-values ≤ 0.05 were considered significant (**** $p < 0.0001$). Flow cytometry results were expressed as the mean MFI ± SEM ($\times 10^4$) from 3 to 5 independent experiments with 2 to 4 biological replicates per experiment. The *p*-values were determined by a one-way ANOVA followed by Tukey's multiple comparison test and comparing the data to H_2O_2 - or AAPH-treated cells. The *p*-values ≤ 0.05 were considered significant (* $p < 0.01$, *** $p < 0.001$, and **** $p < 0.0001$).

3.4. RWE Affects Activation of Key Regulators in the DNA Damage Response Pathway

DNA damage, whether single- or double-stranded breaks, results in activation of the DNA damage response (DDR) pathway. The two main pathways activated as a result of genomic damage are the ATM (ataxia telangiectasia-mutated)/Chk2 (checkpoint kinase 2) and RAD3-related (ATR)/Chk1 (checkpoint kinase 1) pathways. ATM and ATR proteins phosphorylate downstream histone H2AX (γH2AX), which then recruits other ATM and ATR substrates, notably Chk2 and Chk1 proteins. These proteins can then modulate the activity of key cell cycle regulators through the activation of transcription factor p53 [37,38]. Once activated, this triggers the G1/S, S, and G2/M checkpoints, thereby blocking cell cycle progression to enable either DNA repair or cell death induction. In order to investigate the effect of RWE on these DNA damage pathways, the

expression of key proteins and their phosphorylation states were analyzed by Western blot in ARPE-19.

First, we observed that H_2O_2 affects the ATM/Chk2 pathway. As shown in Figure 5A, H_2O_2 increases the phosphorylation of ATM and Chk2 by 14- and 15-fold, respectively, and a pretreatment with RWE is able to prevent these phosphorylations. Indeed, RWE prevents the phosphorylation of ATM even at the lowest concentration (around 65%) and, also, the phosphorylation of Chk2 in a dose-dependent manner (around 37% at 30 and 50 μg/mL and 62% at 100 μg/mL) (Figure 5C). Similarly, the pretreatment with RSV is also able to decrease the phosphorylation of ATM and Chk2 (around 60%). Similar results were observed with the phosphorylation of p53, with a significant increase of p53 phosphorylation induced by H_2O_2 by around 10-fold, and a pretreatment with RWE is able to reduce this phosphorylation at the strongest concentration (62% at 100 μg/mL). Interestingly, RSV is not able to significantly reduce the phosphorylation of p53. Then, we investigated the ATR/Chk1 pathway, and as shown in Figure 5A,C, H_2O_2 did not affect the expression and phosphorylation of ATR and Chk1. Nevertheless, a pretreatment with RWE at the strongest concentration (100 μg/mL) or RSV (20 μM) was able to significantly decrease the phosphorylation of Chk1 even below the basal control level.

In the same way, we studied the impact of AAPH treatment on the ATM/Chk2 and ATR/Chk1 pathways. Contrary to H_2O_2, AAPH does not impact the expression or the phosphorylation of ATM, ATR, Chk1, and p53 (Figure 5B). However, AAPH induces the phosphorylation of Chk2 2.5-fold, and the pretreatment with the highest concentration of RWE or with RSV is able to reduce this phosphorylation by around 45% (Figure 5B,D). Very interestingly, AAPH does not impact the expression or the phosphorylation of p53; however, the pretreatment with the highest concentration of RWE is able to reduce the phosphorylation of p53 by 56% compared to the control cells (Figure 5D).

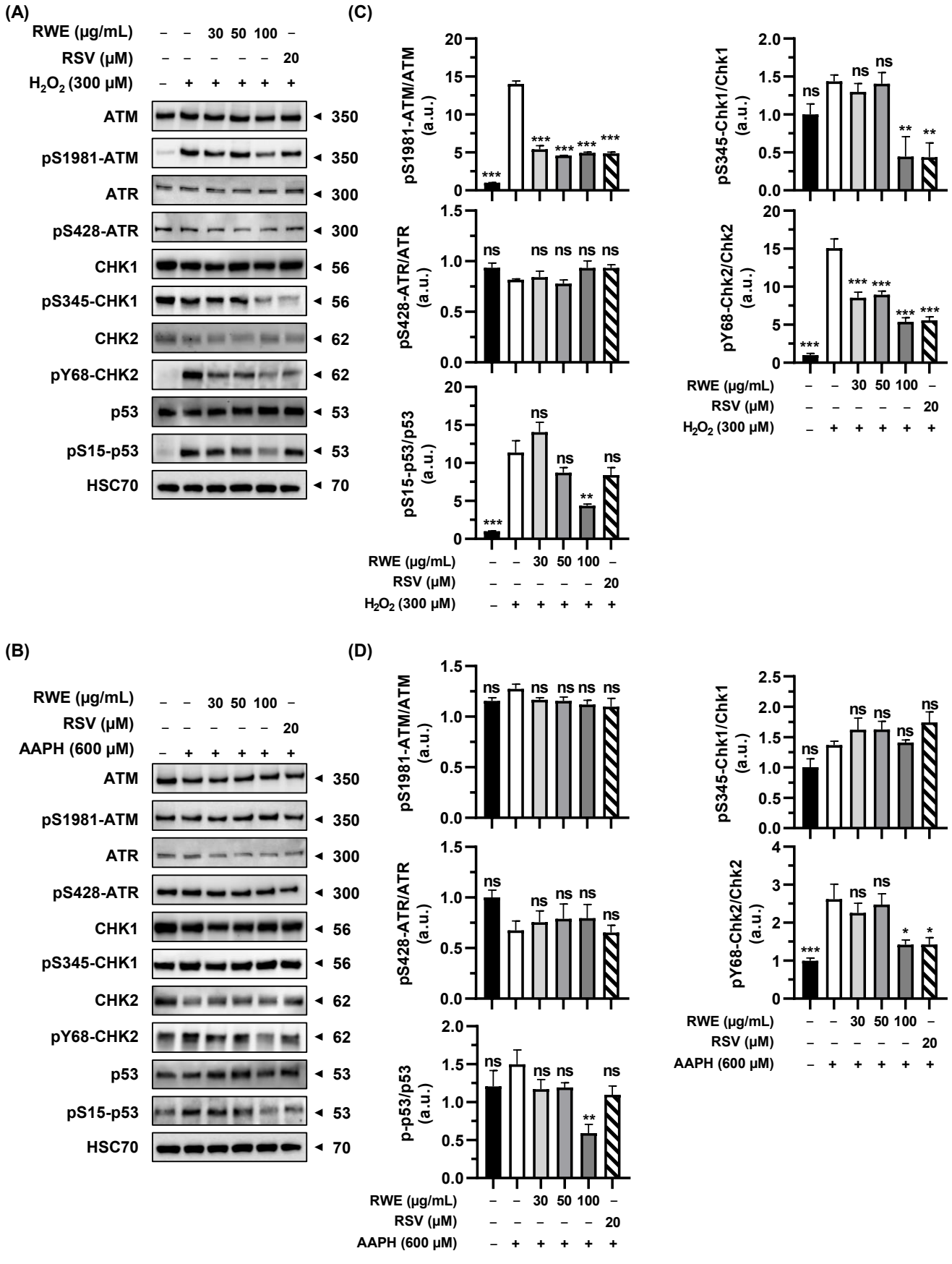
(A)
RWE (µg/mL) – – 30 50 100 –
RSV (µM) – – – – – 20
H2O2 (300 µM) – + + + + +
ATM 350
pS1981-ATM 350
ATR 300
pS428-ATR 300
CHK1 56
pS345-CHK1 56
CHK2 62
pY68-CHK2 62
p53 53
pS15-p53 53
HSC70 70
(B)
RWE (µg/mL) – – 30 50 100 –
RSV (µM) – – – – – 20
AAPH (600 µM) – + + + + +
ATM 350
pS1981-ATM 350
ATR 300
pS428-ATR 300
CHK1 56
pS345-CHK1 56
CHK2 62
pY68-CHK2 62
p53 53
pS15-p53 53
HSC70 70
(C)
pS1981-ATM/ATM (a.u.)
pS428-ATR/ATR (a.u.)
pS15-p53/p53 (a.u.)
pS345-Chk1/Chk1 (a.u.)
pY68-Chk2/Chk2 (a.u.)
RWE (µg/mL) – – 30 50 100 –
RSV (µM) – – – – – 20
H2O2 (300 µM) – + + + + +
(D)
pS1981-ATM/ATM (a.u.)
pS428-ATR/ATR (a.u.)
p-p53/p53 (a.u.)
pS345-Chk1/Chk1 (a.u.)
pY68-Chk2/Chk2 (a.u.)
RWE (µg/mL) – – 30 50 100 –
RSV (µM) – – – – – 20
AAPH (600 µM) – + + + + +

Figure 5. RWE affects H_2O_2 - and AAPH-induced activation of key regulators of the DNA damage response (DDR) pathway in ARPE-19. Cells were treated with increasing concentrations of RWE (30, 50, and 100 μg/mL); RSV (20 μM); or the vehicle alone (0.1% ethanol 70%) for 24 h and were thereafter treated for 6 h with (A) H_2O_2 (300 μM) or by (B) AAPH (600 μM). Immunoblots of the key proteins involved in the DDR pathway are representative of three independent experiments. HSC70 was used as an internal loading control and was used for protein expression normalization. (C,D) Histograms corresponding to protein expression quantification. Data are the mean ratios between phosphorylated and total forms ± SEM (arbitrary units, u.a.) of 3 to 5 independent experiments. The *p*-value was determined by a one-way ANOVA followed by Tukey's multiple comparison test comparing the data to H_2O_2 - or AAPH-treated cells. *** $p < 0.001$, ** $p < 0.01$, * $p < 0.05$, and ns: nonsignificant.

3.5. RWE Prevents H_2O_2- and LPS/IFN-γ-Induced Inflammation in RPE Cells and Macrophages

It is well known that oxidative stress through ROS production and DNA damage contributes to inflammatory processes. Indeed, cigarette smoke concentrate induces ROS production and γH2AX nuclear foci in ARPE-19 cells, which are associated with the upregulation of proinflammatory cytokines IL-6 and IL-8 [39]. Indeed, RPE cells are involved in the regulation of the immune response in the retina, and dysfunctions in the RPE can lead to the secretion of proinflammatory cytokines such as IL-6 and IL-8, which maintain a proinflammatory environment [40]. These cytokines are crucial in AMD pathogenesis. Indeed, IL-6 has proangiogenic properties, the intraocular concentration of this cytokine being more closely correlated to the occurrence of macular edema than VEGF-A [41]. In this context, we have explored the RWE ability to prevent the secretion of IL-6 and IL-8 induced by oxidative stress (i.e., H_2O_2) in ARPE-19 cells.

As expected, the treatment of cells with 300 μM of H_2O_2 for 6 h induced a strong secretion of IL-6 2.5-fold compared to the control. This latter was strongly reduced to the basal control levels by the pretreatment of cells with RWE 30 μg/mL and was even decreased to lower levels when using 50 and 100 μg/mL of RWE (reduction by 44% and 49%, respectively, compared to the control) (Figure 6A).

RSV is also usually described as an anti-inflammatory compound. In these oxidative stress conditions, polyphenol was able to decrease IL-6 secretion but at a lower level than RWE by 37% compared to H_2O_2 (Figure 6A). Similarly, IL-8 secretion was completely decreased with RWE pretreatment (Figure 6B). Indeed, ARPE-19 cells overproduce IL-8 under oxidative stress with H_2O_2 2.5-fold compared to the control, which is completely returned to the basal level when RPE cells are pretreated with 30 or 50 μg/mL of RWE (Figure 6B). In view of these results, we then explored the capacity of RWE to counteract an overproduction of proinflammatory cytokines not by oxidative stress but by a common inducer of inflammation, such as a combination with lipopolysaccharide (LPS) and interferon gamma (IFN-γ). The quantification of IL-6 and IL-8 secretion by RPE cells revealed that LPS/IFN-γ increases IL-6 secretion 5-fold compared to the control (Figure 6D) and around 4.3-fold for IL-8 compared to the control (Figure 6E), without inducing any cytotoxicity (Figure 6C). The pretreatment of cells with RWE strongly decreases IL-6

production at the same basal level of the control with 50 and 100 μg/mL (Figure 6D). Very interestingly, RWE pretreatment decreases IL-8 secretion below the basal control level from 30 μg/mL and strongly decreases under the basal levels at 50 and 100 μg/mL (Figure 6E).

These proinflammatory cytokines, which are produced in RPE cells under the effect of stress activators, are found in the aqueous humor of patients with AMD [42], and their levels have been correlated with neovascular retinal activity [43]. However, RPE cells are not the only immunosuppressive cells playing a role in the proinflammatory state seen in this disease. During AMD, monocytes from the blood circulation are recruited to the retina and choroid, where they differentiate into macrophages, especially into proinflammatory "M1"- type macrophages [15]. This type of macrophages is activated by multiple signals, including bacterial toxins such as LPS, and they secrete, in particular, proinflammatory cytokines such as IL-6 and IL-8 [44]. Considering the important role played by proinflammatory M1 macrophages in AMD progression, we next assessed whether the modulation of IL secretion by RWE in RPE cells could be similar in these immune cells. To this end, we isolated human peripheral blood mononuclear cells (PBMC) from four different male donors that we pre-differentiated with GM-CSF for 6 days. Thereafter, the cells were pretreated for 24 h with increasing concentrations of RWE (30, 50, and 100 μg/mL); RSV (20 μM); or with the vehicle alone before activating monocytes into M1 macrophages with LPS and IFN-γ. After 4 h of stimulation, the macrophages were treated for an additional 20 h with increasing concentrations of RWE or RSV, as previously described. At the end of the treatments, the supernatants were collected to measure the IL-6 and IL-8 secretion levels by ELISA (Figure 7B,C), and the cells were stained with crystal violet to assess the cell viability (Figure 7A). As expected, the treatment with LPS/IFN-γ induced IL-6 secretion that increased by 200-fold compared to the control with no significant toxicity (Figure 7A) and that was lowered in a dose-dependent manner with RWE (65%, 73%, and 76% at 30, 50, and 100 μg/mL, respectively) (Figure 7B). RSV decreased IL-6 secretion slowly compared to the different RWE concentrations, with 43% compared to LPS/IFN-γ (Figure 7B). Similarly, IL-8 secretion was increased by LPS/IFN-γ by around 50-fold compared to the control. Similar to IL-6, IL-8 secretion was inhibited in a dose-dependent manner by RWE, with 35%, 56%, and 84% at 30, 50, and 100 μg/mL, respectively (Figure 7C). As with ARPE-19, pretreatment with 20 μM of RSV decreased the production of the two proinflammatory cytokines compared to cells under stress conditions but at a lower level than with RWE treatment (43% for IL-6 and 25% for IL-8) (Figure 7B,C)

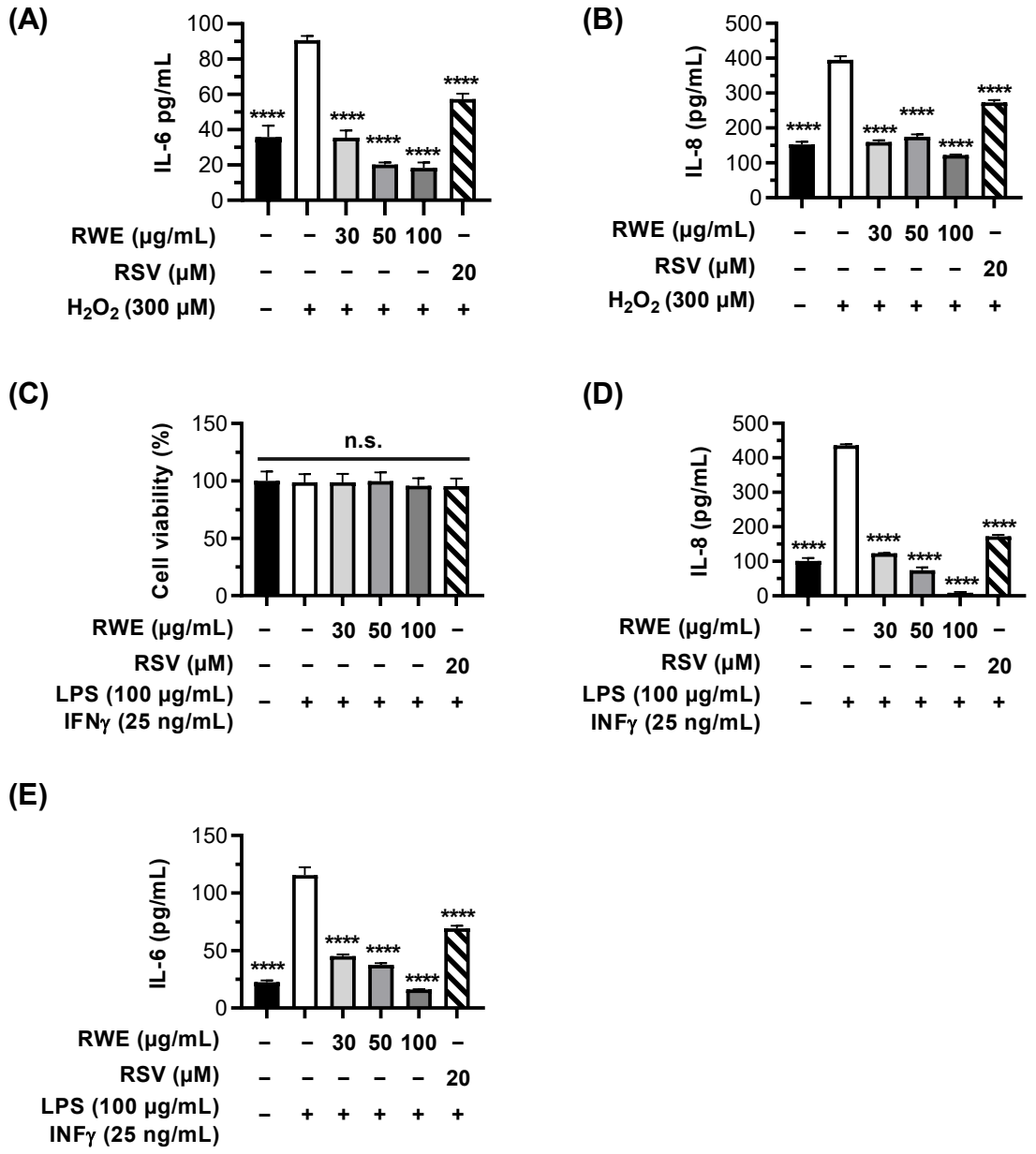

Figure 6. Anti-inflammatory effects of RWE on the secretion of proinflammatory cytokines IL-6 and IL-8 in ARPE-19 cells. Cells were treated with increasing concentrations of RWE (30, 50, and 100 µg/mL); RSV (20 µM); or the vehicle alone (0.1% ethanol 70%). After 24 h of treatment, the cells were incubated for 6 h with (A,B) H_2O_2 (300 µM) or with (C–E) LPS (100 µg/mL) and IFN-γ (25 ng/mL). The levels of (A,D) IL-6 and (B,E) IL-8 were measured by ELISA. Data were expressed as the mean in pg/mL ± SEM of 3–5 independent experiments (2–4 biological replicates per independent experiment). The *p*-values were determined by a one-way ANOVA followed by Tukey's multiple comparison test comparing the data to H_2O_2 - or LPS/IFN-γ-treated cells. The *p*-values ≤ 0.05 were considered significant (**** $p < 0.0001$). (C) Cell viability was measured by crystal violet staining. Data were expressed as the mean percentage relative to the control cells (treated with the vehicles alone) ± SEM of three independent experiments (4 biological replicates per independent experiment). The *p*-values were determined by a one-way ANOVA followed by Tukey's multiple comparison test. The *p*-values ≤ 0.05 were considered significant (n.s. nonsignificant).

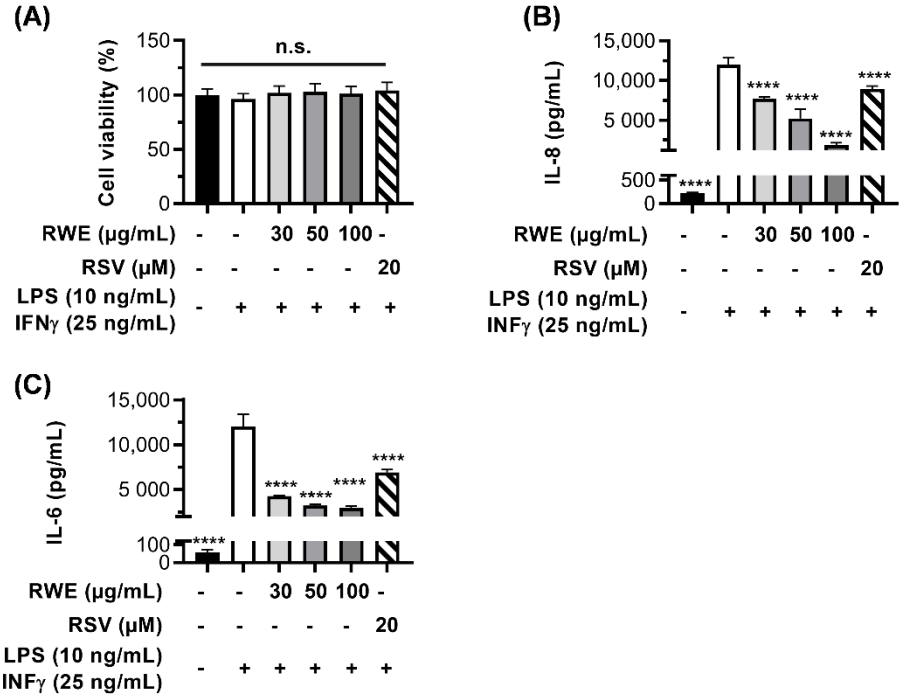

Figure 7. Anti-inflammatory effects of RWE on the secretion of proinflammatory cytokines IL-6 and IL-8 in human macrophages. After 6 days of culture, human PBMC were treated with increasing concentration of RWE (30, 50, and 100 µg/mL); RSV (20 µM); or the vehicle alone (0.1% ethanol 70%). After 24 h of treatment, the cells were incubated with LPS (10 ng/mL) and IFN-γ (25 ng/mL) to polarize cells into M1 macrophages or incubated with the vehicle alone. After 4 h of stimulation with LPS and IFN-γ, increasing concentrations of RWE (30, 50, and 100 µg/mL); RSV (20 µM); or the vehicle alone (0.1% ethanol 70%) were added into the medium for an additional 20 h. At the end of the treatments, the cells' viability was assessed with crystal violet staining (A), and the supernatants were collected to measure by ELISA the secreted levels of (B) IL-6 and (C) IL-8. For the ELISA assays, the data were expressed as the mean in pg/mL ± SEM of 3–5 independent experiments (2–4 biological replicates per independent experiment). The *p*-value was determined by a one-way ANOVA followed by Tukey's multiple comparison test. **** *p*-value < 0.0001 comparing the data to LPS/IFN-γ-treated cells. For cell viability, data were expressed as the mean percentage relative to the control cells (treated with the vehicles alone) ± SEM of three independent experiments (4 biological replicates per independent experiment). The *p*-values were determined by a one-way ANOVA followed by Tukey's multiple comparison test. (n.s. nonsignificant).

4. Discussion

Age-related macular degeneration (AMD) is the leading cause of central vision impairment in patients over the age of 65. This multifactorial disease is caused by both environmental and genetic risk factors [23]: smoking; air pollution; ultraviolet radiation; metabolic diseases (e.g., obesity, hypertension, and diabetes); consumption of dietary fats [24–27]; and genetic polymorphisms such as cfh and arms2/hrta1 genes [28]. These factors can trigger AMD through the production of free radicals that create oxidative stress and inflammation in the retina. Both oxidative stress and inflammation are known for playing a critical role in the initiation and development of AMD [45]. Retinal pigment epithelial (RPE) cells are responsible for maintaining the retina homeostasis by providing

nutritional and structural support; therefore, RPE are the primary target for AMD-associated oxidative stress [46]. RSV, a potent antioxidant compound, may be effective in reducing the risk of AMD in a same way that common antioxidants found in fruits and vegetables (vitamins C and E and carotenoids) have been shown to delay or prevent the development of ocular diseases [47].

Some studies have shown that food supplementation with resveratrol could have beneficial properties against eye disease [22], i.e., by reducing laser-induced choroidal neovascularization (CNV) in mice [48]. Furthermore, other polyphenols found in red wine (such as quercetin, epicatechin, and malvidin) have been reported to have potential positive effects in AMD by exerting antioxidant, anti-inflammatory, and antiangiogenic effects in both in vitro and in animal models of AMD [49–53]. In this context, we used a red wine extract (RWE) enriched with various properly identified and characterized polyphenols, and we describe, for the first time, the potential use of RWE to prevent early events, such as ROS production and proinflammatory IL secretion, in a human RPE cell line (ARPE-19).

It Is well established that polyphenols can both scavenge ROS and regulate signaling pathways involved in oxidative stress, inflammation, and angiogenesis. Indeed, the structure of polyphenol compounds is characterized by a poly hydroxyl group on an aromatic ring, which allows them to exhibit the radical scavenging of NO· and OH· [34]. In addition to their direct action on ROS, polyphenols also have biological functions by regulating the mitochondrial respiratory chain [54,55] and endogenous antioxidant enzymes such as superoxide dismutase, catalase, and glutathione peroxidase or various targets such as nuclear factor erythroid 2-related factor 2 (Nrf2) and the mammalian forkhead transcription factors of the O class (FOXOs) that are involved in the transcription of target antioxidant gene expression [34]. Among these polyphenols, the biological activities of RSV as an antioxidant and anti-inflammatory compound have been well described [56,57], particularly in the context of various ocular dysfunctions [22]. Furthermore, recent studies have shown that this hydroxystilbene is also able to act synergistically with other polyphenols to counteract many deleterious processes. It has now been clearly demonstrated that polyphenolic compounds that are said to have synergistic activities are highly effective against oxidation, inflammation, myocardial infarction, and a variety of other conditions [58–61]. In addition, natural polyphenols act synergistically with existing clinically approved drugs to improve anticancer activity [37,62–64]. We have addressed, in many pathological conditions, the potential use of a mixture from red wine that contains various polyphenols. We were thus able to reveal that the qualitative and quantitative compositions of polyphenols were decisive in the biological activity of these polyphenolic mixtures, because depending on the presence or absence of certain compounds, we observed synergistic effects, additives, or even opposing antagonistic effects [29]. Similarly, we were able to demonstrate, in a previous study on antitumor activity, that the relative concentrations of these compounds were also decisive and that it was the mixture from the dry red wine extract richest in polyphenols that exhibited the best antitumor activity in a model of chemo-induced

carcinogenesis in rats [29]. Very interestingly, these extracts were able to alter tumor angiogenesis in many models through the reduction of VEGF-A [29,65,66]. This proangiogenic factor has a major importance in the progression of AMD and poor clinical prognosis. Se recently showed that the extract enriched in polyphenols was also able to reduce the secretion of VEGF-A in a retinal model of ARPE-19 cells by disturbing the VEGF-R2/mitogen-activated protein kinase (MAPK) signaling pathway [30]. This pathway is not the only one that leads to the overproduction of VEGF-A, and early AMD events can contribute significantly to VEGF-A production and, thus, to the triggering of angiogenesis, as observed during oxidative stress [39] or chronic inflammation [67,68].

Oxidative stress is the first step of AMD. It can lead to cell injury such as DNA damage, triggering RPE cell dysfunction. By inducing ROS production, nuclear damage appears in RPE cells, leading to phosphorylated-histone 2AX-immunoreactive (γH2AX) nuclear foci, which trigger an increase in the p53 protein [39]. The present study highlights that RWE was able to prevent H_2O_2- or AAPH-induced oxidative stress in human ARPE-19 RPE cells in a dose-dependent manner and, thus, protect RPE cells against DNA damage, as demonstrated by the decrease in γH2AX. Subsequently, this protective effect is associated with a downregulation of the DDR pathway involving the ATM/Chk2 and ATR/Chk1 proteins. Very interestingly, as observed in previous studies, RWE was more efficient than RSV alone in preventing oxidative stress and DNA damage, suggesting a potential synergy between polyphenol compounds at very low concentrations.

It is well known that oxidative stress resulting from ROS production and DNA damage contributes to inflammatory processes. Indeed, during aging or exposure to exogenous and endogenous factors, ROS production and γH2AX nuclear foci are induced in RPE cells in association with an upregulation of proinflammatory cytokines, particularly IL-6 and IL-8 [39]. Furthermore, drusen formed during the AMD process contain numerous proinflammatory interleukins and plasmatic proteins (such as C-reactive protein (CRP)) involved in acute inflammation [69]. Indeed, it has been shown that the plasma CRP levels are higher in patients with AMD. Similarly, high levels of IL-6 have been associated with the progression of AMD. Furthermore, many anatomopathological studies have demonstrated the presence of inflammatory cells from the early stage of AMD, notably preceding the appearance of retinal lesions. Particularly, mononuclear phagocytes are present at the edge of atrophic zones and are responsible for the degeneration of photoreceptors. Therefore, there is an amplification loop for inflammation, since there is chronic inflammation of the cells in the RPE that progressively alters their function and results in the formation of drusen. In our study, we show that RWE was able to prevent the secretion of proinflammatory cytokines (IL-6 and IL-8) in RPE cells induced by oxidative stress and by LPS, but RWE was also able to prevent these same cytokines in inflammatory cells such as macrophages. Interestingly, in these two cell types, RSV alone was able to prevent the secretion of IL-6 and IL-8, but the effect was not as marked as for RWE. Overall, RWE and RSV alone can be beneficial in the prevention of the events leading to AMD, but RWE appears to be more efficient.

Overall, these results, which were obtained using a polyphenolic cocktail on a human retinal cell line (ARPE-19) and human macrophages, pave the way for future studies. Our findings suggest that this formula may reduce or prevent events associated with AMD, thus slowing the progression of AMD and preventing the formation of new vessels. Nonetheless, as polyphenols are subjected to intensive metabolism by phase I/phase II enzymes [70–72], further studies are required to evaluate the ability of such a polyphenolic formulation to prevent AMD onset or progression and to analyze RWE metabolite profiles in target tissues using a mass spectrometry approach [48].

5. Conclusions

Our study demonstrated, for the first time, that a red wine extract (RWE) enriched in various polyphenols could counteract the early events of AMD, such as ROS production and proinflammatory IL secretion, in a human RPE cell line (ARPE-19). We showed that RWE can have an antiangiogenic effect and that it can prevent ROS and protect cells from DNA damage through the downregulation of key factors in the DNA damage response pathway, such as ATM, Chk2, and p53. These antioxidant effects are enhanced by antiinflammatory benefits. Moreover, RWE and RSV are able to counteract the secretion of proinflammatory cytokines induced in ARPE-19 cells and human macrophages. These in vitro findings pave the way for further in vivo and clinical investigations on the health benefits of polyphenols and their metabolites.

Supplementary Materials: The following supporting information can be downloaded at: https:// www.mdpi.com/article/10.3390/cells12101408/s1, Figure S1: Effects of RWE on H_2O_2-induced protein expression of Nrf2 transcription factor and Heme-Oxygenase 1 (HO-1) in ARPE-19. Cells were treated with increasing concentrations of RWE (30, 50, 100 μg/mL), RSV (20 μM) or vehicle alone (0.1% ethanol 70%) for 24 h, and were thereafter treated for 6 h with H_2O_2 (300 μM). Immunoblots of Nrf2 and HO-1 are representative of three independent experiments. HSC70 was used as an internal loading control; Figure S2: Flow cytometry gating Strategies. Live cells Were stain withe Fixable viability staining (FVS 520). Gray histogram represents H2AX staining in ARPE-19 after treatment.

Author Contributions: C.C., M.P. and F.H. performed the experiments and analyzed the data; J.V.-F. and T.R. investigated the qualitative and quantitative polyphenols compositions; C.C., F.H., V.A. and D.D. wrote the manuscript; and V.A. and D.D. supervised the experiments and supervised the overall project. All authors have read and agreed to the published version of the manuscript.

Funding: C.C. was supported by grants from the "Fonds Européen de Développement Régional" (FEDER) and the "Bureau interprofessionnel des Vins de Bourgogne" (BIVB). M.P. was supported by grants from ANRT no. 2021/1248 by the French government. This work was supported by a French government grant managed by the French National Research Agency under the program "Investissements d'Avenir", reference ANR-11-

LABX-0021, and was supported by grants from the “Conseil Régional de Bourgogne”, the “Fonds Européen de Développement Régional” (FEDER), the “Bureau interprofessionnel des Vins de Bourgogne” (BIVB).

Institutional Review Board Statement: Not applicable. Informed Consent Statement: Not applicable. Data Availability Statement: The authors declare that all data supporting the findings of this study are available within the article and the Supplementary Materials.

Acknowledgments: The authors thank the Imaflow platform for the flow cytometry analysis, Ruth Hornedo Ortega for supplying the malvidin 3-glucoside standard and thank the Bordeaux Metabolome Facility and the MetaboHUB (ANR11-INBS-0010) Project, and Suzanne Rankin (CHU Dijon) for the editing and critical reading of the manuscript.

Conflicts of Interest: The authors declare no conflict of interest.

References

1. Friedman, D.S.; O'Colmain, B.J.; Muñoz, B.; Tomany, S.C.; McCarty, C.; De Jong, P.T.V.M.; Nemesure, B.; Mitchell, P.; Kempen, J.; Congdon, N. Prevalence of age-related macular degeneration in the United States. *Arch. Ophthalmol.* **2004**, *122*, 564–572. https://doi.org/10.1001/archopht.122.4.564.
2. Klein, R.; Klein, B.E.; Tomany, S.C.; Meuer, S.M.; Huang, G.-H. Ten-year incidence and progression of age-related maculopathy: The Beaver Dam eye study. *Ophthalmology* **2002**, *109*, 1767–1779. https://doi.org/10.1016/s0161-6420(02)01146-6.
3. Fleckenstein, M.; Keenan, T.D.L.; Guymer, R.H.; Chakravarthy, U.; Schmitz-Valckenberg, S.; Klaver, C.C.; Wong, W.T.; Chew, E.Y. Age-related macular degeneration. *Nat. Rev. Dis. Prim.* **2021**, *7*, 31. https://doi.org/10.1038/s41572-021-00265-2.
4. Somasundaran, S.; Constable, I.J.; Mellough, C.B.; Carvalho, L.S. Retinal pigment epithelium and age-related macular degeneration: A review of major disease mechanisms. *Clin. Exp. Ophthalmol.* **2020**, *48*, 1043–1056. https://doi.org/10.1111/ceo.13834.
5. Bressler, N.M.; Bressler, S.B.; Congdon, N.G.; Ferris, F.L., 3rd; Friedman, D.S.; Klein, R.; Lindblad, A.S.; Milton, R.C.; Seddon, J.M.; Age-Related Eye Disease Study Research Group Potential Public Health Impact of Age-Related Eye Disease Study Results: AREDS report no. 11. *Arch. Ophthalmol.* **2003**, *121*, 1621–1624. https://doi.org/10.1001/archopht.121.11.1621.
6. Ammar, M.J.; Hsu, J.; Chiang, A.; Ho, A.C.; Regillo, C.D. Age-related macular degeneration therapy: A review. *Curr. Opin. Ophthalmol.* **2020**, *31*, 215–221. https://doi.org/10.1097/icu.0000000000000657.
7. Nowak, J.Z. Age-related macular degeneration (AMD): Pathogenesis and therapy. *Pharmacol. Rep.* **2006**, *58*, 353–363.
8. Amadio, M.; Govoni, S.; Pascale, A. Targeting VEGF in eye neovascularization: What's new?: A comprehensive review on current therapies and oligonucleotide-based interventions under development. *Pharmacol. Res.* **2015**, *103*, 253–269. https://doi.org/10.1016/j.phrs.2015.11.027.

9. Haibe, Y.; Kreidieh, M.; El Hajj, H.; Khalifeh, I.; Mukherji, D.; Temraz, S.; Shamseddine, A. Resistance Mechanisms to Anti-angiogenic Therapies in Cancer. *Front. Oncol.* **2020**, *10*, 221. https://doi.org/10.3389/fonc.2020.00221.
10. Mettu, P.S.; Allingham, M.J.; Cousins, S.W. Incomplete response to Anti-VEGF therapy in neovascular AMD: Exploring disease mechanisms and therapeutic opportunities. *Prog. Retin. Eye Res.* **2021**, *82*, 100906. https://doi.org/10.1016/j.preteyeres.2020.100906.
11. Abokyi, S.; To, C.-H.; Lam, T.T.; Tse, D.Y. Central Role of Oxidative Stress in Age-Related Macular Degeneration: Evidence from a Review of the Molecular Mechanisms and Animal Models. *Oxidative Med. Cell. Longev.* **2020**, *2020*, 7901270. https://doi.org/10.1155/2020/7901270.
12. Ruan, Y.; Jiang, S.; Gericke, A. Age-Related Macular Degeneration: Role of Oxidative Stress and Blood Vessels. *Int. J. Mol. Sci.* **2021**, *22*, 1296. https://doi.org/10.3390/ijms22031296.
13. Toma, C.; De Cillà, S.; Palumbo, A.; Garhwal, D.P.; Grossini, E. Oxidative and Nitrosative Stress in Age-Related Macular Degeneration: A Review of Their Role in Different Stages of Disease. *Antioxidants* **2021**, *10*, 653. https://doi.org/10.3390/antiox10050653.
14. van Lookeren Campagne, M.; LeCouter, J.; Yaspan, B.L.; Ye, W. Mechanisms of age-related macular degeneration and therapeutic opportunities. *J. Pathol.* **2014**, *232*, 151–164. https://doi.org/10.1002/path.4266.
15. Ambati, J.; Atkinson, J.P.; Gelfand, B.D. Immunology of age-related macular degeneration. *Nat. Rev. Immunol.* **2013**, *13*, 438–451. https://doi.org/10.1038/nri3459.
16. Blasiak, J.; Pawlowska, E.; Sobczuk, A.; Szczepanska, J.; Kaarniranta, K. The Aging Stress Response and Its Implication for AMD Pathogenesis. *Int. J. Mol. Sci.* **2020**, *21*, 8840. https://doi.org/10.3390/ijms21228840.
17. Mukhtar, S.; Ambati, B.K. The value of nutritional supplements in treating Age-Related Macular Degeneration: A review of the literature. *Int. Ophthalmol.* **2019**, *39*, 2975–2983. https://doi.org/10.1007/s10792-019-01140-6.
18. Delmas, D.; Jannin, B.; Latruffe, N. Resveratrol: Preventing properties against vascular alterations and ageing. *Mol. Nutr. Food Res.* **2005**, *49*, 377–395. https://doi.org/10.1002/mnfr.200400098.
19. Delmas, D.; Lancon, A.; Colin, D.; Jannin, B.; Latruffe, N. Resveratrol as a Chemopreventive Agent: A Promising Molecule for Fighting Cancer. *Curr. Drug Targets* **2006**, *7*, 423–442. https://doi.org/10.2174/138945006776359331.
20. Delmas, D.; Limagne, E.; Ghiringhelli, F.; Aires, V. Immune Th17 lymphocytes play a critical role in the multiple beneficial properties of resveratrol. *Food Chem. Toxicol.* **2020**, *137*, 111091. https://doi.org/10.1016/j.fct.2019.111091.
21. Delmas, D.; Solary, E.; Latruffe, N. Resveratrol, a Phytochemical Inducer of Multiple Cell Death Pathways: Apoptosis, Autophagy and Mitotic Catastrophe. *Curr. Med. Chem.* **2011**, *18*, 1100–1121. https://doi.org/10.2174/092986711795029708.
22. Delmas, D.; Cornebise, C.; Courtaut, F.; Xiao, J.; Aires, V. New Highlights of Resveratrol: A Review of Properties against Ocular Diseases. *Int. J. Mol. Sci.* **2021**, *22*, 1295. https://doi.org/10.3390/ijms22031295.
23. AREDS. Risk factors associated with age-related macular degeneration. A case-control study in the age-related eye disease study: Age-Related Eye Disease Study Report Number 3. *Ophthalmology* **2000**, *107*, 2224–2232. https://doi.org/S0161642000004097.
24. Seddon, J.M.; Willett, W.C.; Speizer, F.E.; Hankinson, S.E. A Prospective Study of Cigarette Smoking and Age-Related Macular Degeneration in Women. *JAMA* **1996**, *276*, 1141–1146. https://doi.org/10.1001/jama.1996.03540140029022.

25. Cackett, P.; Yeo, I.; Cheung, C.M.G.; Vithana, E.N.; Wong, D.; Tay, W.T.; Tai, E.S.; Aung, T.; Wong, T.Y. Relationship of Smoking and Cardiovascular Risk Factors with Polypoidal Choroidal Vasculopathy and Age-related Macular Degeneration in Chinese Persons. *Ophthalmology* **2011**, *118*, 846–852. https://doi.org/10.1016/j.ophtha.2010.09.026.
26. Seddon, J.M.; George, S.; Rosner, B. Cigarette Smoking, Fish Consumption, Omega-3 Fatty Acid Intake, and Associations with age-related macular degeneration: The US Twin Study of Age-Related Macular Degeneration. *Arch. Ophthalmol.* **2006**, *124*, 995–1001. https://doi.org/10.1001/archopht.124.7.995.
27. Seddon, J.M.; Cote, J.; Davis, N.; Rosner, B. Progression of Age-Related Macular Degeneration: Association with body mass index, waist circumference, and waist-hip ratio. *Arch. Ophthalmol.* **2003**, *121*, 785–792. https://doi.org/10.1001/archopht.121.6.785.
28. Chen, Y.; Bedell, M.; Zhang, K. Age-related Macular Degeneration: Genetic and Environmental Factors of Disease. *Mol. Interv.* **2010**, *10*, 271–281. https://doi.org/10.1124/mi.10.5.4.
29. Mazué, F.; Delmas, D.; Murillo, G.; Saleiro, D.; Limagne, E.; Latruffe, N. Differential protective effects of red wine polyphenol extracts (RWEs) on colon carcinogenesis. *Food Funct.* **2014**, *5*, 663–670. https://doi.org/10.1039/c3fo60417a.
30. Cornebise, C.; Courtaut, F.; Taillandier-Coindard, M.; Valls-Fonayet, J.; Richard, T.; Monchaud, D.; Aires, V.; Delmas, D. Red Wine Extract Inhibits VEGF Secretion and Its Signaling Pathway in Retinal ARPE-19 Cells to Potentially Disrupt AMD. *Molecules* **2020**, *25*, 5564. https://doi.org/10.3390/molecules25235564.
31. Shen, S.; Kapphahn, R.J.; Zhang, M.; Qian, S.; Montezuma, S.R.; Shang, P.; Ferrington, D.A.; Qu, J. Quantitative Proteomics of Human Retinal Pigment Epithelium Reveals Key Regulators for the Pathogenesis of Age-Related Macular Degeneration. *Int. J. Mol. Sci.* **2023**, *24*, 3252. https://doi.org/10.3390/ijms24043252.
32. Chalons, P.; Courtaut, F.; Limagne, E.; Chalmin, F.; Cantos-Villar, E.; Richard, T.; Auger, C.; Chabert, P.; Schini-Kerth, V.; Ghiringhelli, F.; et al. Red Wine Extract Disrupts Th17 Lymphocyte Differentiation in a Colorectal Cancer Context. *Mol. Nutr. Food Res.* **2020**, *64*, e1901286. https://doi.org/10.1002/mnfr.201901286.
33. Chalons, P.; Amor, S.; Courtaut, F.; Cantos-Villar, E.; Richard, T.; Auger, C.; Chabert, P.; Schni-Kerth, V.; Aires, V.; Delmas, D. Study of Potential Anti-Inflammatory Effects of Red Wine Extract and Resveratrol through a Modulation of Interleukin-1-Beta in Macrophages. *Nutrients* **2018**, *10*, 1856. https://doi.org/10.3390/nu10121856.
34. Chu, A.J. Quarter-Century Explorations of Bioactive Polyphenols: Diverse Health Benefits. *Front Biosci (Landmark Ed)* **2022**, *27*, 134, doi:10.31083/j.fbl2704134.
35. Podhorecka, M.; Skladanowski, A.; Bozko, P. H2AX Phosphorylation: Its Role in DNA Damage Response and Cancer Therapy. *J. Nucleic Acids* **2010**, *2010*, 1–9. https://doi.org/10.4061/2010/920161.
36. Sharma, A.; Singh, K.; Almasan, A. Histone H2AX Phosphorylation: A Marker for DNA Damage. *Methods Mol. Biol.* **2012**, *920*, 613–626. https://doi.org/10.1007/978-1-61779-998-3_40.
37. Aires, V.; Limagne, E.; Cotte, A.K.; Latruffe, N.; Ghiringhelli, F.; Delmas, D. Resveratrol metabolites inhibit human metastatic colon cancer cells progression and synergize with chemotherapeutic drugs to induce cell death. *Mol. Nutr. Food Res.* **2013**, *57*, 1170–1181. https://doi.org/10.1002/mnfr.201200766.
38. Colin, D.J.; Limagne, E.; Ragot, K.; Lizard, G.; Ghiringhelli, F.; Solary, E.; Chauffert, B.; Latruffe, N.; Delmas, D. The role of reactive oxygen species and subsequent DNA-damage response in the emergence of resistance towards resveratrol in colon cancer models. *Cell Death Dis.* **2014**, *5*, e1533. https://doi.org/10.1038/cddis.2014.486.

39. Marazita, M.C.; Dugour, A.; Marquioni-Ramella, M.D.; Figueroa, J.M.; Suburo, A.M. Oxidative stress-induced premature senescence dysregulates VEGF and CFH expression in retinal pigment epithelial cells: Implications for Age-related Macular Degeneration. *Redox Biol.* **2016**, *7*, 78–87. https://doi.org/10.1016/j.redox.2015.11.011.
40. Reinisalo, M.; Karlund, A.; Koskela, A.; Kaarniranta, K.; Karjalainen, R.O. Polyphenol Stilbenes: Molecular Mechanisms of Defence against Oxidative Stress and Aging-Related Diseases. *Oxidative Med. Cell. Longev.* **2015**, *2015*, 340520. https://doi.org/10.1155/2015/340520.
41. Chalam, K.V.; Grover, S.; Sambhav, K.; Balaiya, S.; Murthy, R.K. Aqueous Interleukin-6 Levels Are Superior to Vascular Endothelial Growth Factor in Predicting Therapeutic Response to Bevacizumab in Age-Related Macular Degeneration. *J. Ophthalmol.* **2014**, *2014*, 502174. https://doi.org/10.1155/2014/502174.
42. Jonas, J.B.; Tao, Y.; Neumaier, M.; Findeisen, P. Cytokine concentration in aqueous humour of eyes with exudative age-related macular degeneration. *Acta Ophthalmol.* **2012**, *90*, e381–e388. https://doi.org/10.1111/j.1755-3768.2012.02414.x.
43. Roh, M.I.; Kim, H.S.; Song, J.H.; Lim, J.B.; Koh, H.J.; Kwon, O.W. Concentration of cytokines in the aqueous humor of patients with naive, recurrent and regressed CNV associated with amd after bevacizumab treatment. *Retina* **2009**, *29*, 523–529. https://doi.org/10.1097/iae.0b013e318195cb15.
44. Tan, W.; Zou, J.; Yoshida, S.; Jiang, B.; Zhou, Y. The Role of Inflammation in Age-Related Macular Degeneration. *Int. J. Biol. Sci.* **2020**, *16*, 2989–3001. https://doi.org/10.7150/ijbs.49890.
45. Jarrett, S.G.; Boulton, M.E. Consequences of oxidative stress in age-related macular degeneration. *Mol. Aspects Med.* **2012**, *33*, 399-417, doi:S0098-2997(12)00038-6 [pii]
46. Cai, J.; Nelson, K.C.; Wu, M.; Sternberg, P., Jr.; Jones, D.P. Oxidative damage and protection of the RPE. *Prog. Retin. Eye Res.* **2000**, *19*, 205–221. https://doi.org/10.1016/s1350-9462(99)00009-9.
47. Age-Related Eye Disease Study Research Group. A randomized, placebo-controlled, clinical trial of high-dose supplementation with vitamins C and E, beta carotene, and zinc for age-related macular degeneration and vision loss: AREDS report no. 8. *Arch. Ophthalmol.* **2001**, *119*, 1417–1436. https://doi.org/10.1001/archopht.119.10.1417
48. Courtaut, F.; Aires, V.; Acar, N.; Bretillon, L.; Guerrera, I.C.; Chhuon, C.; de Barros, J.-P.P.; Olmiere, C.; Delmas, D. RESVEGA, a Nutraceutical Omega-3/Resveratrol Supplementation, Reduces Angiogenesis in a Preclinical Mouse Model of Choroidal Neovascularization. *Int. J. Mol. Sci.* **2021**, *22*, 11023. https://doi.org/10.3390/ijms222011023.
49. Chang, Y.-Y.; Lee, Y.-J.; Hsu, M.-Y.; Wang, M.; Tsou, S.-C.; Chen, C.-C.; Lin, J.-A.; Hsiao, Y.-P.; Lin, H.-W. Protective Effect of Quercetin on Sodium Iodate-Induced Retinal Apoptosis through the Reactive Oxygen Species-Mediated Mitochondrion-Dependent Pathway. *Int. J. Mol. Sci.* **2021**, *22*, 4056. https://doi.org/10.3390/ijms22084056.
50. Shao, Y.; Yu, H.; Yang, Y.; Li, M.; Hang, L.; Xu, X. A Solid Dispersion of Quercetin Shows Enhanced Nrf2 Activation and Protective Effects against Oxidative Injury in a Mouse Model of Dry Age-Related Macular Degeneration. *Oxidative Med. Cell. Longev.* **2019**, *2019*, 479571. https://doi.org/10.1155/2019/1479571.
51. Mansoor, S.; Gupta, N.; Luczy-Bachman, G.; Limb, G.A.; Kuppermann, B.D.; Kenney, M.C. Protective effects of memantine and epicatechin on catechol-induced toxicity on Müller cells in vitro. *Toxicology* **2010**, *271*, 107–114. https://doi.org/10.1016/j.tox.2010.03.013.
52. Ni, T.; Yang, W.; Xing, Y. Protective effects of delphinidin against H2O2–induced oxidative injuries in human retinal pigment epithelial cells. *Biosci. Rep.* **2019**, *39*, BSR20190689. https://doi.org/10.1042/bsr20190689.

53. Wang, Y.; Huo, Y.; Zhao, L.; Lu, F.; Wang, O.; Yang, X.; Ji, B.; Zhou, F. Cyanidin-3-glucoside and its phenolic acid metabolites attenuate visible light-induced retinal degeneration in vivo via activation of Nrf2/HO-1 pathway and NF-κB suppression. *Mol. Nutr. Food Res.* **2016**, *60*, 1564–1577. https://doi.org/10.1002/mnfr.201501048.
54. Dabrowska, A.; Zajac, M.; Bednarczyk, P.; Lukasiak, A. Effect of Quercetin on mitoBK$_{Ca}$ Channel and Mitochondrial Function in Human Bronchial Epithelial Cells Exposed to Particulate Matter. *Int. J. Mol. Sci.* **2022**, *24*, 638. https://doi.org/10.3390/ijms24010638.
55. Gherardi, G.; Corbioli, G.; Ruzza, F.; Rizzuto, R. CoQ_{10} and Resveratrol Effects to Ameliorate Aged-Related Mitochondrial Dysfunctions. *Nutrients* **2022**, *14*, 4326. https://doi.org/10.3390/nu14204326.
56. Sheu, J.-N.; Liao, W.-C.; Wu, U.-I.; Shyu, L.-Y.; Mai, F.-D.; Chen, L.-Y.; Chen, M.-J.; Youn, S.-C.; Chang, H.-M. Resveratrol suppresses calcium-mediated microglial activation and rescues hippocampal neurons of adult rats following acute bacterial meningitis. *Comp. Immunol. Microbiol. Infect. Dis.* **2013**, *36*, 137–148. https://doi.org/10.1016/j.cimid.2012.11.002.
57. Sheu, S.-J.; Liu, N.-C.; Ou, C.-C.; Bee, Y.-S.; Chen, S.-C.; Lin, H.-C.; Chan, J.Y.H. Resveratrol Stimulates Mitochondrial Bioenergetics to Protect Retinal Pigment Epithelial Cells From Oxidative Damage. *Investig. Opthalmol. Vis. Sci.* **2013**, *54*, 6426–6438. https://doi.org/10.1167/iovs.13-12024.
58. Ramata-Stunda, A.; Petriņa, Z.; Valkovska, V.; Borodušķis, M.; Gibnere, L.; Gurkovska, E.; Nikolajeva, V. Synergistic Effect of Polyphenol-Rich Complex of Plant and Green Propolis Extracts with Antibiotics against Respiratory Infections Causing Bacteria. *Antibiotics* **2022**, *11*, 160. https://doi.org/10.3390/antibiotics11020160.
59. Zhang, L.; McClements, D.J.; Wei, Z.; Wang, G.; Liu, X.; Liu, F. Delivery of synergistic polyphenol combinations using biopolymer-based systems: Advances in physicochemical properties, stability and bioavailability. *Crit. Rev. Food Sci. Nutr.* **2020**, *60*, 2083–2097. https://doi.org/10.1080/10408398.2019.1630358.
60. Pacifici, F.; Salimei, C.; Pastore, D.; Malatesta, G.; Ricordi, C.; Donadel, G.; Bellia, A.; Rovella, V.; Tafani, M.; Garaci, E.; et al. The Protective Effect of a Unique Mix of Polyphenols and Micronutrients against Neurodegeneration Induced by an In Vitro Model of Parkinson's Disease. *Int. J. Mol. Sci.* **2022**, *23*, 3110. https://doi.org/10.3390/ijms23063110.
61. Li, H.; Christman, L.M.; Li, R.; Gu, L. Synergic interactions between polyphenols and gut microbiota in mitigating inflammatory bowel diseases. *Food Funct.* **2020**, *11*, 4878–4891. https://doi.org/10.1039/d0fo00713g.
62. Patra, S.; Pradhan, B.; Nayak, R.; Behera, C.; Das, S.; Patra, S.K.; Efferth, T.; Jena, M.; Bhutia, S.K. Dietary polyphenols in chemoprevention and synergistic effect in cancer: Clinical evidences and molecular mechanisms of action. *Phytomedicine* **2021**, *90*, 153554. https://doi.org/10.1016/j.phymed.2021.153554.
63. Aires, V.; Brassart, B.; Carlier, A.; Scagliarini, A.; Mandard, S.; Limagne, E.; Solary, E.; Martiny, L.; Tarpin, M.; Delmas, D. A role for peroxisome proliferator-activated receptor gamma in resveratrol-induced colon cancer cell apoptosis. *Mol. Nutr. Food Res.* **2014**, *58*, 1785–1794. https://doi.org/10.1002/mnfr.201300962.
64. Colin, D.; Gimazane, A.; Lizard, G.; Izard, J.-C.; Solary, E.; Latruffe, N.; Delmas, D. Effects of resveratrol analogs on cell cycle progression, cell cycle associated proteins and 5fluoro-uracil sensitivity in human derived colon cancer cells. *Int. J. Cancer* **2009**, *124*, 2780–2788. https://doi.org/10.1002/ijc.24264.
65. Walter, A.; Etienne-Selloum, N.; Brasse, D.; Khallouf, H.; Bronner, C.; Rio, M.-C.; Beretz, A.; Schini-Kerth, V.B. Intake of grape-derived polyphenols reduces C26 tumor growth by

inhibiting angiogenesis and inducing apoptosis. *FASEB J.* **2010**, *24*, 3360–3369. https://doi.org/10.1096/fj.09-149419.
66. Sun, H.; Zhang, Y.; Shen, Y.; Zhu, Y.; Wang, H.; Xu, Z. Inhibitory Effects of Red Wine on Lipid Oxidation in Fish Oil Emulsion and Angiogenesis in Zebrafish Embryo. *J. Food Sci.* **2017**, *82*, 781–786. https://doi.org/10.1111/1750-3841.13651.
67. Sato, T.; Takeuchi, M.; Karasawa, Y.; Enoki, T.; Ito, M. Intraocular inflammatory cytokines in patients with neovascular age-related macular degeneration before and after initiation of intravitreal injection of anti-VEGF inhibitor. *Sci. Rep.* **2018**, *8*, 1–10. https://doi.org/10.1038/s41598-018-19594-6.
68. de Oliveira Dias, J.R.; Rodrigues, E.B.; Maia, M.; Magalhães, O., Jr.; Penha, F.M.; Farah, M.E. Cytokines in neovascular age-related macular degeneration: Fundamentals of targeted combination therapy. *Br. J. Ophthalmol.* **2011**, *95*, 1631–1637. https://doi.org/10.1136/bjo.2010.186361.
69. Johnson, L.V.; Ozaki, S.; Staples, M.K.; Erickson, P.A.; Anderson, D.H. A Potential Role for Immune Complex Pathogenesis in Drusen Formation. *Exp. Eye Res.* **2000**, *70*, 441–449. https://doi.org/10.1006/exer.1999.0798.
70. Patel, K.R.; Scott, E.; Brown, V.A.; Gescher, A.J.; Steward, W.P.; Brown, K. Clinical trials of resveratrol. *Ann. N. Y. Acad. Sci.* **2011**, *1215*, 161–169. https://doi.org/10.1111/j.1749-6632.2010.05853.x.
71. Andreadi, C.; Britton, R.G.; Patel, K.R.; Brown, K. Resveratrol-sulfates provide an intracellular reservoir for generation of parent resveratrol, which induces autophagy in cancer cells. *Autophagy* **2014**, *10*, 524–525. https://doi.org/10.4161/auto.27593.
72. Patel, K.R.; Brown, V.A.; Jones, D.J.; Britton, R.G.; Hemingway, D.; Miller, A.S.; West, K.P.; Booth, T.D.; Perloff, M.; Crowell, J.A.; et al. Clinical Pharmacology of Resveratrol and Its Metabolites in Colorectal Cancer Patients. *Cancer Res.* **2010**, *70*, 7392–7399. https://doi.org/10.1158/0008-5472.can-10-2027.

Supplementary Figure S1

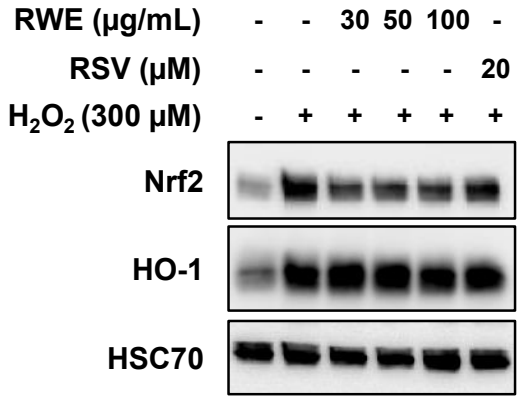

Supplementary Figure S1. Effects of RWE on H_2O_2-induced protein expression of Nrf2 transcription factor and Heme-Oxygenase 1 (HO-1) in ARPE-19. Cells were treated with increasing concentrations of RWE (30, 50, 100 µg/mL), RSV (20 µM) or vehicle alone (0.1% ethanol 70%) for 24 h, and were thereafter treated for 6 h with H_2O_2 (300 µM). Immunoblots of Nrf2 and HO-1 are representative of three independent experiments. HSC70 was used as an internal loading control.

Supplementary Figure S2

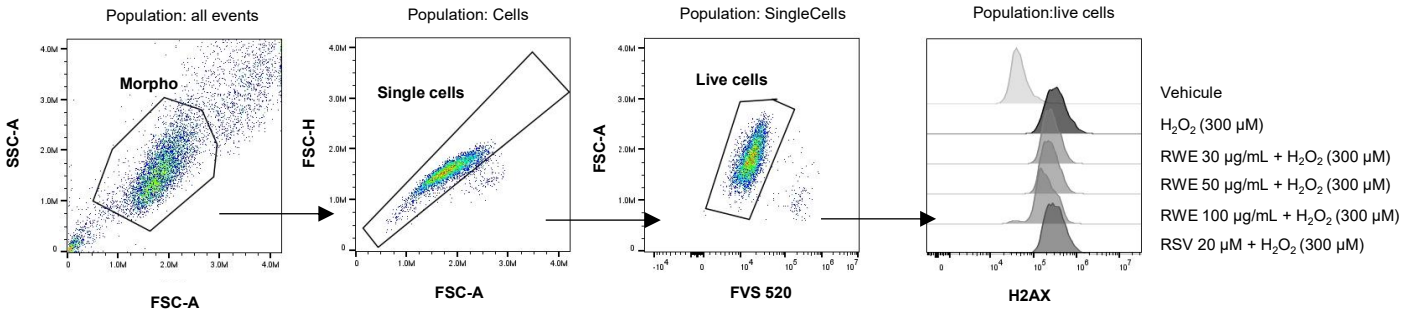

Supplementary Figure S2. Flow cytometry gating Strategies. Live cells Were stain withe Fixable viability staining (FVS 520). Gray histogram represents H2AX staining in ARPE-19 after treatment.

D. Résultats complémentaires

D.1. Caractère anti-angiogénique du RWE

Les résultats des deux précédents articles montrent que RWE inhibe fortement la sécrétion de VEGF-A en condition basale, mais aussi lorsqu'elle est induite par VEGF recombinant (rVEGF) ou par un stress oxydant (H_2O_2). Cette inhibition de sécrétion est associée à une inhibition de l'expression de l'ARNm de VEGF-A lors d'une induction par rVEGF et par H_2O_2. Dans les deux cas, **RWE inhibe de manière dose dépendante l'expression de l'ARNm de VEGF-A** (Figure 24A,B).

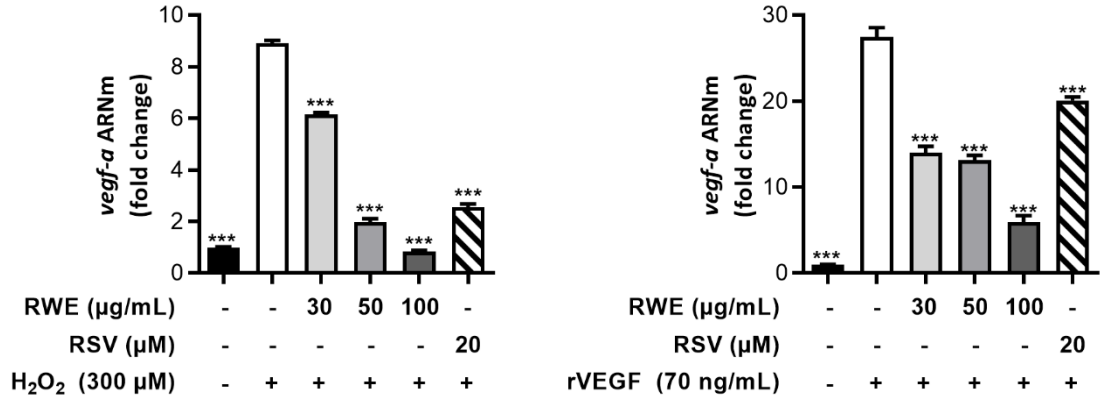

Figure 24. L'extrait sec de vin rouge altère l'expression de l'ARNm de VEGF-A induit dans les cellules ARPE-19

Les cellules ont été traitées avec différentes concentrations d'extrait sec de vin rouge (*Red wine extract* : RWE ; 30; 50; 100 µg/mL) ou de resvératrol (RSV, 20 µM). Après 24 h, les cellules ont été traitées durant 6 h avec **(A)** du peroxyde d'hydrogène (H_2O_2 ; 300 µM), **(B)** VEGF recombinant (rVEGF, 70 ng/mL). L'expression d'ARNm de VEGF-A a été mesurée par qPCR. Le gène L27 a été utilisé comme référence. Les résultats sont exprimés en valeurs moyennes rapportées aux cellules contrôles (traitées avec le solvant) ± SEM de trois expériences indépendantes (u.a. : unité arbitraire). Les *p*-values ont été calculées par un test ANOVA suivi d'un test de Dunnett. ** p<0,01; *** p<0,0001 (valeurs comparées aux valeurs des cellules traitées avec H_2O_2 , rVEGF).

Afin d'étudier le mécanisme d'action de RWE lors d'une induction de la sécrétion de VEGF-A par le rVEGF, l'expression protéique ainsi que la phosphorylation du récepteur VEGF-R2 ont été mesurées par immunobling. Ainsi, nous pouvons observer que le rVEGF semble induire une augmentation de l'expression de VEGF-R2 ainsi que de sa phosphorylation sur la tyrosine 1054 alors que la tyrosine 951 n'a pas été impactée. Nous pouvons observer que le **RWE semble être capable d'inhiber l'expression de VEGF-R2 ainsi que sa phosphorylation**

sur la tyrosine 1054 (Figure 25). Cependant, des expériences supplémentaires sont nécessaires afin de confirmer et de compléter ces résultats.

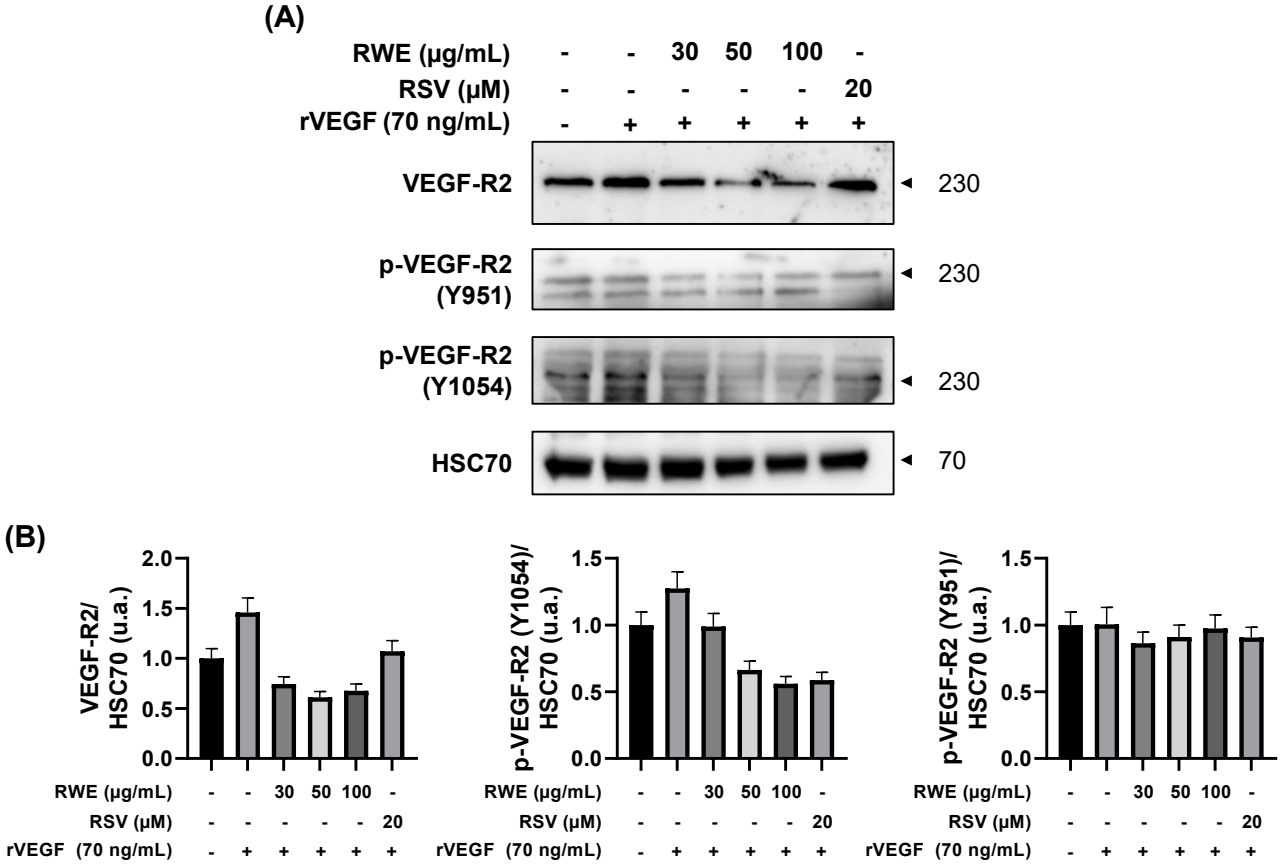

Figure 25. L'extrait sec de vin rouge module la phosphorylation du récepteur VEGF-R2 induite par rVEGF

Les cellules ARPE-19 ont été traitées avec différentes concentrations d'extrait sec de vin rouge (*Red wine extract* : RWE ; 30; 50; 100 µg/mL) ou de resvératrol (RSV, 20 µM). Après 24 h, les cellules ont été traitées durant 6 h avec du VEGF recombinant (rVEGF, 70 ng/mL). Les expressions protéiques ont été mesurées par immunoblotting. **(A)** L'image est représentative de 2 expériences indépendantes. **(B)** Les expressions des protéines ont été normalisées par rapport au contrôle de charge HSC70 et sont exprimées en unité arbitraire (u.a.). Les valeurs sont exprimées en valeur moyenne rapportée au contrôle ± SEM de 2 expériences indépendantes.

Dans la physiopathologie de la DMLA, l'angiogenèse et l'inflammation sont deux processus intrinsèquement liés. En effet, l'induction de l'inflammation dans les cellules de l'EPR peut induire la sécrétion du VEGF-A afin de participer à la formation de nouveaux vaisseaux permettant le recrutement de cellules immunitaires circulantes. Ainsi, le **LPS** semble induire fortement **l'expression d'ARNm ainsi que la sécrétion de VEGF-A** dans les cellules ARPE-19

(Figure 26). Le **RWE semble prévenir de manière dose dépendante l'induction de l'expression d'ARNm ainsi que la sécrétion de VEGF-A** (Figure 26).

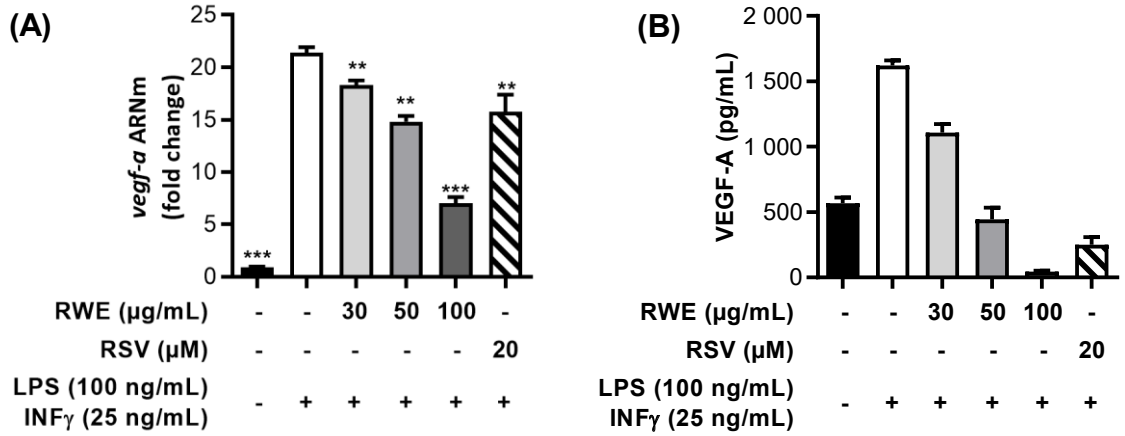

Figure 26. L'extrait sec de vin rouge semble inhiber la sécrétion de VEGF-A induite lors d'une inflammation dans les cellules ARPE-19

Les cellules ont été traitées avec différentes concentrations d'extrait sec de vin rouge (*Red wine extract* : RWE , 30; 50; 100 µg/mL) ou de resvératrol (RSV, 20 µM). Après 24 h, elles ont été traitées durant 6 heures avec du LPS (100 ng/mL) et de l'INFγ (25 ng/mL). **(A)** L'expression d'ARNm de VEGF a été mesurée par qPCR. Le gène L27 a été utilisé comme référence. Les résultats sont exprimés en pourcentages moyens rapportés aux cellules contrôles (traitées avec le solvant) ± SEM de deux expériences indépendantes (u.a. : unité arbitraire). **(B)** la sécrétion de VEGF-A a été mesurée par ELISA. Les résultats sont exprimés en valeurs moyennes ± SEM de trois expériences indépendantes.

D.2. Caractère anti-inflammatoire du RWE dans les cellules de l'EPR

Il est maintenant bien avéré que l'inflammation et le stress oxydant sont deux processus intrinsèquement liés dans l'initiation de la DMLA. Ainsi, la production d'ERO peut induire des dommages contribuant aux processus inflammatoires. L'étude du caractère anti-inflammatoire du RWE sur les cellules de l'EPR (ARPE-19) a permis de montrer qu'il était capable d'inhiber la sécrétion de cytokines pro-inflammatoires (IL-6 et IL-8) lors d'une induction par stress oxydant (H_2O_2) (Cornebise et al., 2023). Quand est-il lors d'un stress oxydant généré par l'AAPH ? Afin d'étudier l'impact de l'AAPH sur l'inflammation, une concentration d'AAPH induisant un fort stress oxydant (cf figure 2F de l'article Cornebise et al., 2023) à savoir 600 µM d'AAPH a été utilisée. **L'AAPH n'impacte pas la sécrétion de cytokines pro-inflammatoires (IL-6 et IL-8)** avec les doses et les temps de traitements utilisés (Figure 27).

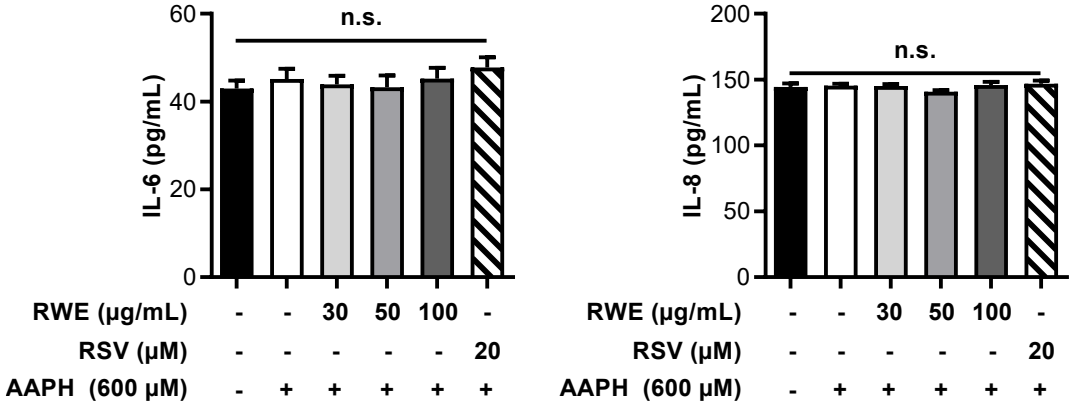

Figure 27. Le stress oxydant induit par AAPH n'altère pas la sécrétion de cytokines pro-inflammatoires dans les cellules ARPE-19

Les cellules ARPE-19 ont été traitées durant 24 h avec différentes concentrations d'extrait sec de vin rouge (*Red wine extract* : RWE, 30 ; 50 ; 100 µg/mL) ou 20 µM de RSV. A la suite de ce traitement, les cellules ont été incubées 6 h avec 600 µM d'AAPH. A la fin des traitements, les sécrétions d'interleukines 6 et 8 (IL-6 et IL-8) ont été mesurées par ELISA. Les résultats sont exprimés en valeurs moyennes ± SEM de trois expériences indépendantes (u.a. : unité arbitraire). Les *p*-values ont été calculées par un test ANOVA suivi d'un test de Dunnett. *p*-value ≤ 0,05 a été considérée comme significative, n.s. = non significatif (valeurs comparées aux valeurs des cellules traitées avec AAPH).

De plus, les résultats montrés dans l'article précédent montrent que l'extrait sec de vin rouge prévient la sécrétion de l'IL-6 et de l'IL-8 lorsqu'elles sont induites par du peroxyde d'hydrogène ou par du LPS (cf figure 6 de l'article). En outre, l'inhibition de la sécrétion de ces cytokines RWE altère aussi l'expression de leur ARNm (Figure 28). En effet, **RWE inhibe de manière dose dépendante l'expression d'IL-6 et d'IL-8** induite par du peroxyde d'hydrogène (Figure 28A). La concentration la plus élevée de RWE (100 µg/ml) permet d'inhiber l'expression d'IL-6 et d'IL-8 et ce à un niveau inférieur aux taux basaux (H_2O_2). De plus, RWE inhibe aussi l'expression d'une autre chimiokine pro-inflammatoire, la chimiotactique monocytaire-1 (MCP-1), qui est notamment impliquée dans le recrutement des macrophages circulants. Ainsi, RWE inhibe l'expression d'ARNm de cette dernière de manière dose dépendante. Tout comme pour l'expression de l'IL-6 et de l'IL-8, la concentration la plus élevée de **RWE est capable de diminuer l'expression de MCP-1** à un taux inférieur aux taux basaux. Si l'on compare l'effet du RSV seul à celui du RWE, on remarque qu'il inhibe fortement l'expression de MCP-1. Et bien qu'il inhibe significativement l'expression d'IL-6 et d'IL-8, son effet est moins important que ceux du RWE aux doses les plus élevées. Ces résultats sont en

accord avec ceux de l'article où l'on observe que l'inhibition de la sécrétion d'IL-6 et d'IL-8 par le RSV seul est moins importante que celle induite par RWE.

De manière similaire, **RWE inhibe l'expression d'IL-6, IL-8 et MCP-1 lorsqu'elles sont induites par LPS** (Figure 28C). RWE inhibe l'expression d'IL-6, même à la concentration la plus faible, RWE permet le retour à un taux basal d'ARNm d'IL-6. De plus, il inhibe de manière dose dépendante l'expression d'IL-8 et de MCP-1 (Figure 28C). Comme précédemment, le RSV seul inhibe l'expression de ces cytokines, mais son effet reste moins important que celui du RWE.

De plus, en lien avec les résultats de la Figure 27, **AAPH n'impacte pas l'expression d'IL-6, IL-8 et MCP-1** (Figure 28B).

Ces résultats suggèrent que **RWE pourrait réduire l'inflammation lorsqu'elle est induite dans un contexte pathologique tel que la DMLA**. De plus, si l'on compare l'effet du RSV seul à celui du RWE, on peut penser que certains polyphénols autres que le RSV peuvent être bénéfiques ou bien dûs à sa vaste diversité polyphénolique, certains composés agissent en synergie.

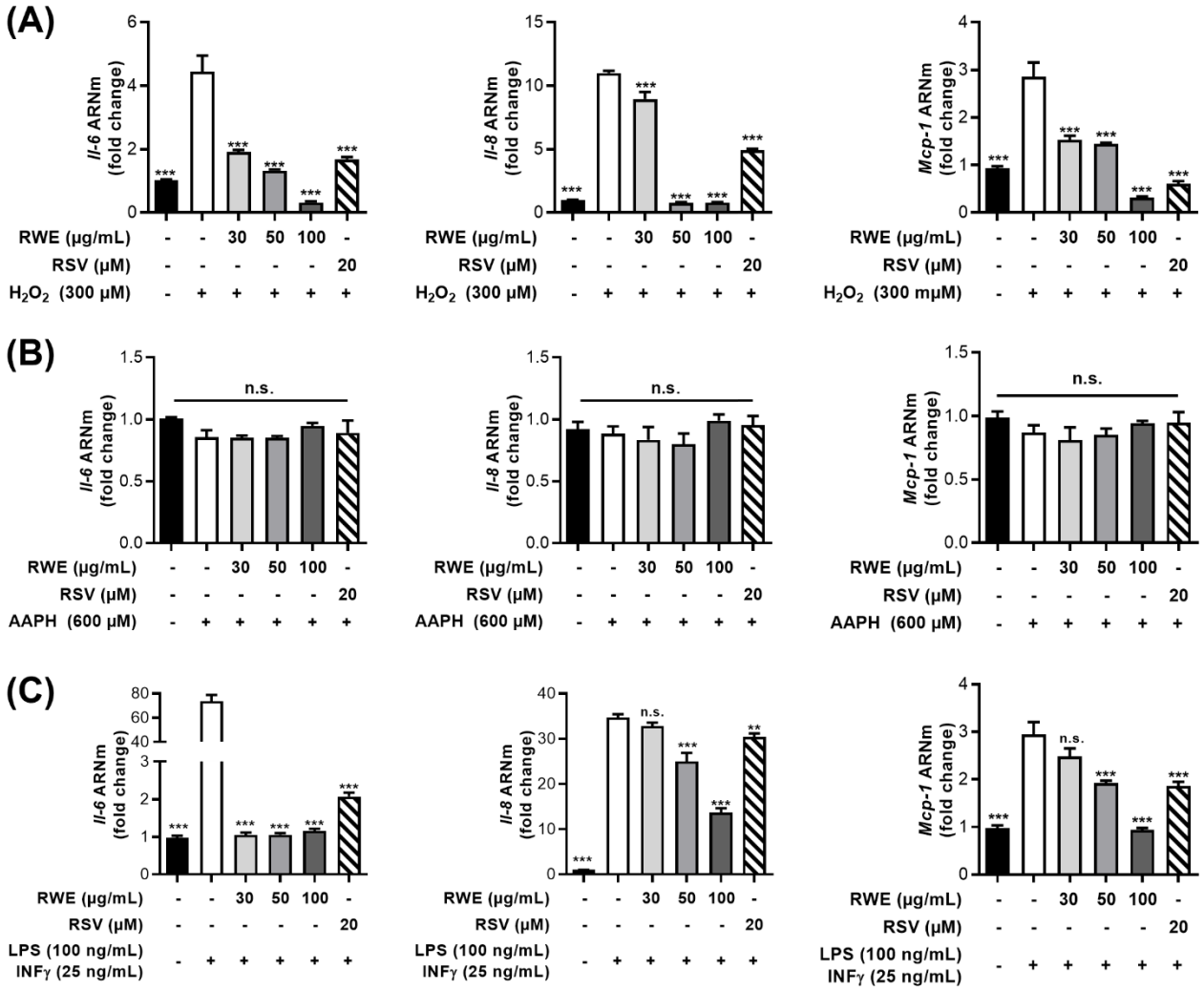

Figure 28. L'extrait sec de vin rouge prévient l'inflammation dans les cellules ARPE-19

Les cellules ont été traitées avec différentes concentrations d'extrait sec de vin rouge (*Red wine extract* : RWE ; 30; 50; 100 µg/mL) ou de resvératrol (RSV, 20 µM). Après 24 h, les cellules ont été traitées avec **(A)** du peroxyde d'hydrogène (H_2O_2 ; 300 µM), **(B)** AAPH (600 µM) ou **(C)** LPS (100 ng/mL) et INFγ (25 ng/mL). Après 6h de traitement, l'expression d'ARNm d'IL-6, IL-8 et MCP-1 (Chimiotactiques monocytaire-1) ont été mesurées par qPCR. Le gène L27 a été utilisé comme référence. Les résultats sont exprimés en pourcentages moyens rapportés aux cellules contrôles (traitées avec le solvant) ± SEM de trois expériences indépendantes (u.a. : unité arbitraire). Les *p*-values ont été calculées par un test ANOVA suivi d'un test de Dunnett. *p*-value ≤ 0,05 a été considérée comme significative, n.s. = non significatif; **p*<0,05; ***p*<0,01; *** *p*<0,0001 (valeurs comparées aux valeurs des cellules traitées avec H_2O_2, AAPH ou LPS et l'INFγ).

Au sein des cellules de l'EPR, l'inflammation est principalement régulée par la voie de Nf κB. En effet, les ERO peuvent induire cette voie et ainsi augmenter la production et la sécrétion d'interleukines pro-inflammatoires (IL-6 et IL-8). Nous pouvons voir Figure 29 que lorsque les cellules ARPE-19 sont traitées durant 6 h avec 300 µM d'**H_2O_2, l'expression de p65 semble**

être fortement induite, cependant, nous n'observons pas de différence de l'expression de p50. En accord avec les résultats précédents, **RWE semble pouvoir réduire de manière dose dépendante la surexpression de p65**. Ainsi, il semblerait que RWE puisse agir sur des protéines clés impliquées dans les voies régulant ces cytokines. Cependant, des expériences supplémentaires sont nécessaires afin de confirmer et de compléter ces résultats.

Figure 29. RWE semble inhiber l'expression de p65 induite par un stress oxydant dans les cellules ARPE-19

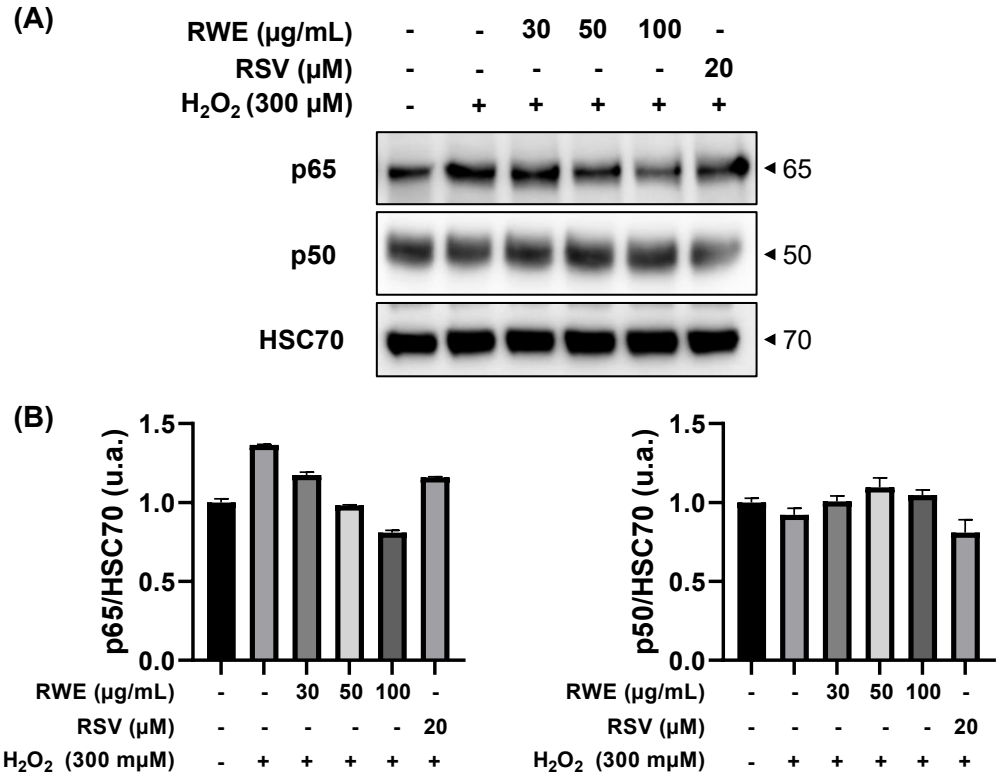

Les cellules ont été traitées avec différentes concentrations d'extrait sec de vin rouge (*Red wine extract* : RWE ; 30; 50; 100 µg/mL) ou de resvératrol (RSV, 20 µM). Après 24 h, les cellules ont été traitées avec du peroxyde d'hydrogène (H_2O_2 ; 300 µM). **(A)** L'image est représentative de 2 expériences indépendantes. **(B)** Les expressions des protéines ont été normalisées par rapport au contrôle de charge HSC70 et sont exprimées en unité arbitraire (u.a.). Les valeurs sont exprimées en valeur moyenne rapportée au contrôle ± SEM de 2 expériences indépendantes.

D.3. Caractère anti-inflammatoire du RWE dans les macrophages pro-inflammatoires

Les cellules de l'EPR ne sont pas les seules cellules influant sur l'inflammation rétinienne. En effet, les patients atteints de DMLA présentent une forte **accumulation de macrophages**.

Ainsi, les précédents résultats (figure 7 de l'article Cornebise et al., 2023) montrent que RWE inhibe la sécrétion de cytokines pro-inflammatoires (IL-6 et IL-8) dans les macrophages humains pro-inflammatoires. Afin de compléter cette étude des effets bénéfiques du RWE sur les cellules immunitaires, l'innocuité de l'extrait et du RSV seul a été vérifiée. Après 24 h de traitement, aucun impact n'a été observé sur la viabilité cellulaire (Figure 30).

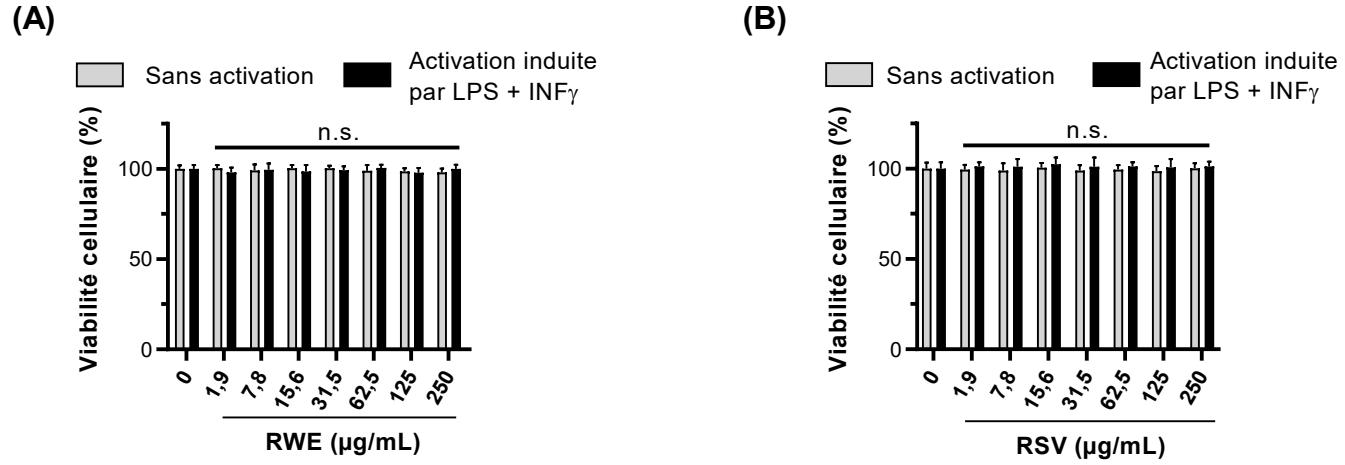

Figure 30. Mesure de l'innocuité de l'extrait sec de vin rouge (RWE) et du resvératrol (RSV) sur des monocytes humains

Des monocytes humains ont été isolés à partir de cellules mononucléées du sang périphérique (PBMC) provenant de sang de patients sains. Après 6 jours de cultures, les monocytes ont été activés ou non en macrophages pro-inflammatoires avec du LPS (10 ng/mL) et de l'Interféron γ (INF γ 25 ng/mL) durant 4h. A la fin du traitement, les cellules ont été traitées avec des concentrations croissantes (0; 1,9; 7,8; 15,6; 31,5; 62,5; 125; 250 µM) de **(A)** extrait sec de vin rouge (RWE) ou de **(B)** resvératrol (RSV) durant 20 h supplémentaires. Les résultats sont exprimés en pourcentages moyens rapportés aux cellules contrôles (traitées avec le solvant) ± SEM de trois expériences indépendantes. Les *p*-values ont été calculées par un test ANOVA suivi d'un test de Dunnett. *p*-value ≤ 0,05 a été considérée comme significative, n.s. = non significatif.

Comme décrit précédemment, le RWE peut prévenir la sécrétion de cytokine pro-inflammatoire, IL-6 et IL-8 (cf figure 7 de l'article Cornebise et al., 2023). De plus, il prévient aussi **l'expression d'ARNm** de ces cytokines ainsi que l'expression d'ARNm de MCP-1 et ce de manière dose dépendante (Figure 31). De plus, si l'on compare son effet à celui du RSV seul on constate qu'il réduit de manière plus importante l'expression de ces cytokines pro-inflammatoires. De plus, RWE **augmente l'expression d'ARNm de l'interleukine anti-inflammatoire (IL-10)** (Figure 31). En effet, l'activation des macrophages en phénotype pro-inflammatoire induit une diminution significative d'IL-10. RWE permet d'augmenter de manière dose dépendante cette expression. Le RSV seul n'est pas capable d'altérer l'expression d'ARNm d'IL-10. De plus, si l'on regarde un des marqueurs des macrophages anti-

inflammatoires CD206, on observe que l'activation par le LPS diminue drastiquement son expression et que RWE est capable de prévenir cette diminution (Figure 31). Ainsi, **il semblerait que RWE puisse non seulement prévenir l'augmentation de l'expression de cytokines pro-inflammatoire, mais aussi d'impacter des marqueurs anti-inflammatoires**. Ainsi, un prétraitement avec du RWE pourrait **prévenir** le phénotype pro-inflammatoire des macrophages.

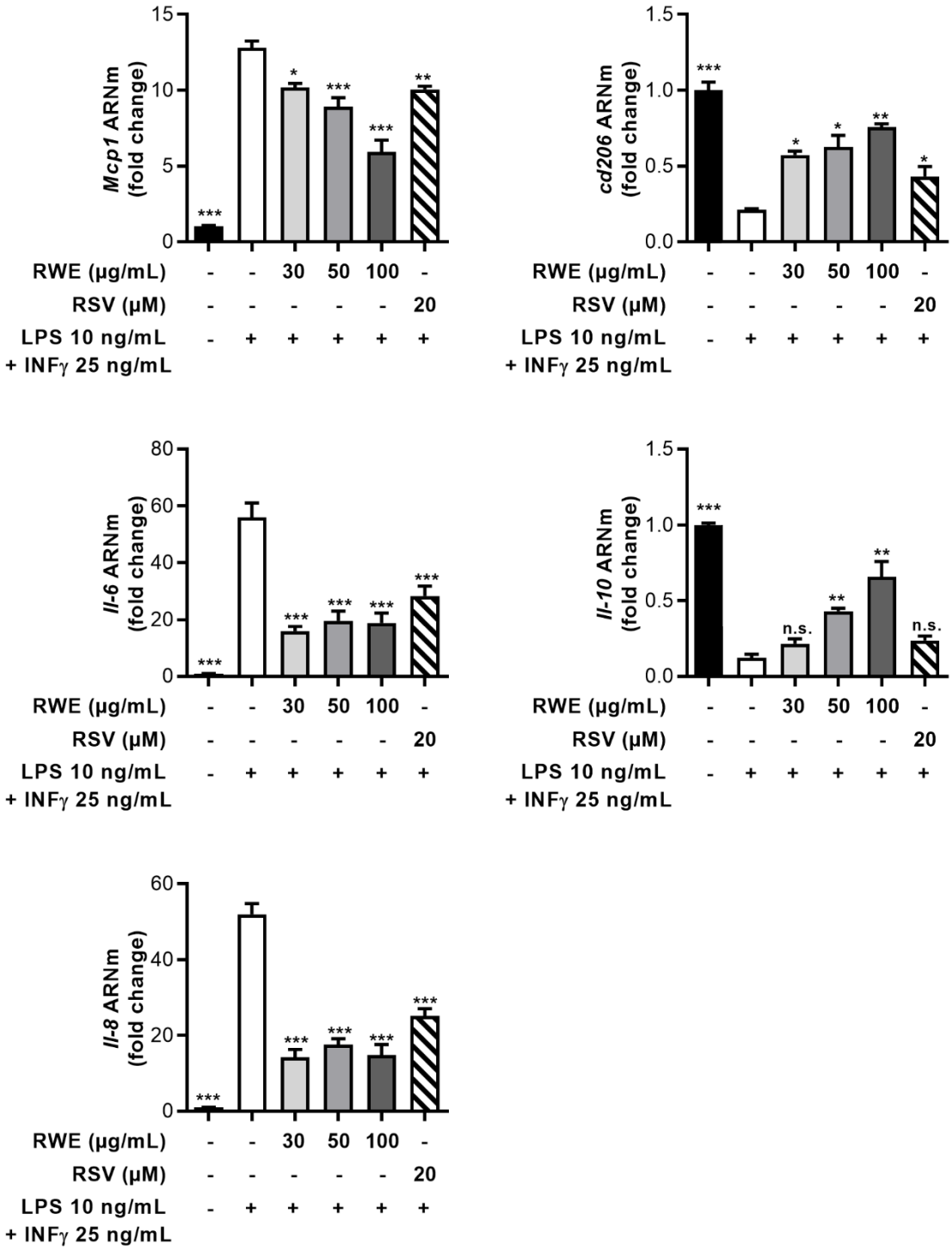

Figure 31. L'extrait sec de vin rouge prévient l'inflammation dans les macrophages pro-inflammatoires.

Des monocytes humains ont été isolés à partir de cellules mononucléées du sang périphérique (PBMC) provenant de sang de patients sains. Après 6 jours de cultures, les cellules ont été traitées avec différentes concentrations d'extrait sec de vin rouge (Red wine extract : RWE ; 30; 50; 100 µg/mL) ou de resvératrol (RSV, 20 µM). Après 24 h, les cellules ont été traitées avec du LPS (10 ng/mL) et de l'INFγ (25 ng/mL). Après 4h de stimulation, des différentes concentrations d'extrait sec de vin rouge (Red wine extract : RWE ; 30; 50; 100 µg/mL) ou de resvératrol (RSV, 20 µM) ont été ajouter aux milieux de culture. A la fin des traitements, l'expression d'ARNm a été mesurée par qPCR. Le gène L27 a été utilisé comme référence. Les résultats sont exprimés en valeurs moyennes rapportées aux

cellules contrôles (traitées avec le solvant) ± SEM de trois expériences indépendantes. Les *p*-values ont été calculées par un test ANOVA suivi d'un test de Dunnett. *p*-value ≤ 0,05 a été considérée comme significative, n.s. = non significatif;** $p<0,01$; *** $p<0,0001$ valeurs comparées aux valeurs des cellules traitées avec le LPS et l'INFγ.

Par la suite, nous nous sommes demandé si l'extrait sec de vin rouge était capable **d'inhiber** le phénotype pro-inflammatoire des macrophages ? C'est-à-dire est-ce que le RWE pourrait être efficace comme **traitement curatif** contre une inflammation déjà installée. Ainsi, les macrophages ont été dans un premier temps activés avec du LPS et de l'INFγ afin d'induire un phénotype pro-inflammatoire. Puis différentes concentrations de RWE ou de RSV ont été rajoutées dans le milieu de culture pour 24 h supplémentaires. A la fin du traitement, la sécrétion ainsi que l'expression de cytokines pro- et anti-inflammatoires ont été mesurées. **RWE inhibe de manière dose dépendante la sécrétion d'IL-6 et d'IL-8** (Figure 32A). Cette inhibition est associée à une **inhibition de l'expression d'ARNm d'IL-6, d'IL-8 ainsi que MCP-1**. Si l'on regarde IL-10, une cytokine anti-inflammatoire, on constate que ni RWE ni le RSV seul n'impactent son expression. De plus, le marqueur CD206 n'est pas non plus impacté par RWE et RSV. Ainsi, **il semblerait que RWE puisse limiter l'inflammation *via* la diminution de cytokines pro-inflammatoires. Cependant, il ne semble pas être capable d'induire des cytokines anti-inflammatoires lorsque les macrophages sont déjà activés en phénotype pro-inflammatoire**.

Ces résultats suggèrent que RWE pourrait réduire de manière indirecte l'inflammation au niveau de l'épithélium rétinien pigmentaire, mais aussi de manière plus directe sur les cellules de l'immunité (macrophages pro-inflammatoires). De plus, il semble être capable de prévenir l'inflammation, mais aussi de la diminuer lorsque celle-ci est déjà en place.

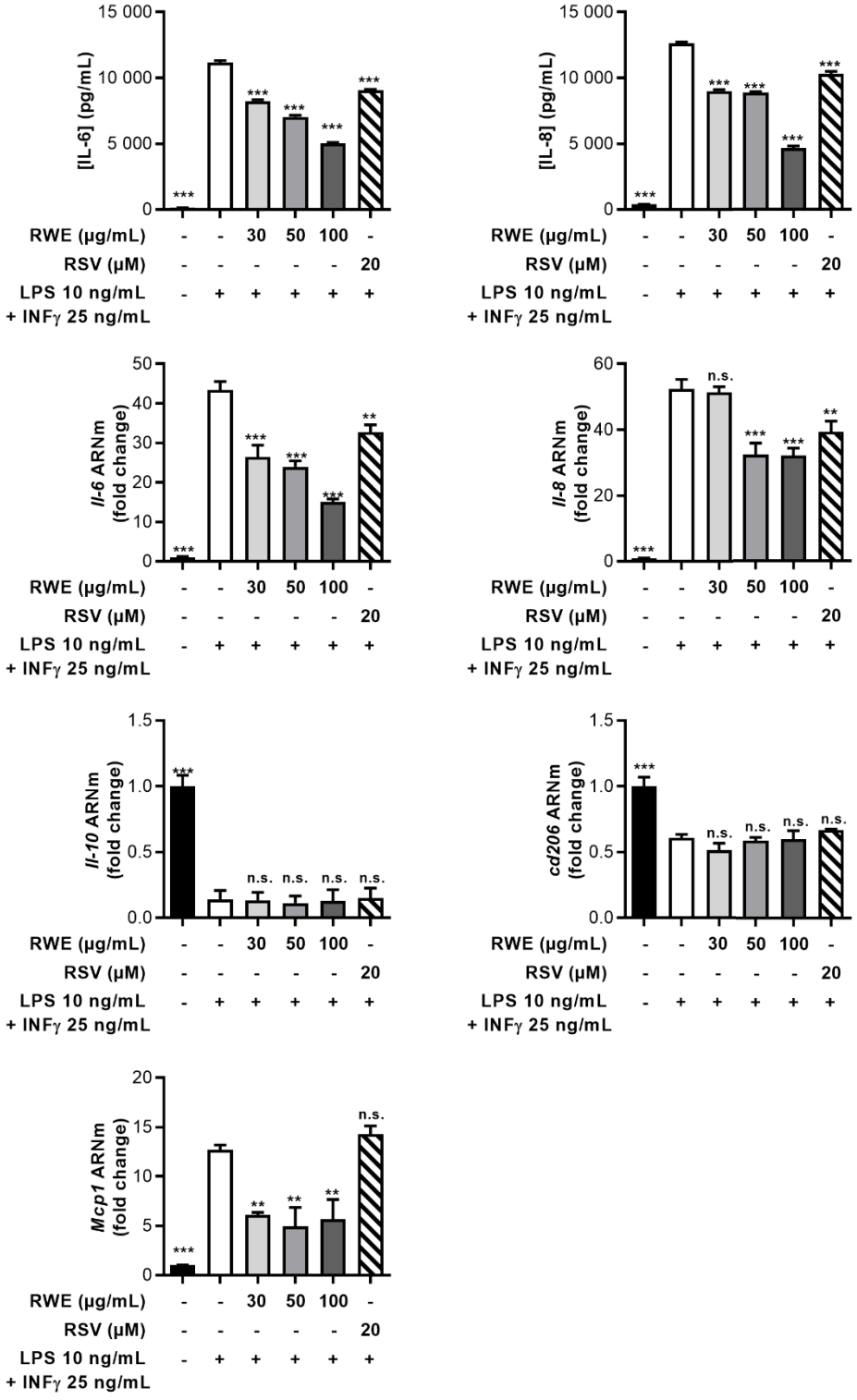

Figure 32. L'extrait sec de vin rouge inhibe l'inflammation dans les macrophages pro-inflammatoires humains

Après 6 jours de cultures, les cellules ont été incubées avec du LPS (10 ng/mL) et de l'INFγ (25 ng/mL) afin de les polariser en macrophages pro-inflammatoires. Après 24 h, différentes concentrations d'extrait sec de vin rouge (*red wine extract* : RWE (30; 50; 100 µg/mL) ou de RSV (20 µM) ont été ajoutés dans les milieux de culture durant 24 h. **(A)** la sécrétion d'IL-6 et d'IL-8 a été mesurée par ELISA. Les résultats sont exprimés ± SEM de trois expériences indépendantes. **(B)** L'expression d'ARNm a été mesurée par qPCR. Le gène L27 a été utilisé comme référence. Les résultats sont exprimés en valeurs moyennes rapportées aux cellules contrôles (traitées avec le solvant) ± SEM de trois expériences

indépendantes. Les *p*-values ont été calculées par un test ANOVA suivi d'un test de Dunnett. *p*-value ≤ 0,05 a été considérée comme significative, n.s. = non significatif;**p<0,01; *** p<0,0001 valeurs comparées aux valeurs des cellules traitées avec le LPS et l'INFγ.

D.4. Les cellules ARPE-19 "différenciées"

La lignée cellulaire ARPE-19 indifférenciée est très largement utilisée afin d'étudier les maladies oculaires telles que la DMLA. En effet, elle fournit une alternative fiable à l'EPR natif (Dunn et al., 1996; Samuel et al., 2017). Cependant, lors des différents passages, les cellules ARPE-19 perdent une partie de leur phénotype, elles ne sont plus polarisées et l'expression de certains gènes tels que rpe65 et rlbp1 est très fortement diminuée. Ainsi, certaines études ont montré que certaines conditions de cultures cellulaires permettaient de **différencier les cellules ARPE-19 afin de rétablir un phénotype fonctionnel et morphologique similaire à l'EPR physiologique** (Dunn et al., 1996; Samuel et al., 2017). Nous avons donc voulu étudier l'effet du RWE ainsi que celui du RSV sur les cellules ARPE-19 lorsque celles-ci étaient différenciées. Ainsi, dans un premier temps, nous avons vérifié que les cellules ARPE-19 cultivées à confluence durant 8 semaines dans un milieu réduit en sérum exprimaient de manière importante des gènes marqueurs du phénotype différencié à savoir rlbp*1* et *rpe65*. On peut voir Figure 33 (A) que ces gènes sont très fortement exprimés dans les cellules différenciées comparativement aux cellules indifférenciées. Dans un second temps, **l'innocuité du RWE et du RSV** a été vérifiée dans ce modèle cellulaire. Après différenciation, les cellules ARPE-19 ont été traitées par des concentrations croissantes de RWE et de RSV allant de 0 à 250 µg/mL. **Après 24 h et 48 h de traitement aucun impact n'a été observé sur la viabilité cellulaire** (Figure 33).

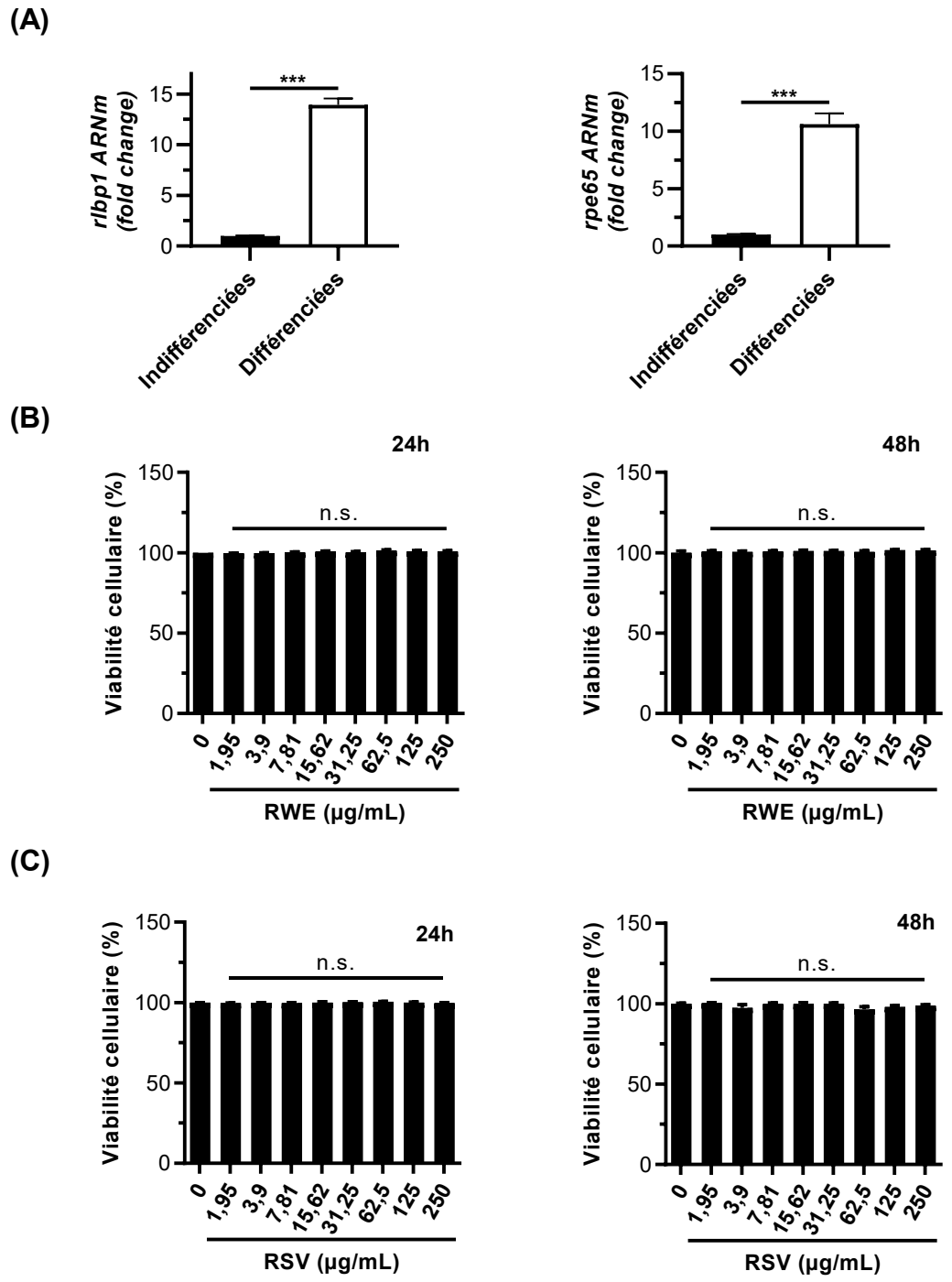

Figure 33. Différenciation des cellules ARPE-19

(A) Expression de gènes marqueurs de la différenciation des cellules ARPE-19. Les cellules ARPE-19 ont été maintenues dans du milieu culture supplémenté avec 1 % de sérum de veau fœtal (SVF) durant 24h pour les cellules indifférenciées et 8 semaines pour les cellules différenciées. L'expression des gènes rlbp1 et rpe65 a ensuite été mesurée par qPCR. Les résultats sont rapportés à l'expression des cellules indifférenciées ± SD. Les *p*-values ont été calculées par un t-test. *** $p<0,001$. **(B-C)** Après 2 mois de culture à confluence, les cellules ARPE-19 ont été traitées durant 24 et 48h avec des doses croissantes (0; 1,95; 3,9; 7,81; 15,62; 31,25; 62,5; 125; 250) de **(B)** RWE et de **(C)** RSV. Les valeurs sont exprimées en pourcentages moyens rapportés aux cellules contrôles ± SEM. Les *p*-values ont été calculées par un test ANOVA à un facteur. n.s. = non significatif.

Par la suite, nous avons souhaité vérifier le pouvoir anti-oxydant de l'extrait sec de vin rouge et du resvératrol sur les ARPE-19 lorsque ces dernières étaient différenciées. Pour cela, trois doses de RWE ont été choisies à savoir 30, 50, 100 µg/mL et une dose de RSV (20 µM). Celles-ci sont les mêmes qui ont été utilisées sur les ARPE-19 indifférenciées dans les études précédentes.

Afin d'étudier le caractère anti-oxydant du RWE et du RSV, nous avons cherché dans un premier temps à déterminer les doses de peroxyde d'hydrogène et d'AAPH capables d'induire des ERO dans les cellules ARPE-19 différenciées. La capacité de ces derniers à induire la d'ERO a été mesurée à l'aide d'une sonde fluorescente (DCFDA). Nos résultats montrent que **ni peroxyde d'hydrogène ni l'AAPH ne présentent d'effet cytotoxicité sur les cellules ARPE-19 différenciées** et ce même aux concentrations les plus élevées (Figure 34A,C). Néanmoins, ils **induisent de manière dose dépendante la production ERO** (Figure 34B,D). Afin d'étudier le caractère anti-oxydant du RWE, nous avons sélectionné une concentration de peroxyde d'hydrogène (3 mM) et une concentration d'AAPH (1,2 mM). Ces concentrations induisent une forte augmentation d'ERO (+900 % pour 3 mM d'H_2O_2 et + 1 100 % pour 1,2 mM d'AAPH). Ainsi, les cellules différenciées ont été traitées 24 h avec différentes concentrations de RWE (30, 50, 100 µM) ou avec 20 µM de RSV. Puis, la production d'ERO a été induite avec 3 mM de peroxyde d'hydrogène ou 1,2 mM d'AAPH. Comme attendu, on observe Figure 34E,G que les différents traitements n'impactent par la viabilité cellulaire. Néanmoins, la production d'ERO est quant à elle altérée. Dans les deux cas, avec **H_2O_2 et AAPH, on observe que l'induction de la production d'ERO est inhibé par RWE** (Figure 34F,H). En effet, même à la concentration la plus faible, RWE permet le retour à un niveau basal d'ERO lorsque ces derniers sont induits par H_2O_2. Lorsque la production d'ERO est induite par AAPH, RWE inhibe leur production de manière dose dépendante. La dose la plus faible de RWE (30 µg) ne permet pas de diminuer les ERO. Néanmoins, les doses les plus fortes, RWE 50 et 100 µg, permettent de diminuer d'environ 40% et 64% la production d'ERO. Si l'on regarde l'effet du RSV seul, on constate que bien qu'il soit capable d'inhiber la production d'ERO induite par l'AAPH et par l'H_2O_2, son effet est dans les deux cas moins importants que l'effet du RWE.

Ces résultats confirment le caractère anti-oxydant du RWE et corroborent les résultats obtenus sur les cellules ARPE-19 indifférenciées (Cornebise et al., 2023).

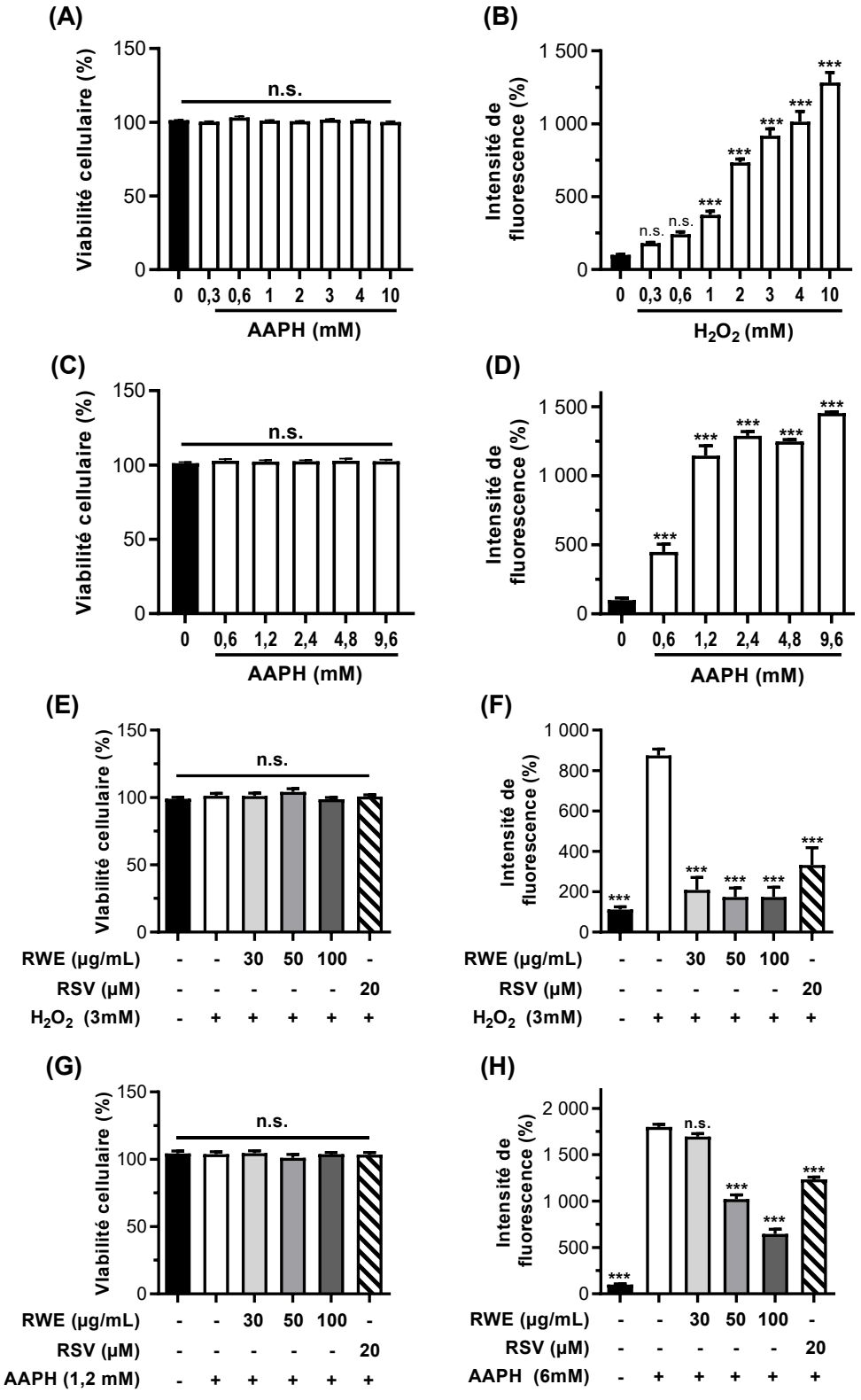

Figure 34. L'extrait sec de vin rouge prévient le stress oxydant dans les cellules ARPE-19 différenciées

Les cellules ARPE-19 ont été différenciées durant 8 semaines dans du milieu réduit en sérum (1%). (A-D) Les cellules ont été traitées avec des doses croissantes de **(A,B)** H_2O_2 (0; 0,3; 0,6; 1; 2 ; 3; 4; 10 mM) ou **(C,D)** d'AAPH (2,20 -Azobis(2-methylpropionamidine) dihydrochloride) (0,6 ; 1,2 ; 2,4 ; 4,8 ;

9,6 mM). Après 6h de traitement, les cellules ont été incubées avec la sonde DCFDA sensible aux espèces réactives de l'oxygène (ERO), (50 μM) durant 30 min. Après rinçage, la viabilité cellulaire a été mesurée par cristal violet **(A,C)** et les ERO ont été mesurés grâce à l'intensité de fluorescence de la sonde DCFDA (em/ex : 490/520) **(B,D)**. Les résultats sont exprimés en pourcentages moyens rapportés aux cellules contrôles ± SEM. Les *p*-values ont été calculées par un test ANOVA suivi d'un test de Dunnett. *p*-value ≤ 0,05 a été considérée comme significative, n.s. = non significatif ; **p< 0,01 ; *** *p*<0,001. **(E-H)** Les cellules ont été traitées avec différentes doses d'extrait sec de vin rouge (*red wine extract* : RWE; 30; 50; 100 μM) ou avec 20 μM de resvératrol (RSV). Après 24h de traitement, les cellules ont été incubées avec 50 μM de DCFDA durant 30min. Après rinçage, les cellules ont été traitées **(E,F)** avec de l'H_2O_2 (3mM) ou **(G,H)** avec de l'AAPH (1,2 mM) durant 6h. A la fin des traitements, la viabilité cellulaire a été mesurée par cristal violet **(E,G)** et l'intensité de fluorescence a été mesurée (em/ex : 490/520)**(F,H)**. Les résultats sont exprimés en pourcentages moyens rapportés aux cellules contrôles ± SEM. Les *p*-values ont été calculées par un test ANOVA suivi d'un test de Dunnett. *p*-value ≤ 0,05 a été considérée comme significative, n.s. = non significatif, ***p< 0,001 comparé aux valeurs des cellules traitées avec H_2O_2.

Discussion et Perspectives

La dégénérescence maculaire liée à l'âge (DMLA) est la première cause de handicap visuelle dans les pays développés. Sa prévalence augmente considérablement avec l'âge, ce qui, combiné au vieillissement de la population mondiale, se traduit par une augmentation constante du nombre de personnes touchées par cette maladie. Ainsi, diminuer ou ralentir sa progression est devenu un enjeu majeur de santé publique. Des études épidémiologiques de grande ampleur ont permis de montrer que l'alimentation joue un rôle prépondérant dans la progression de cette maladie. Dans la majorité des cas, la DMLA est une maladie unilatérale (qui ne touche qu'un seul œil). Il a été montré qu'une alimentation riche en anti-oxydants et en oméga-3 permet de ralentir la progression de la maladie dans l'œil atteint et prévenir sa survenue dans l'œil sain. Dans ce contexte, nous avons axé notre étude sur les effets bénéfiques d'un cocktail riche en molécules anti-oxydante à savoir un extrait sec de vin rouge enrichi en polyphénols.

Le caractère anti-angiogénique du RWE

En condition basale

La forme la plus sévère de la maladie est caractérisée par une néo-angiogenèse aberrante qui va venir perturber l'homéostasie de la rétine. Cette néo-angiogenèse induite par le facteur de croissance *Vascular Endothelial Growth Factor A* (VEGF-A) mène à la formation de nouveaux vaisseaux au sein de la rétine. Le VEGF-A est la cible principale des traitements actuels qui visent à l'inhiber à l'aide d'anticorps bloquants injectés directement dans l'œil. Les traitements ne sont efficaces que lors de la phase active de la maladie, c'est-à-dire lors de la formation de nouveaux vaisseaux. De plus, ces traitements sont très lourds pour les patients, certains vont présenter une résistance aux traitements. De nouvelles études se sont donc orientées sur des molécules connues dans le domaine de la santé qui pourraient être utilisées dans le cadre de la DMLA. Ainsi, les polyphénols, connus pour les activités pléiotropiques dans diverses maladies telles que le cancer, semblent être de bons candidats. En effet, le plus emblématique des polyphénols, le resvératrol (RVS), est bien connu pour ses bénéfices anti-angiogéniques dans le cadre du cancer notamment. Dans notre étude, nous avons utilisé un extrait sec de vin rouge enrichi en polyphénols contenant une part non négligeable de RSV. Nous nous sommes donc intéressés au caractère anti-angiogénique du RWE et nous avons pu montrer qu'il permettait de diminuer la sécrétion ainsi que la signalisation intracellulaire du VEGF-A

(Figure 35). Cette étude a été réalisée *in vitro*, dans une lignée cellulaire saine de l'épithélium pigmentaire rétinien (ARPE-19). Ainsi, le RWE semble prévenir l'angiogenèse dans les cellules saines, quand est-il lors que l'angiogenèse est induite ?

En condition pathologique

Afin de mimer la condition pathologique, nous avons utilisé du VEGF recombinant (rVEGF) afin d'induire la sécrétion du VEFG-A par les cellules ARPE-19. Nous avons pu montrer que même lors d'une induction, le RWE est capable de prévenir la sécrétion du VEGF-A. La signalisation cellulaire du VEGF-A débute par la phosphorylation de son récepteur (VEGF-R2) qui induit une cascade de phosphorylation menant à l'augmentation transcriptionnelle du VEGF-A ainsi qu'à sa sécrétion. Nos résultats ont montré qu'en condition basale, RWE diminue l'expression protéique du récepteur VEGF-R2, mais aussi la phosphorylation de la tyrosine 951 de ce dernier. Etonnamment, nos résultats préliminaires montrent que le rVEGF induit l'expression de VEGF-R2, mais pas sa phosphorylation sur la tyrosine 951. VEGF-R2 possède de nombreuses tyrosines pouvant être phosphorylées lors de sa liaison avec le VEGF-A. Ainsi, nous avons pu constater que rVEGF induisait la phosphorylation d'une autre tyrosine, la tyrosine 1054 du récepteur VEGF-R. La phosphorylation des tyrosines 951 (Y951) et 1054 (Y1054 vont toutes les deux activer la même cascade phosphorylation menant *in fine* à la production et sécrétion du VEGF-A (Figure 35). Néanmoins, la phosphorylation de Y10544 augmente l'activité du récepteur (Wang et al., 2020), il serait donc intéressant de poursuivre nos investigations afin de vérifier que la phosphorylation de Y1054 induit la phosphorylation de protéines telles que ERK1/2 et MEK pour lesquelles nous avons montré que RWE diminuait leur phosphorylation en condition basale. Pour la suite de l'étude, il est primordial de vérifier le caractère anti-angiogénique du RWE *in vivo*. En effet, il est possible d'induire une angiogenèse au niveau de la rétine à l'aide d'impacts lasers sur la rétine. Nous pourrions donc impacter un seul œil afin de mimer une DMLA unilatérale avec un œil pathologique et un œil sain. Cela nous permettrait de vérifier que le RWE est anti-angiogénique en condition pathologique et que ses effets anti-angiogénique ne sont pas délétères dans un œil sain. Les précédents travaux de recherche de notre équipe ont permis de montrer qu'une supplémentation en resvératrol de 35 jours (14 jours en amont des impacts lasers puis durant 21 jours post impacts lasers) permettait de réduire l'angiogenèse induite.

Le caractère anti-oxydant du RWE

Les polyphénols sont principalement connus pour leur effet anti-oxydant. En effet, leur structure chimique leur permet de capter les radicaux libres et ainsi de diminuer le stress oxydant. Etonnamment, nos résultats ont montré qu'en condition non pathologique, le RWE n'affecte pas la quantité intracellulaire d'ERO. Cependant, en condition pathologique, le RWE diminue drastiquement les ERO. Nous avons montré que le RWE prévenait la production d'ERO induite dans les cellules ARPE-19 par du peroxyde d'hydrogène ou par de l'AAPH.

Il est important de rappeler que bien que des niveaux élevés d'ERO soient délétères pour les cellules, un niveau modéré est qu'en a lui nécessaire dans la signalisation cellulaire (Migdal and Serres, 2011; Zuo et al., 2022). Ainsi, il semblerait que le RWE ne soit capable d'influer sur le stress oxydant qu'en condition pathologique et n'interfère pas avec la signalisation cellulaire physiologique.

Nos résultats ont été obtenus dans une lignée cellulaire immortalisée issue d'un homme âgé de 19 ans. Bien que ce modèle cellulaire soit couramment utilisé dans l'étude des maladies oculaires telles que la DMLA, il présente quelques désavantages. En effet, le vieillissement cellulaire impacte fortement la DMLA, il a notamment été montré que l'efficacité des défenses anti-oxydantes diminue avec l'âge (Barouki, 2006) et participe à l'augmentation du stress oxydant au sein de la rétine. Ainsi, il serait intéressant d'étudier l'effet du RWE sur le stress oxydant basal présent dans des cellules de cultures primaires d'épithélium pigmentaire rétinien (RPE) provenant de donneurs âgés (haRPE) (Fisher et al., 2022). De plus, nous pourrions compléter cette étude par la mesure de l'activité des enzymes anti-oxydantes telles que la superoxyde dismutase et la catalase. Au cours de ce projet, nous avons essayé de les mesurer néanmoins, nous ne sommes pas parvenus à montrer une modification de l'activité de ces enzymes, et ce malgré l'induction d'un stress oxydant important (Figure 36).

Enfin, nous n'avons étudié le caractère anti-oxydant du RWE que dans un modèle in vitro, il conviendrait donc de confirmer ces résultats dans un modèle pré-clinique. Pour cela, nous pourrions supplémenter des souris avec du RWE durant plusieurs semaines avant de les exposer à une forte intensité lumineuse afin d'induire des dommages à la rétine (Abokyi et al., 2020). Par ailleurs, un stress oxydant pourrait aussi être induit par de la fumée de cigarette (Abokyi et al., 2020; Hamilton et al., 2012), ainsi, nous pourrions étudier les effets protecteurs

du RWE. L'étude d'un stress oxydant induit par la fumée de cigarette est très intéressante, car les études AREDS ont montré qu'une supplémentation en bêta-carotène augmentait le risque de cancer du poumon chez les patients fumeurs. Ainsi, il serait important de vérifier que le RWE n'a pas le même effet délétère.

Le caractère anti-inflammatoire du RWE

L'inflammation et le stress oxydant sont deux processus intrinsèquement liés dans la pathologie de la DMLA. En effet, il a été montré que les dommages induits par un stress oxydant mènent à l'installation et au maintien d'un environnement pro-inflammatoire (Marazita et al., 2016). Ainsi, notre étude a permis de montrer que le RWE prévenait l'inflammation induite par un stress oxydant dans les cellules de l'EPR. Le RWE prévient la sécrétion d'interleukines pro-inflammatoires (IL-6 et IL-8). De plus, il permet aussi de prévenir l'expression de l'ARNm de MCP-1 qui est une chimiokine impliquée dans le recrutement des macrophages. En effet, les cellules de l'EPR peuvent sécréter MCP-1 afin de favoriser le recrutement de macrophages pro-inflammatoires au niveau de la rétine. Il a notamment été montré que les patients atteints de DMLA présentent une accumulation de macrophages au sein de la rétine ce qui participe au maintien d'un environnement pro-inflammatoire. Dans ce contexte, nous avons étudié le cratère anti-inflammatoire du RWE sur des macrophages primaires humains de phénotypes pro-inflammatoires (M1). Nos résultats ont démontré que le RWE était capable de prévenir l'inflammation induite dans ces macrophages et même de réduire une inflammation déjà établie chez les macrophages pro-inflammatoires. Nos résultats ont montré que le RWE pouvait altérer l'expression d'ARNm de marqueurs phénotypiques des macrophages pro- et anti-inflammatoire (macrophages de type M1 et M2), pour la suite de l'étude, il conviendrait de caractériser le phénotype des macrophages grâce à l'expression membranaire de ces marqueurs. Ainsi, cela permettrait de déterminer si le RWE est capable d'inverser le phénotype pro-inflammatoire en anti-inflammatoire.

Nos résultats ont été obtenus *in vitro*, nous avons pour projet d'étayer ces résultats en utilisant un modèle *in vivo*. Pour cela, nous avons supplémenté durant 42 jours des souris C57BL/J avec du RWE ou du RSV. Après 21 jours de supplémentation, une inflammation chronique a été induite durant 21 jours supplémentaires par des injections de LPS (Figure 38).

Pour la suite de l'étude, nous prévoyons d'analyser les taux de cytokines au niveau de la rétine afin de voir si le RWE est capable *in vivo* de diminuer l'inflammation. Enfin, nous pourrions aussi envisager d'étudier l'effet anti-inflammatoire du RWE lorsqu'une inflammation est déjà établie. Pour cela, nous pourrions induire une inflammation chronique durant quelques jours avant de commencer la supplémentation des souris.

RWE versus RSV

Le resvératrol est l'un des polyphénols les plus emblématiques, il a notamment été beaucoup étudié dans le cancer où il a été montré qu'il possède un fort pouvoir anti-angiogénique. Pour la suite, des études menées dans le cadre de la DMLA ont permis de démontrer que ce polyphénol pouvait aussi être bénéfique dans des maladies oculaires (Delmas et al., 2021). Ainsi, nous avons utilisé, dans le cadre de notre étude, le resvératrol comme composé de référence afin de comparer ses effets à celui de notre extrait polyphénolique de vin rouge. Nos résultats mettent en avant que le RWE possède des effets supérieurs à ceux du resvératrol seul. Il est important de rappeler que dans notre étude, la quantité de resvératrol contenue dans l'extrait (20,5 nM pour la dose la plus forte) est très nettement inférieure à celle utilisée pour le resvératrol seul (20 μM). En outre, certaines études ont montré que le RSV pouvait agir en synergie avec d'autres polyphénols. Il a été démontré que l'activité synergique du resvératrol avec d'autres polyphénols pouvait être très efficace contre le stress oxydant et l'inflammation (58-61). Il a été démontré au niveau clinique que la synergie des polyphénols pouvait être utilisée dans la lutte contre le cancer. Les précédentes études de notre équipe de recherche ont mis en évidence que lorsque le RSV est utilisé avec deux autres polyphénols à savoir la quercétine et la catéchine, ils agissent en synergie et présentent un effet anti-tumoral synergique comparé à l'utilisation de polyphénol seul. Ces trois polyphénols étant dans le RWE, il serait intéressant de déterminer si ces trois composés agissent en synergie dans un contexte de DMLA. La composition polyphénolique des vins étant très variable en fonction des processus de vinification, des conditions climatiques, du cépage, de la région, des conditions de conservation, etc. Dans l'optique d'utiliser le RWE comme complément alimentaire, il serait intéressant d'identifier les polyphénols responsables de l'effet du RWE afin de créer une formulation avec ces derniers.

En parallèle des synergies des polyphénols présents dans le RWE, il est crucial d'étudier sa biodisponibilité avant d'envisager son utilisation dans le domaine clinique. En effet, bien que les polyphénols suscitent un fort intérêt dans le domaine de la santé, leur faible biodisponibilité constitue un frein majeur à leur utilisation en clinique. Les polyphénols et notamment le resvératrol présentent une faible biodisponibilité c'est-à-dire qu'un faible pourcentage de la molécule administrée est retrouvé dans la circulation générale. Deux processus physiologiques sont responsables de cette biodisponibilité, à savoir l'absorption intestinale et le métabolisme. La biodisponibilité des polyphénols est très variable en fonction de leur nature (Tableau 8). La diversité polyphénolique ainsi que les potentiels synergies des composés du RWE pourrait permettre de contrebalancer leur faible biodisponibilité et ainsi permettre de réduire les doses administrées. Néanmoins, il serait nécessaire de faire des analyses plus poussées afin de déterminer les doses nécessaires à une efficacité optimale dans le cadre de la DMLA. Il a été démontré qu'une supplémentation de 12 semaines avec 450 mg/jour de resvératrol permettait de réduire la néoangiogenèse chez des patient atteint de DMLA (Lin et al., 2016). De plus, il a été montré que parfois les doses les plus faibles de RSV pouvaient avoir une efficacité supérieure aux doses les plus fortes (Cai et al., 2015). Cela peut s'expliquer par la capacité du resvératrol et de ses métabolites à s'accumuler dans les tissus. Ces métabolites peuvent être actifs (Aires et al., 2013) ou servir de réservoir de molécules de resvératrol grâce aux sulfates et aux glucuronides (Lin et al., 2012). Ainsi, il serait intéressant, dans le cadre de l'expérience *in vivo* décrite précédemment (Figure 38) de mesurer par CLHP les taux circulant de polyphénols dans le sang ainsi que ceux retrouvés au niveau de la rétine afin de déterminer une dose optimale de RWE permettant de protéger la rétine. De plus, si la synergie de certains composés du RWE est mise en évidence, il sera intéressant de regarder la biodisponibilité des molécules synergiques afin de pouvoir envisager une formulation administrée à homme.

Formulation oméga-3 et anti-oxydants

Les études cliniques de l'AREDS ont permis de montrer qu'une formulation riche en oméga-3 était bénéfique dans la prévention de la DMLA. Ainsi, notre équipe de recherche s'est intéressée à une formulation contenant du resvératrol ainsi que des oméga-3 (Resvega ®). Les travaux de Courtaut et al., réalisés dans un modèle murin de néovascularisations

choroïdiennes ont montré que le Resvega® diminuait la formation de nouveaux vaisseaux, et ce de manière plus importante que le RSV seul utilisé à dose équivalente (Courtaut et al., 2021a). De plus, ces travaux ont été complétés par une étude *in vitro* qui a montré que le Resvega® diminuait l'expression protéique de protéines clés impliquées dans la sécrétion de VEGF-A (Courtaut et al., 2021b). Ainsi, après l'étude et l'identification des composés responsables de l'action du RWE, il serait intéressant d'ajouter des oméga-3 à cette formulation et de comparer les effets de cette dernière à ceux du RWE seul.

De plus, nos travaux ont aussi montré que le Resvega® pouvait prolonger les effets de l'avastin®. En effet, nous avons montré in vivo que le Resvega® pouvait prolonger la diminution de la sécrétion de VEGF-A induite par l'avastin et que cette diminution était accompagnée de la diminution l'expression de protéines clés impliquées dans la pathologie de la DMLA telles que p65 et p50 (Sghaier et al., 2022). Etant donné que nous avons montré que le RWE pouvait aussi impacter p65, il serait intéressant de voir s'il est aussi capable de prolonger les effets de l'avastin® dans un premier temps in vitro dans les cellules ARPE-19 puis dans un second temps dans un modèle murin de néovascularisation induite par impact laser.

Conclusion

Cette étude a mis en évidence qu'un extrait de vin rouge enrichi en polyphénols pouvait contrer les événements précoces de la dégénérescence maculaire liée à l'âge (DMLA), à savoir le stress oxydant, l'inflammation et l'angiogenèse dans un modèle in vitro de cellules de l'épithélium pigmentaire rétinien (ARPE-19). Les résultats de cette étude montrent qu'en condition basale le RWE inhibe la sécrétion ainsi que la voie de signalisation du facteur de croissance VEGF-A impliqué dans la DMLA néovasculaire (Figure 35). Ces résultats ont été confirmés en condition pathologique. Nous avons aussi montré que le RWE prévient le stress oxydant ainsi que ses dommages lorsque ce dernier est induit dans les cellules de l'EPR. De plus, nous avons aussi étudié le cratère anti-inflammatoire du RWE dans les cellules de l'EPR ainsi que dans des macrophages humains pro-inflammatoires. Ainsi, nous avons pu montrer que le RWE permettait non seulement de prévenir l'inflammation au sein des macrophages pro-inflammatoires, mais aussi de la diminuer lorsque celle-ci est déjà établie dans les cellules. Ces résultats *in vitro* sont prometteurs et ouvrent la voie à de futures études pré-cliniques sur

les bienfaits potentiels des polyphénols et de leurs métabolites dans la prévention et le ralentissement de la progression de la DMLA.

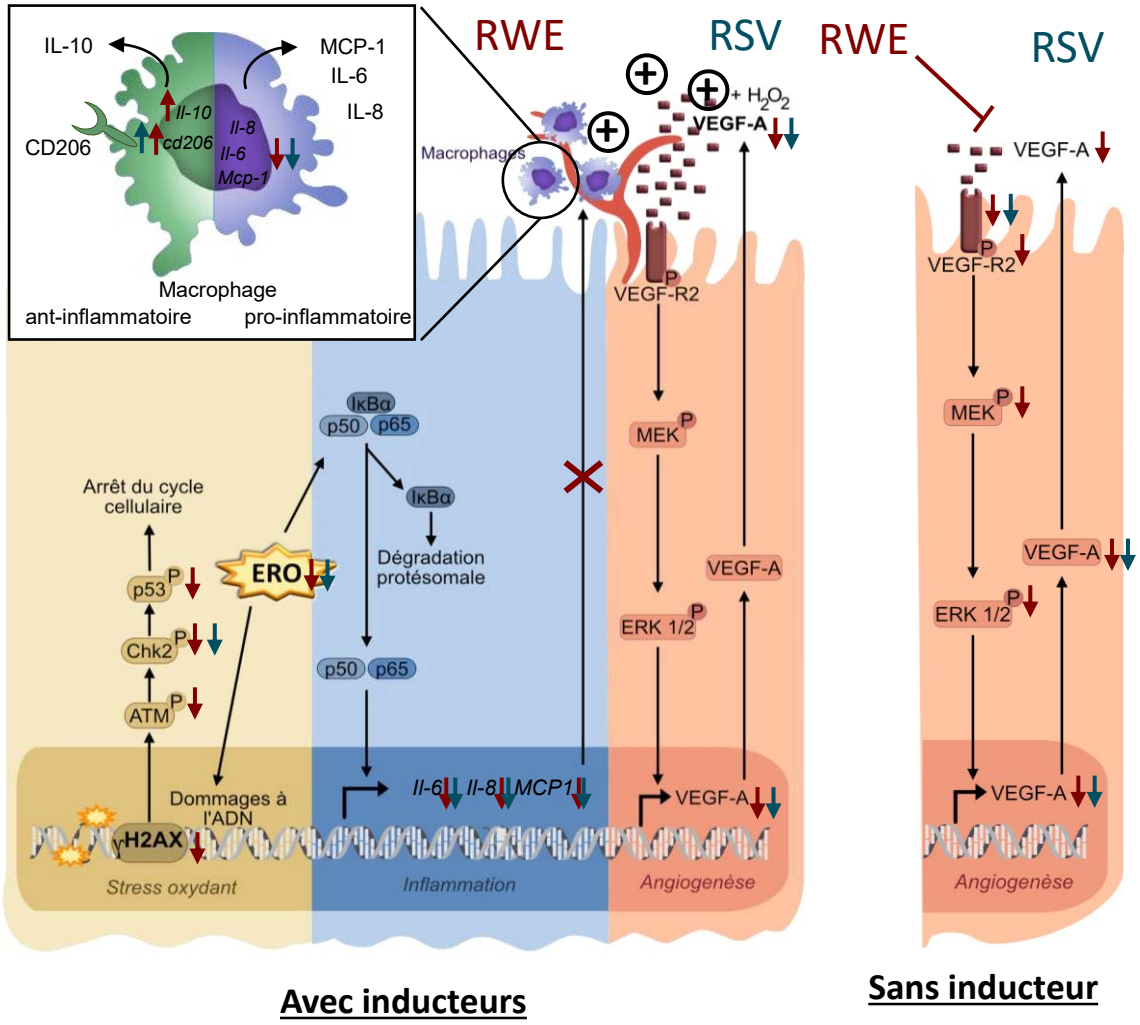

Figure 35. Effet de l'extrait sec de vin rouge sur les cellules de l'épithélium pigmentaire rétinien.
En condition pathologique, l'extrait sec de vin rouge (*Red wine extract* : RWE) diminue la production d'espèces réactives de l'oxygène (ERO) induite par un stress exogène et ainsi prévient les dommages à l'ADN ainsi que la phosphorylation de protéines clés impliquées dans la régulation des dommages à l'ADN. Le RWE prévient l'expression d'ARNm de cytokines (IL-6, IL-8, MCP-1 et VEGF-A) impliquées dans la physiopathologie de la DMLA. En condition basale, le RWE inhibe l'expression d'ARNm et la sécrétion de VEGF-A ainsi que sa voie de signalisation. (AAPH : 2,20 -Azobis(2-methylpropionamidine) dihydrochloride ; LPS : Lipopolysaccharide ; INF : Interféron ; VEGF-A : *Vascular Endothelial Growth Factor* ; VEGF-R2 : *Vascular Endothelial Growth Factor receptor 2).*

Références

Abokyi, S., To, C.-H., Lam, T.T., Tse, D.Y., 2020. Central Role of Oxidative Stress in Age-Related Macular Degeneration: Evidence from a Review of the Molecular Mechanisms and Animal Models. Oxid. Med. Cell. Longev. 2020, e7901270. https://doi.org/10.1155/2020/7901270

Adair, T.H., Montani, J.-P., 2010. Overview of Angiogenesis, in: Angiogenesis. Morgan & Claypool Life Sciences.

Age-Related Eye Disease Study Research Group, 2001. A randomized, placebo-controlled, clinical trial of high-dose supplementation with vitamins C and E, beta carotene, and zinc for age-related macular degeneration and vision loss: AREDS report no. 8. Arch. Ophthalmol. Chic. Ill 1960 119, 1417–1436. https://doi.org/10.1001/archopht.119.10.1417

Ahuja, I., Kissen, R., Bones, A.M., 2012. Phytoalexins in defense against pathogens. Trends Plant Sci. 17, 73–90. https://doi.org/10.1016/j.tplants.2011.11.002

Akhtar-Schäfer, I., Wang, L., Krohne, T.U., Xu, H., Langmann, T., 2018. Modulation of three key innate immune pathways for the most common retinal degenerative diseases. EMBO Mol. Med. 10, e8259. https://doi.org/10.15252/emmm.201708259

Ambati, J., Atkinson, J.P., Gelfand, B.D., 2013. Immunology of age-related macular degeneration. Nat. Rev. Immunol. 13, 438–451. https://doi.org/10.1038/nri3459

Aron, P.M., Kennedy, J.A., 2008. Flavan-3-ols: Nature, occurrence and biological activity. Mol. Nutr. Food Res. 52, 79–104. https://doi.org/10.1002/mnfr.200700137

Austin, B.A., Liu, B., Li, Z., Nussenblatt, R.B., 2009. Biologically active fibronectin fragments stimulate release of MCP-1 and catabolic cytokines from murine retinal pigment epithelium. Invest. Ophthalmol. Vis. Sci. 50, 2896–2902. https://doi.org/10.1167/iovs.08-2495

Ban, Y., Rizzolo, L.J., 2000. Regulation of glucose transporters during development of the retinal pigment epithelium. Brain Res. Dev. Brain Res. 121, 89–95. https://doi.org/10.1016/s0165-3806(00)00028-6

Barouki, R., 2006. Stress oxydant et vieillissement. médecine/sciences 22, 266–272. https://doi.org/10.1051/medsci/2006223266

Behar-Cohen, F., 2018. [AMD and complement pathway in 2017]. Rev. Med. Suisse 14, 64–69.

Behar-Cohen, F., Kowalczuk, L., Keller, N., Savoldelli, M., Azan, F., Jeanny, J.-C., 2009. Anatomie de la rétine. EMC - Ophtalmol. 6, 1–14. https://doi.org/10.1016/S0246-0343(09)30048-9

Behnke, V., Wolf, A., Langmann, T., 2020. The role of lymphocytes and phagocytes in age-related macular degeneration (AMD). Cell. Mol. Life Sci. 77, 781–788. https://doi.org/10.1007/s00018-019-03419-4

Bell, J.R., Donovan, J.L., Wong, R., Waterhouse, A.L., German, J.B., Walzem, R.L., Kasim-Karakas, S.E., 2000. (+)-Catechin in human plasma after ingestion of a single serving of reconstituted red wine. Am. J. Clin. Nutr. 71, 103–108. https://doi.org/10.1093/ajcn/71.1.103

Belmouhand, M., Rothenbuehler, S.P., Dabbah, S., Bjerager, J., Sander, B., Hjelmborg, J.B., Dalgård, C., Jensen, R., Larsen, M., 2022. Small hard drusen and associated factors in early seniority. PLOS ONE 17, e0279279. https://doi.org/10.1371/journal.pone.0279279

Bhattarai, N., Korhonen, E., Toppila, M., Koskela, A., Kaarniranta, K., Mysore, Y., Kauppinen, A., 2020. Resvega Alleviates Hydroquinone-Induced Oxidative Stress in ARPE-19 Cells. Int. J. Mol. Sci. 21, 2066. https://doi.org/10.3390/ijms21062066

Bhosale, P.B., Ha, S.E., Vetrivel, P., Kim, H.H., Kim, S.M., Kim, G.S., 2020. Functions of polyphenols and its anticancer properties in biomedical research: a narrative review. Transl. Cancer Res. 9, 7619–7631. https://doi.org/10.21037/tcr-20-2359

Blaauwgeers, H.G., Holtkamp, G.M., Rutten, H., Witmer, A.N., Koolwijk, P., Partanen, T.A., Alitalo, K., Kroon, M.E., Kijlstra, A., van Hinsbergh, V.W., Schlingemann, R.O., 1999. Polarized vascular endothelial growth factor secretion by human retinal pigment epithelium and localization of vascular endothelial growth factor receptors on the inner choriocapillaris. Evidence for a trophic paracrine relation. Am. J. Pathol. 155, 421–428. https://doi.org/10.1016/S0002-9440(10)65138-3

Blasiak, J., Pawlowska, E., Sobczuk, A., Szczepanska, J., Kaarniranta, K., 2020. The Aging Stress Response and Its Implication for AMD Pathogenesis. Int. J. Mol. Sci. 21, 8840. https://doi.org/10.3390/ijms21228840

Blasiak, J., Piechota, M., Pawlowska, E., Szatkowska, M., Sikora, E., Kaarniranta, K., 2017. Cellular Senescence in Age-Related Macular Degeneration: Can Autophagy and DNA Damage Response Play a Role? Oxid. Med. Cell. Longev. 2017, 5293258. https://doi.org/10.1155/2017/5293258

Boesze-Battaglia, K., Goldberg, A.F.X., 2002. Photoreceptor renewal: a role for peripherin/rds. Int. Rev. Cytol. 217, 183–225. https://doi.org/10.1016/s0074-7696(02)17015-x

Boije, H., Shirazi Fard, S., Edqvist, P.-H., Hallböök, F., 2016. Horizontal Cells, the Odd Ones Out in the Retina, Give Insights into Development and Disease. Front. Neuroanat. 10, 77. https://doi.org/10.3389/fnana.2016.00077

Bonilha, V.L., Bell, B.A., DeBenedictis, M.J., Hagstrom, S.A., Fishman, G.A., Hollyfield, J.G., 2020. Cellular Changes in Retinas From Patients With BEST1 Mutations. Front. Cell Dev. Biol. 8, 573330. https://doi.org/10.3389/fcell.2020.573330

Boucher, J.M., Clark, R.P., Chong, D.C., Citrin, K.M., Wylie, L.A., Bautch, V.L., 2017. Dynamic alterations in decoy VEGF receptor-1 stability regulate angiogenesis. Nat. Commun. 8, 15699. https://doi.org/10.1038/ncomms15699

Bringmann, A., Pannicke, T., Grosche, J., Francke, M., Wiedemann, P., Skatchkov, S.N., Osborne, N.N., Reichenbach, A., 2006. Müller cells in the healthy and diseased retina. Prog. Retin. Eye Res. 25, 397–424. https://doi.org/10.1016/j.preteyeres.2006.05.003

Bub, A., Watzl, B., Heeb, D., Rechkemmer, G., Briviba, K., 2001. Malvidin-3-glucoside bioavailability in humans after ingestion of red wine, dealcoholized red wine and red grape juice. Eur. J. Nutr. 40, 113–120. https://doi.org/10.1007/s003940170011

Caccetta, R.A., Croft, K.D., Beilin, L.J., Puddey, I.B., 2000. Ingestion of red wine significantly increases plasma phenolic acid concentrations but does not acutely affect ex vivo lipoprotein oxidizability. Am. J. Clin. Nutr. 71, 67–74. https://doi.org/10.1093/ajcn/71.1.67

Careri, M., Corradini, C., Elviri, L., Nicoletti, I., Zagnoni, I., 2003. Direct HPLC analysis of quercetin and trans-resveratrol in red wine, grape, and winemaking byproducts. J. Agric. Food Chem. 51, 5226–5231. https://doi.org/10.1021/jf034149g

Carmeliet, P., Jain, R.K., 2011. Molecular mechanisms and clinical applications of angiogenesis. Nature 473, 298–307. https://doi.org/10.1038/nature10144

Cartron, E., Fouret, G., Carbonneau, M.-A., Lauret, C., Michel, F., Monnier, L., Descomps, B., Léger, C.L., 2003. Red-wine beneficial long-term effect on lipids but not on antioxidant characteristics in plasma in a study comparing three types of wine--description of two O-methylated derivatives of gallic acid in humans. Free Radic. Res. 37, 1021–1035. https://doi.org/10.1080/10715760310001598097

Chakravarthy, U., McKay, G.J., de Jong, P.T.V.M., Rahu, M., Seland, J., Soubrane, G., Tomazzoli, L., Topouzis, F., Vingerling, J.R., Vioque, J., Young, I.S., Sofat, R., Hingorani, A.D., Fletcher, A.E., 2013. ARMS2 increases the risk of early and late age-related macular degeneration in the European Eye Study. Ophthalmology 120, 342–348. https://doi.org/10.1016/j.ophtha.2012.08.004

Chalam, K.V., Grover, S., Sambhav, K., Balaiya, S., Murthy, R.K., 2014. Aqueous Interleukin-6 Levels Are Superior to Vascular Endothelial Growth Factor in Predicting Therapeutic Response to Bevacizumab in Age-Related Macular Degeneration. J. Ophthalmol. 2014, 502174. https://doi.org/10.1155/2014/502174

Chalam, K.V., Khetpal, V., Rusovici, R., Balaiya, S., 2011. A review: role of ultraviolet radiation in age-related macular degeneration. Eye Contact Lens 37, 225–232. https://doi.org/10.1097/ICL.0b013e31821fbd3e

Chalons, P., Amor, S., Courtaut, F., Cantos-Villar, E., Richard, T., Auger, C., Chabert, P., Schni-Kerth, V., Aires, V., Delmas, D., 2018. Study of Potential Anti-Inflammatory Effects of Red Wine Extract

and Resveratrol through a Modulation of Interleukin-1-Beta in Macrophages. Nutrients 10, 1856. https://doi.org/10.3390/nu10121856

Chalons, P., Courtaut, F., Limagne, E., Chalmin, F., Cantos-Villar, E., Richard, T., Auger, C., Chabert, P., Schini-Kerth, V., Ghiringhelli, F., Aires, V., Delmas, D., 2020. Red Wine Extract Disrupts Th17 Lymphocyte Differentiation in a Colorectal Cancer Context. Mol. Nutr. Food Res. 64, e1901286. https://doi.org/10.1002/mnfr.201901286

Chan, C.-M., Huang, C.-H., Li, H.-J., Hsiao, C.-Y., Su, C.-C., Lee, P.-L., Hung, C.-F., 2015. Protective Effects of Resveratrol against UVA-Induced Damage in ARPE19 Cells. Int. J. Mol. Sci. 16, 5789–5802. https://doi.org/10.3390/ijms16035789

Chen, H., Yu, K.-D., Xu, G.-Z., 2012. Association between Variant Y402H in Age-Related Macular Degeneration (AMD) Susceptibility Gene CFH and Treatment Response of AMD: A Meta-Analysis. PLoS ONE 7, e42464. https://doi.org/10.1371/journal.pone.0042464

Chen, L., Messinger, J.D., Kar, D., Duncan, J.L., Curcio, C.A., 2021. Biometrics, Impact, and Significance of Basal Linear Deposit and Subretinal Drusenoid Deposit in Age-Related Macular Degeneration. Invest. Ophthalmol. Vis. Sci. 62, 33. https://doi.org/10.1167/iovs.62.1.33

Chen, X., Han, R., Hao, P., Wang, L., Liu, M., Jin, M., Kong, D., Li, X., 2018. Nepetin inhibits IL-1β induced inflammation via NF-κB and MAPKs signaling pathways in ARPE-19 cells. Biomed. Pharmacother. 101, 87–93. https://doi.org/10.1016/j.biopha.2018.02.054

Como, C.N., Cervantes, C., Pawlikowski, B., Siegenthaler, J., 2023. Retinoic acid signaling in mouse retina endothelial cells is required for early angiogenic growth. Differ. Res. Biol. Divers. 130, 16–27. https://doi.org/10.1016/j.diff.2022.12.002

Courtaut, F., Aires, V., Acar, N., Bretillon, L., Guerrera, I.C., Chhuon, C., Pais de Barros, J.-P., Olmiere, C., Delmas, D., 2021a. RESVEGA, a Nutraceutical Omega-3/Resveratrol Supplementation, Reduces Angiogenesis in a Preclinical Mouse Model of Choroidal Neovascularization. Int. J. Mol. Sci. 22, 11023. https://doi.org/10.3390/ijms222011023

Courtaut, F., Scagliarini, A., Aires, V., Cornebise, C., Pais de Barros, J.-P., Olmiere, C., Delmas, D., 2021b. VEGF-R2/Caveolin-1 Pathway of Undifferentiated ARPE-19 Retina Cells: A Potential Target as Anti-VEGF-A Therapy in Wet AMD by Resvega, an Omega-3/Polyphenol Combination. Int. J. Mol. Sci. 22, 6590. https://doi.org/10.3390/ijms22126590

Cunha-Vaz, J., Bernardes, R., Lobo, C., 2011. Blood-retinal barrier. Eur. J. Ophthalmol. 21 Suppl 6, S3-9. https://doi.org/10.5301/EJO.2010.6049

Curcio, C.A., Sloan, K.R., Kalina, R.E., Hendrickson, A.E., 1990. Human photoreceptor topography. J. Comp. Neurol. 292, 497–523. https://doi.org/10.1002/cne.902920402

Datta, S., Cano, M., Ebrahimi, K., Wang, L., Handa, J.T., 2017. The Impact of Oxidative Stress and Inflammation on RPE Degeneration in Non-neovascular AMD. Prog. Retin. Eye Res. 60, 201–218. https://doi.org/10.1016/j.preteyeres.2017.03.002

Delmas, D., Cornebise, C., Courtaut, F., Xiao, J., Aires, V., 2021. New Highlights of Resveratrol: A Review of Properties against Ocular Diseases. Int. J. Mol. Sci. 22, 1295. https://doi.org/10.3390/ijms22031295

Delmas, D., Jannin, B., Latruffe, N., 2005. Resveratrol: Preventing properties against vascular alterations and ageing. Mol. Nutr. Food Res. 49, 377–395. https://doi.org/10.1002/mnfr.200400098

Delmas, D., Lancon, A., Colin, D., Jannin, B., Latruffe, N., 2006. Resveratrol as a Chemopreventive Agent: A Promising Molecule for Fighting Cancer. Curr. Drug Targets 7, 423–442. https://doi.org/10.2174/138945006776359331

Delmas, D., Limagne, E., Ghiringhelli, F., Aires, V., 2020. Immune Th17 lymphocytes play a critical role in the multiple beneficial properties of resveratrol. Food Chem. Toxicol. 137, 111091. https://doi.org/10.1016/j.fct.2019.111091

Delmas, D., Solary, E., Latruffe, N., 2011. Resveratrol, a Phytochemical Inducer of Multiple Cell Death Pathways: Apoptosis, Autophagy and Mitotic Catastrophe. Curr. Med. Chem. 18, 1100–1121. https://doi.org/10.2174/092986711795029708

DelMonte, D.W., Kim, T., 2011. Anatomy and physiology of the cornea. J. Cataract Refract. Surg. 37, 588–598. https://doi.org/10.1016/j.jcrs.2010.12.037

Demb, J.B., Zaghloul, K., Haarsma, L., Sterling, P., 2001. Bipolar cells contribute to nonlinear spatial summation in the brisk-transient (Y) ganglion cell in mammalian retina. J. Neurosci. Off. J. Soc. Neurosci. 21, 7447–7454. https://doi.org/10.1523/JNEUROSCI.21-19-07447.2001

Deng, Y., Qiao, L., Du, M., Qu, C., Wan, L., Li, J., Huang, L., 2021. Age-related macular degeneration: Epidemiology, genetics, pathophysiology, diagnosis, and targeted therapy. Genes Dis. 9, 62–79. https://doi.org/10.1016/j.gendis.2021.02.009

Dinc, E., Ayaz, L., Kurt, A.H., 2017. Protective Effect of Combined Caffeic Acid Phenethyl Ester and Bevacizumab Against Hydrogen Peroxide-Induced Oxidative Stress in Human RPE Cells. Curr. Eye Res. 42, 1659–1666. https://doi.org/10.1080/02713683.2017.1368085

Dixon, M.A., Greferath, U., Fletcher, E.L., Jobling, A.I., 2021. The Contribution of Microglia to the Development and Maturation of the Visual System. Front. Cell. Neurosci. 15, 659843. https://doi.org/10.3389/fncel.2021.659843

Donovan, J.L., Bell, J.R., Kasim-Karakas, S., German, J.B., Walzem, R.L., Hansen, R.J., Waterhouse, A.L., 1999. Catechin is present as metabolites in human plasma after consumption of red wine. J. Nutr. 129, 1662–1668. https://doi.org/10.1093/jn/129.9.1662

Dugas, B., Charbonnier, S., Baarine, M., Ragot, K., Delmas, D., Ménétrier, F., Lherminier, J., Malvitte, L., Khalfaoui, T., Bron, A., Creuzot-Garcher, C., Latruffe, N., Lizard, G., 2010. Effects of oxysterols on cell viability, inflammatory cytokines, VEGF, and reactive oxygen species production on human retinal cells: cytoprotective effects and prevention of VEGF secretion by resveratrol. Eur. J. Nutr. 49, 435–446. https://doi.org/10.1007/s00394-010-0102-2

Dumond, A., Demange, L., Pagès, G., 2020. Les neuropilines - Des cibles pertinentes pour améliorer le traitement des cancers. médecine/sciences 36, 487–496. https://doi.org/10.1051/medsci/2020080

Dunn, K.C., Aotaki-Keen, A.E., Putkey, F.R., Hjelmeland, L.M., 1996. ARPE-19, a human retinal pigment epithelial cell line with differentiated properties. Exp. Eye Res. 62, 155–169. https://doi.org/10.1006/exer.1996.0020

Erlund, I., Kosonen, T., Alfthan, G., Mäenpää, J., Perttunen, K., Kenraali, J., Parantainen, J., Aro, A., 2000. Pharmacokinetics of quercetin from quercetin aglycone and rutin in healthy volunteers. Eur. J. Clin. Pharmacol. 56, 545–553. https://doi.org/10.1007/s002280000197

Esser, S., Wolburg, K., Wolburg, H., Breier, G., Kurzchalia, T., Risau, W., 1998. Vascular Endothelial Growth Factor Induces Endothelial Fenestrations In Vitro. J. Cell Biol. 140, 947. https://doi.org/10.1083/jcb.140.4.947

Ezzat, M.-K., Hann, C.R., Vuk-Pavlovic, S., Pulido, J.S., 2008. Immune cells in the human choroid. Br. J. Ophthalmol. 92, 976–980. https://doi.org/10.1136/bjo.2007.129742

Faber, C., Singh, A., Krüger Falk, M., Juel, H.B., Sørensen, T.L., Nissen, M.H., 2013. Age-related macular degeneration is associated with increased proportion of CD56(+) T cells in peripheral blood. Ophthalmology 120, 2310–2316. https://doi.org/10.1016/j.ophtha.2013.04.014

Fahey, E., Doyle, S.L., 2019. IL-1 Family Cytokine Regulation of Vascular Permeability and Angiogenesis. Front. Immunol. 10, 1426. https://doi.org/10.3389/fimmu.2019.01426

Farneti, B., Masuero, D., Costa, F., Magnago, P., Malnoy, M., Costa, G., Vrhovsek, U., Mattivi, F., 2015. Is there room for improving the nutraceutical composition of apple? J. Agric. Food Chem. 63, 2750–2759. https://doi.org/10.1021/acs.jafc.5b00291

Ferrara, N., 2004. Vascular endothelial growth factor: basic science and clinical progress. Endocr. Rev. 25, 581–611. https://doi.org/10.1210/er.2003-0027

Finch, C.E., Ruvkun, G., 2001. The genetics of aging. Annu. Rev. Genomics Hum. Genet. 2, 435–462. https://doi.org/10.1146/annurev.genom.2.1.435

Fisher, C.R., Ebeling, M.C., Geng, Z., Kapphahn, R.J., Roehrich, H., Montezuma, S.R., Dutton, J.R., Ferrington, D.A., 2022. Human iPSC- and Primary-Retinal Pigment Epithelial Cells for Modeling Age-Related Macular Degeneration. Antioxidants 11, 605. https://doi.org/10.3390/antiox11040605

Folkman, J., 1971. Tumor angiogenesis: therapeutic implications. N. Engl. J. Med. 285, 1182–1186. https://doi.org/10.1056/NEJM197111182852108

Ford, K.M., Saint-Geniez, M., Walshe, T., Zahr, A., D'Amore, P.A., 2011. Expression and Role of VEGF in the Adult Retinal Pigment Epithelium. Invest. Ophthalmol. Vis. Sci. 52, 9478–9487. https://doi.org/10.1167/iovs.11-8353

Frank, R.N., Amin, R.H., Eliott, D., Puklin, J.E., Abrams, G.W., 1996. Basic fibroblast growth factor and vascular endothelial growth factor are present in epiretinal and choroidal neovascular membranes. Am. J. Ophthalmol. 122, 393–403. https://doi.org/10.1016/s0002-9394(14)72066-5

Fritsche, L.G., Chen, W., Schu, M., Yaspan, B.L., Yu, Y., Thorleifsson, G., Zack, D.J., Arakawa, S., Cipriani, V., Ripke, S., Igo, R.P., Buitendijk, G.H.S., Sim, X., Weeks, D.E., Guymer, R.H., Merriam, J.E., Francis, P.J., Hannum, G., Agarwal, A., Armbrecht, A.M., Audo, I., Aung, T., Barile, G.R., Benchaboune, M., Bird, A.C., Bishop, P.N., Branham, K.E., Brooks, M., Brucker, A.J., Cade, W.H., Cain, M.S., Campochiaro, P.A., Chan, C.-C., Cheng, C.-Y., Chew, E.Y., Chin, K.A., Chowers, I., Clayton, D.G., Cojocaru, R., Conley, Y.P., Cornes, B.K., Daly, M.J., Dhillon, B., Edwards, A.O., Evangelou, E., Fagerness, J., Ferreyra, H.A., Friedman, J.S., Geirsdottir, A., George, R.J., Gieger, C., Gupta, N., Hagstrom, S.A., Harding, S.P., Haritoglou, C., Heckenlively, J.R., Holz, F.G., Hughes, G., Ioannidis, J.P.A., Ishibashi, T., Joseph, P., Jun, G., Kamatani, Y., Katsanis, N., N Keilhauer, C., Khan, J.C., Kim, I.K., Kiyohara, Y., Klein, B.E.K., Klein, R., Kovach, J.L., Kozak, I., Lee, C.J., Lee, K.E., Lichtner, P., Lotery, A.J., Meitinger, T., Mitchell, P., Mohand-Saïd, S., Moore, A.T., Morgan, D.J., Morrison, M.A., Myers, C.E., Naj, A.C., Nakamura, Y., Okada, Y., Orlin, A., Ortube, M.C., Othman, M.I., Pappas, C., Park, K.H., Pauer, G.J.T., Peachey, N.S., Poch, O., Priya, R.R., Reynolds, R., Richardson, A.J., Ripp, R., Rudolph, G., Ryu, E., Sahel, J.-A., Schaumberg, D.A., Scholl, H.P.N., Schwartz, S.G., Scott, W.K., Shahid, H., Sigurdsson, H., Silvestri, G., Sivakumaran, T.A., Smith, R.T., Sobrin, L., Souied, E.H., Stambolian, D.E., Stefansson, H., Sturgill-Short, G.M., Takahashi, A., Tosakulwong, N., Truitt, B.J., Tsironi, E.E., Uitterlinden, A.G., van Duijn, C.M., Vijaya, L., Vingerling, J.R., Vithana, E.N., Webster, A.R., Wichmann, H.-E., Winkler, T.W., Wong, T.Y., Wright, A.F., Zelenika, D., Zhang, M., Zhao, L., Zhang, K., Klein, M.L., Hageman, G.S., Lathrop, G.M., Stefansson, K., Allikmets, R., Baird, P.N., Gorin, M.B., Wang, J.J., Klaver, C.C.W., Seddon, J.M., Pericak-Vance, M.A., Iyengar, S.K., Yates, J.R.W., Swaroop, A., Weber, B.H.F., Kubo, M., Deangelis, M.M., Léveillard, T., Thorsteinsdottir, U., Haines, J.L., Farrer, L.A., Heid, I.M., Abecasis, G.R., AMD Gene Consortium, 2013. Seven new loci associated with age-related macular degeneration. Nat. Genet. 45, 433–439, 439e1-2. https://doi.org/10.1038/ng.2578

Fritsche, L.G., Igl, W., Bailey, J.N.C., Grassmann, F., Sengupta, S., Bragg-Gresham, J.L., Burdon, K.P., Hebbring, S.J., Wen, C., Gorski, M., Kim, I.K., Cho, D., Zack, D., Souied, E., Scholl, H.P.N., Bala, E., Lee, K.E., Hunter, D.J., Sardell, R.J., Mitchell, P., Merriam, J.E., Cipriani, V., Hoffman, J.D., Schick, T., Lechanteur, Y.T.E., Guymer, R.H., Johnson, M.P., Jiang, Y., Stanton, C.M., Buitendijk, G.H.S., Zhan, X., Kwong, A.M., Boleda, A., Brooks, M., Gieser, L., Ratnapriya, R., Branham, K.E., Foerster, J.R., Heckenlively, J.R., Othman, M.I., Vote, B.J., Liang, H.H., Souzeau, E., McAllister, I.L., Isaacs, T., Hall, J., Lake, S., Mackey, D.A., Constable, I.J., Craig, J.E., Kitchner, T.E., Yang, Z., Su, Z., Luo, H., Chen, D., Ouyang, H., Flagg, K., Lin, D., Mao, G., Ferreyra, H., Stark, K., von Strachwitz, C.N., Wolf, A., Brandl, C., Rudolph, G., Olden, M., Morrison, M.A., Morgan, D.J., Schu, M., Ahn, J., Silvestri, G., Tsironi, E.E., Park, K.H., Farrer, L.A., Orlin, A., Brucker, A., Li, M., Curcio, C.A., Mohand-Saïd, S., Sahel, J.-A., Audo, I., Benchaboune, M., Cree, A.J., Rennie, C.A., Goverdhan, S.V., Grunin, M., Hagbi-Levi, S., Campochiaro, P., Katsanis, N., Holz, F.G., Blond, F., Blanché, H., Deleuze, J.-F., Igo, R.P., Truitt, B., Peachey, N.S., Meuer, S.M., Myers, C.E., Moore, E.L., Klein, R., Hauser, M.A., Postel, E.A., Courtenay, M.D., Schwartz, S.G., Kovach, J.L., Scott, W.K., Liew, G., Tan, A.G., Gopinath, B., Merriam, J.C., Smith, R.T., Khan, J.C., Shahid, H., Moore, A.T., McGrath, J.A., Laux, R., Brantley, M.A., Agarwal, A., Ersoy, L., Caramoy, A., Langmann, T., Saksens, N.T.M., de Jong, E.K., Hoyng, C.B., Cain, M.S., Richardson, A.J., Martin, T.M., Blangero, J., Weeks, D.E., Dhillon, B., van Duijn, C.M., Doheny,

K.F., Romm, J., Klaver, C.C.W., Hayward, C., Gorin, M.B., Klein, M.L., Baird, P.N., den Hollander, A.I., Fauser, S., Yates, J.R.W., Allikmets, R., Wang, J.J., Schaumberg, D.A., Klein, B.E.K., Hagstrom, S.A., Chowers, I., Lotery, A.J., Léveillard, T., Zhang, K., Brilliant, M.H., Hewitt, A.W., Swaroop, A., Chew, E.Y., Pericak-Vance, M.A., DeAngelis, M., Stambolian, D., Haines, J.L., Iyengar, S.K., Weber, B.H.F., Abecasis, G.R., Heid, I.M., 2016. A large genome-wide association study of age-related macular degeneration highlights contributions of rare and common variants. Nat. Genet. 48, 134–143. https://doi.org/10.1038/ng.3448

Fu, Y., 1995. Phototransduction in Rods and Cones, in: Kolb, H., Fernandez, E., Nelson, R. (Eds.), Webvision: The Organization of the Retina and Visual System. University of Utah Health Sciences Center, Salt Lake City (UT).

Gao, F., Wang, L., Wu, B., Ou, Q., Tian, H., Xu, J., Jin, C., Zhang, J., Wang, J., Lu, L., Xu, G.-T., 2022. Elimination of senescent cells inhibits epithelial-mesenchymal transition of retinal pigment epithelial cells. Exp. Eye Res. 223, 109207. https://doi.org/10.1016/j.exer.2022.109207

Garcia-Alonso, M., Minihane, A.-M., Rimbach, G., Rivas-Gonzalo, J.C., de Pascual-Teresa, S., 2009. Red wine anthocyanins are rapidly absorbed in humans and affect monocyte chemoattractant protein 1 levels and antioxidant capacity of plasma. J. Nutr. Biochem. 20, 521–529. https://doi.org/10.1016/j.jnutbio.2008.05.011

Goldberg, D.M., Yan, J., Soleas, G.J., 2003. Absorption of three wine-related polyphenols in three different matrices by healthy subjects. Clin. Biochem. 36, 79–87. https://doi.org/10.1016/s0009-9120(02)00397-1

Gopinath, B., Liew, G., Kifley, A., Flood, V.M., Joachim, N., Lewis, J.R., Hodgson, J.M., Mitchell, P., 2018. Dietary flavonoids and the prevalence and 15-y incidence of age-related macular degeneration. Am. J. Clin. Nutr. 108, 381–387. https://doi.org/10.1093/ajcn/nqy114

Graefe, E.U., Wittig, J., Mueller, S., Riethling, A.K., Uehleke, B., Drewelow, B., Pforte, H., Jacobasch, G., Derendorf, H., Veit, M., 2001. Pharmacokinetics and bioavailability of quercetin glycosides in humans. J. Clin. Pharmacol. 41, 492–499. https://doi.org/10.1177/00912700122010366

Graw, J., 2010. Chapter Ten - Eye Development, in: Koopman, P. (Ed.), Current Topics in Developmental Biology, Organogenesis in Development. Academic Press, pp. 343–386. https://doi.org/10.1016/S0070-2153(10)90010-0

Green, W.R., Enger, C., 1993. Age-related macular degeneration histopathologic studies. The 1992 Lorenz E. Zimmerman Lecture. Ophthalmology 100, 1519–1535. https://doi.org/10.1016/s0161-6420(93)31466-1

Guillonneau, X., Eandi, C.M., Paques, M., Sahel, J.-A., Sapieha, P., Sennlaub, F., 2017. On phagocytes and macular degeneration. Prog. Retin. Eye Res. 61, 98–128. https://doi.org/10.1016/j.preteyeres.2017.06.002

Hallam, T.M., Cox, T.E., Smith-Jackson, K., Brocklebank, V., Baral, A.J., Tzoumas, N., Steel, D.H., Wong, E.K.S., Shuttleworth, V.G., Lotery, A.J., Harris, C.L., Marchbank, K.J., Kavanagh, D., 2022. A novel method for real-time analysis of the complement C3b:FH:FI complex reveals dominant negative CFI variants in age-related macular degeneration. Front. Immunol. 13, 1028760. https://doi.org/10.3389/fimmu.2022.1028760

Hamilton, R.T., Walsh, M.E., Van Remmen, H., 2012. Mouse Models of Oxidative Stress Indicate a Role for Modulating Healthy Aging. J. Clin. Exp. Pathol. Suppl 4, 005. https://doi.org/10.4172/2161-0681.S4-005

Hammadi, S., Tzoumas, N., Ferrara, M., Meschede, I.P., Lo, K., Harris, C., Lako, M., Steel, D.H., 2023. Bruch's Membrane: A Key Consideration with Complement-Based Therapies for Age-Related Macular Degeneration. J. Clin. Med. 12, 2870. https://doi.org/10.3390/jcm12082870

Hao, Y., Liu, J., Wang, Z., Yu, L.L., Wang, J., 2019. Piceatannol Protects Human Retinal Pigment Epithelial Cells against Hydrogen Peroxide Induced Oxidative Stress and Apoptosis through Modulating PI3K/Akt Signaling Pathway. Nutrients 11, 1515. https://doi.org/10.3390/nu11071515

Harman, D., 1981. The aging process. Proc. Natl. Acad. Sci. U. S. A. 78, 7124–7128. https://doi.org/10.1073/pnas.78.11.7124

Hart, K.M., Abbott, C., Ly, A., Kalff, S., Lek, J.J., Milston, R., Page, G., Robertson, B., Ayton, L., 2020. Optometry Australia's chairside reference for the diagnosis and management of age-related macular degeneration. Clin. Exp. Optom. 103, 254–264. https://doi.org/10.1111/cxo.12964

Hashizume, K., Hirasawa, M., Imamura, Y., Noda, S., Shimizu, T., Shinoda, K., Kurihara, T., Noda, K., Ozawa, Y., Ishida, S., Miyake, Y., Shirasawa, T., Tsubota, K., 2008. Retinal Dysfunction and Progressive Retinal Cell Death in SOD1-Deficient Mice. Am. J. Pathol. 172, 1325–1331. https://doi.org/10.2353/ajpath.2008.070730

He, J., Giusti, M.M., 2010. Anthocyanins: natural colorants with health-promoting properties. Annu. Rev. Food Sci. Technol. 1, 163–187. https://doi.org/10.1146/annurev.food.080708.100754

Ho, V.C., Fong, G.-H., 2015. Vasculogenesis and Angiogenesis in VEGF Receptor-1 Deficient Mice. Methods Mol. Biol. Clifton NJ 1332, 161–176. https://doi.org/10.1007/978-1-4939-2917-7_12

Hsu, M.-Y., Hsiao, Y.-P., Lin, Y.-T., Chen, C., Lee, C.-M., Liao, W.-C., Tsou, S.-C., Lin, H.-W., Chang, Y.-Y., 2021. Quercetin Alleviates the Accumulation of Superoxide in Sodium Iodate-Induced Retinal Autophagy by Regulating Mitochondrial Reactive Oxygen Species Homeostasis through Enhanced Deacetyl-SOD2 via the Nrf2-PGC-1α-Sirt1 Pathway. Antioxid. Basel Switz. 10, 1125. https://doi.org/10.3390/antiox10071125

Hu, M.L., Quinn, J., Xue, K., 2021. Interactions between Apolipoprotein E Metabolism and Retinal Inflammation in Age-Related Macular Degeneration. Life 11, 635. https://doi.org/10.3390/life11070635

Hurst, W.J., Glinski, J.A., Miller, K.B., Apgar, J., Davey, M.H., Stuart, D.A., 2008. Survey of the trans-resveratrol and trans-piceid content of cocoa-containing and chocolate products. J. Agric. Food Chem. 56, 8374–8378. https://doi.org/10.1021/jf801297w

Hussain, A.A., Lee, Y., Zhang, J.-J., Marshall, J., 2011. Disturbed matrix metalloproteinase activity of Bruch's membrane in age-related macular degeneration. Invest. Ophthalmol. Vis. Sci. 52, 4459–4466. https://doi.org/10.1167/iovs.10-6678

Hyttinen, J.M.T., Viiri, J., Kaarniranta, K., Błasiak, J., 2018. Mitochondrial quality control in AMD: does mitophagy play a pivotal role? Cell. Mol. Life Sci. 75, 2991–3008. https://doi.org/10.1007/s00018-018-2843-7

Imanishi, S., Tomita, Y., Negishi, K., Tsubota, K., Kurihara, T., 2023. Molecular and Cellular Regulations in the Development of the Choroidal Circulation System. Int. J. Mol. Sci. 24, 5371. https://doi.org/10.3390/ijms24065371

Ivanov, I.V., Mappes, T., Schaupp, P., Lappe, C., Wahl, S., 2018. Ultraviolet radiation oxidative stress affects eye health. J. Biophotonics 11, e201700377. https://doi.org/10.1002/jbio.201700377

Jackson, G.R., Owsley, C., Curcio, C.A., 2002. Photoreceptor degeneration and dysfunction in aging and age-related maculopathy. Ageing Res. Rev. 1, 381–396. https://doi.org/10.1016/s1568-1637(02)00007-7

Jampol, L.M., Glassman, A.R., Sun, J., 2020. Evaluation and Care of Patients with Diabetic Retinopathy. N. Engl. J. Med. 382, 1629–1637. https://doi.org/10.1056/NEJMra1909637

Jeandet, P., Bessis, R., Maume, B.F., Sbaghi, M., 1993. Analysis of resveratrol in Burgundy wines. J. Wine Res. 4, 79–85. https://doi.org/10.1080/09571269308717954

Jin, M., Li, S., Nusinowitz, S., Lloyd, M., Hu, J., Radu, R.A., Bok, D., Travis, G.H., 2009. The Role of Interphotoreceptor Retinoid-Binding Protein on the Translocation of Visual Retinoids and Function of Cone Photoreceptors. J. Neurosci. 29, 1486–1495. https://doi.org/10.1523/JNEUROSCI.3882-08.2009

Jin, X., Wang, C., Wu, W., Liu, T., Ji, B., Zhou, F., 2018. Cyanidin-3-glucoside Alleviates 4-Hydroxyhexenal-Induced NLRP3 Inflammasome Activation via JNK-c-Jun/AP-1 Pathway in Human Retinal Pigment Epithelial Cells. J. Immunol. Res. 2018, 5604610. https://doi.org/10.1155/2018/5604610

Kaiser, P., 2009. Prospective evaluation of visual acuity assessment: a comparison of snellen versus ETDRS charts in clinical practice (An AOS Thesis). Trans. Am. Ophthalmol. Soc.

Kang, J.-H., Choung, S.-Y., 2016. Protective effects of resveratrol and its analogs on age-related macular degeneration in vitro. Arch. Pharm. Res. 39, 1703–1715. https://doi.org/10.1007/s12272-016-0839-0

Karkkainen, M.J., Haiko, P., Sainio, K., Partanen, J., Taipale, J., Petrova, T.V., Jeltsch, M., Jackson, D.G., Talikka, M., Rauvala, H., Betsholtz, C., Alitalo, K., 2004. Vascular endothelial growth factor C is required for sprouting of the first lymphatic vessels from embryonic veins. Nat. Immunol. 5, 74–80. https://doi.org/10.1038/ni1013

Karunadharma, P.P., Nordgaard, C.L., Olsen, T.W., Ferrington, D.A., 2010. Mitochondrial DNA Damage as a Potential Mechanism for Age-Related Macular Degeneration. Invest. Ophthalmol. Vis. Sci. 51, 5470–5479. https://doi.org/10.1167/iovs.10-5429

Kauppinen, A., Paterno, J.J., Blasiak, J., Salminen, A., Kaarniranta, K., 2016. Inflammation and its role in age-related macular degeneration. Cell. Mol. Life Sci. 73, 1765–1786. https://doi.org/10.1007/s00018-016-2147-8

Kaushik, V., Gessa, L., Kumar, N., Fernandes, H., 2023. Towards a New Biomarker for Diabetic Retinopathy: Exploring RBP3 Structure and Retinoids Binding for Functional Imaging of Eyes In Vivo. Int. J. Mol. Sci. 24, 4408. https://doi.org/10.3390/ijms24054408

Kciuk, M., Marciniak, B., Mojzych, M., Kontek, R., 2020. Focus on UV-Induced DNA Damage and Repair-Disease Relevance and Protective Strategies. Int. J. Mol. Sci. 21, 7264. https://doi.org/10.3390/ijms21197264

Kels, B.D., Grzybowski, A., Grant-Kels, J.M., 2015. Human ocular anatomy. Clin. Dermatol. 33, 140–146. https://doi.org/10.1016/j.clindermatol.2014.10.006

Kensler, T.W., Wakabayashi, N., Biswal, S., 2007. Cell survival responses to environmental stresses via the Keap1-Nrf2-ARE pathway. Annu. Rev. Pharmacol. Toxicol. 47, 89–116. https://doi.org/10.1146/annurev.pharmtox.46.120604.141046

Kim, Jeong Hun, Lee, B.J., Kim, Jin Hyoung, Yu, Y.S., Kim, K.-W., 2009. Anti-angiogenic effect of caffeic acid on retinal neovascularization. Vascul. Pharmacol. 51, 262–267. https://doi.org/10.1016/j.vph.2009.06.010

King, R.E., Kent, K.D., Bomser, J.A., 2005. Resveratrol reduces oxidation and proliferation of human retinal pigment epithelial cells via extracellular signal-regulated kinase inhibition. Chem. Biol. Interact. 151, 143–149. https://doi.org/10.1016/j.cbi.2004.11.003

Klaver, C.C., Kliffen, M., van Duijn, C.M., Hofman, A., Cruts, M., Grobbee, D.E., van Broeckhoven, C., de Jong, P.T., 1998. Genetic association of apolipoprotein E with age-related macular degeneration. Am. J. Hum. Genet. 63, 200–206. https://doi.org/10.1086/301901

Klein, R.J., Zeiss, C., Chew, E.Y., Tsai, J.-Y., Sackler, R.S., Haynes, C., Henning, A.K., SanGiovanni, J.P., Mane, S.M., Mayne, S.T., Bracken, M.B., Ferris, F.L., Ott, J., Barnstable, C., Hoh, J., 2005. Complement factor H polymorphism in age-related macular degeneration. Science 308, 385–389. https://doi.org/10.1126/science.1109557

Klettner, A., Roider, J., 2021. Retinal Pigment Epithelium Expressed Toll-like Receptors and Their Potential Role in Age-Related Macular Degeneration. Int. J. Mol. Sci. 22, 8387. https://doi.org/10.3390/ijms22168387

Kode, A., Rajendrasozhan, S., Caito, S., Yang, S.-R., Megson, I.L., Rahman, I., 2008. Resveratrol induces glutathione synthesis by activation of Nrf2 and protects against cigarette smoke-mediated oxidative stress in human lung epithelial cells. Am. J. Physiol. Lung Cell. Mol. Physiol. 294, L478-488. https://doi.org/10.1152/ajplung.00361.2007

Korb, C.A., Beck, S., Wolters, D., Lorenz, K., Pfeiffer, N., Grus, F.H., 2023a. Serum Autoantibodies in Patients with Dry and Wet Age-Related Macular Degeneration. J. Clin. Med. 12, 1590. https://doi.org/10.3390/jcm12041590

Korb, C.A., Lackner, K.J., Wolters, D., Schuster, A.K., Nickels, S., Beutgen, V.M., Münzel, T., Wild, P.S., Beutel, M.E., Schmidtmann, I., Pfeiffer, N., Grus, F.H., 2023b. Association of autoantibody levels

with different stages of age-related macular degeneration (AMD): Results from the population-based Gutenberg Health Study (GHS). Graefes Arch. Clin. Exp. Ophthalmol. Albrecht Von Graefes Arch. Klin. Exp. Ophthalmol. https://doi.org/10.1007/s00417-023-06085-2

Kozhevnikova, O.S., Fursova, A.Z., Derbeneva, A.S., Nikulich, I.F., Tarasov, M.S., Devyatkin, V.A., Rumyantseva, Y.V., Telegina, D.V., Kolosova, N.G., 2022. Association between Polymorphisms in CFH, ARMS2, CFI, and C3 Genes and Response to Anti-VEGF Treatment in Neovascular Age-Related Macular Degeneration. Biomedicines 10, 1658. https://doi.org/10.3390/biomedicines10071658

Krogh Nielsen, M., Subhi, Y., Molbech, C.R., Falk, M.K., Nissen, M.H., Sørensen, T.L., 2019. Systemic Levels of Interleukin-6 Correlate With Progression Rate of Geographic Atrophy Secondary to Age-Related Macular Degeneration. Invest. Ophthalmol. Vis. Sci. 60, 202–208. https://doi.org/10.1167/iovs.18-25878

Kubicka-Trząska, A., Żuber-Łaskawiec, K., Dziedzina, S., Sanak, M., Romanowska-Dixon, B., Karska-Basta, I., 2022. Genetic Variants of Complement Factor H Y402H (rs1061170), C2 R102G (rs2230199), and C3 E318D (rs9332739) and Response to Intravitreal Anti-VEGF Treatment in Patients with Exudative Age-Related Macular Degeneration. Medicina (Mex.) 58, 658. https://doi.org/10.3390/medicina58050658

Ladoux, A., Frelin, C., 1993. Hypoxia is a strong inducer of vascular endothelial growth factor mRNA expression in the heart. Biochem. Biophys. Res. Commun. 195, 1005–1010. https://doi.org/10.1006/bbrc.1993.2144

Lechner, J., Chen, M., Hogg, R.E., Toth, L., Silvestri, G., Chakravarthy, U., Xu, H., 2017. Peripheral blood mononuclear cells from neovascular age-related macular degeneration patients produce higher levels of chemokines CCL2 (MCP-1) and CXCL8 (IL-8). J. Neuroinflammation 14, 42. https://doi.org/10.1186/s12974-017-0820-y

Lee, A.Y., Raya, A.K., Kymes, S.M., Shiels, A., Brantley, M.A., 2009. Pharmacogenetics of complement factor H (Y402H) and treatment of exudative age-related macular degeneration with ranibizumab. Br. J. Ophthalmol. 93, 610–613. https://doi.org/10.1136/bjo.2008.150995

Lee, M., Yun, S., Lee, H., Yang, J., 2017. Quercetin Mitigates Inflammatory Responses Induced by Vascular Endothelial Growth Factor in Mouse Retinal Photoreceptor Cells through Suppression of Nuclear Factor Kappa B. Int. J. Mol. Sci. 18, 2497. https://doi.org/10.3390/ijms18112497

Lee, S.J., Roh, Y.J., Kim, J.E., Jin, Y.J., Song, H.J., Seol, A., Park, S.H., Douangdeuane, B., Souliya, O., Choi, S.I., Hwang, D.Y., 2023. Protective Effects of Dipterocarpus tuberculatus in Blue Light-Induced Macular Degeneration in A2E-Laden ARPE19 Cells and Retina of Balb/c Mice. Antioxid. Basel Switz. 12, 329. https://doi.org/10.3390/antiox12020329

Leonard, S.S., Xia, C., Jiang, B.-H., Stinefelt, B., Klandorf, H., Harris, G.K., Shi, X., 2003. Resveratrol scavenges reactive oxygen species and effects radical-induced cellular responses. Biochem. Biophys. Res. Commun. 309, 1017–1026. https://doi.org/10.1016/j.bbrc.2003.08.105

Leveziel, N., Puche, N., Zerbib, J., Benlian, P., Coscas, G., Soubrane, G., Souied, E., 2010. Génétique de la dégénérescence maculaire liée à l'âge. médecine/sciences 26, 505–515. https://doi.org/10.1051/medsci/2010265509

Leveziel, N., Soubrane, G., Souied, E.H., 2009. Anti-VEGF : applications pratiques en ophtalmologie. médecine/sciences 25, 1105–1107. https://doi.org/10.1051/medsci/200925121105

Li, Z., Xie, H., Tang, C., Feng, L., Ke, C., Xu, Y., Su, H., Yao, S., Ye, Y., 2023. Flavonoids from the roots and rhizomes of Sophoratonkinensis and their in vitro anti-SARS-CoV-2 activity. Chin. J. Nat. Med. 21, 65–80. https://doi.org/10.1016/S1875-5364(23)60386-3

Lin, C.-T., Sun, X.-Y., Lin, A.-X., 2016. Supplementation with high-dose trans-resveratrol improves ultrafiltration in peritoneal dialysis patients: a prospective, randomized, double-blind study. Ren. Fail. 38, 214–221. https://doi.org/10.3109/0886022X.2015.1128236

Liu, X., Zheng, F., Li, S., Wang, Z., Wang, X., Wen, L., He, Y., 2021. Malvidin and its derivatives exhibit antioxidant properties by inhibiting MAPK signaling pathways to reduce endoplasmic

reticulum stress in ARPE-19 cells. Food Funct. 12, 7198–7213. https://doi.org/10.1039/d1fo01345a

Lopez, P.F., Sippy, B.D., Lambert, H.M., Thach, A.B., Hinton, D.R., 1996. Transdifferentiated retinal pigment epithelial cells are immunoreactive for vascular endothelial growth factor in surgically excised age-related macular degeneration-related choroidal neovascular membranes. Invest. Ophthalmol. Vis. Sci. 37, 855–868.

Lorés-Motta, L., van Asten, F., Muether, P.S., Smailhodzic, D., Groenewoud, J.M., Omar, A., Chen, J., Koenekoop, R.K., Fauser, S., Hoyng, C.B., den Hollander, A.I., de Jong, E.K., 2016. A genetic variant in NRP1 is associated with worse response to ranibizumab treatment in neovascular age-related macular degeneration. Pharmacogenet. Genomics 26, 20–27. https://doi.org/10.1097/FPC.0000000000000180

Lyons, M.M., Yu, C., Toma, R.B., Cho, S.Y., Reiboldt, W., Lee, J., van Breemen, R.B., 2003. Resveratrol in raw and baked blueberries and bilberries. J. Agric. Food Chem. 51, 5867–5870. https://doi.org/10.1021/jf034150f

Mammadzada, P., Corredoira, P.M., André, H., 2020. The role of hypoxia-inducible factors in neovascular age-related macular degeneration: a gene therapy perspective. Cell. Mol. Life Sci. 77, 819–833. https://doi.org/10.1007/s00018-019-03422-9

Manach, C., Scalbert, A., Morand, C., Rémésy, C., Jiménez, L., 2004. Polyphenols: food sources and bioavailability. Am. J. Clin. Nutr. 79, 727–747. https://doi.org/10.1093/ajcn/79.5.727

Manley, A., Meshkat, B.I., Jablonski, M.M., Hollingsworth, T.J., 2023. Cellular and Molecular Mechanisms of Pathogenesis Underlying Inherited Retinal Dystrophies. Biomolecules 13, 271. https://doi.org/10.3390/biom13020271

Mao, J., Chen, N., Zhang, S., Fang, Y., Zheng, Z., Wu, S., Ye, X., Chen, Yijing, Chen, Yiqi, Shen, L., 2022. Association between inflammatory cytokines in the aqueous humor and hyperreflective foci on optical coherence tomography in patients with neovascular age-related macular degeneration and polypoidal choroidal vasculopathy. Front. Med. 9, 973025. https://doi.org/10.3389/fmed.2022.973025

Marazita, M.C., Dugour, A., Marquioni-Ramella, M.D., Figueroa, J.M., Suburo, A.M., 2016. Oxidative stress-induced premature senescence dysregulates VEGF and CFH expression in retinal pigment epithelial cells: Implications for Age-related Macular Degeneration. Redox Biol. 7, 78–87. https://doi.org/10.1016/j.redox.2015.11.011

McDougal, D.H., Gamlin, P.D., 2015. Autonomic control of the eye. Compr. Physiol. 5, 439–473. https://doi.org/10.1002/cphy.c140014

McGeough, M.D., Pena, C.A., Mueller, J.L., Pociask, D.A., Broderick, L., Hoffman, H.M., Brydges, S.D., 2012. Cutting edge: IL-6 is a marker of inflammation with no direct role in inflammasome-mediated mouse models. J. Immunol. Baltim. Md 1950 189, 2707–2711. https://doi.org/10.4049/jimmunol.1101737

Mendes, D., Oliveira, M.M., Moreira, P.I., Coutinho, J., Nunes, F.M., Pereira, D.M., Valentão, P., Andrade, P.B., Videira, R.A., 2018. Beneficial effects of white wine polyphenols-enriched diet on Alzheimer's disease-like pathology. J. Nutr. Biochem. 55, 165–177. https://doi.org/10.1016/j.jnutbio.2018.02.001

Migdal, C., Serres, M., 2011. Espèces réactives de l'oxygène et stress oxydant. médecine/sciences 27, 405–412. https://doi.org/10.1051/medsci/2011274017

Moiseyev, G., Chen, Y., Takahashi, Y., Wu, B.X., Ma, J., 2005. RPE65 is the isomerohydrolase in the retinoid visual cycle. Proc. Natl. Acad. Sci. U. S. A. 102, 12413–12418. https://doi.org/10.1073/pnas.0503460102

Murenu, E., Gerhardt, M.-J., Biel, M., Michalakis, S., 2022. More than meets the eye: The role of microglia in healthy and diseased retina. Front. Immunol. 13, 1006897. https://doi.org/10.3389/fimmu.2022.1006897

Natoli, R., Fernando, N., Madigan, M., Chu-Tan, J.A., Valter, K., Provis, J., Rutar, M., 2017. Microglia-derived IL-1β promotes chemokine expression by Müller cells and RPE in focal retinal degeneration. Mol. Neurodegener. 12, 31. https://doi.org/10.1186/s13024-017-0175-y

Neal, S.E., Buehne, K.L., Besley, N.A., Yang, P., Silinski, P., Hong, J., Ryde, I.T., Meyer, J.N., Jaffe, G.J., 2020. Resveratrol Protects Against Hydroquinone-Induced Oxidative Threat in Retinal Pigment Epithelial Cells. Invest. Ophthalmol. Vis. Sci. 61, 32. https://doi.org/10.1167/iovs.61.4.32

Neekhra, A., Tran, J., Esfahani, P.R., Schneider, K., Pham, K., Sharma, A., Chwa, M., Luthra, S., Gramajo, A.L., Mansoor, S., Kuppermann, B.D., Kenney, M.C., 2020. Memantine, Simvastatin, and Epicatechin Inhibit 7-Ketocholesterol-induced Apoptosis in Retinal Pigment Epithelial Cells But Not Neurosensory Retinal Cells In Vitro. J. Ophthalmic Vis. Res. 15, 470–480. https://doi.org/10.18502/jovr.v15i4.7781

Negre-Salvayre, A., Coatrieux, C., Ingueneau, C., Salvayre, R., 2008. Advanced lipid peroxidation end products in oxidative damage to proteins. Potential role in diseases and therapeutic prospects for the inhibitors. Br. J. Pharmacol. 153, 6–20. https://doi.org/10.1038/sj.bjp.0707395

Nguyen, K.H., Patel, B.C., Tadi, P., 2023. Anatomy, Head and Neck: Eye Retina, in: StatPearls. StatPearls Publishing, Treasure Island (FL).

Ni, T., Yang, W., Xing, Y., 2019. Protective effects of delphinidin against H2O2-induced oxidative injuries in human retinal pigment epithelial cells. Biosci. Rep. 39, BSR20190689. https://doi.org/10.1042/BSR20190689

Nickla, D.L., Wallman, J., 2010. The multifunctional choroid. Prog. Retin. Eye Res. 29, 144–168. https://doi.org/10.1016/j.preteyeres.2009.12.002

Nitzsche, B., Rong, W.W., Goede, A., Hoffmann, B., Scarpa, F., Kuebler, W.M., Secomb, T.W., Pries, A.R., 2022. Coalescent angiogenesis-evidence for a novel concept of vascular network maturation. Angiogenesis 25, 35–45. https://doi.org/10.1007/s10456-021-09824-3

Noell, W.K., Walker, V.S., Kang, B.S., Berman, S., 1966. Retinal damage by light in rats. Invest. Ophthalmol. 5, 450–473.

Ogawa, K., Urata, K., Suzuki, Y., Sugamoto, K., Goto, Y., Nakayama, T., Nishiyama, K., Kunitake, H., Yamasaki, M., 2023. Blueberry stem extract and stem active components prevent blue light-emitting diode light-induced retinal photoreceptor cell damage in vitro. Biosci. Biotechnol. Biochem. 87, 378–388. https://doi.org/10.1093/bbb/zbad001

Parage, C., Tavares, R., Réty, S., Baltenweck-Guyot, R., Poutaraud, A., Renault, L., Heintz, D., Lugan, R., Marais, G.A.B., Aubourg, S., Hugueney, P., 2012. Structural, Functional, and Evolutionary Analysis of the Unusually Large Stilbene Synthase Gene Family in Grapevine. Plant Physiol. 160, 1407–1419. https://doi.org/10.1104/pp.112.202705

Patil, A.J., Gramajo, A.L., Sharma, A., Seigel, G.M., Kuppermann, B.D., Kenney, M.C., 2009. Differential effects of nicotine on retinal and vascular cells in vitro. Toxicology 259, 69–76. https://doi.org/10.1016/j.tox.2009.02.004

Pazgal, I., Boycov, O., Shpilberg, O., Okon, E., Bairey, O., 2007. Expression of VEGF-C, VEGF-D and their receptor VEGFR-3 in diffuse large B-cell lymphomas. Leuk. Lymphoma 48, 2213–2220. https://doi.org/10.1080/10428190701632822

Peng, M., Zhou, X., Yao, F., Li, H., Song, W., Xiong, S., Xia, X., 2022. (-)-Epicatechin Provides Neuroprotection in Sodium Iodate-Induced Retinal Degeneration. Front. Med. 9, 879901. https://doi.org/10.3389/fmed.2022.879901

Peng, T.-I., Yu, P.-R., Chen, J.-Y., Wang, H.-L., Wu, H.-Y., Wei, Y.-H., Jou, M.-J., 2006. Visualizing common deletion of mitochondrial DNA-augmented mitochondrial reactive oxygen species generation and apoptosis upon oxidative stress. Biochim. Biophys. Acta BBA - Mol. Basis Dis., Mitochondria in Diseases and Therapeutics 1762, 241–255. https://doi.org/10.1016/j.bbadis.2005.10.008

Pescarmona, R., Foray, A.-P., Garnier, L., 2023. Exploration immunologique de l'œil. Rev. Francoph. Lab. 2023, 61–67. https://doi.org/10.1016/S1773-035X(23)00111-9

Philp, N.J., Wang, D., Yoon, H., Hjelmeland, L.M., 2003. Polarized expression of monocarboxylate transporters in human retinal pigment epithelium and ARPE-19 cells. Invest. Ophthalmol. Vis. Sci. 44, 1716–1721. https://doi.org/10.1167/iovs.02-0287

Pietta, P., Minoggio, M., Bramati, L., 2003. Plant Polyphenols: Structure, Occurrence and Bioactivity, in: Rahman, A. (Ed.), Studies in Natural Products Chemistry, Bioactive Natural Products (Part I). Elsevier, pp. 257–312. https://doi.org/10.1016/S1572-5995(03)80143-6

Pittalà, V., Fidilio, A., Lazzara, F., Platania, C.B.M., Salerno, L., Foresti, R., Drago, F., Bucolo, C., 2017. Effects of Novel Nitric Oxide-Releasing Molecules against Oxidative Stress on Retinal Pigmented Epithelial Cells. Oxid. Med. Cell. Longev. 2017, 1420892. https://doi.org/10.1155/2017/1420892

Plafker, S.M., O'Mealey, G.B., Szweda, L.I., 2012. MECHANISMS FOR COUNTERING OXIDATIVE STRESS AND DAMAGE IN RETINAL PIGMENT EPITHELIUM. Int. Rev. Cell Mol. Biol. 298, 135–177. https://doi.org/10.1016/B978-0-12-394309-5.00004-3

Rambaran, T.F., 2020. Nanopolyphenols: a review of their encapsulation and anti-diabetic effects. SN Appl. Sci. 2, 1335. https://doi.org/10.1007/s42452-020-3110-8

Rider, P., Carmi, Y., Guttman, O., Braiman, A., Cohen, I., Voronov, E., White, M.R., Dinarello, C.A., Apte, R.N., 2011. IL-1α and IL-1β recruit different myeloid cells and promote different stages of sterile inflammation. J. Immunol. Baltim. Md 1950 187, 4835–4843. https://doi.org/10.4049/jimmunol.1102048

Rittié, L., Berton, A., Monboisse, J.C., Hornebeck, W., Gillery, P., 1999. Decreased contraction of glycated collagen lattices coincides with impaired matrix metalloproteinase production. Biochem. Biophys. Res. Commun. 264, 488–492. https://doi.org/10.1006/bbrc.1999.1519

Robinson, C.J., Stringer, S.E., 2001. The splice variants of vascular endothelial growth factor (VEGF) and their receptors. J. Cell Sci. 114, 853–865. https://doi.org/10.1242/jcs.114.5.853

Romero-Pérez, A.I., Lamuela-Raventós, R.M., Buxaderas, S., Carmen de la Torre-Boronat, M., 1996. Resveratrol and Piceid as Varietal Markers of White Wines. J. Agric. Food Chem. 44, 1975–1978. https://doi.org/10.1021/jf960211g

Roubeix, C., Sahel, J.-A., Guillonneau, X., Delarasse, C., Sennlaub, F., 2020. Sur les origines inflammatoires de la DMLA. médecine/sciences 36, 886–892. https://doi.org/10.1051/medsci/2020159

Ruan, Y., Jiang, S., Gericke, A., 2021. Age-Related Macular Degeneration: Role of Oxidative Stress and Blood Vessels. Int. J. Mol. Sci. 22, 1296. https://doi.org/10.3390/ijms22031296

Sakurai, E., Anand, A., Ambati, B.K., van Rooijen, N., Ambati, J., 2003. Macrophage depletion inhibits experimental choroidal neovascularization. Invest. Ophthalmol. Vis. Sci. 44, 3578–3585. https://doi.org/10.1167/iovs.03-0097

Samra, Y.A., Zaidi, Y., Rajpurohit, P., Raghavan, R., Cai, L., Kaddour-Djebbar, I., Tawfik, A., 2023. Warburg Effect as a Novel Mechanism for Homocysteine-Induced Features of Age-Related Macular Degeneration. Int. J. Mol. Sci. 24, 1071. https://doi.org/10.3390/ijms24021071

Samuel, W., Jaworski, C., Postnikova, Olga.A., Kutty, R.K., Duncan, T., Tan, L.X., Poliakov, E., Lakkaraju, A., Redmond, T.M., 2017. Appropriately differentiated ARPE-19 cells regain phenotype and gene expression profiles similar to those of native RPE cells. Mol. Vis. 23, 60–89.

Sanders, T.H., McMichael, R.W., Hendrix, K.W., 2000. Occurrence of resveratrol in edible peanuts. J. Agric. Food Chem. 48, 1243–1246. https://doi.org/10.1021/jf990737b

Sarks, S.H., Arnold, J.J., Killingsworth, M.C., Sarks, J.P., 1999. Early drusen formation in the normal and aging eye and their relation to age related maculopathy: a clinicopathological study. Br. J. Ophthalmol. 83, 358–368. https://doi.org/10.1136/bjo.83.3.358

Sawadogo, A., 2023. Outils d'évaluation de la qualité d'un paramétrage de propriétés visuelles : cas des textures couleur.

Selhorst, J.B., Chen, Y., 2009. The optic nerve. Semin. Neurol. 29, 29–35. https://doi.org/10.1055/s-0028-1124020

Sennlaub, F., Auvynet, C., Calippe, B., Lavalette, S., Poupel, L., Hu, S.J., Dominguez, E., Camelo, S., Levy, O., Guyon, E., Saederup, N., Charo, I.F., Rooijen, N.V., Nandrot, E., Bourges, J.-L., Behar-Cohen, F., Sahel, J.-A., Guillonneau, X., Raoul, W., Combadiere, C., 2013. CCR2(+) monocytes infiltrate atrophic lesions in age-related macular disease and mediate photoreceptor degeneration in experimental subretinal inflammation in Cx3cr1 deficient mice. EMBO Mol. Med. 5, 1775–1793. https://doi.org/10.1002/emmm.201302692

Serag, A., Salem, M.A., Gong, S., Wu, J.-L., Farag, M.A., 2023. Decoding Metabolic Reprogramming in Plants under Pathogen Attacks, a Comprehensive Review of Emerging Metabolomics Technologies to Maximize Their Applications. Metabolites 13, 424. https://doi.org/10.3390/metabo13030424

Sghaier, R., Perus, M., Cornebise, C., Courtaut, F., Scagliarini, A., Olmiere, C., Aires, V., Hermetet, F., Delmas, D., 2022. Resvega, a Nutraceutical Preparation, Affects NFκB Pathway and Prolongs the Anti-VEGF Effect of Bevacizumab in Undifferentiated ARPE-19 Retina Cells. Int. J. Mol. Sci. 23, 11704. https://doi.org/10.3390/ijms231911704

Shanmuganathan, S., Angayarkanni, N., 2018. Chebulagic acid Chebulinic acid and Gallic acid, the active principles of Triphala, inhibit TNFα induced pro-angiogenic and pro-inflammatory activities in retinal capillary endothelial cells by inhibiting p38, ERK and NFkB phosphorylation. Vascul. Pharmacol. 108, 23–35. https://doi.org/10.1016/j.vph.2018.04.005

Sharma, D., Zachary, I., Jia, H., 2023. Mechanisms of Acquired Resistance to Anti-VEGF Therapy for Neovascular Eye Diseases. Invest. Ophthalmol. Vis. Sci. 64, 28. https://doi.org/10.1167/iovs.64.5.28

Shen, S., Kapphahn, R.J., Zhang, M., Qian, S., Montezuma, S.R., Shang, P., Ferrington, D.A., Qu, J., 2023. Quantitative Proteomics of Human Retinal Pigment Epithelium Reveals Key Regulators for the Pathogenesis of Age-Related Macular Degeneration. Int. J. Mol. Sci. 24, 3252. https://doi.org/10.3390/ijms24043252

Sheu, S.-J., Liu, N.-C., Chen, J.-L., 2010. Resveratrol protects human retinal pigment epithelial cells from acrolein-induced damage. J. Ocul. Pharmacol. Ther. Off. J. Assoc. Ocul. Pharmacol. Ther. 26, 231–236. https://doi.org/10.1089/jop.2009.0137

Shibuya, M., 2001. Structure and dual function of vascular endothelial growth factor receptor-1 (Flt-1). Int. J. Biochem. Cell Biol. 33, 409–420. https://doi.org/10.1016/s1357-2725(01)00026-7

Silván, J.M., Reguero, M., de Pascual-Teresa, S., 2016. A protective effect of anthocyanins and xanthophylls on UVB-induced damage in retinal pigment epithelial cells. Food Funct. 7, 1067–1076. https://doi.org/10.1039/c5fo01368b

Simonetti, P., Gardana, C., Pietta, P., 2001. Plasma levels of caffeic acid and antioxidant status after red wine intake. J. Agric. Food Chem. 49, 5964–5968. https://doi.org/10.1021/jf010546k

Simonetti, Paolo, Gardana, C., Pietta, P., 2001. Caffeic acid as biomarker of red wine intake, in: Methods in Enzymology, Flavonoids and Other Polyphenols. Academic Press, pp. 122–130. https://doi.org/10.1016/S0076-6879(01)35237-0

Snell, R.S., Lemp, M.A., 2013. Clinical Anatomy of the Eye. John Wiley & Sons.

Soleas, G.J., Yan, J., Goldberg, D.M., 2001a. Measurement of trans-resveratrol, (+)-catechin, and quercetin in rat and human blood and urine by gas chromatography with mass selective detection. Methods Enzymol. 335, 130–145. https://doi.org/10.1016/s0076-6879(01)35238-2

Soleas, G.J., Yan, J., Goldberg, D.M., 2001b. Ultrasensitive assay for three polyphenols (catechin, quercetin and resveratrol) and their conjugates in biological fluids utilizing gas chromatography with mass selective detection. J. Chromatogr. B. Biomed. Sci. App. 757, 161–172. https://doi.org/10.1016/s0378-4347(01)00142-6

Sparrow, J.R., Boulton, M., 2005. RPE lipofuscin and its role in retinal pathobiology. Exp. Eye Res. 80, 595–606. https://doi.org/10.1016/j.exer.2005.01.007

Stacker, S.A., Williams, S.P., Karnezis, T., Shayan, R., Fox, S.B., Achen, M.G., 2014. Lymphangiogenesis and lymphatic vessel remodelling in cancer. Nat. Rev. Cancer 14, 159–172. https://doi.org/10.1038/nrc3677

Stamer, W.D., Bok, D., Hu, J., Jaffe, G.J., McKay, B.S., 2003. Aquaporin-1 channels in human retinal pigment epithelium: role in transepithelial water movement. Invest. Ophthalmol. Vis. Sci. 44, 2803–2808. https://doi.org/10.1167/iovs.03-0001

Subhi, Y., Lykke Sørensen, T., 2017. New neovascular age-related macular degeneration is associated with systemic leucocyte activity. Acta Ophthalmol. (Copenh.) 95, 472–480. https://doi.org/10.1111/aos.13330

Subhi, Y., Nielsen, M.K., Molbech, C.R., Oishi, A., Singh, A., Nissen, M.H., Sørensen, T.L., 2017. T-cell differentiation and CD56+ levels in polypoidal choroidal vasculopathy and neovascular age-related macular degeneration. Aging 9, 2436–2452. https://doi.org/10.18632/aging.101329

Sun, M., Yu, T., Zhao, J., Zhu, X., Xin, W., Zhang, F., Zhang, L., 2023. Role of flavonoids in age-related macular degeneration. Biomed. Pharmacother. 159, 114259. https://doi.org/10.1016/j.biopha.2023.114259

Supanji, S., Romdhoniyyah, D.F., Sasongko, M.B., Agni, A.N., Wardhana, F.S., Widayanti, T.W., Prayogo, M.E., Perdamaian, A.B.I., Dianratri, A., Kawaichi, M., Oka, C., 2021. Associations of ARMS2 and CFH Gene Polymorphisms with Neovascular Age-Related Macular Degeneration. Clin. Ophthalmol. Auckl. NZ 15, 1101–1108. https://doi.org/10.2147/OPTH.S298310

Szaflik, J.P., Janik-Papis, K., Synowiec, E., Ksiazek, D., Zaras, M., Wozniak, K., Szaflik, J., Blasiak, J., 2009. DNA damage and repair in age-related macular degeneration. Mutat. Res. 669, 169–176. https://doi.org/10.1016/j.mrfmmm.2009.06.008

Tammela, T., Zarkada, G., Wallgard, E., Murtomäki, A., Suchting, S., Wirzenius, M., Waltari, M., Hellström, M., Schomber, T., Peltonen, R., Freitas, C., Duarte, A., Isoniemi, H., Laakkonen, P., Christofori, G., Ylä-Herttuala, S., Shibuya, M., Pytowski, B., Eichmann, A., Betsholtz, C., Alitalo, K., 2008. Blocking VEGFR-3 suppresses angiogenic sprouting and vascular network formation. Nature 454, 656–660. https://doi.org/10.1038/nature07083

Taylor, A.W., Hsu, S., Ng, T.F., 2021. The Role of Retinal Pigment Epithelial Cells in Regulation of Macrophages/Microglial Cells in Retinal Immunobiology. Front. Immunol. 12, 724601. https://doi.org/10.3389/fimmu.2021.724601

Terakita, A., 2005. The opsins. Genome Biol. 6, 213. https://doi.org/10.1186/gb-2005-6-3-213

Terao, R., Ahmed, T., Suzumura, A., Terasaki, H., 2022. Oxidative Stress-Induced Cellular Senescence in Aging Retina and Age-Related Macular Degeneration. Antioxid. Basel Switz. 11, 2189. https://doi.org/10.3390/antiox11112189

Toma, C., De Cillà, S., Palumbo, A., Garhwal, D.P., Grossini, E., 2021. Oxidative and Nitrosative Stress in Age-Related Macular Degeneration: A Review of Their Role in Different Stages of Disease. Antioxid. Basel Switz. 10, 653. https://doi.org/10.3390/antiox10050653

Tomani, J.C.D., Kagisha, V., Tchinda, A.T., Jansen, O., Ledoux, A., Vanhamme, L., Frederich, M., Muganga, R., Souopgui, J., 2020. The Inhibition of NLRP3 Inflammasome and IL-6 Production by Hibiscus noldeae Baker f. Derived Constituents Provides a Link to Its Anti-Inflammatory Therapeutic Potentials. Mol. Basel Switz. 25, 4693. https://doi.org/10.3390/molecules25204693

Torres, A.K., Jara, C., Llanquinao, J., Lira, M., Cortés-Díaz, D., Tapia-Rojas, C., 2023. Mitochondrial Bioenergetics, Redox Balance, and Calcium Homeostasis Dysfunction with Defective Ultrastructure and Quality Control in the Hippocampus of Aged Female C57BL/6J Mice. Int. J. Mol. Sci. 24, 5476. https://doi.org/10.3390/ijms24065476

Treps, L., Gavard, J., 2015. L'angiogenèse tumorale - Quand l'arbre de vie tourne mal. médecine/sciences 31, 989–995. https://doi.org/10.1051/medsci/20153111013

Ulhaq, Z.S., Soraya, G.V., Budu, null, Wulandari, L.R., 2020. The role of IL-6-174 G/C polymorphism and intraocular IL-6 levels in the pathogenesis of ocular diseases: a systematic review and meta-analysis. Sci. Rep. 10, 17453. https://doi.org/10.1038/s41598-020-74203-9

United Nations, 2022. World Population Prospects 2022.

van Lookeren Campagne, M., LeCouter, J., Yaspan, B.L., Ye, W., 2014. Mechanisms of age-related macular degeneration and therapeutic opportunities. J. Pathol. 232, 151–164. https://doi.org/10.1002/path.4266

Veltmann, M., Hollborn, M., Reichenbach, A., Wiedemann, P., Kohen, L., Bringmann, A., 2016. Osmotic Induction of Angiogenic Growth Factor Expression in Human Retinal Pigment Epithelial Cells. PloS One 11, e0147312. https://doi.org/10.1371/journal.pone.0147312

Vilkeviciute, A., Cebatoriene, D., Kriauciuniene, L., Liutkeviciene, R., 2022. VEGFA Haplotype and VEGF-A and VEGF-R2 Protein Associations with Exudative Age-Related Macular Degeneration. Cells 11, 996. https://doi.org/10.3390/cells11060996

von Hanno, T., Lade, A.C., Mathiesen, E.B., Peto, T., Njølstad, I., Bertelsen, G., 2017. Macular thickness in healthy eyes of adults (N = 4508) and relation to sex, age and refraction: the Tromsø Eye Study (2007–2008). Acta Ophthalmol. (Copenh.) 95, 262–269. https://doi.org/10.1111/aos.13337

Walle, T., Hsieh, F., DeLegge, M.H., Oatis, J.E., Walle, U.K., 2004. High absorption but very low bioavailability of oral resveratrol in humans. Drug Metab. Dispos. Biol. Fate Chem. 32, 1377–1382. https://doi.org/10.1124/dmd.104.000885

Walter, A., Etienne-Selloum, N., Brasse, D., Khallouf, H., Bronner, C., Rio, M.-C., Beretz, A., Schini-Kerth, V.B., 2010. Intake of grape-derived polyphenols reduces C26 tumor growth by inhibiting angiogenesis and inducing apoptosis. FASEB J. Off. Publ. Fed. Am. Soc. Exp. Biol. 24, 3360–3369. https://doi.org/10.1096/fj.09-149419

Wang, J.-H., Wong, R.C.B., Liu, G.-S., 2023. Retinal Aging Transcriptome and Cellular Landscape in Association With the Progression of Age-Related Macular Degeneration. Invest. Ophthalmol. Vis. Sci. 64, 32. https://doi.org/10.1167/iovs.64.4.32

Wang, X., Bove, A.M., Simone, G., Ma, B., 2020. Molecular Bases of VEGFR-2-Mediated Physiological Function and Pathological Role. Front. Cell Dev. Biol. 8, 599281. https://doi.org/10.3389/fcell.2020.599281

Warjri, G.B., Senthil, S., 2022. Imaging of the Ciliary Body: A Major Review. Semin. Ophthalmol. 37, 711–723. https://doi.org/10.1080/08820538.2022.2085515

Weiskirchen, S., Weiskirchen, R., 2016. Resveratrol: How Much Wine Do You Have to Drink to Stay Healthy?123. Adv. Nutr. 7, 706–718. https://doi.org/10.3945/an.115.011627

Weng, S., Mao, L., Gong, Y., Sun, T., Gu, Q., 2017. Role of quercetin in protecting ARPE-19 cells against H2O2-induced injury via nuclear factor erythroid 2 like 2 pathway activation and endoplasmic reticulum stress inhibition. Mol. Med. Rep. 16, 3461–3468. https://doi.org/10.3892/mmr.2017.6964

Wong, W.L., Su, X., Li, X., Cheung, C.M.G., Klein, R., Cheng, C.-Y., Wong, T.Y., 2014. Global prevalence of age-related macular degeneration and disease burden projection for 2020 and 2040: a systematic review and meta-analysis. Lancet Glob. Health 2, e106-116. https://doi.org/10.1016/S2214-109X(13)70145-1

Wooff, Y., Man, S.M., Aggio-Bruce, R., Natoli, R., Fernando, N., 2019. IL-1 Family Members Mediate Cell Death, Inflammation and Angiogenesis in Retinal Degenerative Diseases. Front. Immunol. 10, 1618. https://doi.org/10.3389/fimmu.2019.01618

Yang, S., Zhao, J., Sun, X., 2016. Resistance to anti-VEGF therapy in neovascular age-related macular degeneration: a comprehensive review. Drug Des. Devel. Ther. 10, 1857–1867. https://doi.org/10.2147/DDDT.S97653

Yang, S., Zhou, J., Li, D., 2021. Functions and Diseases of the Retinal Pigment Epithelium. Front. Pharmacol. 12, 727870. https://doi.org/10.3389/fphar.2021.727870

Yang, Y., Wu, Z.-Z., Cheng, Y.-L., Lin, W., Qu, C., 2019. Resveratrol protects against oxidative damage of retinal pigment epithelium cells by modulating SOD/MDA activity and activating Bcl-2 expression. Eur. Rev. Med. Pharmacol. Sci. 23, 378–388. https://doi.org/10.26355/eurrev_201901_16786

Young, R.W., 1971. The renewal of rod and cone outer segments in the rhesus monkey. J. Cell Biol. 49, 303–318. https://doi.org/10.1083/jcb.49.2.303

Yu, D.-Y., Cringle, S.J., 2005. Retinal degeneration and local oxygen metabolism. Exp. Eye Res. 80, 745–751. https://doi.org/10.1016/j.exer.2005.01.018

Zehetner, C., Bechrakis, N.E., Stattin, M., Kirchmair, R., Ulmer, H., Kralinger, M.T., Kieselbach, G.F., 2015. Systemic counterregulatory response of placental growth factor levels to intravitreal aflibercept therapy. Invest. Ophthalmol. Vis. Sci. 56, 3279–3286. https://doi.org/10.1167/iovs.15-16686

Zhang, F., Tang, Z., Hou, X., Lennartsson, J., Li, Y., Koch, A.W., Scotney, P., Lee, C., Arjunan, P., Dong, L., Kumar, A., Rissanen, T.T., Wang, B., Nagai, N., Fons, P., Fariss, R., Zhang, Y., Wawrousek, E., Tansey, G., Raber, J., Fong, G.-H., Ding, H., Greenberg, D.A., Becker, K.G., Herbert, J.-M., Nash, A., Yla-Herttuala, S., Cao, Y., Watts, R.J., Li, X., 2009. VEGF-B is dispensable for blood vessel growth but critical for their survival, and VEGF-B targeting inhibits pathological angiogenesis. Proc. Natl. Acad. Sci. U. S. A. 106, 6152–6157. https://doi.org/10.1073/pnas.0813061106

Zhang, H., Davies, K.J.A., Forman, H.J., 2015. Oxidative stress response and Nrf2 signaling in aging. Free Radic. Biol. Med. 88, 314–336. https://doi.org/10.1016/j.freeradbiomed.2015.05.036

Zhao, N., Kulkarni, S., Zhang, S., Linville, R.M., Chung, T.D., Guo, Z., Jamieson, J.J., Norman, D., Liang, L., Pessell, A.F., Searson, P., 2023. Modeling angiogenesis in the human brain in a tissue-engineered post-capillary venule. Angiogenesis 26, 203–216. https://doi.org/10.1007/s10456-023-09868-7

Zhou, D.-D., Luo, M., Huang, S.-Y., Saimaiti, A., Shang, A., Gan, R.-Y., Li, H.-B., 2021. Effects and Mechanisms of Resveratrol on Aging and Age-Related Diseases. Oxid. Med. Cell. Longev. 2021, e9932218. https://doi.org/10.1155/2021/9932218

Zhu, Q., Liu, M., He, Y., Yang, B., 2019. Quercetin protect cigarette smoke extracts induced inflammation and apoptosis in RPE cells. Artif. Cells Nanomedicine Biotechnol. 47, 2010–2015. https://doi.org/10.1080/21691401.2019.1608217

Zouache, M.A., 2022. Variability in Retinal Neuron Populations and Associated Variations in Mass Transport Systems of the Retina in Health and Aging. Front. Aging Neurosci. 14, 778404. https://doi.org/10.3389/fnagi.2022.778404

Zuo, J., Zhang, Z., Luo, M., Zhou, L., Nice, E.C., Zhang, W., Wang, C., Huang, C., 2022. Redox signaling at the crossroads of human health and disease. MedComm 3, e127. https://doi.org/10.1002/mco2.127

Annexes

Annexe 1 : Mesure de l'activité enzymatique de la catalase et de la superoxide dismustase

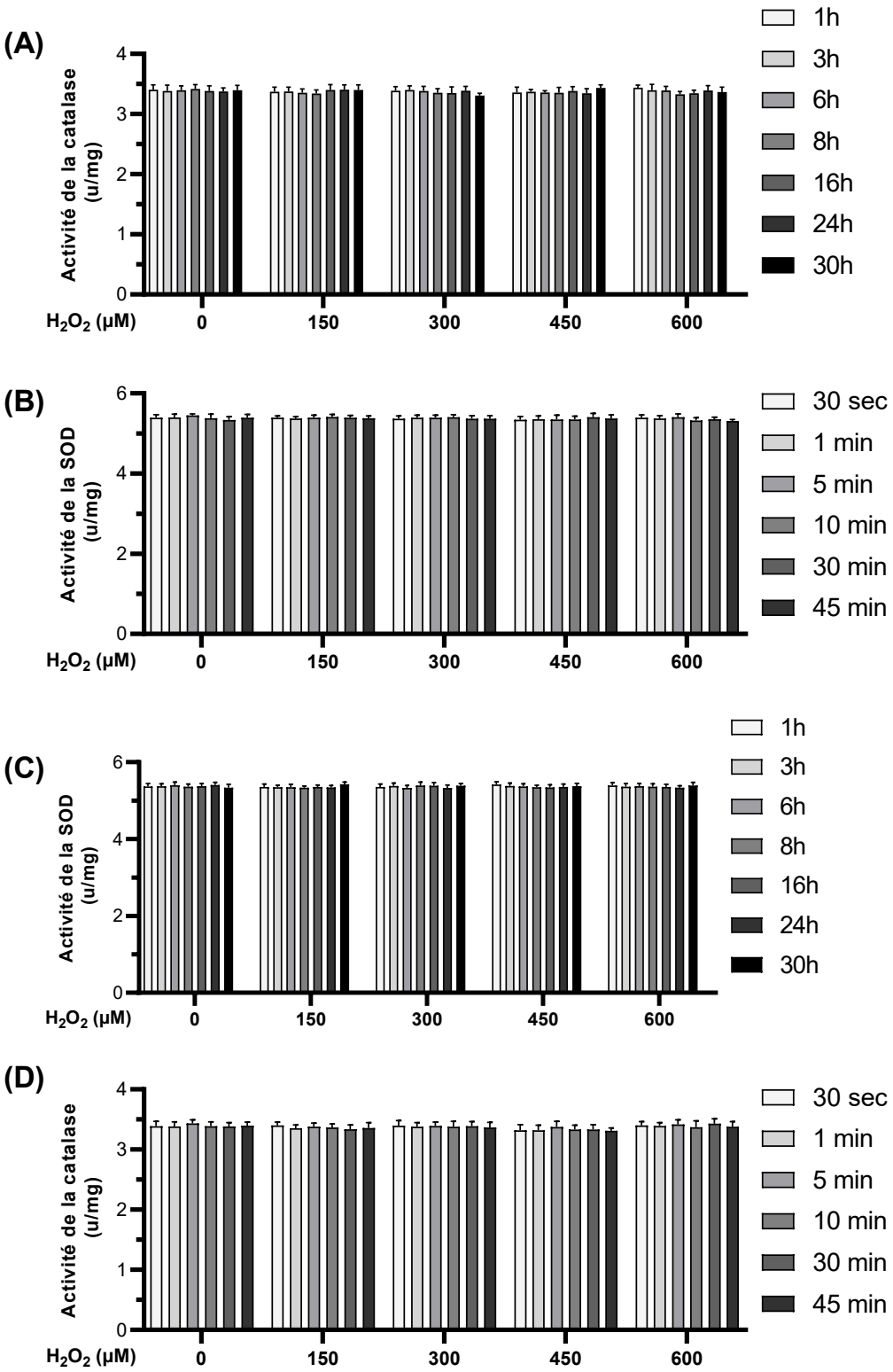

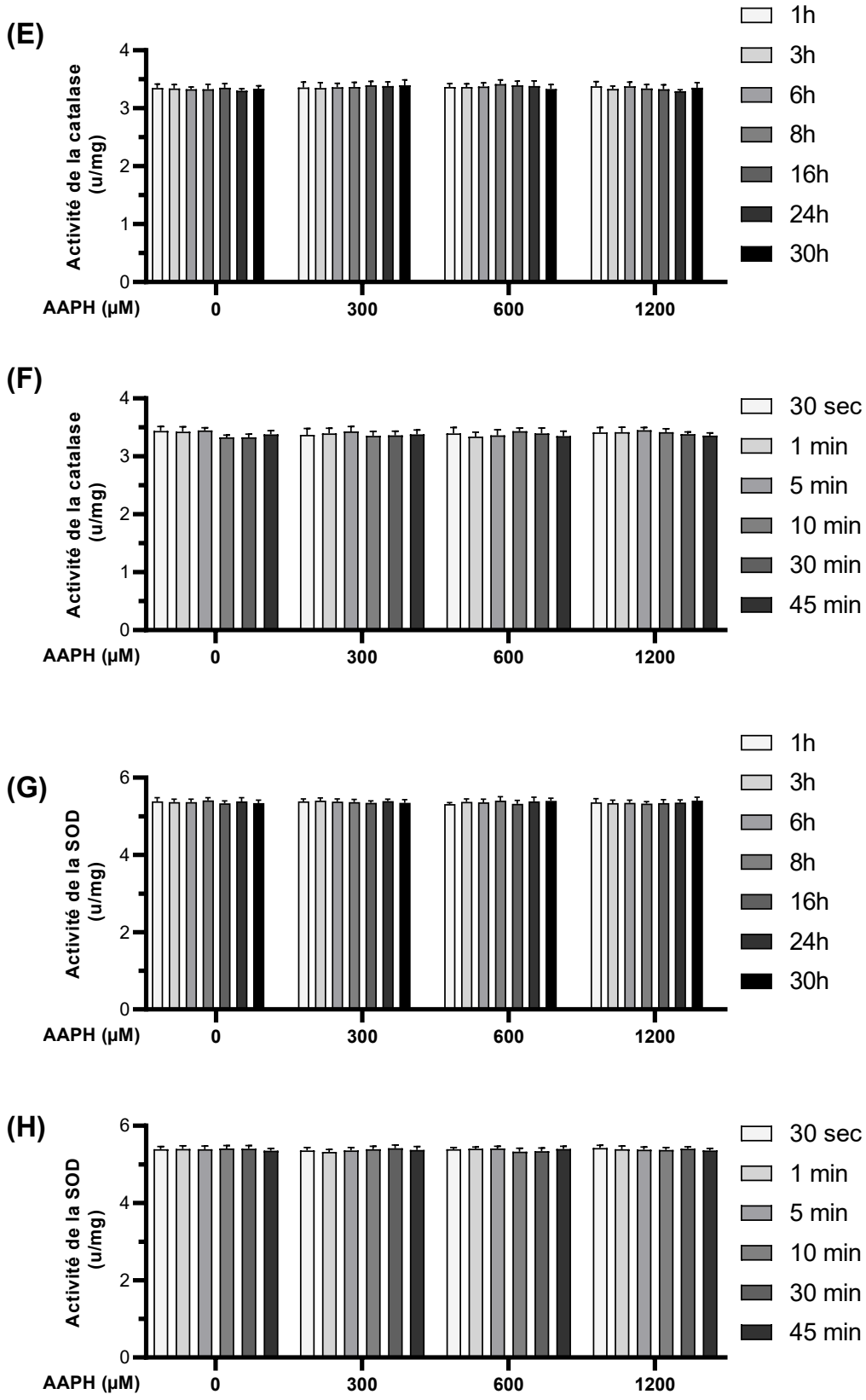

Figure 36. Mesure de l'activité enzymatique de la superoxyde dismutase et de la catalase dans les cellules ARPE-19

(A-D) Les cellules ARPE-19 ont été traitées avec des concentrations croissantes de peroxyde d'hydrogène (H_2O_2 : 0 ; 150 ; 300 ; 450 ; 600 μM) durant 1, 3, 6, 8, 16, 24, et 30 h **(A,B)** ou durant 30 secondes, 1, 5, 10, 30, 45 min **(C,D)**. **(A-D)** Les cellules ARPE-19 ont été traitées avec des concentrations croissantes de d'AAPH (0 ; 300; 600 ; 1200 μM) durant 1, 3, 6, 8, 16, 24, et 30 h **(E,F)** ou durant 30 secondes, 1, 5, 10, 30, 45 min **(G,H)**. A la fin des traitements l'activité enzymatique de la catalase et de la superoxide dismutase ont été mesurées par fluorescence. Les résultats sont exprimés en valeur moyenne ±SEM de 3 expériences indépendantes.

Annexe 2 : Mesure de la viabilité cellulaire (MTS assay)

Afin de confirmer les mesures de viabilité cellulaire réalisées par coloration au cristal violet, la viabilité cellulaire a été mesurée à l'aide d'un test MTS.

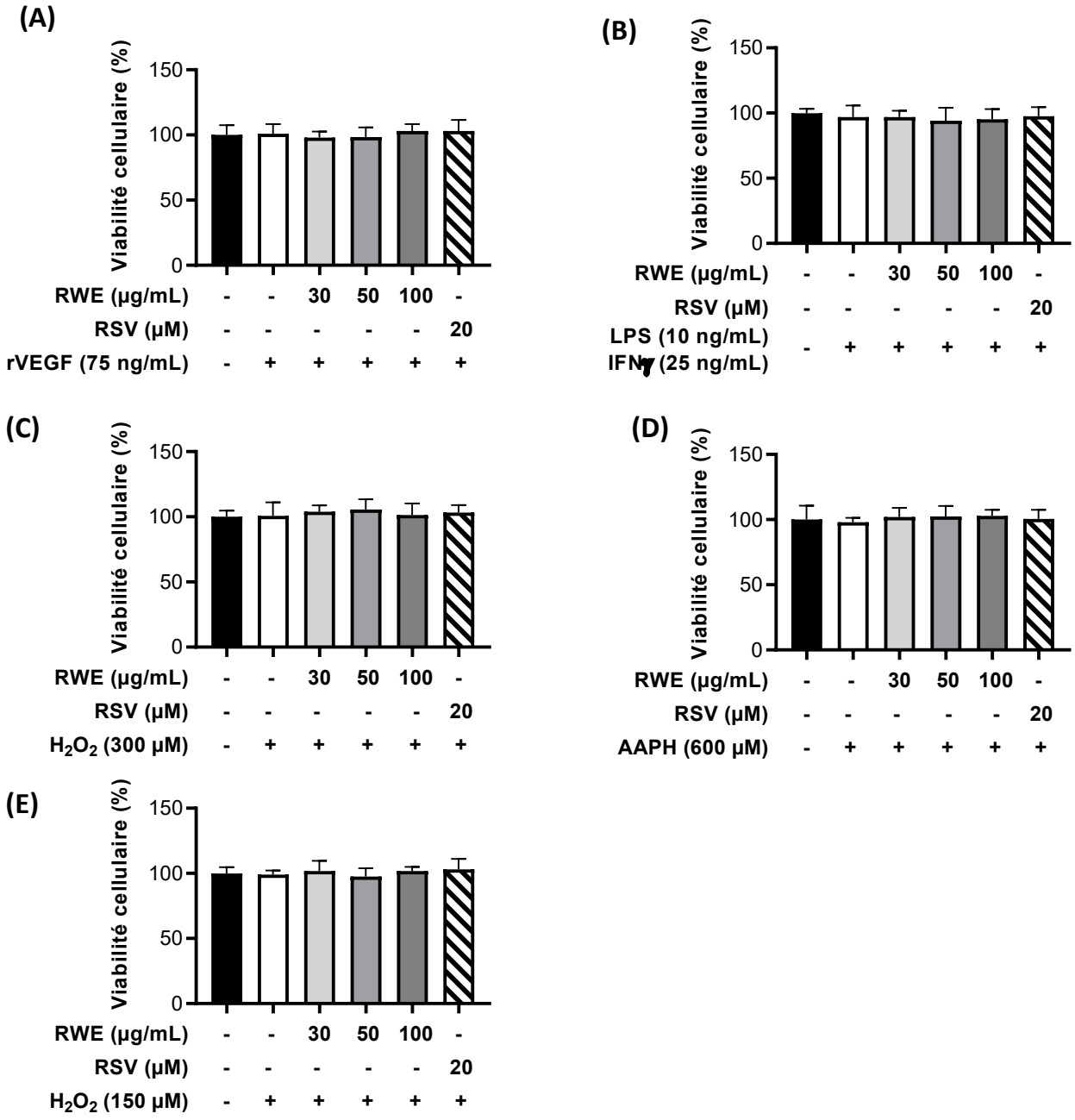

Figure 37. Viabilité cellulaire mesurée par le test MTS

Les cellules ARPE-19 ont été traitées 24 h avec une concentration croissante de RWE (30, 50, 100 µg/mL), de RSV (20 µM) ou avec le véhicule. Les cellules ont ensuite été traitées durant 6 h avec les traitements suivants **(A)** au rVEGF (75 ng/mL) **(B)** LPS (100 µg/mL) et de l'IFN-γ (25 ng/mL), **(C)** H_2O_2 (300 µM), **(D)** AAPH (600 µM). **(E)** Les cellules ARPE-19 ont été traitées 24 h avec des concentrations croissantes de RWE (30, 50, 100 µg/mL), de RSV (20 µM) ou avec le véhicule après 24 h de traitement au H_2O_2 (150 µM). A la fin des traitements, la viabilité cellulaire a été mesurée par le test MTS (Promega). Les résultats sont exprimés en valeur moyenne +/- SEM partir de 3 expériences indépendantes.

Annexe 3 : Expérimentation *in vivo*

Tous les animaux ont été nourris et maintenus en accord selon la FELASA (Federation for Laboratory Animal Science Associations) et le Guide du Comité d'Ethique de l'Expérimentation Animale (Université de Bourgogne-Franche-Comté, France) (Numéro d'Autorisation de projet utilisant des animaux à des fins scientifiques #39970-2022122214245926 v2).

Supplémentations et traitements

Des souris femelles C57/BL6J âgées de 7 semaines ont été obtenues auprès des laboratoires Charles Rivers. Après réception, les souris ont été acclimatées durant une semaine avant le début des expérimentations. Les souris ont été réparties par groupe de traitements (10 souris par groupe, Tableau 6) afin d'avoir un groupe de traitement par cage. Le resvératrol et le RWE ont été dissous dans du DMSO afin de préparer des solutions mères à 182,4 mg/mL pour le resvératrol et 400 mg/mL pour le RWE. Ces solutions mères ont par la suite été diluées dans de l'huile de maïs afin d'avoir (pour une souris de 25g) 250 µL d'huile contenant 2,5 mg de RWE (équivalent à 100 mg/Kg) ou 114 µg (équivalent à 4,56 mg/Kg) de RSV ou la quantité équivalente de DMSO. Les supplémentations ont été administrées par gavage de manière journalière durant 42 jours. Après les pemiers 21 jours de supplémentation, des injections intrapéritonéales de LPS ont été administrées tous les deux jours en complément de la supplémentation pour 21 jours supplémentaires (Figure 38). Un suivi du poids des animaux a été réalisé 2 fois par semaine lors des 21 premiers jours de supplémentation puis 3 fois par semaine jusqu'à la fin de l'expérimentation.

Tableau 6. Description des différents groupes de traitements

Supplémentation	***Traitement***
DMSO (solvant)	PBS (solvant)
DMSO (solvant)	LPS (300 µg/Kg/j)
Extrait sec de vin rouge (100 mg/Kg/j)	LPS (300 µg/Kg/j)
Resvératrol (4,56 mg/Kg/j)	LPS (300 µg/Kg/j)

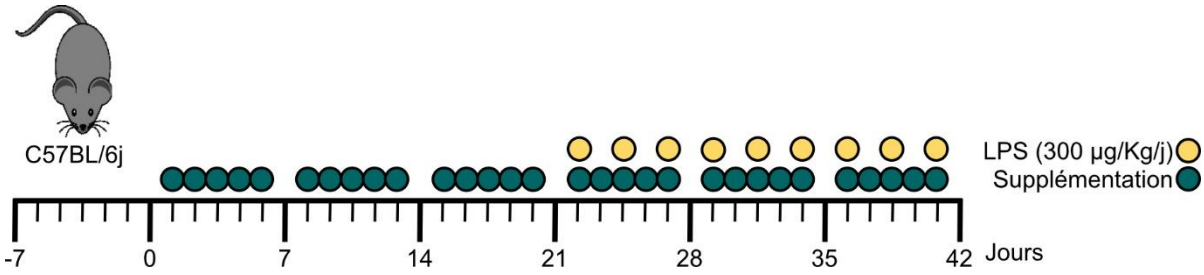

Figure 38. Plan chronologique des supplémentations et des traitements réalisés au cours de l'expérimentation *in vivo*

Suivi du poids

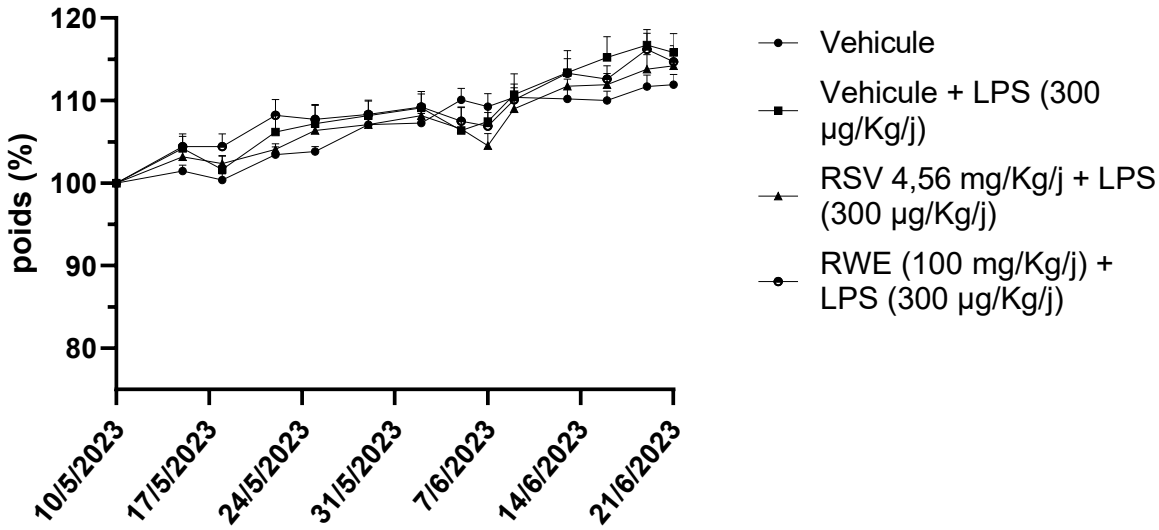

Figure 39. Suivie du poids des souris supplémentées avec de l'extrait sec de vin rouge ou du resvératrol

Les souris C57BL/6j ont été supplémentées durant 42 jours avec de l'extrait sec de vin rouge (RWE ; 100 mg/kg/j), avec du resvératrol (RSV ; 4,56 mg/Kg/j) ou avec le véhicule (contrôle solvant). Après 21 jours de traitement, les souris ont reçu une injection intrapéritonéale de LPS (300 µg/Kg/j) tous les deux jours et ce jusqu'à la fin de la supplémentation. Les valeurs sont exprimées comme la valeur moyenne ± SEM (n=10).

Annexe 4 : Concentrations molaires des différents composants du RWE

Tableau 7. Equivalences en µM des concentrations des différents constituants du RWE, correspondant aux concentrations de traitements (RWE 30, 50 et 100 µg/mL)

			RWE 30 µg/mL	RWE 50 µg/mL	RWE 100 µg/mL
	mg/g d'extrait	Ecartype	Concentrations équivalentes en µM		
Acides phénoliques	5,125033333	0,312489114			
Acide gallique	2,407165333	0,098658521	4,2449424E-07	7,0749040E-07	1,4149808E-06
Acide caftarique	2,593417333	0,212497535	2,4918416E-07	4,1530693E-07	8,3061386E-07
Acide caféique	0,124450667	0,001333059	2,0723357E-08	3,4538928E-08	6,9077857E-08
Flavan-3-ols	3,777605333	0,11303737			
Catéchine	0,909881333	0,01609645	9,4041342E-08	1,5673557E-07	3,1347114E-07
Epicatechine	0,333022667	0,018740346	3,4418576E-08	5,7364293E-08	1,1472859E-07
Procyanidine B1	1,672489333	0,051785487	8,4398116E-08	1,4066353E-07	2,8132705E-07
Procyanidine B2	0,499285333	0,009538886	2,5195223E-08	4,1992038E-08	8,3984076E-08
Procyanidine B3	0,18766	0,004490856	9,4698066E-09	1,5783011E-08	3,1566022E-08
Procyanidine B4	0,175266667	0,012385344	8,8444071E-09	1,4740678E-08	2,9481357E-08
Flavonols	0,234866667	0,008637527			
Quercetine	0,196261333	0,008009241	1,9480935E-08	3,2468226E-08	6,4936451E-08
Quercetine 3-glucuronide	0,026977333	0,000424836	1,6917224E-09	2,8195373E-09	5,6390747E-09
Quercetine 3-rhamnoside	0,011628	0,00020345	7,7800080E-10	1,2966680E-09	2,5933360E-09
Stilbenes	0,560926667	0,020076636			
c-Resvératrol	0,157010667	0,006700417	2,0636670E-08	3,4394451E-08	6,8788901E-08
t-Resvératrol	0,046902667	0,002034775	6,1646440E-09	1,0274407E-08	2,0548813E-08
C-Picéide	0,045781333	0,001383886	3,5182130E-09	5,8636884E-09	1,1727377E-08
t-Picéide	0,012506667	0,000490426	9,6111481E-10	1,6018580E-09	3,2037160E-09
t-Picéatanol	0,015308	0,00092509	1,8802611E-09	3,1337684E-09	6,2675369E-09
c-E-viniférine	0,001209333	0,000273242	7,9823982E-11	1,3303997E-10	2,6607994E-10
E-viniférine	0,006797333	0,000197315	4,4869848E-10	7,4783081E-10	1,4956616E-09
w-viniférine	0,003570667	4,77214E-05	2,3570313E-10	3,9283854E-10	7,8567709E-10
Pallidol	0,057369333	0,001616774	3,7870046E-09	6,3116744E-09	1,2623349E-08
Parthenocissine	0,034785333	0,001777514	2,2960616E-09	3,8267693E-09	7,6535387E-09
Isohopéaphenol	0,179685333	0,004629475	5,9439409E-09	9,9065682E-09	1,9813136E-08
Anthocyanines	1,053611232	0,022986367			
Delphindine 3-glucoside	0,144862361	0,00231157	8,6771640E-09	1,4461940E-08	2,8923880E-08
Cyanidine 3-glucoside	0,005531417	0,00066672	3,4226240E-10	5,7043734E-10	1,1408747E-09
Petunidine 3-glucoside	0,073599644	0,005294567	4,2885237E-09	7,1475395E-09	1,4295079E-08
Peonidine 3-glucoside	0,112014628	0,005607353	6,7362363E-09	1,1227061E-08	2,2454121E-08
Malvidine 3-glucoside	0,717603182	0,009106157	4,0704297E-08	6,7840494E-08	1,3568099E-07

Annexe 5 : Biodisponibilité des polyphénols issu de vin rouge chez l'homme

Tableau 8. Biodisponibilité des polyphénols du vin administrés par voie orale chez l'homme

Composé	*Dose administrée*	*C (µM)*	*Référence*
Acide caféique	55 µg/Kg	0,084	(Caccetta et al., 2000)
Acide caféique	0,9-2,7	0,007-0,03	(P. Simonetti et al., 2001a)
Acide caféique	1,8 mg	0,04-0,06	(Paolo Simonetti et al., 2001b)
Acide gallique	4 mg	1,57	(Cartron et al., 2003)
Acide gallique	47 µg/Kg	0,176	(Caccetta et al., 2000)
Malvidine-3-glycoside	68 mg	0,0014	(Bub et al., 2001)
Quercetine 4'glucoside	100 mg	4,5	(Graefe et al., 2001)
Quercetine	8 ; 20 ; 50 mg	0,14 ; 0,22 ; 0,29	(Erlund et al., 2000)
Quercetine	0,14 mg/Kg	0,15-0,42	(Goldberg et al., 2003)
Catechine	35 mg	0,077	(Bell et al., 2000)
Catechine	35 mg	0,091	(Donovan et al., 1999)
Peonidine-3-glucoside	15 mg	0,008	(Garcia-Alonso et al., 2009)
Malvidine-3-glucoside	80 mg	0,0042	(Garcia-Alonso et al., 2009)
Resvératrol	25 mg	1,5-7,1	(Soleas et al., 2001a, 2001b)
Resvératrol	25 mg/ 70 Kg	1,83-2,06	(Goldberg et al., 2003)
Resvératrol	25 mg/ 70 Kg	2,15	(Walle et al., 2004)

Annexe 6 : Valorisations scientifiques

Liste de publications

Dans le cadre de la thèse

- **Cornebise C**, Perus M, Hermetet F, Valls-Fonayet J, Richard T, Aires V†, Delmas D†. Red Wine Extract Prevents Oxidative Stress and Inflammation in ARPE-19 Retinal Cells. Cells 2023, 12, 1408. https://doi.org/10.3390/cells12101408

- **Cornebise C**†, Courtaut F†, Taillandier-Coindard M, Valls-Fonayet J, Richard T, Monchaud D, Aires V, Delmas D. Red Wine Extract Inhibits VEGF Secretion and Its Signaling Pathway in Retinal ARPE-19 Cells to Potentially Disrupt AMD. Molecules. 2020 Nov 27;25(23):5564. doi: 10.3390/molecules25235564. PMID: 33260857; PMCID: PMC7731402.

- Delmas D, **Cornebise C**, Courtaut F, Xiao J, Aires V. New Highlights of Resveratrol: A Review of Properties against Ocular Diseases. Int J Mol Sci. 2021 Jan 28;22(3):1295. doi: 10.3390/ijms22031295. PMID: 33525499; PMCID: PMC7865717.

Autres publications

- Barboura M, **Cornebise C**†, Hermetet F†, Guerrache A, Selmi M, Salek A, Chekir-Ghedira L‡, Aires V‡, Delmas D‡. Tannic Acid, A Hydrolysable Tannin, Prevents Transforming Growth Factor-β-Induced Epithelial-Mesenchymal Transition to Counteract Colorectal Tumor Growth. Cells. 2022 Nov 17;11(22):3645. doi: 10.3390/cells11223645. PMID: 36429073; PMCID: PMC9688195.

- Sghaier R, Perus M, **Cornebise C**, Courtaut F, Scagliarini A, Olmiere C, Aires V, Hermetet F†, Delmas D†. Resvega, a Nutraceutical Preparation, Affects NFκB Pathway and Prolongs the Anti-VEGF Effect of Bevacizumab in Undifferentiated ARPE-19 Retina Cells. Int J Mol Sci. 2022 Oct 3;23(19):11704. doi: 10.3390/ijms231911704. PMID: 36233006; PMCID: PMC9569823

- Courtaut F†, Scagliarini A†, Aires V†, **Cornebise C**, Pais de Barros JP, Olmiere C, Delmas D. VEGF-R2/Caveolin-1 Pathway of Undifferentiated ARPE-19 Retina Cells: A Potential Target as Anti-VEGF-A Therapy in Wet AMD by Resvega, an Omega-

3/Polyphenol Combination. Int J Mol Sci. 2021 Jun 19;22(12):6590. doi: 10.3390/ijms22126590. PMID: 34205419; PMCID: PMC8234996.

Liste des communications affichées

- **Cornebise C**, Courtaut F, Taillandier M, Valls Fonayet J, Tristan Richard T, Monchaud D, Aires V and Delmas D. « Red wine extract, a polyphenolic cocktail, could prevent age-related macular degeneration by inhibits VEGF secretion and its signaling pathway in human retinal cells. », **The International Conference on Polyphenols and Health 10th, 20-23 Avril 2022, Londres, Royaume Uni –** Poster

- **Cornebise C**, Courtaut F, Taillandier M, Valls Fonayet J, Tristan Richard T, Monchaud D, Aires V and Delmas D, « Red wine extract and resveratrol from grapevines could counteract AMD by inhibiting angiogenesis promoted by VEGF pathway in human retinal cells » **Wine Active Coumpounds**, **29-30 Juin 2022, Dijon, France –** Poster

Financements et prix liés à la thèse

- Bourse mobilité universitaire Nutrition méditerranéen et santé (NMS) 2022, pour assiter au congrès The International Conference on Polyphenols and Health 10th, 20-23 Avril 2022, Londres, Royaume-Uni

- Prix poster au congrès Wine Active Coumpounds, 29-30 Juin 2022, Dijon, France

Annexe 7 : Posters

Red Wine Extract, a polyphenolic cocktail, could prevent age-related macular degeneration by inhibiting VEGF secretion and its signaling pathway in human retinal cells

Clarisse CORNEBISE[1,2], Flavie COURTAUT[1,2], Marie TALLANDIER-COINDARD[1,2], Joseph VALLS FONAYET[3], David MONCHAUD[1,4], Virginie AIRES[1,2], Dominique DELMAS[1,2,5]

1 Université de bourgogne Franche-Comté, F21000 Dijon, France; 2 INSERM Research Center U1231-Cancer and adaptative Immun Response Team, Bioactive Molecules and Health Research Group, F-21000 Dijon, France; 3 Unité de Recherche Oenologies, EA 4577, USC 1366 INRA-ISVV, F-33882 Villenave d'Ornon, France; 4 Institut de Chimie Moléculaire (ICMUB), CNRS UMR6302. UNIC, 121078 Dijon, France, 5 Centre Anticancéreux Georges François Leclerc, 1-21000 Dijon, France.

Contacts : dominique.delmas@u-bourgogne.fr/virginie.aires02@u-bourgogne.fr/clarisse.cornebise@u-bourgogne.fr

Background

Age-related Macular Degeneration (AMD) is the most common cause of irreversible visual impairment in developed countries among people over the age of 50. AMD is characterized by a progressive loss of photoreceptor in the macula due to damages to the Retinal Pigmented Epithelium (RPE). The most severe form of AMD (wet AMD) is characterized by a choroïdal neoangiogenesis supported by the aberrant signalling pathway and production of the vascular endothelial growth factor A (VEGF-A). To date, the most effective treatment of wet AMD is the intravitreal injection of VEGF-A inhibitor in order to block the angiogenic processes. Although, this treatment has limited sucess and moderate visual outcomes due to major side effects. To prevent or slow the progression of the disease, polyphenols such as Resveratrol (RSV), is as well-characterized anti-oxydant, anti-inflammatory, antiangiogenic and neuroprotecive compound. In this study, we have use a Red Wine Extract (RWE), a polyphenolic cocktail (prepared and analysed as previously described (Chalons *et al.*, 2020)), in order to investigate its potential effects on the secretion of VEGF-A and its signaling pathway in human retinal cells ARPE-19.

Chalons *et al.*, Mol. Nutr. Food Res., 2020.

Aim of the study

Caracterisation of the RWE (a polyphenolic cocktail) and evaluation of its ability to block neoangiogenesis through the modulatation of the secretion and signaling pathway of VEGF-A

Materials and Methods

Qualitative and quantitative analysis of the RWE was performed by High Performance Liquid Chromatography coupled to tandem Mass Spectrometry (HPLC MS-MS).

The human Retinal Pigmented Epithelial (RPE) cell line, ARPE-19, was treated with RWE for 24h in order to :

- ▸Measure the secretion of VEGF-A by ELISA
- ▸Analyse the expression of the key proteins involved in VEGF-A signaling pathway by Western blot.

Wet Age-related Macular Degeneration (AMD)

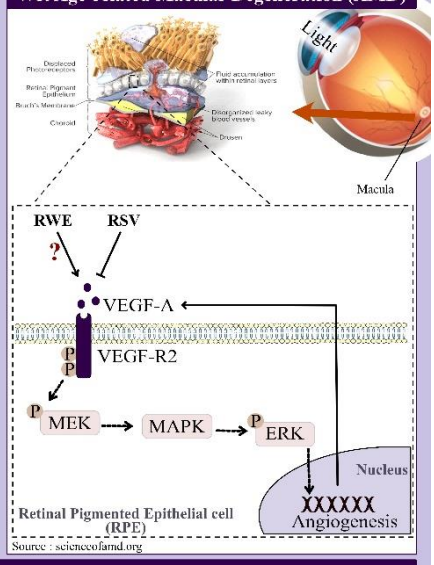

Source : sciencesofarnd.org

Qualitative and Quantitative analysis of RWE and structures of the main polyphenolic compounds

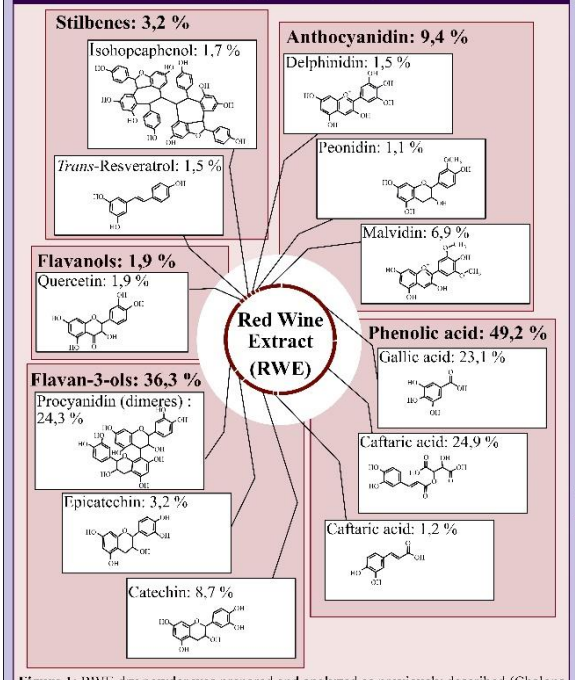

Figure 1: RWE dry powder was prepared and analyzed as previously described (Chalons *et al.*, 2020). Qualitative and Quatitative analysis of phenolic compounds of RWE was performed by HPLC MS-MS. Data are expressed as percentages of total dry extract.

RWE is able to reduce the secretion of VEGF-A through the inhibition of its signaling pathway in RPE cells

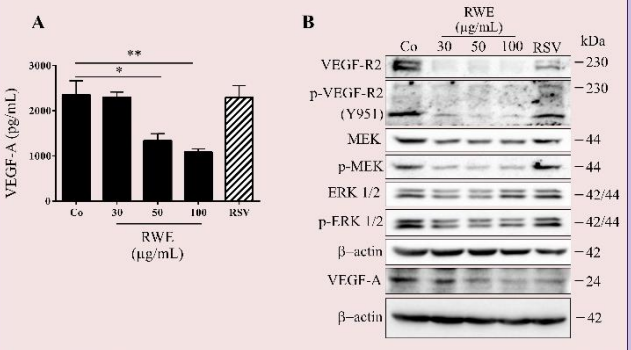

Figure 2: ARPE-19 cells were treated for 24h with various concentration of Red Wine Extract (RWE) and 20 µM of Resveratrol (RSV) **A**. Supernatent were collected. VEGF-A secretion was measured in the cell medium by ELISA. The data mean ± S.D. of four independent experiement with n=10. p values were determined by one-way ANOVA followed by Tukey's multiple comparison test. * – $p < 0.05$; ** – $p < 0.01$. **B**. then were harvest for protein extraction. Protein expression levels were analyzed by western blot. One representative expreriment is shown.

Conclusion

This work shows that RWE is composed of various phenolic compounds which are able to strongly inhibit VEGF-R2 protein expression and its phosphorylated form. This disruption of VEGF-R2 activation through its intracytoplasmic phosphorylation, leads to a decrease in the activation of the downstream MEK and ERK½ signaling pathway. As shown in the immunoblotting, 24 h of treatment with RWE significantly decreases the phosphorylation of MEK and ERK½ in ARPE-19 cells. In contrast to RWE, RSV alone significantly decreases the expression of VEGF-R2 but fails to prevent its phosphorylation, which allows the phosphorylation cascade to take place. These data, thus suggest that RWE could be effective in blocking neoangiogenesis in AMD.

This work was supported by grants from the Bureau Interprofessionnel des Vins de Bourgogne (BIVB), the Conseil Régional Bourgogne, Franche-Comte and the FEDER (European Funding for Regional Economic Development)

Red wine extract and resveratrol from grapevines could counteract AMD by inhibiting angiogenesis promoted by VEGF pathway in human retinal cells

Clarisse CORNEBISE[1,2], Flavie COURTAUT[1,2], Marie TALLANDIER-COINDARD[1,2], Joseph VALLS FONAYET[3], David MONCHAUD[1,4], Virginie AIRES[1,2], Dominique DELMAS[1,2,5]

1 Université de bourgogne Franche-Comté, F21000 Dijon, France; 2 INSERM Research Center U1231-Cancer and adaptative Immun Response Team, Bioactive Molecules and Health Research Group, F-21000 Dijon, France; 3 Unité de Recherche Oenologies, EA 4577, USC 1366 INRA-ISVV, F-33882 Villenave d'Ornon, France; 4 Institut de Chimie Moléculaire (ICMUB), CNRS UMR6302, UNIC, 121078 Dijon, France, 5 Centre Anticancéreux Georges François Leclerc, F-21000 Dijon, France.

Contacts : dominique.delmas@u-bourgogne.fr/virginie.aires02@u-bourgogne.fr/clarisse.cornebise@u-bourgogne.fr

Background

Age-related Macular Degeneration (AMD) is the most common cause of irreversible visual impairment in developed countries among people over the age of 50. AMD is characterized by a progressive loss of photoreceptor in the macula due to damages to the Retinal Pigmented Epithelium (RPE). The most severe form of AMD (wet AMD) is characterized by a choroïdal neoangiogenesis supported by the aberrant signalling pathway and production of the vascular endothelial growth factor A (VEGF-A). To date, the most effective treatment of wet AMD is the intravitreal injection of VEGF-A inhibitor in order to block the angiogenic processes. Although, this treatment has limited sucess and moderate visual outcomes due to major side effects. To prevent or slow the progression of the disease, polyphenols such as Resveratrol (RSV), is as well-characterized anti-oxydant, anti-inflammatory, anti-angiogenic and neuroprotecive compound. In this study, we have use a Red Wine Extract (RWE), a polyphenolic cocktail (prepared and analysed as previously described (Chalons *et al.*, 2020)), in order to investigate its potential effects on the secretion of VEGF-A and its signaling pathway in human retinal cells ARPE-19.

Chalons *et al.*, Mol. Nutr. Food Res., 2020.

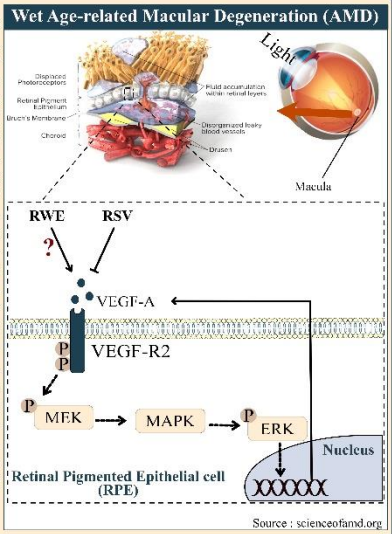

Source : scienceofamd.org

Aim of the study

Caracterisation of the RWE (a polyphenolic cocktail) and evaluation of its ability to block neoangiogenesis through the modulatation of the secretion and signaling pathway of VEGF-A

Materials and Methods

Qualitative and quantitative analysis of the RWE was performed by High Performance Liquid Chromatography coupled to tandem Mass Spectrometry (HPLC MS-MS).

The human Retinal Pigmented Epithelial (RPE) cell line, ARPE-19, was treated with RWE (with indicated concentrations) or RSV 20 µM, in order to :

- Analyse the cytotocicity of RWE and RSV by cristal violet staining
- Measure the secretion of VEGF-A by ELISA
- Analyse the expression of the key proteins involved in VEGF-A signaling pathway by Western blot.

Red Wine extract			
30 µg/mL	50 µg/mL	100 µg/mL	Resveratrol
$6{,}16.10^{-6}$ µM	$10{,}27.10^{-6}$ µM	$20{,}55.10^{-6}$ µM	20 µM

Table 1. Equivalence of RWE concentration in µg/mL to RSV concentration in µM

Extraction and Qualitative and Quantitative analysis of RWE

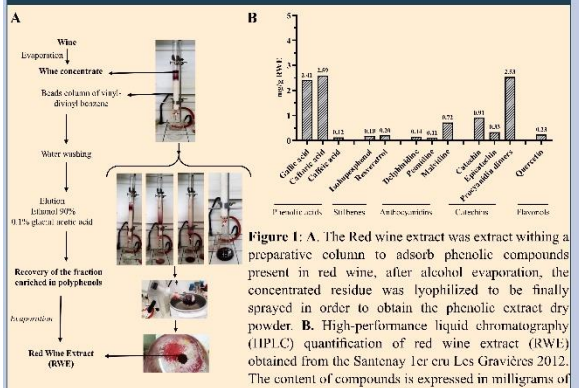

Figure 1: **A.** The Red wine extract was extract withing a preparative column to adsorb phenolic compounds present in red wine, after alcohol evaporation, the concentrated residue was lyophilized to be finally sprayed in order to obtain the phenolic extract dry powder. **B.** High-performance liquid chromatography (HPLC) quantification of red wine extract (RWE) obtained from the Santenay 1er cru Les Gravières 2012. The content of compounds is expressed in milligrams of compound per gram of RWE.

Safety assessment of RWE and RSV on RPE cells

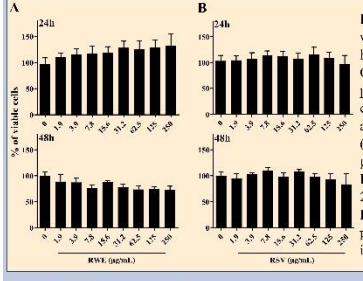

Figure 2: Safety assessment of red wine extract (RWE) and RSV on human retinal cell line ARPE-19. Crystal violet staining was performed in order to analyzed the cell viability of ARPE-19 after 24 and 48h of the (A) RWE treatment (starting concentration up to 250 µg/mL, 1:2 serial dilutions) and (B) RSV (starting concentration up to 250 µg/mL, 1:2 serial dilutions). Data are expressed as mean percentages ± s.d. of three independent experiments.

RWE is able to reduce the secretion of VEGF-A through the inhibition of its signaling pathway in RPE cells

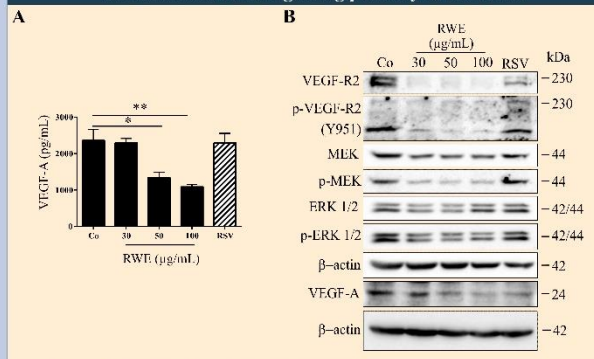

Figure 3: ARPE-19 cells were treated for 24h with various concentration of Red Wine Extract (RWE) and 20 µM of Resveratrol (RSV) **A.** The secretion of VEGF-A was measured in the cell medium by ELISA. The data mean ± S.D. of four independent experiement with n=10. p values were determined by one-way ANOVA followed by Tukey's multiple comparison test. * – $p < 0.05$; ** – $p < 0.01$. **B.** then were harvest for protein extraction. Protein expression levels were analyzed by western blot. One representative expreriment is shown.

Conclusion

This work shows that RWE is composed of various phenolic compounds which are able to strongly inhibit VEGF-R2 protein expression and its phosphorylated form. This disruption of VEGF-R2 activation through its intracytoplasmic phosphorylation, leads to a decrease in the activation of the downstream MEK and ERK½ signaling pathway. As shown in the immunoblotting, 24 h of treatment with RWE significantly decreases the phosphorylation of MEK and ERK½ in ARPE-19 cells. In contrast to RWE, RSV alone significantly decreases the expression of VEGF-R2 but fails to prevent its phosphorylation, which allows the phosphorylation cascade to take place. These data, thus suggest that RWE could be effective in blocking neoangiogenesis in AMD.

This work was supported by grants from the Bureau Interprofessionnel des Vins de Bourgogne (BIVB), the Conseil Régional Bourgogne, Franche-Comte and the FEDER (European Funding for Regional Economic Development)

Annexe 8 : Article : Tannic Acid, A Hydrolysable Tannin, Prevents Transforming Growth Factor-β-Induced Epithelial-Mesenchymal Transition to Counteract Colorectal Tumor Growth

Mahassen Barboura [1,2,3], Clarisse Cornebise [1,2,†] , François Hermetet [1,2,†] , Abderrahmane Guerrache [1,4] , Mouna Selmi [3] , Abir Salek [3] , Leila Chekir-Ghedira [3,‡];Virginie Aires [1,2,‡] and Dominique Delmas [1,2,5,*,‡]

1 UFR des Sciences de Santé, Université de Bourgogne, 21000 Dijon, France
2 INSERM Research Center U1231—Cancer and Adaptive Immune Response Team, Bioactive Molecules and Health Research Group, 21000 Dijon, France
3 Research Unit Bioactive Natural Products and Biotechnology UR17ES49, Faculty of Dental Medicine of Monastir, University of Monastir, Avicenne street, Monastir 5000, Tunisia
4 INSERM Research Center U1231—DesCartes Team, 21000 Dijon, France
5 Centre Anticancéreux Georges François Leclerc Center, 21000 Dijon, France
* Correspondence: dominique.delmas@u-bourgogne.fr; Tel.: +33-380-39-32-26
† These authors contributed equally to this work.
‡ Senior authors coshared this work.

Résumé : Malgré les avancées thérapeutiques réalisées dans la prise en charge des patients atteints de cancer colorectal (CCR), le pronostic à cinq ans reste mauvais. La résistance des cellules cancéreuses colorectales résulte en partie de leurs caractéristiques phénotypiques en lien avec la transition épithélial-mésenchymateuse (EMT). Dans la présente étude, nous avons exploré la capacité d'un polyphénol, l'acide tannique (AT), à contrer la prolifération et l'invasion des cellules CCR en altérant l'EMT. Nous avons mis en évidence que l'AT diminue la viabilité des cellules humaines de CCR (SW480 et SW620) et des cellules murines de CCR (CT26). De plus, l'AT inhibe leur adhésion en présence de composants de la matrice extracellulaire, en particulier en présence de collagène de type I et IV, et de fibronectine. En outre, ces propriétés ont été associées à la capacité de l'AT à perturber la migration et l'invasion des cellules CCR, qui sont induites par le *transforming growth factor-β* (TGF-β). Au niveau moléculaire, l'AT favorise l'inversion de la transition épithéliale-mésenchymateuse en réprimant les marqueurs mésenchymateux (Slug, Snail, ZEB1 et N-cadhérine) et en réexprimant les marqueurs épithéliaux (E-cadhérine et β-caténine). Ces effets pourraient résulter d'une perturbation de la voie de signalisation non canonique induite par le TGF-β1, où l'AT diminue fortement la phosphorylation de la kinase régulée par le signal extracellulaire ERK1/2, P38 et les protéines AKT qui sont bien connues pour contribuer à l'EMT, à la motilité cellulaire et à l'acquisition de propriétés invasives par les cellules tumorales. De manière très intéressante, notre étude préclinique menée sur des souris porteuses de cellules tumorales murines sous-cutanées du côlon (CT26) a montré que l'AT pouvait réduire de manière significative la vitesse de croissance des tumeurs.

Mots clés : polyphénols, acide tannique, cancer colorectal, chimioprévention

cells

MDPI

Article

Tannic Acid, A Hydrolysable Tannin, Prevents Transforming Growth Factor-β-Induced Epithelial–Mesenchymal Transition to Counteract Colorectal Tumor Growth

Mahassen Barboura [1,2,3], Clarisse Cornebise [1,2,†], François Hermetet [1,2,†], Abderrahmane Guerrache [1,4], Mouna Selmi [3], Abir Salek [3], Leila Chekir-Ghedira [3,‡], Virginie Aires [1,2,‡] and Dominique Delmas [1,2,5,*,‡]

1 UFR des Sciences de Santé, Université de Bourgogne, 21000 Dijon, France
2 INSERM Research Center U1231—Cancer and Adaptive Immune Response Team, Bioactive Molecules and Health Research Group, 21000 Dijon, France
3 Research Unit Bioactive Natural Products and Biotechnology UR17ES49, Faculty of Dental Medicine of Monastir, University of Monastir, Avicenne street, Monastir 5000, Tunisia
4 INSERM Research Center U1231—DesCartes Team, 21000 Dijon, France
5 Centre Anticancéreux Georges François Leclerc Center, 21000 Dijon, France
* Correspondence: dominique.delmas@u-bourgogne.fr; Tel.: +33-380-39-32-26
† These authors contributed equally to this work.
‡ Senior authors coshared this work.

Abstract: Despite the medico-surgical progress that has been made in the management of patients with colorectal cancer (CRC), the prognosis at five years remains poor. This resistance of cancer cells partly results from their phenotypic characteristics in connection with the epithelial–mesenchymal transition (EMT). In the present study, we have explored the ability of a polyphenol, tannic acid (TA), to counteract CRC cell proliferation and invasion through an action on the EMT. We highlight that TA decreases human SW480 and SW620 CRC cell and murine CT26 CRC cell viability, and TA inhibits their adhesion in the presence of important factors comprising the extracellular matrix, particularly in the presence of collagen type I and IV, and fibronectin. Moreover, these properties were associated with TA's ability to disrupt CRC cell migration and invasion, which are induced by transforming growth factor-β (TGF-β), as evidence in the video microscopy experiments showing that TA blocks the TGF-β1-induced migration of SW480 and CT26 cells. At the molecular level, TA promotes a reversal of the epithelial–mesenchymal transition by repressing the mesenchymal markers (i.e., Slug, Snail, ZEB1, and N-cadherin) and re-expressing the epithelial markers (i.e., E-cadherin and β-catenin). These effects could result from a disruption of the non-canonical signaling pathway that is induced by TGF-β1, where TA strongly decreases the phosphorylation of extracellular-signal regulated kinase ERK1/2, P38 and the AKT proteins that are well known to contribute to the EMT, the cell motility, and the acquisition of invasive properties by tumor cells. Very interestingly, a preclinical study of mice with subcutaneous murine tumor colon CT26 cells has shown that TA was able to significantly delay the growth of tumors without hepato- and nephrotoxicities.

Keywords: polyphenol; tannic acid; colon cancer; EMT; chemoprevention

Citation: Barboura, M.; Cornebise, C.; Hermetet, F.; Guerrache, A.; Selmi, M.; Salek, A.; Chekir-Ghedira, L.; Aires, V.; Delmas, D. Tannic Acid, A Hydrolysable Tannin, Prevents Transforming Growth Factor-β-Induced Epithelial–Mesenchymal Transition to Counteract Colorectal Tumor Growth. *Cells* **2022**, *11*, 3645. https://doi.org/10.3390/cells11223645

Academic Editor: Natália Cruz-Martins

Received: 19 October 2022
Accepted: 14 November 2022
Published: 17 November 2022

1. Introduction

Colorectal cancer (CRC) represents a global health threat owing to its high incidence, mortality rates, and morbidity [1]. It is the third most commonly diagnosed cancer and the second most common cause of cancer-related death in both men and women [2,3]. This unfavorable prognosis partly results from the fact that colon cancer is a tumor with a high metastatic propensity. The tumor invasion and metastasis in the middle and late stages are the root causes of treatment failure and poor therapeutic efficacy [4,5]. Among the molecular mechanisms leading to the process of metastasis, the epithelial–mesenchymal transition (EMT) plays a fundamental role. This is a complex dynamic process by which

the epithelial cells dedifferentiate into a more mobile mesenchymal cell phenotype. Indeed, the EMT is one of the fundamental molecular steps in the process of tumor progression and distant metastasis, which facilitate the invasion and migration in different cancers, and is correlated with a poor prognosis in CRC [6]. During the EMT, the epithelial cells lose epithelial characteristics such as polarity and specialized cell-to-cell contact, and acquire a mesenchymal phenotype with increased migratory and invasiveness abilities [7]. During this process, the epithelial cells lose the expression of cell–cell adhesion proteins, including E-cadherin and β-catenin, and acquire the expression of mesenchymal markers, including vimentin and N-cadherin [8]. This mechanism is also characterized by the activation of various transcription factors, which include Snail, Slug, and Zinc finger E-box-binding homeobox (ZEB) 1/2 [7]. Snail and Slug are mainly known for their involvement in the EMT, where they repress the expression of the epithelial markers, such as E-cadherin and Claudin-1, and increase the expression of the mesenchymal markers, such as ZEB1 and MMP-9 [9,10]. Several oncogenic pathways that respond to extracellular cues have been shown to contribute to the EMT of the carcinoma cells, such as transforming growth factor-β (TGF-β), bone morphogenetic protein (BMP), Wnt/β-catenin, Notch, and Hedgehog signaling pathways. TGF-β is the first EMT inducer that has been described in normal mammary epithelial cells [11], and it plays a crucial role in tumor metastasis. Thus, the inhibitors of the TGF-β signaling pathway have become attractive tools as strategies to prevent tumor progression [12].

In this context, we and others have shown the potential ability of natural compounds to act in a chemopreventive or a chemosensitization strategy [13–17]. Indeed, many in vitro and in vivo studies in animals have shown that these natural molecules are able to block all of the stages of carcinogenesis and can also sensitize tumor cells to many anticancer agents, thus increasing their chemotherapeutic potential. At the cellular and molecular levels, polyphenols can act at the DNA level and can modulate many of the signaling pathways that are involved in cell death, inflammation, and angiogenesis, as well as in the metabolism [13,18–21]. Due to their ability to act as anti- and pro-oxidant molecules, polyphenols could also contribute to limiting certain fundamental aspects of tumorigenesis and resistance mechanisms by acting on the cellular redox balance [21]. In later stages, these natural bioactive compounds could also act on multiple cell processes or conditions that are known to be involved in cancer progression, such as altered tumor metabolism and a pro-inflammatory microenvironment, migration, invasion, angiogenesis, and metastatic spread. In relation to this latter aspect, various natural compounds exhibit an inhibitory action on the EMT [22]. Among these natural compounds that could participate to a chemosensitization strategy and act on EMT, tannic acid (TA) could be a good candidate. This hydrolysable tannin is present in several natural sources, such as grapes, green tea, and coffee [23], and a myriad of pharmaceutical and biological applications in the medical field has been well recognized [24]. Among these effects, potential anticancer activities against several solid malignancies, such as lung, liver, pancreatic, breast, ovarian, and colorectal cancers, have been reported [25]. A recent study has shown that, in pulmonary fibrosis, TA could repress TGF-β signaling and the subsequent EMT process in lung epithelial cells [26]. However, the potential effect of TA on the EMT in CRC and its chemopreventive properties still remain to be defined and deserve further investigation.

In the present study, we first investigated whether TA was able to counteract the processes of cell migration and invasion in human SW480 and murine CT26 CRC cells lines. We show the ability of TA to significantly decrease both the adhesion and the TGF-β-induced proliferation of CRC cells. Moreover, TA inhibits the TGF-β1-induced motility of metastatic colon cancer cells in vitro, and this inhibition is associated with a decrease in the mesenchymal biomarkers and an increase in epithelial protein expression. Our in vivo efficacy studies demonstrate a tumor regression in the mice that were supplemented with TA without toxicity. These findings provide new evidence that TA could be a robust and promising tool in the development of innovative chemoprevention strategies.

2. Materials and Methods

2.1. Cell Culture and Treatments

SW480 (RRID: CVCL_0546), SW620 (RRID: CVCL_0547) human, and CT26 (RRID: CVCL_7254) murine adenocarcinoma cell lines were purchased from ATCC (Rockville, MD, USA) and were maintained in RPMI medium (Life Technologies, Gaithersburg, MD, USA) that was supplemented with 10% fetal bovine serum (FBS) (Life Technologies). All cell lines were cultured in a humidified chamber at 37 °C with 5% CO_2.

2.2. Drugs, Antibodies, and Chemical Reagents

Tannic acid (TA) was obtained from Sigma-Aldrich laboratory (St. Quentin Fallavier, France) and a stock solution was prepared in dimethyl sulfoxide (DMSO). Antibodies targeting E-cadherin, N-cadherin, β-catenin, ZEB1, Slug, Snail, P38 MAPK, phospho (p) P38 MAPK, ERK1/2, phospho (p) ERK1/2, AKT, phospho (p) AKT, and GAPDH were used.

2.3. Crystal Violet Staining Assay

Cell viability was determined using crystal violet (CV) (4-[(4-dimethylaminophenyl)-phenyl-methyl]-N,N-dimethyl-aniline) to stain the DNA, as described previously [27,28]. Cells were seeded in triplicates in 96 well plates in RPMI + 10% FBS at the density of 2, 2.5, and 3 × 10^4, respectively, and incubated for 24 h in 5% CO_2 atmosphere and 95% humidity at 37 °C. Then, the cells were treated at 24 h, 48 h, and 72 h, with increasing concentrations of TA (1:2 serial dilutions; starting concentration 100 µM). As a control, cells were treated with the vehicle alone (DMSO 0.1%). After the treatment, the cells were washed with phosphate-buffered saline (PBS) 1×, and then fixed and stained with a CV solution (crystal violet 2.3%, ammonium oxalate 0.1%, ethyl alcohol 20%, 5 min), and rinsed with water. After extensive washing of the cells with water, CV was finally solubilised in 33% acetic acid. The absorbance was measured at 590 nm using a BiochromAsys UVM 340 spectrophotometer. The assays were carried out in three independent experiments. The results were expressed as a percentage of cell viability reffering to those treated with vehicle alone (control) assumed as 100% and using the following equation: Cell viability (%) = 100 − [(Absorbance control − Absorbance test/Absorbance control) × 100]. The dose–response curves were then plotted using GraphPad Prism software (v8.3.0), in order to determine, at the different times of treatment, the 50% inhibitory concentrations (IC_{50}, concentration of a molecule inducing 50% of toxicity on a given cell population) after an adjustment of the data by a non-linear regression with 4 parameters.

2.4. Cell Adhesion Assay

Cell adhesion was determined using a method described in [29]. Briefly, 96-well plates were pre-coated with fibronectin (1 µg/mL, Sigma-Aldrich, St. Louis, MO, USA) in Hank's buffer (Welgene Inc., Daegu, Republic of Korea), collagen I (20 µL, 5 g/mL, 0.01 M HCl in PBS), collagen IV (10 µg/mL in PBS), or poly-L-lysine (50 µg/mL), and allowed to adhere for 1 h at 37 °C. BSA (1% diluted in PBS) was added to each well for 1 h. The wells were washed twice with PBS and left to dry for a further 2 h. The cells were suspended in serum complete media containing TA at different concentrations and then plated into wells. After 48 h, the non-adherent cells were removed by media aspiration. The adherent cells were stained with 0.1% CV for 10 min at room temperature (RT), dissolved with 1% sodium dodecyl sulfate (Sigma-Aldrich), and then quantified by measuring the absorbance at 540 nm using a plate reader (Bio-Rad Laboratories).

2.5. Migration Using Wound-Healing Assay and Incucyte Device

A wound-healing assay was carried out to evaluate the effect of TA on cell migration. Cells were grown in six-well plates overnight until confluence. When the cells reached confluency, a wound was made by scratching the monolayer of cells using a sterile plastic 10 µL pipette tip. Then, the cells were rinsed with PBS to remove any free-floating cells and debris. Serum-free cell medium was then added, and culture plates were incubated

at 37 °C in the presence of TA for 48 h. Images of the scratched areas were captured with an inverted microscope (Olympus IX-71, Manchester, UK). Experiments were performed in triplicate for each condition and cell line. The average widths of the wounds at 0 h, 24 h, and 48 h time points were measured using Image-J software (NIH). The distance (D) migrated by the cells was calculated as follows: D = (size of the wound at t = 0 h—size of the wound at t = 24 h or 48 h). We next evaluated the effect of TA on TGF-β1-induced cell migration using the *IncuCyte® S3* Live-Cell Analysis System (Essen BioScience, Ann Arbor, MI, USA). The SW480 and CT26 cells were seeded in 96-well plates at 8×10^4 and 3×10^5 cells/well, respectively, in 100 µL of complete RPMI and incubated for 6 h at 37 °C and 5% CO_2. Then, they were serum starved (0.5% FBS) overnight. A homogeneous wide wound in the cell monolayer of each well was performed using the Wound Maker (Essen BioScience, Ann Arbor, MI, USA). The cells were washed twice with HBSS and then treated with TGF-β1 (10 ng/mL) in the presence or absence of TA (0.8 µM) for 72 h. The untreated cells served as the controls (solvents alone, Co). The plate was placed at 37 °C in the presence of 5% CO_2 in the *IncuCyte®* system and the cell migration was recorded every 2 h by phase-contrast scanning (10× objective) for 72 h. The wound recovery area at each time point was analyzed and the percentages of the wound relative density was determined with the using Incucyte®*S3* Software update (V2021B).

2.6. Migration and Invasion Using Transwell Assay

Cells were seeded in Transwell® chambers with an 8.0 µm Pore Polyester Membrane Insert (3464, Corning, Fisher Scientific S.A.S, Illkirch, France) for migration and invasion assays. For the migration assay, the treated cells in the serum-free medium were plated in uncoated inserts and incubated for 48 h. For the invasion assay, the inserts were pre-coated with 100 µL of Matrigel® (Matrigel® Basement Membrane Matrix, 354,234, Corning, NY, USA), and the treated cells were plated in the serum-free medium, as described above, for an incubation period of 48 h. A total of 500 µL of culture medium containing 10% FBS was added to the lower chamber. The cells attached to the bottom of the membrane were fixed with 4% paraformaldehyde, then were stained with 5% CV (Sigma-Aldrich). After 2 washes of the membrane, the CV was finally solubilized in 33% acetic acid. The absorbance was measured at 590 nm using a BiochromAsys UVM 340 spectrophotometer. Three independent experiments were performed in triplicates.

2.7. Western Blotting

Western blotting analysis was performed as described previously [30]. Cells were seeded into 75 cm^2 flasks 24 h before treatment, then were serum starved (1% FBS) overnight. The following day, the SW480 and the CT26 cells were treated with solvents alone (control cells) or were co-treated with TA (0.8 µM) and/or TGFβ-1 (10 ng/mL) for 48 h. After treatment, the cells were lysed with radio-immunoprecipitation assay (RIPA) buffer supplemented with a complete phosphatase and protease inhibitor cocktail (Roche, Boulogne Billancourt, France). An equal amount of protein was resolved by SDS-PAGE and transferred to nitrocellulose membranes (Amersham, Les Ulis, France). The membranes were saturated with 5% (*w/v*) nonfat dry milk for 1 h, and incubated with primary antibodies against N-cadherin (1:1000), E-cadherin (1:1000), β-catenin (1:1000), Slug (1:1000), Snail (1:1000), ZEB1 (1:1000), ERK1/2 (1:1000), p-ERK1/2 (1:1000), AKT (1:1000), p-AKT (1:1000), P38 (1:1000), p-P38 (1:1000), and GAPDH (1:3000) overnight at 4 °C. Primary antibodies were detected using horseradish peroxidase (HRP)-conjugated appropriate secondary antibodies (Cell Signaling Technologies, Ozyme, Saint-Cyr-l'Ecole, France), followed by exposure to Enhanced Chemiluminescence (ECL) (Santa Cruz Biotechnology, Heidelberg, Germany). A signal was acquired with a ChemiDocTM XRS + imaging system (Bio-Rad, Marnes-la-Coquette, France), and blots were analyzed with Image Lab™ v6.0.1 software (Bio-Rad, Marnes-la-Coquette, France).

2.8. Animal Studies

A total of 15 male BALB/c mice (8 weeks old and weighing ≈ 25 g) were housed according to the Council of the European Communities (86/609/EEC; 24 November 1986) Directives regulating the welfare of experimental animals, and experiments were approved by the Life Sciences and Health Research Ethics Committee (cer-svs) of the Institute of Biotechnology (University of Monastir, Tunisia; ethical approval no. 2021/02/I/CER-SVS/ISBM; 9 January 2021). The mice were maintained in a pathogen-free environment (24 °C and 50% humidity) on a 12 h light/12 h dark cycle, with food and water supplied ad libitum throughout the experimental period. The mice were allowed to acclimatize under the laboratory conditions for 1 week before being used for the experiments. CT26 colon cancer cells (10^6, suspended in 200 µL of PBS) were subcutaneously (s.c.) injected into their right hind leg. One week after tumor cell injection, the mice were separated into the following three experimental groups: vehicle (as a control), TA, and 5-FU (n = 5 per group). For all groups, DMSO was used at the final concentration of 0.1% and the control group received a saline solution with 0.1% of DMSO (Sigma-Aldrich, St. Quentin Fallavier, France, reference 67-68-5). In group 1, mice were treated with TA diluted in 0.1% DMSO, which was administered 3 times per week by intraperitoneal injection (15 mg/kg). In group 2, mice were treated with 5-FU in 0.1% DMSO once per week by intraperitoneal injection (15 mg/kg). The mice in the control group were administered a sterile saline solution with the same timing and dosing schedule as that used for the other treatment groups. The tumor volumes (TV) and body weights of the mice were measured every 2 days. TV was calculated using the following formula: TV (mm^3) = $\frac{1}{2} \times (D \times d^2)$, where D is the longest and d is shortest diameter.

2.9. Biochemical Assay

Blood samples were collected from the sacrificed mice. The serum samples were analyzed by the Biochemistry Department laboratory of the University Hospital Center (UHC) FarhatHached (Sousse, Tunisia). The aspartate transaminase (ASAT), alanine transaminase (ALAT), and creatinine (CR) levels were determined by automated analysis using a commercial Cobas Integra kit (Roche, Boulogne-Billancourt, France).

2.10. Satistical Analyses

The data are expressed as mean ± standard deviation (SD), or standard error of the mean (SEM), as indicated in the figure legends. Statistical analysis was carried out with Prism GraphPad8.0 Prism software (GraphPad Software, La Jolla, San Diego, CA, USA). Statistical comparisons among groups were performed using one-way and two-way analysis of variance (ANOVA), followed by Tukey's test for multiple comparison. The p-values ≤ 0.05 were considered significant (* $p < 0.05$, ** $p < 0.01$, *** $p < 0.001$, and **** $p < 0.0001$).

3. Results

3.1. TA Inhibits the Proliferation of Colorectal Carcinoma Cells

In order to determine whether TA presents potential chemopreventive properties against CRC, we first evaluated its cytotoxic effect on two human colorectal carcinoma cells lines, which were SW480 and its metastatic derived cell line SW620, and a murine CT26 CRC cell line was used in order to further explore the effect of TA in an in vivo model. Using the CV assays, we observed that TA induced a dose- and time-dependent cytotoxic effect, the latter of which being more pronounced from 48 h of treatment, using TA concentrations ranging from 0 to 100 µM (Figure 1). Indeed, the inhibitory concentration of 50% (IC_{50}) that was obtained after 48 h of treatment was found to be of 12 µM and 44 µM for SW480 and SW620, respectively, and was of 11 µM for the murine CT26 cells, the latter of which being the most sensitive cell line (Figure 1, Table 1). Based on these values at 48 h of treatment, we chose the following IC_{50}-related doses for subsequent experiments: 0.5 fold IC_{50} (1/2 IC_{50}), IC_{50}, and 2 fold IC_{50} (2 IC_{50}). In order to study the EMT, we focused on the two cell

lines that were found to be most sensitive to TA, which were the SW480 and CT26 cells. The SW620 cells displayed lower sensitivity to TA, and as they have a metastatic phenotype (they are derived from a metastasis of the same tumor from which SW480 cells are derived), they were not used in the following experiments aiming to evaluate the inhibitory potential of TA on the EMT.

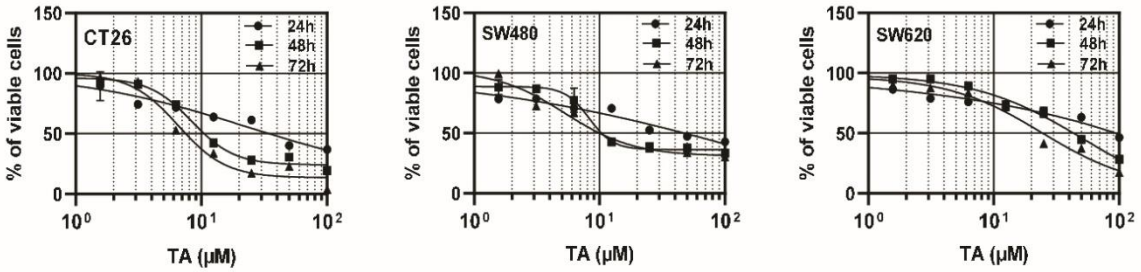

Figure 1. TA decreases the viability of CT26, SW480, and SW620 CRC cells in a dose- and time-dependent manner. Cells were exposed to increasing concentrations of TA (from 0 to 100 µM) for 24 h, 48 h, and 72 h. Cell viability was determined by CV assay and expressed as a percentage of the control (DMSO). Dose–response curves were plotted at the different treatment time points in the 3 cell lines with 4-parameter non-linear regression using GraphPad prism software. Each point of the curves represents the mean percentage of viable cells ± SD of 3 independent experiments, with 5 replicates per condition.

Table 1. TA IC_{50} values were determined after 24 h, 48 h, and 72 h of treatment in CRC cell lines. Statistical significance was determined by one-way ANOVA, followed by Tukey's test for multiple comparison. *** p <0.001, **** p <0.0001 vs. CT26 cells at 24 h; #### p <0.0001 vs. SW480 cells at 24 h; $$$ p <0.001, $$$$ p <0.0001 vs. CT26 cells at 48 h; ££££ p <0.0001 vs. SW480 cells at 48 h; ¥¥¥¥ p < 0.0001 vs. CT26 cells at 72 h; and &&&& p < 0.0001 vs. SW480 cells at 72 h.

Time of Treatment (h)	Cell Line		
	CT26	SW480	SW620
24	34.48 ± 1.20	48.49 ± 1.68 ***	88.17 ± 2.77 ****, ####
48	11.16 ± 0.14	12.16 ± 0.11 $$$	44.20 ± 0.20 $$$$, ££££
72	7.61 ± 0.14	9.40 ± 0.08 ¥¥¥¥	25.75 ± 0.02 ¥¥¥¥, &&&&

3.2. TA Inhibits Colorectal Carcinoma Cell Adhesion

Before studying the EMT, we evaluated the capacity of TA to modulate the adhesion of CRC cells in the presence of three important factors of the extracellular matrix (ECM). Indeed, for example, an ECM that is rich in type I collagen has been shown to confer a tumor phenotype to untransformed pancreatic ductal cells [31]. In a same manner, fibronectin induces the EMT in CRC cells and plays a pivotal role in promoting CRC metastasis [32]. A recent review has summarized the ECM content in the stroma surrounding the primary CRC and presented a quantitative comparison of the identified components with those from a normal colon [33]. In the light of these elements, we tested the efficiency of TA to decrease the adhesion capacity of CRC cells in the presence of the following three major compounds, that are found increased during EMT process: collagen type I and IV, and fibronectin. We next evaluated the specific adhesion and the nonspecific cell adhesion using collagen I and IV or fibronectin pre-coated wells, respectively, and poly-L-lysine pre-coated wells. The CRC cells' capacity to adhere to these differentially pre-coated wells was evaluated after 48 h of seeding and with a prior treatment of the cells for 30 min in the presence or absence of TA, which was used at three concentrations, based on the IC_{50} values that were determined at 48 h (Table 1). In these experimental settings, we observed that TA was able to significantly decrease the percentage of cell adhesion only in the presence of the collagen

I and IV, and fibronectin for the SW480 and CT26 cell lines in a concentration-dependent manner (Figure 2). It is interesting to note that no effect was observed on cell adhesion to the integrin-independent substrate, the poly-L-lysine.

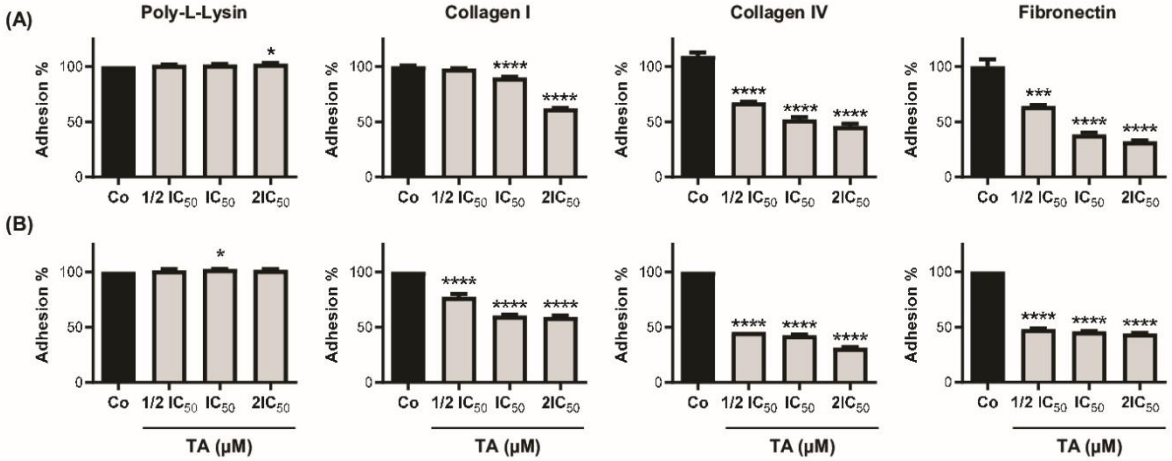

Figure 2. TA inhibits CRC cell adhesion. SW480 (**A**) and CT26 (**B**) cells were exposed for 30 min to 3 different IC_{50}-related doses of TA (SW480 cells: IC_{50} = 12 µM, $\frac{1}{2}$ IC_{50} = 6 µM, and $2IC_{50}$ = 24 µM; CT26 cells: IC_{50} = 11 µM, $\frac{1}{2}$ IC_{50} = 5.5 µM, and $2IC_{50}$ = 22 µM) and seeded on poly-L-Lysin, type I or type IV collagen (collagen I and collagen IV, respectively), and fibronectin pre-coated wells to evaluate ECM protein-dependent cell adhesion. After 48 h, the percentage of attached cells was determined by CV assay. The results are expressed as the percentage of solvent control (DMSO, Co) (mean ± SD) of 3 independent experiments performed in triplicate per condition. Statistical significance was determined by one-way ANOVA, followed by Tukey's test for multiple comparison tests, with $p < 0.05$ (*), $p < 0.001$ (***), and $p < 0.0001$ (****) vs. the corresponding control group.

3.3. TA Inhibits Cell Migration

Metastasis development involves multiple biological mechanisms, including an increase in cell motility. For this reason, the migratory capacity of SW480 and CT26 cells was assessed with wound-healing assays. Confluent cell monolayers were scratched and then the recolonization of the latter was monitored at specific time points (24 h and 48 h) by microscopy or by video microscopy for 72 h. The concentrations of TA that were used for the wound-healing treatments were $\frac{1}{2}$ IC_{50}, IC_{50}, and $2IC_{50}$, as determined previously in Figure 1 and Table 1 for the two cell lines. As shown in Figure 3, TA inhibited SW480 and CT26-cell migration after 48 h of incubation in a dose-dependent manner, with an inhibition rate of >80% in SW480 and 50% in CT26. In addition, the result from the transwell migration assay was in line with the data from the scratch assay. In Figure 4A, TA efficiently inhibited SW480 and CT26-cell migration in a dose-dependent-manner and the inhibition rates after 48 h of treatment were >72% in SW480 and 50% in CT26 cells.

3.4. TA Inhibits TGF-β1-Induced Motility of Metastatic Colon Cancer Cells In Vitro

The effects of TA on TGF-β1 induced cell migration were further studied using a real-time cell imaging system (IncuCyte® S3 Live-Cell Imaging System, Essen BioScience, Ann Arbor, MI, USA). As shown in Figure 3C,D, TA blocked the TGF-β1-induced migration of the SW480 and CT26 cells. Through the EMT, the cells acquire migratory and invasive capacity. The migration and invasion of cells are the essential steps to form metastatic foci. Thus, we next determined the effects of TA on the invasion and migration that was induced by TGF-β1. As shown in Figure 4B,C, TA blocked the TGF-β1-induced invasion and migration of the SW480 and CT26 CRC cells.

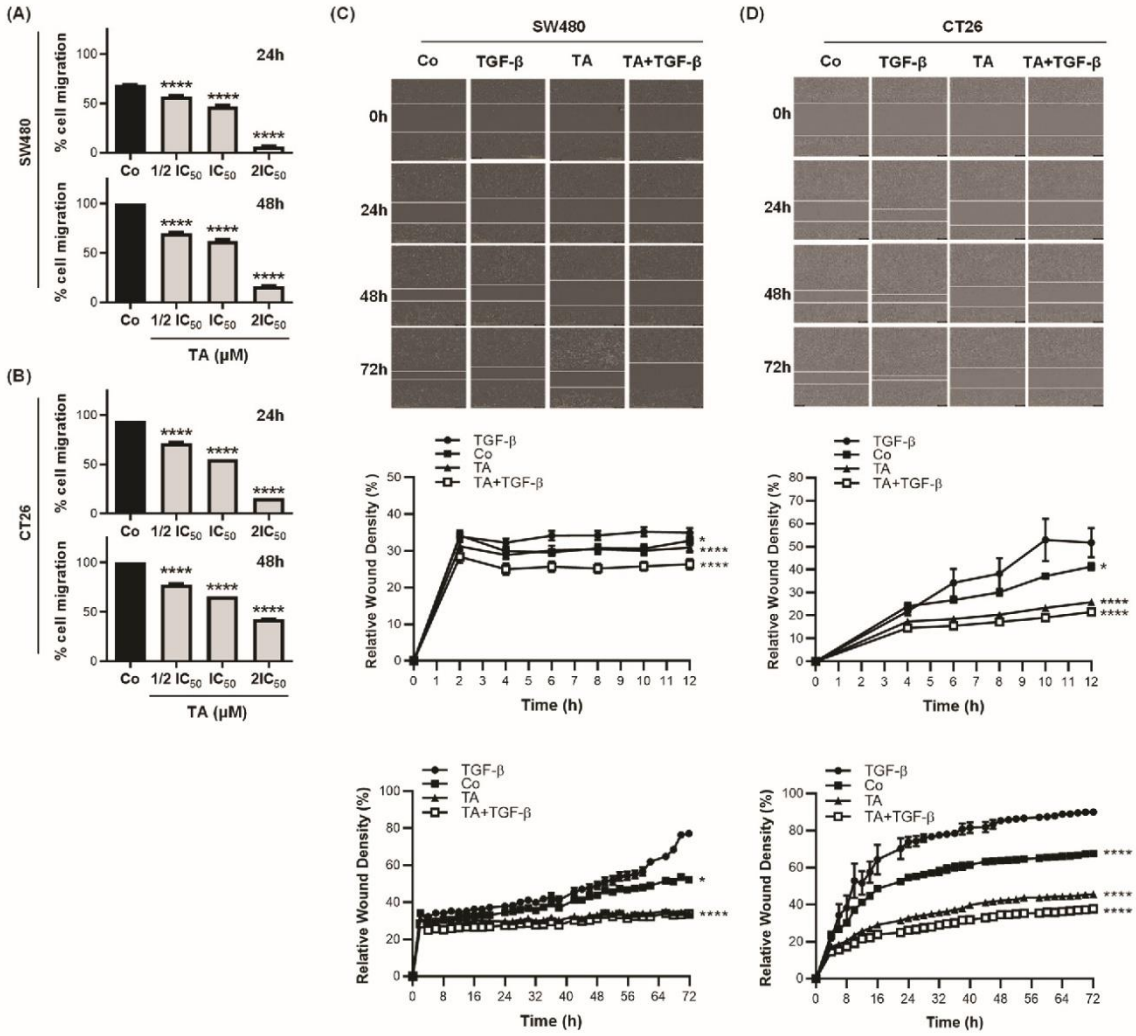

Figure 3. TA decreases the basal and TGF-β-induced migratory abilities of CRC cells. (**A**,**B**) Confluent SW480 and CT26 cell monolayers were subjected to scratch wounding and then cultured in RPMI medium with 0.5% FBS only (Control, Co), or in the presence of TA (SW480 cells: IC_{50} = 12 μM, $\frac{1}{2}$ IC_{50} = 6 μM, and $2IC_{50}$ = 24 μM; CT26 cells: IC_{50} = 11 μM, $\frac{1}{2}$ IC_{50} = 5.5 μM, and $2IC_{50}$ = 22 μM). The percentages of the wound recovery area at 24 h and 48 h, reflecting cell migration, were calculated as described in the Materials and Methods Section and are expressed as the mean ± SD of 3 experiments (n = 3) carried out in 3 replicates per condition. Statistical significance was determined by one-way ANOVA, followed by Tukey's test for multiple comparison tests, with **** $p \leq 0.0001$, vs. the corresponding control group. (**C**,**D**) Confluent SW480 and CT26 cell monolayers were subjected to scratch wounding and then cultured in RPMI medium with 0.5% FBS only (Control, Co), or in the presence of TA (0.8 μM), TGF-β (10 ng/mL), or TA and TGF-β (TA + TGF-β). The percentages of the wound recovery area over time (up to 72 h), reflecting cell migration, were calculated as described in the Materials and Methods Section and are expressed as the mean ± SD of 3 experiments (n = 3) carried out in 3 replicates per condition. (**C**,**D**, top panel). Representative photomicrographs (10× objective) of the wounds at 0 h (initial wounds), and at 24 h, 48 h, and 72 h were taken using the IncuCyte® S3 Live-Cell Analysis System. The dotted lines represent the migration front lines. Statistical significance was determined by one-way ANOVA, followed by Tukey's test for multiple comparison tests, with * $p < 0.05$, **** $p < 0.0001$, vs. TGF-β group.

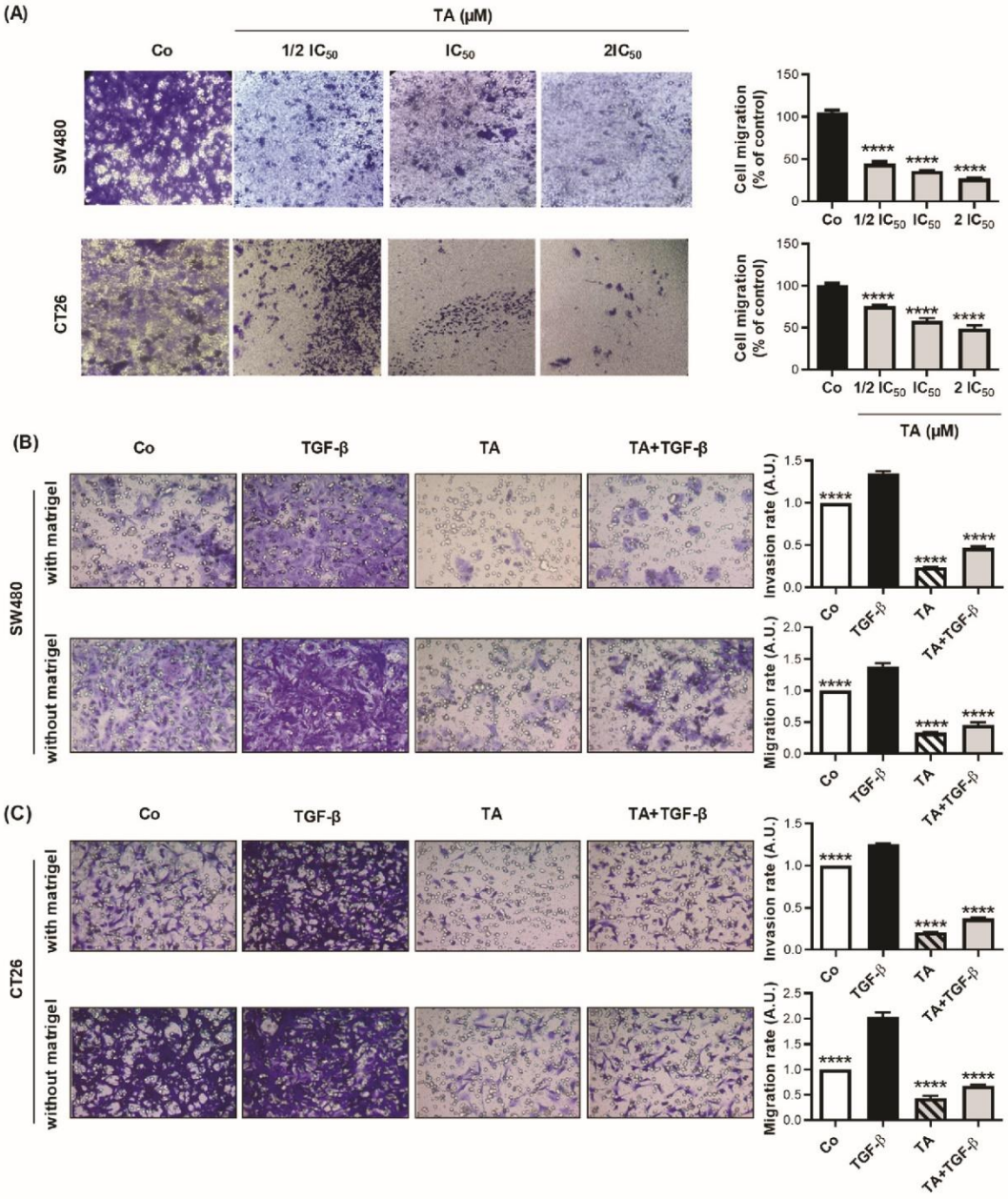

Figure 4. TA decreases the basal and TGF-β-induced migration abilities and invasiveness of CRC cells. SW480 and CT26 cells were seeded into the upper filters (migration assay) or on Matrigel-precoated filters (invasion assay) of Boyden chambers and incubated at 37 °C in complete RPMI medium only (Control, Co), or in the presence of TA (0.8 µM), TGF-β (10 ng/mL), or a combination of both (TA + TGF-β). After 48 h, cells that had migrated to the bottom of the filter were stained using CV and photographed. The cell migration ability was determined by measurement of CV absorbance at 540 nm after solubilization in 33% acetic acid. (**A**) Representative photomicrographs (10× objective) of the trans-well migration assays on the left panel. The right panel represents the cell migration rate normalized as a percentage of control (100%). Representative photomicrographs (10× objective) of the trans-well Matrigel invasion (upper row) and migration (bottom row) assays are on the left panel

for (**B**) SW480 and (**C**) CT26 cell lines. The right panel represents the cell invasion (upper) and migration (bottom) rates normalized to the control. Results are expressed as mean ± SD of 3 independent experiments (n = 3) carried out in 3 replicates per condition. Statistical significance was determined by one-way ANOVA, followed by Tukey's test for multiple comparison tests, with **** $p \leq 0.0001$, vs. the corresponding control group.

3.5. TA Restores Epithelial Markers Expressionin CRC Cells

The migratory capacity of cancer cells is necessary for metastasis and the acquisition of metastatic capability is associated with the EMT in cancer cells. During the process of EMT, the epithelial cells lose cell-to-cell contacts and gain the expression of mesenchymal factors, enabling migration and invasion into the surrounding stroma in order to facilitate metastasis. In this process, E-cadherin and β-catenin loss are relatively common in cancers of epithelial origin, such as colon cancer. In order to investigate the effect of TA on the TGF-β1-induced EMT, the protein expression of the epithelial markers, such as β-catenin and E-cadherin, was analyzed in SW480 and CT26 cells (Figure 5).

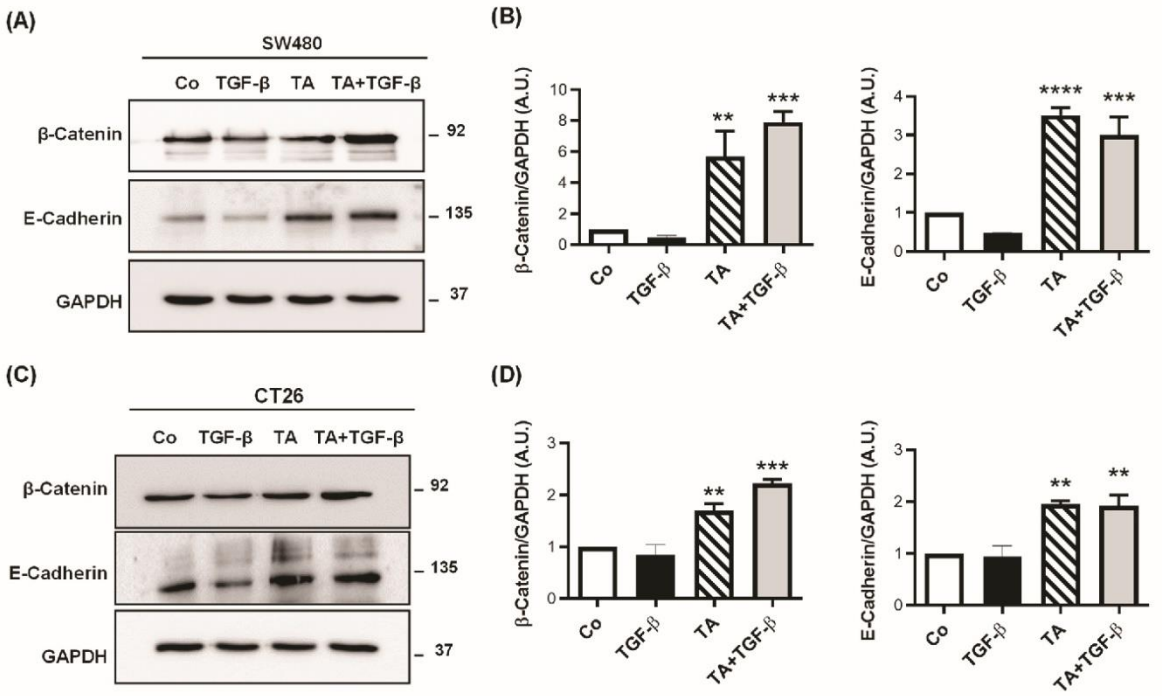

Figure 5. TA inhibits the TGF-β-induced decrease in epithelial marker expression in SW480 and CT26 cells. Serum-starved SW480 and CT26 cells were treated with TA (0.8 μM), TGF-β (10 ng/mL), or a combination of both (TA + TGF-β) for 48 h. Vehicle-treated cells served as the control (Co). Representative immunoblot and densitometry quantification analysis of EMT markers β-catenin and E-cadherin in SW480 (**A**,**B**) and CT26 (**C**,**D**) after 48 h of treatments. The band intensity was quantified using GAPDH as an internal loading control, and quantification values were normalized to the control. Results are expressed as mean ± SD of 3 independent experiments (n = 3). Statistical significance was determined by one-way ANOVA, followed by Tukey's test for multiple comparison tests, with ** $p < 0.01$, *** $p < 0.001$, and **** $p < 0.0001$, vs. the corresponding TGF-β1 group.

First of all, we observed that TA, at the IC_{50}, significantly increases the protein expression of β-catenin and E-cadherin after 48 h of treatment in SW480 cells (Figure 5A,B). Very interestingly, when SW480 cells are cotreated with TGF-β1 and TA over 48 h, the increases in the two epithelial markers are maintained at the induction levels similar to

those that were obtained with TA alone (Figure 5A,B). In the same way, similar results are observed in CT26 cells, with a weak but significant TA of β-catenin and E-cadherin expression, compared to the control (Figure 5C,D). As observed in the SW480 cells, the protein expression level of β-catenin and E-cadherin was very similar to TA alone when cotreated with TA and TGF-β1 in the CT26 cells (Figure 5C,D).

3.6. TA Inhibits Mesenchymal Marker Expression in Colorectal Cancer Cells

Mesenchymal markers, such as Slug, Snail1, and ZEB1, enable EMT through various mechanisms [34]. They act by either repressing the transcription of genes coding for proteins of adherent junctions, such as E-cadherin [35], or by activating the expression of mesenchymal genes (N-cadherin, vimentin), which are involved in cytoskeleton remodeling and enzyme production, promoting cell motility and basal lamina degradation. In the present study, we highlight that TA was able to both decrease the protein expression of the transcription factors Slug, Snail1, and ZEB1 in basal conditions and also counteract their TGF-β1-induced expression (Figure 6).

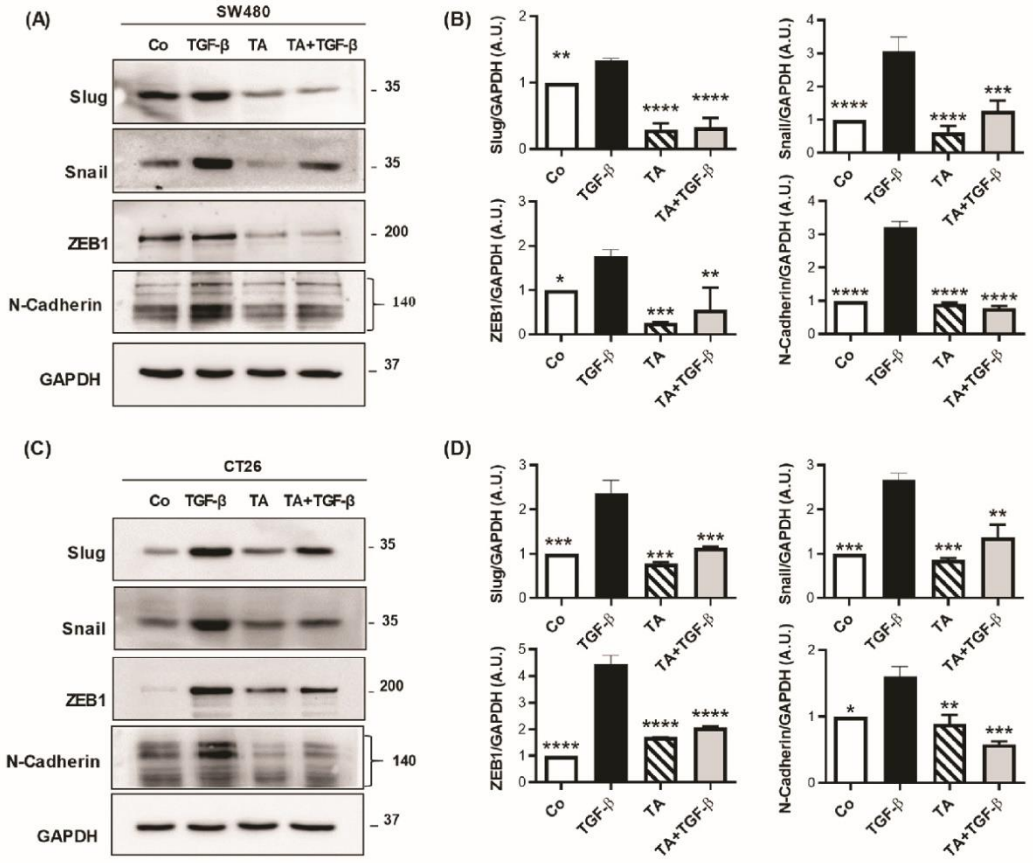

Figure 6. TA inhibits TGF-β-induced mesenchymal marker expression in SW480 and CT26 cells. Serum-starved SW480 and CT26 cells were treated with TA (0.8 μM), TGF-β (10 ng/mL), or a combination of both (TA + TGF-β) for 48 h. Vehicle-treated cells served as the control (Co). Representative immunoblot and densitometry quantification analysis of EMT markers Slug, Snail, ZEB1, and N-cadherin in SW480 (**A**,**B**) and CT26 (**C**,**D**) after 48 h of treatment. The band intensity was quantified using GAPDH as an internal loading control, and quantification values were normalized to the control. Results are expressed as mean ± SD of 3 independent experiments (n = 3). Statistical significance was determined by one-way ANOVA, followed by Tukey's test for multiple comparison tests, with * $p \leq 0.05$, ** $p < 0.01$, *** $p < 0.001$, and **** $p < 0.0001$, vs. the corresponding TGF-β1 group.

The transcription factors, Slug, Snail, and ZEB1 were significantly decreased with TA treatment alone, as compared to the control by 70, 40, and 65%, respectively, in SW480 cells (Figure 6A,B). As expected, and previously described in the literature, TGF-β1 induces a strong expression of all of the transcriptional factors (Slug, Snail, and ZEB1), as well as N-cadherin (Figure 6A,B). Interestingly, when SW480 cells are cotreated with TGF-β1 and TA over 48 h, we observed a strong inhibition of all of the TGF-β1-induced epithelial markers in the SW480 cells by 90% (Slug), 60% (Snail), 68% (ZEB1), and 78% (N-cadherin), as compared to TGF-β1 alone (Figure 6A,B). These effects of TA on TGF-β1-induced epithelial markers in the SW480 cells were also observed in the CT26 cells (Figure 6C,D). Overall, our data provide in vitro evidence that TA prevents the epithelial cells from transitioning to a mesenchymal-like phenotype induced by TGF-β1 treatment.

3.7. TA Antagonizes TGF-β1-Mediated Smad-Independent Signaling Pathways

Activation of Smad-dependent and/or independent signaling pathways are reported to be critical for TGF-β-induced EMT [36]. In order to further explore the mechanism underlying the antifibrotic effects of TA, overnight serum-starved SW480 and CT26 cells were stimulated with TGF-β1 for 48 h in the presence or absence of TA. We investigated the influence of TA on other non-Smad pathways, such as mitogen-activated protein kinase (MAPK), signaling (P38 and ERK), and AKT signaling pathways.

Firstly, as expected, the TGF-β1 treatment alone induced the phosphorylation of ERK1/2, P38, and AKT protein, without modulation of their expression level (Figure 7). Very interestingly, the treatment of SW480 and CT26 cells for 48 h with TA alone, or in combination with TGF-β1, strongly decreased phosphorylated forms of ERK1/2, P38, and AKT (Figure 7). Collectively, our results have indicated that TA inhibits TGF-β1-induced EMT through the inhibition of non-Smad signaling pathways.

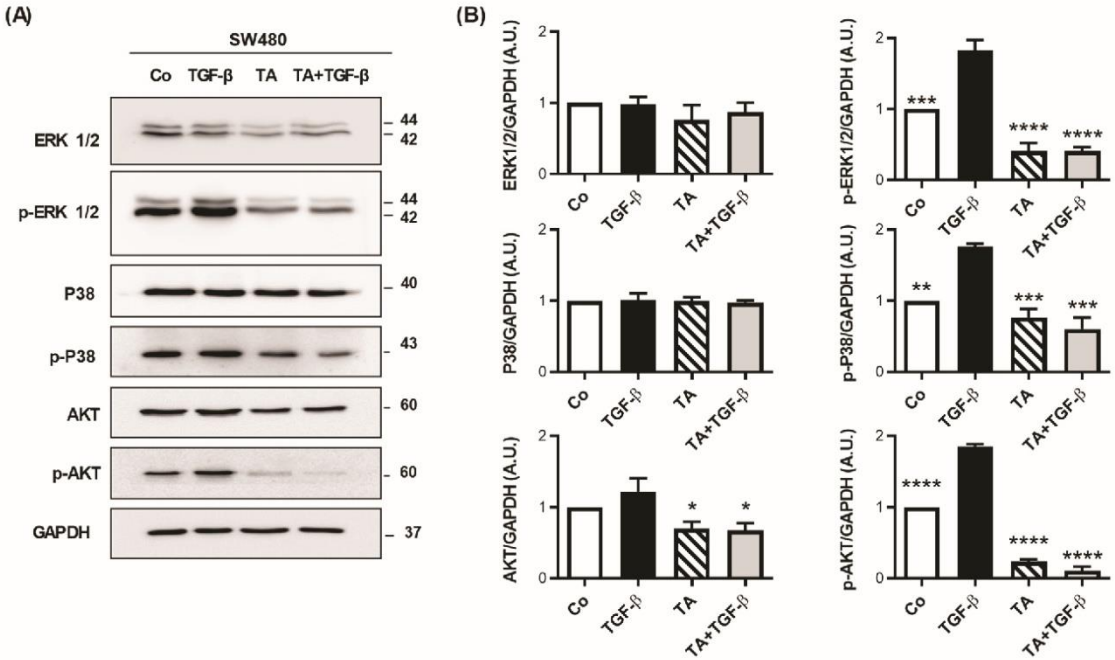

Figure 7. *Cont.*

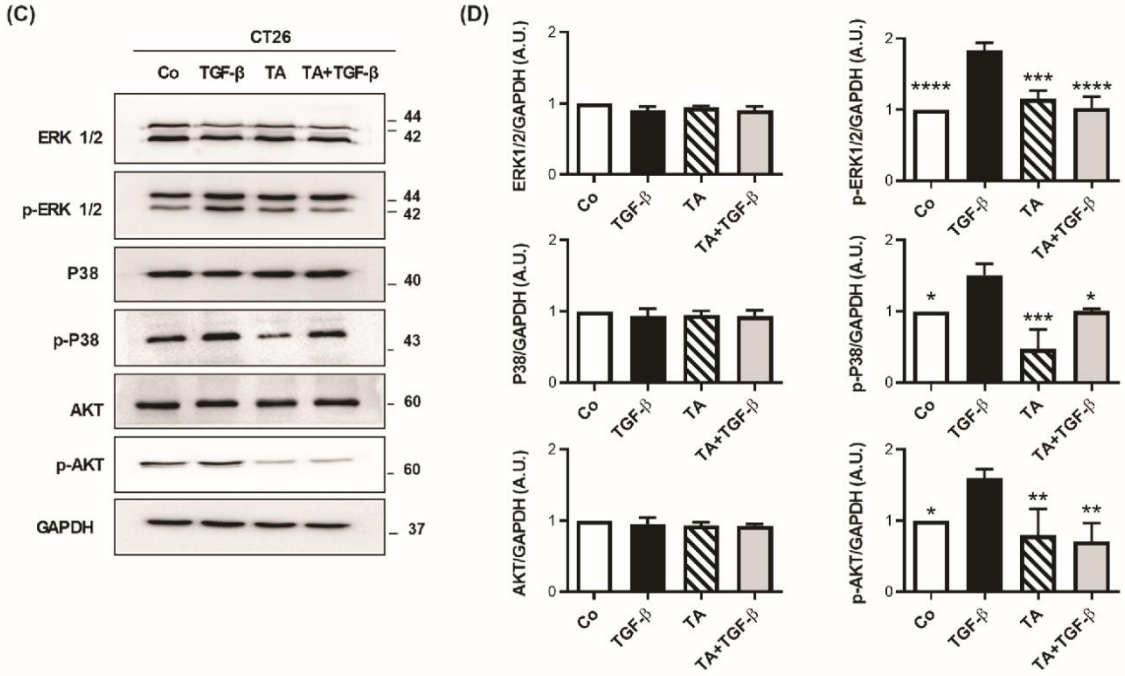

Figure 7. TA blocks TGF-β-induced non-Smad-dependent signaling pathways in SW480 and CT26 cells. Serum-starved SW480 and CT26 cells were treated with TA (0.8 µM), TGF-β (10 ng/mL), or a combination of both (TA + TGF-β) for 48 h. Vehicle-treated cells served as the control (Co). Representative immunoblot and densitometry quantification analysis of total and phosphorylated (*p*-) $ERK_{1/2}$, P38, and AKT in SW480 (**A**,**B**) and CT26 (**C**,**D**) cells after 48 h of treatments. The band intensity was quantified using GAPDH as an internal loading control, and quantification values were normalized to the control. Results are expressed as mean ± SD of 3 independent experiments (n = 3). Statistical significance was determined by one-way ANOVA, followed by Tukey's test for multiple comparison tests, with * $p < 0.05$, ** $p < 0.01$, *** $p < 0.001$, and **** $p < 0.0001$, vs. the corresponding TGF-β1 group.

3.8. TA Prevents Murine Colon Carcinoma Growth

In order to determine whether TA is able to prevent tumor progression, we used a syngeneic model of CT26 tumors that were subcutaneously injected into BALB/c, which we challenged three times per week, either with a fixed amount of TA (15 mg/kg), or 5-FU (15 mg/kg) or with sterile saline solution for the control group. Our results showed that, comparatively to the control mouse group, TA was able to significantly delay the growth of tumors (Figure 8A,B). As expected, the 5-FU-related side effects were associated with rises in alanine transaminase (ALT), aspartate transaminase (ASAT), and creatinine (CR) levels in the blood samples from mouse group that was treated with the chemotherapeutic agent (Figure 8C). Very surprisingly, the treatment with TA decreased the expression of these three markers of toxicity (Figure 8C), suggesting that the antitumor effect of TA was not associated with a toxicity, as observed in the 5-FU-treated mice (Figure 8C).

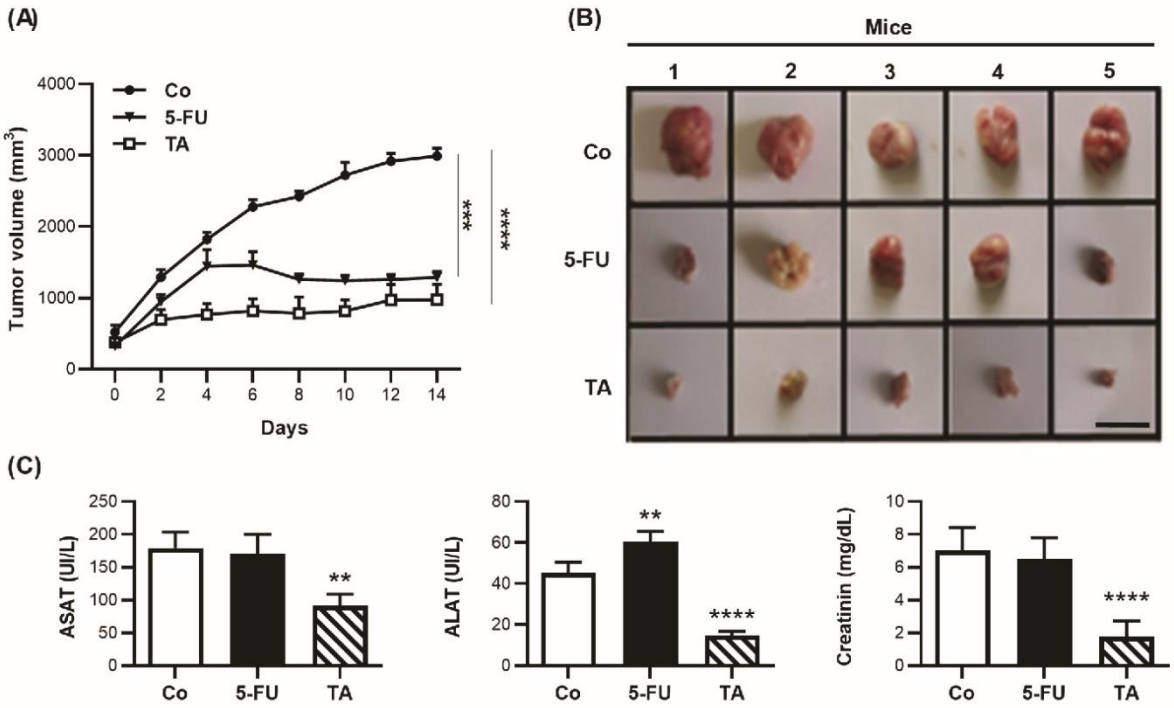

Figure 8. TA inhibits tumor growth without hepato- and nephrotoxicities in vivo. (**A**) One week after tumor cell injection, CT26 subcutaneous tumor-bearing BALB/c mice were treated (day 0 on the graph) with sterile saline solution (control group (Co, ●), 5-FU (15 mg/kg, ▼), or TA (15 mg/kg, □), (n = 5 mice per group)), and the treatment was continuing at a rate of one injection every 2 days. The evolution of tumor volumes (mm^3) in time was determined. (**B**) Images of tumors harvested from the mice on day 14 (scale bar = 1 cm). (**C**) Measurement of serum aspartate transaminase (ASAT), alanine transaminase (ALT), and creatinine levels in Co, 5-FU-, or TA-treated mice. The data are (**A**) medians ± SEM or (**C**) means ± SD of 3 independent experiments (n = 3). Statistical significance was determined by one-way ANOVA, followed by Tukey's test for multiple comparison tests, with ** $p < 0.01$, *** $p < 0.001$, and **** $p < 0.0001$, vs. the corresponding control group.

4. Discussion

Colorectal cancer (CRC) is the second most lethal cancer and the third most prevalent malignant tumor worldwide [3]. Despite the innovation and supportive care in cancer over the last several decades, which increase the overall survival rate of patients due to better cancer prevention, early detection, and treatments, the prognosis of CRC remains unsatisfactory, especially for patients with metastatic lesions [37].

This therapeutic failure can result from numerous phenomena that are linked to the host, to the cancerous cells themselves, which can present an intrinsic or an acquired resistance, or even to the tumor microenvironment. Many studies demonstrate that this would play a primordial role in the progression of the metastatic phenotype and in the acquisition of the phenomenon of chemoresistance.

The re-emergence of nutraceutical and plant/diet extracts, or the formulation of a mixture of them, as a promising field of investigation for the identification of innovative anticancer treatments provide a challenging opportunity to further explore the link between nutritional agents and tumor growth and spreading metastasis.

In this context, we show for the first time that a polyphenol, such as TA, could affect the microenvironment through a disruption of the EMT in CRC cells. We provide a mechanism by which TA affects the migration and the adhesion of CRC cells via a decrease in mesenchymal biomarkers and an increase in epithelial proteins under TGF-β1 treatment.

These events were associated with a TA-induced inhibition of the key regulators of the non-Smad pathways, such as mitogen-activated protein kinase (MAPK), signaling (P38 and ERK), and AKT signaling pathways (Figure 9). By these methods, the supplementation of mice with TA led to tumor regression without toxicity.

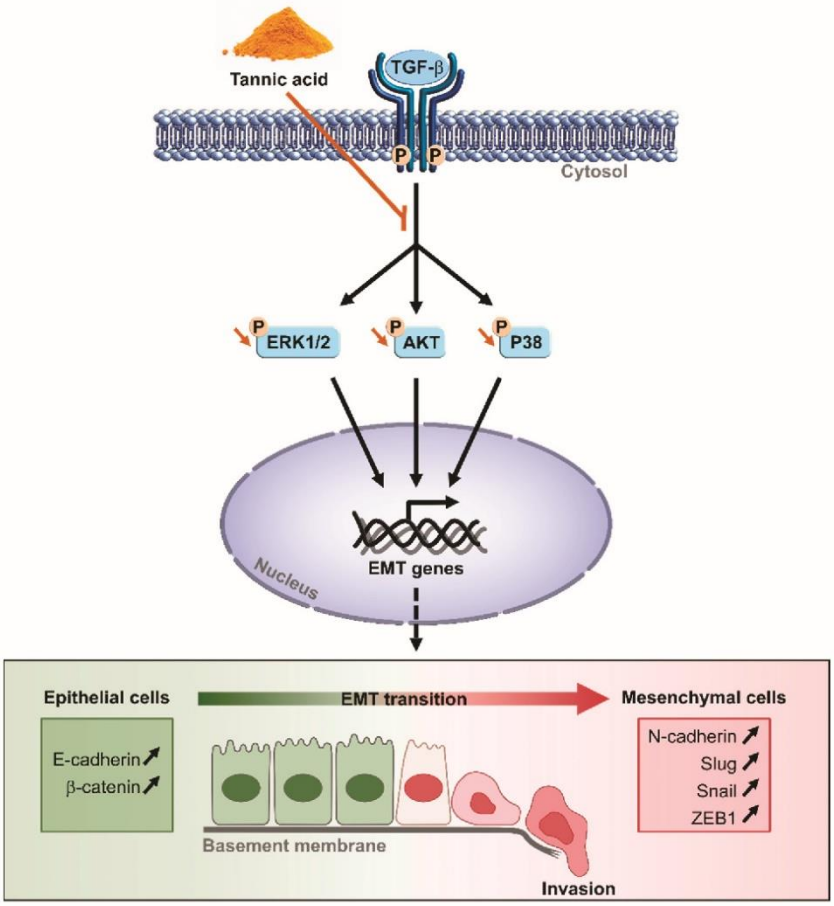

Figure 9. Tannic acid inhibits the epithelial–mesenchymal transition (EMT) of CRC cells by disrupting TGF-β1-mediated Smad-independent signaling pathways. Briefly, tannic acid decreases the phosphorylation of ERK1/2, AKT, and P38, and subsequently prevents invasion mediated by EMT.

EMT is characterized by the occurrence of morphological and phenotypic changes allowing cancer cells to acquire the properties of mesenchymal cells. Recent work suggests the involvement of the EMT in the phenomenon of chemoresistance in CRC [38,39]. From a molecular point of view, the establishment of the mesenchymal phenotype requires modifications of the genetic program that is carried out by ZEB1, Twist, and Snail [40]. In the epithelial cells, the transcription factor Snail is phosphorylated on serine residues by glycogen synthase kinase 3 beta (GSK3β), which constitutes a poly-ubiquitination signal, leading to the degradation of Snail by the proteasome [41]. In the present study, we show that TA was able to strongly decrease both the basal expression of Snail and ZEB1, compared to untreated SW480 and CT26 CRC cells, as well as their expression that is induced by the TGF-β1 (Figure 6). Snail regulates the expression of a large number of proteins. It decreases the expression of the epithelial markers, such as E-cadherin, Claudin-1, and occludin, and activates the expression of the mesenchymal markers, such as fibronectin, vitronectin, and N-cadherin [42]. The transcription factor ZEB acts as a repressor of the transcription of genes coding for the cell junction proteins [43] and also stimulates the

expression of N-cadherin [42]. Thus, by its action on Snail and ZEB1, TA also decreases the basal expression of N-cadherin and the expression that is induced by TGF-β1 (Figure 6). Very interestingly, TA affects another important mesenchymal factor, the Slug protein, which has been found to be overexpressed in many cancers, including breast and lung cancers, leukemia, glioblastoma, and hepatocarcinoma, but also CRC [22,24,26,44,45]. This protein contributes to the loss of cell adhesion and polarity by repressing the adhesion proteins. These alterations give the cells the ability to migrate and invade the surrounding tissues and neighboring organs. One of its transcriptional targets is E-cadherin [42]. It is well known that Slug represses the expression of various epithelial genes, such as cytokeratins, occludin, and zonulaoccludens, which are genes that are involved in tight junctions. This transcription factor also initiates the EMT by altering the organization of the desmosomes by repressing the expression of desmoplakin and desmoglein, as well as the cadherins, which are the constituent elements of the desmosomes [46]. In addition, it can activate the transcription of the mesenchymal genes indirectly or directly, such as fibronectin, vimentin, and N-cadherin, depending on the cell type and the cell signals that are transduced [42]. Some studies have demonstrated the existence of cooperation between EMT transcription factors in the inhibition of E-cadherin. Indeed, one of the transcriptional targets of Slug is the ZEB1 protein, which is capable of directly activating the transcription of N-cadherin and vimentin in melanoma [47]. Likewise, TA impacts N-cadherin by decreasing its protein expression and, conversely, by increasing that of epithelial E-cadherin, both at a basal level and under TGF-β1 stimulation (Figures 5 and 6). The E-cadherin is usually located in the adherent junctions and in the basolateral plasma membrane, where, by its extracellular end, it allows interactions between two neighboring cells. Within the same time, the intracytoplasmic region of E-cadherin interacts with the actin cytoskeleton via α- and β-catenins [48]. This complex, therefore, ensures cellular stability and enables the reorganization of the cytoskeleton. In addition to its intercellular adhesion function, E-cadherin transmits signals by interacting with β-catenin [49]. The repression of E-cadherin transcription is mediated by transcription factors, including Snail1, Snail2, ZEB1, ZEB2, and Twist. These E-cadherin transcriptional repressors are generally expressed after the activation of the signaling pathways that are mediated by EMT-inducing factors (i.e., TGF-β1). Consequently, TA increased both E-cadherin and β-catenin in the CRC cells that were used in this study (Figure 5).

Moreover, TA action on Slug is likely to be linked to its anti-migration and anti-invasion properties. Indeed, Slug has been associated with a wide spectrum of biological functions, including motility, migration, invasion, adipogenesis, stem phenotype, and survival. In pathophysiological conditions, these mechanisms contribute to promoting tumor progression, aggressiveness, and also the emergence of metastases. The EMT aids tumor cells in their transition from an epithelial morphology to a motile and invasive mesenchymal phenotype, and then assists tumor cells to cross or disrupt the basal lamina barrier and invade the neighboring tissue. Several studies showed the anti-migratory and anti-invasiveness potential of TA in breast, prostate, and non-small-cell lung cancer cells [44,45,50–52]. To the best of our knowledge, our study is the first one that demonstrates that TA significantly abrogated the TGF-β1-induced migration and the invasion capability of CRC cells in vitro, using both murine CT26 and human SW480 cell lines.

Among the signaling pathways that are involved in the EMT process, many are those activated by the TGF-β receptor (TGF-βR). This can stimulate the PI3K/AKT and Smad2/3 pathways that are involved in the repression or the activation of genes coding for proteins involved in the EMT [7]. The TGF-βR signaling pathways lead to the dissolution of cell junctions and, subsequently, to cellular morphological changes [53]. TGF-β1 can also induce the MAPK pathway that is involved in the EMT [54]. In this context, TGF-β1 triggers the activation of the MAPKs, ERK1, and ERK2, in order to promote the expression of Snail and Rho-GTPases, which are a family of G proteins that are involved in the dynamics of the actin cytoskeleton during the migration process. Thus, the MAPK pathway contributes to the establishment of the EMT, cell motility, and the acquisition of the invasive properties

of tumor cells [55]. Similar activation of the PI3K/AKT pathway leads to the inhibition of the GSK3β protein, which subsequently favors the stabilization of β-catenin and the transcription factor, leading ultimately to the modulation of the genes controlling the EMT. Very interestingly, we have shown that TA was able to target different signaling pathways through both the diminution and the activation of ERK1/2, AKT, and P38 kinases (Figure 7). Together, these events contribute to strongly delaying the tumor growth in mice, as demonstrated by the action of TA in the mice that were grafted with CT26 CRC cells.

5. Conclusions

Based on functional assays using both human and murine cancer cells, in this study we have explored the anti-metastatic impact of TA on CRC. Our results demonstrate that TA decreases cell motility/invasiveness by reducing the expression of the mesenchymal biomarkers β-catenin and E-cadherin, and by increasing that of the epithelial markers Slug, Snail, ZEB1, and N-cadherin. These molecular events were associated in vivo with a tumor regression in mice that were supplemented with TA, without apparent signs of hepato- and nephrotoxicities. These findings pave the way for the recommendation of nutraceutical TA or tannin-containing foods as preventive agents and potential adjuvants and as a complementary approach to conventional treatments in order to improve treatment outcomes.

Author Contributions: M.B., C.C., F.H., A.G., M.S. and A.S. performed the experiments and analyzed the data; L.C.-G., V.A. and D.D. supervised the experiments; F.H., L.C.-G., V.A. and D.D. wrote the manuscript; V.A. and D.D. supervised the overall project. All authors have read and agreed to the published version of the manuscript.

Funding: This work was supported by a French Government grant managed by the French National Research Agency under the program "Investissements d'Avenir", reference ANR-11-LABX-0021, and was supported by grants from the "Conseil Régional de Bourgogne" and the "Fonds Européen de Développement Régional" (FEDER). The authors acknowledge the Tunisian Higher Education and Scientific Research Ministry for the financial support of this study.

Institutional Review Board Statement: Not applicable.

Informed Consent Statement: Not applicable.

Data Availability Statement: The authors declare that all data supporting the findings of this study are available within the article.

Conflicts of Interest: The authors declare no conflict of interest.

References

1. Favoriti, P.; Carbone, G.; Greco, M.; Pirozzi, F.; Pirozzi, R.E.M.; Corcione, F. Worldwide burden of colorectal cancer: A review. *Updates Surg.* **2016**, *68*, 7–11. [CrossRef]
2. Abdel-Samad, R.; Aouad, P.; Darwiche, N. Natural and synthetic retinoids in preclinical colorectal cancer models. *Anti-Cancer Drugs* **2019**, *30*, 655–669. [CrossRef]
3. Siegel, R.L.; Miller, K.D.; Jemal, A. Cancer statistics, 2019. *CA Cancer J. Clin.* **2019**, *69*, 7–34. [CrossRef]
4. Diepenbruck, M.; Christofori, G. Epithelial–mesenchymal transition (EMT) and metastasis: Yes, no, maybe? *Curr. Opin. Cell Biol.* **2016**, *43*, 7–13. [CrossRef]
5. Vences-Catalán, F.; Levy, S. Immune targeting of tetraspanins involved in cell invasion and metastasis. *Front. Immunol.* **2018**, *9*, 1277. [CrossRef]
6. Spaderna, S.; Schmalhofer, O.; Hlubek, F.; Berx, G.; Eger, A.; Merkel, S.; Jung, A.; Kirchner, T.; Brabletz, T. A transient, EMT-linked loss of basement membranes indicates metastasis and poor survival in colorectal cancer. *Gastroenterology* **2006**, *131*, 830–840. [CrossRef]
7. Lamouille, S.; Xu, J.; Derynck, R. Molecular mechanisms of epithelial–mesenchymal transition. *Nat. Rev. Mol. Cell Biol.* **2014**, *15*, 178–196. [CrossRef]
8. Savagner, P. The epithelial–mesenchymal transition (EMT) phenomenon. *Ann. Oncol.* **2010**, *21*, vii89–vii92. [CrossRef]
9. Batlle, E.; Sancho, E.; Francí, C.; Domínguez, D.; Monfar, M.; Baulida, J.; García de Herreros, A. The transcription factor snail is a repressor of E-cadherin gene expression in epithelial tumour cells. *Nat. Cell Biol.* **2000**, *2*, 84–89. [CrossRef]

10. Kurrey, N.; Amit, K.; Bapat, S. Snail and Slug are major determinants of ovarian cancer invasiveness at the transcription level. *Gynecol. Oncol.* **2005**, *97*, 155–165. [CrossRef]
11. Tsuji, T.; Ibaragi, S.; Hu, G.-f. Epithelial-mesenchymal transition and cell cooperativity in metastasis. *Cancer Res.* **2009**, *69*, 7135–7139. [CrossRef]
12. Derynck, R.; Akhurst, R.J.; Balmain, A. TGF-beta signaling in tumor suppression and cancer progression. *Nat. Genet.* **2001**, *29*, 117–129. [CrossRef]
13. Aires, V.; Limagne, E.; Cotte, A.K.; Latruffe, N.; Ghiringhelli, F.; Delmas, D. Resveratrol metabolites inhibit human metastatic colon cancer cells progression and synergize with chemotherapeutic drugs to induce cell death. *Mol. Nutr. Food Res.* **2013**, *57*, 1170–1181. [CrossRef]
14. Colin, D.; Gimazane, A.; Lizard, G.; Izard, J.C.; Solary, E.; Latruffe, N.; Delmas, D. Effects of resveratrol analogs on cell cycle progression, cell cycle associated proteins and 5fluoro-uracil sensitivity in human derived colon cancer cells. *Int. J. Cancer* **2009**, *124*, 2780–2788. [CrossRef]
15. Delmas, D. Silymarin and Derivatives: From Biosynthesis to Health Benefits. *Molecules* **2020**, *25*, 2415. [CrossRef]
16. Delmas, D.; Xiao, J.; Vejux, A.; Aires, V. Silymarin and Cancer: A Dual Strategy in Both in Chemoprevention and Chemosensitivity. *Molecules* **2020**, *25*, 2009. [CrossRef]
17. Sioud, F.; Amor, S.; Toumia, I.B.; Lahmar, A.; Aires, V.; Chekir-Ghedira, L.; Delmas, D. A New Highlight of Ephedra alata Decne Properties as Potential Adjuvant in Combination with Cisplatin to Induce Cell Death of 4T1 Breast Cancer Cells In Vitro and In Vivo. *Cells* **2020**, *9*, 362. [CrossRef]
18. Aires, V.; Delmas, D. Common pathways in health benefit properties of RSV in cardiovascular diseases, cancers and degenerative pathologies. *Curr. Pharm. Biotechnol.* **2015**, *16*, 219–244. [CrossRef]
19. Kasala, E.R.; Bodduluru, L.N.; Madana, R.M.; V, A.K.; Gogoi, R.; Barua, C.C. Chemopreventive and therapeutic potential of chrysin in cancer: Mechanistic perspectives. *Toxicol. Lett.* **2015**, *233*, 214–225. [CrossRef]
20. Ko, J.H.; Sethi, G.; Um, J.Y.; Shanmugam, M.K.; Arfuso, F.; Kumar, A.P.; Bishayee, A.; Ahn, K.S. The Role of Resveratrol in Cancer Therapy. *Int. J. Mol. Sci.* **2017**, *18*, 2589. [CrossRef]
21. Stevens, J.F.; Revel, J.S.; Maier, C.S. Mitochondria-Centric Review of Polyphenol Bioactivity in Cancer Models. *Antioxid Redox Signal* **2018**, *29*, 1589–1611. [CrossRef]
22. Avila-Carrasco, L.; Majano, P.; Sanchez-Tomero, J.A.; Selgas, R.; Lopez-Cabrera, M.; Aguilera, A.; Gonzalez Mateo, G. Natural Plants Compounds as Modulators of Epithelial-to-Mesenchymal Transition. *Front Pharm.* **2019**, *10*, 715. [CrossRef]
23. Kuo, M.-L.; Lee, K.-C.; Lin, J.-K. Genotoxicities of nitropyrenes and their modulation by apigenin, tannic acid, ellagic acid and indole-3-carbinol in the Salmonella and CHO systems. *Mutat. Res./Fundam. Mol. Mech. Mutagenes.* **1992**, *270*, 87–95. [CrossRef]
24. Chung, K.T.; Wong, T.Y.; Wei, C.I.; Huang, Y.W.; Lin, Y. Tannins and human health: A review. *Crit. Rev. Food Sci. Nutr.* **1998**, *38*, 421–464. [CrossRef]
25. Youness, R.A.; Kamel, R.; Elkasabgy, N.A.; Shao, P.; Farag, M.A. Recent advances in tannic acid (gallotannin) anticancer activities and drug delivery systems for efficacy improvement; a comprehensive review. *Molecules* **2021**, *26*, 1486. [CrossRef]
26. Pattarayan, D.; Sivanantham, A.; Krishnaswami, V.; Loganathan, L.; Palanichamy, R.; Natesan, S.; Muthusamy, K.; Rajasekaran, S. Tannic acid attenuates TGF-beta1-induced epithelial-to-mesenchymal transition by effectively intervening TGF-beta signaling in lung epithelial cells. *J. Cell. Physiol.* **2018**, *233*, 2513–2525. [CrossRef]
27. Yang, Y.I.; Jung, D.W.; Bai, D.G.; Yoo, G.S.; Choi, J.K. Counterion-dye staining method for DNA in agarose gels using crystal violet and methyl orange. *Electrophoresis* **2001**, *22*, 855–859. [CrossRef]
28. Reid, K.J.; Lang, K.; Froscio, S.; Humpage, A.J.; Young, F.M. Undifferentiated murine embryonic stem cells used to model the effects of the blue–green algal toxin cylindrospermopsin on preimplantation embryonic cell proliferation. *Toxicon* **2015**, *106*, 79–88. [CrossRef]
29. Kwak, Y.; Ju, J. Inhibitory activities of Perilla frutescens britton leaf extract against the growth, migration, and adhesion of human cancer cells. *Nutr. Res. Pract.* **2015**, *9*, 11–16. [CrossRef]
30. Li, S.; Chen, M.; Wu, H.; Li, Y.; Tollefsbol, T.O. Maternal epigenetic regulation contributes to prevention of estrogen receptor–negative mammary cancer with broccoli sprout consumption. *Cancer Prev. Res.* **2020**, *13*, 449–462. [CrossRef]
31. Ottaviano, A.J.; Sun, L.; Ananthanarayanan, V.; Munshi, H.G. Extracellular matrix-mediated membrane-type 1 matrix metalloproteinase expression in pancreatic ductal cells is regulated by transforming growth factor-beta1. *Cancer Res.* **2006**, *66*, 7032–7040. [CrossRef]
32. Ou, J.; Peng, Y.; Deng, J.; Miao, H.; Zhou, J.; Zha, L.; Zhou, R.; Yu, L.; Shi, H.; Liang, H. Endothelial cell-derived fibronectin extra domain A promotes colorectal cancer metastasis via inducing epithelial-mesenchymal transition. *Carcinogenesis* **2014**, *35*, 1661–1670. [CrossRef]
33. Karlsson, S.; Nystrom, H. The extracellular matrix in colorectal cancer and its metastatic settling—Alterations and biological implications. *Crit. Rev. Oncol. Hematol.* **2022**, *175*, 103712. [CrossRef]
34. Cano, A.; Perez-Moreno, M.A.; Rodrigo, I.; Locascio, A.; Blanco, M.J.; del Barrio, M.G.; Portillo, F.; Nieto, M.A. The transcription factor snail controls epithelial-mesenchymal transitions by repressing E-cadherin expression. *Nat. Cell Biol.* **2000**, *2*, 76–83. [CrossRef]
35. Onder, T.T.; Gupta, P.B.; Mani, S.A.; Yang, J.; Lander, E.S.; Weinberg, R.A. Loss of E-cadherin promotes metastasis via multiple downstream transcriptional pathways. *Cancer Res.* **2008**, *68*, 3645–3654. [CrossRef]

36. Derynck, R.; Zhang, Y.E. Smad-dependent and Smad-independent pathways in TGF-β family signalling. *Nature* **2003**, *425*, 577–584. [CrossRef]
37. Provenzale, D.; Gupta, S.; Ahnen, D.J.; Markowitz, A.J.; Chung, D.C.; Mayer, R.J.; Regenbogen, S.E.; Blanco, A.M.; Bray, T.; Cooper, G.; et al. NCCN Guidelines Insights: Colorectal Cancer Screening, Version 1.2018. *J. Natl. Compr. Cancer Netw.* **2018**, *16*, 939–949. [CrossRef]
38. Escalante, P.I.; Quinones, L.A.; Contreras, H.R. Epithelial-Mesenchymal Transition and MicroRNAs in Colorectal Cancer Chemoresistance to FOLFOX. *Pharmaceutics* **2021**, *13*, 75. [CrossRef]
39. Cheng, M.; Jiang, Y.; Yang, H.; Zhao, D.; Li, L.; Liu, X. FLNA promotes chemoresistance of colorectal cancer through inducing epithelial-mesenchymal transition and smad2 signaling pathway. *Am. J. Cancer Res.* **2020**, *10*, 403–423.
40. De Craene, B.; Berx, G. Regulatory networks defining EMT during cancer initiation and progression. *Nat. Rev. Cancer* **2013**, *13*, 97–110. [CrossRef]
41. Zhou, B.P.; Deng, J.; Xia, W.; Xu, J.; Li, Y.M.; Gunduz, M.; Hung, M.C. Dual regulation of Snail by GSK-3beta-mediated phosphorylation in control of epithelial-mesenchymal transition. *Nat. Cell Biol.* **2004**, *6*, 931–940. [CrossRef]
42. Peinado, H.; Olmeda, D.; Cano, A. Snail, Zeb and bHLH factors in tumour progression: An alliance against the epithelial phenotype? *Nat. Rev. Cancer* **2007**, *7*, 415–428. [CrossRef]
43. Sanchez-Tillo, E.; Lazaro, A.; Torrent, R.; Cuatrecasas, M.; Vaquero, E.C.; Castells, A.; Engel, P.; Postigo, A. ZEB1 represses E-cadherin and induces an EMT by recruiting the SWI/SNF chromatin-remodeling protein BRG1. *Oncogene* **2010**, *29*, 3490–3500. [CrossRef]
44. Hatami, E.; PK, B.N.; Sikander, M.; Dhasmana, A.; Chauhan, S.C.; Jaggi, M.; Yallapu, M.M. Tannic Acid Exhibits Antiangiogenesis Activity in Nonsmall-Cell Lung Cancer Cells. *ACS Omega* **2022**, *7*, 23939–23949. [CrossRef]
45. Karakurt, S.; Adali, O. Tannic Acid Inhibits Proliferation, Migration, Invasion of Prostate Cancer and Modulates Drug Metabolizing and Antioxidant Enzymes. *Anti-Cancer Agents Med. Chem.* **2016**, *16*, 781–789. [CrossRef]
46. Savagner, P.; Yamada, K.M.; Thiery, J.P. The zinc-finger protein slug causes desmosome dissociation, an initial and necessary step for growth factor-induced epithelial-mesenchymal transition. *J. Cell Biol.* **1997**, *137*, 1403–1419. [CrossRef]
47. Wels, C.; Joshi, S.; Koefinger, P.; Bergler, H.; Schaider, H. Transcriptional activation of ZEB1 by Slug leads to cooperative regulation of the epithelial-mesenchymal transition-like phenotype in melanoma. *J. Investig. Dermatol.* **2011**, *131*, 1877–1885. [CrossRef]
48. Yilmaz, M.; Christofori, G. EMT, the cytoskeleton, and cancer cell invasion. *Cancer Metast. Rev.* **2009**, *28*, 15–33. [CrossRef]
49. Comoglio, P.M.; Boccaccio, C.; Trusolino, L. Interactions between growth factor receptors and adhesion molecules: Breaking the rules. *Curr. Opin. Cell Biol.* **2003**, *15*, 565–571. [CrossRef]
50. Booth, B.W.; Inskeep, B.D.; Shah, H.; Park, J.P.; Hay, E.J.; Burg, K.J. Tannic Acid preferentially targets estrogen receptor-positive breast cancer. *Int. J. Breast Cancer* **2013**, *2013*, 369609. [CrossRef]
51. Nie, F.; Liang, Y.; Jiang, B.; Li, X.; Xun, H.; He, W.; Lau, H.T.; Ma, X. Apoptotic effect of tannic acid on fatty acid synthase over-expressed human breast cancer cells. *Tumour Biol.* **2016**, *37*, 2137–2143. [CrossRef]
52. Nagesh, P.K.B.; Hatami, E.; Chowdhury, P.; Kashyap, V.K.; Khan, S.; Hafeez, B.B.; Chauhan, S.C.; Jaggi, M.; Yallapu, M.M. Tannic Acid Induces Endoplasmic Reticulum Stress-Mediated Apoptosis in Prostate Cancer. *Cancers* **2018**, *10*, 68. [CrossRef]
53. Ridley, A.J. Life at the leading edge. *Cell* **2011**, *145*, 1012–1022. [CrossRef]
54. Moustakas, A.; Heldin, C.H. Non-Smad TGF-beta signals. *J. Cell Sci.* **2005**, *118*, 3573–3584. [CrossRef]
55. Makrodouli, E.; Oikonomou, E.; Koc, M.; Andera, L.; Sasazuki, T.; Shirasawa, S.; Pintzas, A. BRAF and RAS oncogenes regulate Rho GTPase pathways to mediate migration and invasion properties in human colon cancer cells: A comparative study. *Mol. Cancer* **2011**, *10*, 118. [CrossRef]

Annexe 9 : Article : Resvega, a Nutraceutical Preparation, Affects NFκB Pathway and Prolongs the Anti-VEGF Effect of Bevacizumab in Undifferentiated ARPE-19 Retina Cells

Randa Sghaier[1,2] Maude Perus[1,2] Clarisse Cornebise[1,2] Flavie Courtaut[1,2] Alessandra Scagliarini[1,2] Céline Olmiere[3] Virginie Aires[1,2] François Hermetet[1,2,†] et Dominique Delmas[1,2,4,*†5,*,‡]

1 UFR des Sciences de Santé, Université de Bourgogne, 21000 Dijon, France
2 INSERM Research Center U1231—Cancer and Adaptive Immune Response Team, Bioactive Molecules and Health Research Group, 21000 Dijon, France
3 Laboratoires Théa ®, 12 Rue Louis-Blériot, 63000 Clermont-Ferrand, France
4 Centre Anticancéreux Georges François Leclerc Center, 21000 Dijon, France
* Correspondence: dominique.delmas@u-bourgogne.fr; Tel.: +33-380-39-32-26
† These authors contributed equally to this work

Résumé : La dégénérescence maculaire liée à l'âge (DMLA) est une maladie oculaire irréversible qui affecte la rétine. Malgré les avancées thérapeutiques et l'utilisation d'anticorps dirigés contre le facteur de croissance VEGF-A, des mécanismes de résistance diminuent fortement leur efficacité. Dans cette étude, nous avons étudié si une formulation nutraceutique composée d'acides gras oméga-3 et de resvératrol, appelée Resvega®, était capable de perturber la sécrétion de VEGF-A dans les cellules rétiniennes humaines ARPE-19. Nous avons constaté que Resvega® inhibe la sécrétion de VEGF-A en diminuant les voies de signalisation PI3KAKT-mTOR et NFκB. Dans la voie de signalisation NFκB, le Resvega® inhibe la phosphorylation de l'inhibiteur de NFκB, IκB, qui peut lier les dimères de NFκB et les séquestrer dans le cytoplasme. Ainsi, les sous-unités NFκB ne peuvent pas migrer vers le noyau où elles se lient normalement à l'ADN et stimulent la transcription de gènes cibles tels que le VEGF-A. Le complexe IκB kinase (IKK) est également affecté par Resvega® puisque la formulation nutraceutique diminue à la fois les sous-unités IKKα et IKKβ et la sous-unité IKKγ qui sont nécessaires à la stimulation de l'IKK. De manière très intéressante, nous avons mis en évidence que Resvega® pourrait prolonger l'effet anti-angiogénique d'Avastin®, qui est un agent anti-VEGF généralement utilisé dans la pratique clinique. Nos résultats suggèrent que Resvega® pourrait avoir un intérêt potentiel en tant que supplémentation nutritionnelle contre la DMLA.

Mots clés : DMLA, angiogenèse, maladies oculaires, anti-VEGF, oméga-3, resvératrol.

International Journal of
Molecular Sciences

MDPI

Article

Resvega, a Nutraceutical Preparation, Affects NFκB Pathway and Prolongs the Anti-VEGF Effect of Bevacizumab in Undifferentiated ARPE-19 Retina Cells

Randa Sghaier [1,2], Maude Perus [1,2], Clarisse Cornebise [1,2], Flavie Courtaut [1,2], Alessandra Scagliarini [1,2], Céline Olmiere [3], Virginie Aires [1,2], François Hermetet [1,2,†] and Dominique Delmas [1,2,4,*,†]

1 UFR des Sciences de Santé, Université de Bourgogne, 21000 Dijon, France
2 INSERM Research Center U1231—Cancer and Adaptive Immune Response Team, Bioactive Molecules and Health Research Group, 21000 Dijon, France
3 Laboratoires Théa®, 12 Rue Louis-Blériot, 63000 Clermont-Ferrand, France
4 Centre Anticancéreux Georges François Leclerc Center, 21000 Dijon, France
* Correspondence: dominique.delmas@u-bourgogne.fr; Tel.: +33-380-39-32-26
† These authors contributed equally to this work.

Abstract: Age-related macular degeneration (AMD) is an irreversible chronic degenerative pathology that affects the retina. Despite therapeutic advances thanks to the use of anti-vascular endothelial growth factor (VEGF) agents, resistance mechanisms have been found to accentuate the visual deficit. In the present study, we explored whether a nutraceutical formulation composed of omega-3 fatty acids and resveratrol, called Resvega®, was able to disrupt VEGF-A secretion in human ARPE-19 retina cells. We found that Resvega® inhibits VEGF-A secretion through decreases in both the PI3K-AKT-mTOR and NFκB signaling pathways. In NFκB signaling pathways, Resvega® inhibits the phosphorylation of the inhibitor of NFκB, IκB, which can bind NFκB dimers and sequester them in the cytoplasm. Thus, the NFκB subunits cannot migrate to the nucleus where they normally bind and stimulate the transcription of target genes such as VEGF-A. The IκB kinase complex (IKK) is also affected by Resvega® since the nutraceutical formulation decreases both IKKα and IKKβ subunits and the IKKγ subunit which is required for the stimulation of IKK. Very interestingly, we highlight that Resvega® could prolong the anti-angiogenic effect of Avastin®, which is an anti-VEGF agent typically used in clinical practice. Our results suggest that Resvega® may have potential interest as nutritional supplementation against AMD.

Keywords: AMD; angiogenesis; ocular diseases; anti-VEGF; Resvega; omega-3 fatty acids; resveratrol

Citation: Sghaier, R.; Perus, M.; Cornebise, C.; Courtaut, F.; Scagliarini, A.; Olmiere, C.; Aires, V.; Hermetet, F.; Delmas, D. Resvega, a Nutraceutical Preparation, Affects NFκB Pathway and Prolongs the Anti-VEGF Effect of Bevacizumab in Undifferentiated ARPE-19 Retina Cells. *Int. J. Mol. Sci.* **2022**, *23*, 11704. https://doi.org/10.3390/ijms231911704

Academic Editor: Stephanie C. Joachim

Received: 6 September 2022
Accepted: 30 September 2022
Published: 3 October 2022

1. Introduction

Age-related macular degeneration (AMD) is the eye disease most often responsible for severe vision loss in people older than 60. It is characterized by the progressive onset of neurodegeneration of the photoreceptor-retinal pigment epithelium (RPE) complex. RPE cells play a key role in the development of the different types of AMD. In fact, in age-related maculopathy, there is an accumulation of precursors, drusen, of variable shape, size and number, the most probable origin of which is the accumulation of residues of phagocytosis of the photoreceptors by cells of the RPE. This is then accompanied by an alteration of the RPE, with phenomena of hyper- or hypo-pigmentation [1]. In the atrophic or "dry" form, there is a progressive loss of RPE cells, due to the degeneration of the latter by apoptosis, which leads secondarily to the disappearance of the choriocapillaris, then of the photoreceptors in the macular region and finally, the severe loss of vision. Geographic atrophy occurs when the cell loss can no longer be compensated for by the spreading of the remaining cells that previously maintained the continuity of the epithelium [2]. Finally, in wet or exudative or even neovascular AMD (nAMD), the newly formed vessels are more

fragile and lead to a diffusion of serum and blood, causing hemorrhages within the retina, which disrupts its organization, with, in particular, the appearance of exudates, intraretinal edema, scars or retinal detachments. In the absence of treatments, the exudates through the new choroidal vessels, cause the destruction of the photoreceptors [3]. All forms combined, it is the main cause of visual impairment in the elderly in industrialized countries, with more than 1 million affected individuals in France (approximately 8% of the population) and several hundred million worldwide [4]. There are generally three major clinical forms, but the term AMD corresponds to the most advanced stages of the pathology. So-called exudative or "wet" or nAMD, characterized by aberrant neoangiogenesis of the choroid and very rapid progression, affects only 10 to 15% of patients but accounts for 90% of severe vision loss [1,3]. The multiple molecular mechanisms underlying AMD are complex and still poorly understood. However, the major components involved in the pathogenesis of AMD are significant oxidative stress associated with the aging process, which appears to be the triggering factor for the pathology [5–8], and chronic inflammation eventually leading to the formation of the new choroidal vessels (choroidal neovascularization or CNV) observed in the most advanced and severe stages of the disease [9,10]. None of the clinical stages of AMD can be effectively prevented, treated or cured. Counseling patients on the importance of a healthy lifestyle including smoking cessation and a healthy diet is an important part of patient care. Since the 2000s, nAMD (the most severe form) has been treated with repeated intravitreal injections of antibodies (bevacizumab), humanized antibody fragment (ranibizumab), recombinant fusion protein (aflibercept) or, more recently, humanized single-chain antibody fragment (brolucizumab), directed against vascular endothelial growth factor (VEGF), the major angiogenesis-regulating factor (on average 7 injections per year) [11–15]. These targeted therapies have shown efficacy in stabilizing or even reversing the progression of the disease, but they do not constitute a definitive cure. They are indicated in the active phases of new vessel development but are not effective on healed or highly advanced forms, which implies that the diagnosis should be made in the early stages. In addition, recurrent fluid or exudation may persist despite anti-VEGF treatment. Thus, patients with refractory or recurrent AMD (approximately 1/3 of patients) may develop resistance mechanisms over the long term, leading to a reduction in therapeutic efficacy [16,17]. Moreover, the large number of repeated injections of anti-VEGF treatments required to maintain efficacy constitutes a heavy economic burden. It therefore seems urgent to develop new therapeutic strategies to block the neoangiogenic process, or to identify compounds capable of increasing the effectiveness of anti-VEGFs or making it possible to space out the injections.

Faced with this major public health problem, numerous studies and pharmaceutical companies have attempted to develop other VEGF inhibitors, which is the key factor in controlling neoangiogenesis, analogous to what is well known in models of tumor angiogenesis. In this field, we have highlighted the potential interest of a nutraceutical, Resvega® (RGA), containing both resveratrol (RSV) and ω-3 fatty acids (eicosapentaenoic acid (EPA), docosahexaenoic acid (DHA)). This new formulation, based on the Age-Related Eye Disease Study 1 (AREDS-1) recommendations concerning the use of ω-3 fatty acids, was able to counteract angiogenesis in a preclinical mouse model of CNV [18]. Indeed, the combination of RSV and ω-3 fatty acids was able to decrease laser-induced CNV in mice, and a proteomic analysis of retinas revealed that mice supplemented with RGA present a specific enrichment in negative regulation of epithelial cell migration clusters in the retinas, including negative vasculature development, blood vessel development, angiogenesis, blood vessel morphogenesis and negative regulation of epithelial cell proliferation [18]. Very interestingly, the observed benefit relative to angiogenesis development produced by the omega-3 (ω-3) fatty acids/RSV combination was better than ω-3 fatty acids or RSV alone. A potential molecular explanation was recently suggested by some authors showing that RGA could reduce inflammation [19] and oxidative stress [20], and, on the contrary, induce autophagy [21] in retinal cell models. Very recently, we have demonstrated that the ω-3 fatty acids/RSV combination interferes with the transcriptional regulation of genes

coding both for VEGF-R2 and VEGF-A [22]. Nevertheless, the molecular mechanisms by which RGA prevents angiogenesis in retina cells is still unclear.

In this novel study, we show the ability of an ω-3 fatty acids/RSV combination to counteract VEGF-A production over time due to an alteration of the AKT/PI3K and NFκB pathways. More specifically, RGA reduces the inhibitor of the κB (IκB) kinase (IKK) regulator complex that controls the future of NFκB, and the subunits P65 and P50 are diminished in nuclear fractions of the ARPE-19 retina cells treated with the nutraceutical formulation. Disruption of these two important angiogenesis signaling pathways increases the sensitivity of retina cells to anti-VEGF treatment. Pretreatment with RGA helps to prolong the treatment effect of Avastin®, an anti-VEGF commonly used in clinics to treat AMD patients. This finding provides evidence that this ω-3 fatty acids/RSV formulation could be used as a new therapeutic strategy in combination or not with anti-VEGF treatments in AMD therapy.

2. Results

2.1. RGA Inhibits VEGF-A Secretion over Time in Human ARPE-19 Retina Cells

One of the pro-angiogenic factors playing a major role in the development, progression and complications of AMD is vascular endothelial growth factor A (VEGF-A). VEGF-A is strongly involved in the abnormal growth of blood vessels and the increase in vascular permeability that leads to loss of vision [23]. We have previously been able to show that RGA supplementation was able to decrease VEGF secretion in an in vivo mouse model [18]. In undifferentiated human ARPE-19 retinal cells mimicking the cells affected by AMD [24], this nutraceutical formulation was also able to reduce the secretion of VEGF by approximately 20% after 24 h of treatment, without affecting cell viability [22]. Firstly, in this same human retinal cell model that is widely used to test the efficacy of anti-angiogenic compounds, we tested whether the anti-angiogenic effect of RGA lasted over time, increased or, on the contrary, decreased. For these experiments, ARPE-19 cells were treated with RGA over 72 h and, interestingly, ω-3 fatty acids/RSV formulation at 12 µM reduced VEGF-A secretion over time, as shown by the ELISA method (Figure 1). This reduction was accentuated from 48 h of treatment to reach a maximum difference at 72 h of treatment, where the formulation inhibited VEGF secretion by 64.6% compared to the control (Figure 1A). It is important to note that RGA (12 µM) has no significant impact on the cellular viability of human ARPE-19 retinal cells as a function of incubation time (kinetics observed between 0 h and 72 h) (Figure 1B).

Furthermore, the integrity of human retinal–endothelial barrier (REB) is maintained by tight junctions of the RPE cells in particular, which create a very tight monolayer, so that macromolecules cannot easily penetrate between the cells forming the retinal unit [25]. These tight junction proteins such as zonula occludens-1 (ZO-1) are essential to maintain retinal homeostasis and to conserve choroid microenvironment. Thereby, the loss of tight junctions, connected to the actin cytoskeleton through ZO-1, leads to retinal-barrier disruption, which is associated with the AMD-pathogenicity [25,26]. To explore the role of RGA in human RPE barrier integrity and permeability, we investigate its impact on the expression of the essential tight junctions' proteins. Immunoblotting analysis revealed that RGA maintains ZO-1 expression in ARPE-19 cells.

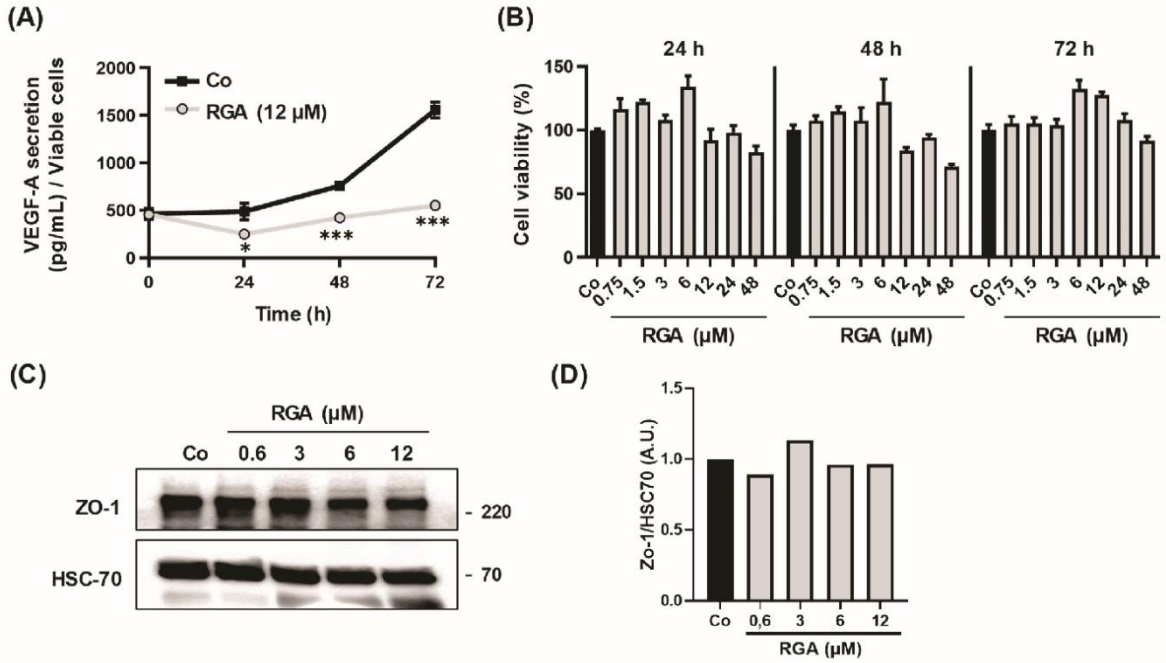

Figure 1. RGA formulation disrupts VEGF-A secretion over time in human ARPE-19 retina cells. (**A**) ARPE-19 retina cells were treated for 24, 48 and 72 h without serum with vehicle as control (Co) or with RGA (12 µM). VEGF-A secretion was measured in cell medium by ELISA assay. The data are mean ± S.D. of four independent experiments with n = 10. *p* values were determined by one-way ANOVA followed by Tukey's multiple comparison test of treatments vs. control. * $p < 0.05$, and *** $p < 0.001$. (**B**) ARPE-19 cells were treated with 12 µM of RGA at 37 °C for 24, 48 and 72 h. The percentage of cell viability was determined by crystal violet assay. Results are expressed as a percentage of control (mean ± SD of three independent experiments with n = 10). (**C**) Immunoblot analysis of ZO-1 in RGA treated ARPE-19 cells with increasing concentration (0.6, 3, 6, 12 µM) or with vehicle (Co) for 24 h. HSC-70 was used as a loading control. (**D**) Densitometry quantification of western blotting. Data are expressed as the mean fold induction compared to control (Co).

2.2. RGA Disrupts AKT/mTOR Signaling Pathway

We next explored the mechanisms underlying the inhibitory effect of RGA on VEGF-A production. The very fine regulation of angiogenesis involves numerous pathways following activation by VEGF-A of its main receptor, VEGF-R2. Once activated, it in turn triggers many intracellular signaling pathways. These include, in particular, the ERK1/2 pathway on which we have shown that RGA has an effect [22], but also other pathways, for instance the PI3K-AKT-mTOR pathway, which is crucial for cell survival, regulation of vasomotion and angiogenesis [27,28] In order to understand the impact of RGA on VEGF-A pathway through PI3K-AKT-mTOR, we investigated its effect on the expression of key proteins involved in the signaling cascade. Immunoblotting analysis revealed that RGA strongly decreases phosphorylation of c-RAF, in a concentration-dependent manner, as well as the protein expression of PI3K, AKT, mTOR and their respective phosphorylated forms (Figure 2A,B).

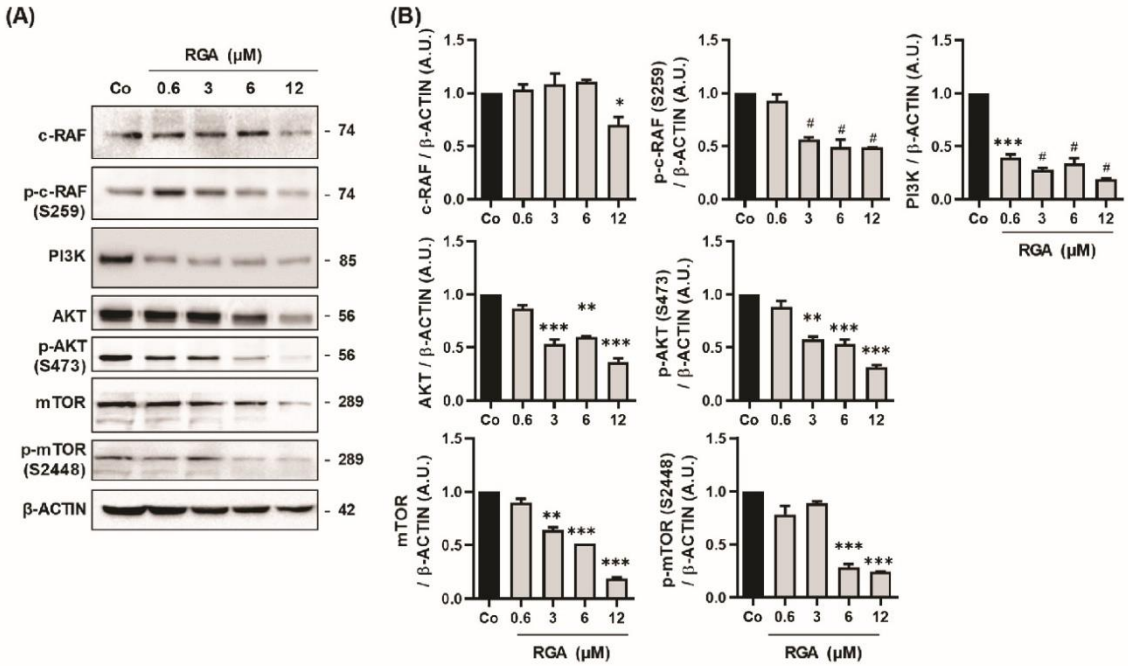

Figure 2. RSV/ω-3 fatty acids combination disrupts PI3K-AKT-mTOR signaling pathway. (**A**) Immunoblot analysis of c-RAF, phospho-c-RAF (p-RAF), PI3K, AKT, phospho-AKT (p-AKT), mTOR, phospho-mTOR (p-mTOR) in RGA-treated ARPE-19 cells with increasing concentration (0.6, 3, 6, 12 μM) or with vehicle (Co) for 24 h. β-ACTIN was used as a loading control. (**B**) Densitometry quantification of western blotting. Data are expressed as the mean fold induction ± SEM of three independent experiments. *p*-values were determined by a one-way ANOVA followed by Tukey's multiple comparison test of treatments vs. control. * $p < 0.05$, ** $p < 0.01$, *** $p < 0.001$, and # $p < 0.0001$.

2.3. RGA Inhibits NFκB Subunits and Its Kinase Inhibitor IκB

It is well established that AKT regulates the phosphorylation of many proteins downstream of the PI3K-AKT-mTOR signaling pathway, such as the NFκB transcriptional complex, which plays an essential role in the transcriptional activation of the gene encoding the VEGF-A protein in human retina cells. This nuclear transcriptional factor is a multimeric complex constituted of the isoform P65 and P50 which is formed from a cytosolic precursor P105 protein. In response to multiple stimuli such as oxidative stress, reactive oxygen species (ROS) or inflammatory cytokines, the NFκB inhibitory factor, IκB, is rapidly phosphorylated, which results in its degradation and allows the activation of NFκB. This allows the release of NFκB dimer (P50/P65) and its translocation into the nucleus, where it binds to promoters of various target genes. In order to analyze the potential effect of RGA on these factors, ARPE-19 cells were treated with increasing concentrations of RGA. Immunoblotting analyses revealed that RGA decreases both P50 and its precursor P105 by around 66% and 84%, respectively, at 12 μM of RGA compared to the control (Figure 3A,B). Similarly, RGA diminished in a concentration-dependent manner the expression of P65 and its phosphorylated form by 77% and 34%, respectively, compared to the control. Interestingly, RGA strongly inhibited both IκB and its phosphorylation, suggesting a potential repercussion on the cellular distribution of NFκB subunits (Figure 3A,B).

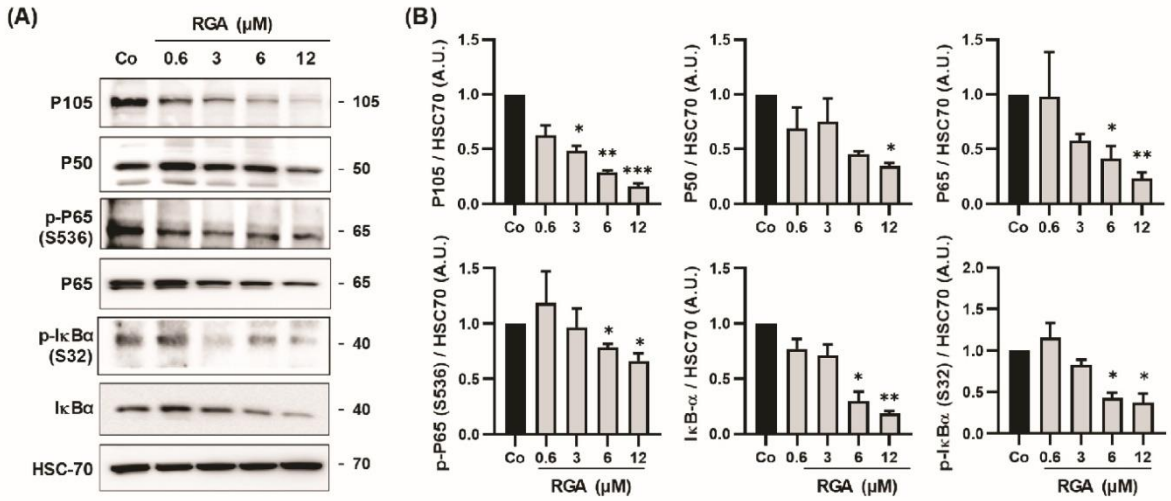

Figure 3. RSV/ω-3 fatty acids combination decreases NFκB complex protein expression. (**A**) Immunoblot analysis of P105, P50, phospho-P65, (p-P65), P65, phospho-IκBα (p-IκBα), IκBα in RGA-treated ARPE-19 cells with increasing concentration (0.6, 3, 6, 12 μM) or with vehicle (Co) for 24 h. HSC-70 was used as a loading control. (**B**) Densitometry quantification of western blotting. Data are expressed as the mean fold induction ± SEM of three independent experiments. *p* values were determined by a one-way ANOVA followed by Tukey's multiple comparison test of treatments vs. control. * $p < 0.05$, ** $p < 0.01$ and *** $p < 0.001$.

2.4. RGA Inhibits Nuclear Relocalization of Dimer P65/P50 Subunits of NFκB

In the processes of angiogenesis observed in AMD, the canonical NFκB activation pathway mainly applies to the dimers formed by the P65 and P50 subunits. Under normal conditions, the P65/P50 dimers are sequestered in the cytoplasm in an inactive form by their association with the inhibitory IκB proteins (inhibitor of NFkB). NFκB activation in response to a stimulus leads to the phosphorylation of IκB, and results in IκB ubiquitination and degradation. As a consequence, free P65/P50 dimers translocate into the nucleus to activate the transcription of specific target genes such as the gene coding for VEGF-A. Because RGA strongly inhibited the phosphorylation of IκB (Figure 3), this action could lead to a cytosolic sequestration of the P65/P50 subunits, thus preventing the dimer from playing its role as a transcriptional factor on the gene coding for VEGF-A in the nucleus of retinal cells. To assess the ability of RGA to prevent the relocalization of nuclear factors into the nucleus, we performed immunoblotting from a nucleus/cytoplasm extraction where poly (ADP-ribose) polymerase-1 (PARP-1) and heat shock cognate (HSC-70) proteins were used as controls for the nuclear and cytosolic fractions, respectively (Figure 4). While P50 was indeed expressed in the nuclear fraction in the control (Co), RGA decreased, in a concentration-dependent manner, the amount of this protein in the nuclear fractions compared with the control, reaching around 36.7% at 12μM of RGA (Figure 4A,B). The precursor of P50, P105, is more expressed in the cytosolic fraction, which is its normal localization, compared to the nuclear fraction. In both cytosolic and nuclear fractions, RGA treatment strongly decreased its protein expression by 12.6% and 34.0%, respectively, at 12 μM of RGA (Figure 4A,B). Similar to P50, the subunit P65 and its phosphorylated form (p-P65) were also strongly diminished in nuclear fractions compared with the control, by 26.3% and 9.8%, respectively, at 12 μM of RGA (Figure 4A,B).

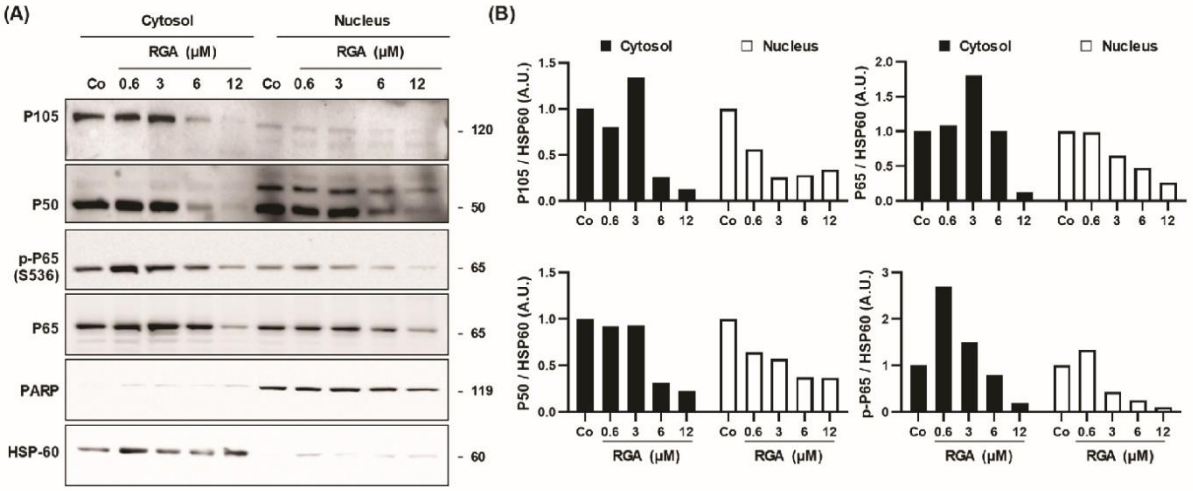

Figure 4. RGA disturbs the translocation of the P65 and P50 dimer subunits of NFkB into the nucleus of ARPE-19 cells. (**A**). Representative blot of P105, P50, P65 protein expression in concentration range of RGA (0.6, 3, 6, 12 μM)-treated or not (Co) ARPE-19 cells for 24 h. Nuclear fractions and cytosolic fractions are shown from three independent experiments. (**B**) Densitometry quantification of western blotting from the representative nuclear and cytosolic immunoblotting. Data are expressed as the mean fold induction.

2.5. RGA Inhibits Subunits of IκB Kinase

Sequestration into the nucleus of NFκB subunits is under the double control of a multimolecular complex called IκB kinase (IKK). Indeed, this heterotrimercomplex kinase IKK controls the phosphorylation of inhibitors of κB (IκB) [29,30]. The two homologous kinases, IKKα and IKKβ subunits (85 and 87 kDa, respectively), form the IKK complex with the unrelated regulatory 52-kDa subunit IKKγ [31], also known as NEMO (NF-κB essential modulator) [32]. This complex is responsible for the phosphorylation of IκBα, which leads to its degradation and the release of the transcription factor NF-κB. RGA disrupts both the IκB phosphorylation (Figure 3) and diminishes the nuclear translocation of p65 and p50 and their phosphorylated forms, respectively (Figure 4). We then sought to determine whether the effects induced by RGA after 24 h of treatment were associated with a modulation of the key proteins constituting the IKK complex, which control the fate of NFκB. Immunoblotting revealed that RGA strongly decreases, in a concentration-dependent manner, the two subunit kinases IKKα and IKKβ and the phosphorylated form of the homodimer phospho-IKKαβ (p-IKKαβ). Inhibition was significant in all cases at 12 μM (Figure 5A,B). Very interestingly, IKKγ, which is required for the stimulation of IKK by upstream signals, was also strongly decreased by the concentration range of RGA (Figure 5A,B).

Altogether, the first data set demonstrated that RGA formulation is able to affect the canonical NFκB activation pathway by decreasing both the protein expression of P65/P50 dimers and their phosphorylated forms, but also to affect key regulators controlling their cellular distribution. This effect, which is induced by the RGA, then makes it possible to reduce the translocation of P65 and P50 in the nucleus and thus to prevent their role as nuclear transcriptional factors.

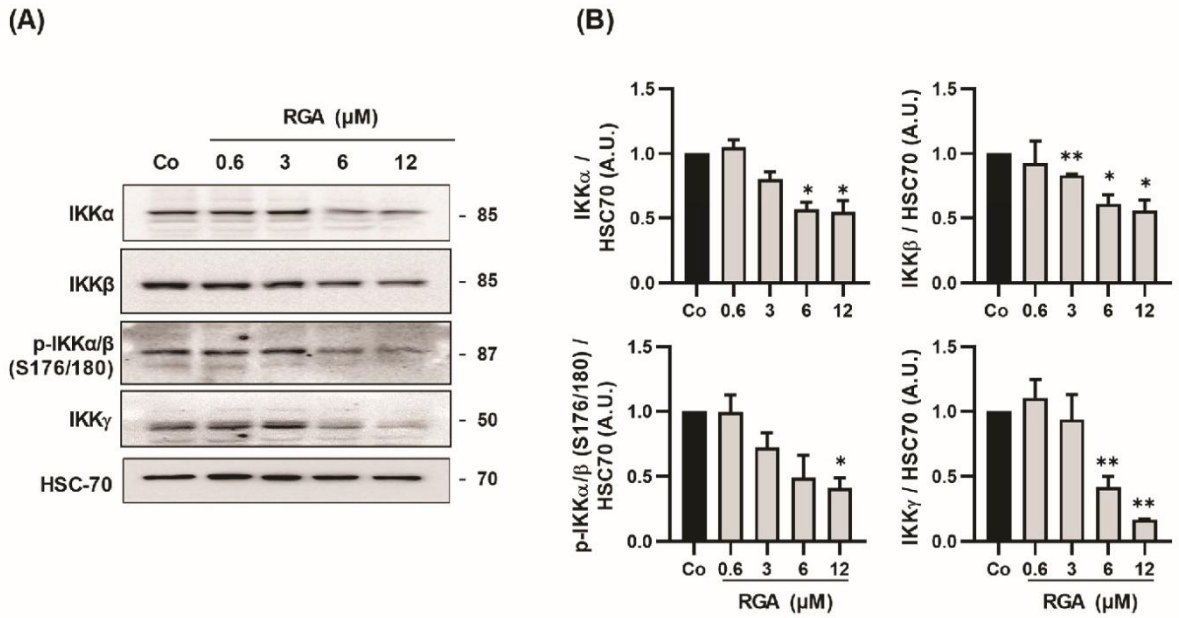

Figure 5. The RSV/ω-3 fatty acids combination decreases subunits of IκB complex protein expression. (**A**) Immunoblot analysis of IKKα, IKKβ, phospho-IKKαβ (p-IKKαβ), IKKγ in RGA-treated ARPE-19 cells with increasing concentrations (0.6, 3, 6, 12 μM) or with vehicle (Co) for 24 h. HSC-70 was used as a loading control. (**B**) Densitometry quantification of western blotting. Data are expressed as the mean fold induction ± SEM of three independent experiments. *p* values were determined by a one-way ANOVA followed by Tukey's multiple comparison test of treatments vs. control. * $p < 0.05$ and ** $p < 0.01$.

2.6. RGA Sensitizes AREP-19 Retina Cells to the Anti-Angiogenic Effect of Bevacizumab

Because RGA induces VEGF-A secretion inhibition, at least involving the NFκB and PI3K-AKT-mTOR signaling pathways, the ω-3 fatty acids/RSV combination could sensitize human ARPE-19 retina cells to the anti-angiogenic effect of an anti-VEGF such as bevacizumab (Avastin®). We therefore examined whether RGA at 12 μM could delay the VEGF-A inhibitory effect of Avastin® on ARPE-19. To explore this hypothesis, we pretreated ARPE-19 for 72 h at 12 μM and then exposed retina cells for 24 h to Avastin® at 100 ng/mL before assessment of VEGF-A secretion at 96 and 120 h, which is the retinal cell culture time limit in our experiments (Figure 6A). Levels of VEGF-A secreted by ARPE-19 cells shown that RGA decreases VEGF-A from 58% and Avastin® from 87% and the combination of RGA with Avastin® is similar to Avastin® alone (Figure 6B). But very interestingly, when the VEGF-A was measured 24 h later, the level had risen by around 15% with Avastin® alone, whereas, in the cells pretreated with RGA, the anti-angiogenic effect of Avastin® prolonged the inhibition at a level comparable to that observed 24 h earlier i.e., 91% of inhibition (Figure 6B).

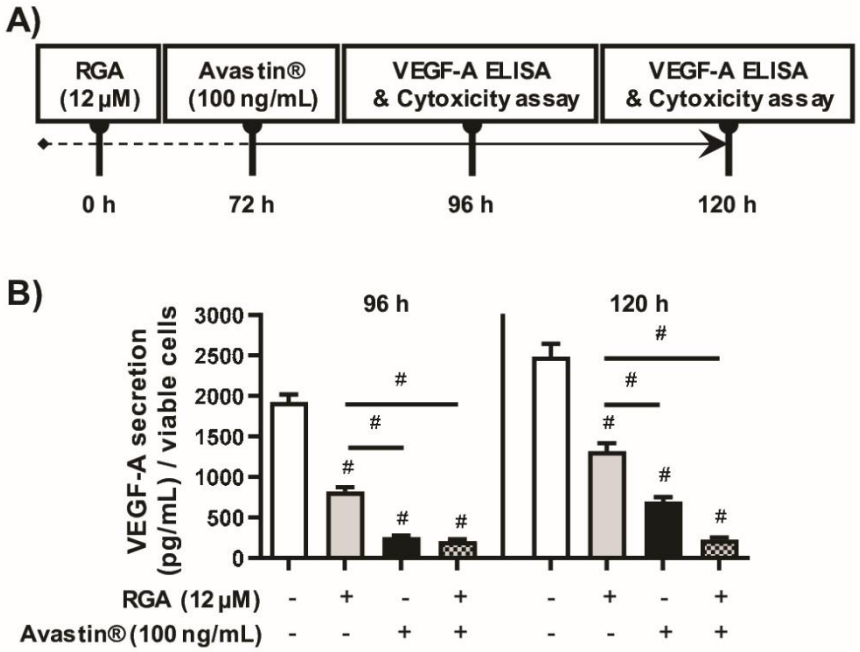

Figure 6. RSV/ω-3 fatty acids prolong the VEGF-A inhibition induced by Avastin®. (**A**) Experimental workflow. After 24 h of culture, ARPE-19 retina cells were treated with 12 µM of RGA or with vehicle during 72 h, and then exposed to Avastin® at 100 ng/mL during 24 or 48 h. At each time point, the level of VEGF-A secreted was measured by ELISA assay as well as the percentage of viable cells by crystal violet assay. (**B**) Histograms of the concentration of secreted VEGF-A (pg/mL) normalized to cell viability after 24 or 48 h or treatment with Avastin® (100 ng/mL) in ARPE-19 retina cells, and pretreated or not with RGA (12 µM). Data are expressed as the mean fold induction ± SEM of the three independent experiments. *p* values were determined by a one-way ANOVA followed by Tukey's multiple comparison test to 2 groups (control group vs. treatment group and treatment group vs. treatment group). # $p < 0.0001$.

3. Discussion

Age-related macular degeneration (AMD) is a disabling degenerative disease that reduces visual acuity in patients after the age of 50. Despite the development of new therapies to counteract neoangiogenesis through the development of anti-VEGF antibodies or agents (i.e., ranibizumab, aflibercept, bevacizumab, etc.) [33], treatment failure still occurs due to side effects and resistance. Herein, for the first time, through the use of a potential anti-angiogenic nutraceutical combining ω-3 fatty acids and RSV (Resvega®; RGA), we provide a mechanism by which RGA counteracts VEGF-A secretion through a modulation of the PI3K-AKT-mTOR pathway, disturbing the canonical pathway of NFκB and its regular IKK complex. These new insights complement the full spectrum of action of RGA on signaling pathways, which we and others have recently begun to describe. We previously demonstrated that RGA, as anti-VEGF formulation, prevents activation of the MAPK signaling pathway in ARP19 cells [18,22]. In total, the RGA-mediated disruption of these two important angiogenesis signaling pathways (i.e., PI3K-AKT-mTOR and MAPK signaling pathways) likely lead a prolongation of anti-angiogenic properties of bevacizumab (Avastin®), an anti-VEGF often used to treat AMD (Figure 7).

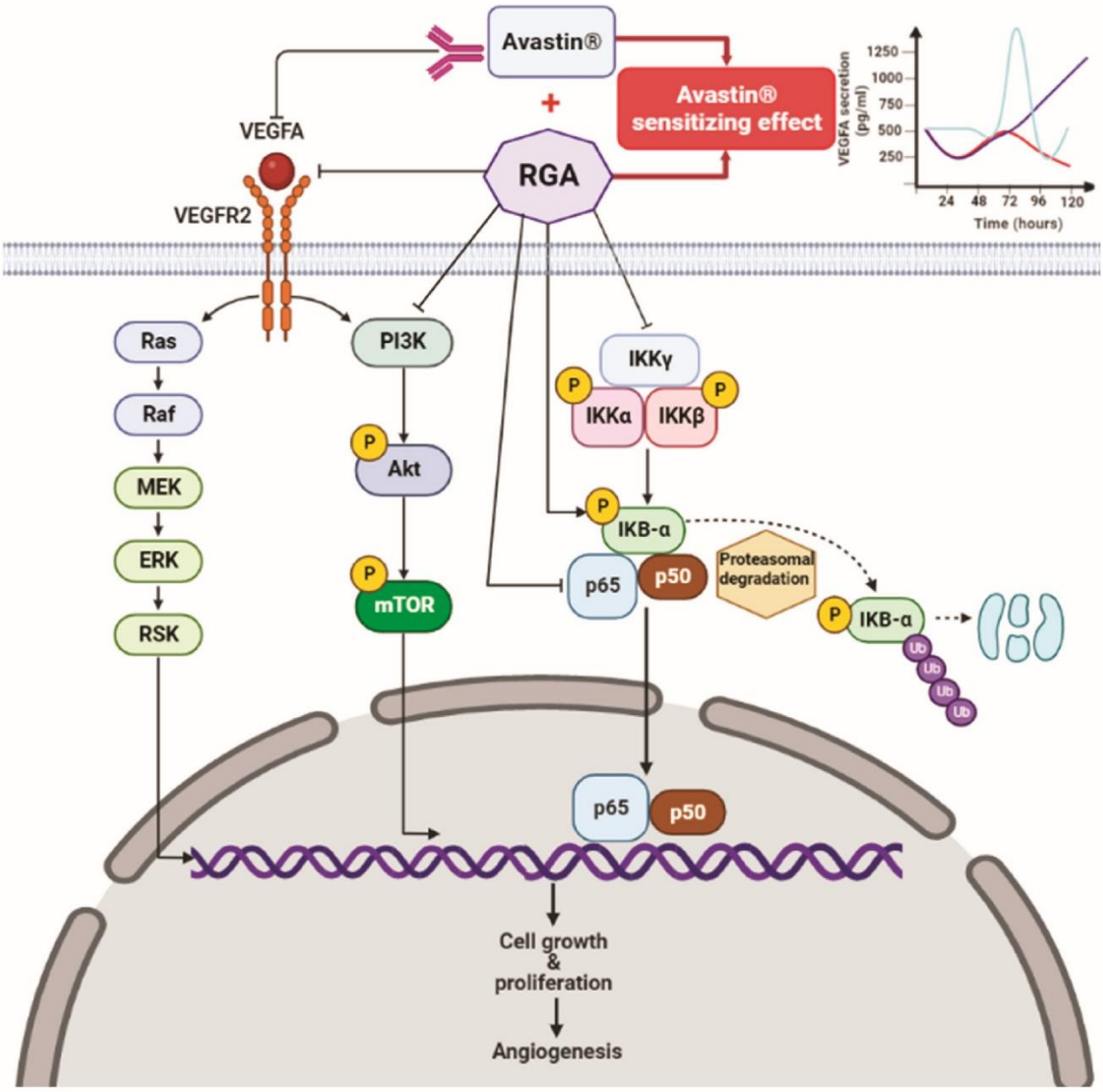

Figure 7. Schematic illustration of the novel proposed mechanisms of the anti-angiogenic impact of Resvega® (RGA), which is able to target several angiogenesis molecular pathways in human ARPE-19 retina cell model. RGA counteracts angiogenic VEGF-A production through an alteration of the AKT/PI3K and NFκB pathways. In detail, RGA reduces the regulator complex IKK controlling the downstream NFκB subunits P65 and P50 belonging and their nuclear/cytosolic localization. This new RGA-targeted pathway complements data on the impact of RGA, which we have previously demonstrated to be involved in preventing activation of the MAPK signaling pathway in ARP19 cells [22]. The disruption of these two important angiogenesis signaling pathways likely leads to a sensitization of retina cells to the anti-VEGF treatment, resulting in an increased ability of Avastin® to decrease VEGF-A secretion over time.

The phosphorylation of AKT leads to the expression of inflammatory cytokines (IL-6, IL-8, IL-18), which support the inflammatory environment involved in AMD pathogenesis, and contributes to VEGF secretion by the inflammatory-induced angiogenesis process [34]. Previous study has revealed that RGA, as an anti-inflammatory formulation, could modulate the expression of inflammatory cytokines such as IL-6 and IL-8 [20]. Our results

suggest that RGA-mediated decreases in AKT phosphorylation may underlie the anti-inflammatory ability of RGA. If we determine here for the first time, to our knowledge, the ability of a nutraceutical containing both RSV and ω-3 fatty acids to increase ability of Avastin® to decrease VEGF-A secretion over time, other studies will be necessary to mechanistically explore the impact of RGA/Avastin® in ARPE 19 and to expand the use of RGA in combination with others anti-VEGF agents such as ranibizumab, aflibercept or brolucizumab.

AMD, which is a chronic, progressive and disabling retinal degenerative disease is characterized by two evolutionary forms: an exudative form, also called the "wet form", and a dry form. In the exudative forms, nutritional supplementation can be associated with drug treatments. Indeed, the results of the Age-Related Eye Disease Study 1 (AREDS-1), a multicenter, randomized controlled clinical trial, showed the benefit of using large doses of micronutrients in the early stages of the disease [35]. The importance of doses of micronutrients, well beyond dietary intake, and the prospect of a therapeutic effect have illustrated a novel concept in ophthalmology that appeared at the beginning of the 2000s, that of health food. Various nutraceutical combinations have been developed, for example Longevinex® which is a polyphenol combination including RSV and quercetin. A clinical trial in elderly patients in the USA showed that an oral administration of this polyphenol combination reduced neovascularisation, and the authors saw objective retinal and visual restoration similar to anti-VEGF therapy [36–38]. The drug treatments inhibiting the VEGF pathway are only effective in progressive exudative forms (wet forms, representing only 20% of clinical forms of AMD) and they are administered intravitreally. Their contraindications, useful clinical effects and undesirable effects stem from the route of administration and the effects of inhibiting VEGF (risk of infection, hemorrhage, etc.). Moreover, retinal cells are able to put resistance systems into place in order to produce VEGF-A regardless of the anti-VGF used. Indeed, various signaling pathways are induced to produce more VEGF-A, amplifying its secretion. Among these cellular pathways, the PI3K-AKT-mTOR pathway seems to be a target that could be used to disturb VEGF-A production. Various studies have shown in in vivo tumor models, that targeting this signaling pathway reduces angiogenesis and microvascular density [39,40]. In a similar manner, in the eye, inhibition of this pathway has been described as a new strategy to manage neovascularization in a variety of ocular diseases [41]. For example, recent studies have shown that the use of a selective inhibitor of class I PI3K and mTOR pathways blocks vascular leakage and reduces CNV lesion size in a laser-induced model of neovascular AMD [42]. Therefore, a combination of anti-VEGF with a nutraceutical such as RGA resulting from ω-3 fatty acids and RSV could act on the PI3K-AKT-mTOR pathway. The combination of the two therapies would thus aim to enhance the disease-modifying properties of the treatment of wet AMD. We show in the present study that RGA is able to inhibit the key protein of this signaling pathway by reducing the phosphorylation of mTOR as well as AKT and the PI3K protein (Figure 2). Subsequent to this inhibition, the NFκB pathway was also affected. RGA was therefore able to act both on the NFκB complex by reducing the protein expression of each subunit (P50 and P65) and on the IκB protein, which is a key protein in the NFκB complex (Figure 3). By inhibiting the phosphorylation of the NFκB complex, IκB can bind NFκB dimers and sequester them in the cytoplasm (Figures 3 and 4). As a result, the NFκB subunits cannot migrate to the nucleus where they normally bind to and stimulate the transcription of target genes such as VEGF-A. Interestingly, another checkpoint controlling activation of NFκB, the IKK complex, is also affected by RGA, since the ω-3 fatty acids/RSV combination decreases both two subunits of IκB complex protein expression (IKKα and IKKβ) and the subunit IKKγ which is required for the stimulation of IKK (Figure 5). The decreases in VEGF-A secretion and the PI3K-AKT-mTOR-NFκB pathway by RGA reinforce the results of a recent laser-induced CNV in mouse model study in which supplementation for 14 days with RGA significantly reduced CNV development [18]. These in vivo results were also supported by a global proteome analysis on lasered retinas where we identified a specific enrichment in negative regulation of epithelial cell migration cluster in the retinas

from mice supplemented with RGA, including negative vasculature development, negative blood vessel development, negative angiogenesis and blood vessel morphogenesis and negative regulation of epithelial cell proliferation [18]. It is worth noting that the pharmacokinetics of RGA demonstrated that after 21 days of RGA supplementation in mice, both RSV aglycons, but mainly RSV metabolites (especially RSV-3-O-sulfate, RSV-4′-O glucuronide and 3-O-glucuronide), were found in the retina and in the posterior pole [18].

Thus, by targeting relevant pathways, the ω-3 fatty acids/RSV combination could enhance or prolong the effect of anti-VEGF-A. To support this hypothesis, a pretreatment of retina cells with RGA followed by a treatment with 100 ng/mL of bevacizumab (Avastin®) made it possible to lengthen the inhibitory effect of Avastin® on VEGF-A production (Figure 6). These important preliminary results, obtained using a combination of a nutraceutical and an anti-VEGF agent on a human retina cell line, pave the way for future studies because it may reduce the undesirable effects of anti-VEGF antibodies and prolong their effect. Furthermore, a recent study was able to show that RSV alone was able to reverse the adverse effect of bevacizumab in ARPE-19 retinal cell [43]. Studies are ongoing to determine whether a combination of ω-3 fatty acids and RSV could also reverse this side effect and enhance the effect of bevacizumab in in vivo models.

4. Materials and Methods

4.1. Cell Culture and Treatment

Human retinal pigmented epithelial cell line (ARPE-19) were obtained from the American Type Culture Collection (ATCC, Manassas, VA, USA). ARPE-19 were cultured in Dulbecco's modified Eagle's F12 medium (DMEM/F12) supplemented with 10% fetal bovine serum (FBS; Dutscher, Brumath, France), 1% penicillin/streptomycin at 37 °C in a 5% CO_2 incubator and passaged twice per week or before they reach 80–85% confluency. These undifferentiated ARPE-19 cells spontaneously produce human RPE cell lines with normal karyology, which form polarized epithelial monolayers [44]. The cells were seeded for the different tests, at a constant density of 17,000 cells/cm^2, to obtain identical experimental conditions.

After 24 h of cell culture, the culture medium was removed and cells were washed twice with Hank's Balanced Salt Solution (HBSS, Dutscher, Brumath, France) and then incubated in DMEM/F12 with 1% FBS and 1% penicillin/streptomycin (Unit/mL) for 24 h. The cells were further incubated with Dimethyl Sulfoxide (DMSO), used as control, or increasing concentration of Resvega® (RGA, Laboratoires Théa®, Clermont-Ferrand, France) (0, 6, 3, 6 and 12 µM) for 24 h. RGA is a nutraceutical formulation composed of Vitamin C 240 mg; Vitamin E 30 mg; Zinc 12.5 mg; Cu 1 mg; EPA 380 mg; DHA 190 mg; Lutein 10 mg; Zeaxanthin 2 mg; trans-RSV 30 mg).

Avastin® (also called Bevacizumab; 25 mg/mL) was provided by Roche and used at a concentration of 100 ng/mL (dilution in DMEM/F12 medium with 1% FBS and 1% penicillin/streptomycin for treatment of the cells for 24 h and 48 h, with or without 72 h RGA pretreatment.

4.2. ELISA

The cells were seeded in a 96-well plate (5600 cells/well) 24 h before being treated or not in a final volume of 100 µL of cell culture media per well. Cell culture supernatants were assayed by ELISA for human VEGF-A (BMS277-2 Invitrogen, Waltham, MA, USA), according to the manufacturer's protocol. Briefly, 50 µL of supernatant of each condition were diluted with 50 µL of sample diluent, loaded onto each well of 96 well plates coated with anti-human VEGF-A antibody, and finally incubated at room temperature on a microplate shaker for 2 h. After washing, 100 µL of biotin conjugated anti-human VEGF-A with horseradish peroxidase (HRP) was added and incubated for 1 h at room temperature, followed by 100 µL of substrate incubation. After 15 min, the absorbance was then measured at 450 nm using a Biochrom Assay UVM340 microplate reader.

4.3. Antibodies

For Western-Blot analyses, the following antibodies were used: c-RAF Rabbit pAb #9422 (1:1000); Phospho-c-RAF (Ser259) Rabbit pAb #9421(1:100); PI3K Rabbit pAb #4292 (1:1000); AKT Rabbit pAb#9272 (1:1000); Phospho-AKT (Ser473) Rabbit pAb #9271 (1:1000); mTOR (L27D4) Mouse mAb #4517 (1:1000); Phospho-mTOR (Ser2448) Rabbit pAb#2971(1:1000); β-ACTIN Mouse mAb#A1978(1:10,000); NF-κB1 p105/p50 (D4P4D) Rabbit mAb #13586 (1:1000); NF-κB p65 (D14E12) XP® Rabbit mAb #8242 (1:1000); Phospho-NF-κB p65 (Ser536) (93H1) Rabbit mAb #3033 (1:1000); IκBα (L35A5) Mouse mAb #4814 (1:1000); Phospho-IκBα (Ser32) (14D4) Rabbit mAb #2859 (1:1000); IKKα Rabbit pAb #2682 (1:1000); IKKβ (D30C6) Rabbit mAb #8943(1:1000); IKKγ (DA10-12) Mouse mAb #2695 (1:1000); Phospho-IKKα/β (Ser176/180) (16A6) Rabbit mAb #2697 (1:1000); ZO-1 Rabbit pAb #13663 (1:1000). For ARPE-19 subcellular fractionation approach, the purity of cytoplasmic and nuclear fractions was determined with HSP60 (D6F1) XP® Rabbit mAb #12165 (1:1000) and poly (ADP-ribose) polymerase-1 (PARP-1) (PARP) (Rabbit mAb# 9542 (1:1000), respectively. All antibodies were purchased from Cell signaling (Ozyme, Saint-Cyr-l'École, France) excluding 71 kDa heat shock cognate (HSC-70) Mouse mAb# sc7298 (1:10,000), which was purchased from Santa Cruz Biotechnology (Nanterre, France).

4.4. Western Blot Analysis

ARPE-19 cells were collected, washed with cold 1X phosphate-buffered saline (PBS Dutshcher, brumath France) centrifugate (5 min, 300× *g*, 4 °C), and then incubated for 30 min on ice with RIPA buffer (Radioimmunoprecipitation Assay buffer, 50 mM Tris-HCl, 150 mM sodium chloride, 0.5% sodium deoxycholate, 1% NP40 and 0.1% sodium dodecyl sulfate, pH 8) containing a protease inhibitor cocktail (Roche, Boulogne-Billancourt, France) a phosphatase inhibitor, sodium fluoride (50 mM) and a protease inhibitor, phenylmethylsulfonyl fluoride (PMSF; 100 µM, Sigma-Aldrich, St. Quentin Fallavier, France). After centrifugation (20 min, 16,000× *g*, 4 °C), the cell debris were eliminated and the protein concentrations were assessed using QuantiPro TM BCA kit (Bicinchoninic Acid; Sigma Aldrich, St. Louis, MO, USA). Samples were adjusted into denaturing loading buffer (50 mM Tris-HCl, 10% glycerol, 5% 2-mercaptoethanol, 2% sodium dodecyl sulfate, pH 6.8 and 0.1% bromophenol blue) and then denatured for 5 min at 95 °C prior to separation. Twenty micrograms of protein were separated on a 10% SDS-PAGE gel, and then transferred onto a nitrocellulose membrane. Nonspecific binding sites were blocked by incubation, for 1 h at room temperature, with 5% non-fat milk powder in PBST (PBS, 0.1% Tween 20, pH 7.2) before overnight incubation at 4 °C with specific primary antibodies which are diluted at 1:1000 in 5% milk-PBST or 5% BSA-PBST. Then, membranes were washed three times for 10 min, with PBST and subsequently incubated at room temperature for 1 h with appropriate horseradish peroxidase (HRP)-conjugated secondary antibodies (Jackson ImmunoResearch, Interchim, Montlucon, France) followed by exposure to enhanced chemiluminescence detection to ECL (Bio-Rad, Marnes-la-Coquette, France). Digital chemiluminescence images were acquired with a ChemiDocTM XRS+ imaging system (Biorad, Marnes-la-coquette, France). Blot analysis and/or band intensity determination was carried out with Image LabTM Software 6.0.1 (Biorad, Marnes-la-coquette, France).

4.5. Nuclear and Cytoplasmic Fraction Isolation

The cells were lysed in buffer (NE-PER; Pierce Biotechnology, Rockford, IL, USA), supplemented with a protease inhibitor cocktail (Halt; Pierce Biotechnology, Rockford, IL, USA), according to the manufacturer's protocol. Protein concentrations were determined (BCA Kit; Pierce Biotechnology) before being loaded onto polyacrylamide gels.

4.6. Densitometry and Statistical Significance

The densitometry of blots was performed with ImageJ software (National Institutes of Health). Unless indicated in the legends of figures, the reported values represent the means of triplicate from one representative experiment repeated three times +/− SD.

Statistical analysis was carried out with Prism GraphPad6.0 Prism software (GraphPad Software, La Jolla, San Diego, CA, USA). Data are shown as means ± standard deviation (SD) for triplicate assay samples of three independent experiments. The difference between mean values was determined by a one-way ANOVA followed by Tukey's test for multiple comparisons. p-values < 0.05 were considered significant (* $p < 0.05$, ** $p < 0.01$, *** $p < 0.001$ and # $p < 0.0001$).

5. Conclusions

In this study, we showed that a nutraceutical enriched with ω-3 fatty acids and resveratrol, a polyphenol, could decrease VEGF-A secretion in retinal cells through a disruption of the PI3K-AKT-mTOR signaling axis and NFκB pathways. These first results were associated with a prolongation of the anti-angiogenic effect of Avastin®, an anti-VEGF usually used in clinical practice to treat AMD. Nonetheless, further investigations are needed to demonstrate the potential use of Resvega® as nutritional supplementation with anti-VEGF antibodies against AMD, especially in preclinical models.

Author Contributions: R.S., M.P., C.C., F.C., A.S., V.A. and F.H. performed the experiments and analyzed the data; C.O. helped in setting up the project; F.H. and D.D. supervised experiments and wrote the manuscript. D.D. supervised the overall project. All authors have read and agreed to the published version of the manuscript.

Funding: This work was supported by grants from the ANRT N°2016/0003, ANRT N° n°2021/1248, by a French Government grant managed by the French National Research Agency under the program "Investissements d'Avenir", reference ANR-11-LABX-0021, the Conseil Régional Bourgogne, Franche-Comte (PARI grant) and the FEDER (European Funding for Regional Economic Development).

Institutional Review Board Statement: Not applicable.

Informed Consent Statement: Not applicable.

Data Availability Statement: The authors declare that all data supporting the findings of this study are available within the article.

Acknowledgments: The authors are grateful to Suzanne Rankin (CHU Dijon) for editing and critical reading of this manuscript.

Conflicts of Interest: C.O. is an employee of Laboratoires THEA.

References

1. Somasundaran, S.; Constable, I.J.; Mellough, C.B.; Carvalho, L.S. Retinal pigment epithelium and age-related macular degeneration: A review of major disease mechanisms. *Clin. Exp. Ophthalmol.* **2020**, *48*, 1043–1056. [CrossRef] [PubMed]
2. Mahmoudzadeh, R.; Hinkle, J.W.; Hsu, J.; Garg, S.J. Emerging treatments for geographic atrophy in age-related macular degeneration. *Curr. Opin. Ophthalmol.* **2021**, *32*, 294–300. [CrossRef] [PubMed]
3. Fleckenstein, M.; Keenan, T.D.L.; Guymer, R.H.; Chakravarthy, U.; Schmitz-Valckenberg, S.; Klaver, C.C.; Wong, W.T.; Chew, E.Y. Age-related macular degeneration. *Nat. Rev. Dis. Primers* **2021**, *7*, 31. [CrossRef] [PubMed]
4. Lim, L.S.; Mitchell, P.; Seddon, J.M.; Holz, F.G.; Wong, T.Y. Age-related macular degeneration. *Lancet* **2012**, *379*, 1728–1738. [CrossRef]
5. Abokyi, S.; To, C.H.; Lam, T.T.; Tse, D.Y. Central Role of Oxidative Stress in Age-Related Macular Degeneration: Evidence from a Review of the Molecular Mechanisms and Animal Models. *Oxidative Med. Cell. Longev.* **2020**, *2020*, 7901270. [CrossRef]
6. Ruan, Y.; Jiang, S.; Gericke, A. Age-Related Macular Degeneration: Role of Oxidative Stress and Blood Vessels. *Int. J. Mol. Sci.* **2021**, *22*, 1296. [CrossRef]
7. Toma, C.; De Cilla, S.; Palumbo, A.; Garhwal, D.P.; Grossini, E. Oxidative and Nitrosative Stress in Age-Related Macular Degeneration: A Review of Their Role in Different Stages of Disease. *Antioxidants* **2021**, *10*, 653. [CrossRef]
8. van Lookeren Campagne, M.; LeCouter, J.; Yaspan, B.L.; Ye, W. Mechanisms of age-related macular degeneration and therapeutic opportunities. *J. Pathol.* **2014**, *232*, 151–164. [CrossRef]
9. Ambati, J.; Atkinson, J.P.; Gelfand, B.D. Immunology of age-related macular degeneration. *Nat. Rev. Immunol.* **2013**, *13*, 438–451. [CrossRef]
10. Blasiak, J.; Pawlowska, E.; Sobczuk, A.; Szczepanska, J.; Kaarniranta, K. The Aging Stress Response and Its Implication for AMD Pathogenesis. *Int. J. Mol. Sci.* **2020**, *21*, 8840. [CrossRef]

11. Amadio, M.; Govoni, S.; Pascale, A. Targeting VEGF in eye neovascularization: What's new?: A comprehensive review on current therapies and oligonucleotide-based interventions under development. *Pharmacol. Res.* **2016**, *103*, 253–269. [CrossRef] [PubMed]
12. Ammar, M.J.; Hsu, J.; Chiang, A.; Ho, A.C.; Regillo, C.D. Age-related macular degeneration therapy: A review. *Curr. Opin. Ophthalmol.* **2020**, *31*, 215–221. [CrossRef] [PubMed]
13. Nowak, J.Z. Age-related macular degeneration (AMD): Pathogenesis and therapy. *Pharmacol. Rep.* **2006**, *58*, 353–363.
14. Musial-Kopiejka, M.; Polanowska, K.; Dobrowolski, D.; Krysik, K.; Wylegala, E.; Grabarek, B.O.; Lyssek-Boron, A. The Effectiveness of Brolucizumab and Aflibercept in Patients with Neovascular Age-Related Macular Degeneration. *Int. J. Environ. Res. Public Health* **2022**, *19*, 2303. [CrossRef] [PubMed]
15. Tan, C.S.; Ngo, W.K.; Chay, I.W.; Ting, D.S.; Sadda, S.R. Neovascular Age-Related Macular Degeneration (nAMD): A Review of Emerging Treatment Options. *Clin. Ophthalmol.* **2022**, *16*, 917–933. [CrossRef]
16. Haibe, Y.; Kreidieh, M.; El Hajj, H.; Khalifeh, I.; Mukherji, D.; Temraz, S.; Shamseddine, A. Resistance Mechanisms to Anti-angiogenic Therapies in Cancer. *Front. Oncol.* **2020**, *10*, 221. [CrossRef] [PubMed]
17. Mettu, P.S.; Allingham, M.J.; Cousins, S.W. Incomplete response to Anti-VEGF therapy in neovascular AMD: Exploring disease mechanisms and therapeutic opportunities. *Prog. Retin. Eye Res.* **2021**, *82*, 100906. [CrossRef]
18. Courtaut, F.; Aires, V.; Acar, N.; Bretillon, L.; Guerrera, I.C.; Chhuon, C.; Pais de Barros, J.P.; Olmiere, C.; Delmas, D. RESVEGA, a Nutraceutical Omega-3/Resveratrol Supplementation, Reduces Angiogenesis in a Preclinical Mouse Model of Choroidal Neovascularization. *Int. J. Mol. Sci.* **2021**, *22*, 11023. [CrossRef]
19. Bhattarai, N.; Piippo, N.; Ranta-Aho, S.; Mysore, Y.; Kaarniranta, K.; Kauppinen, A. Effects of Resvega on Inflammasome Activation in Conjunction with Dysfunctional Intracellular Clearance in Retinal Pigment Epithelial (RPE) Cells. *Antioxidants* **2021**, *10*, 67. [CrossRef]
20. Bhattarai, N.; Korhonen, E.; Toppila, M.; Koskela, A.; Kaarniranta, K.; Mysore, Y.; Kauppinen, A. Resvega Alleviates Hydroquinone-Induced Oxidative Stress in ARPE-19 Cells. *Int. J. Mol. Sci.* **2020**, *21*, 2066. [CrossRef]
21. Koskela, A.; Reinisalo, M.; Petrovski, G.; Sinha, D.; Olmiere, C.; Karjalainen, R.; Kaarniranta, K. Nutraceutical with Resveratrol and Omega-3 Fatty Acids Induces Autophagy in ARPE-19 Cells. *Nutrients* **2016**, *8*, 284. [CrossRef] [PubMed]
22. Courtaut, F.; Scagliarini, A.; Aires, V.; Cornebise, C.; Pais de Barros, J.P.; Olmiere, C.; Delmas, D. VEGF-R2/Caveolin-1 Pathway of Undifferentiated ARPE-19 Retina Cells: A Potential Target as Anti-VEGF-A Therapy in Wet AMD by Resvega, an Omega-3/Polyphenol Combination. *Int. J. Mol. Sci.* **2021**, *22*, 6590. [CrossRef] [PubMed]
23. Ferrara, N. Vascular endothelial growth factor and age-related macular degeneration: From basic science to therapy. *Nat. Med.* **2010**, *16*, 1107–1111. [CrossRef]
24. Ablonczy, Z.; Dahrouj, M.; Tang, P.H.; Liu, Y.; Sambamurti, K.; Marmorstein, A.D.; Crosson, C.E. Human retinal pigment epithelium cells as functional models for the RPE in vivo. *Investig. Ophthalmol. Vis. Sci.* **2011**, *52*, 8614–8620. [CrossRef] [PubMed]
25. Watson, M.I.; Barabas, P.; McGahon, M.; McMahon, M.; Fuchs, M.A.; Curtis, T.M.; Simpson, D.A. Single-cell transcriptomic profiling provides insights into retinal endothelial barrier properties. *Mol. Vis.* **2020**, *26*, 766–779.
26. Rizzolo, L.J. Development and role of tight junctions in the retinal pigment epithelium. *Int. Rev. Cytol.* **2007**, *258*, 195–234. [CrossRef]
27. Graupera, M.; Guillermet-Guibert, J.; Foukas, L.C.; Phng, L.K.; Cain, R.J.; Salpekar, A.; Pearce, W.; Meek, S.; Millan, J.; Cutillas, P.R.; et al. Angiogenesis selectively requires the p110alpha isoform of PI3K to control endothelial cell migration. *Nature* **2008**, *453*, 662–666. [CrossRef]
28. Fukumura, D.; Gohongi, T.; Kadambi, A.; Izumi, Y.; Ang, J.; Yun, C.O.; Buerk, D.G.; Huang, P.L.; Jain, R.K. Predominant role of endothelial nitric oxide synthase in vascular endothelial growth factor-induced angiogenesis and vascular permeability. *Proc. Natl. Acad. Sci. USA* **2001**, *98*, 2604–2609. [CrossRef]
29. DiDonato, J.A.; Hayakawa, M.; Rothwarf, D.M.; Zandi, E.; Karin, M. A cytokine-responsive IkappaB kinase that activates the transcription factor NF-kappaB. *Nature* **1997**, *388*, 548–554. [CrossRef]
30. Mercurio, F.; Zhu, H.; Murray, B.W.; Shevchenko, A.; Bennett, B.L.; Li, J.; Young, D.B.; Barbosa, M.; Mann, M.; Manning, A.; et al. IKK-1 and IKK-2: Cytokine-activated IkappaB kinases essential for NF-kappaB activation. *Science* **1997**, *278*, 860–866. [CrossRef]
31. Rothwarf, D.M.; Zandi, E.; Natoli, G.; Karin, M. IKK-gamma is an essential regulatory subunit of the IkappaB kinase complex. *Nature* **1998**, *395*, 297–300. [CrossRef] [PubMed]
32. Yamaoka, S.; Courtois, G.; Bessia, C.; Whiteside, S.T.; Weil, R.; Agou, F.; Kirk, H.E.; Kay, R.J.; Israel, A. Complementation cloning of NEMO, a component of the IkappaB kinase complex essential for NF-kappaB activation. *Cell* **1998**, *93*, 1231–1240. [CrossRef]
33. Keane, P.A.; Sadda, S.R. Development of Anti-VEGF Therapies for Intraocular Use: A Guide for Clinicians. *J. Ophthalmol.* **2012**, *2012*, 483034. [CrossRef]
34. Fontaine, V.; Fournie, M.; Monteiro, E.; Boumedine, T.; Balducci, C.; Guibout, L.; Latil, M.; Sahel, J.A.; Veillet, S.; Dilda, P.J.; et al. A2E-induced inflammation and angiogenesis in RPE cells in vitro are modulated by PPAR-alpha, -beta/delta, -gamma, and RXR antagonists and by norbixin. *Aging* **2021**, *13*, 22040–22058. [CrossRef]
35. Marshall, L.L.; Roach, J.M. Prevention and treatment of age-related macular degeneration: An update for pharmacists. *Consult. Pharm* **2013**, *28*, 723–737. [CrossRef] [PubMed]
36. Richer, S.; Cho, J.; Stiles, W.; Levin, M.; Wrobel, J.S.; Sinai, M.; Thomas, C. Retinal Spectral Domain Optical Coherence Tomography in Early Atrophic Age-Related Macular Degeneration (AMD) and a New Metric for Objective Evaluation of the Efficacy of Ocular Nutrition. *Nutrients* **2013**, *4*, 1812–1827. [CrossRef] [PubMed]

37. Richer, S.; Patel, S.; Sockanathan, S.; Ulanski, L.J., 2nd; Miller, L.; Podella, C. Resveratrol based oral nutritional supplement produces long-term beneficial effects on structure and visual function in human patients. *Nutrients* **2014**, *6*, 4404–4420. [CrossRef]
38. Richer, S.; Stiles, W.; Ulanski, L.; Carroll, D.; Podella, C. Observation of human retinal remodeling in octogenarians with a resveratrol based nutritional supplement. *Nutrients* **2013**, *5*, 1989–2005. [CrossRef]
39. Liu, M.; Howes, A.; Lesperance, J.; Stallcup, W.B.; Hauser, C.A.; Kadoya, K.; Oshima, R.G.; Abraham, R.T. Antitumor activity of rapamycin in a transgenic mouse model of ErbB2-dependent human breast cancer. *Cancer Res.* **2005**, *65*, 5325–5336. [CrossRef]
40. Saito, K.; Matsumoto, S.; Yasui, H.; Devasahayam, N.; Subramanian, S.; Munasinghe, J.P.; Patel, V.; Gutkind, J.S.; Mitchell, J.B.; Krishna, M.C. Longitudinal imaging studies of tumor microenvironment in mice treated with the mTOR inhibitor rapamycin. *PLoS ONE* **2012**, *7*, e49456. [CrossRef]
41. Liegl, R.; Koenig, S.; Siedlecki, J.; Haritoglou, C.; Kampik, A.; Kernt, M. Temsirolimus inhibits proliferation and migration in retinal pigment epithelial and endothelial cells via mTOR inhibition and decreases VEGF and PDGF expression. *PLoS ONE* **2014**, *9*, e88203. [CrossRef]
42. Ma, J.; Sun, Y.; Lopez, F.J.; Adamson, P.; Kurali, E.; Lashkari, K. Blockage of PI3K/mTOR Pathways Inhibits Laser-Induced Choroidal Neovascularization and Improves Outcomes Relative to VEGF-A Suppression Alone. *Invest. Ophthalmol. Vis. Sci.* **2016**, *57*, 3138–3144. [CrossRef]
43. Subramani, M.; Ponnalagu, M.; Krishna, L.; Jeyabalan, N.; Chevour, P.; Sharma, A.; Jayadev, C.; Shetty, R.; Begum, N.; Archunan, G.; et al. Resveratrol reverses the adverse effects of bevacizumab on cultured ARPE-19 cells. *Sci. Rep.* **2017**, *7*, 12242. [CrossRef] [PubMed]
44. Dunn, K.C.; Aotaki-Keen, A.E.; Putkey, F.R.; Hjelmeland, L.M. ARPE-19, a human retinal pigment epithelial cell line with differentiated properties. *Exp. Eye Res.* **1996**, *62*, 155–169. [CrossRef] [PubMed]

Annexe 10 : Article :VEGF-R2/Caveolin-1 Pathway of Undifferentiated ARPE-19 Retina Cells: A Potential Target as Anti-VEGF-A Therapy in Wet AMD by Resvega, an Omega-3/Polyphenol Combination

Flavie Courtaut[1,2,†], Alessandra Scagliarini[1,2,†] , Virginie Aires[1,2,†] , Clarisse Cornebise[1,2], Jean-Paul Pais de Barros[1,2,3], Céline Olmiere[4] and Dominique Delmas[1,2,5,*]

1 Université de Bourgogne Franche-Comté, 21000 Dijon, France; flavie.courtaut@gmail.com (F.C.); alescaglia@gmail.com (A.S.); virginie.aires02@u-bourgogne.fr (V.A.); clarisse.cornebise@gmail.com (C.C.); jppais@u-bourgogne.fr (J.-P.P.d.B.)
2 INSERM Research Center U1231—Cancer and Adaptive Immune Response Team, Bioactive Molecules and Health Research Group, 21000 Dijon, France
3 Lipidomic Analytical Platform, 21000 Dijon, France
4 Laboratoires Thea, 12 Rue Louis-Blériot, 63000 Clermont-Ferrand, France; celine.olmiere@theaopeninnovation.com
5 Centre Anticancéreux Georges François Leclerc Center, 21000 Dijon, France
* Correspondence: dominique.delmas@u-bourgogne.fr; Tel.: +33-380-39-32-26
† These authors contributed equally of this work

Résumé : La dégénérescence maculaire liée à l'âge (DMLA) est l'une des principales causes de handicap visuel chez les adultes âgés de 55 ans et plus. Malgré les thérapies actuelles, la progression de la maladie est souvent observée sans inversion de la qualité de la vision. Dans cette étude, nous avons cherché à savoir si, dans les cellules rétiniennes ARPE-19 indifférenciées, la voie du récepteurs du VEGF (VEGF-R)/caveoline-1 (Cav-1) pouvait être altérée. Nous soulignons que Resvega®, une combinaison d'acides gras oméga-3 et d'un anti-oxydant, le resvératrol, inhibe la sécrétion de VEGF-A *in vitro* en perturbant la dissociation du complexe VEGF-R2/Cav-1 dans les radaux lipidiques et empêche par la suite l'activation des MAPK. En outre, l'analyse ChIP de l'ADN révèle que cette combinaison empêche l'interaction entre AP-1 et les promoteurs des gènes vegf-a et vegf-r2. Par ces voies, Resvega pourrait présenter un intérêt potentiel en tant que complément nutritionnel contre la DMLA.

Mots clés : DMLA, angiogenèse, maladies oculaires, VEGF, Récepteur au VEGF, oméga-3, resvératrol.

International Journal of
Molecular Sciences

MDPI

Article

VEGF-R2/Caveolin-1 Pathway of Undifferentiated ARPE-19 Retina Cells: A Potential Target as Anti-VEGF-A Therapy in Wet AMD by Resvega, an Omega-3/Polyphenol Combination

Flavie Courtaut [1,2,†], Alessandra Scagliarini [1,2,†], Virginie Aires [1,2,†], Clarisse Cornebise [1,2], Jean-Paul Pais de Barros [1,2,3], Céline Olmiere [4] and Dominique Delmas [1,2,5,*]

1 Université de Bourgogne Franche-Comté, 21000 Dijon, France; flavie.courtaut@gmail.com (F.C.); alescaglia@gmail.com (A.S.); virginie.aires02@u-bourgogne.fr (V.A.); clarisse.cornebise@gmail.com (C.C.); jppais@u-bourgogne.fr (J.-P.P.d.B.)
2 INSERM Research Center U1231—Cancer and Adaptive Immune Response Team, Bioactive Molecules and Health Research Group, 21000 Dijon, France
3 Lipidomic Analytical Platform, 21000 Dijon, France
4 Laboratoires Thea, 12 Rue Louis-Blériot, 63000 Clermont-Ferrand, France; celine.olmiere@theaopeninnovation.com
5 Centre Anticancéreux Georges François Leclerc Center, 21000 Dijon, France
* Correspondence: dominique.delmas@u-bourgogne.fr; Tel.: +33-380-39-32-26
† These authors contributed equally of this work.

Citation: Courtaut, F.; Scagliarini, A.; Aires, V.; Cornebise, C.; Pais de Barros, J.-P.; Olmiere, C.; Delmas, D. VEGF-R2/Caveolin-1 Pathway of Undifferentiated ARPE-19 Retina Cells: A Potential Target as Anti-VEGF-A Therapy in Wet AMD by Resvega, an Omega-3/Polyphenol Combination. *Int. J. Mol. Sci.* **2021**, *22*, 6590. https://doi.org/10.3390/ijms22126590

Academic Editors: Janusz Blasiak and Kai Kaarniranta

Received: 22 May 2021
Accepted: 15 June 2021
Published: 19 June 2021

Abstract: Age-related macular degeneration (AMD) is one of the main causes of deterioration in vision in adults aged 55 and older. In spite of therapies, the progression of the disease is often observed without reverse vision quality. In the present study, we explored whether, in undifferentiated ARPE-19 retinal cells, a disruption of the VEGF receptors (VEGF-R)/caveolin-1 (Cav-1)/protein kinases pathway could be a target for counteracting VEGF secretion. We highlight that Resvega®, a combination of omega-3 fatty acids with an antioxidant, resveratrol, inhibits VEGF-A secretion in vitro by disrupting the dissociation of the VEGF-R2/Cav-1 complex into rafts and subsequently preventing MAPK activation. Moreover, DNA ChIP analysis reveals that this combination prevents the interaction between AP-1 and *vegf-a* and *vegf-r2* gene promoters. By these pathways, Resvega could present a potential interest as nutritional complementation against AMD.

Keywords: AMD; angiogenesis; ocular diseases; VEGF; VEGF-receptor; omega-3 fatty acids; resveratrol

1. Introduction

Among the degenerative pathologies linked to age, eye diseases represent a significant part, and in particular age-related macular degeneration (AMD), which is one of the main causes of deterioration in vision in adults aged 55 and older in developed countries with an obvious negative impact on quality of life [1]. This disease is characterized by damage to the macula, the central area of the retina, which allows for fine or central vision. AMD is characterized by different key steps such as oxidative damage, lipofuscin accumulation, and impaired activity or function of the retinal pigmented epithelium (RPE). Subsequently, increased cell death is observed along with inflammation, which is activated by the accumulation of extracellular and intracellular debris. Finally, there is the development of atrophy ("dry AMD") or of so-called new vessels in the macular region that seem to play a very important role in the complications associated with "wet AMD". The first warning signs—deformation of straight lines, abrupt decrease in visual acuity or contrasts, dark central spot—should lead to prompt consultation at an ophthalmologist. It is usually classed into one of two forms. For the atrophic form, only nutritional supplementation is currently given since no therapies have been shown to be effective. The aim of the non-exudative AMD treatment is to delay the loss of visual function. The second form is

a wet or "exudative" or "neovascular" form. The abnormal vessels are fragile and allow the serum to diffuse, which can cause serious detachment and lead to hemorrhage. The disease progression will depend on the type and location of these abnormal vessels, the possible occurrence of retinal uplifts, bleeding, and the response to treatment. It is crucial to detect the first signs of exudative macular degeneration because the earlier the diagnosis is made, the more effective the treatment. As AMD involves several factors such as oxidative stress, inflammation, and angiogenesis, antioxidants as vitamin E or fatty acids, especially poly-unsaturated acids (PUFA), could be used as supplementation to protect against AMD through their antioxidant power. In this way, the Age-Related Eye Disease Study 1 (AREDS-1), a multicenter, randomized controlled clinical trial, demonstrated that oral nutritional supplementation of a combination of vitamin C, vitamin E, β-carotene, zinc oxide, and cupric oxide in patients with intermediate or advanced AMD in one eye had a 25% relative risk reduction over 5 years of developing advanced AMD. The risk of vision loss of three or more lines was reduced by 19% with this supplementation [2]. Moreover, a French study (NAT1, Nutritional AMD Treatment 1) showed that lesions due to AMD were stabilized in patients supplemented with a PUFA, the docosahexaenoic acid (DHA) [3]. Alongside a preventive supplementation with nutraceuticals, therapies used for wet AMD aim to inhibit abnormal growth of blood vessels with laser photocoagulation or vascular endothelial growth factor (VEGF) inhibitors that are injected into the eye; however, some side effects and progression of AMD have been observed, and anti-VEGF-A therapies do not reverse vision quality.

Faced with this major public health problem, numerous studies and pharmaceutical companies have attempted to develop other inhibitors of VEGF, which is the key factor controlling neoangiogenesis analogous to what is well known in models of tumor angiogenesis. Indeed, the molecular mechanisms by which VEGF induces activation of kinase cascades from the different isoforms of its receptor, VEGF-R, are well described. More specifically, some authors have been able to show the importance of constitutive proteins from lipid rafts, such as the caveolin-1 (Cav-1) protein, in the early activation phase induced by VEGF in cancer models [4]. The binding of the latter to the extracellular domain of its receptor induces a signaling pathway initiated in low-density caveolar membrane domains and requires the dissociation of the receptor to Cav-1. The latter acts as a negative regulator of VEG-R2 activity under basal conditions and as a substrate that is tyrosine-phosphorylated under activating conditions [4].

Herein, we sought to fill the gap in the literature concerning the link between retinal cells and the disruption of the fine molecular mechanism involved in VEGF cascades. To this end, we explored in retinal cells mimicking the AMD phenotype whether a disruption in the sequence of VEGF-R/Cav-1/protein kinase activation could be a potential target for counteracting VEGF secretion in retinal cells and, subsequently, AMD progression. We use a specific nutraceutical, Resvega®, which in comparison to the AREDS formulations, Resvega® (RSG) has resveratrol (RSV) as an additional component [5,6]. In this study, we highlight in retinal cells with an AMD phenotype that VEGF-R2 is dissociated to Cav-1 to activate the Raf–mitogen-activated protein kinase (MAPK)–extracellular signal-regulated kinases 1/2 (ERK1/2) oncogenic signaling pathway. The nutraceutical composed of both omega-3 fatty acids (ω3) and resveratrol (RSV), a polyphenol of grapevines, strongly favors VEGF-R2/Cav-1 association and decreases the active phosphorylated form of Cav-1. These events lead to inhibition of the oncogenic signaling pathway and target the transcriptional activation of *vegf-r2* and *vegf* gene expression. Subsequently, protein expressions are altered, and the VEGF-VEGF-R2 loop is inhibited.

2. Results

2.1. Combination of Resveratrol/ω3 Fatty Acid Inhibits VEGF Pathway in ARPE-19 Cells

The progression and complication of AMD result from excessive angiogenesis, where the vascular endothelial growth factor A (VEGF-A) plays a key role by contributing to the abnormal growth of blood vessels and an increase in vascular permeability that leads

to loss of vision [7]. Due to the ability of RSV to limit production of VEGF in various models of cancer and retinal cells [8–10], we determined the ability of a nutraceutical, Resvega® (RSG) containing both RSV and ω3 fatty acids (EPA: eicosapentaenoic acid, DHA: docosahexaenoic acid), to decrease the production of VEGF-A in ARPE-19, a retinal cell model spontaneously producing VEGF and mimicking the AMD phenotype [11]. For these experiments, we use undifferentiated ARPE-19 retinal cells mimicking cells affected by AMD [12] and that are widely used to test the effect of various molecules and anti-angiogenic compounds, including RSG and RSV [13,14]. Before evaluating VEGF secretion, we first assessed the toxicity of RSG and RSV on undifferentiated ARPE-19 retinal cells. In order to examine the effects of RSG, it was added to cells at concentrations that corresponded to RSV concentrations 0.6; 1.5; 3; 6; 12; 25 μM, since beyond this concentration, RSG has been shown to decrease metabolic activity (especially at 50 and 100 μM) [14]. It appears that neither RSV nor RSG has a significant impact on the cellular viability of human retinal cells ARPE-19 after 24 h of treatment with a range of increasing concentrations from 0 up to 25 μM (Figure 1A). The absence of toxicity of resveratrol at the concentrations used confirms our data published previously on this cellular model [15]. In view of these first results, RSG was therefore used at these non-toxic concentrations (0.6; 3; 6; 12 μM) during the 24 h of treatment in the ARPE-19 cell line, and RSV serves as a positive control for the concentration of 20 μM.

In basal conditions, it appeared that a 24 h treatment with RSV (20 μM) did not decrease VEGF-A secretion from these cells and even slightly increased it (Figure 1B). Very surprisingly, a combination of ω3/RSV at a very low dose of RSV (12 μM) showed a significant decrease in VEGF-A secretion from retinal ARPE-19 cells compared with the control or with RSV alone (Figure 1B). This inhibitory action induced by RSG is more important when retinal cells are previously pretreated with a well-known inducer of VEFG-A secretion such as H_2O_2. Indeed, when the retinal cells are subjected to continuous but non-toxic oxidative stress, there is an overproduction of VEGF-A by H_2O_2 (200 μM), which is almost tripled compared with the control (Figure 1C). However, when ARPE-19 cells are cotreated with RSG, the overproduction of VEGF-A is reduced by 43% compared with H_2O_2 treatment alone. In comparison with RSV that decreases modestly by 27%, the H_2O_2-induced VEGF-A secretion, RSG, appeared to be the most effective in reducing VEGF-A secretion (Figure 1C).

Secretion of VEGF by retinal cells results from an activation of the signaling pathway involving VEGF-specific tyrosine kinase receptors whose activation loop results from a phosphorylation cascade through the induction of successive kinases [16]. In order to evaluate the impact of the ω3 fatty acids/RSV combination on the activating phosphorylation pathway, we next investigated the influence of the different treatments on global protein phosphorylation in ARPE-19 cells. By using an antibody targeting the total phosphorylation sites, we showed in the same basal conditions that only RSG was able to decrease global protein phosphorylation compared with the control (Supplementary Figure S1A). As expected, when retinal cells were stimulated with a recombinant VEGF-A at 10 ng/mL, a high global phosphorylation level is observed in control cells. The VEGF-A increasing effect on phosphorylation level is lowered when cells are pre-treated for 24 h with RSG (Supplementary Figure S1B). This overall decrease in VEGF-induced phosphorylation suggests that the signaling pathway involving the activation of multiple kinase cascades may be affected. Indeed, in the canonic pathway, VEGF-A can bind to two distinct VEGF receptors (VEGF-R) with tyrosine kinase domains leading to homo- or hetero- dimer formation: VEGF-R1, also known as fms-like tyrosine kinase (Flt-1) and VEGF-R2, also known as fetal liver kinase (Flk-1/KDR) [17]. In retinal cells, VEGF binds to VEGF-R2, leading to the dimerization of the receptor and the activation of its intracellular domain through the phosphorylation of tyrosine residues. Once activated, the signaling cascade is triggered, allowing for the recruitment and activation of various factors leading to the transcriptional activation of the gene coding for VEGF and consequently to its production. We found that a treatment with a ω-3/RSV combination (RSG) for 24 h was able to significantly decrease

in a concentration-dependent manner the expressions of VEGF-R1 and -R2 compared to the control (Figure 1D). More interestingly, the 6 μM RSG treatment induced a more significant decrease of VEGFR2 than RSV alone at a concentration of 20 μM (Figure 1D).

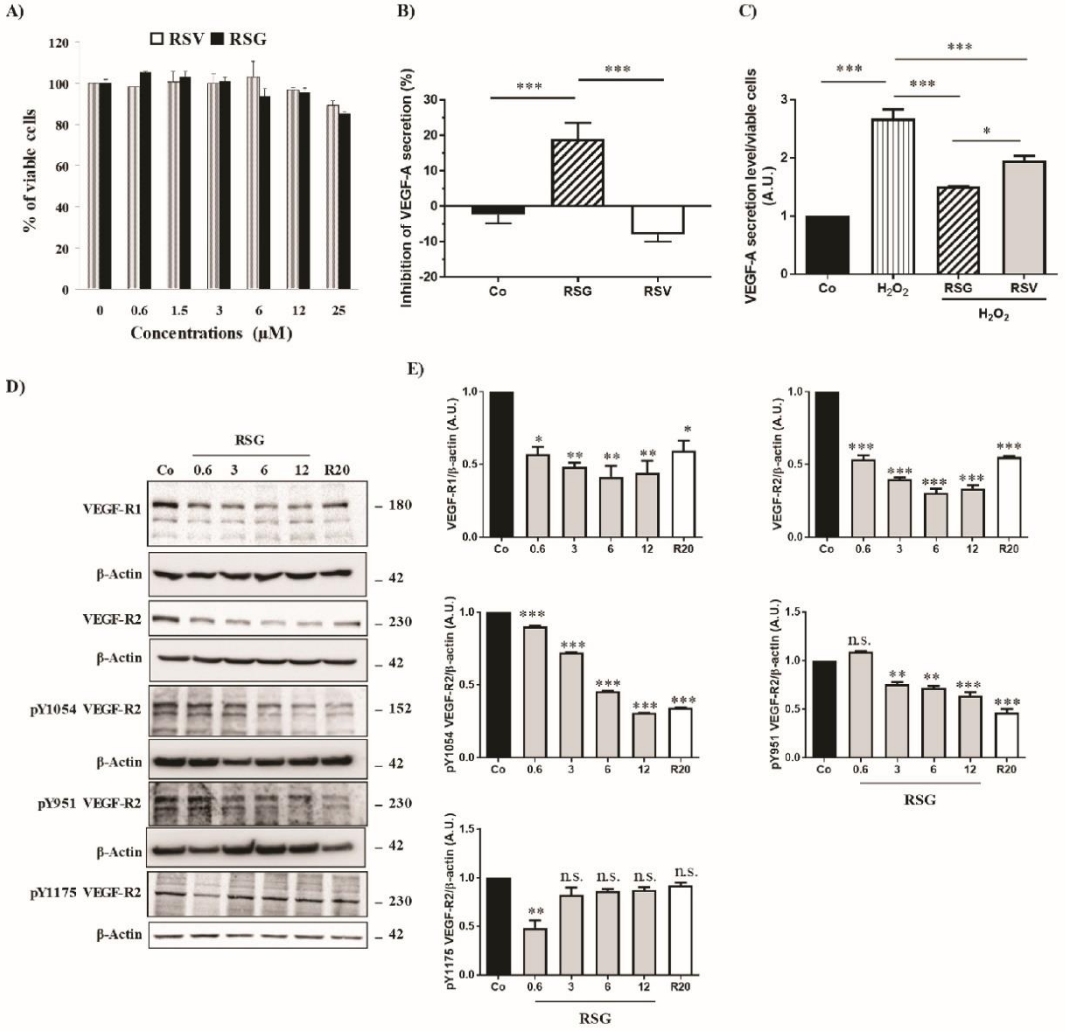

Figure 1. RSV/ω3 fatty acids combination disrupts VEGF-A secretion and inhibits phosphorylation of its receptor. (**A**) Determination of RSG and RSV effects on human retinal ARPE-19 cells. After treatment of ARPE-19 cells with increasing of RSG (0; 0.6; 3; 6; and 12 μM) or RSV (20 μM) concentrations at 37 °C for 24 h, the percentage of cell viability was determined by crystal violet assay. Results are expressed as a percentage of control (mean ± standard deviation of three independent experiments with $n = 10$). (**B**) ARPE-19 retina cells were treated for 24 h without serum with RSG (12 μM) or RSV (20 μM). VEGF-A secretion was measured in cell medium by ELISA. The data are mean ± S.D. of four independent experiments with $n = 10$. p values were determined by one-way ANOVA followed by Tukey's multiple comparison test. * = $p < 0.05$; ** = $p < 0.01$; *** = $p < 0.001$. (**C**) ARPE-19 retina cells were treated without (Co) or with H_2O_2 (200 μM) for 24 h in combination or not with RSG (12 μM) or RSV (20 μM). As in (A) VEGF-A secretion was measured in cell medium by ELISA. The data are mean ± S.D. of four independent experiments with $n = 10$. p values were determined by one-way ANOVA followed by Tukey's multiple comparison test. * = $p < 0.05$; ** = $p < 0.01$; *** = $p < 0.001$. (**D**) Immunoblot analysis of VEGF-R1, VEGF-R2, phospho Y1054 VEGF-R2, phospho Y951 VEGF-R2, phospho Y115 VEGF-R2 in ARPE-19 cell line after treatment without (Co) or with RSG (0.6, 3, 6, 12 μM) or with RSV (20 μM) for 24 h. β-actin was used as the loading control. (**E**) Densitometry quantification of western blots. Data are expressed as the mean fold induction ± SEM of three independent experiments. p values were determined by a one-way ANOVA followed by Tukey's multiple comparison test. * $p < 0.05$, ** $p < 0.01$, *** $p < 0.001$ and n.s.: not significant.

VEGF-R2 is the receptor most involved in the signaling cascade through the phosphorylation of its intracytoplasmic domain. Different tyrosine (Y) sites of VEGF-R2 are particularly important—Y1175, Y1054, and Y951—for kinase regulation and vascular permeability [18]. We investigated among these phosphorylation sites which ones could be more affected by the different treatments. We found that RSG drastically decreased VEGF-R2 activation by decreasing the phosphorylation of both Y1054 and Y951 tyrosyl residues with a very clear inhibition for Y1054, as compared with the control (Figure 1D,E). In the same manner, p-Y951 VEGF-R2 was significantly decreased through RSG treatment from 3 µM of ω-3/RSV combination (Figure 1D,E). The Y1175 phosphorylation site seems not to be affected by the different treatments.

2.2. VEGFR Signaling Pathway Is Disrupted via Lipid Rafts

We next explored the mechanisms underlying the regulation of VEGF-R2 activity, which is poorly understood, especially in retinal cells. Several reports have suggested that VEGF-R2 may be localized in detergent-resistant membranes (DRM) known as lipid rafts, playing the role of a signaling platform to initiate a cascade of kinases in endothelial cells [4]. Then, VEGF-R2 is endocytosed within small invaginations (caveolae) mainly formed by caveolin, a constitutive protein of lipid rafts. Since caveolin-1 (Cav-1) is highly expressed in the eye [19] and is up-regulated during ocular neovascularization [20], we next explored the impact of the treatments with RSG and RSV on Cav-1 protein expression and its active phosphorylated form. Immunoblotting analysis revealed that RSG slightly decreases Cav-1 protein expression and, more importantly, its phosphorylated form in a concentration-dependent manner (Figure 2A). To better characterize the link with lipid rafts, by using both anti-VEGF-R2 and anti-Cav-1 Abs, we chose to use the 0.6 µM concentration for RSG, because the latter is the lowest concentration allowing both a decrease in the VEGF-R2 while maintaining the expression of Cav-1 in order to be able to observe their potential localization. We first confirmed by fluorescence microscopy in retinal ARPE-19 cells a strong decrease in VEGF-R2 expression, and we also saw a well-localized fluorescence (Figure 2B). However, very interestingly, we found that VEGF-R2 colocalized with the raft-associated protein Cav-1 at the surface of RSG-treated retinal cells, as shown by a few yellow spots on the overlay, which is not observed in control cells (Figure 2B).

These points are particularly important since it has been previously shown in aortic bovine endothelial cells (BAEC) that phospho-Cav-1 functions as a scaffolding protein for the VEGF-mediated signaling pathway [21], and the egress of VEGF-R2 from caveolae/lipid rafts is concurrent with the tyrosine phosphorylation of caveolin-1 [4]. Thus, these two events, decreasing the active form of Cav-1 and maintaining VEGF-R2 with Cav-1-associated in lipid rafts, could contribute to the ability of RSG to maintain the inactive form of VEGF-R2 associated with Cav-1 in lipid rafts. To better characterize the involvement of lipid rafts in this VEGF-R signaling pathway in retinal cells, we isolated lipid rafts from ARPE-19 treated with the different compounds. Lysates of ARPE-19 exposed or not for 24 h to RSG or RSV were fractionated on a sucrose gradient, and the lipid content of each fraction was determined by HPLC-coupled mass spectrometry to identify sphingomyelin- and cholesterol-enriched fractions corresponding to lipid rafts (Figure 2C). Further, immunoblotting of flotillin and the two isoforms of caveolin, Cav-1 and Cav-2, confirmed the lipid raft enrichment in fractions 3, 4, and 5 (Figure 2D). Immunoblot analysis of receptors to VEGF indicated that VEGF-R2 was almost undetectable in lipid raft fractions (3, 4, and 5) in control cells, as shown by the western blot and qualitative analysis of three independent experiments, while rafts marker proteins were perfectly localized in these fractions rich in cholesterol and sphingomyelin (Figure 2C,D). Conversely, RSG and RSV treatments strongly relocalized VEGF-R2 into fractions 3, 4, and 5, corresponding to lipid rafts, especially in fraction 4 where Cav-1 was mainly detected (Figure 2D,E). Thus, these results reinforced microscopy observations in which RSG colocalized with Cav-1 into lipid rafts (Figure 2B). Activation of the VEGF-R2 signaling pathway involves the dissociation of VEGF-R2 to Cav-1, leading to Cav-1 phosphorylation, which induces a

Int. J. Mol. Sci. **2021**, *22*, 6590

kinase cascade as shown previously in bovine BAEC cells [4]. Thus, by being delocalized in lipid rafts at a distance from Cav-1, the VEGF-R2 signaling pathway could be reduced or even inhibited by treatment with RSG. In order to verify this hypothesis, we analyzed if RSG could modulate these phosphorylation cascades.

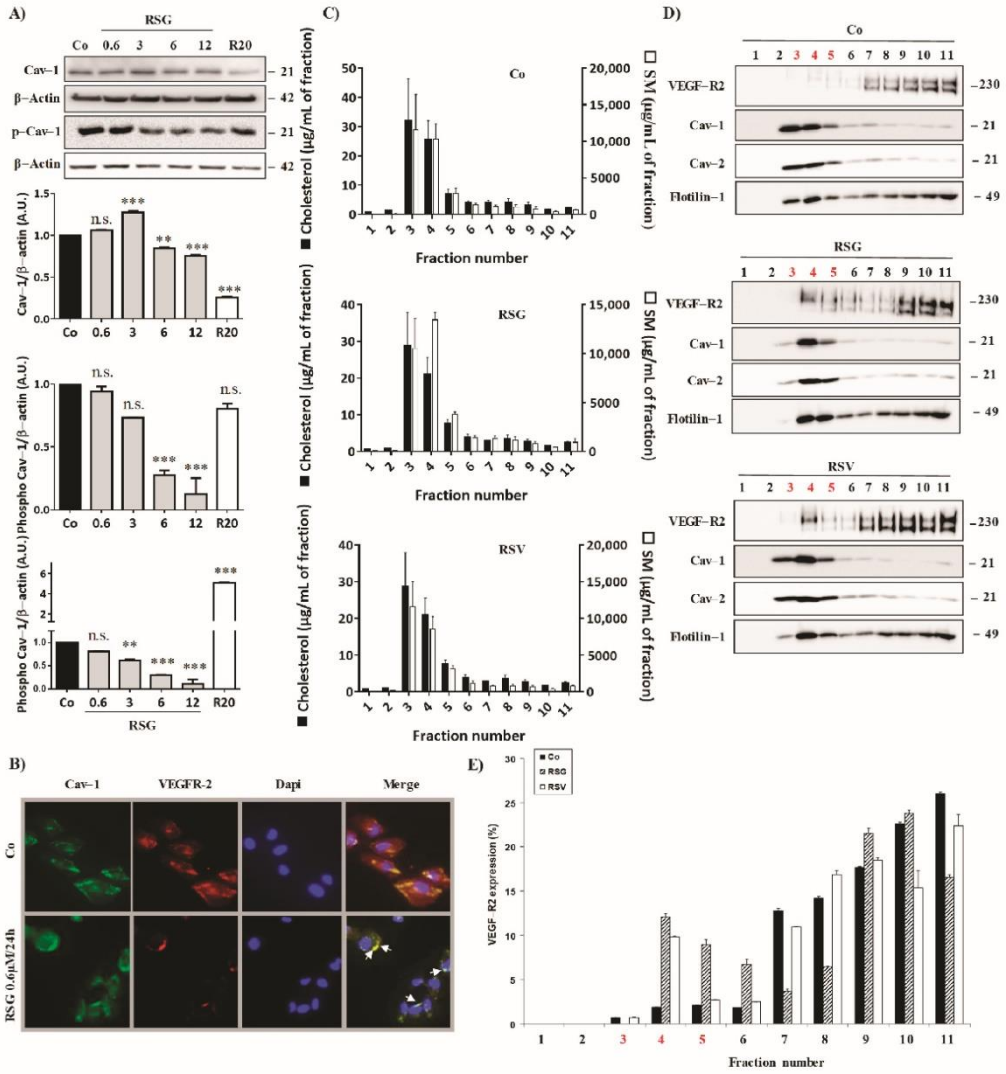

Figure 2. Disruption of VEGF-R2/Cav-1 dissociation into lipid rafts by RSV/ω3 fatty acids combination. (**A**) ARPE-19 retina cells were treated for 24 h by increasing concentrations of RSG (0.6, 3, 6, 12 μM) or with RSV (20 μM) for 24 h. A representative blot of Cav-1 and phospho-Cav-1 (p-Cav-1) is shown from three independent experiments. β-actin was used as a loading control. Densitometry quantification of western blotting is expressed as the mean fold induction ± SEM of three independent experiments. *p* values were determined by a one-way ANOVA followed by Tukey's multiple comparison test. ** $p < 0.01$, *** $p < 0.001$ and n.s.: not significant. (**B**) ARPE-19 cells were left untreated (Co) or treated with 0.6 μM RSG for 24 h before fluorescence microscopy analysis of caveolin-1 (Cav-1) and VEGF-R2 coexpression. A representative image of three independent experiments is shown. (**C**) Lipid composition of ARPE-19 cell lysate fractions after RSG (12 μM) or RSV (20 μM) treatment for 24 h. Cholesterol (black bars) and sphingomyelin (white bars) were expressed in μg/mL of a fraction. Data are expressed as the mean fold induction ± SEM of three independent experiments. (**D**) The representative blot of the expression of indicated proteins in the above-defined fractions is shown from three independent experiments. (**E**) Densitometry quantification of western blotting. Data are expressed as the mean fold induction ± SEM of three independent experiments.

2.3. ω-3. Fatty Acids/RSV Combination-Inhibited VEGF-R2 Activation Is Associated with Disruption of MAPK Pathway Activation

When tyrosine kinase domains are autophosphorylated in their cytoplasmic domains, the downstream signal can be triggered to initiate and activate the signaling pathway [16]. The Raf-mitogen-activated protein kinase (MAPK)-extracellular signal-regulated kinases (ERK1/2) represents an important oncogenic signaling pathway to target the transcriptional activation of *vegf-r2* and *vegf* gene expression and, subsequently, protein expression [22]. We observed that RSG strongly decreased in a concentration-dependent manner the different protein kinases involved and their phosphorylated forms, as shown for Raf, MEK, and ERK1/2 protein expression (Figure 3A,B). Once again, as compared with RSV alone, RSG had a better effect on inhibiting this sequence of kinase activation.

Altogether, these first data demonstrate that RSG containing the ω-3 fatty acids/RSV combination act in synergy to alter the signaling pathway of VEGF-R2 in human retinal cells mimicking the AMD phenotype.

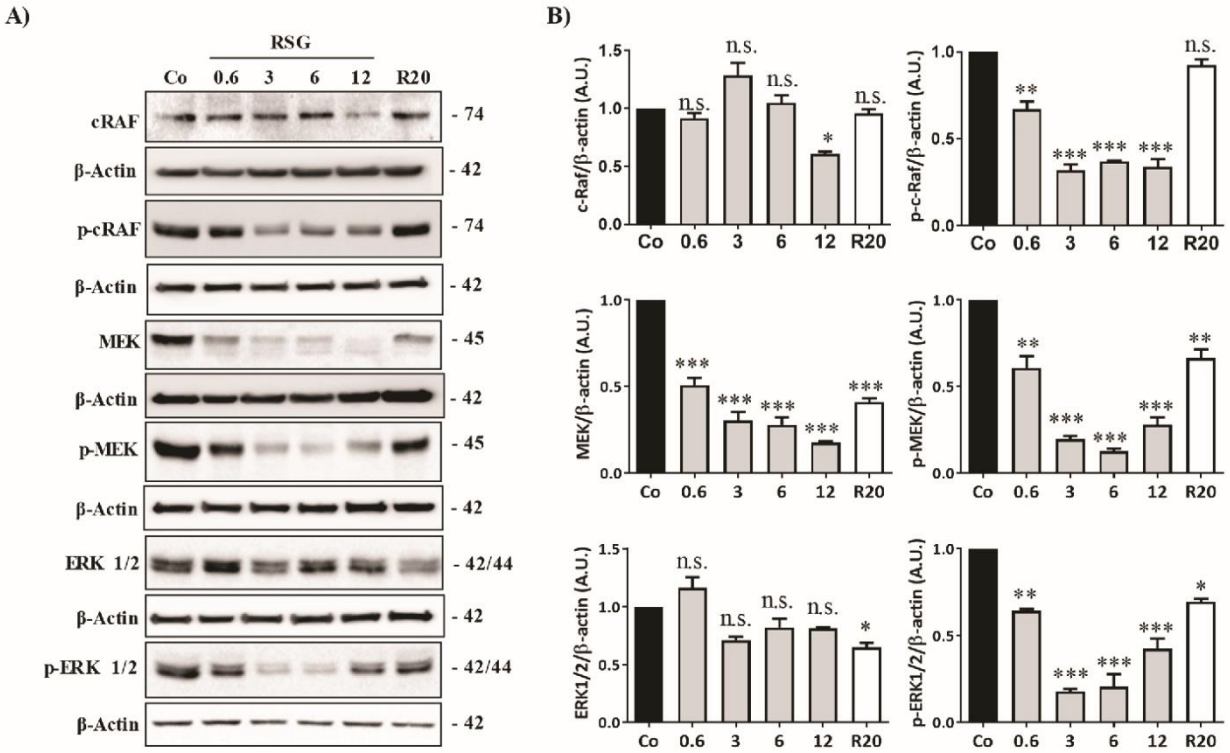

Figure 3. RSG affects the Raf-MAP kinases pathway in retinal cells. (**A**) Immunoblot analysis of c-Raf, phospho c-Raf (p-Raf), MEK, phospho MEK (p-MEK), ERK 1/2, phospho-ERK 1/2 (p ERK 1/2) in RSG-treated ARPE-19 cells with increasing concentration (0.6, 3, 6, 12 μM) or with RSV (20 μM) for 24 h. β-actin was used as a loading control. (**B**) Densitometry quantification of western blotting. Data are expressed as the mean fold induction ± SEM of three independent experiments. P values were determined by a one-way ANOVA followed by Tukey's multiple comparison test. * $p < 0.05$, ** $p < 0.01$ and *** $p < 0.001$, n.s.: not significant.

2.4. ω-3. Fatty Acids/RSV Combination Affects c-Jun/c-Fos Signaling Pathways and Their Relocalization into the Nucleus

Disruption of the intracellular signaling pathway involved in VEGF-R2 by RSG, especially the members of the classic MAPK cascades (MEK, ERK1/2), could affect the ultimate nuclear factors such as c-Jun and c-Fos. These transcriptional factors can form a homodimerization between c-Jun or a heterodimerization between c-Jun and c-Fos, leading to the

formation of the transcription factor activator protein 1 (AP-1) complex [23]. Transcriptional activity of AP-1 complexes is primarily mediated by induction of their expression and regulated by post-translational modification, particularly their phosphorylation by MAP kinase family members such as ERK 1/2. Considering the most important role played by this transcriptional factor, we next assessed whether the previous modulation of MAPK by RSG could have an impact on c-Jun and c-Fos protein and gene expression and determined the potential key role of AP-1 in RSG actions. To this end, we treated retinal cells with RSG and RSV for 24 h. We observed a strong decrease in both *c-jun* and *c-fos* mRNA expression with RSG, which was more significant after 24 h of treatment (Figure 4A). This decrease in gene expression was associated with a strong decrease in c-Jun and c-Fos protein expression in a concentration-dependent manner with RSG, which was also observed with 24 h of treatment with RSV (Figure 4B,C). Post-translational events are important for the increase in transcriptional activity of c-Jun of c-Fos, such as increases of phosphorylation on their serine sites in their transactivation domain [24,25]. Very surprisingly, no treatments modulated the phosphorylation of c-Fos; however, RSG strongly disrupted phosphorylation of c-Jun (Figure 4B,C). Indeed, using specific Abs against serine residues of c-Jun, we observed a decrease in phospho Ser63-c-Jun with RSG and RSV and a slight modulation of phospho Ser73-c-Jun at 12 µM of RSG (Figure 4B,C).

Phosphorylation at Ser 63 and 73 is crucial for the role of c-Jun. Indeed, the transcriptional activity of c-Jun is increased by phosphorylation of these two serines in the transactivation domain that are mediated by MAP kinases [24,25]. To act as transcriptional factors and to form the homo- or heterodimer AP-1, c-Jun and its phosphorylated forms must be translocated into the nucleus to response elements of target genes.

Fluorescence microscopy analysis confirmed the decrease in the proteins of interest but showed that RSG abolished the migration of the transcriptional factors, c-Jun, and its phosphorylated forms Ser 63 and Ser73, into the nucleus (Figure 5A). Indeed, RSG halved the c-Jun protein amount compared with the control and the other treatments (Figure 5A).

To assess this relevant property of RSG in preventing the relocalization of nuclear factors into the nucleus, we performed immunoblotting from a nucleus/cytoplasm extraction where poly(ADP-ribose) polymerase-1 (PARP-1) and heat shock cognate (HSC70) proteins are used as controls for the nuclear and cytosolic fractions, respectively. While c-Jun and its active phosphorylated forms are mainly in the nucleus, as demonstrated in the control, RSG strongly decreases the amount of c-Jun protein in these nuclear fractions compared with the control by 44% (Figure 5B). In a similar manner for its phosphorylated forms, phospho-Ser63-c-Jun both strongly decreased in the nucleus fractions (RSG −67%) and strongly increased in the cytosolic fractions (Figure 5B). Surprisingly, RSV increased phospho-Ser63-c-Jun both in nuclear and cytosolic fractions compared with the control. On the other hand, phospho-Ser73-c-Jun also clearly decreased through RSG treatment in nuclear fractions compared with the control by 75% as well as through RSV by 80%, respectively (Figure 5B).

Collectively, these results indicate that a functional VEGF-R2 allows for the activation of a cascade of kinases, leading to the migration into the nucleus of the nuclear factors necessary for the AP-1 complex formation, which could play a role as a transcriptional activator of target genes. Conversely, treatment with a nutraceutical such as RSG keeps the VEGF-R2 complex in an inactive form and inactivates the Raf-MEK-ERK pathway, but also abolishes the translocation of c-Jun in the nucleus.

Int. J. Mol. Sci. 2021, 22, 6590

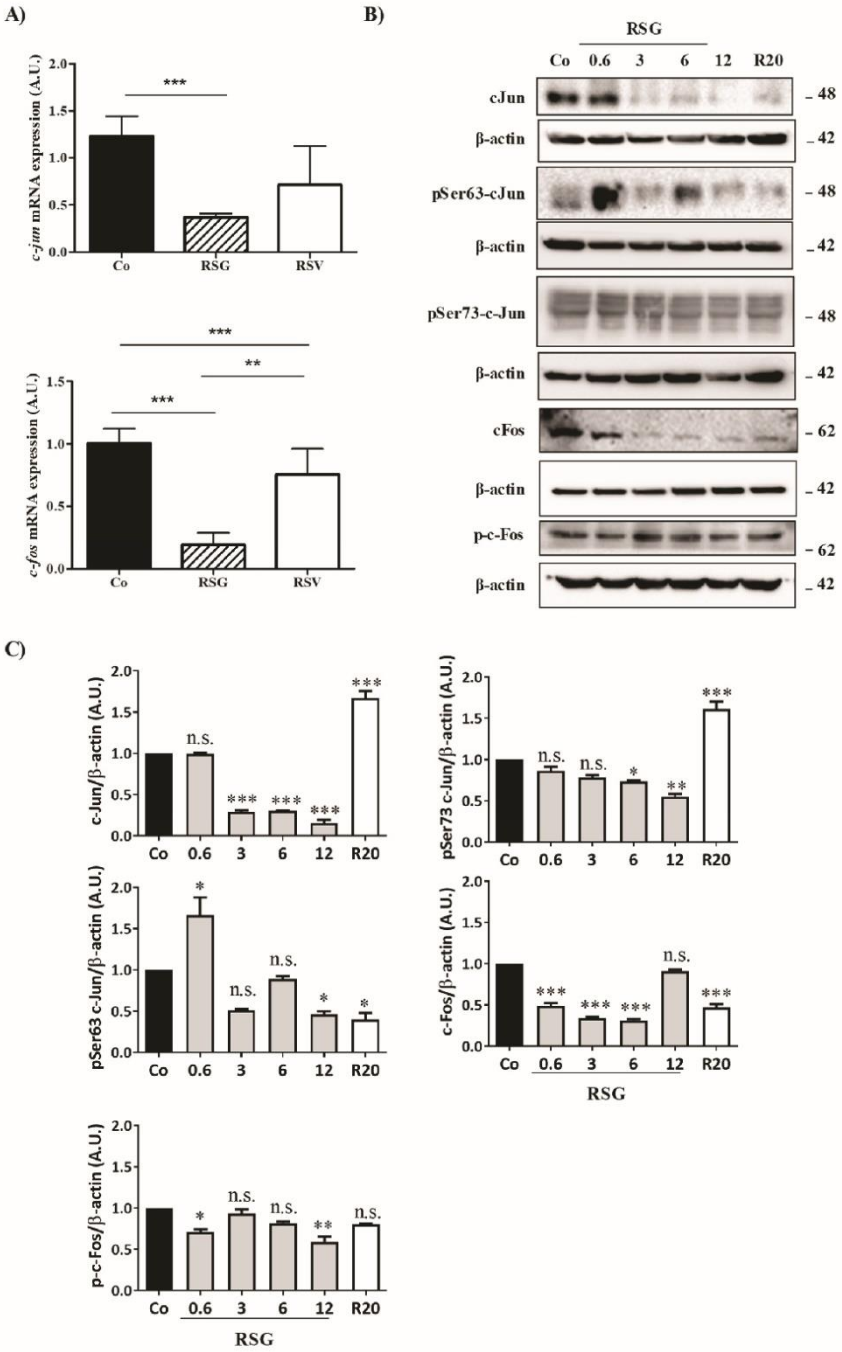

Figure 4. RSG down-regulates nuclear transcriptional factors c-Jun and c-Fos and their phosphorylated forms. (**A**) RT-qPCR mRNA expression analysis of *c-jun* and *c-fos*. Data represent three independent experiments. Data are expressed as the mean fold induction ± SEM of three independent experiments. *p* values were determined by a one-way ANOVA followed by Tukey's multiple comparison test. * $p < 0.05$, ** $p < 0.01$, *** $p < 0.001$ and n.s.: not significant. (**B**) Immunoblot analysis of c-Jun, phospho Ser63 c-Jun (pSer63 c-Jun), phospho Ser73 c-Jun (pSer73 c-Jun), c-Fos, phospho-c-Fos (p-c-Fos) in RSG-treated ARPE-19 cells with increasing concentration (0.6, 3, 6, 12 μM) or with RSV (20 μM) for 24 h. β-actin was used as the loading control. (**C**) Densitometry quantification of western blotting. Data are expressed as the mean fold induction ± SEM of three independent experiments. *p* values were determined by a one-way ANOVA followed by Tukey's multiple comparison test. * $p < 0.05$, ** $p < 0.01$ and *** $p < 0.001$.

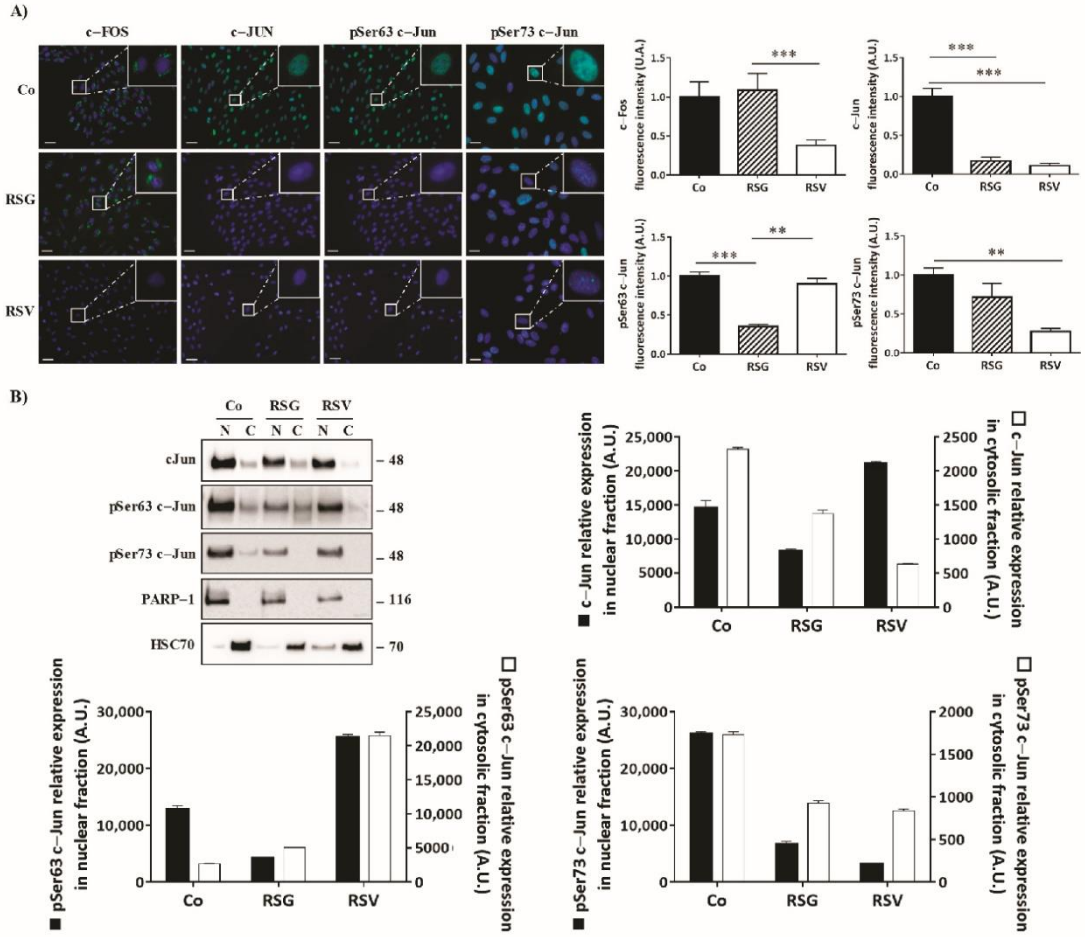

Figure 5. RSG inhibits the translocation of phosphorylated c-Jun forms into the nucleus of ARPE-19 cells. (**A**) Immunofluorescence analysis of expression and localization of c-Fos, c-Jun, and phospho Ser63 c-Jun, phospho Ser 73 c-Jun into untreated (Co) or treated ARPE-19 retina cells with RSG (12 µM) or with RSV (20 µM) for 24 h. Left panel, representative images of specific proteins expression (green fluorescence) counterstaining with Hoechst 33342 (nuclei, blue). Right panel quantification of a specific protein on merged pictures (300 cells per line) with Image J software. *p* values were determined by a one-way ANOVA followed by Tukey's multiple comparison test. ** $p < 0.01$, *** $p < 0.001$ and n.s.: not significant. (**B**) Representative blot of c-Jun, phospho Ser63 c-Jun (pSer63 c-Jun), phospho Ser73 c-Jun (pSer73 c-Jun) protein expression in RSG (12 µM)-treated ARPE-19 cells or with RSV (20 µM) for 24 h. Nuclear fractions (N) and cytosolic (C) fractions are shown from three independent experiments. Densitometry quantification of western blotting. Data are expressed as the mean fold induction ± SEM of three independent experiments. *p* values were determined by a one-way ANOVA followed by Tukey's multiple comparison test. ** $p < 0.01$ and *** $p < 0.001$.

2.5. ω-3. Fatty Acids/RSV Combination Antagonizes AP-1 Binding Sites on VEGF and VEGF-r2 Promoter Genes and Their Transcription

Activation of the Ras-MEK-ERK signaling pathway is known to up-regulate VEGF expression and also its receptor, VEGF-R2, in various models, particularly in cancer models, to promote angiogenesis [26]. A disruption of the final elements such as translocation of AP-1 into the nucleus should alter its transcriptional activity on the promoter of *vegf* and *vegf-r2* genes and subsequently must strongly affect the VEGF/VEGF-R2 autocrine feed-forward loop triggering angiogenesis. Alteration of c-Fos and especially c-Jun and its phosphorylated forms by RSG led us to explore whether this ω-3 fatty acids/RSV combination could antagonize the positive effect of the AP-1 transactivation factor on the

promoters of the *vegf* and *vegf-r2* genes. Accordingly, AP-1 chromatin immunoprecipitation (ChIP) assay on five putative binding sites of the *vegf* promoter gene (Figure 6A, upper panel) using nuclear extracts of human retinal ARPE-19 cells treated or not treated with nutraceuticals RSG and RSV for 24 h showed that AP-1 on the *vegf* promoter (binding site 3 (B.S.3)) is dramatically impeded by RSG compared with the control or with RSV (no enrichment was observed on B.1; B.S.2; B.S. 4; B.S.5) (Figure 6A). This antagonization of AP-1 to bind and to activate the transcription of the *vegf* promoter gene was subsequently associated with a decrease in *vegf* mRNA levels after treatment with RSG (Figure 6B). The gene of the VEGF-R2 protein possesses in its proximal promoter region multiple AP-1 binding sites that could be involved in the nutraceutical action (Figure 6C, upper panel). As previously, the AP-1 ChIP assay on the six putative binding sites on the *vegf-r2* promoter gene showed that AP-1 on the *vegf-r2* promoter (binding sites 5 (B.S.5) and 6 (B.S.6)) is affected by RSG, with a stronger effect on (B.S.5) than (B.S.6) compared with the control (no enrichment was observed on B.1; B.S.2; B.S.3; B.S.4) (Figure 6C). RSV also seemed to disrupt and antagonize AP-1 binding sites (Figure 6C). In a similar manner to the *vegf* gene expression, this action induced by RSG and RSV led to a strong decrease in the *vegf-r2* mRNA levels (Figure 6D).

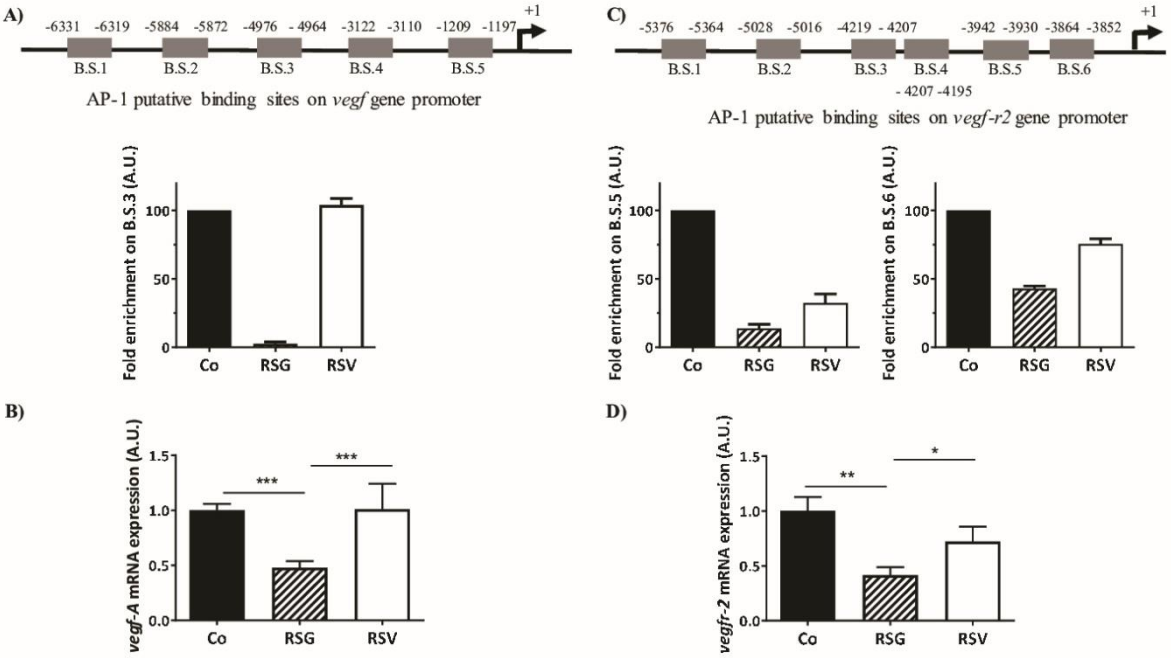

Figure 6. RSG inhibits *vegf-a* and *vegf-r2* mRNA expressions through a disruption of the AP-1 binding sites. ARPE-19 cells were untreated (Co) or treated with RSG (12 μM) or with RSV (20 μM) for 24 h. (**A**) Upper panel, analysis on the putative binding sites of AP-1 on the *vegf-a* gene promoter. Down panel, ChIP analysis of the interaction between AP-1 and the *vegf* promoter in ARPE-19 cells. Analysis of the putative B.S.3 for AP-1 on the *vegf* promoter (−4976 −4964) is shown. For the putative B.S.1, B.S.2, B.S.4, and B.S.5, any amplification was obtained. (**B**) RT-qPCR mRNA expression analysis of *vegf-a*. Data represent three independent experiments. Data are expressed as the mean fold induction ± SEM of three independent experiments. *p* values were determined by a one-way ANOVA followed by Tukey's multiple comparison test. * $p < 0.05$, ** $p < 0.01$ and *** $p < 0.001$. (**C**) Upper panel, analysis of the putative binding sites of AP-1 on the *vegf-r2* gene promoter. Down panel, ChIP analysis of the interaction between AP-1 and the *vegf-r2* promoter in ARPE-19 cells. Analysis of the putative B.S.5 and B.S.6 for AP-1 on the *vegf-r2* promoter (−3942, −3930, and −3864, −3852, respectively) is shown. For the putative B.S.1, B.S.2, B.S.3, and B.S.4, any amplification was obtained. (**D**) RT-qPCR mRNA expression analysis of *vegf-r2*. Data represent three independent experiments. Data are expressed as the mean fold induction ± SEM of three independent experiments. *p* values were determined by a one-way ANOVA followed by Tukey's multiple comparison test. * $p < 0.05$, ** $p < 0.01$ and *** $p < 0.001$.

Together, these data highlight a potential role of RSG as a nutraceutical composed of polyphenols and ω-3 fatty acids to counteract the progression of AMD through a pleiotropic action in the retina by targeting key regulators of neoangiogenesis in retina cells.

3. Discussion

Despite an increasing number of reports highlighting the key role of VEGF-A in the development of blood vessels in tumors and other tissues undergoing abnormal angiogenesis [27,28], and the development of new anti-VEGF antibodies to counteract neovascularization, especially in advanced cancers or in ocular diseases (i.e., ranibizumab, bevacizumab, aflibercept, etc.) [29], side effects and the progression of AMD continue to be observed and lead to treatment failures. Furthermore, some studies have suggested a role for caveolin-1 (Cav-1), a protein of lipid rafts, in the regulation of the VEGF-R pathway in prostate cancer and endothelial cells [4,30]. Indeed, Cav-1 regulates VEGF-stimulated VEGF-R2 autophosphorylation and the activation of downstream angiogenic signaling, possibly through compartmentalization of specific signaling molecules. Caveolae and lipid rafts act as platforms for the negative modulation of VEGF signal transduction cascades in various cancer models (Figure 7) [4,31]. However, no direct links between VEGF-R2, Cav-1, their localization into lipid rafts, and the full mechanism induced in ocular degenerative diseases such as AMD have been provided so far. Herein, for the first time, through the use of potential anti-angiogenic nutraceuticals, we provide a mechanism by which a ω-3 fatty acids/RSV combination (RSG) can counteract VEGF secretion through modulation of the link between VEGF-R2 and Cav-1 into lipid rafts and the repercussions on the downstream signaling cascade.

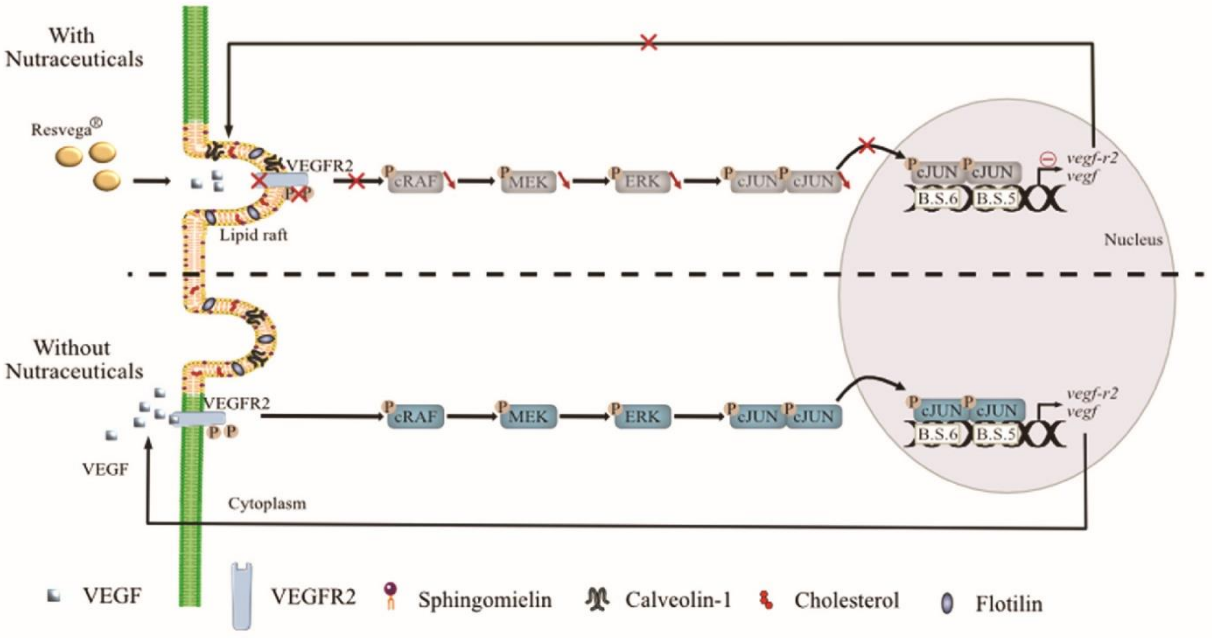

Figure 7. Suggested model to counteract VEGF-A secretion in retinal cells with AMD phenotype by nutraceuticals. Contrary to the physiopathological mechanism observed in retinal cells mimicking AMD, nutraceutical with resveratrol/ω3 fatty acids combination promotes (1) VEGF-R2 relocalization into lipid rafts and its binding with Cav-1, a constitutive protein of lipid rafts. This VEGF-R2-Cav-1 association, which acts as a negative regulator of the VEGF-A signaling cascade, prevents (2) the activation of MAP kinase pathway and subsequently decreases (3) phosphorylation of transcriptional nuclear factors such as c-Jun. Reduction of phospho-c-Jun level is associated with a (4) disruption of c-Jun into the nucleus. Furthermore, nutraceuticals also seemed to disrupt and antagonize AP-1 binding sites on the promoters of *vegf* and *vegfr* genes and contribute to the decrease in their mRNA and protein levels.

The pathological process of AMD leads to progressive destruction of the neurosensory macular area, involving the RPE, Bruch's membrane, and the choroid. Different stages of the disease have been described with the manifestation of retinal abnormalities and the appearance of drusen (extracellular deposit of lipid, cellular debris, and protein) near the fovea, while late stages present with geographic atrophy or CNV. Angiogenesis, namely, the development of new blood vessels from pre-existing vasculature, plays a crucial role in neovascular AMD where pro-angiogenic VEGF-A had been shown to be involved in the development of CNV [32]. Based on their use in treatments for various cancers with metastasis, VEGF inhibitors have revolutionized the care of vasoproliferative ophthalmologic disease, but some side effects are observed. Subsequently, new alternatives and compounds have been researched to improve the management of this serious disease. For many years, various studies have sought alternatives or therapeutic supplements in order to prevent the occurrence of the disease or its progression. In this way, the Age-Related Eye Disease Study 1 (AREDS-1), a multicenter, randomized controlled clinical trial, demonstrated that oral nutritional supplementation of a combination of vitamin C (500 mg), vitamin E (400 UI), β-carotene (15 mg), zinc oxide (80 mg), and cupric oxide (2 mg) in patients with intermediate or advanced AMD in one eye had a 25% relative risk reduction of developing advanced AMD in the eye over 5 years. The risk of vision loss of three or more lines was reduced by 19% with this treatment. Moreover, several epidemiological studies demonstrated that carotenoid intake reduced the risk of advanced AMD and that a lutein- and zeaxanthin-based diet might protect against intermediate AMD in female patients. Thus, the objective of the second AREDS (AREDS-2) was to determine whether the addition of lutein/zeaxanthin and omega-3 fatty acids (docosahexaenoic (DHA) and eicosapentaenoic acids (EPA)) would further reduce progression to late-stage AMD. The addition of lutein + zeaxanthin, DHA + EPA, or lutein + zeaxanthin and DHA + EPA to the complete AREDS formulation did not further reduce the risk of progression to advanced AMD [2,5]. Moreover, because of the potential increased incidence of lung cancer in former smokers, lutein + zeaxanthin could be an appropriate carotenoid substitute in the AREDS formulation [5]. Nevertheless, other studies have shown that long-chain poly-unsaturated fatty acids could protect against AMD [3]. Indeed, a meta-analysis suggests that ω-3 fatty acids such as DHA, which are essential dietary compounds found in fish such as salmon or tuna, could reduce the risk of both early and late AMD [33]. In the same manner, other natural compounds, such as polyphenols, could act on the different molecular steps of AMD through their pleiotropic actions such as their antioxidant, anti-inflammatory, and anti-angiogenic properties [34–36]. These phytomolecules have cellular targets similar to those of the new drugs developed by pharmaceutical companies, and more than 1600 patents are currently reported concerning flavonoids and 3000 patents concerning polyphenols. One of the best known is the polyphenol resveratrol (RSV), which is a *trans*-3,4′,5-trihydroxystilbene and seems to be of great interest for the prevention of various pathologies. Indeed, RSV presents a myriad of health benefits and acts at multiple levels such as cellular signaling, enzymatic pathways, apoptosis, and gene expression to prevent or to fight coronary heart damage, cancers, or degenerative diseases (see for review [37–39]). It is well described that RSV can reduce cancer progression through an anti-angiogenic action [40]. This last property involved inhibition of VEGF at gene and protein expression levels through an NFκB-mediated mechanism, as we and others have previously shown in various cancer types such as melanoma or colon cancers [41,42]. More specifically, we have shown in retinal cells that RSV was able to reduce VEGF secretion induced by oxysterols and subsequently to counteract their toxic effects [15]. Recently, a clinical trial realized in the United States in octogenarian patients has shown that oral administration of a polyphenol combination including resveratrol and quercetin reduces neovascularization, and the authors saw objective retinal and visual restoration, similar to anti-VEGF therapy [43,44]. Based on these findings, we compared the action of resveratrol alone (RSV) with the ω-3 fatty acids/RSV combination (RSG) on human retinal cells mimicking the AMD phenotype with a VEGF secretion. Interestingly, the ω-3

fatty acids/RSV combination showed a synergic anti-angiogenic action compared with the two drugs alone, particularly when VEGF-inducers stimulated retinal cells. These results are in accordance with a previous study showing that RSG inhibited retinal endothelial tube formation. In fact, a concentration range of Resvega (25, 50, and 100 μM) reduced the ability of endothelial cells obtained from a human umbilical vein (HUVEC) and of monkey retinal endothelial cells (RF/6A) to form networks on matrigel [45]). Moreover, we demonstrate that RSG strongly decreased both VEGF-R2 activation through its tyrosine phosphorylation but also decreased Cav-1 phosphorylation. Cav-1 is expressed in ocular types, including vascular cells, RPE, and the lens epithelium (Figure 7) [46,47]. In the eye, Cav-1 plays an essential role in modulating angiogenic signaling where VEGF-R2 is localized into caveolae. Morais et al. showed that Cav-1 expression promotes VEGF-induced corneal angiogenesis [48]. Very interestingly, the ω-3 fatty acids/RSV combination (RSG), by decreasing the phosphorylation of Cav-1 into the residue Y14, altered the main function of phospho-Cav-1 that acts as a scaffolding protein for VEGF-mediated signaling by serving as a docking site for phospho-tyrosine-binding molecules [30]. Moreover, we observed that the ω-3 fatty acids/RSV combination reinforced the association between VEGF-R2 and Cav-1 into lipid rafts and subsequently disturbed the autophosphorylation of VEGF-R2 and activation of the downstream signaling cascade. According to the central role of the Raf-MAPK-ERK oncogenic signaling pathway in the control of transcription of VEGF-R2 and VEGF expression, we observed an important property of RSG that was able to inhibit the transcription of these genes (Figure 7). Indeed, we highlight that RSG was able to alter nuclear relocalization into the nucleus of nuclear transcriptional factors such as c-Jun and its phosphorylated form. This effect was reinforced by the fact that RSG was able to prevent the binding of the AP-1 complex on the response elements controlling gene transcription of *vegf-r2* and *vegf*. Subsequently, protein and gene expressions were reduced by the ω-3 fatty acids/RSV combination.

4. Materials and Methods

4.1. Cell Cultured and Viability Assays

The human retinal pigmented epithelial cell line ARPE-19, purchased from the American Type Culture Collection (Manassas, VA, USA), was maintained in Dulbecco's Modified Eagle's F12 medium (DMEM/F12) supplemented with 10% fetal bovine serum (Dutscher, Brumath, France), 1% penicillin/streptomycin in a humidified atmosphere of 5% CO_2 at 37 °C. These undifferentiated ARPE-19 cells are spontaneously arising human RPE (retinal pigment epithelium) cell lines with normal karyology, which form polarized epithelial monolayers [49]. ARPE-19 has structural and functional properties characteristic of RPE cells in vivo. They both express some markers of RPE cells such as rpe65 and rlbp1 and various genes involved in the production of VEGF (i.e., rpe65, rlbp1, vegf, kdr, serpinf 1, pnp1). Due to these properties, ARPE-19 cells are considered as retinal cells, mimicking the AMD phenotype. Cells were seeded and grown to a sub-confluence of 60–70% in normoxia. After seeding for 24 h, the medium was removed, and the cells were washed once with Hank's Balanced Salt Solution (HBSS, Dutscher, Brumath, France) before re-incubating in DMEMF12 with 1% FBS and 1% penicillin/streptomycin. The following day, cells were treated with DMSO, Resvega® (Laboratoires Théa, Clermont-Ferrand, France), or Resveratrol (Sigma Aldrich, St. Quentin Fallavier, France). The viability assays were assessed by crystal violet staining (Sigma Aldrich, St. Quentin Fallavier, France). Briefly, retinal cells were seeded into 96-well plates and treated with increasing concentrations of RSG (Resvega®: Vitamin C 240 mg; E 30 mg; Zinc 12.5 mg; Cu 1 mg, EPA 380 mg; DHA 190 mg; Lutein 10 mg; Zeaxanthin 2 mg; *trans*-resveratrol 30 mg), and RSV for 0.5, 1, 2, 4, 6, 8, 24, 48, and 72 h. After 24 h of culture, at the end of the treatment, cells were washed with phosphate-buffered saline (PBS), fixed with ethanol for 10 min at 4°C, and then stained with a crystal violet solution (0.5% (*w/v*) crystal violet in 25% (*v/v*) methanol) for 15 min at room temperature. Cells were then gently rinsed with water, and absorbance was measured

at 590 nm using a Biochrom Assays UVM 340 microplate reader, following extraction of the dye using an acetic acid 33% solution.

4.2. ELISA

Cell culture supernatants were assayed by ELISA for human VEGF-A (BMS277-2 Invitrogen, Waltham, MA, USA), according to the manufacturer's protocol.

4.3. Western Blot Analysis

ARPE-19 cells washed with cold 1X phosphate-buffered saline (PBS Dutscher, Brumath, France) were either lysed in Boiling buffer (SDS sodium dodecyl sulfate 1%, orthovanadate 1 mM, Tris 10 mM (pH 7.4)) with protease inhibitors (Roche, Boulogne-Billancourt, France) for 30 min on ice. Then, the lysates were sonicated for 6/7 sec at 30% amplitude. Protein concentrations were measured using a BCA assay kit (Thermo Fisher Scientific, IllKirch-Graffenstaden, France). As for total protein, 25 to 60 µg were loaded onto 10% polyacrylamide gel. Proteins were resolved by SDS-PAGE and transferred to nitrocellulose membranes (Amersham, Les Ulis, France). Blots were then saturated in 5% milk (1 h at RT) before overnight incubation at 4 °C with specific primary antibodies (Supplementary Table S1). All primary antibodies were diluted at 1:1000 in 5% *w*/*v* non-fat milk or 5% BSA. Primary antibodies were detected using horseradish peroxidase (HRP)-conjugated appropriate secondary antibodies (Cell Signaling Technologies, IllKirch-Graffenstaden, France) followed by exposure to ECL (Santa Cruz Biotechnology, Nanterre, France). Signal was acquired with a ChemiDoc™ XRS+ imaging system (Biorad, Marnes-la-coquette, France), and blots were analyzed with Image Lab™ Software 5.1.2 (Biorad, Marnes-la-coquette, France).

4.4. Immunofluorescent Labelling and Staining of Cells

ARPE-19 cells cultured on coverslips were washed with cold PBS and fixed with 4% paraformaldehyde (PFA) for 10 min at room temperature, followed by permeabilization with cold methanol. The samples were blocked with 3% BSA 0.2% Saponin (47036, Sigma Aldrich) for 20 min at room temperature. Cells were incubated with primary antibody diluted 1:200 overnight at 4 °C. After washing with PBS, samples were incubated with secondary Alexa 488 or 568 coupled anti-rabbit (Life Technologies, Saint Aubin, France) diluted 1:1000 with BSA/Saponin buffer. After extensive washing, coverslips were mounted on a drop of Mounting Medium ProLong® containing DAPI (Molecular Probes, ThermoFisher Scientific, Strasbourg, France) in the dark for 1 h. Slides were imaged using a CDD equipped upright microscope (Zeiss, Marly le Roi, France) and 63×, 1.4 NA objective.

4.5. Lipid Rafts Isolation and Biochemical Characterization

Retinal cells were grown in 175 cm^2 dishes and treated for 24 h with or without treatments (RSG 12 µM, NUT 12 µM, and RSV 20 µM). Cells were washed with ice-cold PBS, harvested by scraping in 2 mL of ice-cold Tris-NaCl-EDTA buffer (TNE; 150 nM NaCl, 20 mM Tris (pH 7.4) and 1 mM EDTA) containing 1% (*w*/*v*) Lubrol, and vortexed. After 30 min of incubation on ice, cells were homogenized further by passing the lysate at least 25 times through a 21-gauge needle. Lysates were transferred to centrifuge tubes and mixed with 2 mL of 80% (*w*/*v*) sucrose in TNE. On top of this, 3.5 mL of 35% (*w*/*v*) and 3.5 mL of 5% (*w*/*v*) sucrose in TNE were successively loaded, resulting in a discontinuous gradient. All solutions contained a complete protease inhibition cocktail (Roche Applied Bioscience). The samples were centrifuged at 39,000 rpm for 20 h at 4 °C, and 1 mL fractions were collected from the top of the gradient. Then, 60 µL of each fraction was subjected to SDS-polyacrylamide gel electrophoresis and immunoblotted. Lipids were extracted and analyzed as described [50] in the indicated conditions. Expression profiles of both flotillin and caveolin-2, described as rafts markers, were analyzed in each fraction by western blotting.

4.6. Lipidomic Analysis of Lipid Rafts

For targeted analysis of cholesterol and sphingomyelins, 25 µL and 50 µL of rafts fractions were used by GCMS and LCMSMS, respectively, as previously described [51].

4.7. RNA Extraction and Quantitative PCR Analysis

Total cellular RNA was extracted with TRIzol® RNA Isolation Reagent (Ambion). RNA (300 ng) was reverse transcribed into cDNA using M-MLV Reverse Transcriptase, random primers, and RNAseOUT inhibitor (Invitrogen). cDNA was quantified by real-time PCR with the Power SYBR Green PCR Master Mix (Applied Biosystems; Warrington, UK) on a 7500 Fast Real-Time PCR detection system (Applied Biosystems). Relative mRNA levels were determined by the ΔΔCt method and normalized to the expression levels of human or mouse *Actb.* Primer sequences used are listed in the following Table 1.

Table 1. Primers used for RT-qPCR analysis.

Gene	Forward Sequence	Reverse Sequence
h-Beta-actin	5′-TCCACCTTCCAGCAGATGTG-3′	5′-GCATTTGCGGTGGACGAT-3′
h-vegf-a	5′-ATCTTCAAGCCATCCTGTGTG-3′	5′-GAGGTTTGATCCGCATAATCTG-3′
h-vegf-r1	5′-GAAATCACCTACGTGCCGGA-3′	5′-ACGTTCAGATGGTGGCCAAT-3′
h-vegf-r22	5′-CCAGCAAAAGCAGGGAGTCTGT-3′	5′-TGTCTGTGTCATCGGAGTGATATCC-3′
h-c-fos	5′-TTATCTCCAGAAGAAGAAGAGAAAAGGAGAATC-3′	5′-AGGGCCAGCAGCGTGGGTGAGCTGAGCGAGTCA-3′
h-c-jun	5′-CAGCCAGGTCGGCAGTATAG-3′	5′-GGGACTCTGCCACTTGTCTC-3′
h-c-jun #3 (vegf)	5′-GAGCAGCGAAAGCGACAG-3′	5′-TGTCTGTCTGTCTGTCCGTCA-3′
h-c-jun #5 (vegf-r2)	5′-CACACCACACAGATGTGCAA-3′	5′-CCAATGCCAGTTAATTTCTGA-3′
h-c-jun #6 (vegf-r2)	5′-TCAGAAATTAACTGGCATTGG-3′	5′-AGACCCAGGGATATTCTGACA-3′

4.8. Nuclear and Cytoplasmic Fraction Isolation

The cells were lysed in buffer (NE-PER; Pierce Biotechnology, Rockford, IL, USA) supplemented with a protease inhibitor cocktail (Halt; Pierce Biotechnology, Rockford, IL, USA), according to the manufacturer's protocol. Protein concentrations were determined (BCA Kit; Pierce Biotechnology) before being loaded onto polyacrylamide gels.

4.9. DNA ChIP Assay

Cells are prepared according to the truChIPTM Shearing Kit protocol (Covaris), collected, and rinsed using cold PBS 1 X. Cell pellets were fixed using buffer A and using 1% formaldehyde. After 10 min with stirring, we add buffer E then the cells are centrifuged (500 G, 5 min, room temperature). After two washes with PBS 1 X, buffer B is added to lyse plasma membranes (10 min with stirring at 4 °C). Then, cells are centrifuged, and the pellets resuspended in washing buffer C (10 min at 4 °C). The nuclei are recovered by centrifugation (1700 G, 5 min at 4 °C). The nuclear pellet is resuspended in the D3 buffer and transferred to milliTUBE AFA Fiber tubes (Covaris, Woburn, MA, USA). The samples are then ultrasound (3 sessions of 12 min). After this nuclear preparation, ChIP was conducted according to the manufacturer's instruction: ChIP-IT® Express Enzymatic (Active Motif, La Hulpe, Belgium) protocol. After dosing the chromatin, we carry out an incubation of 50 µg of chromatin with the magnetic beads, a supplied ChIP buffer, and the anti-VEGFR-2 (Cell Signaling, Danvers, MA, USA) or anti-VEGF (Cell signaling) antibodies overnight at 4 °C. The beads are then washed several times, and the chromatin is eluted using a buffer. The DNA obtained can be used immediately in PCR or stored at −20 °C. The sequences of the oligonucleotides used are described in Table 1.

4.10. Densitometry and Statistical Significance

The densitometry of blots was realized by the use of ImageJ software (National Institutes of Health). Unless indicated in the legends of figures, the reported values represent the means of triplicate from one representative experiment repeated three times +/− SD. Statistical significance was determined using the Mann–Whitney test at * $p < 0.05$, ** $p < 0.01$ or *** $p < 0.001$.

5. Conclusions

In this study, we showed that a nutraceutical enriched in omega-3 and in a polyphenol, resveratrol, could decrease VEGF-A secretion for retinal cells through a disruption of the MAP kinase pathway and the transcription of gene encoding to VEGF-R2 and VEGF proteins. Nonetheless, further investigations must be performed to demonstrate the potential use of Resvega as nutritional complementation against AMD, especially regarding whether these anti-angiogenic effects are confirmed in preclinical models of AMD.

Supplementary Materials: The following are available online at https://www.mdpi.com/article/10.3390/ijms22126590/s1, Figure S1: RSG decreases expression of global phosphorylation, Table S1: Antibodies.

Author Contributions: F.C., A.S., V.A. and C.C. performed the experiments and analyzed the data; J.-P.P.d.B. designed the lipidomic methods and supervised the lipidomic experiments, C.O. helped in setting up the project; D.D. wrote the manuscript and supervised the overall project. All authors have read and agreed to the published version of the manuscript.

Funding: This work was supported by grants from the ANRT N°2016/0003, by a French Government grant managed by the French National Research Agency under the program "Investissements d'Avenir", reference ANR-11-LABX-0021, the Conseil Régional Bourgogne, Franche-Comte (PARI grant) and the FEDER (European Funding for Regional Economic Development).

Institutional Review Board Statement: Not applicable.

Informed Consent Statement: Not applicable.

Data Availability Statement: The authors declare that all data supporting the findings of this study are available within the article.

Acknowledgments: The authors thank Isabella Athanassiou for her valuable English corrections and thank Victoria Bergas for her help with lipidomic analysis.

Conflicts of Interest: C.O. is an employee of Laboratoires THEA.

References

1. Lim, L.S.; Mitchell, P.; Seddon, J.M.; Holz, F.G.; Wong, T.Y. Age-related macular degeneration. *Lancet* **2012**, *379*, 1728–1738. [CrossRef]
2. Marshall, L.L.; Roach, J.M. Prevention and treatment of age-related macular degeneration: An update for pharmacists. *Consult. Pharm.* **2013**, *28*, 723–737. [CrossRef] [PubMed]
3. Querques, G.; Benlian, P.; Chanu, B.; Portal, C.; Coscas, G.; Soubrane, G.; Souied, E.H. Nutritional AMD treatment phase I (NAT-1): Feasibility of oral DHA supplementation in age-related macular degeneration. *Eur. J. Ophthalmol.* **2009**, *19*, 100–106. [CrossRef] [PubMed]
4. Labrecque, L.; Royal, I.; Surprenant, D.S.; Patterson, C.; Gingras, D.; Beliveau, R. Regulation of vascular endothelial growth factor receptor-2 activity by caveolin-1 and plasma membrane cholesterol. *Mol. Biol. Cell* **2003**, *14*, 334–347. [CrossRef] [PubMed]
5. Age-Related Eye Disease Study 2 Research Group. Lutein + zeaxanthin and omega-3 fatty acids for age-related macular degeneration: The Age-Related Eye Disease Study 2 (AREDS2) randomized clinical trial. *JAMA* **2013**, *309*, 2005–2015. [CrossRef]
6. Age-Related Eye Disease Study Research Group. The Age-Related Eye Disease Study (AREDS): Design implications. AREDS report no. 1. *Control. Clin. Trials* **1999**, *20*, 573–600. [CrossRef]
7. Ferrara, N. Vascular endothelial growth factor and age-related macular degeneration: From basic science to therapy. *Nat. Med.* **2010**, *16*, 1107–1111. [CrossRef]
8. Zhang, H.; He, S.; Spee, C.; Ishikawa, K.; Hinton, D.R. SIRT1 mediated inhibition of VEGF/VEGFR2 signaling by Resveratrol and its relevance to choroidal neovascularization. *Cytokine* **2015**, *76*, 549–552. [CrossRef]

9. Seong, H.; Ryu, J.; Jeong, J.Y.; Chung, I.Y.; Han, Y.S.; Hwang, S.H.; Park, J.M.; Kang, S.S.; Seo, S.W. Resveratrol suppresses vascular endothelial growth factor secretion via inhibition of CXC-chemokine receptor 4 expression in ARPE-19 cells. *Mol. Med. Rep.* **2015**, *12*, 1479–1484. [CrossRef]
10. Wu, H.; He, L.; Shi, J.; Hou, X.; Zhang, H.; Zhang, X.; An, Q.; Fan, F. Resveratrol inhibits VEGF-induced angiogenesis in human endothelial cells associated with suppression of aerobic glycolysis via modulation of PKM2 nuclear translocation. *Clin. Exp. Pharmacol. Physiol.* **2018**, *45*, 1265–1273. [CrossRef]
11. Miller, J.W.; Adamis, A.P.; Aiello, L.P. Vascular endothelial growth factor in ocular neovascularization and proliferative diabetic retinopathy. *Diabetes. Metab. Rev.* **1997**, *13*, 37–50. [CrossRef]
12. Ablonczy, Z.; Dahrouj, M.; Tang, P.H.; Liu, Y.; Sambamurti, K.; Marmorstein, A.D.; Crosson, C.E. Human retinal pigment epithelium cells as functional models for the RPE in vivo. *Invest. Ophthalmol. Vis. Sci.* **2011**, *52*, 8614–8620. [CrossRef]
13. Bhattarai, N.; Korhonen, E.; Toppila, M.; Koskela, A.; Kaarniranta, K.; Mysore, Y.; Kauppinen, A. Resvega alleviates hydroquinone-induced oxidative stress in ARPE-19 cells. *Int. J. Mol. Sci.* **2020**, *21*, 2066. [CrossRef] [PubMed]
14. Bhattarai, N.; Piippo, N.; Ranta-Aho, S.; Mysore, Y.; Kaarniranta, K.; Kauppinen, A. Effects of resvega on inflammasome activation in conjunction with dysfunctional intracellular clearance in Retinal Pigment Epithelial (RPE) Cells. *Antioxidants* **2021**, *10*, 67. [CrossRef] [PubMed]
15. Dugas, B.; Charbonnier, S.; Baarine, M.; Ragot, K.; Delmas, D.; Menetrier, F.; Lherminier, J.; Malvitte, L.; Khalfaoui, T.; Bron, A.; et al. Effects of oxysterols on cell viability, inflammatory cytokines, VEGF, and reactive oxygen species production on human retinal cells: Cytoprotective effects and prevention of VEGF secretion by resveratrol. *Eur. J. Nutr.* **2010**, *49*, 435–446. [CrossRef]
16. Koch, S.; Tugues, S.; Li, X.; Gualandi, L.; Claesson-Welsh, L. Signal transduction by vascular endothelial growth factor receptors. *Biochem. J.* **2011**, *437*, 169–183. [CrossRef] [PubMed]
17. Abhinand, C.S.; Raju, R.; Soumya, S.J.; Arya, P.S.; Sudhakaran, P.R. VEGF-A/VEGFR2 signaling network in endothelial cells relevant to angiogenesis. *J. Cell. Commun. Signal* **2016**, *10*, 347–354. [CrossRef] [PubMed]
18. Matsumoto, T.; Mugishima, H. Signal transduction via vascular endothelial growth factor (VEGF) receptors and their roles in atherogenesis. *J. Atheroscler. Thromb.* **2006**, *13*, 130–135. [CrossRef]
19. Gu, X.; Reagan, A.; Yen, A.; Bhatti, F.; Cohen, A.W.; Elliott, M.H. Spatial and temporal localization of caveolin-1 protein in the developing retina. *Adv. Exp. Med. Biol.* **2014**, *801*, 15–21. [CrossRef] [PubMed]
20. Jiang, Y.; Lin, X.; Tang, Z.; Lee, C.; Tian, G.; Du, Y.; Yin, X.; Ren, X.; Huang, L.; Ye, Z.; et al. Critical role of caveolin-1 in ocular neovascularization and multitargeted antiangiogenic effects of cavtratin via JNK. *Proc. Natl. Acad. Sci. USA* **2017**, *114*, 10737–10742. [CrossRef] [PubMed]
21. Ikeda, S.; Ushio-Fukai, M.; Zuo, L.; Tojo, T.; Dikalov, S.; Patrushev, N.A.; Alexander, R.W. Novel role of ARF6 in vascular endothelial growth factor-induced signaling and angiogenesis. *Circ. Res.* **2005**, *96*, 467–475. [CrossRef]
22. Song, M.; Finley, S.D. Mechanistic insight into activation of MAPK signaling by pro-angiogenic factors. *BMC Syst. Biol.* **2018**, *12*, 145. [CrossRef]
23. Jia, J.; Ye, T.; Cui, P.; Hua, Q.; Zeng, H.; Zhao, D. AP-1 transcription factor mediates VEGF-induced endothelial cell migration and proliferation. *Microvasc. Res.* **2016**, *105*, 103–108. [CrossRef]
24. Smeal, T.; Binetruy, B.; Mercola, D.A.; Birrer, M.; Karin, M. Oncogenic and transcriptional cooperation with Ha-Ras requires phosphorylation of c-Jun on serines 63 and 73. *Nature* **1991**, *354*, 494–496. [CrossRef]
25. Pulverer, B.J.; Kyriakis, J.M.; Avruch, J.; Nikolakaki, E.; Woodgett, J.R. Phosphorylation of c-jun mediated by MAP kinases. *Nature* **1991**, *353*, 670–674. [CrossRef]
26. Milanini, J.; Vinals, F.; Pouyssegur, J.; Pages, G. p42/p44 MAP kinase module plays a key role in the transcriptional regulation of the vascular endothelial growth factor gene in fibroblasts. *J. Biol. Chem.* **1998**, *273*, 18165–18172. [CrossRef] [PubMed]
27. Carmeliet, P.; Jain, R.K. Molecular mechanisms and clinical applications of angiogenesis. *Nature* **2011**, *473*, 298–307. [CrossRef]
28. Carmeliet, P.; Jain, R.K. Angiogenesis in cancer and other diseases. *Nature* **2000**, *407*, 249–257. [CrossRef] [PubMed]
29. Keane, P.A.; Sadda, S.R. Development of Anti-VEGF Therapies for Intraocular Use: A Guide for Clinicians. *J. Ophthalmol.* **2012**, *2012*, 483034. [CrossRef] [PubMed]
30. Tahir, S.A.; Park, S.; Thompson, T.C. Caveolin-1 regulates VEGF-stimulated angiogenic activities in prostate cancer and endothelial cells. *Cancer Biol. Ther.* **2009**, *8*, 2286–2296. [CrossRef]
31. Caliceti, C.; Zambonin, L.; Rizzo, B.; Fiorentini, D.; Vieceli Dalla Sega, F.; Hrelia, S.; Prata, C. Role of plasma membrane caveolae/lipid rafts in VEGF-induced redox signaling in human leukemia cells. *BioMed Res. Int.* **2014**, *2014*, 857504. [CrossRef]
32. Spilsbury, K.; Garrett, K.L.; Shen, W.Y.; Constable, I.J.; Rakoczy, P.E. Overexpression of vascular endothelial growth factor (VEGF) in the retinal pigment epithelium leads to the development of choroidal neovascularization. *Am. J. Pathol.* **2000**, *157*, 135–144. [CrossRef]
33. Chong, E.W.; Kreis, A.J.; Wong, T.Y.; Simpson, J.A.; Guymer, R.H. Dietary omega-3 fatty acid and fish intake in the primary prevention of age-related macular degeneration: A systematic review and meta-analysis. *Arch. Ophthalmol.* **2008**, *126*, 826–833. [CrossRef]
34. Pandey, K.B.; Rizvi, S.I. Plant polyphenols as dietary antioxidants in human health and disease. *Oxidative Med. Cell. Longev.* **2009**, *2*, 270–278. [CrossRef] [PubMed]
35. Cao, Y.; Cao, R.; Brakenhielm, E. Antiangiogenic mechanisms of diet-derived polyphenols. *J. Nutr. Biochem.* **2002**, *13*, 380–390. [CrossRef]

36. Ghiringhelli, F.; Rebe, C.; Hichami, A.; Delmas, D. Immunomodulation and anti-inflammatory roles of polyphenols as anticancer agents. *Anticancer. Agents Med. Chem.* **2012**, *12*, 852–873. [CrossRef] [PubMed]
37. Delmas, D.; Jannin, B.; Latruffe, N. Resveratrol: Preventing properties against vascular alterations and ageing. *Mol. Nutr. Food Res.* **2005**, *49*, 377–395. [CrossRef]
38. Delmas, D.; Lancon, A.; Colin, D.; Jannin, B.; Latruffe, N. Resveratrol as a chemopreventive agent: A promising molecule for fighting cancer. *Curr. Drug Targets* **2006**, *7*, 423–442. [CrossRef]
39. Delmas, D.; Solary, E.; Latruffe, N. Resveratrol, a phytochemical inducer of multiple cell death pathways: Apoptosis, autophagy and mitotic catastrophe. *Curr. Med. Chem.* **2011**, *18*, 1100–1121. [CrossRef]
40. Kimura, Y.; Okuda, H. Resveratrol isolated from Polygonum cuspidatum root prevents tumor growth and metastasis to lung and tumor-induced neovascularization in Lewis lung carcinoma-bearing mice. *J. Nutr.* **2001**, *131*, 1844–1849. [CrossRef]
41. Yu, H.B.; Zhang, H.F.; Zhang, X.; Li, D.Y.; Xue, H.Z.; Pan, C.E.; Zhao, S.H. Resveratrol inhibits VEGF expression of human hepatocellular carcinoma cells through a NF-kappa B-mediated mechanism. *Hepatogastroenterology* **2010**, *57*, 1241–1246. [PubMed]
42. Limagne, E.; Thibaudin, M.; Euvrard, R.; Berger, H.; Chalons, P.; Vegan, F.; Humblin, E.; Boidot, R.; Rebe, C.; Derangere, V.; et al. Sirtuin-1 Activation Controls Tumor Growth by Impeding Th17 Differentiation via STAT3 Deacetylation. *Cell Rep.* **2017**, *19*, 746–759. [CrossRef] [PubMed]
43. Richer, S.; Patel, S.; Sockanathan, S.; Ulanski, L.J., 2nd; Miller, L.; Podella, C. Resveratrol based oral nutritional supplement produces long-term beneficial effects on structure and visual function in human patients. *Nutrients* **2014**, *6*, 4404. [CrossRef] [PubMed]
44. Richer, S.; Stiles, W.; Ulanski, L.; Carroll, D.; Podella, C. Observation of human retinal remodeling in octogenarians with a resveratrol based nutritional supplement. *Nutrients* **2013**, *5*, 1989. [CrossRef]
45. Olmiere, C.; Clerc, A.; Leconte, L. RESVEGA, by the presence of Resveratrol, inhibits retinal endothelial tube formation. *Acta Ophtalmol.* **2013**, *91*. [CrossRef]
46. Feng, Y.; Venema, V.J.; Venema, R.C.; Tsai, N.; Caldwell, R.B. VEGF induces nuclear translocation of Flk-1/KDR, endothelial nitric oxide synthase, and caveolin-1 in vascular endothelial cells. *Biochem. Biophys. Res. Commun.* **1999**, *256*, 192–197. [CrossRef]
47. Mora, R.C.; Bonilha, V.L.; Shin, B.C.; Hu, J.; Cohen-Gould, L.; Bok, D.; Rodriguez-Boulan, E. Bipolar assembly of caveolae in retinal pigment epithelium. *Am. J. Physiol. Cell Physiol.* **2006**, *290*, C832–C843. [CrossRef]
48. Morais, C.; Ebrahem, Q.; Anand-Apte, B.; Parat, M.O. Altered angiogenesis in caveolin-1 gene-deficient mice is restored by ablation of endothelial nitric oxide synthase. *Am. J. Pathol.* **2012**, *180*, 1702–1714. [CrossRef] [PubMed]
49. Dunn, K.C.; Aotaki-Keen, A.E.; Putkey, F.R.; Hjelmeland, L.M. ARPE-19, a human retinal pigment epithelial cell line with differentiated properties. *Exp. Eye Res.* **1996**, *62*, 155–169. [CrossRef]
50. Delmas, D.; Rebe, C.; Lacour, S.; Filomenko, R.; Athias, A.; Gambert, P.; Cherkaoui-Malki, M.; Jannin, B.; Dubrez-Daloz, L.; Latruffe, N.; et al. Resveratrol-induced apoptosis is associated with Fas redistribution in the rafts and the formation of a death-inducing signaling complex in colon cancer cells. *J. Biol. Chem.* **2003**, *278*, 41482–41490. [CrossRef]
51. Blondelle, J.; Pais de Barros, J.P.; Pilot-Storck, F.; Tiret, L. Targeted Lipidomic Analysis of Myoblasts by GC-MS and LC-MS/MS. *Methods Mol. Biol.* **2017**, *1668*, 39–60. [CrossRef] [PubMed]

ÉCOLE DOCTORALE
Environnements - Santé
Bourgogne | Franche-Comté

Titre : Polyphénols de la vigne et du vin et dégénérescence maculaire liée à l'âge

Mots clés : Polyphénols, extrait sec de vin rouge, resvératrol, DMLA, maladies oculaires

Résumé : La dégénérescence maculaire liée à l'âge (DMLA) constitue la première cause de handicap visuel dans les pays industrialisés. Bien que les traitements actuels se focalisent sur les stades avancés de la maladie, des études récentes mettent en évidence l'importance des traitements préventifs et d'une alimentation riche en anti-oxydants pour prévenir l'apparition de la maladie. Cette thèse a pour objectif d'évaluer les propriétés antioxydantes, anti-inflammatoires et anti-angiogéniques d'un cocktail polyphénolique, à savoir un extrait sec de vin rouge (RWE) ainsi qu'une d'un polyphénol seul, le resvératrol (RSV). Les résultats de cette étude ont démontré que le RWE prévenait la sécrétion et la voie de signalisation du facteur de croissance endothéliale VEGF-A, impliqué dans la néo-angiogenèse caractéristique de la forme la plus sévère de la DMLA. De plus, cette thèse a mis en évidence les effets protecteurs du RWE sur les événements précoces et initiateurs de la maladie. En effet, le caractère anti-oxydant du RWE permet non seulement de diminuer le stress oxydant, mais aussi de prévenir leurs dommages dans les cellules rétiniennes. Par ailleurs, le RWE a montré un fort pouvoir anti-inflammatoire dans les cellules rétiniennes, et aussi dans les cellules immunitaires. Enfin, les résultats de cette étude ont permis de montrer que les caractères pléiotropiques du RWE sont supérieurs à ceux du RSV seul. Ces résultats prometteurs soulignent l'intérêt des polyphénols dans la lutte contre la DMLA.

Title : Vine and wine polyphenols and age-related macular degeneration

Keywords : polyphenols, red wine extract, resvetarol, AMD, ocular diseases

Résumé : Age-related macular degeneration (AMD) is the leading cause of visual impairment in industrialized countries. Ours days, treatments target advanced stages of the disease. However, recent studies highlight the importance of preventive treatments and an antioxidant-rich diet in order to prevent the disease. The aim of this thesis was to evaluate the anti-oxidant, anti-inflammatory and anti-angiogenic properties of a polyphenolic cocktail, a red wine dry extract (RWE) and a polyphenol, resveratrol (RSV). The results of this study demonstrated that RWE prevented the secretion and the signaling pathway of the endothelial growth factor VEGF-A, involved in the neo-angiogenesis characteristic of the most severe form of AMD. In addition, this thesis highlighted the protective effects of RWE on early, disease-initiating events. RWE's anti-oxidant properties not only reduces oxidative stress, but also prevents their damage on retinal cells. In addition, RWE showed strong anti-inflammatory properties in retinal cells, as well as in immune cells. Finally, the results of this study showed that the properties of RWE were superior to those of RSV alone. These promising results underline the value of polyphenols cocktails in the fight against AMD.